



U.S. Department
of Transportation

**National Highway
Traffic Safety
Administration**



DOT HS 812 091

April 2021

Potential Alternative Methodology for Evaluating Flammability of Interior Automotive Materials

DISCLAIMER

This publication is distributed by the U.S. Department of Transportation, National Highway Traffic Safety Administration, in the interest of information exchange. The opinions, findings, and conclusions expressed in this publication are those of the authors and not necessarily those of the Department of Transportation or the National Highway Traffic Safety Administration. The United States Government assumes no liability for its contents or use thereof. If trade or manufacturers' names or products are mentioned, it is because they are considered essential to the object of the publications and should not be construed as an endorsement. The United States Government does not endorse products or manufacturers.

NOTE: This report is published in the interest of advancing motor vehicle safety research. While the report provides results from research or tests using specifically identified motor vehicle and child restraint system models, it is not intended to make conclusions about the safety performance or safety compliance of those motor vehicles or child restraints, and no such conclusions should be drawn.

Suggested APA Format Citation:

Huczek, J., Janssens, M., Cabiness, S., Friedman, K., Mattos, G., & Stephenson, R. (2021, April). *Potential alternative methodology for evaluating flammability of interior automotive materials* (Report No. DOT HS 812 091). National Highway Traffic Safety Administration.

Technical Report Documentation Page

1. Report No. DOT HS 812 091	2. Government Accession No.	3. Recipient's Catalog No.	
4. Title and Subtitle Potential Alternative Methodology for Evaluating Flammability of Interior Automotive Materials		5. Report Date April 2021	
		6. Performing Organization Code	
7. Authors Jason P. Huczek, Marc L. Janssens, Spring Cabiness (SwRI); Keith Friedman, Garrett Mattos, Rhoads Stephenson (FRC)		8. Performing Organization Report No.	
9. Performing Organization Name and Address Southwest Research Institute Fire Technology Department 6220 Culebra Road, B143 San Antonio, TX 78238		10. Work Unit No. (TRAVIS)	
		11. Contract or Grant No.	
12. Sponsoring Agency Name and Address National Highway Traffic Safety Administration 1200 New Jersey Avenue SE Washington, DC 20590		13. Type of Report and Period Covered Final Report	
		14. Sponsoring Agency Code	
15. Supplementary Notes			
16. Abstract This paper describes results of an ongoing research program conducted at Southwest Research Institute for the National Highway Traffic Safety Administration. The purpose of the research is to improve the repeatability and reproducibility of evaluating the flammability of interior materials that are difficult to test according to FMVSS No. 302 (e.g., rigid non-planar materials, parts smaller than the FMVSS No. 302 specimen size, etc.). The goal is to identify an alternative existing small-scale fire test method for which FMVSS No. 302 equivalent pass/fail criteria can be established. Three alternative small-scale test methods were considered. The microscale combustion calorimeter as described in ASTM D7309 was found to be the most promising.			
17. Key Words FMVSS No. 302, flammability, interior materials, child restraint systems, motorcoach, passenger vehicle, flamespread, transportation, MCC, ASTM D7309		18. Distribution Statement Document is available to the public from the National Technical Information Service, www.ntis.gov .	
19 Security Classif. (of this report) Unclassified	20. Security Classif. (of this page) Unclassified	21 No. of Pages 325	22. Price

Form DOT F 1700.7 (8-72)

Reproduction of completed page authorized

Table of Contents

Introduction	1
Background	2
Regulatory Background	2
Program Structure Overview	3
Test Method Review	4
Vehicle Fires Field Data	6
Fire Cause and Origin and Propagation Paths	6
Task 2.1 Methodology	6
Task 2.1 Results	6
Major Fire Characteristics and Materials.....	9
Task 2.2 Methodology	9
Task 2.2 Results	9
Bench-Scale Material Testing	12
Test Material Selection and Procurement	12
Test Material Properties	15
FMVSS No. 302 Testing.....	17
ASTM D3801 Testing.....	19
ASTM E1354 Testing.....	20
ASTM D7309 Testing.....	22
Full-Scale Bus Seat Testing per ASTM E2574	25
ASTM E2574 Overview	25
Test Chamber	25
Ignition Sources	26
Procedure	27
Optional Calorimetry Measurements.....	28
First Series of Testing	29
Second Series of Testing.....	30
Child Restraint System Testing	34
Child Restraint Systems	34
Experimental Plan.....	35
Bench-Scale Testing	36
Open Calorimetry Testing.....	36
Calorimetry Results	38

Analysis.....	41
Chemical Composition Testing.....	42
Equipment and Methodology.....	42
Sample Processing Procedure.....	43
First Stage of Chemical Composition Testing.....	44
Second Stage of Chemical Composition Testing.....	47
Smoke Toxicity Testing	51
Methodology Approach	51
Test Plan.....	51
Baseline Tests	52
Experimental Apparatus and Procedure.....	54
Test Results.....	56
Small-Scale Flammability Test Data Analysis	58
ASTM D3801.....	58
ASTM E1354 (cone calorimeter).....	60
ASTM D7309 (MCC).....	61
Alternative Methodology Development	62
MCC Test Results and Material Properties Used in the Analysis	62
Method for Estimating T_{ig}	67
Estimating T_{ig} for Materials With a Single Peak in the Q(T) Curve	67
Estimating T_{ig} for Materials With Multiple Peaks in the Q(T) Curve	70
Statistical Analysis.....	71
Development of MCC Parameter-Based FMVSS No. 302 Pass/Fail Prediction Limits	72
Development of Physics-Based Pass/Fail Prediction Limits	74
Pass/Fail Criteria for the Alternative Methodology.....	76
Improving Repeatability for Layered Materials.....	82
Conclusions.....	84
Vehicle Fire Field Data.....	84
Bench-Scale Testing	84
School Bus and Motorcoach Seat Testing per ASTM E2574.....	84
Child Restraint System Research.....	84
Chemical Composition Testing.....	84
Alternative Methodology Development	85
Smoke Toxicity Testing.....	85

References.....	86
Appendix A: Test Method Review Matrix.....	A-1
Appendix B: Vehicle Fires Field Data – FRC Report	B-1
Appendix C: FMVSS 302 Data.....	C-1
Appendix D: ASTM D3801 Data	D-1
Appendix E: ASTM E1354 Data	E-1
Appendix F: ASTM D7309 Data	F-1
Appendix G: ASTM E2574 Data.....	G-1
Appendix H: Child Restraint Seat Calorimetry Data	H-1
Appendix I: Chemical Composition Data.....	I-1
Appendix J: Ignition Temperature Analysis.....	J-1

Figures

Figure 1. Passenger vehicle fire area of origin (NASS CDS 1995-2015)	7
Figure 2. Passenger vehicle interior component damaged by fire (NASS CDS - 228 cases).....	8
Figure 3. Case summary of crash-induced fire resulting in flamespread over the dash	8
Figure 4. Proportion of vehicle fires in fatal crashes by initial contact point (FARS 1991-2015)	10
Figure 5. Vehicle fire rate by vehicle age in fatal crashes (FARS 1991-2015)	11
Figure 6. Vehicle availability and preference ranking in terms of fire involvement and fire rate.	13
Figure 7. Material procurement – Selected photographs for passenger vehicles	14
Figure 8. Material procurement – Selected photographs for motorcoach and school buses	15
Figure 9. Schematic of FMVSS No. 302 test apparatus	18
Figure 10. Schematic of ASTM D3801 test apparatus	19
Figure 11. Schematic of ASTM E1354 (cone calorimeter) test apparatus	21
Figure 12. Schematic of ASTM D7309 (MCC) test apparatus.....	23
Figure 13. Specific heat release rate versus MCC pyrolysis chamber temperature curve.....	23
Figure 14. ASTM E2574 test chamber schematic	25
Figure 15. Photograph of SwRI test chamber for ASTM E2574.....	26
Figure 16. Schematics of top burner Specified in ASTM E2574	26
Figure 17. Schematics of under seat burner specified in ASTM E2574.....	27
Figure 18. Schematic of standard calorimeter hood and exhaust duct	28
Figure 19. Photograph of SwRI test chamber under large calorimeter.....	28
Figure 20. Pre (left) and post (right) test photographs of Bluebird school bus seat	29
Figure 21. Pre (left) and post (right) test photographs of Trans Tech school bus seat	29
Figure 22. Post-test photographs of Starcraft school bus seats.....	30
Figure 23. Pre (left) and post (right) test photographs from Test 1 of Second Series	30
Figure 24. Pre (left) and post (right) test photographs from Test 2 of Second Series	31
Figure 25. Pre (left) and post (right) test photographs from Test 3 of Second Series	31
Figure 26. Pre (left) and post (right) test photographs from Test 4 of Second Series	31
Figure 27. Pre (left) and post (right) test photographs from Test 5 of Second Series	32
Figure 28. Heat release rate comparison for ASTM E2574 Testing.....	33
Figure 29. Schematic of furniture calorimeter apparatus.....	37
Figure 30. Photograph of CRS test setup (Britax CRS pictured)	37
Figure 31. CRS heat release rate comparison (seat and base)	38
Figure 32. CRS heat release rate comparison (seat only)	38
Figure 33. CRS heat release rate comparison (base only)	39
Figure 34. FTIR Spectrometer (left) and Diamond ATR Module (right).....	43
Figure 35. Polyurethane Foam control sample spectra comparison results.....	48
Figure 36. Polypropylene control sample spectra comparison results.....	48
Figure 37. ABS control sample spectra comparison results	48

Figure 38. Required oxygen flow rates for the MC padding	52
Figure 39. Required oxygen flow rates for the MC Blue Seat backing.....	53
Figure 40. Required oxygen flow rates for the MC green seat cover	53
Figure 41. Schematic of modified MCC apparatus for smoke toxicity measurements	54
Figure 42. Clear sample bag connected to FTIR for gas analysis	55
Figure 43. Example FTIR spectra graph used for gas analysis.....	55
Figure 44. ASTM D3801 V-rating versus η_c from Lyon et al.	59
Figure 45. ASTM D3801 V-rating versus η_c based on present work.....	60
Figure 46. ASTM E1354 HRR _{peak} versus T_{ig} for three sets of automotive material	61
Figure 47. Typical Q(t) curve measured in the MCC	63
Figure 48. Corresponding Q(T) curve	63
Figure 49. MCC Q(T) curves for the motor coach luggage rack door	68
Figure 50. SP PPM Fit to Q(T) curves for the motor coach luggage rack door	69
Figure 51. Solver fit to Q(T) curves for the motor coach luggage rack door	69
Figure 52. Pass/fail limit for η_c (green circles are materials with $\eta_c \leq 200 \text{ J/g}\cdot\text{K}$).....	73
Figure 53. Pass/fail Limit for η_c (green circles are materials with $\eta_c \leq 200 \text{ J/g}\cdot\text{K}$)	73
Figure 54. FMVSS No. 302 burn rate as a Function of $\rho\delta(T_{ig} - T_a)$	75
Figure 55. Establishing $\rho\delta(T_{ig} - T_a)$ lower limit to predict failure in FMVSS No. 302.....	75
Figure 56. Correlation (or lack thereof) between FMVSS No. 302 burn rate and FGC.....	80
Figure 57. Relationship between T_1 and T_{ig}	80

Tables

Table 1: Work Tasks.....	3
Table 2: Final Selection of Test Methods for Evaluation.....	4
Table 3: Vehicle Fire Incidents by Year (NFIRS 2010-2014).....	9
Table 4: Summary of Material Properties for School Bus, Motorcoach, and Passenger Vehicle Test Specimens	16
Table 5: Summary of Material Properties for Thin Materials, Water Mist Foams, and Child Restraint System Materials	17
Table 6: FMVSS No. 302 Test Results Legend.....	18
Table 7: ASTM D3801 Rating Classification.....	20
Table 8: ASTM D3801 Test Results Legend.....	20
Table 9: ASTM E1354 Test Results Legend	22
Table 10: ASTM D7309 Test Results Legend.....	24
Table 11: ASTM E2574 Test Series 1 – Flame Spread Observations	29
Table 12: ASTM E2574 Test Series 2 – Flame Spread Observations	30
Table 13: ASTM E2574 Test Results Data Summary	32
Table 14: ASTM E2574 Test Results Legend	32
Table 15: Photographs of Child Restraint Systems	35
Table 16: Close-Up View of Selected Child Seat Components	35
Table 17: Summary Test Results for CRS Testing.....	40
Table 18: CRS Testing per ASTM E2067 Results Legend	41
Table 19: Stage 1 Chemical Composition Results – Passenger Vehicle Samples.....	45
Table 20: Stage 1 Chemical Composition Results – School Bus Seat Samples.....	45
Table 21: Stage 1 Chemical Composition Results – Child Restraint System Samples	46
Table 22: Stage 1 Chemical Composition Results – Motorcoach Samples.....	46
Table 23: Stage 1 Chemical Composition Results – Control Samples.....	47
Table 24: Stage 2 Chemical Composition Testing – Positive FR Control Samples.....	47
Table 25: Stage 2 Chemical Composition Testing – Final Results	49
Table 26: FR Chemical Composition Results Legend.....	50
Table 27: Test Matrix for Smoke/Toxicity Testing	51
Table 28: Summary Test Results for Smoke Toxicity Testing.....	56
Table 29: Comparison of Selected ASTM D3801, FMVSS No.302 and MCC Results	59
Table 30: Comparison of Selected ASTM E1354 and FMVSS No. 302 Results.....	61
Table 31: Compilation of Data Used in the Development of the Alternative Methodology	64
Table 32: Independent Variables Correlation Matrix	71
Table 33: Data for Materials With $\eta_c > 200$ J/g·K and $T_{ig} < 310^\circ\text{C}$ That Pass FMVSS No. 302	74
Table 34: Expected/Predicted FMVSS No. 302 Performance for the Materials Tested in the MCC ³	77

Table 35: Effect of Tested Surface on FMVSS No. 302 Performance.....	82
Table 36: Comparison of MCC Data for the Surface Layer Versus the Full Product.....	82
Table 37: Comparison of MCC Data for Knife-Milled Versus Cryo-Milled Specimens.....	83

Executive Summary

The National Highway Traffic Safety Administration awarded a contract to Southwest Research Institute (SwRI) to conduct research and testing in the interest of flammability of interior materials.

The purpose of the research was to improve the repeatability and reproducibility of evaluating the flammability of interior materials that are difficult to test per Federal Motor Vehicle Safety Standard (FMVSS) No. 302, Flammability of interior materials, (e.g., rigid non-planar materials, parts smaller than the FMVSS No. 302 specimen size, etc.). The goal was to identify an alternative, existing, small-scale fire test method for which FMVSS No. 302 equivalent pass/fail criteria can be established. The outcome of the program is potential test procedures and performance criteria that demonstrate improved repeatability over tests conducted to meet the current requirements of FMVSS No. 302. This report describes the work plan tasks and results of this research program.

The material flammability test standards used in this project were identified based on a literature review. Approximately two dozen of the most common small-open-flame test methods and approximately 10 of the most common radiant heat exposure methods that are currently used for some regulatory purpose were included in the review.

Based on this review, 4 bench-scale test methods, including the FMVSS No. 302 test method, were chosen for further evaluation, in addition to the intermediate-scale standardized test applicable to school bus seats. The results of testing per these methods are discussed in the report and there is an emphasis on the microscale combustion calorimetry (MCC) apparatus, standardized in ASTM D7309, *Standard Test Method for Determining Flammability Characteristics of Plastics and Other Solid Materials Using Microscale Combustion Calorimetry*, as a potential alternative methodology to the current FMVSS No. 302 test procedure. This method is especially useful for automotive materials that cannot be easily constructed into a specimen size and shape required by FMVSS No. 302.

Vehicle fires in the United States were investigated using the National Fire Incident Reporting System, Version 5 (NFIRS-5), National Automotive Sampling System (NASS), General Estimates System (GES), Fatality Analysis Reporting System (FARS), and NASS Crashworthiness Data System (CDS) datasets from 1991 to 2015. The investigation provided information on the frequency and characteristics of vehicle fires, including the cause, origins, and propagation paths of passenger compartment fires. A detailed analysis was conducted of 202 crashes resulting in vehicle fires.

Testing of interior automotive materials from passenger vehicles, a motorcoach, school buses, and several common materials was conducted per the four selected test methods for evaluation. In addition to the standard bench-scale testing, separate subtasks we carried out investigating specific areas of interest, including standard school bus seat testing, child restraint system testing, chemical composition testing, and smoke toxicity testing.

An analysis of the data obtained from bench-scale testing resulted in the selection of the MCC as the apparent most suitable method to serve as an alternative to FMVSS No. 302. Two sets of criteria were developed to determine, based on MCC test data and the thickness and density of the material, whether a material will pass the FMVSS No. 302 test. One test parameter used in this determination (surface temperature at ignition) is obtained from a complex analysis of the MCC data. An alternative parameter can be directly obtained from MCC data is suggested to make the method more user-friendly without much loss in its predictive capability of FMVSS No. 302 performance.

Introduction

The National Highway Traffic Safety Administration awarded a contract to Southwest Research Institute to conduct research and testing in the interest of flammability of interior materials.

The purpose of the research was to investigate possible ways to improve the repeatability and reproducibility of evaluating the flammability of interior materials that are difficult to test per FMVSS No. 302, Flammability of Interior Materials, (e.g., rigid non-planar materials, parts smaller than the FMVSS No. 302 specimen size, etc.). The goal was to identify an existing small-scale fire test method that does not have the FMVSS No. 302 limitations, and for which equivalent pass/fail criteria can be established. The outcomes of the program are identified test procedures and performance criteria that demonstrate improved repeatability over tests conducted to meet the current requirements of FMVSS No. 302. This report describes the work plan tasks and results of this research program.

Background

This section provides a discussion of the regulatory background and provides details on the project structure, specific tasks and layout of this report.

Regulatory Background

FMVSS No. 302, Flammability of Interior Materials, specifies burn resistance requirements for materials used in the occupant compartments of motor vehicles (49 CFR § 571.302). The standard was established in 1972 to reduce deaths and injuries caused by vehicle fires, especially those started from sources such as matches or cigarettes. The standard applies to passenger cars, child seats, multi-purpose vehicles, trucks, and buses. FMVSS No. 302 requires that any single or composite material within 13 mm of the occupant compartment air space, and cut to a thickness of up to 13 mm, shall not burn at a rate of more than 102 mm per minute when tested under the conditions of the standard. Specimens are tested within a metal cabinet in a horizontal test fixture. The ignition source is a Bunsen burner and a natural gas flame.

According to the National Fire Protection Agency's report (Ahrens, 2020) on vehicle fire trends and patterns, annual deaths and injuries from vehicle fires have dropped by more than half from 1980 to 2018. It is encouraging that fire frequency has been steadily diminishing.

FMVSS No. 302 went into effect on September 1, 1972, and has been amended with only minor changes to test procedures and definitions since then. As a result of the research, regulations, and industry standards developed over the past 40 years since FMVSS No. 302 was enacted, consideration is given to the current relevance of the standard, and to more recently developed evaluation methods and criteria.

Technical equivalents to FMVSS No. 302 were adopted by ISO (1989) in 1976/1989, ASTM (2020) in 1990, and SAE International (2019) in 1995. All these standards have been consistently reaffirmed and carried through revisions without changes to 2019.

In 1995 and 1999 the Federal Aviation Administration (14 CFR § 25.853) and the Federal Railroad Administration (49 CFR § 238.103) issued fire protection regulations for compartment interior materials. These regulations require many more tests, including, for example, vertical burn tests, and cone calorimeter tests, which provide several measurements (smoke emission, heat release rate, etc.). FAA has additional requirements for planes with passenger capacities of 20 or more.

The National Transportation Safety Board (NTSB) has issued safety recommendations to NHTSA to adopt more rigorous fire standards after the deadly Wilmer, Texas (Sept. 23, 2005), and Orland, California (April 10, 2014), motorcoach fires (NTSB, 2004a, 2004b). NHTSA sponsored research programs at the National Institute of Standards and Technology (NIST) and SwRI to evaluate fire detection, suppression, and exterior hardening materials for motorcoaches in order to extend egress time from burning vehicles (Johnson & Yang, 2007; Huczek & Blais, 2015). As part of those evaluations, both interior and exterior materials of motorcoaches were tested to different fire test standards. Several studies conducted since 1995 have also provided data characterizing passenger vehicle fires and methods to evaluate fire performance of components and materials used in vehicle construction (Janssens, 2008; Battipaglia et al., 2003; Miller et al., 2003).

Program Structure Overview

The focus of this research was to evaluate potential improvements to enhance the relevance, repeatability, and objectivity of FMVSS No. 302 for interior materials of passenger vehicles and motorcoaches.

Table 1 shows a breakdown of the work plan tasks designed to reach this objective. Tasks 4-7 are supplemental research topics that are tangentially related to the main focus of the project, but do not directly impact the analysis of the bench-scale data or development of the alternative test methodology and procedure.

Table 1: Work Tasks

Task Number	Task Description
1	Test Method Review
2	Statistical Analysis
2.1	Fire Cause and Origin and Propagation Paths
2.2	Major Fire Characteristics and Materials
3	Bench-Scale Material Testing
3.1	Test Material Procurement (NHTSA)
3.2	Test Matrix Development
3.3	FMVSS No. 302 Testing
3.4	ASTM D3801 Testing
3.5	ASTM E1354 Testing
3.6	ASTM D7309 Testing
4	ASTM E2574 Testing (Full-Scale Bus Seat Testing)
5	Child Restraint Seat Testing per ASTM E2067
6	Chemical Composition Testing
7	Smoke Toxicity Testing
8	Data Analysis
8.1	FMVSS No. 302 Testing
8.2	ASTM D3801 Testing
8.3	ASTM E1354 Testing
8.4	ASTM D7309 Testing
9	Alternative Methodology Development
10	Lab Procedure for Alternative Regulatory Test per ASTM D7309

Test Method Review

The material flammability test standards used in this project have been identified based on a literature review. Approximately two dozen of the most common small-open-flame test methods that are currently used for some regulatory purpose were included in the review. Approximately 10 of the most common radiant heat exposure test methods that are currently used for some regulatory purpose were included in the review.

Based on this review, 4 bench-scale test methods were chosen for further evaluation, in addition to the intermediate-scale standardized test applicable to school bus seats.

Table 2 provides the designation and title of each test method selected.

A matrix describing the results of this review has been created and is presented in Appendix A of this report. Table A-1 gives a summary of the most common small-open-flame test methods that are currently used for some regulatory purpose. These methods are referred to as “Small Flame Exposure” test methods. Table A-2 gives a summary of the most common radiant heat exposure test methods that are currently used for some regulatory purpose. These methods are referred to as “Radiant Exposure” test methods. Table A-3 gives a summary of the advantages and disadvantages to the various test methods outlined in Tables A-1 and A-2.

Table 2: Final Selection of Test Methods for Evaluation

Test Method Designation	Test Method Title
49 CFR § 571.302	FMVSS No. 302, Flammability of Interior Materials
ASTM D3801-10	Standard Test Method for Measuring the Comparative Burning Characteristics of Solid Plastics in a Vertical Position
ASTM E1354-16a	Standard Test Method for Heat and Visible Smoke Release Rates for Materials and Products Using an Oxygen Consumption Calorimeter
ASTM D7309-13	Standard Test Method for Determining Flammability Characteristics of Plastics and Other Solid Materials Using Microscale Combustion Calorimetry
ASTM E2574/ E2574M - 12a	Standard Test Method for Fire Testing of School Bus Seat Assemblies

Brief summaries of each of the test methods are provided below.

FMVSS No. 302 is the baseline comparison test and existing regulatory requirement. Other technically equivalent methods to FMVSS No. 302 were considered in the test method review and are included by proxy with the existing regulatory test. The project team decided it was unnecessary to conduct separate tests according to these various equivalent methods and that it would be more useful to focus the amount of available testing as described in this report.

ASTM D3801 is a small-flame test, conducted in the vertical position, and is technically equivalent to the 20 mm (50W) Vertical Burning Test (V-0, V-1, or V-2) of ANSI/UL 94. There are numerous options available for selection of a vertically oriented small-flame test. This specific method was chosen for two primary reasons. First, since this method is equivalent to subsections of UL 94, it is expected that most plastic materials used in the automotive industry will have already been evaluated to this method and as a result, this potential change is not expected to be significantly onerous to the industry. Second, this specific ASTM method was chosen, since precision (repeatability and reproducibility) data is available and published in the standard, and it focuses on the vertical tests in UL 94.

ASTM E1354 standardizes the use of the cone calorimeter in fire testing. The cone calorimeter was identified in a previous research program (Battipaglia et al., 2003) as a potential candidate to modernize the flammability requirements of FMVSS No. 302 and may still be a useful alternative to explore in the current project, with a specific emphasis on repeatability, reproducibility and sample preparation considerations. This type of test method is a technical improvement on small-flame test methods, since quantitative data is the direct output, which can be related to fire hazard of the material for specific fire scenarios.

ASTM D7309 describes another apparatus that provides quantitative data, which can be related to fire hazard. In addition, the output from this test method has been correlated with some success to other test methods, such as ASTM E1354 and UL 94 (Lyon & Walters, 2006). This apparatus and test method were not yet developed during the previous SwRI project and offer some potential improvements as well as new challenges. The sample size for this method is a few milligrams, as opposed to a 4 × 14-in sample for FMVSS No. 302. This is helpful for evaluating materials that are difficult to fit into the current required sample configuration. However, some data analysis will be required in this project to relate results from a very small sample to the performance of materials in their end-use conditions in a vehicle.

ASTM E2574 describes standardized testing of school bus seats. This is essentially equivalent to the National Safety Council Standard (school bus seat upholstery fire block test, approved by the National Conference on School Transportation as part of the National Standards for School Buses and National Standards for School Bus Operations), with the exception of replacement of the fire source (paper grocery bag with crumpled paper) with a gas burner, which greatly improves the repeatability and reproducibility of the method.

Vehicle Fires Field Data

Task 2.1 and 2.2 were both related to a review of vehicle fire statistics. Vehicle fires in the United States were investigated using the National Fire Incident Reporting System, Version 5 (NFIRS-5), NASS, GES, FARS, and CDS datasets from 1991 to 2015. The investigation provided information on the frequency and characteristics of vehicle fires, including the cause, origins, and propagation paths of passenger compartment fires. A detailed analysis was conducted of 202 crashes resulting in a vehicle fire.

The full report on vehicle fire field data is provided in Appendix B to this report. The following subsections of this report provide a few highlights of the results for the two primary focus areas of this analysis.

Fire Cause and Origin and Propagation Paths

Task 2.1 Methodology

The objective in this task was to further characterize the cause and origins of passenger compartment fires. Attention was also given to school buses and motorcoaches to examine how they differ from passenger vehicles.

NFIRS-5 data was reviewed, such as ignition source, type of material first ignited, type of material contributing most to flame spread, cause of ignition, factors contributing to ignition, variations by passenger vehicle type, etc. In addition, text fields will be reviewed exploring whether descriptive information of value to this study is present. NASS-CDS will be reviewed for crash induced fire information including fire occurrence and origin of fire. Propagation paths, compartment openings and general geometry will be obtained from existing representative vehicle models.

Task 2.1 Results

An in-depth investigation of crashes involving fires in the NASS CDS highlighted some characteristics of passenger vehicle fires. Frontal crashes were the predominant crash mode resulting in fires and the engine compartment was most often indicated as the fire origin area. Figure 1 illustrates the fire areas of origin for the NASS CDS dataset.

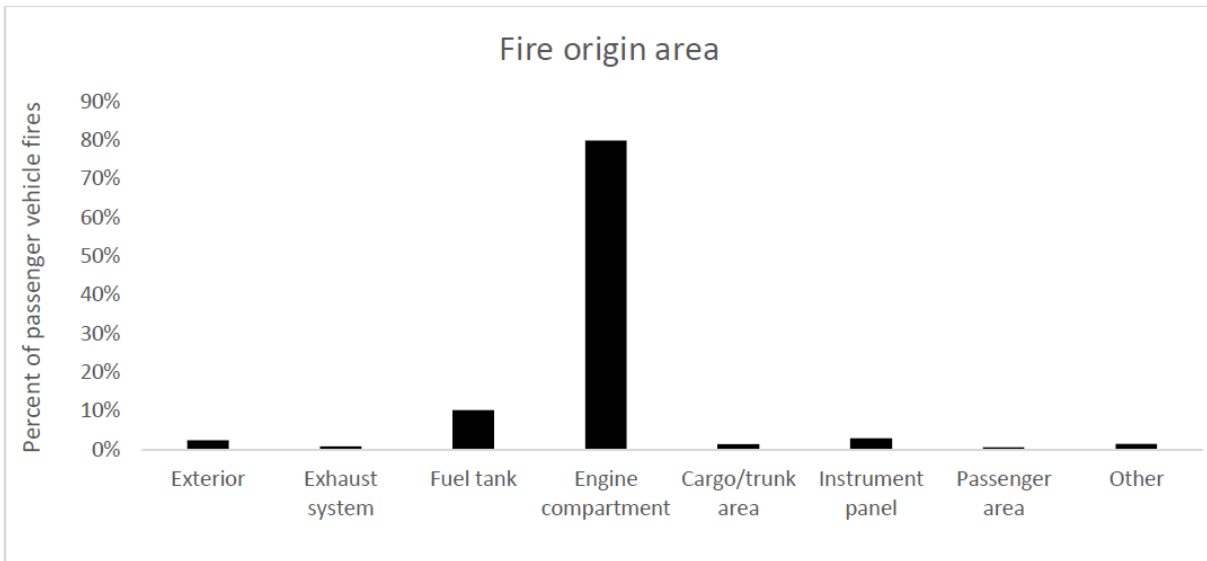


Figure 1. Passenger vehicle fire area of origin (NASS CDS 1995-2015)

In vehicle fires originating in the engine compartment the method of fire ingress into the passenger compartment was most often through the windshield and over the dash. It appears that the fire progresses through the windshield, which was either damaged by crash forces or thermal effects, and then ignites the vehicle interior, often the top of the dash. The fire then moves upward and rearward through the interior of the vehicle. In general, this includes in order of decreasing frequency, fire damage to the top dash, sun visor, front headliner, mid dash, steering wheel, mid headliner, steering wheel air bag, and front seat backs.

A secondary method of ingress into the passenger compartment may include propagation through a damaged firewall, though evidence for this was rarely directly observed. Another common scenario for ingress was through the rear of the vehicle often associated with rear impact damage. Figure 2 shows the interior components damaged by fire from the NASS CDS dataset.

Summaries of 202 fire crashes from the NASS CDS are presented in Appendix B to the FRC Report. These summaries include a link to the online case viewer, a brief police crash report narrative, a preliminary estimation of fire ingress area, and photos of the subject vehicle. Figure 3 shows an example of a summary of a crash resulting in over the dash flamespread.

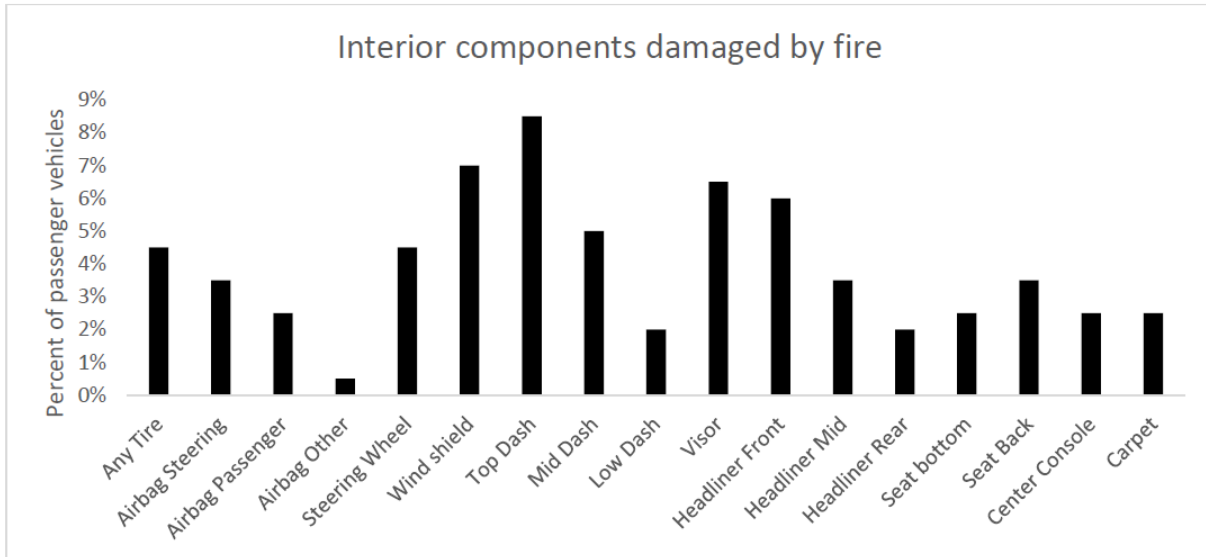


Figure 2. Passenger vehicle interior component damaged by fire (NASS CDS - 228 cases)

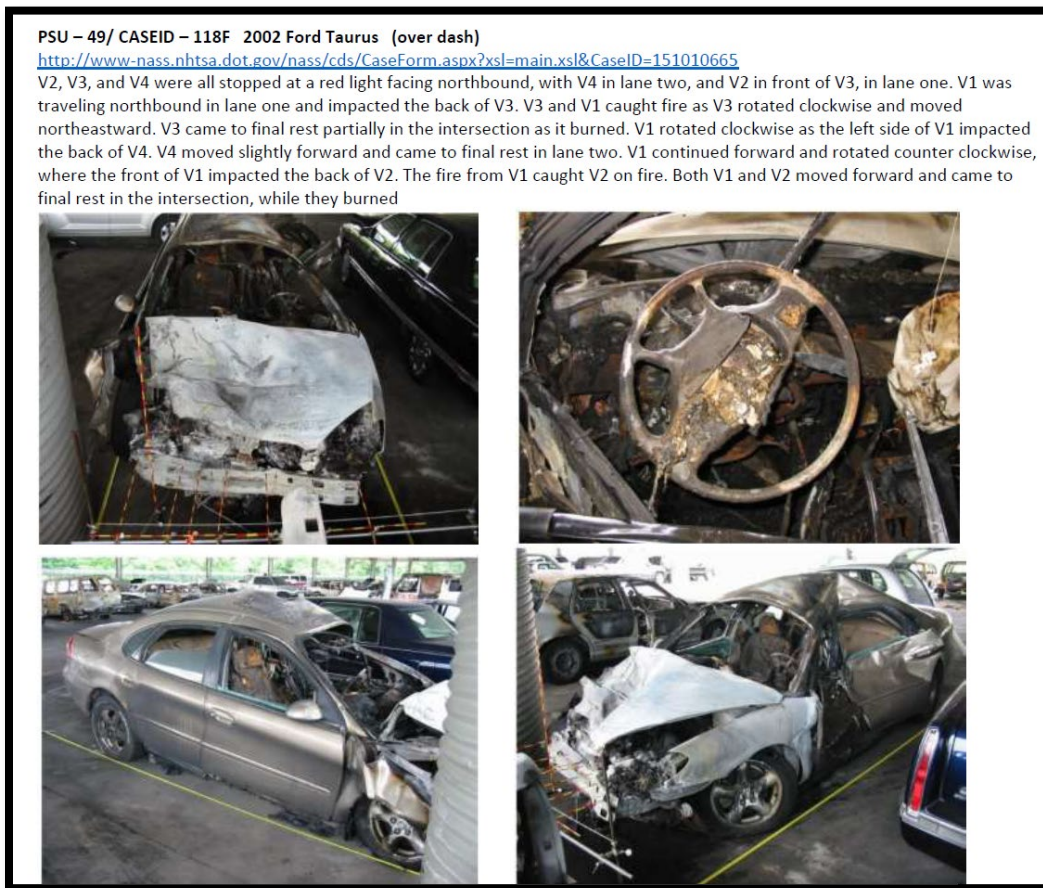


Figure 3. Case summary of crash-induced fire resulting in flame spread over the dash

Major Fire Characteristics and Materials

Task 2.2 Methodology

In this task the frequencies of vehicle fires by make, model and year were identified using NFIRS-5. Fire incidence by vehicle type nationally was confirmed using GES and FARS information to check the relative frequencies observed in NFIRS-5.

A characterization of the materials types and volumes present by vehicle type and origin location was determined through analysis of these databases. The distribution of these materials was assessed by location within vehicles representative of each vehicle type.

Task 2.2 Results

The total number of passenger vehicle fires that occurred in the United States decreased from 2010 to 2014. The total number of all fire incidents reported in NFIRS during this period also decreased, thus the passenger vehicle fire rate, per all fire incidents, was generally stable over this period. At the same time the number and rate, per all fire incidents, of heavy-truck fires increased. The number of bus fires trended along with the decrease in all fire incidents reported in NFIRS. Table 3 summarizes the vehicle fire data in the NFIRS-5 dataset.

Table 3: Vehicle Fire Incidents by Year (NFIRS 2010-2014)

NFIRS Incident Year	All Fire Incidents	Passenger Vehicle Fires		Heavy-Truck Fires		Bus Fires	
		n	%	n	%	n	%
2010	663,333	94,966	14.32	5,288	0.80	607	0.09
2011	671,329	91,330	13.60	5,570	0.83	601	0.09
2012	599,879	84,424	14.07	5,216	0.87	521	0.09
2013	554,671	83,225	15.00	5,678	1.02	525	0.09
2014	596,521	84,123	14.10	6,146	1.03	532	0.09
Total	3,085,733	437,068	14.16	27,898	0.90	2,786	0.09

In general, the rate of vehicle fires, per crash, decreased overall year by year. However, crash severity and other factors affect fire involvement. Vehicle fires are characterized by areas of origin, heat sources, items and materials burned, as well as basic crash factors. The results are disaggregated, where applicable, by general vehicle type including light duty passenger vehicles, medium/heavy trucks, and buses.

The number and rate, per police-reported crash, of passenger vehicle fires has decreased over the past decade. This is true for all passenger vehicle fires as well as crash-related fires. However, the rate of fire involvement for passenger vehicles involved in fatal crashes has increased over the past 26 years. This is likely due to improved vehicle crashworthiness that has resulted in a

relative increase in the severity of fatal crashes over the same time; i.e., occupants of contemporary vehicles are surviving more severe crashes than those in older vehicles. Thus, this result is likely more indicative that fire involvement increases with crash severity than with crash year or model year.

The overall number of heavy-truck fires, with or without crash-involvement, has increased according to the last 5 years of NFIRS data. Yet, like passenger vehicles, there has been a reduction in the number and rate of crash-involved heavy-truck fires. Bus fire and crash exposure was relatively low and no real trend was observed.

Vehicle fires were most often initiated without crash involvement. Approximately 1.6 percent of passenger vehicle fires and 1.9 percent of heavy-truck fires were associated with some type of collision. Crash events were only coded as being a factor in 0.3 percent of bus fires.

The characteristics of all vehicle fires were generally similar across all vehicle types and databases. For vehicles involved in collisions, fires most often originated in the engine compartment due to frontal impact damage. The passenger area was only noted as relatively common area of fire origin for events in which crashes were not a factor. Heavy-truck fires, in general, most frequently originated in the engine compartment or cargo area. However, in crash-related heavy-truck fires the fuel tank and fuel lines were noted as the area of origin 10 times more often than in non-crash-related heavy-truck fires. Figure 4 shows the proportion of vehicle fires sorted by initial contact point.

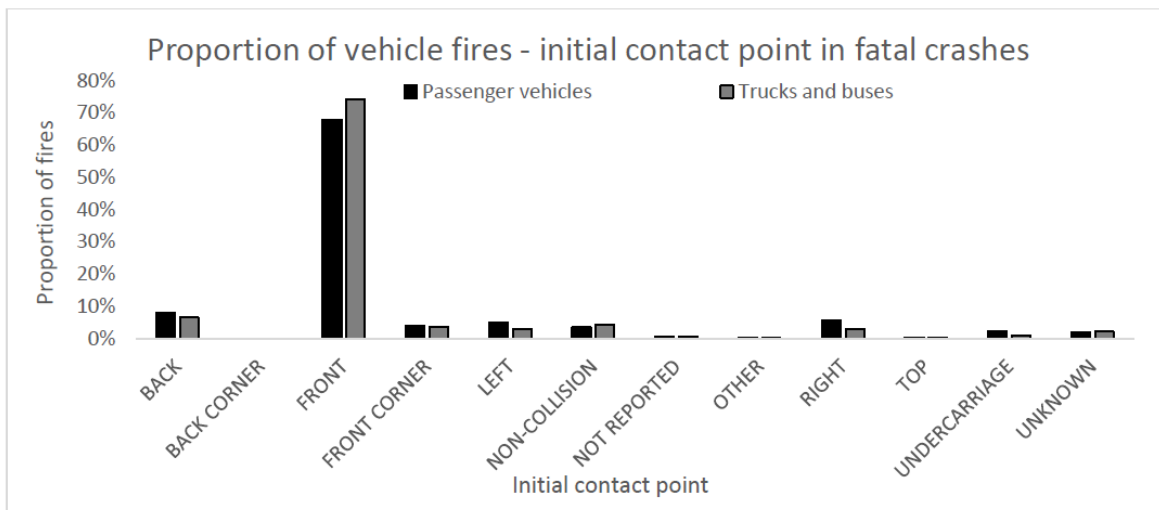


Figure 4. Proportion of vehicle fires in fatal crashes by initial contact point (FARS 1991-2015)

The types of materials that burned consisted mostly of flammable liquids in the engine compartment or fuel lines, electrical wires, tires, and interior fabrics. Operating equipment was, by far, the main source of heat attributed to initiating the fire. Overheated tires were also noted as a common heat source. Vehicle seats made up a relatively large proportion of items first ignited in passenger vehicles. However, vehicle seats were rarely coded as the first item ignited when passenger vehicle fires were restricted to those in which a collision was identified as factor contributing to the fire.

The fire rate, per crash, was found to vary widely for different vehicle makes and models. This may be due to several factors such as driver demographics, engine compartment and firewall design, and types of materials used throughout the vehicle. Vehicle age was also noted to be associated with fire involvement rates for both passenger vehicles and heavy trucks. Interestingly, the rate of fire involvement increased with vehicle age for passenger vehicles while it decreased with vehicle age for heavy trucks. Figure 5 illustrates these trends of vehicle age by type of vehicle.

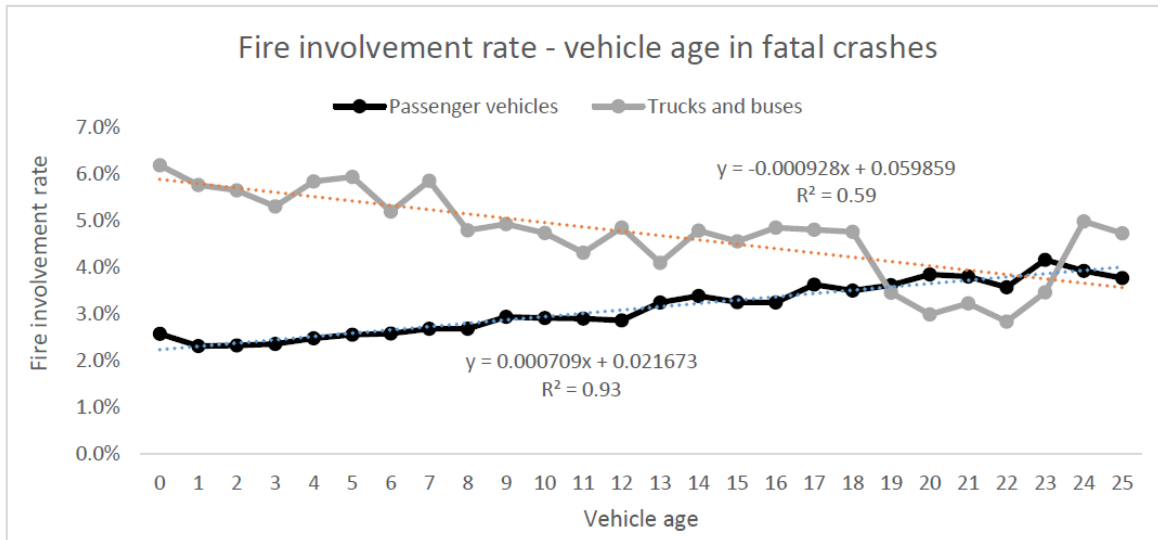


Figure 5. Vehicle fire rate by vehicle age in fatal crashes (FARS 1991-2015)

A summary of the fire involvement frequency and fire involvement rate for the top 30 passenger vehicles involved in fatal and police-reported crashes was developed from review of the datasets. This list was cross-referenced with the list of tested vehicles that were potentially available from NHTSA for collection of materials and this is summarized in Appendix A of the FRC report. Based on the information collected regarding frequencies and relevance a list of potential passenger car, child seat, school bus, and motorcoach interior components was selected for evaluation and comparison in project tasks. Further details will be provided in subsequent sections about these selected materials for testing.

Bench-Scale Material Testing

The following subsections provide details on the test material selection and procurement. Additional information about each test method is also provided, as well as some discussion of test parameters such as required sample preparation, sample conditioning, incident heat flux, and required replicate testing.

Test Material Selection and Procurement

Figure 6 lists the top 30 vehicle makes/models by fire involvement as determined from the NFIRS, FARS, GES, and CDS databases. The makes and models were cross-referenced with the makes and models that were available to NHTSA to be used in support of the project. The second column lists the total number of test vehicles that were available among all test sites. Available test vehicles were only listed if they corresponded to a top-30-ranked vehicle. The rankings were based on either the total number of fire involvements or the rate of fire involvement.

Note that the model year or generation of the test vehicle may not necessarily be equivalent to the model identified in the data. Also note that for some models, e.g., Ford F-Series, the make model codes do not disaggregate by series level. In the case of the F-Series, a review of Vehicle Identification Numbers (VINs) was undertaken to identify trends by series, i.e., “150”, “250,” etc. F-150s were over-represented compared to all other F-Series pickups.

NHTSA provided all the test samples to SwRI for the standardized fire testing. The results of the statistical review aided in the selection of passenger vehicle test samples from the inventory of vehicles that NHTSA had access to for other required standard tests (e.g., crash testing, air bag testing, etc.). Selection of make and model was based on higher frequency of fires in the statistics, frequency on the road and availability. This included parts from the following 2017 model year vehicles: Chevrolet Camaro, Mercedes E-Class, Ford F150, and Ford F250.

In addition to passenger vehicles, NHTSA provided materials from a Prevost motorcoach and seating material from three school buses (Bluebird, Starcraft, and TransTech). Figure 7 and Figure 8 show photograph arrays of selected materials received for testing in this project.

Year, Make, Model	# of Available Tested Vehicles	NFIRS Ranked by # Fires	NFIRS Ranked by Rate (per 1000 Crashes)	FARS Ranked by # fires	FARS Ranked by fire rate	GES Ranked by # fires (weighted)	GES Ranked by fire rate (weighted)	NASS CDS Ranked by # Major Fires (weighted)	NASS CDS ranked by Major Fire Rate (weighted)
2016 FORD F150 PICKUP	3	1	14	1	25	2			
2016 FORD F250 PICKUP	2	1	14	1	25	2			
2017 Ford F-250 SuperCrew	3	1	14	1	25	2			
2017 Ford F-250	3	1	14	1	25	2			
2017 FORD F250 CREW CAB	3	1	14	1	25	2			
2017 Ford F-250 SuperCab	4	1	14	1	25	2			
2016 NISSAN ALTIMA	1	3	6	4	18	4			
2015 TOYOTA CAMRY	1	7	21	10					
2016 CHEVROLET MALIBU	10	8	20	14		27			
2016 HONDA CIVIC	4	11							
2017 TOYOTA COROLLA	6	14		9					
2016 CHRYSLER 300	1	15	3	23	22			8	15
2017 FORD FUSION	7	16		15		15			12
2016 HYUNDAI SONATA	7	17	19	21					
2017 JEEP WRANGLER UNLIMITED	4	18	7	22	23				
2015 DODGE GRAND CARAVAN	2	19	22	19		11			
2017 FORD ESCAPE	2	23		20					
2017 CHEVROLET CAMARO	7			17	1				
2017 Subaru Impreza	3			26	2	16	17		
2016 CHEVROLET COLORADO	1								
2016 FORD EXPLORER	1								
2017 Cadillac CTS-V	2								
2016 FORD FIESTA	1							1	3
2017 CHRYSLER PACIFICA	9							20	16
2016 DODGE JOURNEY	1							26	
2016 JEEP PATRIOT	1								11
2016 CHEVROLET CRUZE	4				11	12	26		
2017 Nissan Frontier CrewCab	3				30	18	16		
2016 TOYOTA SIENNA	1					24			
2017 NISSAN TITAN	2				24				

Figure 6. Vehicle availability and preference ranking in terms of fire involvement and fire rate

		
Camaro Headliner	Camaro Dashboard	Camaro Seats
		
Mercedes Headliner	Mercedes Dashboard	Mercedes Seats
		
Ford F-150 Headliner	Ford F-150 Dashboard	Ford F-150 Seats
		
Ford F-250 Headliner	Ford F-250 Dashboard	Ford F-250 Seats

Figure 7. Material procurement – Selected photographs for passenger vehicles










		
Motorcoach Luggage Door	Motorcoach Floor Covering	Motorcoach Overall (View Toward Rear of Coach)
		
Motorcoach Luggage Door and Headliner	Motorcoach HVAC Controls at Occupant Seats	Motorcoach Overall (View Toward Front of Coach)
		
Trans Tech School Bus Seats	Starcraft School Bus Seats	Bluebird School Bus Seats

Figure 8. Material procurement – Selected photographs for motorcoach and school buses

As the project continued and the bench-scale data analyzed, it was necessary to procure additional materials to be used as possible control samples. These are referred to as “thin materials” and “water mist foams.”¹ In addition, a separate subtask devoted to investigating child restraint systems was initiated during the project and is discussed in more detail in subsequent sections.

Test Material Properties

Table 4 provides a summary of the relevant properties for test specimens from school buses, a motorcoach and passenger vehicles. Table 5 provides a similar summary for test specimens from thin materials, water mist foams and child restraint systems.

¹ Standard foam used in fire extinguishing tests per FM 5560, Approval Standard for Water Mist Systems (2016). The simulated mattress foam is described in Section G.3.1 and the simulated furniture foam is described in Section G.3.2 of FM 5560.

Table 4: Summary of Material Properties for School Bus, Motorcoach, and Passenger Vehicle Test Specimens

	Material	# of Layers	δ^* (mm)	ρ^{**} (kg/m ³)
School Bus Seats	Blue Bird Seat Cover	2	0.8	1055
	Blue Bird Padding	1	46.2	56
	Starcraft Seat Cover	2	0.8	945
	Starcraft Padding	1	42.0	95
	Trans Tech Seat Cover	2	0.8	1050
	Trans Tech Padding	1	25.4	24
Motorcoach Materials	Green Cover Padding	1	53.0	45
	Green Seat Cover	2	3.6	149
	Blue Seat Backing	2	3.7	247
	Blue Seat Cover	2	3.2	230
	Grey Seat Backing	1	5.2	163
	Luggage Rack Door	2	24.1	258
	Floor Covering	2	2.4	1073
	Headliner	2	4.2	215
	Blue Cover Padding ¹	1	101.6	73
	Blue Cover Padding ¹	1	101.6	73
	Blue Cover Padding ²	1	101.6	73
	Blue Cover Padding ²	1	101.6	73
Motor Vehicle Interior Mats	Ford F250 Carpet	2	15.3	124
	Mercedes Carpet	3	15.0	343
	Ford F250 Dashboard	1	3.4	1000
	Mercedes Dashboard	3	25.3	241
	Camaro Headliner	4	6.7	126
	Ford Headliner	4	16.7	65
	Camaro Seat Cover	3	3.7	165
	Mercedes Seat Cover	1	4.4	265
	Camaro Padding	1	16.8	36
	Mercedes Padding	1	19.0	50

* δ is the actual thickness of the material as received.

* ρ is calculated from the mass and dimensions of the FMVSS No. 302 specimens or a small sample if not tested to FMVSS No. 302.

Table 5: Summary of Material Properties for Thin Materials, Water Mist Foams, and Child Restraint System Materials

Material		# of Layers	δ^* (mm)	ρ^{**} (kg/m ³)
Thin Matls.	Acrylate	1	1.6	1040
	Corrugated Cardboard	1	3.2	155
	Thick HDPE	1	1.6	950
	Thin HDPE	1	0.8	950
	Folder Cardboard	1	0.3	680
WM Foam	SF Test Foam	1	6.4	29
	SF Test Foam	1	12.7	29
	SM Test Foam	1	6.4	33
	SM Test Foam	1	12.7	33
Child Restraint System Materials	Britax Base	1	1.2	629
	Chicco Base	1	2.9	602
	Peg Perego Base	1	2.9	711
	UPPAbaby Base	1	2.8	676
	Britax Fabric	1	0.2	435
	Chicco Fabric	1	0.2	539
	Peg Perego Fabric	1	0.5	284
	UPPAbaby Fabric	1	0.4	665
	Britax Padding	1	15.9	10
	Chicco Padding	1	9.7	26
	Peg Perego Padding	1	11.3	30
	UPPAbaby Padding	1	10.7	24
	Britax Assembly	1	16.1	16
	Chicco Assembly	2	9.9	38
	Peg Perego Assembly	2	11.8	41
UPPAbaby Assembly	2	11.1	46	

FMVSS No. 302 Testing

The primary purpose for the development of FMVSS No. 302 in the early 1970s was to reduce deaths and injuries to passengers caused by fires originating in the passenger compartment of motor vehicles (passenger cars, multipurpose passenger vehicles, trucks and buses). Automotive materials must be tested and meet the test requirements if any portion is within 13 mm (½ in.) of the occupant compartment air space.

Test specimens are prepared to dimensions of 100 × 355 mm (4 × 14 in.), with a maximum thickness of 13 mm (½ in.). The specimen is mounted in a U-shaped frame facing down in the direction that provides the most adverse test results (see Figure 9). Specimens that are less than

50-mm (2-in.) wide are supported in a special frame with wire supports. The frame is placed in a ventilated 200 × 380 × 355-mm (8 × 15 × 14-in.) chamber to protect against drafts.

The gas flow to a Bunsen burner is adjusted to provide a 38 mm (1.5 in.) flame, and the burner is placed 19 mm (¾ in.) below the center of the open end of the frame. The specimen is exposed to the flame for 15 s, and the time is recorded when the flame front reaches a point 38 mm (1.5 in.) from the exposed end. The time for the flame to travel along the underside of the specimen, from a point 38 mm (1.5 in.) from the exposed end of the frame to a point 38 mm (1.5 in.) from the clamped end of the specimen is also recorded. The rate of flame spread is then calculated and must not exceed 102 mm/min (4 in./min) for any of the five specimens tested.

For each different material, a set of five replicate test runs was performed. For materials that had multiple components/layers (e.g., seats), the composite material and/or its components was tested as required by the FMVSS No. 302 standard.

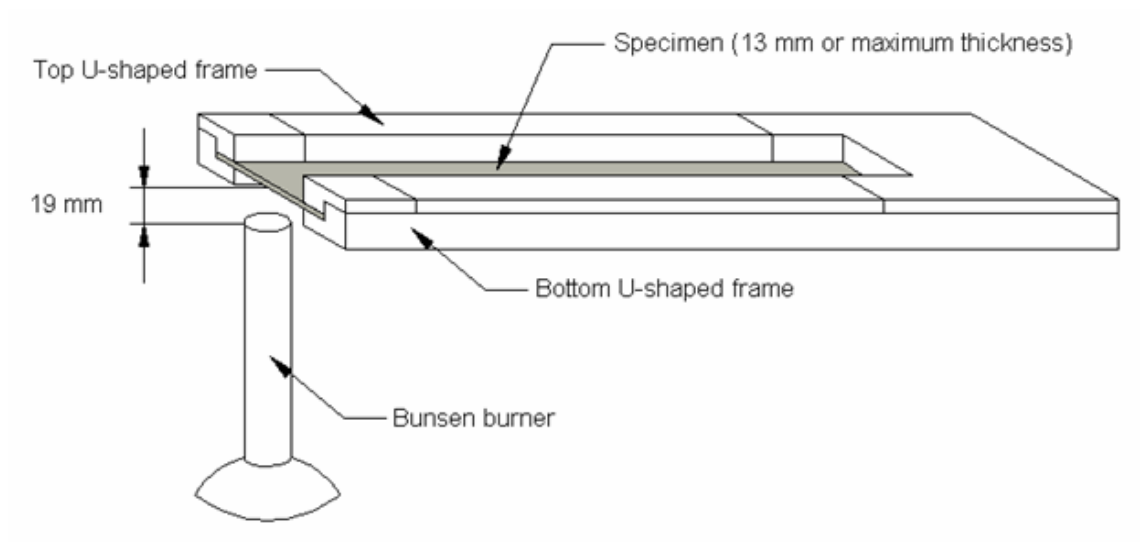


Figure 9. Schematic of FMVSS No. 302 test apparatus

The data gathered from this testing can be referenced in Appendix C and is discussed at length in the data analysis section of this report. Table 6 summarizes the results by vehicle type within Appendix C. Failing results are highlighted pink in the summary tables.

Table 6: FMVSS No. 302 Test Results Legend

Results Description	Appendix C Table Number
FMVSS 302 Results for School Bus Seat Materials	C-1
FMVSS 302 Results for Motorcoach Materials	C-2
FMVSS 302 Results for Vehicle Interior Materials	C-3
FMVSS 302 Results for Vehicle Interior Materials (Backside)	C-4
Thin Materials	C-5
Water Mist Foams	C-6
Child Restraint Seat Foams	C-7

ASTM D3801 Testing

ASTM D3801 is technically equivalent to the first vertical burning test described in the UL 94 (Underwriters Laboratories, 2013) standard, the “20-mm Vertical Burning Test; V-0, V-1, or V-2.” A schematic of the test setup is shown in Figure 10. The V-0, V-1, or V-2 classification is based on the duration of flaming or glowing following the removal of the burner flame, as well as the ignition of cotton by dripping particles from the test specimen.

Specimens measuring 125 mm long by 13 mm wide are suspended vertically and clamped at the top end. A thin layer of cotton is positioned 300 mm below the test specimen to catch any molten material that may drop from the specimen. A 20-mm long flame from a methane burner is applied to the center point on the bottom end of the specimen. The burner is positioned such that the burner barrel is located 9.5 mm below the bottom end of the material specimen. If the material melts, the burner barrel is held at an angle to avoid catching burning droplets that may ignite the cotton.

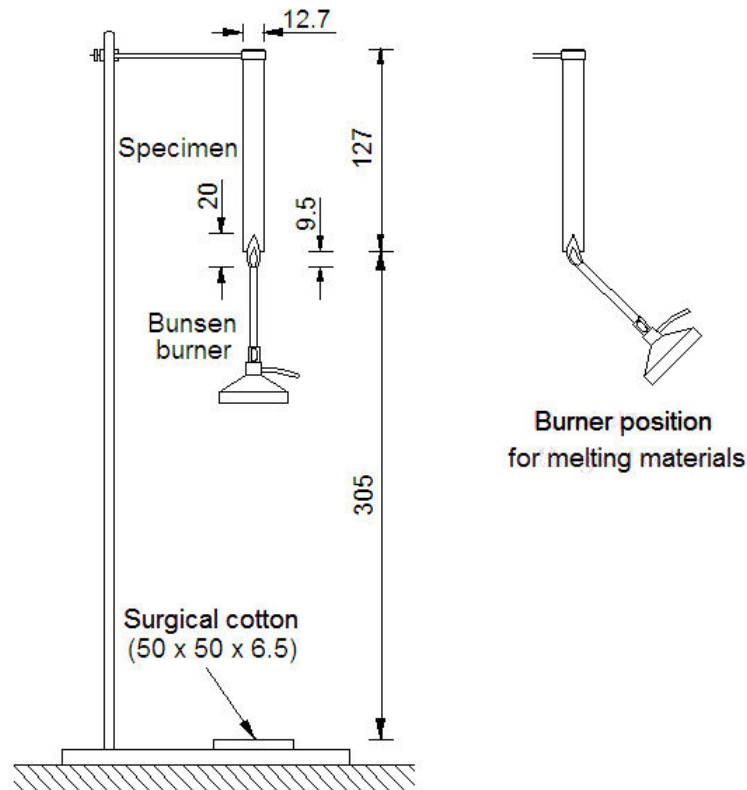


Figure 10. Schematic of ASTM D3801 test apparatus

The flame is maintained for 10 s, and then removed to a distance of at least 150 mm. Upon flame removal, the specimen is observed for flaming and its duration time recorded (t_1). As soon as the flame ceases, the burner flame is reapplied for an additional 10 s, then removed again. Duration of flaming (t_2) and glowing (t_3) after the second flame application are noted. Based on the results for five specimens tested, the material is classified as either V-0, V-1, or V-2 based on the criteria outlined in Table 7.

Table 7: ASTM D3801 Rating Classification

Observation	Classification		
	V-0	V-1	V-2
t ₁ or t ₂ for any specimen	≤10 s	≤30 s	≤30 s
t ₁ + t ₂ for 5 specimens	≤50 s	≤250 s	≤250 s
t ₂ + t ₃ for any specimen	≤30 s	≤60 s	≤60 s
Flame propagation or glowing up to clamp, any specimen	No	No	No
Ignition of cotton	No	No	Yes

For each different material, a set of five replicate test runs was performed. This test method also includes the option to perform tests on two sets of five samples, with the difference between the two sets being how the samples are conditioned prior to testing. In Set A, samples are conditioned in a more common way, at approximately 23 °C and 50 percent relative humidity. For Set B, samples are conditioned at a higher temperature, nominally 70 °C. The fire test procedure is the same for both sets.

This difference between conditioning procedures is related to the expected operating temperature of an appliance, in which a given plastic material is installed. For this project, this could be appropriate for evaluating engine compartment materials. However, for interior materials, it is expected that the more common conditioning procedure is most appropriate. Therefore, all the replicate tests were conducted per the Set A conditioning procedure in ASTM D3801, which is equivalent to the conditioning procedure followed for the other selected test methods.

The data gathered from this testing can be referenced in Appendix D and is further discussed in the data analysis section of this report. Table 8 summarizes the results by vehicle type within Appendix D.

Table 8: ASTM D3801 Test Results Legend

Results Description	Appendix D Table Number
ASTM D3801 Results for School Bus Seat Materials	D-1
ASTM D3801 Results for Motorcoach Materials	D-2
ASTM D3801 Results for Vehicle Interior Materials	D-3

ASTM E1354 Testing

The cone calorimeter is a sophisticated small-scale test apparatus that can measure the heat release rate of materials and products under a wide range of thermal exposure conditions using the oxygen consumption technique (Janssens, 1991). Other useful information obtained from cone calorimeter tests includes time to ignition, mass loss rate, smoke production rate, and effective heat of combustion. The cone calorimeter apparatus, calibration procedure, and test protocol are standardized in the United States as ASTM E1354 and internationally as ISO 5660 (ISO, 2015). A schematic of the apparatus is shown in Figure 11.

At the start of a test, a square specimen of 100 × 100 mm (4 × 4 in.) is placed on the load cell and exposed to a preset radiant heat flux from the electric heater. The heater is in the shape of a truncated cone and can provide heat fluxes to the specimen in the range from 0 to 100 kW/m².

An electric spark ignition source is used for piloted ignition of the pyrolysis gases produced by the heated specimen. The products of combustion and entrained air are collected in a hood and extracted through a duct by a blower. A gas sample is drawn from the exhaust duct and analyzed for oxygen concentration. Smoke production is determined on the basis of the measured light obscuration in the duct using a laser photometer located close to the gas sampling point. Gas temperature at and differential pressure across an orifice plate are used for calculating the mass flow rate of the exhaust gases.

The cone calorimeter was designed to evaluate essentially flat products and materials. Some automotive parts tested in this program did not have a flat surface of 100×100 mm. In these cases specimens had to be pieced together. This appeared to have a minimal effect on the cone calorimeter results for the materials that were tested.

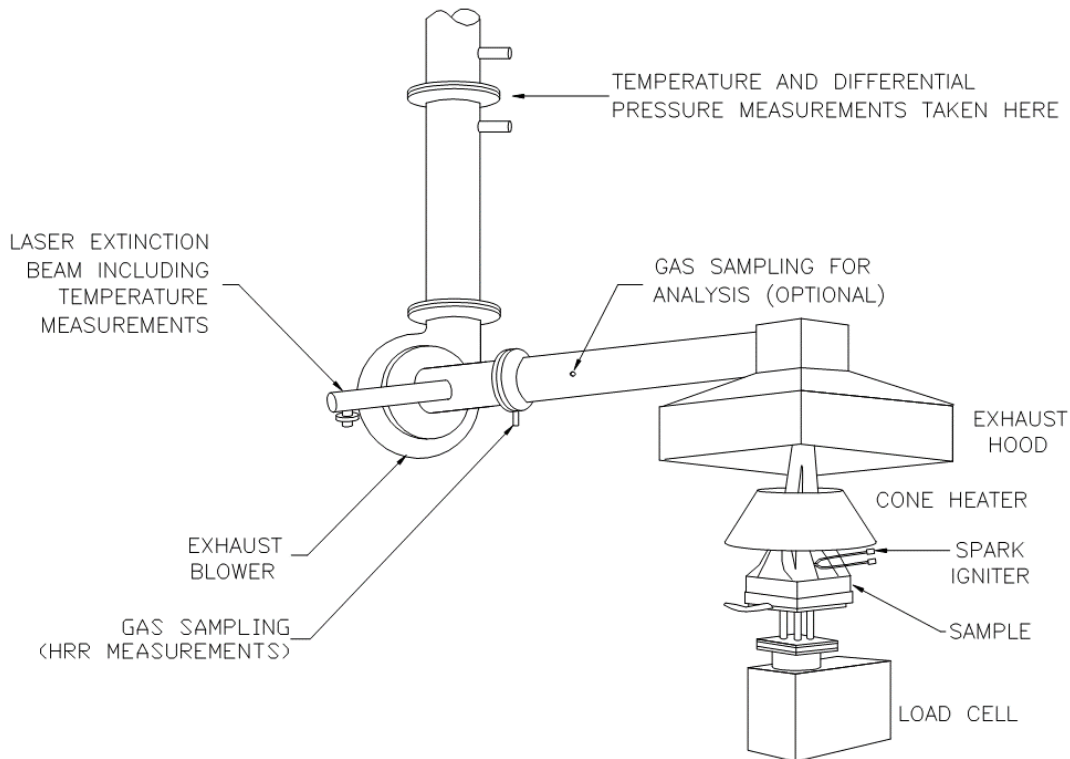


Figure 11. Schematic of ASTM E1354 (cone calorimeter) test apparatus

For each different material, a set of three replicate test runs was performed. For materials that are known to have multiple components/layers (e.g., seats), the components and assembly materials are separated in the tables. For this test, only the assembly is tested, as opposed to the components.

Heat release rate testing was conducted with an incident heat flux level of 35 kW/m^2 , based on prior research noted earlier (SwRI, 2003). Additional tests were conducted to determine ignition times at a variety of heat flux levels, which will be discussed in more detail in the data analysis section of this report.

The data gathered from this testing can be referenced in Appendix E and is further discussed in the data analysis section of this report. Table 9 summarizes the results by vehicle type within Appendix E.

Table 9: ASTM E1354 Test Results Legend

Results Description	Appendix E Table Number
ASTM E1354 Results for School Bus Seat Materials	E-1
ASTM E1354 Results for Motorcoach Materials	E-2
ASTM E1354 Results for Vehicle Interior Materials	E-3

ASTM D7309 Testing

The FAA developed the microscale combustion calorimeter (MCC) to assist with the development of fire-resistant polymers for use in commercial passenger aircraft. A schematic of the MCC is shown in Figure 12. The apparatus is described in more detail in ASTM D7309.

A milligram-size specimen is heated at a constant rate between 0.2 and 2 K/s. Decomposition can take place in nitrogen (method A) or in a mixture of nitrogen and oxygen (method B). When Method A is used, char-forming specimens do not decompose completely and leave a solid residue. In this case, the volatiles are mixed with a metered supply of oxygen in the combustor to obtain the heat release rate of the volatiles. When Method B is used, the organic components of the specimen are completely consumed.

Testing in this project was all conducted at one heating rate, 1 K/s, which is a common recommended heating rate in the test method documentation. In addition, Method A was used for all testing in this project. Method A is more representative of a real fire scenario and is more commonly used.

The primary result of this test method is the heat release rate per mass unit of fuel as a function of time or pyrolysis chamber temperature (as opposed to the heat release rate per unit exposed specimen area as a function of time). The heat release rate per mass unit of fuel is referred to as the specific heat release rate, $Q(t)$, and is expressed in W/g. A typical result of an MCC test is shown in Figure 13.

The following five parameters are calculated when Method A is used:

1. The heat release capacity $\eta_c \equiv Q_{\max}/\beta$ in J/g·K, where Q_{\max} is the maximum value of $Q(t)$ and β is the heating rate in K/s.
2. The heat release temperature T_{\max} in K as the pyrolysis chamber temperature at which $Q(t) = Q_{\max}$.
3. The specific heat of combustion h_c in kJ/g as the area under the $Q(t)$ curve.
4. The pyrolysis residue $Y_p \equiv m_p/m_0$ in g/g, where m_p is the residual mass of the specimen at the end of the test.
5. The specific heat of combustion of the specimen gases $h_{c,\text{gas}} \equiv h_c/(1-Y_p)$ in kJ/g.

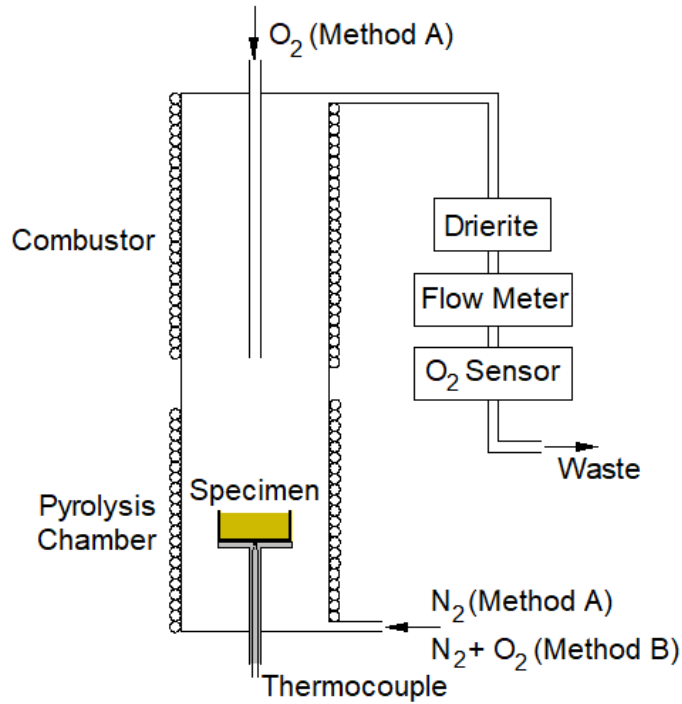


Figure 12. Schematic of ASTM D7309 (MCC) test apparatus

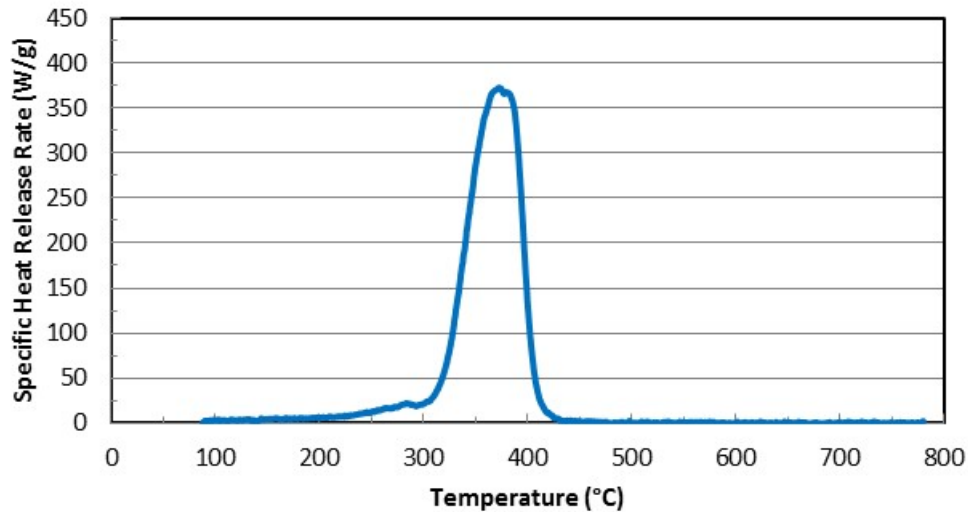


Figure 13. Specific heat release rate versus MCC pyrolysis chamber temperature curve

For each different material, a set of three replicate test runs was performed. For materials that were known to have multiple components/layers (e.g., seats), the components and assembly materials are separated in the tables.

The data gathered from this testing can be referenced in Appendix F and is further discussed in the data analysis section of this report. Table 10 summarizes the results by vehicle type within Appendix F.

Table 10: ASTM D7309 Test Results Legend

Results Description	Appendix F Table Number
ASTM D7309 Results for School Bus Seat Materials	F-1
ASTM D7309 Results for Motorcoach Materials	F-2
ASTM D7309 Results for Motorcoach Blue Cover Seat Padding	F-3
ASTM D7309 Results for Vehicle Interior Materials	F-4
ASTM D7309 Results for Surface Layer of Selected Vehicle Interior Materials	F-5
ASTM D7309 Results for Cryo-Milled Samples of Various Materials	F-6
ASTM D7309 Results for Thin Materials	F-7
ASTM D7309 Results for Water Mist Foams	F-8
ASTM D7309 Results for Britax Parkway and Chicco KeyFit Materials	F-9
ASTM D7309 Results for Peg Perego Primo Viaggio and UP-PAbaby Mesa Materials	F-10

Full-Scale Bus Seat Testing per ASTM E2574

Two series of tests were performed. The first series only considered school bus seats and the second series of tests focused primarily on motorcoach seats, but also considered one school bus seat test. All testing was performed according to ASTM E2574. Some tests were conducted with gas burner and some tests were conducted with paper bag ignition source.

ASTM E2574 Overview

ASTM E2574 describes standardized testing of school bus seats. This is essentially equivalent to the National Safety Council Standard (School bus seat upholstery fire block test, approved by the National Conference on School Transportation as part of the National Standards for School Buses and National Standards for School Bus Operations), with the exception of replacement of the fire source (paper grocery bag with crumpled paper) with a gas burner, which greatly improves the repeatability and reproducibility of the method.

A mock-up of a school bus is constructed with three rows of actual seats. A gas burner ignition source is used (alternative paper bag ignition source described in Appendix X.1 of ASTM E2574). Each standard test consists of two trials. In each trial a gas burner ignition source is placed at a specified location to ignite the middle row of seats and is ignited. A different gas burner is used for the top of the seat and for the bottom of the seat. Once flame extinction has occurred, the time to flame extinction, the extent of fire spread (within the seat and to the other seats if applicable) and the mass loss of the seat are assessed.

Test Chamber

The test chamber is required to be either an actual section of a school bus or a mockup that meets the cross-section requirements shown in the schematic in Figure 14. SwRI uses an actual school bus section for this type of testing and a photograph of that chamber can be seen in Figure 15.

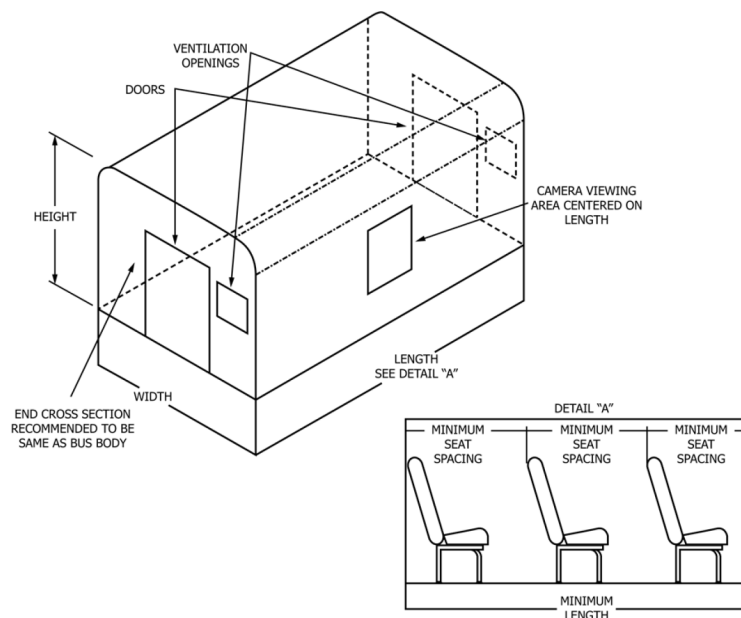


Figure 14. ASTM E2574 test chamber schematic



Figure 15. Photograph of SwRI test chamber for ASTM E2574

Ignition Sources

There are two ignition sources specified in ASTM E2574. The first is for ignition of the top of the seating and a schematic is shown in Figure 16. The second is for ignition under the seating and a schematic is shown in Figure 17.

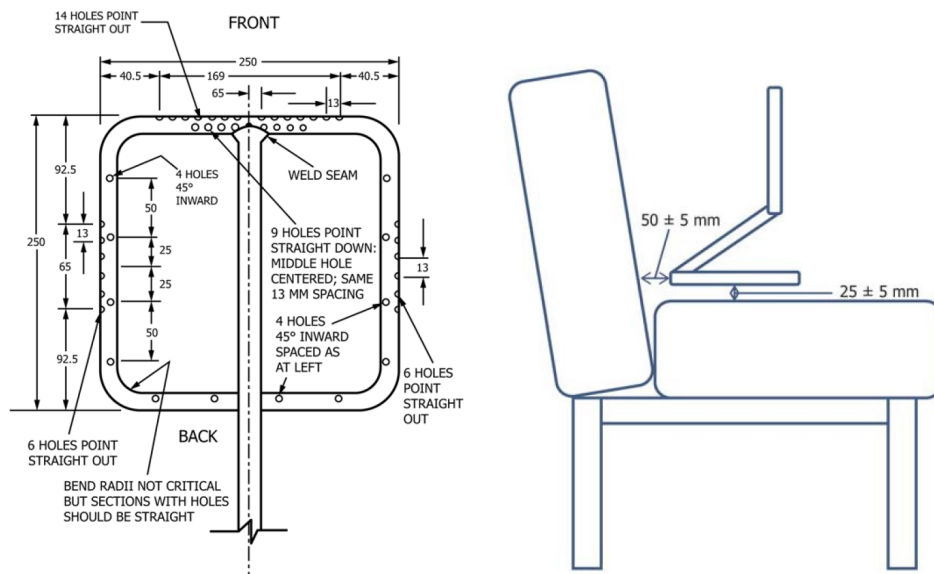


Figure 16. Schematics of top burner specified in ASTM E2574

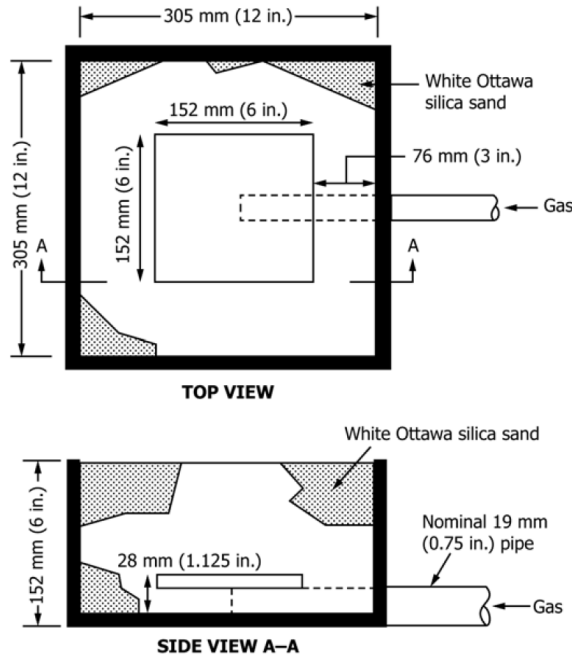


Figure 17. Schematics of under seat burner specified in ASTM E2574

For each ignition source, the same propane flow rate is used, 19.5 L/min, which equates to approximately 29 kW. The burner exposure is 120 s, after which time the gas supply is shut off and observations and measurements are continued to be made.

For a standard test, a set of school bus seats would be tested with both ignition sources. For testing in this project, the top seat ignition scenario was most commonly used, but the under seat ignition source was also used in some tests. This was primarily driven by the available seats for testing.

Procedure

Three rows of seats are installed in the test chamber. The spacing between seat rows is specified to be the minimum spacing recommended by the installer or the spacing required by FMVSS No. 222, "School bus passenger seating and crash protection." For all testing conducted under this project, this spacing was 0.86 m (34 in.) from headrest to headrest, on center.

The test period begins once the ignition source has been ignited and ends once all flaming of the specimen has ceased, including any flaming of the specimen at the ignition source, unless safety considerations dictate an earlier termination. A new set of seats shall be used for each trial.

For each test performed in this project, the following information is reported.

- Time elapsed between ignition and cessation of flaming.
- Whether flame has spread from the seat with the ignition source to adjacent seats or adjacent surfaces.
- Whether melting of the seat materials has occurred and whether it has resulted in flaming drips beneath the seat.

Optional Calorimetry Measurements

The measurement of heat release rate by oxygen consumption calorimetry is optional in ASTM E2574. These measurements were not taken in the first series of tests, but were made in the second series. For those tests, the school bus test chamber was centered under SwRI's large-scale calorimeter. Figure 18 provides a schematic for the calorimeter and Figure 19 shows a photograph of the school bus chamber under the calorimeter.

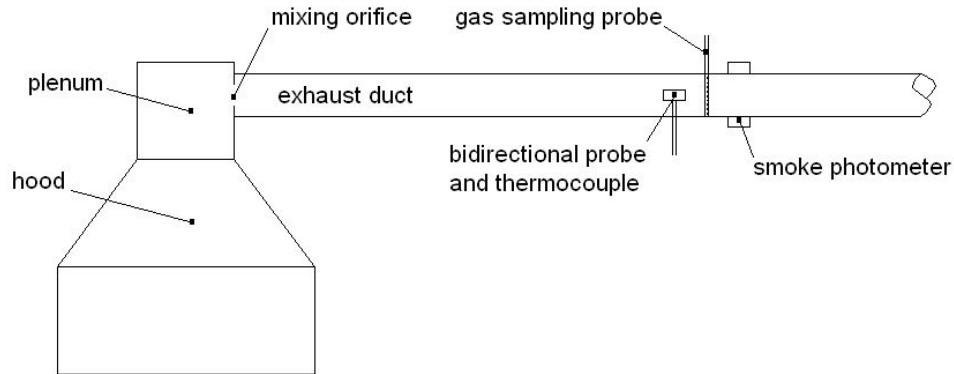


Figure 18. Schematic of standard calorimeter hood and exhaust duct



Figure 19. Photograph of SwRI test chamber under large calorimeter

First Series of Testing

The first series of testing consisted of four tests. Table 11 summarizes the times observed for flame spread to an adjacent row of seats.

In the first test with the Bluebird seats, after the gas burner was turned off, the flames went out. So, Test 2 was quickly started with the under seat burner on the same set of seats. The same result was observed for this ignition source with the Bluebird seats.

Flame spread was observed to adjacent rows of seating in both tests 3 and 4 and each test was terminated early for safety of the laboratory and personnel after the fire intensity grew, which included melting and dripping and resulting pool fires on the floor of the bus test chamber.

Table 11: ASTM E2574 Test Series 1 – Flame Spread Observations

Test No	Test Description	Time to Flame Spread to Adjacent Seat Row
1	Bluebird Seats – Gas Burner – Top Seat Ignition	N/A
2	Bluebird Seats – Gas Burner – Under Seat Ignition	N/A
3	TransTech Seats – Gas Burner – Top Seat Ignition	4:32
4	Starcraft Seats – Gas Burner – Top Seat Ignition	2:15

Figure 20, Figure 21, and Figure 22 show selected photos from this series of testing.



Figure 20. Pre (left) and post (right) test photographs of Bluebird school bus seat



Figure 21. Pre (left) and post (right) test photographs of Trans Tech school bus seat



Figure 22. Post-test photographs of Starcraft school bus seats

Second Series of Testing

It was decided to perform the next series of tests in the calorimetry facility to safely perform the tests and allow the seats to burn out, as well as to collect heat release rate data. The testing focused on the motorcoach seats, however, one test was conducted on the remaining set of Bluebird school bus seats. Table 12 provides a summary of the tests conducted and the time observed for flames to spread to adjacent rows of seating. Melting and dripping was observed in all the tests with motorcoach seats. Figure 23 – Figure 27 show selected photographs from each test.

Table 12: ASTM E2574 Test Series 2 – Flame Spread Observations

Test No	Test Description	Time to Flame Spread to Adjacent Seat Row
1	Motorcoach Green Seats – Gas Burner – Seat Ignition	4:03
2	Motorcoach Green Seats – Paper Bag – Seat Ignition	4:00
3	Motorcoach Blue Seats – Gas Burner – Seat Ignition	6:11
4	Motorcoach Blue Seats – Paper Bag – Seat Ignition	9:00
5	Bluebird Seats – Paper Bag – Seat Ignition	N/A



Figure 23. Pre (left) and post (right) test photographs from Test 1 of second series of testing



Figure 24. Pre (left) and post (right) test photographs from Test 2 of second series of testing



Figure 25. Pre (left) and post (right) test photographs from Test 3 of second series of testing



Figure 26. Pre (left) and post (right) test photographs from Test 4 of second series of testing



Figure 27. Pre (left) and post (right) test photographs from Test 5 of second series of testing
 Table 13 provides a summary of the heat release rate parameters.

Table 13: ASTM E2574 Test Results Data Summary

Test No	Peak Heat Release Rate (kW)	Total Heat Released (MJ)	Peak CO Release Rate (g/s)
1	560	236	1.172
2	422	838	1.267
3	430	854	1.338
4	440	807	2.400
5	37	15	0.030

Figure 28 shows a comparison of the heat release rate curves for the five tests conducted. The nominal peak heat release rate seems to be controlled more by the specified test chamber and the available ventilation.

School bus seats are generally designed to meet the test specifications in ASTM E2574. Therefore, in general, the school bus seats performed better in this testing than the motorcoach seats.

The heat release rate data gathered from the second series of testing can be referenced in Appendix G. Table 14 summarizes the results by seat and ignition source type in Appendix G.

Table 14: ASTM E2574 Test Results Legend

Results Description	Appendix G Table Number
ASTM E2574 Results for MC Green Seats – Top Gas Burner Ignition Source	G-1
ASTM E2574 Results for MC Green Seats – Paper Bag Ignition Source	G-2
ASTM E2574 Results for MC Blue Seats – Top Gas Burner Ignition Source	G-3
ASTM E2574 Results for MC Blue Seats – Paper Bag Ignition Source	G-4
ASTM E2574 Results for Bluebird SB Seats – Paper Bag Ignition Source	G-5

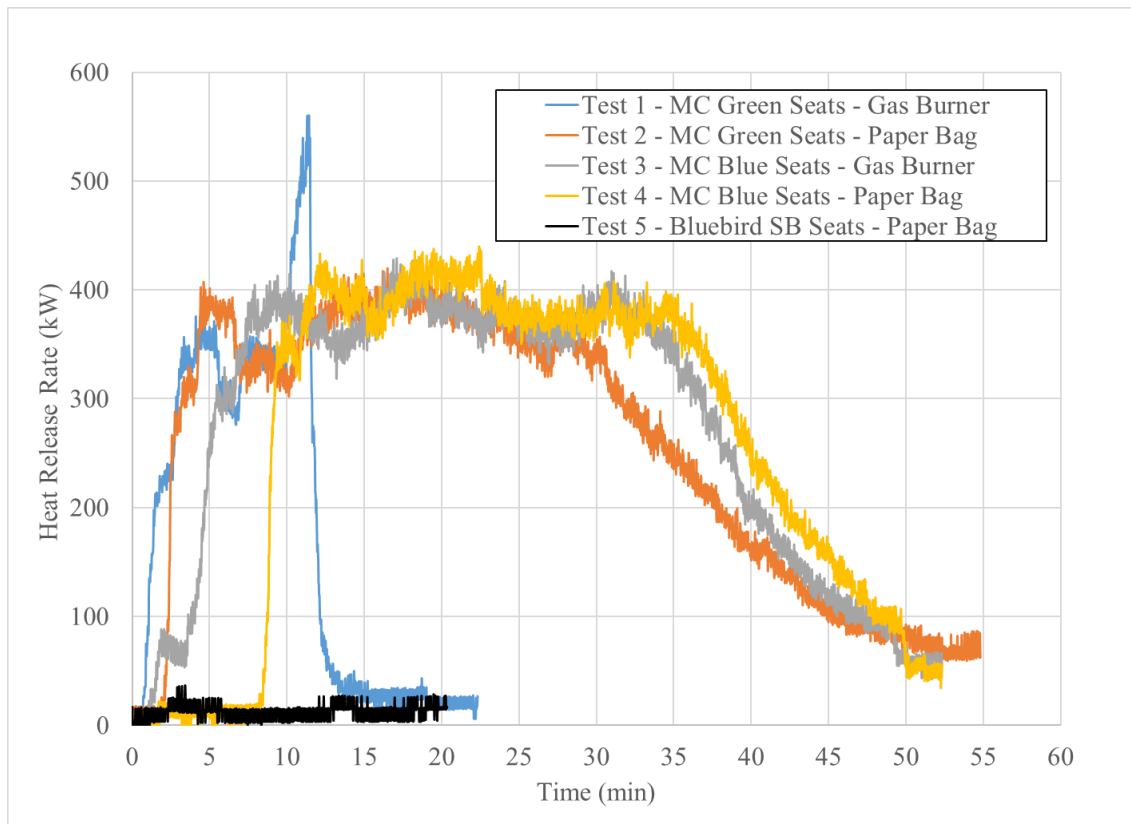


Figure 28. Heat release rate comparison for ASTM E2574 Testing

Child Restraint System Testing

NHTSA was interested in better understanding how fire propagates to child restraints in a motor vehicle fire and the effect of flame retardant chemicals on the ignition and propagation of fire through different types of child restraint materials.

To understand the effect of different material types and material treatments on the propagation of vehicle fires to child restraints in the vehicle, NHTSA funded a separate task to investigate the ignition and flammability of several child restraint models.

NHTSA was also interested in evaluating the performance of different child restraint models (with different flame retardant chemicals or no flame-retardant chemicals) in simulations of a representative real-world vehicle fire where the fire propagates from the front row seats to the rear rows. However, it was not possible to address this within the project scope and remains a good future topic of research.

Child Restraint Systems

Four different child restraint systems (CRS) were tested as detailed below.

- Britax Parkway (High-back booster seat)
- UPPA Baby Mesa (Infant seat – Detachable seat and base)
- Peg Perego Primo Viaggio (Infant seat – Detachable seat and base)
- Chicco KeyFit (Infant seat – Detachable seat and base)




Table 15 shows photographs of each CRS and the seat padding section from which MCC and FMVSS No. 302 specimens were sampled. The top row of the table shows the seat padding section, which is where the seats were ignited in the large-scale tests conducted in 2018. The middle row shows the entire seat for reference and the bottom row identifies the seat make.

Table 15: Photographs of Child Restraint Systems

			
			
Britax	UppaBaby	Peg Perego	Chicco

Table 16 show specific examples of the seating components. It is worth noting that some of the seating has adhesive fixing the fabric to the padding, while others do not. We tested each combination for our research purposes, but in the current guidelines, materials that are adhered together would be tested together in FMVSS No. 302.

Table 16: Close-Up View of Selected Child Seat Components

		
Example of Padding and Seat Fabric (no adhesive)	Example of Rigid Plastic Specimen	Example of Padding and Seat Fabric (adhered together)

Experimental Plan

Testing of these child restraint seats as well as some of their components was conducted in bench-scale and intermediate-scale configurations and methods. The following sections provide more description of the testing and results.

Bench-Scale Testing

FMVSS No. 302 test results for the CRS seat components can be referenced in Table C-7. ASTM D7309 test results for the CRS seat components can be referenced in Tables F-9 and F-10.

Open Calorimetry Testing

A furniture calorimeter was used for this testing, which was conducted in accordance to ASTM E2067, *Standard Practice for Full-Scale Oxygen Consumption Calorimetry Fire Tests*. This standard provides guidance for conducting calorimetry testing using the oxygen consumption principle. A furniture calorimeter consists of a weighing platform that is located on the floor of the laboratory beneath the standard hood (see Figure 29). The object is placed on the platform and ignited with the specified ignition source. The products of combustion are collected in the hood and extracted through the exhaust duct. Measurements of oxygen concentration, flow rate and light transmission in the exhaust duct are used to determine the heat release rate and smoke production rate from the object as a function of time.

Several child restraint seat systems were tested at SwRI to investigate the ignition characteristics of these child restraints in a more realistic fire scenario, as compared to what is described in FMVSS No. 302. The general fire scenario consisted of a small ignition source, starting with a small open flame and increasing until sustained combustion is observed. Upon observing sustained combustion, the flame spread was allowed to develop naturally and heat release rate and smoke production rate were measured.

The ignition sources used are summarized in Section 9.2 of ASTM E3020-16a, *Standard Practice for Ignition Sources*. These are three different sizes of a small propane diffusion flame. The first source is a similar size flame as FMVSS No. 302. The second and third size ignition sources are 3.6 and 7.8 times the size (heat release rate) of the first source, respectively.

A small wood crib ignition source, which is described in Section 11.2.2 of ASTM E3020, was also considered in this testing, as necessary. These alternative wood crib sources provide a larger initial exposure area as well as different fuel chemistry.

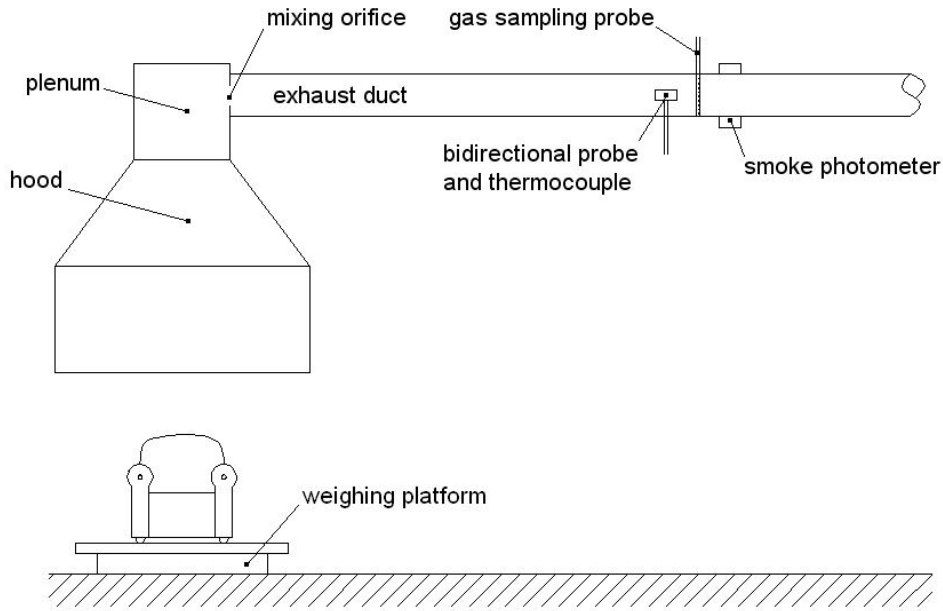


Figure 29. Schematic of furniture calorimeter apparatus

Figure 30 shows a photograph of the basic setup for each test. A CRS was placed on a metal stand, which was on a load cell (scale), centered under a calorimeter. The test was started by determining the minimum ignition source required for sustained ignition. After sustained ignition was observed, the fire growth of the seat was allowed to develop naturally. During each test, several measurements were made, including heat release rate, smoke production rate, mass loss rate, and CO/CO₂ production rates.



Figure 30. Photograph of CRS test setup (Britax CRS pictured)

Calorimetry Results

Table 17 shows a summary of selected test results. Figure 31 shows a summary heat release rate curve for each seat and base tested together. Figure 32 shows a comparison heat release rate curve for the two tests conducted with only a seat (no base) and Figure 33 shows a comparison heat release rate curve for the two tests conducted with only a base (no seat).

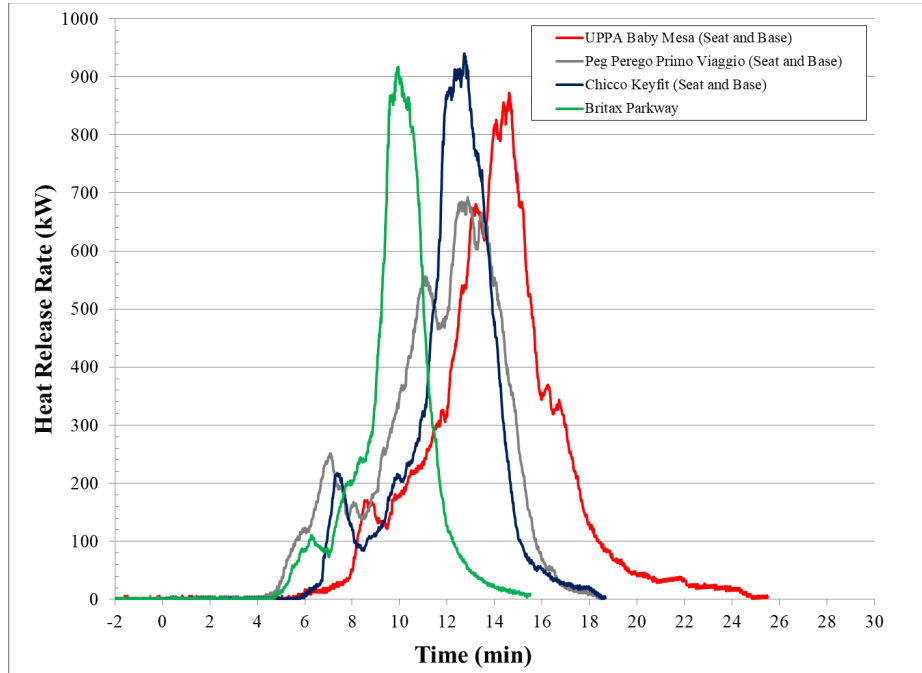


Figure 31. CRS heat release rate comparison (seat and base)

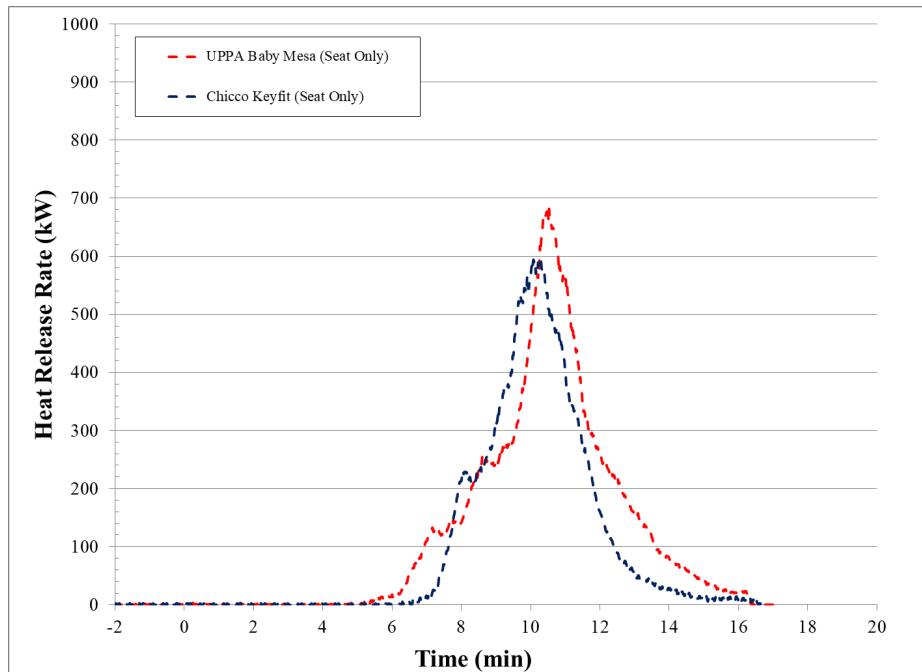


Figure 32. CRS heat release rate comparison (seat only)

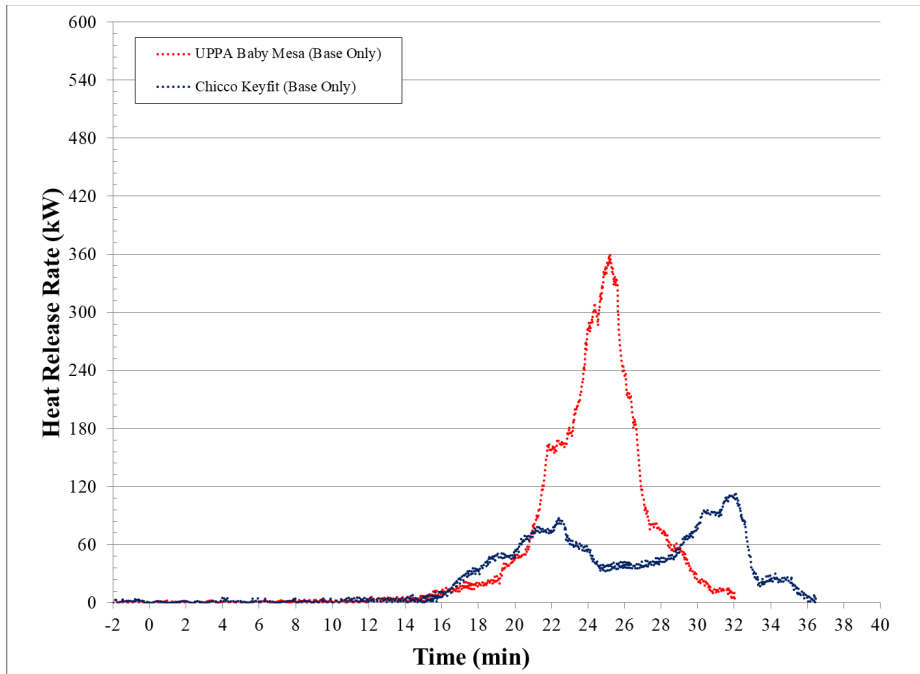


Figure 33. CRS heat release rate comparison (base only)

Table 17: Summary Test Results for CRS Testing

Child Seat ID	Child Seat Test Description	Seat Trial Number	Ignition Source Number Required for Sustained Ignition	Peak Heat Release Rate (kW)	Total Heat Released (MJ)	Effective Heat of Combustion (kJ/g)	Peak Smoke Production Rate (m ² /s)	Total Smoke Released (m ²)
Britax Parkway	High Back Booster	1	2	Note 1	Note 1	Note 1	Note 1	Note 1
	High Back Booster	2	2	588	108	Note 2	5.16	1095
	High Back Booster	3	2	917	147	28.2	5.72	1113
UPPA Baby Mesa	Infant Seat - Seat and Base	1	2	854	241	27.6	7.04	2112
	Infant Seat - Seat and Base	2	2	873	249	29.1	7.59	2267
	Infant Seat - Seat Only	3	2	682	127	28.6	4.29	991
	Infant Seat - Base Only	4	6	360	101	30.4	2.54	628
Peg Perego Primo Viaggio	Infant Seat - Seat and Base	1	1	693	223	30.4	6.11	2059
Chicco KeyFit	Infant Seat - Seat and Base	1	3	940	195	24.7	7.62	1670
	Infant Seat - Seat and Base	2	3	795	176	22.6	6.03	1444
	Infant Seat - Seat Only	3	3	594	105	25.6	4.09	850
	Infant Seat - Base Only	4	6	113	63	29.3	1.15	354

Note 1: The sample collapsed in such a way that it fell off the test stand and the test was aborted, Note 2: Part of the burning sample fell off the test stand and damaged part of the data cable for the load cell. This was repaired prior to the conduct of the remaining tests.

The full set of data gathered from this testing can be referenced in Appendix H. Table 18 summarizes the results by vehicle type within Appendix H.

Table 18: CRS Testing per ASTM E2067 Results Legend

Results Description	Appendix H Figure Number
ASTM E2067 Results for Britax Parkway CRS	H-1
ASTM E2067 Results for Chicco KeyFit CRS	H-2
ASTM E2067 Results for Peg Perego Primo Viaggio CRS	H-3
ASTM E2067 Results for UPPAbaby Mesa CRS	H-4

Analysis

Several high-level observations could be made from these test results. There is variability in the ignition of these seats with a small gas flame. Three child restraints tested could sustain ignition from Ignition Sources 1, 2 and 3 (small, medium, large gas flame). The fourth child restraint ignited with Ignition Source 2 but not with Ignition Source 1. Chemical composition evaluation confirmed that all four child restraints had flame retardant chemicals.

Once sustained ignition is observed, a relatively consistent fire growth is seen between seats and a similar peak heat release rate and total heat released are measured. This is more easily comparable between the UPPA Baby, Peg Perego and Chicco seats since they are the same style of seat.

It is also observed that the infant child restraint bases are more ignition resistant and they also release less heat release once ignited. Based on the results of the UPPA Baby and Chicco seats, it can be seen that most the heat release is coming from the seat as opposed to the base. This may be a result of more FR treatment in the base as compared to the seat or a natural difference between more rigid plastics and foam plastics (or some combination of both). In terms of smoke production, the seats alone make up a larger fraction of the total smoke, as compared to the bases. In general, the smoke production numbers are similar for all child restraints tested.

In the data analysis section of this report, there will be further discussion about the relationship between the bench-scale data from the CRS components and the alternative methodology criteria that has been developed for use with the MCC.

Chemical Composition Testing

NHTSA was interested in confirming the presence of halogenated flame retardants (FR) in the automotive materials previously tested in the current project. This would provide an understanding of the countermeasures used to comply with the current FMVSS No. 302 requirements and their performance in the other test methods evaluated by SwRI.

Fourier transform infrared (FTIR) spectroscopy was the experimental technique used along with the corresponding extensive chemical compound lookup database, which includes several flame-retardant chemicals.

Testing was conducted in two stages. In the first stage, of all the materials analyzed, approximately half were confirmed with high likelihood to contain some FR treatment. In the second stage, it was necessary to conduct additional testing of positive control samples and re-analyze a subset of the previous results.

All testing was conducted in the Applied Physics Division at SwRI and the analyst was not provided any specific information about the chemical composition of the samples prior to or during analysis, with the exception of control samples used in each stage. The results are reported in the following subsections.

Equipment and Methodology

FTIR spectroscopy is an analytical technique used to identify known compounds in a sample. It is based on the concept that when infrared radiation passes through a sample, chemical vapors present in the gas sample will absorb the infrared energy at different wavelengths and at different intensities, which are unique to specific chemical compounds.

Attenuated total reflection (ATR) is a sampling technique used in conjunction with infrared spectroscopy that enables samples to be examined directly in the solid or liquid state without further preparation. ATR uses a property of total internal reflection resulting in an evanescent wave. A beam of infrared light is passed through the ATR crystal in such a way that it reflects at least once off the internal surface in contact with the sample. This reflection forms the evanescent wave that extends into the sample. The penetration depth into the sample is typically between 0.5 and 2 micrometers, with the exact value determined by the wavelength of light, the angle of incidence and the indices of refraction for the ATR crystal and the medium being probed. The number of reflections may be varied by varying the angle of incidence. The beam is then collected by a detector as it exits the crystal.

Most modern infrared spectrometers can be converted to characterize samples via ATR by mounting the ATR accessory in the spectrometer's sample compartment. The accessibility, rapid sample turnaround and ease of ATR-FTIR has led to substantial use by the scientific community.

The testing in this project used these methods with a Thermo Scientific iS50 FT-IR Advanced FTIR spectrometer, which has a built-in diamond ATR module. Figure 34 shows photographs of the FTIR and ATR module used for this project. This hardware is supported by the OMNIC Spectra and annual BioRad KnowItAll license (spectra database),² which is used to confirm

² FTIR Spectrum, SpectraBase, 2019 Bio-Rad Laboratories, Inc.

matches from a given sample to know chemical compounds. This software also has a specific sub-database that is focused on flame retardant chemical compounds and is called FRX.³



Figure 34. FTIR Spectrometer (left) and Diamond ATR Module (right)

Sample Processing Procedure

The following general procedure was followed for chemical composition testing.

1. If sample has multiple layers and various textiles, analyze each individually.
2. Save Omnic spectra as raw data.
3. Analyze the spectra with Bio-Rad Software:
 - a. Search It (all databases)
 - i. Results in the core component of the layer analyzed.
 - ii. Software outputs a Hit Quality Index (HQI) for each match.
 - iii. Looking for a high HQI, 90 percent or better.
 - iv. Does the core component already have a flame retardant embedded within it?
 - v. How well does the spectral comparison fit?
 - b. Search It (FRX-flame retardant database only)
 - i. Will provide a correlation with only the FRX database?
 - ii. Software will force a match, thus HQI value will have to be reviewed as well as peak matches.
 - iii. Cross-reference results with Step 3a.

³ Bio-Rad Spectral Database Index, IR- Flame Retardants- Bio-Rad Sadtler.

- c. Mixture Analysis (all databases)
 - i. Will provide up to 5 components present in the material.
 - ii. A match within the FRX database may not result, if the flame retardant is embedded in the core material and only makes up a small percent of the total weight.
 - iii. Have to review HQI and peak matches, to see if data makes sense. Not all components are seen as true.
- 4. Analyze the spectra manually and cross reference with Step 3 results.
 - a. Look at individual peaks and level of intensity in which it correlates.
 - b. Do the peaks or areas in which the FRX (flame retardant) database does not match up represent the polymer or core component?
 - c. Has the fire retardant peak area shifted and how much of a shift is acceptable?
 - d. Does a peak that matches in FRX not match anywhere else?
 - e. Final analysis should take into consideration the sample as a whole, if it was processed as multiple layers or segments.
 - f. Look for specific flame retardant peaks (Fong, 2017; Shimadzu, 2005) (represented in cm^{-1}):
 - i. C-Cl = 800-600.
 - ii. C-Br = 750-500.
 - iii. P-H = 2440-2275.
 - iv. P=O = 1320-1140 (Foam positive control has peak that overlaps this spectral region).
 - v. Decabromodiphenyl oxide (C12Br10O)= 1360-1340 and 1325.
 - vi. Brominated fingerprint region = 1500-1000.
 - vii. ABS and PP positive control w/Decabromodiphenyl ethane (12%) shows unique peaks around 750-500.

First Stage of Chemical Composition Testing

Table 19 – Table 23 summarize the results for the first stage of chemical composition testing on passenger vehicle, school bus, child restraint seats, motorcoach and control materials. The results showed that most of the materials sampled contain some flame-retardant chemicals, although some additional testing and analysis would be required to confirm this conclusion.

The disposition of each individual material tested, in terms of the likelihood of flame retardant treatment, is framed as “unlikely, plausible, unknown and likely.” If the results are rolled up to “product level,” then it is shown that 10/18 products are “likely” to contain FR treatment, 6/18 products are “plausible” to contain FR treatment and 2/18 products are “unknown.”

Table 19: Stage 1 Chemical Composition Results – Passenger Vehicle Samples

Sample Number	Sample Description	Sample Section Description	Qualitative Results (Unlikely, Plausible,* Unknown,* Likely)	FR in Product?
#1	Camaro 2 of 5 (foam)	light foam	Plausible*	Likely
#2	Camaro 2 of 5 (cover)	gray, light portion	Likely	
#2	Camaro 2 of 5 (cover)	back, dark portion	Plausible*	
#3	Ford F250 (4/5) carpet	fibrous portion	Unknown*	Plausible*
#3	Ford F250 (4/5) carpet	black rubber portion	Plausible*	
#4	Mercedes 1/5 carpet M20174300	gray portion	Plausible	Likely
#4	Mercedes 1/5 carpet M20174300	black portion	Likely	
#5	Camaro (3/5) headliner	gray portion	Plausible*	Likely
#5	Camaro (3/5) headliner	black portion	Likely	
#6	Ford headliner	rigid, gray foam portion	Likely	Likely
#6	Ford headliner	soft gray portion	Plausible*	
#7	Ford F250 dashboard	gray silver of inner compartment	Unknown*	Unknown*
#8	Mercedes dashboard	black rubber portion	Plausible*	Plausible*
#8	Mercedes dashboard	gray foam portion	Plausible*	

*For components that were plausible or unknown, a secondary analysis is recommended, especially if a judgement can't be made at product level (some component of whole product isn't already dispositioned as likely containing FR).

Table 20: Stage 1 Chemical Composition Results – School Bus Seat Samples

Sample Number	Sample Description	Sample Section Description	Qualitative Results (Unlikely / Plausible / Unknown / Likely)	FR in Product?
#18	Bluebird (Cover)	gray portion	Unknown	Plausible
#18	Bluebird (Cover)	gray portion, attached to threading	Plausible	
#19	Bluebird (Padding)	polyurethane foam	Plausible	
#20	Starcraft (Cover)	vinyl cover	Unlikely	Plausible
#21	Starcraft (Padding)	polyether polyurethane foam	Plausible	
#22	TransTech (Cover)	gray portion, attached to threading	Plausible	Plausible
#23	TransTech (Padding)	polyurethane foam portion	Unknown	
#23	TransTech (Padding)	lining portion	Unknown	

Table 21: Stage 1 Chemical Composition Results – Child Restraint System Samples

Sample Number	Sample Description	Sample Section Description	Qualitative Results (Unlikely / Plausible / Unknown / Likely)	FR in Product?
#9	Peg Perego (Foam)	polystyrene foam	Likely	Likely
#15	Peg Perego (Plastic)	rigid plastic	Plausible	
#17	Peg Perego (Cover)	fabric top	Plausible	
#17	Peg Perego (Cover)	cover foam	Likely	
#17	Peg Perego (Cover)	fabric bottom	Plausible	
#10	Britax (Cover)	foam portion	Likely	Likely
#10	Britax (Cover)	fabric portion	Plausible	
#11	Britax (Foam)	polystyrene foam	Likely	
#14	Britax (Plastic)	rigid plastic	Plausible	
#12	UppaBaby (Plastic)	rigid plastic	Unknown	Unknown
#13	UppaBaby (Cover)	foam portion	Unknown	
#13	UppaBaby (Cover)	fabric portion	Unknown	
#16	UppaBaby (Foam)	polypropylene foam	Unknown	

Table 22: Stage 1 Chemical Composition Results – Motorcoach Samples

Sample Number	Sample Description	Sample Section Description	Qualitative Results (Unlikely, Plausible, Unknown, Likely)	FR in Product?
#24	Seat Padding	polyurethane foam	Plausible	Likely
#29	Seat Backing – Gray	whole intact section	Unknown	
#30	Seat Cover – Blue	top portion	Unknown	
#30	Seat Cover – Blue	bottom portion	Unknown	
#31	Seat Cover – Green	top portion	Likely	
#31	Seat Cover – Green	bottom portion	Plausible	
#32	Seat Cover – Patterned Blue	top portion	Unknown	
#32	Seat Cover – Patterned Blue	bottom portion	Likely	
#25	Headliner	top blue portion	Plausible	Plausible
#25	Headliner	bottom portion	Unknown	
#26	Floor Covering	fibrous portion	Unknown	Likely
#26	Floor Covering	rubber portion	Likely	
#27	Luggage Rack Door	foam portion	Likely	Likely
#27	Luggage Rack Door	gray plastic portion	Likely	
#28	HVAC Control Panel	rigid plastic	Likely	Likely

Table 23: Stage 1 Chemical Composition Results – Control Samples

Sample Number	Sample Description	Sample Section Description	Qualitative Results (Unlikely, Plausible, Unknown, Likely)	FR in Product?
Control-1	Manilla Folder	whole, intact	Unlikely	No
Control-2	PMMA	whole, intact	Unlikely	No
Control-3	HDPE	whole, intact	Likely	Yes
Control-4	Thick Cardboard	whole, intact	Unlikely	No

Second Stage of Chemical Composition Testing

To clarify the results of the first stage of chemical composition testing, it was necessary to conduct additional testing of positive FR control samples and re-analyze the previous results. Three different FR-treated control materials were acquired from an FR manufacturer for this task and provides the details.

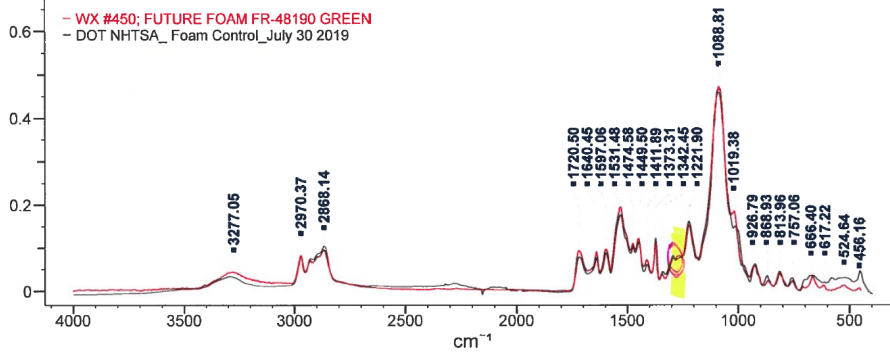
Table 24: Stage 2 Chemical Composition Testing – Positive FR Control Samples

Base Polymer	FR Chemistry Class	Specific FR Chemistry
ABS (Rigid Plastic)	Bromine	Decabromodiphenyl ethane (12%)
PP (Rigid Plastic)	Bromine	Decabromodiphenyl ethane (23%)
PU (Flexible Foam)	Phosphate	Fyrol FR-2 (TDCP) at 5 percent by weight loading: Tris (1, 3-dichloro-2-propyl) phosphate

These materials were analyzed with the same FTIR technique to challenge the standard FR database. Based on these control results, the previous dataset was re-analyzed to investigate whether some of the questionable products can be dispositioned as to the presence (and maybe also what type and loading) of FR treatment.

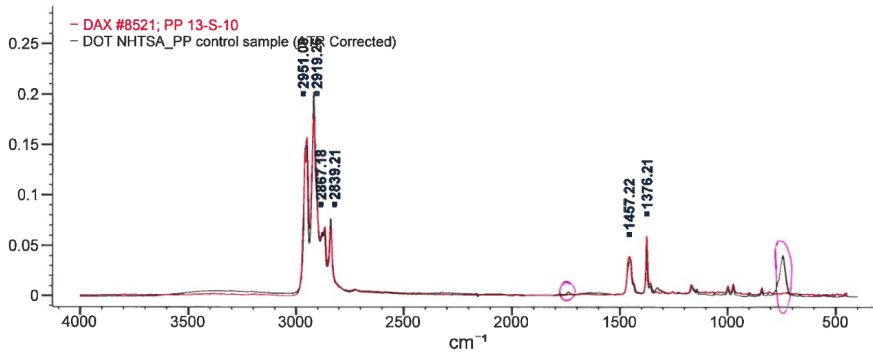
Figure 35, Figure 36, and Figure 37 illustrate the process the analyst used to look for differences between the control sample spectra for PU, PP and ABS, respectively, which contained know amounts of specific FR chemical compounds, and the base polymer spectra in the Bio-Rad database. The outlying peaks identified in these overlaid comparison graphs occur at wavenumbers corresponding to specific chemical bonds that indicate the presence of bromine or phosphate-based FR chemicals.

Based on this updated testing and analysis, 23 out of the 32 materials tested can be confirmed to contain FR treatment. Five of the materials can be confirmed to not contain any FR treatment and four materials remain uncertain. Table 25 provides a summary of the final disposition of all the samples evaluated.



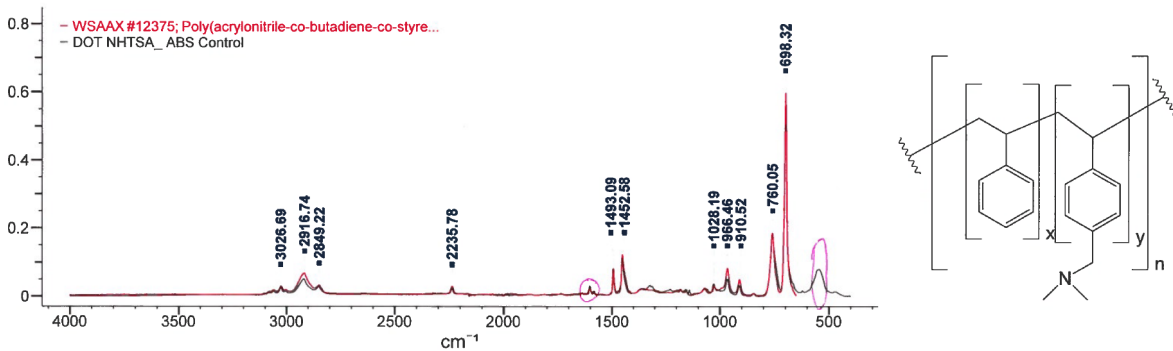
HQI	Tag	Correctio	DB	ID	Name	Spectrum
98.35			WX	450	FUTURE FOAM FR-48190 GREEN	

Figure 35. Polyurethane foam control sample spectra comparison results



HQI	Tag	Correctio	DB	ID	Name	Spectrum
96.21			DAX	8521	PP 13-S-10	

Figure 36. Polypropylene control sample spectra comparison results



HQI	Tag	Correctio	DB	ID	Name	Spectrum
97.51			WSAAX	12375	Poly(acrylonitrile-co-butadiene-co-styrene)	

Figure 37. ABS control sample spectra comparison results

Table 25: Stage 2 Chemical Composition Testing – Final Results

<u>SwRI</u> <u>Sample</u> <u>Number</u>	<u>Sample Designation</u>	<u>FR Assessment</u>	<u>Notes</u>
1	M2017_Camaro 2 of 5 (foam)	Present	1223 cm ⁻¹ peak present like the foam control, representing phosphate peak
2	M20170114_Camaro 2 of 5 (interior upholstery)	Present	
3	4/5 Carpet	Plausible	Do not have a PET or Rubber control with FR for this sample
4	M 1/5 Carpet M20174300	Present	
5	3/5 Head	Present	
6	F-Head	Present	
7	Ford dash	Plausible/ Present	1376-1359 peak; possible shift for Br region, FR assessment changes to present?
8	Dashboard	Plausible/ Present	1372-1345 peak; possible shift for Br region, FR assessment changes to present?
9	Baby Seat_Peg Perego foam	Present	3 peaks in 750-500 cm ⁻¹ region (754, 695, 538)
10	Baby Seat_Britax parking cover	Present	
11	Baby Seat_Britax Parkway foam	Present	No true control for this one, but does have peak at 1328 and 750-500 cm ⁻¹ region (753, 695, 538)
12	Baby Seat_Uppa Baby plastic	Absent	No confirming peaks to illustrate FR present
13	Baby Seat_Uppa Baby cover	Present	
14	Baby Seat_Britax Parkway plastic	Present	1359-1330; possible shift for Br region
15	Baby Seat_Peg Perego plastic	Absent	No confirming peaks to illustrate FR present
16	Baby Seat_Uppa baby foam	Absent	Absent of any FR key peaks
17	Baby Seat_Peg Perego cover	Present	
18	School Bus_Blue Bird cover	Plausible	No comparable control for this sample; possible P peaks
19	School Bus_Blue Bird padding	Present	
20	School Bus_Starcraft cover	Absent	No comparable control for this sample, no key peaks present
21	School Bus_Starcraft padding	Present	
22	School Bus_Trans Tech cover	Plausible/ Present	1382-1365 and 1325; possible Br shift, FR assessment changes to present?
23	School Bus_Trans Tech padding	Plausible/ Present	1373-1340; possible Br shift, FR assessment changes to present?
24	Motorcoach_seat padding	Present	1373-1340
25	Motorcoach_Headliner	Plausible	No comparable control and no key peaks present
26	Motorcoach_Floor covering	Present	
27	Motorocoach_Door of luggage	Present	
28	Motorcoach_HVAC control panel	Present	
29	Motorcoach_Seat Backing gray	Absent	No key peaks present
30	Motorocoach_Seat cover	Plausible	No comparable control and no key peaks present
31	Motorcoach_Seat Cover green	Present	
32	Motorcoach_Seat Cover patterned blue	Plausible/ Present	1408-1340; possible shift on bottom portion sampled, FR assessment changes to present?

The full set of analyst notes from this testing can be referenced in Appendix I.

Table 26 summarizes the results by material type in Appendix I.

Table 26: FR Chemical Composition Results Legend

Results Description	Appendix I Table Number
Chemical Composition Results for Passenger Vehicle Materials	I-1
Chemical Composition Results for School Bus Seat Materials	I-2
Chemical Composition Results for CRS Seat Materials	I-3
Chemical Composition Results for Motorcoach Materials	I-4
Chemical Composition Results for Control Materials	I-5

Smoke Toxicity Testing

In addition to evaluating flammability of automotive materials, NHTSA was interested in evaluating the quantity and toxicity of the smoke produced from burning automotive materials. Of additional interest was the development or implementation of a repeatable and reproducible test procedure to evaluate smoke toxicity of materials.

Methodology Approach

Because the MCC was being considered as an alternative test for the existing FMVSS No. 302 procedure, it was decided to pursue using the MCC for smoke toxicity measurements as well. This has been previously explored by the developers of the MCC at the FAA (Speitel et al., 2017). The same basic approach was taken for this research project. This methodology includes performing several tests, which are conducted across a range of ventilation conditions to assess the generation of toxic compounds in various stages of a real fire. Implementation of the methodology involved the following steps, which are discussed in later sections:

- Baseline testing to obtain the stoichiometric flow rate of oxygen for each of the materials.
- Modification of the MCC setup to allow control of the oxygen and nitrogen flow rate with external flow controllers and collect the exhaust gases in a bag for FTIR analysis.
- Modified MCC testing, FTIR analysis of the gas samples and data processing.

Test Plan

It was decided to focus on a small number of materials from the motorcoach. The main objective of this part of the research is to determine whether this approach may be suitable for assessing smoke toxicity of automotive materials. In addition, the hazard from the smoke toxicity of interior materials is likely more important for motorcoaches, as opposed to passenger vehicles, due to the size and occupant loading of each vehicle type. The three motorcoach (MC) materials listed in Table 27 exhibited the worst performance in the MCC and FMVSS No. 302 testing.

Table 27: Test Matrix for Smoke/Toxicity Testing

Test Series Number	Material ID	Number of Test Trials			
		Baseline Tests (O ₂ Demand)	Phi = 0.5	Phi = 1.0	Phi = 1.5
B1	MC Seat Padding	3			
B2	MC Seat Cover - Green	3			
B3	MC Seat Backing - Blue	3			
1	MC Seat Padding			6	
2	MC Seat Padding				6
3	MC Seat Padding		6		
4	MC Seat Backing - Blue			6	
5	MC Seat Backing - Blue				6
6	MC Seat Backing - Blue		6		
7	MC Seat Cover - Green			6	
8	MC Seat Cover - Green				6
9	MC Seat Cover - Green		6		

Baseline Tests

Prior to running tests at varying ventilation conditions, baseline tests were conducted to determine the oxygen demand for stoichiometric combustion in a standard MCC test. The results of this testing allowed for the calculation of the required oxygen and nitrogen flow rates at specified ventilation conditions, characterized by the equivalence ratio, denoted by Phi. By testing at these different ventilation conditions, the results can be related to real fire scenario conditions (e.g. early fire growth stages, pre-flashover and post-flashover, when different amounts of oxygen are available for combustion during a fire). The required oxygen flow rate, for the different values of Phi, for each of the materials are summarized in Figure 38, Figure 39 and Figure 40.

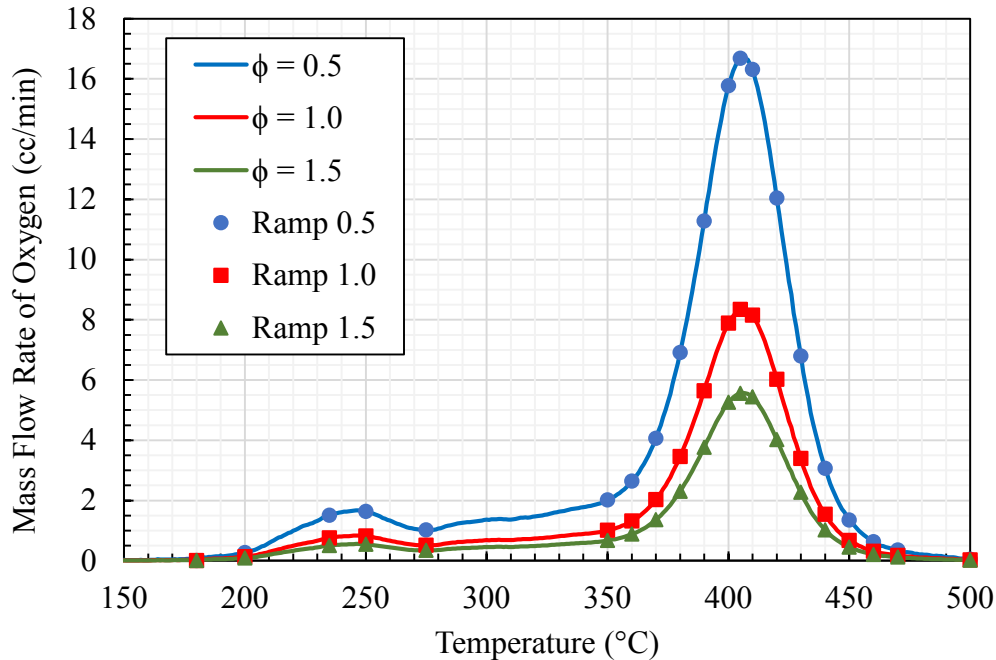


Figure 38. Required oxygen flow rates for the MC padding

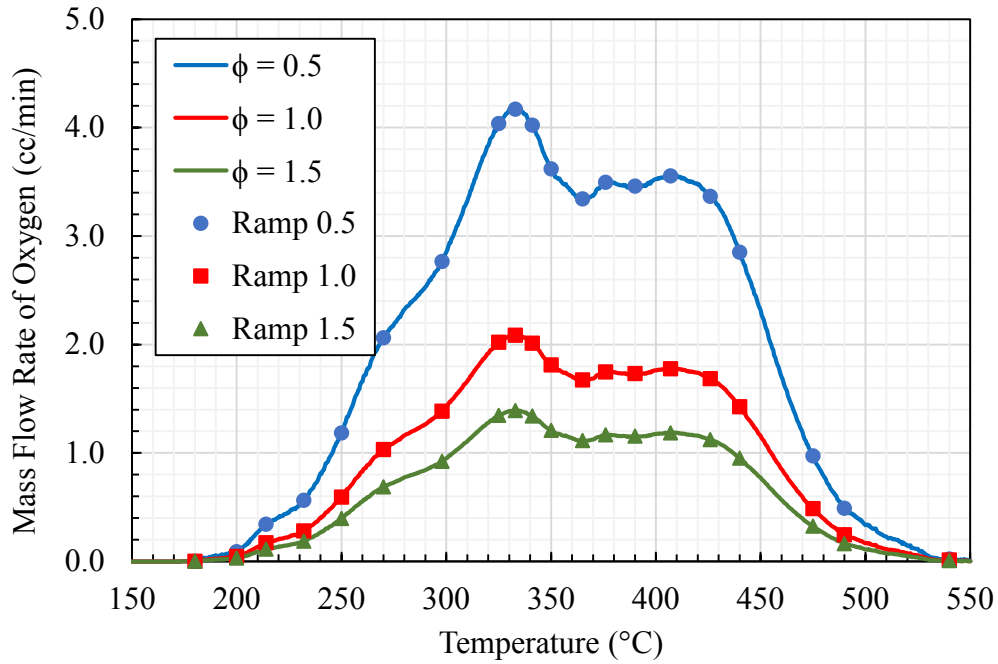


Figure 39. Required oxygen flow rates for the MC Blue Seat backing

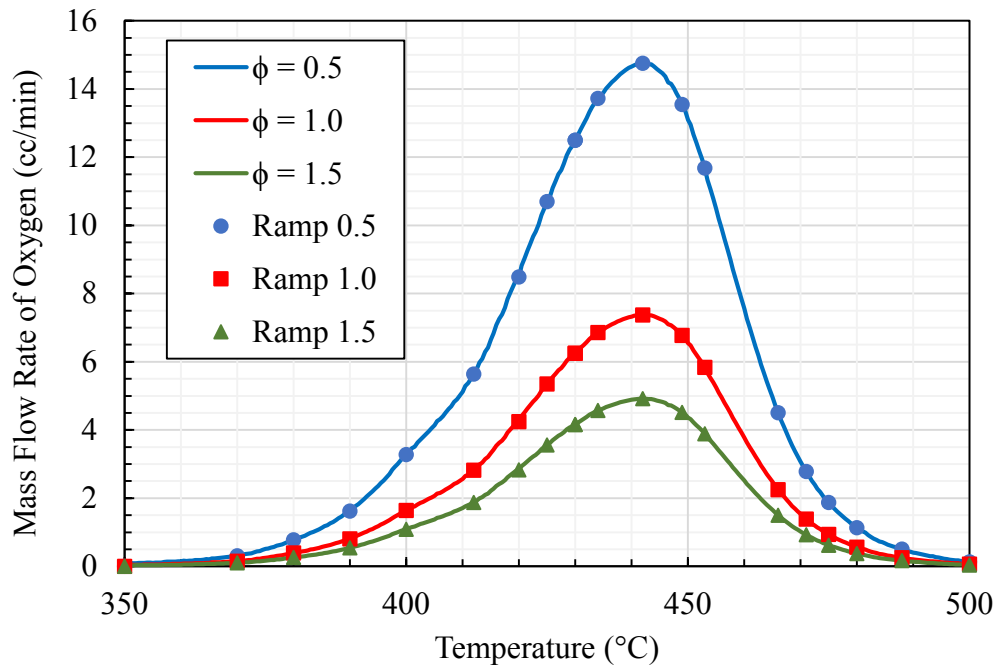


Figure 40. Required oxygen flow rates for the MC Green Seat cover

Experimental Apparatus and Procedure

After the baseline tests were conducted, the apparatus was modified to allow collecting the exhaust gases in an inflatable bag during the active part of an MCC test. After collection was completed (it took several tests for each material to fill the bag), the sample bags were taken to an FTIR and that gas sample was analyzed for toxic compounds from the products of combustion during the test. Figure 41 shows a schematic of the modified MCC, which allowed introducing oxygen and nitrogen throughout the test at different rates than in a standard test (i.e., 20 cc/min for oxygen and 80 cc/min for nitrogen). This was accomplished by using external nitrogen and oxygen flow controllers (shown as colored boxes in Figure 41) that by-passed and were more easily accessible than the internal flow controllers. Figure 44 shows a photograph of the FTIR used to analyze the gas samples collected during testing. Figure 45 shows an example spectrum from the FTIR and identifies the peaks associated with several of the toxic compounds that were detected in this MCC testing of the motorcoach materials.

For a given test run, the standard MCC software was used to initiate the process, except that the external flow controllers were set to flow nitrogen and oxygen at 100 cc/min and 0 cc/min, respectively. When the pyrolysis chamber reached the temperature corresponding to the onset of pyrolysis, i.e., about 180°C for the Padding and Blue Seat Backing (see Figure 38 and Figure 39) and 350°C for the green seat cover (see Figure 40), the ramp function that prescribes the flow rate of oxygen to be supplied to the MCC combustor was initiated. The ramp function then controlled the oxygen flow rates to follow the curves in Figure 38, Figure 39 and Figure 40, while the nitrogen flow rate was adjusted to maintain a total flow rate of 100 cc/min. During this period, the exhaust gases were collected in a sampling bag. The bag was used for multiple runs in order to obtain enough sample gas for FTIR analysis and quantification of the concentrations of common toxic gas components found in products of combustion such as acid gases, carbon monoxide, and hydrogen cyanide.

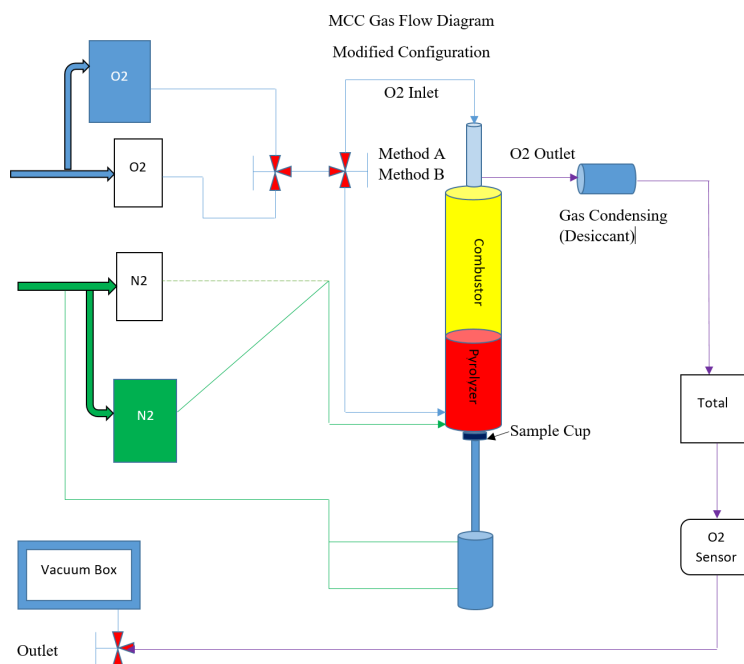


Figure 41. Schematic of modified MCC apparatus for smoke toxicity measurements

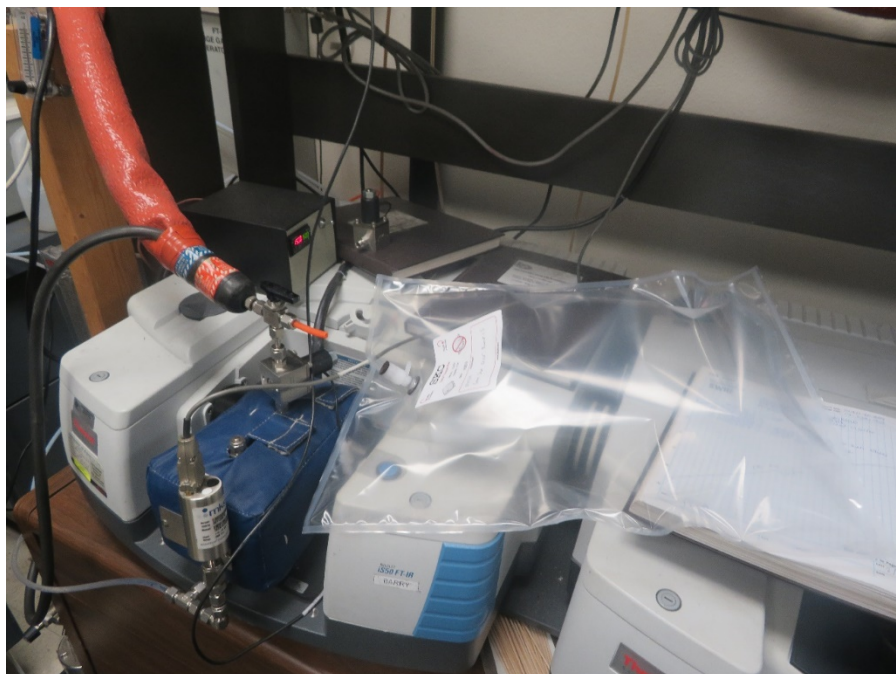


Figure 42. Clear sample bag connected to FTIR for gas analysis

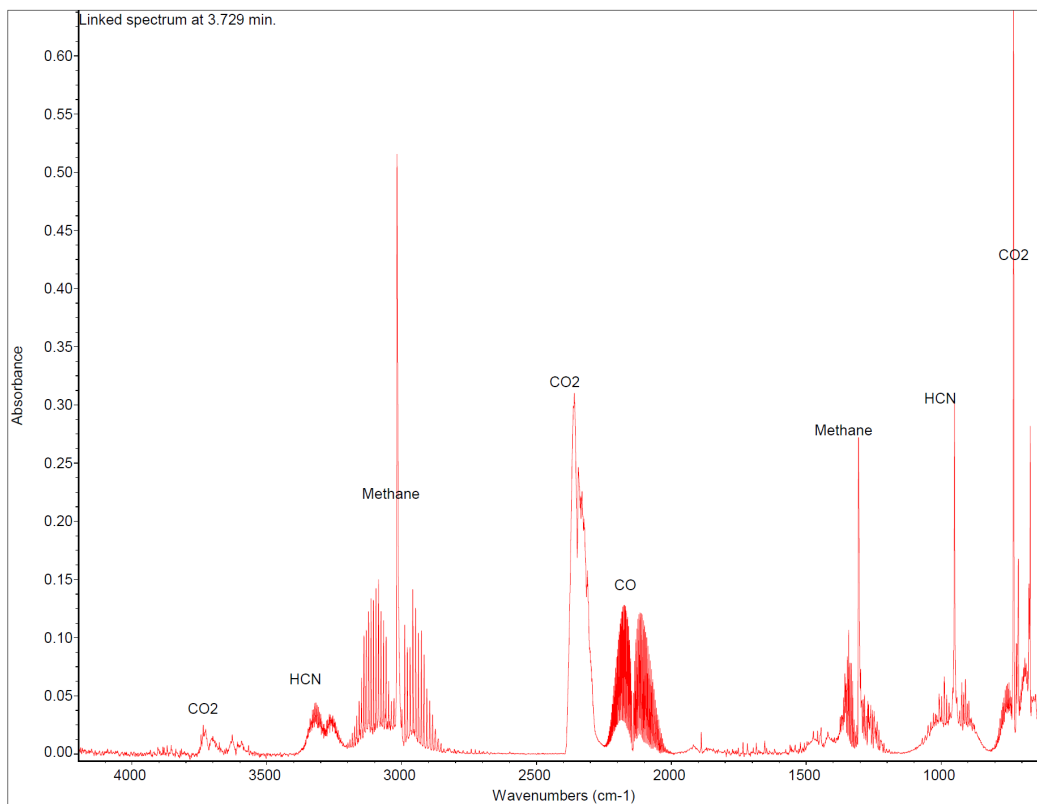


Figure 43. Example FTIR spectra graph used for gas analysis

Test Results

Table 28 provides a summary of the measured concentrations of detected compounds during testing.

Table 28: Summary Test Results for Smoke Toxicity Testing

Material ID	Equivalence Ratio - Phi	Average CO (ppm)	CO Yield (g/g)	Average HCN (ppm)	HCN Yield (g/g)
MC Seat Padding	0.5	1828	0.186	37	0.052
MC Seat Padding	1	2166	0.222	48	0.060
MC Seat Padding	1.5	1974	0.201	38	0.051
MC Seat Backing - Blue	0.5	1406	0.182	52	0.030
MC Seat Backing - Blue	1	1425	0.183	27	0.017
MC Seat Backing - Blue	1.5	1425	0.181	57	0.036
MC Seat Cover - Green	0.5	1429	0.077	0	0.000
MC Seat Cover - Green	1	1799	0.094	7	0.002
MC Seat Cover - Green	1.5	1425	0.074	2	0.001

These volumetric concentrations can be converted to a mass yield of toxic compound generated per unit mass of fuel burned (g/g). Yield data are useful for hazard assessment or modeling calculations. The CO and HCN yields for the three motorcoach materials that were tested are also included in Table 28.

Toxic gas yields generally increase between phi values of 0.5 and 1.5. The yields reported in Table 28 do not follow this trend. A few possible reasons for this inconsistency are briefly discussed below.

- For a significant part of the test duration oxygen was supplied at the low end of the 50 cc/min flow controller range. This made it difficult to control the oxygen flow rate accurately, in particular for the higher phi values and the MC Seat Backing material.
- It was difficult to synchronize the start of the oxygen flow and the onset of pyrolysis, which varied somewhat from test to test.
- Variations in sample composition and mass between tests result in uncertainties of the phi value.
- Six MCC tests were conducted on samples of each material to collect a sufficient gas sample volume for standard FTIR measure in flow-through mode. Perhaps, batch-type sampling, in which the FTIR cell is evacuated and then filled with the exhaust gases generated in a single MCC test, is a better approach and would have resulted in six repeat measurements.

Although the results in terms of yields of CO and HCN as a function of equivalence ratio are inconsistent with data in the literature, the initial smoke toxicity work conducted in this project indicates that it is possible to modify the MCC and make these types of measurements for vehicle materials. However, improvements are needed to obtain data that are consistent with the literature.

Small-Scale Flammability Test Data Analysis

ASTM D3801

The V-rating for the materials tested according to ASTM D3801, together with the FMVSS No. 302 burn rate and the MCC heat release capacity, η_c , are presented in Table 29. Many of the materials tested could not be rated (NR) in accordance with ASTM D3801 V-0, V-1, or V-2 classification because they performed poorly and did not meet the criteria of any of the ratings. This table clearly indicates that an ASTM D3801 V-0 rating is much more difficult to achieve than passing the FMVSS No. 302 test. This is partly due to the more stringent requirements. For example, a V-0 rating does not allow particles or drops that are capable of igniting a cotton wad that is placed below the specimen while FMVSS No. 302 does not take this mechanism of flame spread into account. More importantly, in ASTM D3801 the flame propagates in the upward direction and the spread rate is enhanced by buoyancy effects. In the FMVSS No. 302 test, the flame propagates in the horizontal direction in a relatively quiescent environment and the flame spread rate is largely unaffected by gravity.

The higher severity of the ASTM D3801 is also evident from Figure 44, which shows the lack of correlation between the V rating and the specific heat release capacity, η_c measured in the MCC. From this figure, which is based on data for 110 polymers compiled by Lyon et al. (2009), it can be observed that an η_c of approximately 200 J/g·K is a sufficient condition to achieve a V-0 rating. However, it is also a necessary condition because, while some polymers with a higher η_c have a V-0 rating, many are unrated. Figure 45 shows a similar plot based on the data in Table 29. The fact that η_c is a poor predictor of ASTM D3801 is partly because performance in ASTM D3801 is affected significantly by specimen thickness while MCC data are materials characteristics that are independent of end-use conditions.

Table 29: Comparison of Selected ASTM D3801, FMVSS No.302 and MCC Results

Set	Material Description	V-Rating	Burn Rate (mm/min)	η_c (kJ/g)
School Bus Seats	Blue Bird Seat Cover	V-0	0	169
	Blue Bird Seat Padding	V-2	30	371
	Starcraft Seat Cover	NR	42	125
	Starcraft Seat Padding	NR	22	357
	Trans Tech Seat Cover	V-0	45	129
	Trans Tech Seat Padding	NR	0	350
Motor Coach Materials	Green Cover Seat Padding	NR	23	538
	Seat Cover - Green	NR	38	260
	Seat Backing - Blue	NR	0	93
	Seat Cover - Pattern Blue	NR	0	125
	Seat Backing - Gray	NR	45	936
	Door of Luggage Rack	NR	19	379
	Floor Covering	NR	0	107
	Headliner	NR	0	101
Motor Vehicle Interior	Carpet Ford F250	NR	20	909
	Carpet Mercedes	NR	15	220
	Dashboard Ford F250	NR	19	1112
	Headliner Camaro	NR	38	187
	Headliner Ford	NR	22	138
	Seat Cover Camaro	NR	0	325
	Seat Cover Mercedes	NR	78	269
	Seat Padding Camaro	V-2	44	496
	Seat Padding Mercedes	V-2	0	525

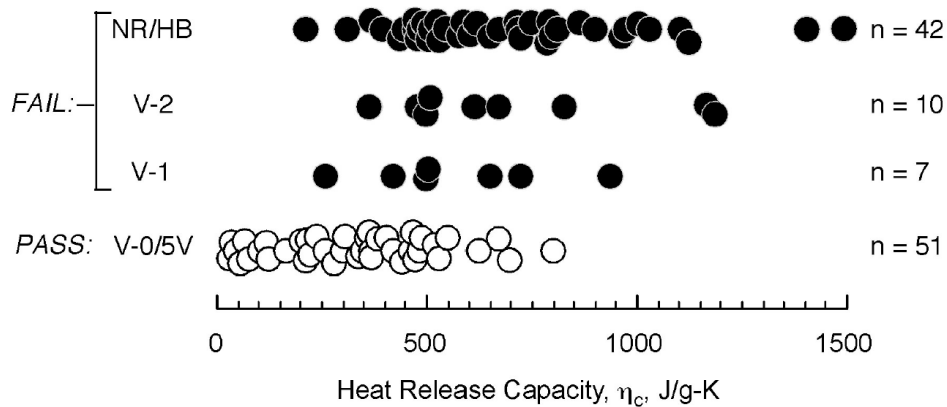


Figure 44. ASTM D3801 V-rating versus η_c from Lyon et al.

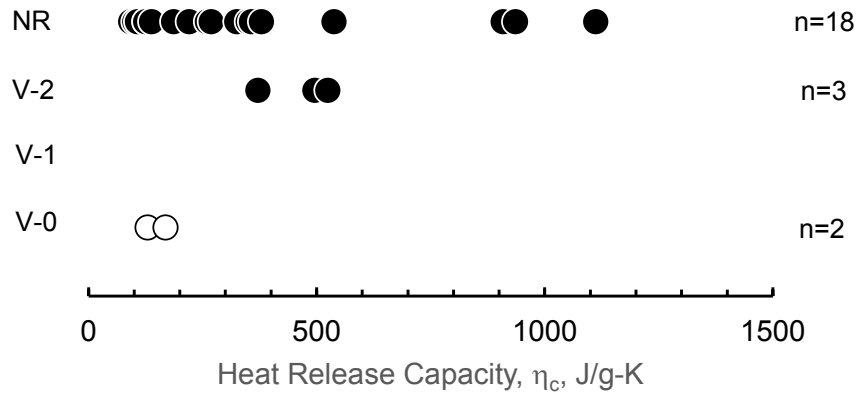


Figure 45. ASTM D3801 V-rating versus η_c based on present work

Several materials with an FMVSS No. 302 burn rate of zero have no V rating. However, the Trans Tech seat cover has a V-0 rating but an FMVSS No. 302 burn rate of 45 mm/min. This lack of correlation together with higher severity of ASTM D3801 make the test unsuitable as an alternative method for materials that are difficult to test in FMVSS No. 302. Moreover, materials that show poor repeatability and reproducibility in FMVSS No. 302 are typically materials for which the FMVSS No. 302 test specimens consist of smaller pieces that need to be tested with steel wire supports. It is likely that for many of these materials it will be difficult to make ASTM D3801 specimens, even though they are (much) smaller than FMVSS No. 302 specimens.

ASTM E1354 (cone calorimeter)

Table 30 provides a comparison between selected results from cone calorimeter testing at a heat flux of 35 kW/m² to the FMVSS burn rate. The cone calorimeter test results are defined as follows: t_{ig} is the time to ignition in seconds from the start of test, HRR_{peak} is the first (or only) peak in the heat release rate curve, HRR_{60} is the average heat release rate over a 60-s period following ignition, THR is the total heat released during entire test, and HOC is the effective heat of combustion.

To determine whether cone calorimeter criteria can be established to predict failure in FMVSS No. 302, Carpenter et al. (2006) developed a plot of HRR_{peak} versus t_{ig} measured in the cone calorimeter at 35 kW/m² for two sets of FMVSS No. 302-compliant automotive materials. The data was obtained from previous studies conducted by NHTSA (Battipaglia et al., 2003) and GM (Miller et al., 2004). The plot developed by Carpenter et al. (2006) is reproduced in Figure 46, which also includes the present data.

Table 30: Comparison of Selected ASTM E1354 and FMVSS No. 302 Results

Set	Material	t_{ig} (s)	HRR_{peak} (kW/m ²)	HRR_{60} (kW/m ²)	THR (MJ/m ²)	HOC (MJ/kg)	Burn Rate (mm/min)
Motor Coach	Seat Backing - Gray	20	440	259	59.7	30.5	45
	Door of Luggage Rack	50	662	443	193.6	28.8	19
	Floor Covering	26	267	208	33.5	14.5	0
	Headliner	38	273	139	12.6	15.0	0
Motor Vehicle Interior	Carpet Ford F250	31	437	262	68.6	31.3	20
	Carpet Mercedes	68	317	243	77.4	29.2	15
	Dashboard Ford F250	54	372	272	151.4	38.5	19
	Dashboard Mercedes	21	396	287	165.0	31.4	38
	Headliner Camaro	7	300	208	17.0	26.5	22
	Headliner Ford	7	343	173	14.6	22.1	0

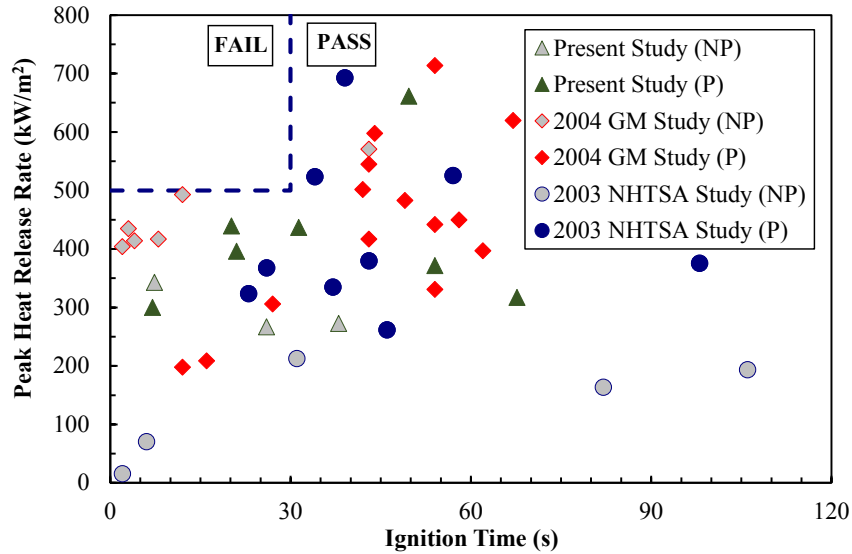


Figure 46. ASTM E1354 HRR_{peak} versus t_{ig} for three sets of automotive material

Materials that are easier to ignite and, once ignited, release heat at a higher rate are expected to perform worse in a small-scale flammability test such as FMVSS No. 302. Figure 46 indicates that, to pass FMVSS No. 302, peak heat release rate must not exceed 500 kW/m² and ignition time must be 30 s or greater. Although these limits are not very challenging, most automotive materials need to be treated with fire retardants or a protective coating to meet them.

ASTM D7309 (MCC)

The analysis of the MCC data is discussed in detail here.

Alternative Methodology Development

Based on the analysis of the ASTM D3801 and ASTM E1354 data discussed in previous sections, the MCC was identified as the best candidate to provide an alternative methodology to FMVSS No. 302. The development of the alternative methodology is the subject of this section.

MCC Test Results and Material Properties Used in the Analysis

The MCC is described in detail in the section on “Bench-Scale Material Testing.” All MCC tests were performed according to Method A in ASTM D7309, i.e., with nitrogen supplied to the pyrolysis chamber and oxygen to the combustor. The following MCC parameters were used in the analysis:

1. The heat release capacity $\eta_c \equiv Q_{\max}/\beta$ in J/g·K, where Q_{\max} is the maximum value of $Q(t)$ in W/g and β is the heating rate in K/s.
2. Q_{\max} as defined above.
3. The heat release temperature T_{\max} in K as the pyrolysis chamber temperature at which $Q(t) = Q_{\max}$.
4. The specific heat of combustion h_c in J/g as the area under the $Q(t)$ curve.

A typical $Q(t)$ curve measured in the MCC and the corresponding $Q(T)$ curve are shown in Figure 47 and Figure 48, respectively. Because the heating rate, β , is close to 1 °C/s, the $Q(T)$ curve is essentially shifted to the right by a ΔT equal to the pyrolysis chamber temperature at the start of data collection ($t = 0$). Figure 48 illustrates how Q_{\max} and T_{\max} are determined and h_c is calculated from the area under the $Q(t)$ curve (or the area under the $Q(T)$ curve divided by β).

In addition, to the four MCC parameters, the analysis also uses the thickness, δ , and density, ρ , of the material and its ignition temperature, T_{ig} . The latter is an important measure of the ease of ignition of the material. T_{ig} can be estimated from the MCC data, but the process is rather involved. A detailed discussion is provided in the next section.

A list of the physical characteristics (δ and ρ), average FMVSS No. 302 burn rate, MCC parameters (η_c , Q_{\max} , T_{\max} , and h_c), and T_{ig} can be found in Table 31. In addition, to columns for these data, there are three additional columns that contain the number of layers the material consists of, the number of observed peaks in the $Q(T)$ curve, and the number of peaks that were considered in the calculations to estimate T_{ig} . The relevance of the number of peaks will become clear in the discussion of the method used to estimate T_{ig} .

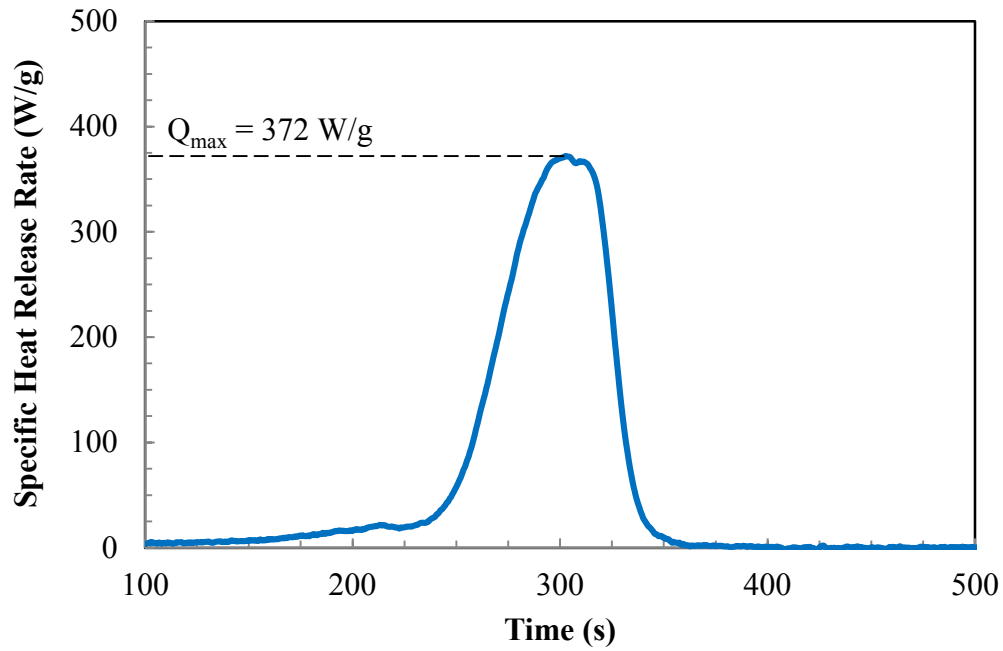


Figure 47. Typical $Q(t)$ curve measured in the MCC

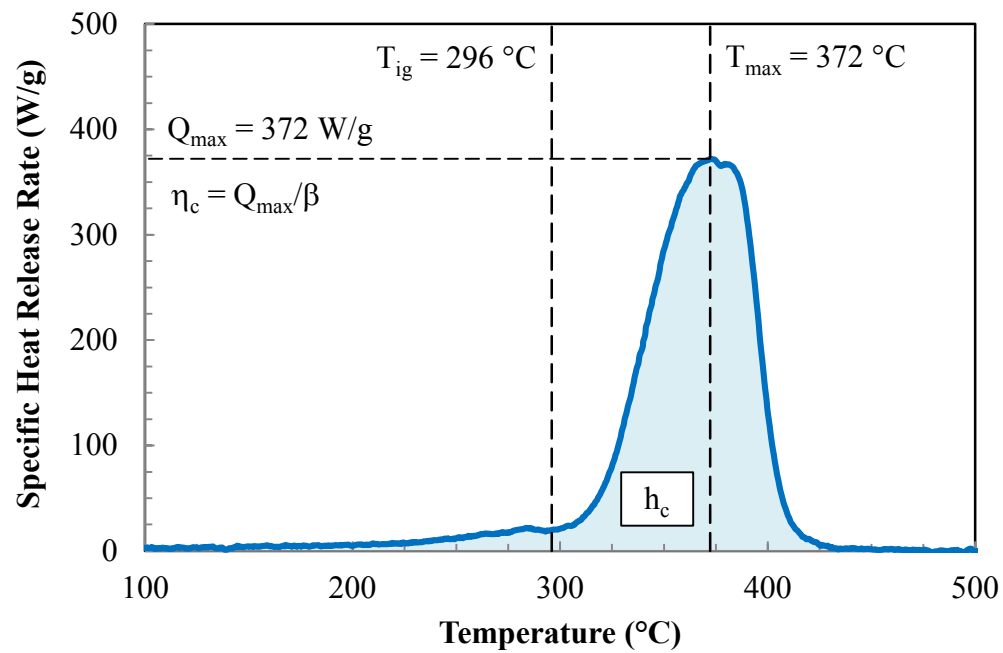


Figure 48. Corresponding $Q(T)$ curve

Table 31: Compilation of Data Used in the Development of the Alternative Methodology

	Material	# of Layers	δ (mm)	ρ (kg/m ³)	Burn Rate (mm/min)	η_c (J/g·K)	Q_{max} (W/g)	T_{max} (°C)	h_c (kJ/g)	No. of Peaks		T_{ig} (°C)
										Obs.	Mod. ³	
School Bus Seats	Blue Bird Seat Cover	2	0.8	1055	0	169	173	250	8.26	4	1P	228
	Blue Bird Padding	1	46.2	56	30	371	376	420	18.6	1	1F	365
	Starcraft Seat Cover	2	0.8	945	42	125	128	296	9.86	3	1F	225
	Starcraft Padding	1	42.0	95	22	357	360	412	16.5	1	1F	364
	Trans Tech Seat Cover	2	0.8	1050	45	129	132	298	9.53	4	1F	235
	Trans Tech Padding	1	25.4	24	0	350	353	410	15.1	1/2	1F	365
Motor Coach Materials	Green Cover Padding	1	53.0	45	23	538	537	355	18.5	1-3	1F	294
	Green Seat Cover	2	3.6	149	38	260	264	444	14.9	2	1F	374
	Blue Seat Backing	2	3.7	247	0	93	93	372	8.67	4	1F	292
	Blue Seat Cover	2	3.2	230	0	125	125	423	12.9	2	1P	276
	Grey Seat Backing	1	5.2	163	45	936	936	489	34.6	1	1F	427
	Luggage Rack Door	2	24.1	258	19	379	384	436	28.3	1	1F	356
	Floor Covering	2	2.4	1073	0	101	109	308	7.19	2	1P	237
	Headliner	2	4.2	215	0	107	103	510	4.01	3	NA ⁴	475
	Blue Cover Padding ¹	1	101.6	73	94	435	432	406	23.3	3	1P	210
	Blue Cover Padding ¹	1	101.6	73	94	448	439	405	23.6	3	1P	205
	Blue Cover Padding ²	1	101.6	73	94	421	417	404	23.9	3	1P	216
	Blue Cover Padding ²	1	101.6	73	94	427	422	405	24.0	3	1P	214
	Motor Vehicle Interior Mats	Ford F250 Carpet	2	15.3	124	20	909	924	482	40.2	1	1F
Mercedes Carpet		3	15.0	343	15	220	224	414	20.4	4	1P	264
Ford F250 Dashboard		1	3.4	1000	19	1112	1066	492	38.0	1	1F	427
Mercedes Dashboard		3	25.3	241	38	322	326	411	25.0	2	1F	311
Camaro Headliner		4	6.7	126	22	198	201	462	22.7	2	1P	229
Ford Headliner		4	16.7	65	0	138	141	425	17.5	3	1P	232
Camaro Seat Cover		3	3.7	165	78	325	328	444	18.1	3	1P	369
Mercedes Seat Cover		1	4.4	265	44	269	275	283	13.3	3	1P	244
Camaro Padding		1	16.8	36	0	496	502	409	21.5	1	1F	352
Mercedes Padding		1	19.0	50	0	525	524	409	23.4	2	1P	301

Table 31: Compilation of Data Used in the Development of the Alternative Methodology
(Continued)

Material		# of Layers	δ (mm)	ρ (kg/m ³)	Burn Rate (mm/min)	η_c (J/g-K)	Q_{max} (W/g)	T_{max} (°C)	h_c (kJ/g)	No. of Peaks		T_{ig} (°C)
										Obs.	Mod. ³	
Surface Layer	Ford F250 Carpet	1				949	950	472	41.2	1	1F	398
	Mercedes Carpet	1				611	606	458	29.3	2	1F	380
	Mercedes Dashboard	1				294	291	383	27.2	2	1F	281
	Camaro Headliner	1				230	228	425	18.6	4	1P	229
	Ford Headliner	1				281	279	441	18.6	4	1P	229
	Camaro Seat Cover	1				385	381	438	16.7	2	1F	381
Thin Mats	Acrylate	1	1.6	1040	42	404	409	400	25.8	2	1F	316
	Corrugated Cardboard	1	3.2	155	61	140	142	364	9.47	2	1F	292
	Thick HDPE	1	1.6	950	36	1156	1176	504	43.4	1	1F	440
	Thin HDPE	1	0.8	950	68	1156	1176	504	43.4	2	1F	440
	Folder Cardboard	1	0.3	680	121	215	216.9	365	10.7	2	1F	306
WM Foam	SF Test Foam	1	6.4	29	142	640	632	385	27.4	3	1P	216
	SF Test Foam	1	12.7	29	101	640	632	385	27.4	3	1P	216
	SM Test Foam	1	6.4	33	117	544	536	387	26.7	3	1P	216
	SM Test Foam	1	12.7	33	82	544	536	387	26.7	3	1P	216
Cryo-milled Specimens	Blue Bird Seat Cover	2	0.8	1055		134	136	310	14.6	4	1P	192
	Blue Bird Padding	1	46.2	56		538	547	401	29.1	3	1P	217
	Blue Bird Padding BS	1	46.2	56		400	407	413	25.4	3	1P	219
	Starcraft Padding	1	42.0	95		383	390	412	26.3	3	1P	218
	Trans Tech Padding	1	25.4	24		403	410	408	29.0	3	1P	227
	Luggage Rack Door	2	24.1	258		623	629	444	37.7	2	1F	370
	Headliner	2	4.2	215		123	125	372	14.0	3	1P	262
	Mercedes Carpet	3	15.0	343		132	138	488	13.8	3	1P	296
	Ford Headliner	4	16.7	65		149	150	401	21.5	3	1P	233
	Camaro Padding	1	16.8	36		498	554	405	28.0	3	1P	229
Acrylate	1	1.6	1040		420	466	389	27.0	2	1F	276	

Table 31: Compilation of Data Used in the Development of the Alternative Methodology
(Continued)

Material	# of Layers	δ (mm)	ρ (kg/m ³)	Burn Rate (mm/min)	η_c (J/g·K)	Q_{max} (W/g)	T_{max} (°C)	h_c (kJ/g)	No. of Peaks		T_{ig} (°C)	
									Obs.	Mod. ³		
Childseat Materials	Britax Base	1	1.2	629		1236	1229	469	44.4	1	1F	409
	Chicco Base	1	2.9	602		1149	1140	470	44.0	1	1F	405
	Peg Perego Base	1	2.9	711		1186	1171	469	44.5	1	1F	407
	UPPAbaby Base	1	2.8	676		1271	1261	471	44.5	1	1F	411
	Britax Fabric	1	0.2	435		334	332	442	15.9	1	1F	379
	Chicco Fabric	1	0.2	539		1246	1234	473	42.8	1	1F	411
	Peg Perego Fabric	1	0.5	284		328	325	441	15.9	1	1F	379
	UPPAbaby Fabric	1	0.4	665		124	123	391	14.7	2	1P	253
	Britax Padding	1	15.9	10		332	329	440	15.6	1	1F	381
	Chicco Padding	1	9.7	26	0	327	321	385	26.1	3	1P	198
	Peg Perego Padding	1	11.3	30	0	513	504	390	25.4	3	1P	212
	UPPAbaby Padding	1	10.7	24	121	571	564	391	27.7	3	1P	220
	Britax Assembly	1	16.1	16		346	344	443	16.1	1	1F	385
	Chicco Assembly	2	9.9	38		268	266	422	33.1	3-4	1P	212
	Peg Perego Assembly	2	11.8	41		222	220	405	19.7	5	1P	225
	UPPAbaby Assembly	2	11.1	46		269	265	401	17.8	3	1P	229

Notes: ¹ Samples taken from various locations inside the padding

² Samples taken at various locations on the surface

³ 1F = fit covers the entire Q(T) curve, 1P = fit covers part of the Q(T) curve corresponding to the first reaction

⁴ Optimization did not converge

Method for Estimating T_{ig}

Implementation of the approach that was used to estimate T_{ig} is relatively straightforward for materials with a single peak in the $Q(T)$ curve (or materials for which only a single peak needs to be considered to estimate T_{ig}). The first subsection therefore uses such a material to illustrate how the method works. The next subsection deals with some of the challenges that are encountered when the $Q(T)$ curve has multiple peaks.

Estimating T_{ig} for Materials With a Single Peak in the $Q(T)$ Curve

The subsection uses the MCC data for the motor coach luggage rack door to illustrate how T_{ig} for a material with a single $Q(T)$ peak can be estimated based on a modified version of a method developed by Lyon and Safronava (2017). The $Q(T)$ curves for the three MCC tests that were conducted on this material are shown in Figure 49.

The rate of conversion of the solid to gaseous fuel in a single step thermal decomposition process can be expressed by the following Arrhenius reaction rate model

$$\frac{d\alpha}{dt} = (1 - \alpha)^n A \exp\left(\frac{-E}{RT}\right) \quad [1]$$

where α is the conversion or degree of advancement of the reaction (varies between 0 and 1), t is time in seconds, n is the reaction order, A is the frequency factor (s^{-1}), E is the activation energy (J/mol), R is the universal gas constant (8.314 J/mol-K), and T is temperature in K. Assuming a constant heat of combustion, which is consistent with the assumption of a single step thermal degradation reaction, α can be expressed as follows

$$\alpha(t) \equiv \frac{\int_0^t Q(\tau) d\tau}{h_c} = \frac{Q_{cumul}(t)}{h_c} \quad [2]$$

where $Q_{cumul}(t)$ is the cumulative specific heat release rate at time t in J/g.

Because α is very small at ignition (typically of the order of 1 or 2 percent based on the calculations presented in Appendix J), neglecting α_{ig} results in conservative [low] estimates for T_{ig} . Equation 1 at ignition can therefore be simplified to

$$h_c \left(\frac{d\alpha}{dt}\right)_{ig} \equiv Q^* \approx h_c A \exp\left(\frac{-E}{RT_{ig}}\right) \quad [3]$$

where Q^* is the specific heat release rate at ignition. Equation 3 can then be rearranged to express T_{ig} as a function of A and E

$$T_{ig} \approx \frac{E}{R \ln\left(\frac{A h_c}{Q^*}\right)} \quad [4]$$

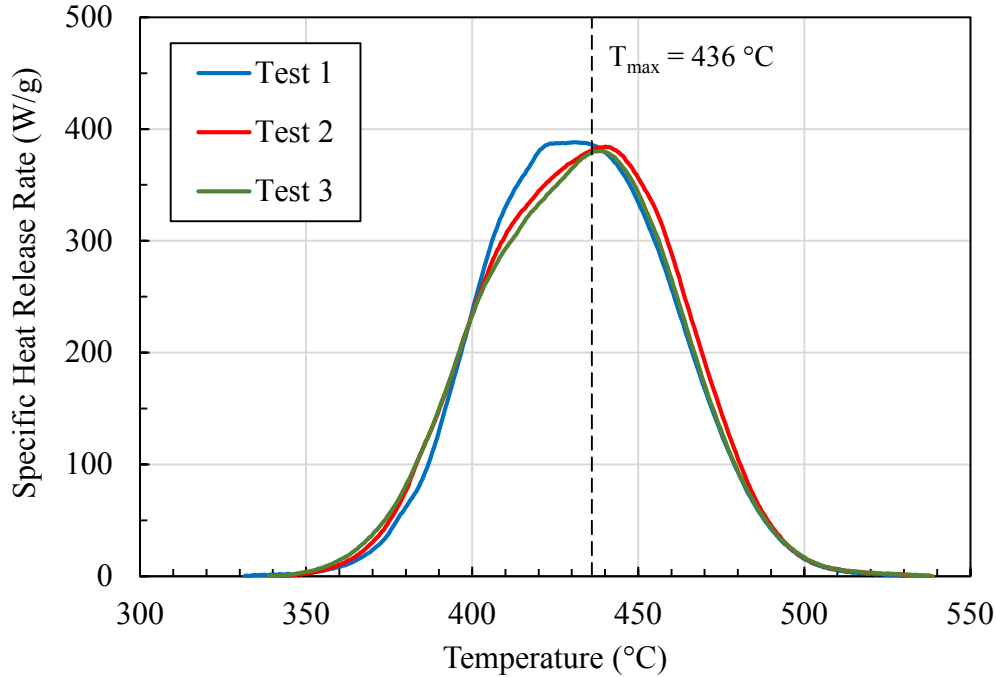


Figure 49. MCC $Q(T)$ curves for the motor coach luggage rack door

Lyon and Safronava calculated Q^* for a typical polymer and obtained a value of 20 W/g corresponding to sustained ignition in the cone calorimeter. They tested specimens of 16 polymers in the cone calorimeter and obtained reasonable agreement between measured or inferred (from the critical heat flux) surface temperatures at sustained piloted ignition and those calculated from Equation 4. A value of 20 W/g for Q^* was used to estimate T_{ig} in the present study.

The single point peak property method (SP PPM) described in another paper by Lyon and Safronava (2013) was used to obtain initial estimates of A and E (with $n=1$). First, E is estimated from Equation 5, and once E is determined, A is calculated from Equation 6.

$$E \approx \frac{Q_{max} e R T_{max}^2}{h_c} - 2 R T_{max} \quad [5]$$

$$A \approx \frac{\beta E}{R T_{max}^2} \exp\left(\frac{E}{R T_{max}}\right) \quad [6]$$

In a final step, the standard Solver in MS Excel was used to refine the A , E , and n . Figure 50 shows the results of the first step (SP PPM), which leads to an estimated T_{ig} of 338°C, which seems low based on a comparison between the SP PPM fit and the measured $Q(T)$ curves at the low end of the temperature range. The Solver solution gives a T_{ig} of 356°C, which is more consistent with the experimental data.

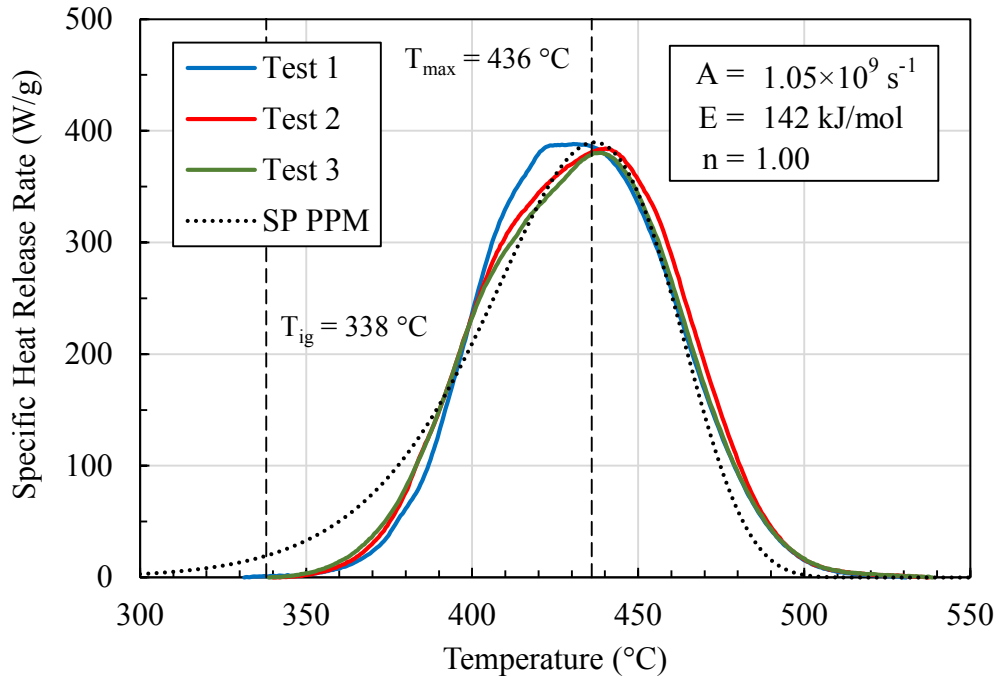


Figure 50. SP PPM Fit to $Q(T)$ curves for the motor coach luggage rack door

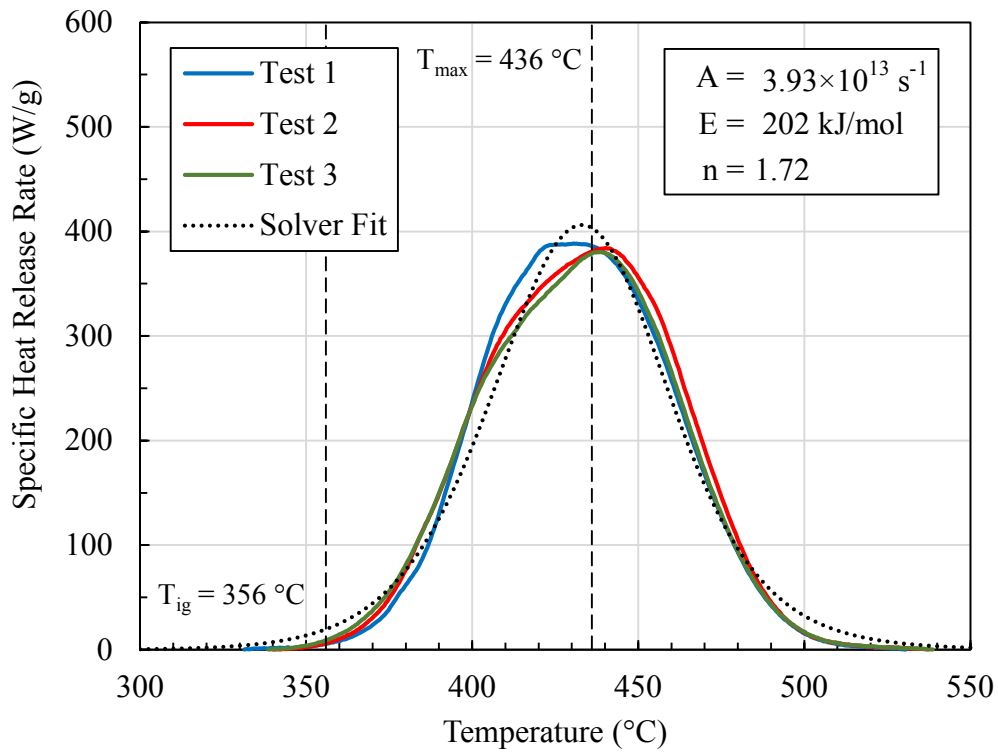


Figure 51. Solver fit to $Q(T)$ curves for the motor coach luggage rack door

Estimating T_{ig} for Materials With Multiple Peaks in the $Q(T)$ Curve

Estimating the kinetic parameters of multiple overlapping Arrhenius reactions is a difficult problem. Over the past 10 years many investigators have developed methods to solve this problem (e.g., Lautenberger and Fernandez-Pello, 2011; Matala et al., 2012; Pau et al., 2013; Li et al., 2014; Yuen, 2018; and Bruns & Leventon, 2020, to name a few). The initial plan was to review these methods and select and customize the method that is most suitable for the purpose of estimating the ignition temperature, which is typically associated with the first thermal degradation reaction that occurs at the low end of the temperature range over which the specimen decomposes. Yuen's approach was chosen as the most practical and potentially suitable for the task at hand.

When multiple overlapping reactions occur (reactions that do not overlap can be modeled as discussed in the previous section), the $Q(t)$ curve is modeled by combining the Arrhenius reaction models (Equation 1) for all contributors to the thermal degradation of the material.

$$Q(t) = h_c \frac{d\alpha}{dt} = h_c \sum_{i=1}^N c_i \frac{d\alpha_i}{dt} = h_c \sum_{i=1}^N c_i (1 - \alpha_i)^{n_i} A_i \exp\left(\frac{-E_i}{RT}\right) \quad [7]$$

where c_i is a weighting factor equal to the contribution of reaction i to the total heat released (h_c). Because the weighting factors must add up to one, a model that involves N reactions requires that $4N - 1$ parameters must be estimated.

The first challenge is to determine how many reactions need to be included in the model. Each reaction results in a peak or shoulder in the $Q(T)$ curve. The number of reactions is relatively easy to determine when the peaks are distinct. The situation is much more difficult when the peaks are not distinct and the reactions have significant overlap.

An algorithm was developed and implemented in Excel using the Solver feature. The algorithm does a good job reproducing the peaks, but often does not provide a good fit near T_{ig} and has difficulties detecting all peaks when there is significant overlap between the reactions. It was therefore, decided to develop an algorithm that only models the first reaction to more easily obtain a more accurate estimate of T_{ig} . The algorithm requires an initial guess of c_1 , but is otherwise very similar to the method for $Q(T)$ curves with a single peak discussed in the previous section. The parameters c_1 , n_1 , A_1 and E_1 are determined by fitting the model to the initial part of the $Q(T)$ curve where it is assumed there is no overlap with another reaction.

This optimization method was used to determine T_{ig} for all materials that were tested in the MCC. The results can be found in Appendix J.

Statistical Analysis

A statistical analysis was conducted of the MCC data obtained for the school bus seat, motor coach, motor vehicle interior and thin materials with the objective of determining whether the FMVSS No. 302 burn rate (BR) can be estimated using the following power law:

$$BR = C (\eta_c)^{n1} (Q_{max})^{n2} (T_{max})^{n3} (h_c)^{n4} (1 - Y_p)^{n5} (h_{c,gas})^{n6} (T_{ig})^{n7} (\delta)^{n8} (\rho)^{n9} \quad [8]$$

The model can be linearized as follows:

$$\ln(BR) = C + \sum_{i=1}^9 n_i X_i \quad [9]$$

where $X_1 = \ln(\eta_c)$, $X_2 = \ln(Q_{max})$, $X_3 = \ln(T_{max})$, $X_4 = \ln(h_c)$, $X_5 = \ln(1 - Y_p)$, $X_6 = \ln(h_{c,gas})$, $X_7 = \ln(T_{ig})$, $X_8 = \ln(\delta)$, and $X_9 = \ln(\rho)$. To reduce the number of independent variables, a principal component and factor analysis was performed. Since $h_{c,gas} = h_c / (1 - Y_p)$, X_5 was removed before the calculations were made. Table 32 shows the correlation matrix between the remaining eight independent variables based on the measured data for the 29 materials in Appendix F, Tables F-1, F-2, F-4 and F-7.

Table 32: Independent Variables Correlation Matrix

	X1	X2	X3	X4	X6	X7	X8	X9
X1	1.0000	0.9981	0.5520	0.9055	0.7340	0.6273	0.2345	-0.1128
X2	0.9981	1.0000	0.5347	0.8948	0.7214	0.6236	0.2138	-0.0923
X3	0.5520	0.5347	1.0000	0.5605	0.3830	0.8998	0.2951	-0.2658
X4	0.9055	0.8948	0.5605	1.0000	0.8682	0.4846	0.2664	-0.0698
X6	0.7340	0.7214	0.3830	0.8682	1.0000	0.2645	0.1882	0.0903
X7	0.6273	0.6236	0.8998	0.4846	0.2645	1.0000	0.2091	-0.2006
X8	0.2345	0.2138	0.2951	0.2664	0.1882	0.2091	1.0000	-0.8071
X9	-0.1128	-0.0923	-0.2658	-0.0698	0.0903	-0.2006	-0.8071	1.0000

The cells with a correlation coefficient of 0.8 or greater are highlighted. This indicates that the independent variables to predict burn rate can be grouped into three subsets of highly correlated variables.

- Subset 1: MCC heat release parameters (η_c , Q_{max} , h_c , and up to a lesser extent $h_{c,gas}$)
- Subset 2: MCC temperature parameters (T_{ig} and T_{max})
- Subset 3: Specimen thickness (δ) and density (ρ)

This is consistent with the results of the factor analysis, which revealed that 84 percent of the variance of the independent variable data set can be explained by the variance of the following three factors.

$$F_1 = (X'_1)^{0.8740}(X'_2)^{0.8694}(X'_4)^{0.9328}(X'_6)^{0.9261} \quad [10a]$$

$$F_2 = (X'_3)^{0.8881}(X'_7)^{0.9471} \quad [10b]$$

$$F_3 = (X'_8)^{-0.9399}(X'_9)^{0.9445} \quad [10c]$$

A linear regression analysis was performed to develop an equation for predicting the FMVSS No. 302 burn rate as a function of the three factors. Although the equation identifies the single failing material (manila file folder cardboard), quantitative prediction of the burn rate is too inaccurate to be useful.

Development of MCC Parameter-Based FMVSS No. 302 Pass/Fail Prediction Limits

The main take away from the principal component and factor analysis is that it should be possible to establish pass/fail limits based on the values of three independent variables, one from each of the three subsets. The heat release capacity, η_c , is a logical choice for the first subset because Lyon et al. have used it to predict with reasonable success whether a material is expected to burn or not burn in various small-scale flammability tests, including FMVSS No. 302 (Lyon et al., 2009). T_{ig} is a logical choice for the second subset because flame spread over the surface of a solid material can be viewed as a series of consecutive ignition events, and T_{ig} is an indicator of the ignition propensity (and therefore flame spread propensity) of a material. Finally, δ is the obvious choice for the third subset because the only material that fails the FMVSS No. 302 test is also one of the thinnest of the 29 materials that were tested.

Manila file folder cardboard is the only material that failed the FMVSS No. 302 test in the set that was used for the statistical analysis. In fact, this material is one of the five “thin” materials that were added to the set in an attempt to include some failures. Two of the five thin materials were made of polyethylene, which is used extensively in motor vehicles. Unfortunately, these materials passed the FMVSS No. 302 test. Untreated plastic foams are likely to fail FMVSS No. 302 (see Table 34), but were not considered because of the unusual fire behavior of this type of materials.

The file folder cardboard material has a η_c of 215 ± 6 J/g·K. Consequently, a maximum η_c of 200 J/g·K (roughly 215 J/g·K minus two standard deviations) is considered as a pass/fail limit. Figure 52 shows, based on this criterion alone, that only 9 of the 29 materials would be expected to pass FMVSS No. 302. To reduce the number of incorrectly predicted failures, an alternative pass/fail criterion is suggested for T_{ig} , in other words, $T_{ig} \geq 310$ °C. The 310 °C limit is based on the fact that T_{ig} for the file folder cardboard is 306°C. Figure 53 shows that including the alternative criterion still results in four materials for which the prediction does not align with FMVSS No. 302 results. The heat release capacity, ignition temperature and thickness for these materials are given in Table 33: Data for Materials With $\eta_c > 200$ J/g·K and $T_{ig} < 310$ °C that Pass FMVSS No. 302 To correctly predict the FMVSS No. 302 pass of these four materials it is suggested to relax the criteria for materials with a thickness of 3.2 mm ($\frac{1}{8}$ in.) or greater, and require that either $\eta_c \leq 300$ J/g·K, or $T_{ig} \geq 290$ °C.

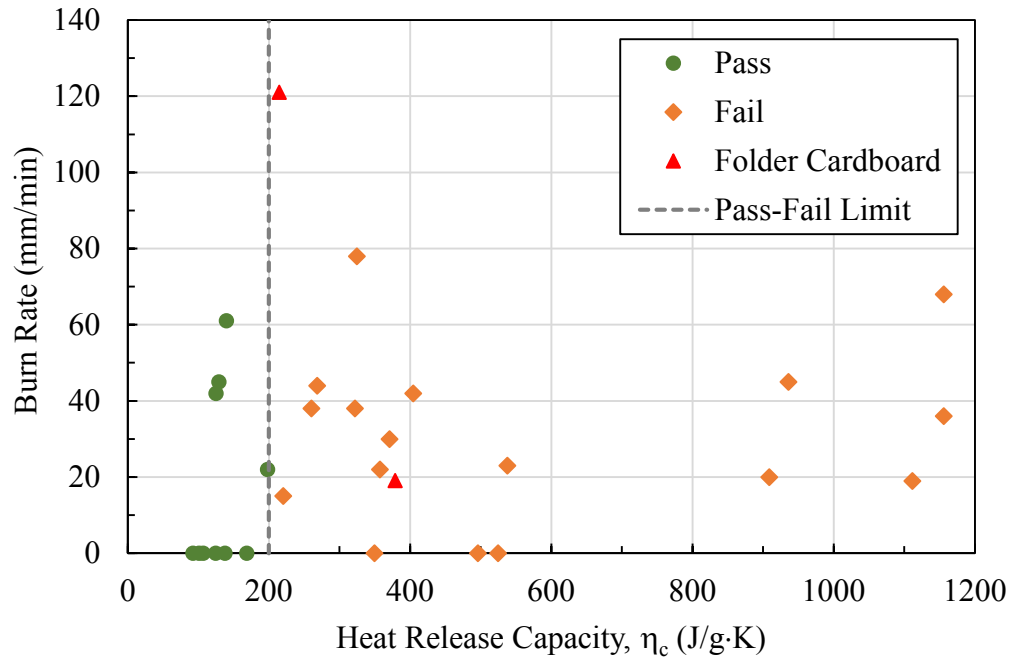


Figure 52. Pass/fail limit for η_c (green circles are materials with $\eta_c \leq 200$ J/g·K)

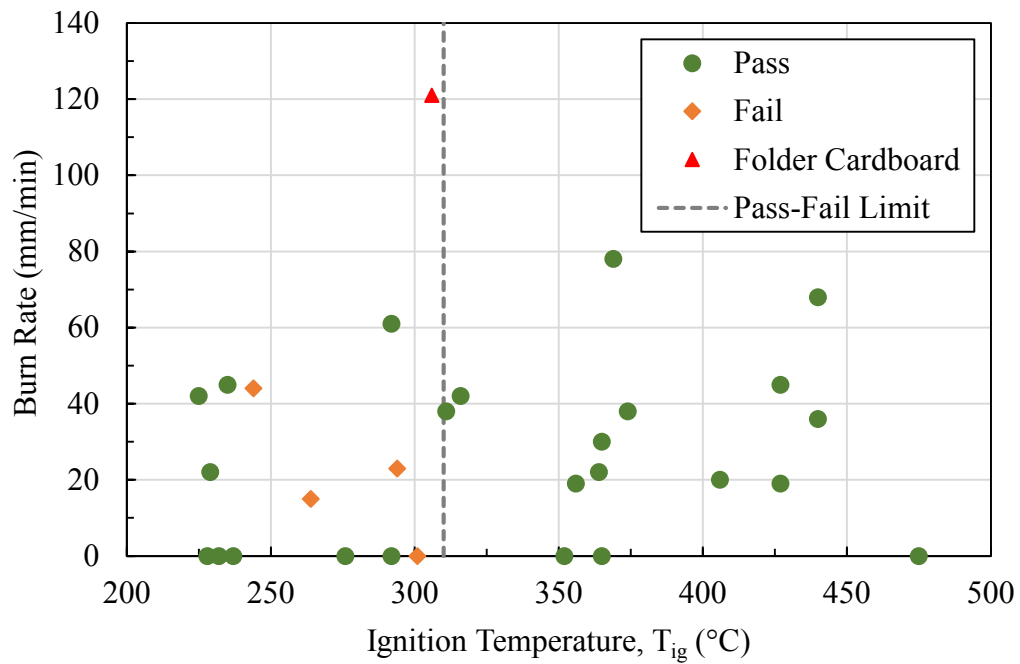


Figure 53. Pass/fail Limit for η_c (green circles are materials with $\eta_c \leq 200$ J/g·K)

Table 33: Data for Materials With $\eta_c > 200 \text{ J/g}\cdot\text{K}$ and $T_{ig} < 310^\circ\text{C}$ That Pass FMVSS No. 302

Material	$\eta_c \text{ (J/g}\cdot\text{K)}$	$T_{ig} \text{ (}^\circ\text{C)}$	$\delta \text{ (mm)}$
Carpet Mercedes	221 ± 23	264 ± 10	15.0
Seat Cover Mercedes	269 ± 17	244 ± 2	4.4
Seat Padding Mercedes	525 ± 1	297 ± 1	19.0
MC Seat Padding	446 ± 7	294 ± 1	53.0

Development of Physics-Based Pass/Fail Prediction Limits

Flame spread over the surface of a specimen in the FMVSS No. 302 test apparatus is essentially in the opposite direction of the entrained air flow. The opposed-flow flame spread rate, V_p , over the surface over a thin sheet of solid material with negligible heat losses from the back side can be estimated from the following relationship (Hasemi, 2016).

$$V_p = \frac{k_g(T_f - T_r)}{\rho c \delta (T_{ig} - T_a)} \quad [11]$$

where k_g is the thermal conductivity of air in $\text{W/m}\cdot\text{K}$, T_f is the flame temperature in $^\circ\text{C}$ or K , T_r is a reference temperature in the same units, ρ is the density of the solid material in kg/m^3 , c is the specific heat of the solid in $\text{J/kg}\cdot\text{K}$, δ is the thickness of the sheet in m , T_{ig} is the ignition temperature in $^\circ\text{C}$ or K and T_a is the ambient (or initial) temperature in the same units. Both k_g and T_f are relatively constant. T_r is between T_a and T_{ig} , closer to the former and well below T_f . Finally, the specific heat of plastics used in the interior of motor vehicles varies over a relatively small range ($1.5 \pm 0.3 \text{ kJ/kg}\cdot\text{K}$ as reported by Miller et al.). Consequently, V_p (or the FMVSS No. 302 burn rate) is expected to be approximately inversely proportional to $\rho\delta(T_{ig} - T_a)$:

$$V_p \approx \frac{C}{\rho\delta(T_{ig} - T_a)} \quad [12]$$

Where C is a constant. Figure 54 shows that the data roughly follow this trend, except for some heavily FR-treated materials that may be relatively easy to ignite, but extinguish immediately or shortly after the burner flame is removed. The value of $\rho\delta(T_{ig} - T_a)$ below which the material is expected to fail FMVSS No. 302 was determined from Equation 11 with $C = 153 \times 56 \approx 8570$, whereby 153 is the mean FMVSS No. 302 burn rate observed for the file folder cardboard plus two standard deviations (see Table C-5 in Appendix C) and 56 is equal to $\rho\delta(T_{ig} - T_a)$ for the same material in $\text{kg}\cdot^\circ\text{C/m}^2$. The limiting value is approximately $85 \text{ kg}\cdot^\circ\text{C/m}^2$.

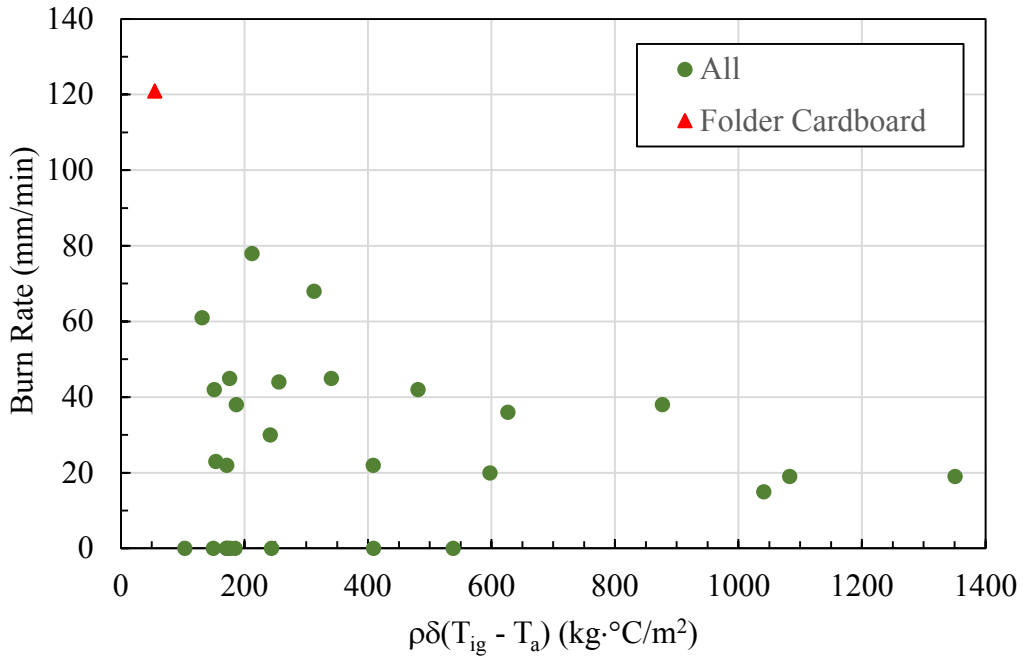


Figure 54. FMVSS No. 302 burn rate as a Function of $\rho\delta(T_{ig} - T_a)$

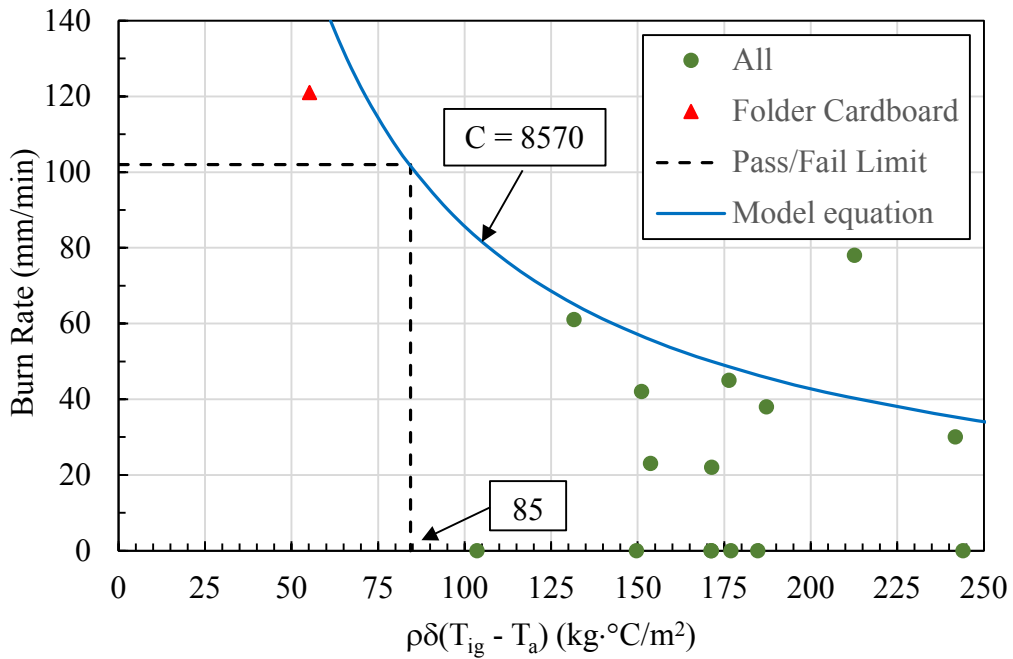


Figure 55. Establishing $\rho\delta(T_{ig} - T_a)$ lower limit to predict failure in FMVSS No. 302

Pass/Fail Criteria for the Alternative Methodology

Two sets of alternative pass/fail criteria have been developed based on the analysis of the MCC data discussed in the previous two sections. These criteria are as follows.

1. MCC parameter-based criteria:

- Materials that are 3.2 mm or less in thickness are predicted to pass the FMVSS No. 302 when at least one of the following criteria is met: $\eta_c \leq 200 \text{ J/g}\cdot\text{K}$ or $T_{ig} \geq 310 \text{ }^\circ\text{C}$.
- Materials that are more than 3.2 mm thick are predicted to pass the FMVSS No. 302 when at least one of the following, less stringent, criteria are met: $\eta_c \leq 300 \text{ J/g}\cdot\text{K}$ or $T_{ig} \geq 310 \text{ }^\circ\text{C}$.

2. Physics-based criterion:

- Materials are predicted to pass the FMVSS 302 if the following criterion is met: $\rho\delta(T_{ig} - T_0) \geq 85 \text{ kg}\cdot\text{K/m}^2$. Note that the thickness in this parameter is set at 12.7 mm if the end-use thickness of the material is greater than 12.7 mm.

A material is predicted to pass FMVSS No. 302 if at least one of the two criteria (MCC parameter-based and the physics-based) presented above is met. Table 34 shows which of the materials tested in the MCC as part of this study predicted to pass FMVSS No. 302. This table does not only present the results of the evaluation based on T_{ig} , but also presents results based on another temperature, T_1 . T_1 corresponds to a cumulative specific heat release equal to 5 percent of the total (= area under the $Q(t)$ curve, which is equal to h_c). This temperature is used by the FAA as a surrogate for the ignition temperature in a recently-developed MCC-based methodology (Safironava et al. 2019) to determine whether small changes to aircraft cabin materials (e.g. because an original component is no longer available) can have a sufficient impact on the material's fire performance so that (expensive) re-qualification will be needed. The assessment is based on the fire growth capacity (FGC) in $\text{J/g}\cdot\text{K}$, which is calculated as follows:

$$\text{FGC} = \left(\frac{h_c}{T_2 - T_1} \right) \left(\frac{T_2 - T_0}{T_1 - T_0} \right) \quad [13]$$

Where T_2 is referred to as the burnout temperature (i.e., the temperature at which the cumulative specific heat release reaches 95% of h_c) and T_0 is the reference temperature (25 °C). T_2 and the FGC are also given in Table 34. Unfortunately, the FGC does not correlate well with the FMVSS No. 302 burn rate (see Figure 56). However, regardless of whether T_{ig} or T_1 are used, the predicted FMVSS No. 302 performance is nearly always the same. The 12.7 mm simulated mattress foam is the only exception. The physics-based parameter predicts a failure based on T_{ig} for this material but predicts a pass when the slightly higher T_1 is used. This is consistent with the fact that this material was a borderline pass.

All methods predict that the Chicco and Peg Perego child restraint padding materials will fail FMVSS No. 302, while they actually passed. However, Table C-7 in Appendix C shows that these materials passed because the flame spread at a rate higher than 102 mm/min, but extinguished within 60 s and did not propagate more than 51 mm (2 in.) beyond the first mark, which is one of the ways to pass the FMVSS No. 302 test.

Table 34: Expected/Predicted FMVSS No. 302 Performance for the Materials Tested in the MCC³

Material		Burn Rate (mm/min)	δ (mm)	ρ (kg/m ³)	η_c (J/g·K)	h_c (kJ/g)	T_{ig} (°C)	T_1 (°C)	T_2 (°C)	FGC (J/g·K)	FMVSS 302 P/F Predictions			
											η_c & T_{ig}	η_c & T_1	$\rho\delta\Delta T_{ig}$	$\rho\delta\Delta T_1$
School Bus Seats	Blue Bird Seat Cover	0	0.80	1055	169	8.3	228	237	327	131	PASS	PASS	176	183
	Blue Bird Padding	30	46.2	56	371	18.6	365	384	452	325	PASS	PASS	245	259
	Starcraft Seat Cover	42	0.80	945	125	9.9	225	238	341	142	PASS	PASS	155	165
	Starcraft Padding	22	42.0	95	357	16.5	364	379	448	285	PASS	PASS	415	433
	Trans Tech Seat Cover	45	0.80	1050	129	9.5	235	245	341	143	PASS	PASS	181	189
	Trans Tech Padding	0	25.4	24	350	15.1	365	382	445	281	PASS	PASS	105	110
Motorcoach Materials	Green Cover Padding	23	53.0	45	538	18.5	294	310	386	309	PASS	PASS	157	166
	Green Seat Cover	38	3.60	149	260	14.9	374	394	468	242	PASS	PASS	190	201
	Blue Seat Backing	0	3.70	247	93	8.7	292	306	439	96	PASS	PASS	249	261
	Blue Seat Cover	0	3.20	230	125	12.9	276	291	467	122	PASS	PASS	188	199
	Grey Seat Backing	45	5.20	163	936	34.6	427	447	506	669	PASS	PASS	345	362
	Luggage Rack Door	19	24.1	258	379	28.3	356	387	477	393	PASS	PASS	1100	1201
	Floor Covering	0	2.37	1073	101	7.2	237	246	336	113	PASS	PASS	551	574
	Headliner	0	4.23	215	107	4.0	475	480	560	59	PASS	PASS	414	418
	Blue Cover Padding ¹	94	101.6	73	435	23.3	210	245	435	229	FAIL	FAIL	176	209
	Blue Cover Padding ¹	94	101.6	73	448	23.6	205	237	434	231	FAIL	FAIL	172	201
	Blue Cover Padding ²	94	101.6	73	421	23.9	216	252	434	236	FAIL	FAIL	182	215
Blue Cover Padding ²	94	101.6	73	427	24.0	214	247	435	236	FAIL	FAIL	180	210	
Motor Vehicle Interior	Ford F250 Carpet	20	15.3	124	909	40.2	406	434	500	707	PASS	PASS	606	650
	Mercedes Carpet	15	15.0	343	220	20.4	264	302	496	179	PASS	PASS	1063	1229
	Ford F250 Dashboard	19	3.36	1000	1112	38.0	427	450	507	756	PASS	PASS	1368	1445
	Mercedes Dashboard	38	25.3	241	322	25.0	311	341	453	302	PASS	PASS	892	984
	Camaro Headliner	22	6.65	126	198	22.7	229	268	489	196	PASS	PASS	176	208
	Ford Headliner	0	16.7	65	138	17.5	232	265	523	141	PASS	PASS	175	203
	Camaro Seat Cover	78	3.74	165	325	18.1	369	388	471	268	PASS	PASS	216	227
	Mercedes Seat Cover	44	4.41	265	269	13.3	244	259	328	250	PASS	PASS	262	280
	Camaro Padding	0	16.8	36	496	21.5	352	377	440	402	PASS	PASS	152	163
	Mercedes Padding	0	19.0	50	525	23.4	301	324	431	297	PASS	PASS	180	195

Table 34: Expected FMVSS No. 302 Performance for the Materials Tested in the MCC (Continued)

Material		Burn Rate (mm/min)	δ (mm)	ρ (kg/m ³)	η_c (J/g·K)	h_c (kJ/g)	T_{ig} (°C)	T_1 (°C)	T_2 (°C)	FGC (J/g·K)	FMVSS 302 P/F Predictions			
											η_c & T_{ig}	η_c & T_1	$\rho\delta T_{ig}$	$\rho\delta T_1$
Surface Layer	Ford F250 Carpet		15.3	124	949	41.2	398	424	494	692	PASS	PASS	595	636
	Mercedes Carpet		15.0	343	611	29.3	380	392	474	437	PASS	PASS	1568	1620
	Mercedes Dashboard		25.3	241	294	27.2	281	301	437	298	PASS	PASS	799	860
	Camaro Headliner		6.70	126	230	18.6	229	259	457	174	PASS	PASS	176	202
	Ford Headliner		16.7	65	281	18.6	229	262	463	171	PASS	PASS	173	200
	Camaro Seat Cover		3.70	165	385	16.7	381	399	465	298	PASS	PASS	220	231
Thin Materials	Acrylate	42	1.59	1040	404	25.8	316	342	417	426	PASS	PASS	489	532
	Corrugated Cardboard	61	3.18	155	140	9.5	292	292	405	119	PASS	PASS	134	134
	Thick HDPE	36	1.59	950	1156	43.4	440	468	517	983	PASS	PASS	634	677
	Thin HDPE	68	0.79	950	1156	43.4	440	468	517	983	PASS	PASS	317	338
	Folder Cardboard	121	0.29	680	215	10.7	306	314	387	183	FAIL	FAIL	56	58
Water Mist	SF Test Foam	142	6.35	29	640	27.4	216	246	408	293	FAIL	FAIL	36	42
	SF Test Foam	101	12.7	29	640	27.4	216	246	408	293	FAIL	FAIL	72	83
	SM Test Foam	117	6.35	33	544	26.7	216	237	410	281	FAIL	FAIL	41	45
	SM Test Foam	82	12.7	33	544	26.7	216	237	410	281	FAIL	FAIL	82	91
Cryomilled Specimens	Blue Bird Seat Cover		0.80	1055	134	14.6	192	207	482	133	PASS	PASS	145	158
	Blue Bird Padding		46.2	56	538	29.1	217	245	423	296	FAIL	FAIL	140	160
	Blue Bird Padding BS		46.2	56	400	25.4	219	245	442	244	FAIL	FAIL	142	160
	Starcraft Padding		42.0	95	383	26.3	218	246	452	247	FAIL	FAIL	239	273
	Trans Tech Padding		25.4	24	187	29.0	227	245	434	285	PASS	PASS	63	69
	Luggage Rack Door		24.1	258	623	37.7	370	400	482	561	PASS	PASS	1146	1244
	Headliner		4.23	215	123	14.0	262	284	462	133	PASS	PASS	220	240
	Mercedes Carpet		15.0	343	132	13.8	296	309	500	121	PASS	PASS	1203	1259
	Ford Headliner		16.7	65	149	21.5	233	260	497	182	PASS	PASS	176	199
	Camaro Padding		16.8	36	498	28.0	229	259	441	274	FAIL	FAIL	96	109
Acrylate		1.59	1040	24	27.0	276	291	411	327	PASS	PASS	423	448	

Table 34: Expected FMVSS No. 302 Performance for the Materials that Tested in the MCC (Continued)

Material	Burn Rate (mm/min)	δ (mm)	ρ (kg/m ³)	η_c (J/g·K)	h_c (kJ/g)	T_{ig} (°C)	T_1 (°C)	T_2 (°C)	FGC (J/g·K)	FMVSS 302 P/F Predictions				
										η_c & T_{ig}	η_c & T_1	$\rho\delta\Delta T_{ig}$	$\rho\delta\Delta T_1$	
Childseat Materials	Britax Base		1.17	629	1236	44.4	409	432	488	901	PASS	PASS	286	303
	Chicco Base		2.90	602	1149	44.0	405	426	487	831	PASS	PASS	672	709
	Peg Perego Base		2.89	711	1186	44.5	407	432	488	904	PASS	PASS	795	846
	UPPAbaby Base		2.79	676	1271	44.5	411	431	488	889	PASS	PASS	738	776
	Britax Fabric		0.22	435	334	15.9	379	399	467	276	PASS	PASS	34	36
	Chicco Fabric		0.22	539	1246	42.8	411	437	488	944	PASS	PASS	46	49
	Peg Perego Fabric		0.51	284	328	15.9	379	398	467	274	PASS	PASS	52	55
	UPPAbaby Fabric		0.38	665	124	14.7	253	273	468	134	PASS	PASS	59	64
	Britax Padding		15.9	10	332	15.6	381	401	469	271	PASS	PASS	45	47
	Chicco Padding	0	9.66	26	327	26.1	198	220	419	265	FAIL	FAIL	46	51
	Peg Perego Padding	0	11.3	30	513	25.4	212	232	408	267	FAIL	FAIL	66	73
	UPPAbaby Padding	121	10.7	24	571	27.7	220	245	410	294	FAIL	FAIL	52	58
	Britax Assembly		16.1	16	346	16.1	385	404	469	291	PASS	PASS	72	76
	Chicco Assembly		9.88	38	268	33.1	212	245	479	291	PASS	PASS	72	84
	Peg Perego Assembly		11.8	41	222	19.7	225	249	455	183	PASS	PASS	100	112
	UPPAbaby Assembly		11.1	46	269	17.8	229	247	428	179	PASS	PASS	107	116

Notes: ¹ Samples taken from various locations inside the padding

² Samples taken at various locations on the surface

³A material is predicted to pass FMVSS No. 302 if at least the MCC parameter-based criteria (η_c , T_{ig}) or the physic-based criterion ($\rho\delta\Delta T_{ig}$) are met. All automotive materials tested using the FMVSS No. 302 test method met the FMVSS No. 302 performance criteria.

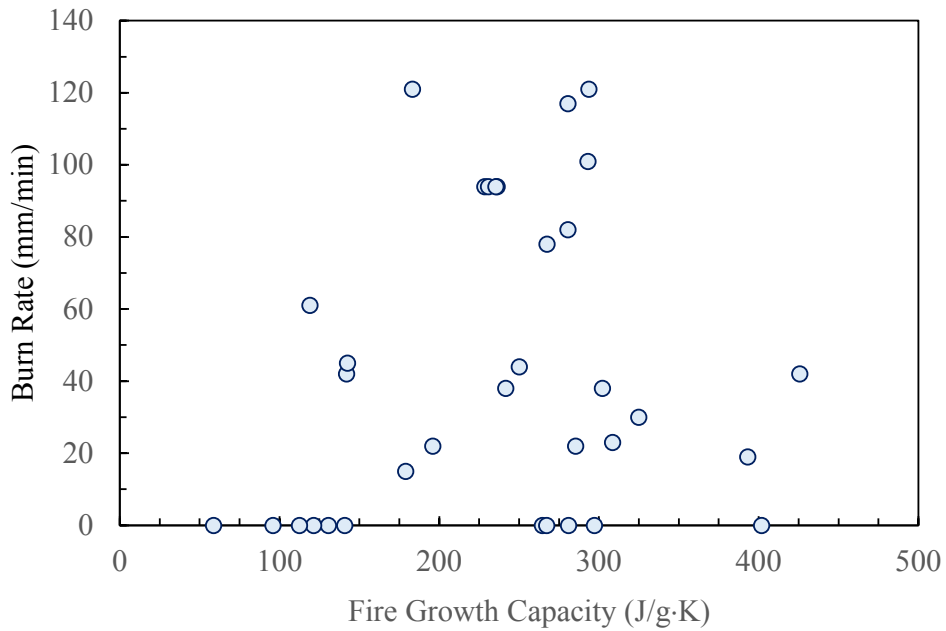


Figure 56. Correlation (or lack thereof) between FMVSS No. 302 burn rate and FGC

The following linear relationship between T_1 and T_{ig} (see Figure 57) could be used to estimate T_{ig} from T_1 , which would address the challenges in determining T_{ig} for materials with a $Q(T)$ curve that has multiple peaks.

$$T_1 = 0.979 T_{ig} + 28.8 \quad \text{or} \quad T_{ig} = 1.021 T_1 - 29.4 \quad [14]$$

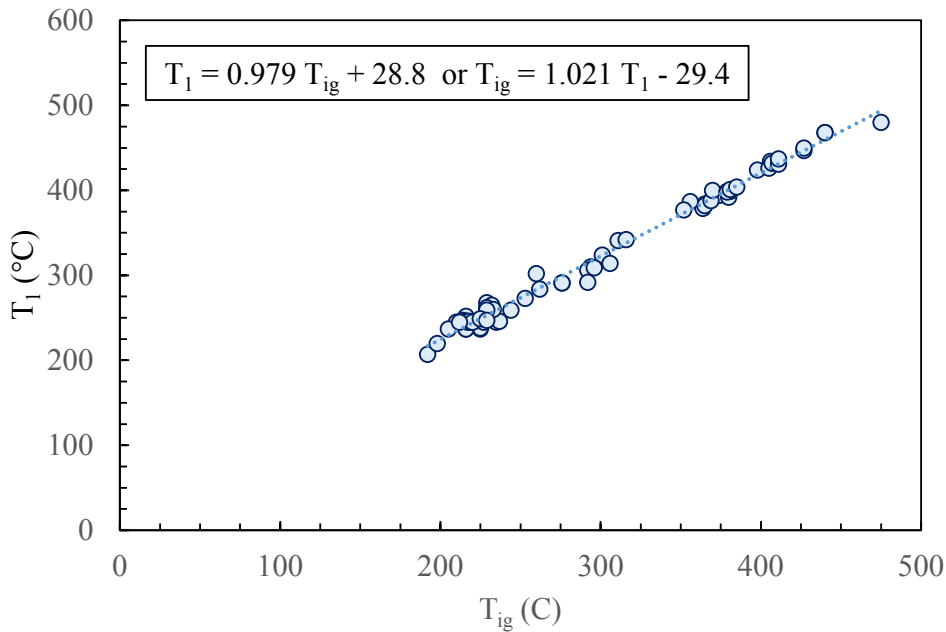


Figure 57. Relationship between T_1 and T_{ig}

Because the process to determine T_{ig} from the kinetic reaction parameters is rather complicated and T_1 easily can be calculated from the MCC data, it is recommended that Equation 14 be used to estimate T_{ig} . Alternatively, T_1 could be used directly in the MCC-based FMVSS No. 302 pass/fail criteria instead of T_{ig} , which has the advantage of eliminating the effect of minor thermal degradation reactions at low temperatures that generate pyrolyzates at an insufficient rate to sustain flaming.

Improving Repeatability for Layered Materials

Although the repeatability of the MCC data is generally very good, there is significant variability between replicate tests for some layered products. This was assumed to be the result of variations in the composition of the MCC specimens. Three types of tests were conducted to explore this further and possibly develop an improved specimen preparation method.

1. For some materials the flame appeared to propagate at a faster rate in the FMVSS No. 302 over the top surface than over the bottom surface of the specimen. Specimens of four materials were tested with the front and backside exposed to the flame. The results are provided in Table 35. Overall, the burn rate appears to be slightly lower when the backside is exposed to the flame but the differences are not significant.

Table 35: Effect of Tested Surface on FMVSS No. 302 Performance

Material Description	Burn Rate (mm/min)	
	Front Side	Back Side
Carpet Ford F250	20	18
Dashboard Ford F250	19	15
Headliner Camaro	22	21
Seat Cover Camaro	78	72

2. MCC tests were conducted on the surface layer of six motor vehicle interior materials. Results are compared to the corresponding data for the complete product in Table 36. The results are very close for four of the six materials. However, there are significant differences in η_c and T_{ig} for the remaining two materials. For this reason, testing the surface layer instead of the complete product does not appear to be an acceptable approach to improve repeatability.

Table 36: Comparison of MCC Data for the Surface Layer Versus the Full Product

Material	Complete Product			Surface Layer		
	η_c (J/g·K)	h_c (kJ/g)	T_{ig} (°C)	η_c (J/g·K)	h_c (kJ/g)	T_{ig} (°C)
Ford F250 Carpet	909	40.2	406	949	41.2	398
Mercedes Carpet	220	20.4	264	611	29.3	380
Mercedes Dashboard	322	25.0	427	294	27.2	281
Camaro Headliner	198	22.7	229	230	18.6	229
Ford Headliner	138	17.5	232	281	18.6	229
Camaro Seat Cover	325	18.1	369	385	16.7	381

3. The third series involved MCC testing of cryo-milled specimens with a particle size between 50 and 300 μm . Cryo-milling is a commonly used method to obtain more representative samples for thermo-gravimetric characterization of refuse derived fuel (Robinson et al., 2016; Bosmans et al., 2014), which has similar challenges, i.e., creating mg-size specimens that are representative of a mixture of fuels with unknown composition.

A comparison of selected MCC data for cryo-milled versus knife-milled specimens can be found in Table 37. Nearly all cryo-milled specimens have a significantly higher h_c , and some have a significantly higher η_c and lower T_{ig} compared to the knife-milled specimens. Cryo-milling was not further considered because it changes the physical structure and adversely affect the fire performance of most materials, which is consistent with findings reported in the literature (Hedman et al.2018).

Table 37: Comparison of MCC Data for Knife-Milled Versus Cryo-Milled Specimens

Material	Knife-Milled Samples			Cryo-Milled Samples		
	η_c (J/g·K)	h_c (kJ/g)	T_{ig} (°C)	η_c (J/g·K)	h_c (kJ/g)	T_{ig} (°C)
Blue Bird Seat Cover	169	8.26	228	134	14.6	192
Blue Bird Padding	371	18.6	365	538	29.1	217
Blue Bird Padding BS				400	25.4	219
Starcraft Padding	357	16.5	364	383	26.3	218
Trans Tech Padding	350	15.1	365	403	29.0	227
Luggage Rack Door	379	28.3	356	623	37.7	370
Headliner	107	4.01	475	123	14.0	262
Mercedes Carpet	220	20.4	264	132	13.8	296
Ford Headliner	138	17.5	232	149	21.5	233
Camaro Padding	496	21.5	352	498	28.0	229
Acrylate	404	25.8	316	420	27.0	276

Conclusions

The following subsections provide summary conclusions related to this research.

Vehicle Fire Field Data

Vehicle fires in the United States were investigated using the National Fire Incident Reporting System, Version 5, NASS, GES, FARS, and NASS CDS datasets from 1991 to 2015. The investigation provided information on the frequency and characteristics of vehicle fires, including the cause, origins, and propagation paths of passenger compartment fires.

Bench-Scale Testing

Testing of interior automotive materials from passenger vehicles, a motorcoach, school buses, as well as several common materials was conducted per the 4 selected test methods for evaluation. These data are summarized in Appendix C – F and will be a resource for future researchers.

School Bus and Motorcoach Seat Testing per ASTM E2574

School bus seats are generally designed to meet the test specifications in ASTM E2574. Therefore, in general, the school bus seats performed better in this testing than the motorcoach seats.

Child Restraint System Research

Testing of child restraint systems yielded interesting results in terms of ignitability and heat release rates for several different types and models.

There is variability in the ignition of these child restraints with a small gas flame. Three child restraints tested sustained ignition from Ignition Sources 1, 2 and 3 (small, medium, large gas flame). A fourth child restraint tested ignited with Ignition Source 2 but not with Ignition Source 1. Chemical composition evaluation confirmed that all four child restraints had flame retardant chemicals.

Once sustained ignition is observed, a relatively consistent fire growth is seen between seats and a similar peak heat release rate and total heat released are measured. This is more easily comparable between the UPPA Baby, Peg Perego, and Chicco seats since they are the same style of seat.

It is also observed that the infant seat bases are more ignition resistant and they also release less heat release once ignited. Based on the results of the UPPA Baby and Chicco seats, it can be seen that the majority of the heat release is coming from the seat as opposed to the base. This could be a result more FR treatment in the base as compared to the seat, or a natural difference between more rigid plastics and foam plastics (or some combination of both). In terms of smoke production, the seats alone make up a larger fraction of the total smoke, as compared to the bases. In general, the smoke production numbers were similar for all the child restraints evaluated.

Chemical Composition Testing

All the materials that were tested in the bench-scale methods were also tested to determine if they were treated with flame retardants. Based on this testing and analysis, 23 out of the 32 materials tested can be confirmed to contain FR treatment. Five materials can be confirmed to not contain any FR treatment and 4 materials remain uncertain.

Alternative Methodology Development

An analysis of the data obtained from bench-scale testing resulted in the selection of the MCC as possibly the most suitable method to achieve the purposes of FMVSS No. 302 of those evaluated. Two sets of criteria were developed to determine, based on MCC test data and the thickness and density of the material, whether a material is predicted to “pass” the FMVSS No. 302 test. A material is predicted to pass the FMVSS No. 302 test if one of the two criteria are met. One of the test parameters that is used in this determination (surface temperature at ignition) is obtained from a relatively complicated analysis of the MCC data. An alternative parameter that can be directly obtained from MCC data is discussed, one that makes the method more user-friendly with little loss in its predictive capability of FMVSS No. 302 performance.

Smoke Toxicity Testing

In addition to evaluating flammability of automotive materials, NHTSA was interested in evaluating the quantity and toxicity of the smoke produced from burning automotive materials. The objective of the smoke toxicity testing was to explore the development or implementation of a repeatable and reproducible test procedure to evaluate smoke toxicity of materials.

Because the MCC was being evaluated, it was decided to pursue using the MCC for smoke toxicity measurements as well. This has been previously explored by the developers of the MCC at the FAA. The same basic approach was taken for this research project. This methodology includes performing several tests, which are conducted across a range of ventilation conditions to assess the generation of toxic compounds in various stages of a real fire.

Three materials from the motorcoach were tested and mass yields of CO and HCN were obtained for each material across a range of ventilation conditions. Although the results in terms of yields of CO and HCN as a function of equivalence ratio are inconsistent with data in the literature, the work conducted in this project indicate that it is possible to modify the MCC and make these types of measurements for vehicle materials. Possible reasons for the inconsistencies have been suggested and provide some ideas for improving the method and addressing the discrepancies.

References

- 14 CFR § 25.853 - Compartment interiors.
- 49 CFR § 238.103 - Fire safety, and associated appendices.
- 49 CFR § 571.302 - Standard No. 302; Flammability of interior materials.
- Ahrens, M. (2020, March). *Vehicle fires*. National Fire Protection Association. www.nfpa.org/-/media/Files/News-and-Research/Fire-statistics-and-reports/US-Fire-Problem/osvehiclefires.pdf
- ASTM International. (2020). D5132-20 Standard test method for horizontal burning rate of polymeric materials used in occupant compartments of motor vehicles. <https://doi.org/10.1520/D5132-20>
- Battipaglia, K. C., Griffith, A. L., Huczek, J. P., Janssens, M. L., Miler, M. A., & Willson, K. R. (2003, October). *Comparison of fire properties of automotive materials and evaluation of performance levels*. National Highway Traffic Safety Administration. Available at https://ntlrepository.blob.core.windows.net/lib/24000/24800/24894/r5804_final.pdf
- Bosmans, A., De Dobbelaere, C., & Helsen, L. (2014, March). Pyrolysis characteristics of excavated waste material processed into refuse derived fuel. *Fuel*, 122: 198-205. DOI: 10.1016/j.fuel.2014.01.019
- Bruns, M. C., & Leventon, I. T. (2020, May 22). Automated fitting of thermogravimetric analysis data. *Fire and Materials*. <https://doi.org/10.1002/fam.2849>
- Carpenter, K., Janssens, M., & Saucedo, A. (2006, April 3-6). *Using the cone calorimeter to predict FMVSS 302 performance of interior and exterior automotive materials*. 2006 SAE World Congress, Fire Safety Session, Detroit, MI.
- Fong, A., Allen, J., & Schneider, Y. (2017). *Determination of flame-retardant materials in plastics using a combination of analytical techniques*. EAG Laboratories.
- Hasemi, Y. (2016). Surface flame spread. in M. J. Hurley, D. T. Gottuk, J. R. Hall Jr., K. Harada, E. D. Kuligowski, M. Puchovsky, J. L. Torero, J. M. Watts Jr., & C. J. Wiecek (eds.), *SFPE handbook of fire protection engineering*, 5th edition, Springer, Chapter 23, pp. 705-723.
- Hedman, T. D., Demko, A. R., & Kalman, J. (2018). Enhanced ignition of milled boron-polytetrafluoroethylene mixtures. *Combustion and Flame*, 198, 112-119.
- Huczek, J. P., & Blais, M. S. (2015, November). *Motorcoach fire safety*. (Report No. DOT HS 812 213). National Highway Traffic Safety Administration. Available at www.nhtsa.gov/Research/Crashworthiness
- International Standardization Organization. (1989). ISO 3795:1989 Road vehicles, and tractors and machinery for agriculture and forestry — Determination of burning behaviour of interior materials.
- ISO. (2015, March). ISO Standard 5660-1:2015, Reaction-to-fire tests — Heat release, smoke production and mass loss rate — Part 1: Heat release rate (cone calorimeter method) and smoke production rate (dynamic measurement).

- Janssens, M., (1991). Measuring Rate of Heat Release by Oxygen Consumption. *Fire Technology*, 27, pp. 234-249.
- Janssens, M. L., (2008, March). *Development of a database of full-scale calorimeter tests of motor vehicle burns*. Motor Vehicle Fire Research Institute.
- Johnsson, E., Yang, & J. (2007). Motorcoach flammability final report, tire fires - Passenger compartment penetration, tenability, mitigation, and material performance (NIST Technical Note 1705). National Institute of Standards and Technology. www.regulations.gov/contentStreamer?documentId=NHTSA-2007-28793-0027&attachmentNumber=1&contentType=pdf
- Lautenberger, C., & Fernandez-Pello, A. C. (2011). Optimization algorithms for material pyrolysis property estimation. *Fire Safety Science*, 10, 751-764.
- Li, K. Y., Huang, X., Fleischmann, C., Rein, G., & Ji, J. (2014). Pyrolysis of medium-density fiberboard: optimized search for kinetics scheme and parameters via a genetic algorithm driven by Kissinger's method. *Energy & fuels*, 28(9), 6130-6139.
- Lyon, R., & Safronava, N. (2013). Comparison of direct methods to determine-the order kinetic parameters of solid thermal decomposition for use in fire models," *Journal of Thermal Analysis and Calorimetry*, 114, 213-227.
- Lyon, R., & Safronava, N. (2017, February 6-8). *Determining ignition temperature using dynamic thermal analysis*. Fire and Materials 15th International Conference, San Francisco, CA, pp. 827-839.
- Lyon, R., & Walters, R. (2006, April 3-6). *Flammability of automotive plastics* (SAE Technical Paper 2006-01-1010). SAE International World Congress 2006, Detroit, MI. <https://doi.org/10.4271/2006-01-1010>.
- Lyon, R., Walters, R., Safronava, N., & Stoliarov, S. (2009, January 26-28). *A statistical model for the results of flammability tests*. Fire and Materials 11th International Conference, San Francisco, CA, pp. 141-159.
- Matala, A., Lautenberger, C., & Hostikka, S. (2012). Generalized direct method for pyrolysis kinetic parameter estimation and comparison to existing methods. *Journal of Fire Sciences*, 30(4), 339-356.
- Miller, M., Janssens, M., & Huczek, J. (2003). *Development of a new procedure to assess the fire hazard of materials used in motor vehicles*. National Highway Traffic Safety Administration.
- National Transportation Safety Board. (2015a, August 4). Safety Recommendation (in re H-07-005 to H-07-008). www.nts.gov/safety/safety-recs/recletters/H07-4-8.pdf
- NTSB. (2015b, August 4). Safety Recommendation (in re H-15-12). www.nts.gov/safety/safety-recs/recletters/H-15-012-013.pdf
- Pau, D. S., Fleischmann, C. M., Spearpoint, M. J., & Li, K. Y. (2013). Determination of kinetic properties of polyurethane foam decomposition for pyrolysis modelling. *Journal of Fire Sciences*, 31(4), 356-384.

- Robinson, T., Bronson, B., Gogolek, P., & Mehrani, P. (2016). Sample preparation for thermo-gravimetric determination and thermo-gravimetric characterization of refuse derived fuel. *Waste Management*, 48, 265-274.
- SAE International. (2019). *Flammability of polymeric interior materials - Horizontal test method J369_201908*. https://doi.org/10.4271/J369_201908
- Safronava, N., Lyon, R., & Walters, R. (2019, May 20-22). *Small-scale test and criterion for flammability of aircraft cabin materials*. 30th Conference on Recent Advances in Flame Retardancy of Polymeric Materials, San Antonio, TX.
- Shimadzu News. (2005, January). *Identification of brominated flame-retardants in polymers*. www.shimadzu.com/an/sites/shimadzu.com.an/files/pim/pim_document_file/applications/application_note/12169/ftir_flame-retardants_news_01_2005_en.pdf
- Speitel, L., Walters, R., & Lyon, R. (2017, February 6-8). Polymer combustion products at constant fuel/oxygen ratios in the microscale combustion calorimeter with FTIR. 15th International Conference and Exhibition on Fire and Materials, San Francisco, CA.
- Underwriters Laboratories. (2013, March 28). UL Standard 94, Tests for Flammability of Plastic Materials for Parts in Devices and Appliances, Edition 6.
- Yuen, A. C. Y., Chen, T. B. Y., Yeoh, G. H., Yang, W., Cheung, S. C. P., Cook, M., & Yip, H. L. (2018). Establishing pyrolysis kinetics for the modelling of the flammability and burning characteristics of solid combustible materials. *Journal of Fire Sciences*, 36(6), 494-517.

Appendix A: Test Method Review Matrix

Table A-1. Summary of “Small Flame Exposure” Test Methods

	Area of Regulation	Summary of Method
FMVSS 302	U.S. DOT uses this method to regulate the flammability of materials used in the interiors of passenger vehicles.	Five specimens, measuring 4 × 14 in. × nominal thickness, in the horizontal position are exposed to a 1½-inch high Bunsen burner flame for 15 s. The rate of flame spread over measured length is observed, and the maximum permitted flame spread rate is 4 in./min.
FAR 25.853	<p>This standard is used to test the materials and components in cabins and holds of transport aircraft in the U.S.</p> <p>It is also recommended in the Federal Register Vol. 47 No. 228, for testing of rail transit upholstery seating material.</p>	<p>Depending on what type of material is being tested, the orientation of the specimen can be vertical, horizontal, at 45°, or at 60°. In each case, three specimens are tested with a Bunsen or Tirrill burner at a specified height and exposed for a specified duration. For each procedure, there are classifications based on burn length, flame spread rate, after flame time, glow time, and flame time of drippings.</p> <p>For rail transit upholstery seating materials, testing is conducted to FAR 25.853 and the flame time cannot exceed 10 s and the burn length cannot exceed 6 inches.</p>
ASTM C1166	Appendix B of Part 238 to the Code of Federal Regulations (CFR) uses this standard test to regulate the flammability performance of elastomeric gaskets and accessories in rail transportation vehicles.	Six specimens, measuring 1 × 18 × ½-in. thick, are exposed to a 38-mm high Bunsen burner flame for 15 or 5 min for dense or cellular materials, respectively. The samples are tested in the vertical position, and the remaining unburned length of the specimen is measured. The average flame propagation for the six runs is reported.
UL 94	This test standard contains several test procedures in different orientations and with slightly different exposures. The UL listing of a given electrical appliance is generally contingent on the classifications of plastics tested in these procedures.	<p>Depending on the type of classification required, materials are tested to UL 94HB, 94V-0, 94V-1, 94V-2, 94HBF, 94HF-1, 94HF-2, 94-5V, 94VTM-0, 94VTM-1, or 94VTM-2.</p> <p>The main difference between all of these different procedures is the orientation of the test specimen. Most of these procedures test two sets of five specimens each, nominally measuring between 5 and 6 in. long and ½ - 2 in. wide with a ½-in. maximum thickness. All of these procedures expose the specimen to a Bunsen or Tirrill burner flame with a height between ¾ and 5 in. long and a duration between 3 and 60 s, depending on the material tested. Each procedure classifies the material by several factors, including average burning rate, self-extinguishment, after flame time, burning droplets, glow or incandescence time, and/or burn-through.</p>

Table A-1. Summary of “Small Flame Exposure” Test Methods (Continued)

	Area of Regulation	Summary of Method
ASTM D2859	This test standard applies to floor coverings installed in buildings.	Eight specimens, each measuring 9 × 9 in., are exposed to the burning of a methenamine tablet, lit with a match. The material passes the test if the charred area is less than or equal to 1 in. from the inner edge of the 8-in. diameter steel plate lying on top of the floor covering sample.
ASTM D635	Building codes use this test to classify the burning behavior of rigid plastics in the horizontal position.	Ten specimens, each 5 × ½-in. × usual thickness, in the horizontal position, are exposed to a 1-in. long Bunsen burner flame for 30 s. The building codes classify a plastic as CC2 if its maximum burning rate is ¼ in./min for a thickness greater than 0.05 in.
ASTM D568	Building codes use this test to classify the burning behavior of rigid plastics in the vertical position.	Ten specimens, each 1 × 18 in., in the vertical position, are exposed to a 1-in. long Bunsen burner flame until the specimen ignites or a maximum of 15 s. Test specimens less than 0.05 inch thick are required to be tested to this procedure, and a passing result is a specimen that is not completely consumed within 2 min.
ASTM D2863	The U.S. Navy uses this test procedure to qualify (in part) composite materials and composite material systems for use in Naval submarines. The National Aeronautics and Space Administration (NASA) also uses this test procedure	15 to 30 specimens are tested for each material qualified in order to systematically bracket the minimum oxygen concentration necessary for combustion. Combustion is defined, for self-supporting polymers, when either the specimen has burned for 3 min or when flames have spread 2 in. below the top of the specimen. For the Navy specification, tests are conducted at 25, 75, and 300°C, and the minimum requirement for qualification is 35, 30, and 21 percent, respectively.
GM 269M	General Motors has proposed using this method to evaluate flammability of engine compartment sound absorbing materials.	A 12 × 4-in. sample with a thickness between 1/16 and 5/16 inch is placed in a frame and mounted at a 45° angle. The whole system is placed on a load cell in an enclosed test chamber. Two infrared heaters, placed parallel to each 4-in. wide side of the test sample are used to preheat both surfaces. After the desired surface temperature is reached, the sample is exposed to a 4-inch high Meeker burner flame for 15 s. If the sample ignites, it is allowed to burn for 5 min or until self-extinguishment. If it does not ignite or self-extinguishes within 10 s of removal of the burner, the ignition procedure is repeated 8 times. Mass loss of the sample is recorded as well as mass of dripping with a second load cell. Other qualitative data and observations are also derived. To date, there is no consensus for pass/fail criteria.

Table A-1. Summary of “Small Flame Exposure” Test Methods (Continued)

	Area of Regulation	Summary of Method
ASTM D5132	Not officially used for regulation of automotive industry, however, technically equivalent to FMVSS 302	ASTM equivalent to FMVSS 302. This method was created, in part, to improve repeatability of the test method.
SAE J 369	Not officially used for regulation of automotive industry, however, technically equivalent to FMVSS 302	SAE equivalent to FMVSS 302.
ISO 3795	Technically equivalent to FMVSS 302 for International community	ISO equivalent to FMVSS 302.
ECE R118	Economic Commission for Europe regulation for flammability requirements of certain categories of motor vehicles	Annex 6 is technically equivalent to FMVSS 302. Annex 7 describes a test to determine the melting behavior of materials. Annex 8 considers a vertical burning test, similar to the method below as well as other vertical small-flame test methods.
14 CFR 25, Appendix F, Part I	Used in FAA regulations for Interior compartments occupied by crew or passengers	Similar to the vertical tests in UL 94 and other vertical small-flame test methods, including Annex 8 of ECE R118

Table A-2. Summary of “Radiant Exposure” Test Methods

	Area of Regulation	Summary of Method
ASTM E906	The FAA uses this standard (FAR 25-61) to qualify interior materials in aircraft.	Three specimens, each measuring 4 × 4 in. nominally, with a maximum thickness of 2 inches are exposed vertically to a radiant ignition source (35 kW/m ²) for 5 min. The heat release rate is measured by a series of temperature measurements, <i>i.e.</i> , a thermopile. According to FAA regulations, materials tested must not have a peak heat release rate of ≥ 65 kW/m ² nor a total heat release of ≥ 65 kW • min/m ² .
ASTM E662 With or Without Toxicity Measurements	The FAA, the Federal Railroad Administration (FRA), and the U. S. Navy use this test method to regulate interior finish materials.	<p><i>FAA</i>: Three vertically oriented specimens are exposed to 25 kW/m² in the presence of a series of 6 multi-flamelet burners. Two burners impinge directly on the sample, and the other four are positioned vertically in the gas stream. Depending on the type of material being tested, there are different requirements for passing the test. In general, the specific optical density of a tested material must be ≤ 100 in the first 90 s of the test and ≤ 200 in the first 4 min. All materials used in the pressurized area of the fuselage must be tested for toxicity. The products of combustion are sampled for concentrations of CO, HCl, HCN, HF, NO_x and SO₂. The FAA has concentration requirements for each compound at 90 s and 4 min.</p> <p><i>FRA</i>: Three specimens are exposed to 25 kW/m² with and without the presence of a series of 6 multi-flamelet burners. Two burners impinge directly on the sample, and the other four are positioned vertically in the gas stream. In general, the specific optical density of a tested material must be ≤ 100 in the first 90 s of the test and ≤ 200 in the first 4 min.</p> <p><i>Navy</i>: Three specimens are exposed to 25 kW/m² with and without the presence of a series of six multi-flamelet burners. Two burners impinge directly on the sample, and the other four are positioned vertically in the gas stream. The maximum optical density must be observed ≤ 200 s into testing.</p>
ASTM E1995	The International Maritime Organization (IMO) uses this test method to regulate interior finish materials.	<i>IMO</i> : Three horizontally oriented specimens are exposed to 25 kW/m ² with and without the presence of a single pilot flame and three specimens are exposed to 50 kW/m ² without the presence of a single pilot flame. In general, the specific optical density of a tested material must be ≤ 200. In addition, the products of combustion are sampled for concentrations of CO, HBr, HCl, HCN, HF, NO _x and SO ₂ . The IMO has maximum concentration requirements for each compound.

Table A-2. Summary of “Radiant Exposure” Test Methods (Continued)

	Area of Regulation	Summary of Method
ASTM E648	The FRA uses this test method to qualify flooring materials on rail transit vehicles.	Three horizontally mounted specimens, each measuring 10 × 41 in. nominally, are exposed to a radiant ignition source ranging from 1 to 10 kW/m ² . A propane pilot is applied perpendicular to the long edge of the sample and ignition and/or flame spread is observed. After a series of tests, the critical heat flux for ignition can be determined. The FRA requires a critical radiant flux of ≥ 5 kW/m ² .
ASTM E162	The FRA uses this test method to qualify most of the component materials installed on rail transit vehicles. The U.S. Navy also uses this standard to approve interior composite material systems for submarine applications.	Four specimens, each measuring 6 × 18 in. nominally, are mounted vertically at 30° to the radiant panel (operating temperature – 670°C). A gas pilot burner is placed at 15 to 20° to the specimen and is applied from a distance of approximately 1¼ inches to the upper edge. The test is run until flame has spread 15 inches down the specimen or a maximum of 15 min has elapsed. A flame spread index (I _s) is calculated from measured flame spread and a heat evolution term, which relates the difference between the time temperature curve of the tested sample to that of a standard reference material. <i>FRA</i> : Depending on the type of material, there are different requirements for I _s . For windows and light diffusers, I _s ≤ 100. For thermal and acoustic insulation, I _s ≤ 25. For most of the other interior materials in a transit vehicle, the maximum I _s allowed is 35. <i>Navy</i> : For interior materials installed in a naval submarine, the maximum allowable value for I _s is 20.
ASTM D3675	This test method is a variant of the ASTM E162. However, it targets the cushioning of seating materials specifically. The FRA uses this test to qualify the cushion of the seating material in transit vehicles.	The test procedure is functionally identical to the ASTM E162, outlined above, with two exceptions: (1) the test specimens are retained in the holder with a sheet of 20-gauge hexagonal steel wire mesh placed against the surface of the test face, (2) the exposure time is equal to the time it takes to spread the full length of the specimen (18 inches) or 15 min, whichever comes first. According to FRA regulations, I _s ≤ 25.

Table A-2. Summary of “Radiant Exposure” Test Methods (Continued)

	Area of Regulation	Summary of Method
ASTM E1317	<p>The IMO uses this test method to qualify interior finishes for use on bulkheads, ceilings, and decks. The test method and acceptance criteria are described in IMO Resolution A.653. IMO Resolution A.687(17) is nearly identical, but only applies to primary deck coverings, and, as such, requires steel as a substrate for the material tested.</p> <p>This same apparatus is used in ASTM E1317.</p>	<p>Three specimens, each measuring 6 × 31½ in., are mounted vertically in a frame and subjected to a radiant ignition source, which is positioned at a 15° angle to the specimen. Specimens of normal thickness < 2 inches are tested at their full thickness adhered to a representative substrate. Specimens of normal thickness > 2 inches are tested with extra material cut away, such that the thickness of the sample tested is 2 inches. An acetylene-air pilot flame is positioned adjacent to the sample, and the length is adjusted to approximately 9 in. The time to ignition is observed, and flame spread is recorded manually by the operator in 2-inch increments. The duration of the test is 10 min if the sample ignites, or until all flaming has ceased, or if flame spreads across the entire length of the specimen.</p> <p>Four key parameters are measured or derived from this testing: the critical flux at extinguishment, the heat for sustained burning, the total heat release, and the peak heat release rate. The IMO has different acceptance criteria for each of these parameters depending on if the tested material is a floor covering or if it is a wall, ceiling, or bulkhead covering.</p>
ASTM E2058	<p>Not currently used in any regulatory manner. However, Factory Mutual (FM) has proposed using this apparatus as a way to quantify the relative material flammability of automotive components. This work is published and available on the NHTSA public docket #3588.</p>	<p>This test method has three separate procedures involving material flammability: an ignition procedure, a combustion test procedure, and a fire propagation procedure. For each procedure, at least 3 specimens, each measuring 4 × 4 in., are exposed to an external heat flux of 0 to 65 kW/m² at an oxygen concentration of 21 to 40 percent by volume.</p> <p>The ignition procedure determines the time required from the application of an externally applied heat flux to a horizontal specimen until ignition of that specimen. Ignition is considered to have occurred when at least 4 s of sustained flaming is observed on or over most of the specimen surface.</p> <p>The combustion procedure is conducted to measure the chemical and convective heat release rates, the mass loss rate, and the effective heat of combustion of a horizontal specimen at a given externally applied heat flux and oxygen concentration (maximum of 40% by volume).</p> <p>The fire propagation test procedure is performed to determine the chemical heat release rate of a vertical specimen during upward fire propagation and burning.</p>

Table A-2. Summary of “Radiant Exposure” Test Methods (Continued)

	Area of Regulation	Summary of Method
ASTM E1354	<p>The IMO and the U.S. Navy use this test method or its International Organization for Standardization (ISO) equivalent (ISO 5660) to qualify material flammability of component and/or composite materials. Appendix B to Part 238 of CFR Title 49 requires testing of materials with small surface areas at 50 kW/m² and to have $t_{ig}/q_{max} \geq 1.5$.</p> <p>In addition, NIST used the cone calorimeter apparatus to test various automotive vehicle components from the interior, engine compartment, and fuel tank areas. This testing was performed as part of the GM-DOT settlement agreement.</p> <p>Similar testing was performed at SwRI for a number of interior automotive parts from a Chevrolet Cavalier. This work was also performed as part of the GM-DOT settlement agreement.</p> <p>An independent study of material flammability of automotive components was published by Dr. Marcelo Hirschler of GBH International, Inc. The main conclusion of this paper was that the flammability (ignitability and heat release rates) of plastics in automobiles is higher than that of generic plastics used in buildings.</p>	<p>This test method exposes a 4 × 4 in. specimen (horizontal or vertical) to a radiant heat flux ranging from 0 to 100 kW/m². Typically, three specimens are tested for repeatability, and the average is reported. This method yields several properties and/or parameters that are relevant to the tested material’s flammability. These include time to ignition, heat release rate (oxygen consumption calorimetry), total heat released, smoke production rate, total smoke released, mass loss rate (burning rate), effective heat of combustion, critical heat flux for ignition, thermal response parameter, and heat of gasification.</p> <p><i>IMO:</i> In the standard for qualifying marine materials for high-speed craft as fire-restricting materials, the IMO requires testing of materials used for furniture or other components, according to ISO 5660, which uses the cone calorimeter apparatus.</p> <p><i>Navy:</i> Uses this test method to qualify materials installed on naval submarines. Several criteria exist for a material’s flammability to be accepted. A series of ignitability tests are performed and, at each specified heat flux (25, 50, 75, and 100 kW/m²), the time to ignition (300, 150, 90, and 60 seconds) is given as a minimum requirement.</p> <p>In addition, maximum peak and average heat release rates are specified for a given heat flux. At 100 kW/m² irradiance, the peak heat release rate must not exceed 150 kW/m² and the average over 300 s must not exceed 120 kW/m². At 75 kW/m² irradiance, the peak heat release rate must not exceed 100 kW/m² and the average over 300 s must not exceed 100 kW/m². At 50 kW/m² irradiance, the peak heat release rate must not exceed 65 kW/m², and the average over 300 s must not exceed 50 kW/m². At 25 kW/m² irradiance, the peak heat release rate must not exceed 50 kW/m², and the average over 300 s must not exceed 50 kW/m².</p> <p>The Navy also uses the cone calorimeter apparatus to measure the concentrations of several products of combustion continuously during a test at 25 kW/m² irradiance. The maximum concentrations allowed of CO, CO₂, HCN, and HCl are 200 ppm, 4 percent by volume, 30 ppm, and 100 ppm, respectively.</p>

Table A-2. Summary of "Radiant Exposure" Test Methods (Continued)

	Area of Regulation	Summary of Method
ASTM D 7309	<p>Microscale combustion calorimeter: this is the apparatus developed at the FAA and is now standardized in ASTM.</p>	<p>This apparatus allows the measurement of very similar types of data as in the cone calorimeter, but with much smaller test specimens (1-5 mg). Typically, three specimens are tested for repeatability, and the average is reported. This method yields several properties and/or parameters that are relevant to the tested material's flammability. These include the specific heat release rate (oxygen consumption calorimetry, J/g), specific heat of combustion of specimen gases (J/g), critical heat flux for ignition, and heat release capacity (J/g-K).</p>

A-3. Summary of Advantages and Disadvantages of Test Methods

	Advantages	Disadvantages
All “Small Flame Exposure” Tests*	Inexpensive screening tool that could be used as a method to separate the average material from the subpar material in terms of flammability.	Does not reflect a “real” fire scenario. The heat exposure is too limited and can yield false positives for various materials.
ASTM E 906	Yields a material’s heat release rate from a radiant heat exposure. This method is more representative of a real fire scenario.	This method measures heat release rate by way of a thermopile. This method of measurement is obsolete. It would be more relevant if oxygen consumption calorimetry were used.
ASTM E662	Provides a standard way to measure the optical density of the smoke produced by a burning material. Can be used effectively as a ranking tool.	Data collected in this test are only relevant to this particular test method; they cannot be extrapolated to the material outside the geometry of the test method. In addition, the static state of the test method may influence the burning rate of the material, <i>i.e.</i> , the buildup of smoke in the test chamber may affect the rate at which a material burns.
ASTM E648	Provides a standard way to measure the flame spread of a burning floor covering. Can be used effectively as a ranking tool.	The data collected in this test are only relevant to this particular test method and its geometry. It does not address how a floor covering might burn and spread flame in full scale when it occurs in the same direction as surrounding air flow.
ASTM D3675	Provides a standard way to measure the flame spread of a burning seat cushion (flexible cellular material). Can be used effectively as a ranking tool.	The data collected in this test are only relevant to this particular test method and its geometry. It does not address how a seat cushion might burn and spread flame in full-scale.
ASTM E162	Provides a standard way to measure the flame spread of a burning wall or ceiling covering. Can be used effectively as a ranking tool.	The data collected in this test are only relevant to this particular test method and its geometry. It does not address how a wall or ceiling covering might burn and spread flame in full-scale.

* Although GM269M includes radiant heat exposure, the advantages and disadvantages of “small flame exposure” tests largely apply to this test also.

Table A-3. Summary of Advantages and Disadvantages of Test Methods (Continued)

	Advantages	Disadvantages
ASTM E1317	Provides a standard way to measure the flame spread of a burning wall or ceiling covering. Can be used effectively as a ranking tool.	The data collected in this test are only relevant to this particular test method and its geometry. This method measures heat release rate by way of a thermopile. This method of measurement is obsolete.
ASTM E2058	Can be operated at a wide range of heat fluxes and oxygen concentrations, which can be varied to simulate various relevant fire scenarios. This test method yields relevant engineering data such as heat release rate, mass loss rate, effective heat of combustion, etc., which can be used as input to fire models as part of a fire risk and hazard assessment.	Due to the use of high-temperature heating lamps, the specimens are required to be blackened, which can influence test results. The gas pilot flame used is not always the best method for igniting pyrolyzates. This test apparatus can require significant maintenance in the way of calibration of instrumentation and various troubleshooting that is inherent with sophisticated apparatuses.
ASTM E1354	Can be operated at a wide range of heat fluxes, which can be varied to simulate various relevant fire scenarios. This test method yields relevant engineering data such as heat release rate, mass loss rate, effective heat of combustion, etc., which can be used as input to fire models as part of a fire risk and hazard assessment.	The flow field over the sample surface complicates the analysis of ignition data. This test apparatus can require significant maintenance in the way of calibration of instrumentation and various troubleshooting that is inherent with sophisticated apparatuses.
ASTM D7309	Can be operated at a wide range of heating rates, which can be varied to simulate various relevant fire scenarios. This test method yields relevant engineering data such as specific heat release rate, specific heat of combustion of specimen gases, etc., which can be used as input to fire models as part of a fire risk and hazard assessment.	Due to the size of the test specimen (1-5 mg), post-processing and analysis of the data is required in order to relate the results to larger-scale fire tests and real fire scenarios.

Appendix B: Vehicle Fires Field Data – FRC Report

1 Executive Summary

Vehicle fires in the United States were investigated using the NFIRS-5, NASS GES, FARS, and NASS CDS datasets from 1991 to 2015.

The total number of passenger vehicle fires that occurred in the United States decreased from 2010 to 2014. The total number of all fire incidents reported in NFIRS during this period also decreased, thus the passenger vehicle fire rate, per all fire incidents, was generally stable over this period. At the same time the number and rate, per all fire incidents, of heavy-truck fires increased. The number of bus fires trended along with the decrease in all fire incidents reported in NFIRS.

In general, the rate of vehicle fires per crash decreased overall year by year. However, crash severity and other factors affect fire involvement. Frontal crashes appear to be the dominant crash mode precipitating fire occurrence. The engine compartment, fuel tank, and fuel line areas are often associated with the area of fire origin for vehicles involved in crashes while the passenger compartment is more often associated with fire initiation in non-collision events. The primary path for fire ingress into the passenger compartment is likely through the windshield though there is also evidence of fires propagating through the rear of the vehicle in instances with and without rear crash damage.

Vehicle fires are characterized in the results below by areas of origin, heat sources, items and materials burned, as well as basic crash factors. The results are disaggregated, where applicable, by general vehicle type including light duty passenger vehicles, medium/heavy trucks, and buses.

A summary of the fire involvement frequency and fire involvement rate for the top 50 passenger vehicles involved in fatal and police-reported crashes is provided. This list is cross-referenced with the list of tested vehicles that are potentially available from the NHTSA for collection of materials and summarized in Appendix A. This list is meant to assist with the selection of vehicle models to use for calorimeter testing such that a selection can be based upon either overall fire exposure or fire involvement rate.

In-depth analyses of 228 passenger vehicle fires were conducted to investigate methods of fire ingress into the occupant compartment. The results of the analysis suggest that the typical path of a fire originating in the engine compartment includes ingress into the occupant compartment via a broken windshield. The distribution and frequency of interior components that were damaged by fire indicate that the fire moves most rapidly in an upward and rearward direction. In general this includes, in order of decreasing frequency, fire damage to the top dash, sun visor, front headliner, mid dash, steering wheel, mid headliner, steering wheel air bag, and front seat backs. Summaries of 202 fire crashes from the NASS CDS are presented in Appendix B. These summaries include a link to the online case viewer, a brief police accident report narrative, a preliminary estimation of fire ingress area, and photos of the subject vehicle.

2 Data

Four different datasets were used to investigate the characteristics of vehicles fires in the United States over the previous 25 years. These are the NFIRS-5, NASS GES, FARS, and the NASS CDS. The filtering and inclusion criteria for each database were prescribed to provide equivalent datasets from which similar results could be obtained, where applicable. However, given the differences in coding methods, definitions, and sampling protocols, some variations in the output datasets were produced as described below.

2.1 Fire occurrence

Fire occurrence is coded in NASS CDS as either minor or major, depending on the extent of fire involvement. Minor fires involve *only one* major area of the vehicle such as the engine, trunk compartment, passenger compartment, undercarriage, or tires. Major fires always involve the passenger compartment and at least one other area. Incidents in which only the passenger compartment is involved, and is totally burned are also coded as Major. In the GES and FARS, fire involvement is either coded as involved or not involved based on the police accident report. In NFIRS, vehicle fires are coded as either source of ignition and burned, not source of ignition and burned, or source of ignition but did not burn. Incidents in which the vehicle was identified as the source of ignition, but did not burn were not included in the analysis. These incidents were not of interest to this work as they include, for example, vehicles causing sparks that ignited a wildfire.

2.2 Filtering Methods

All counts are based on the number of vehicles, not the number of crashes or passengers. In the results generated from the FARS data, vehicles are included whether or not its passengers were fatally injured. A summary of the filtering methods is provided in Table 1.

2.2.1 NASS

Datasets from the GES and CDS were produced using equivalent filtering methods, but different crash years due to changes in coding methods over the years. All cases (vehicles) were weighted based on the ratio inflation factor.

2.2.2 FARS

While the focus of the FARS database is on fatal crashes, not every vehicle in FARS has a fatally injured occupant. This work was focused on the characteristics of all crash-involved vehicles, whether or not their occupants were injured. The results below are based on counts of vehicles rather than crashes since more than one vehicle is often involved in a fatal crash, and, in the case of fire involvement, not all vehicles in a crash catch fire.

2.2.3 NFIRS-5

The NFIRS-5 database is a census of all incidents responded to by approximately 75 percent of U.S. fire departments. Fire departments respond to all manner of incidents including fires, emergency medical services, hazardous material response, and support requests. Incident types are coded using a hierarchy in which the lowest code value is given priority over higher incident type codes that may also be related to the incident. For example, if a vehicle is involved in a

crash and catches fire, the incident is coded as “131: Passenger vehicle fire” rather than “322: Motor vehicle accident.” Therefore, the results of the NFIRS-5 analysis include vehicle fires that resulted from crashes as well as from other causes.

Vehicle model codes are populated by direct text input from the coder. Thus, many typos and variations of model names exist in the database. For example, there were 279 variations of model names for Ford F-Series pickups. In order to reduce the effort required to map vehicle make/model character strings from NFIRS-5 to make/model codes that could be compared across all databases (FARS, CDS, and GES) only the top 50 vehicles involved in fatal crashes (identified from FARS) and the top 50 vehicles involved in police reported crashes (identified from GES) were mapped. An additional restriction was made to limit the mapping to vehicles newer than model year 2005 to provide a list of vehicles representative of the modern fleet. The resulting list of vehicles identified by make/model in NFIRS included 56 unique vehicles due to the overlap between the FARS and GES lists. A total of 2,051 different NFIRS model name variations existed for the 56 unique models included in this summary which had to be mapped to equivalent FARS and NASS MAK_MOD codes. Many vehicle models were coded using generic terms such as “sedan” or “pickup.” The results can, therefore, be assumed to be a conservative estimate of total counts for vehicle fires.

Table B-1. Data Filtering Summary

Dataset	Description	Data Years	Vehicle Model Years	Mobile vehicle/body type	Incident Type
NFIRS-5	Passenger Vehicles	2010-2014	All	10, 11, 22	131: Pass Vehicle Fire
NFIRS-5	Passenger Vehicles – COLLISIONS	2010-2014	All	10, 11, 22	131: Pass Vehicle Fire
NFIRS-5	Heavy Trucks	2010-2014	All	20, 21, 23, 24, 25, 26, 27	132: Road Freight or Transport Vehicle
NFIRS-5	Buses	2010-2014	All	12	131: Pass Vehicle Fire
NFIRS-5	Modern Passenger Vehicles	2010-2014	2006+	10, 11, 22	131: Pass Vehicle Fire
NASS GES		2000-2015	All	< 80, ≠42, 65, 73	n/a
FARS		1991-2015	All	< 80, ≠42, 65, 73	n/a
NASS CDS		1995-2015	All	<= 39	n/a

3 Results

In NFIRS-5, mobile property that is involved in a fire is identified by its type of involvement.

- burned but not ignition source
- burned and was ignition source
- ignition source but did not burn

For all the NFIRS-5 results presented below, only vehicles that burned, irrespective of ignition status, are included. The results for the NFIRS data are broken down by vehicle type; passenger vehicle, heavy truck, and bus. Table 2 summarizes the total number of fires per year for each vehicle type. There was a general decreasing trend in the number of fires for passenger vehicles and buses from 2010 to 2014. On the other hand, heavy trucks were involved in more fires in 2014 than any of the previous 4 years. From 2010 to 2014 the total number of fire incidents coded in NFIRS decreased from more than 660,000 per year to less than 600,000 per year. The rates of vehicle fires per total incidents reported was fairly stable for passenger vehicles and buses, but increased for heavy trucks.

Table B-2. Vehicle Fire Incidents by Year (NFIRS 2010-2014)

NFIRS Incident Year	All Fire Incidents	Passenger Vehicle Fires		Heavy-Truck Fires		Bus Fires	
	n	n	%	n	%	n	%
2010	663,333	94,966	14.32	5,288	0.80	607	0.09
2011	671,329	91,330	13.60	5,570	0.83	601	0.09
2012	599,879	84,424	14.07	5,216	0.87	521	0.09
2013	554,671	83,225	15.00	5,678	1.02	525	0.09
2014	596,521	84,123	14.10	6,146	1.03	532	0.09
Total	3,085,733	437,068	14.16	27,898	0.90	2,786	0.09

3.1 NFIRS-5 (2010-2014; Passenger Vehicles)

The total number of passenger vehicles identified in NFIRS from 2010 to 2014 that burned is listed in Table 3 and disaggregated by fire involvement. Nearly 10 times as many vehicles were coded as being the ignition sources than not.

Table B-3. Vehicle Fire Involvement Type (NFIRS 2010-2014; Passenger Vehicles)

NFIRS Reported Fire Involvement	Passenger Vehicles	
	n	%
Burned but not ignition source	41,499	9.5
Burned and was ignition source	395,569	90.5
Total	437,068	100

For vehicles that were coded as being the ignition source, fires were predominantly identified as originating in the engine compartment, as shown in Figure 1. The fuel tank and cargo/trunk area were rarely identified as the origin of fire for vehicles involved in the ignition. The area of origin for vehicles not involved in the ignition was nearly evenly split among the engine area, passenger area, and areas not related to the vehicle. Exterior areas and the cargo/trunk region made up most of the remainder of known areas. Areas related to fuel tanks or fuel lines were rarely coded for any ignition involvement type.

Operating equipment was the most common determinable primary heat source (Figure 2). Hot objects, open flame, and spread from another first are also notable sources. The detailed breakdown of heat sources (Figure 3) indicates that electrical arcing, radiated heat, flames, and overheated tires are some of the most common heat sources.

Engine fuel and electrical wire are the most frequent items to ignite first (Figures 4 and 5). Vehicle seats are also relatively commonly coded as the first items to ignite. Similar results are recorded in a breakdown of the first material ignited (Figures 6 and 7). The most common materials that ignite first are flammable liquids and gases, plastics, oils, and tires.

The most commonly coded factors contributing to the ignition of a passenger vehicle fire are mechanical or electrical failures (Figure 8). However, the detailed descriptions for these categories are most often coded as ““other.” Collision is only coded as a factor contributing to fire ignition for 1.7 percent of all passenger vehicle fires (Figure 9).

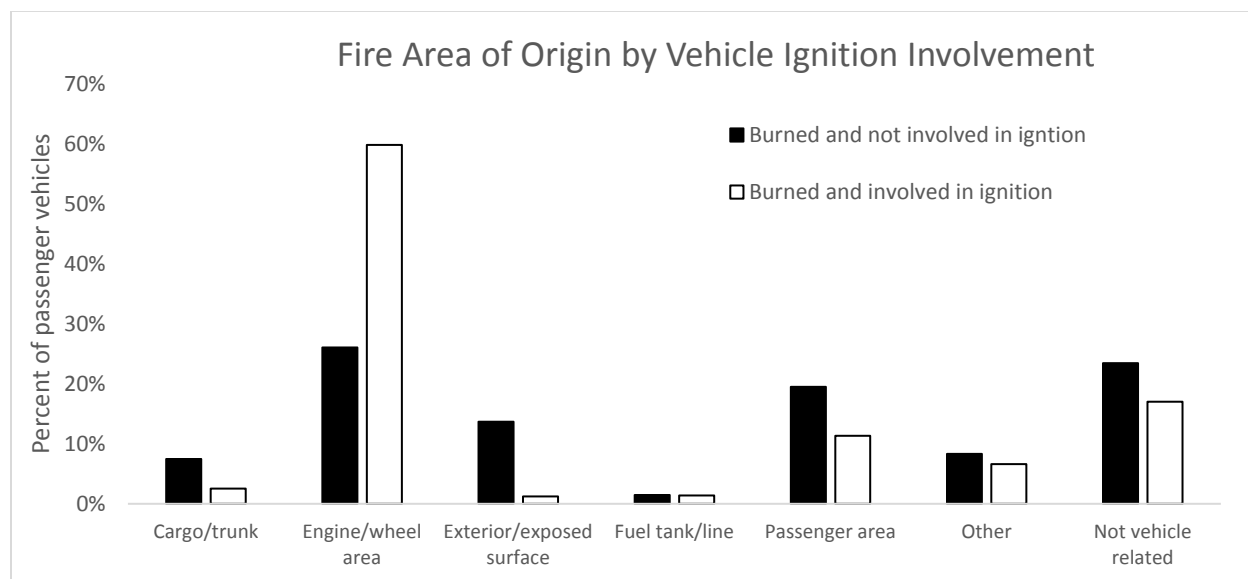


Figure B-1. Area of origin by vehicle involvement type for all passenger vehicles (NFIRS 2010-2014; Passenger Vehicles)

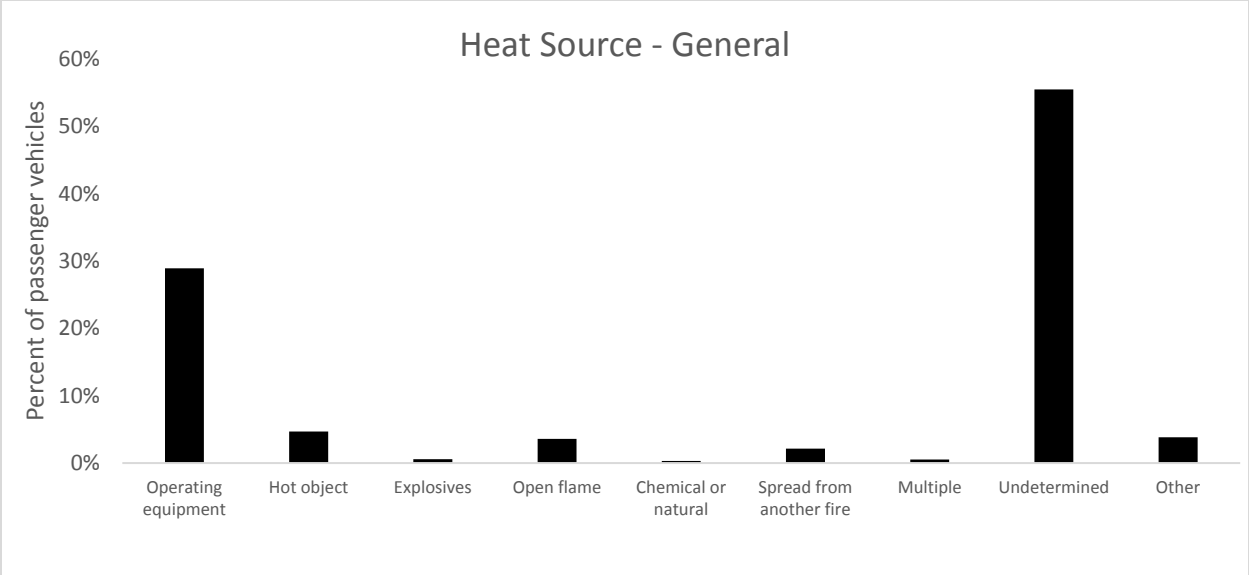


Figure B-2. Heat source that ignited the item first ignited to cause the fire; general description (NFIRS 2010-2014; Passenger Vehicles)

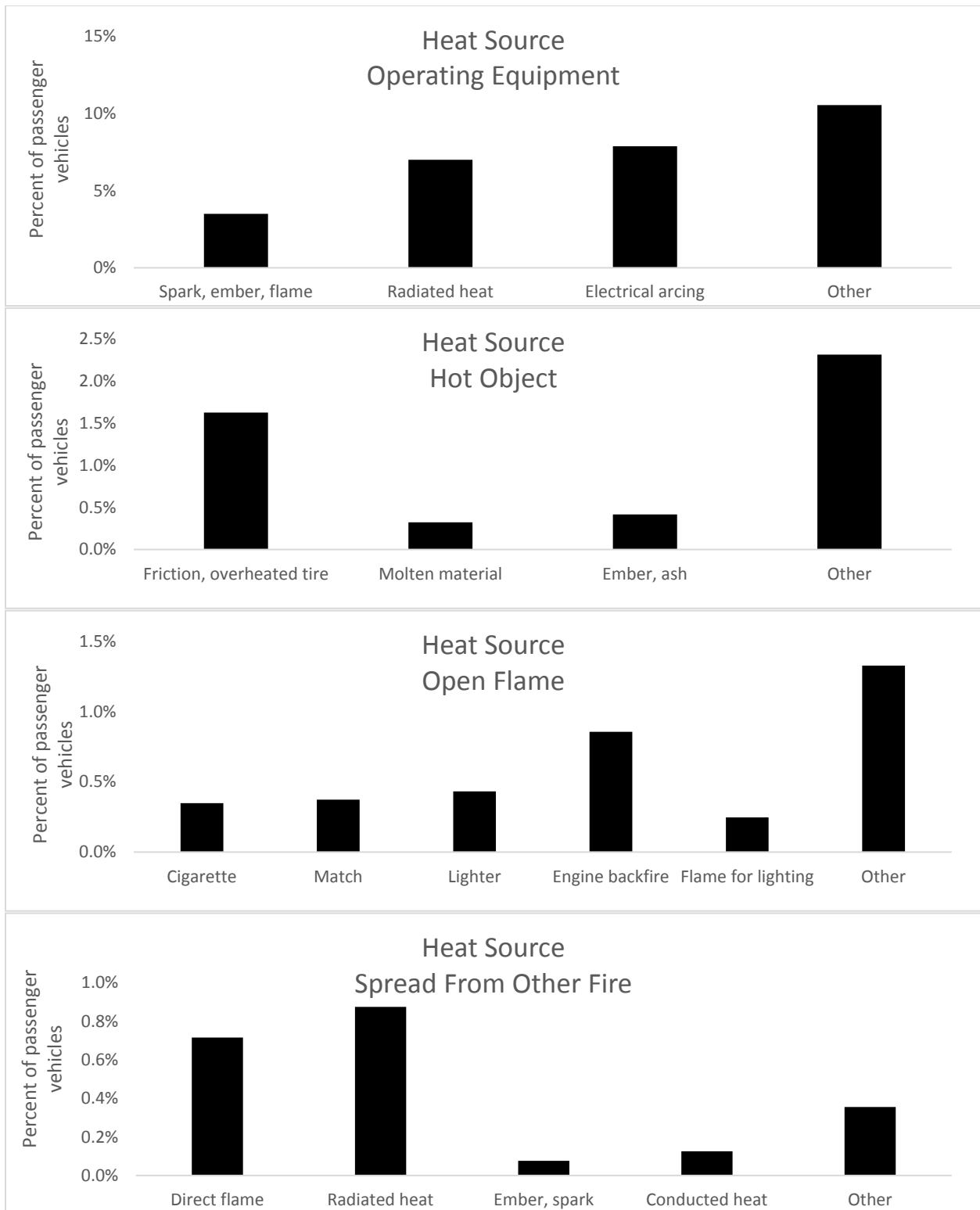


Figure B-3. Heat source that ignited the item first ignited to cause the fire; detailed description of top 4 known general sources (NFIRS 2010-2014; Passenger Vehicles)

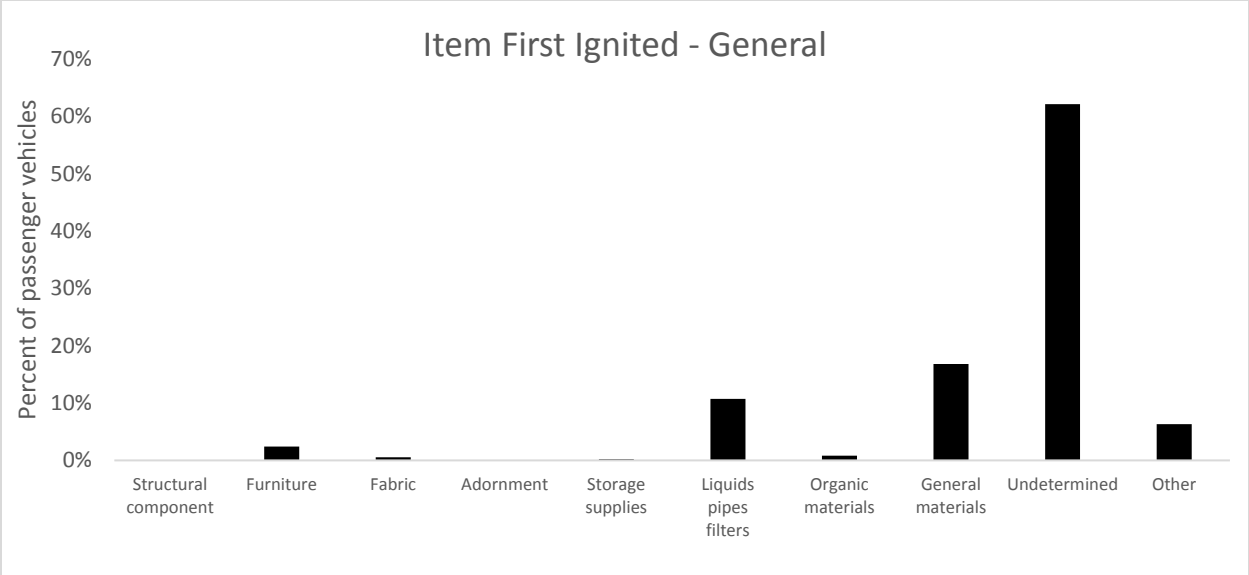


Figure B-4. Item first ignited; general description (NFIRS 2010-2014; Passenger Vehicles)

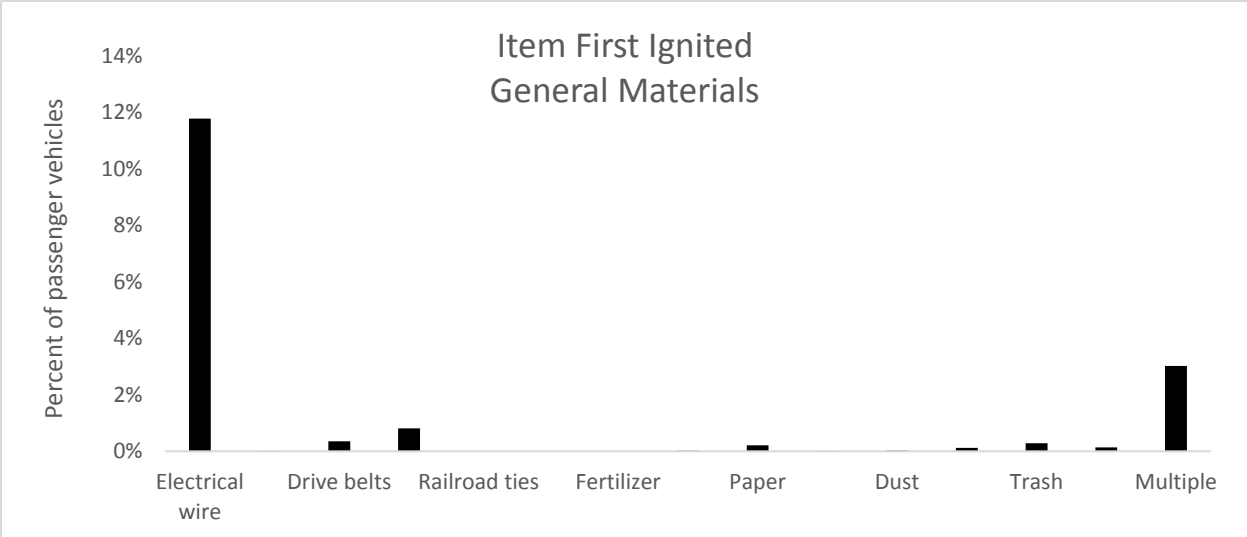
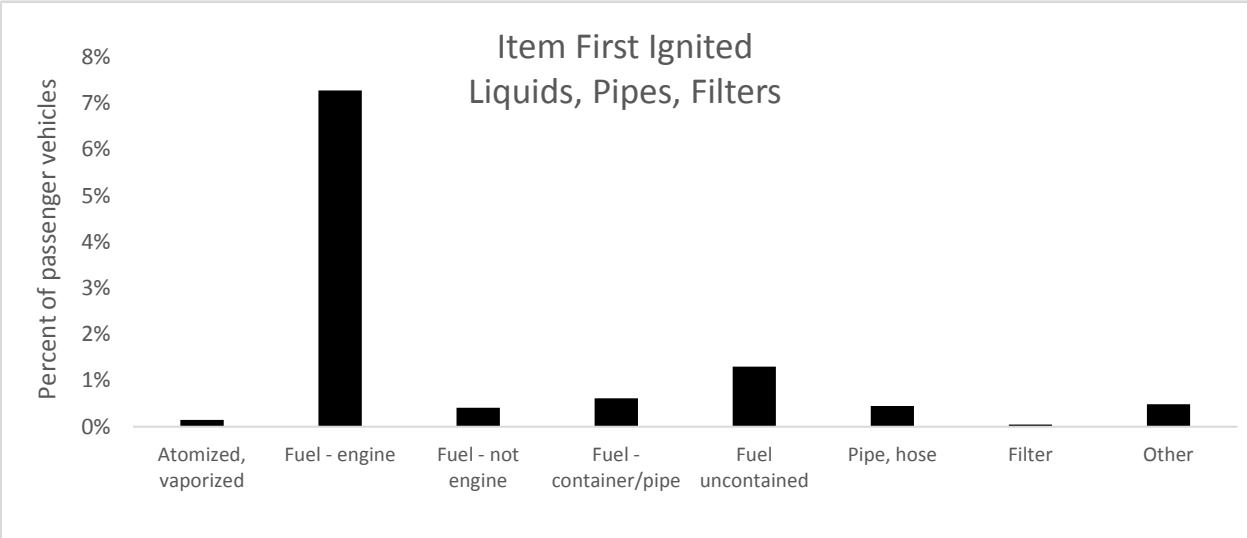
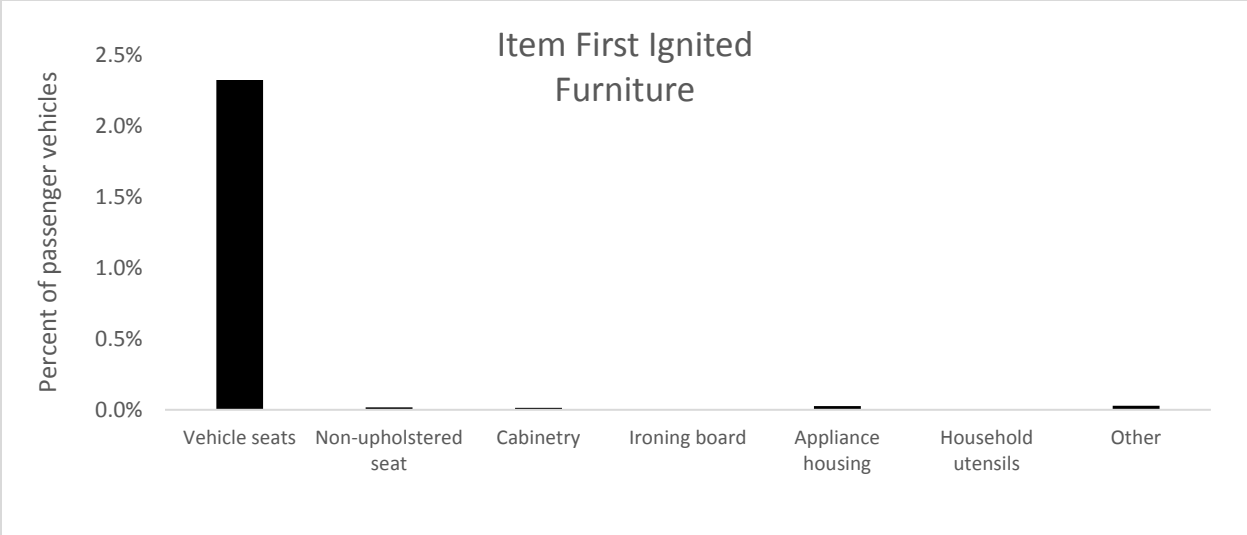


Figure B-5. Item first ignited; detailed description of top 3 known general items (NFIRS 2010-2014; Passenger Vehicles)

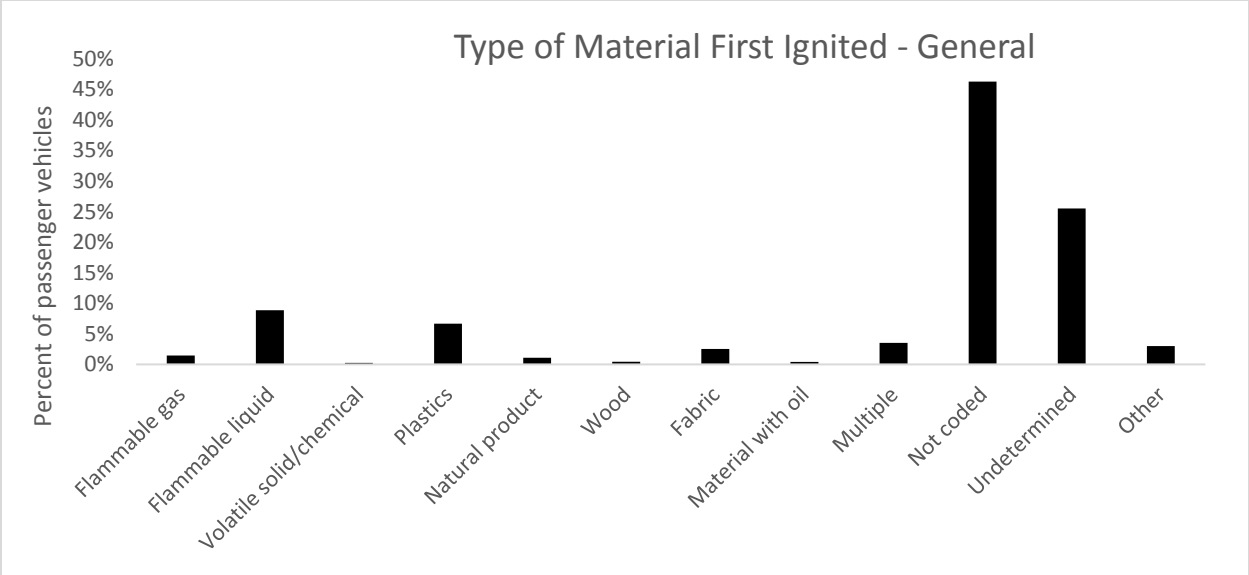


Figure B-6. Type of material first ignited by the heat source; general description (NFIRS 2010-2014; Passenger Vehicles)

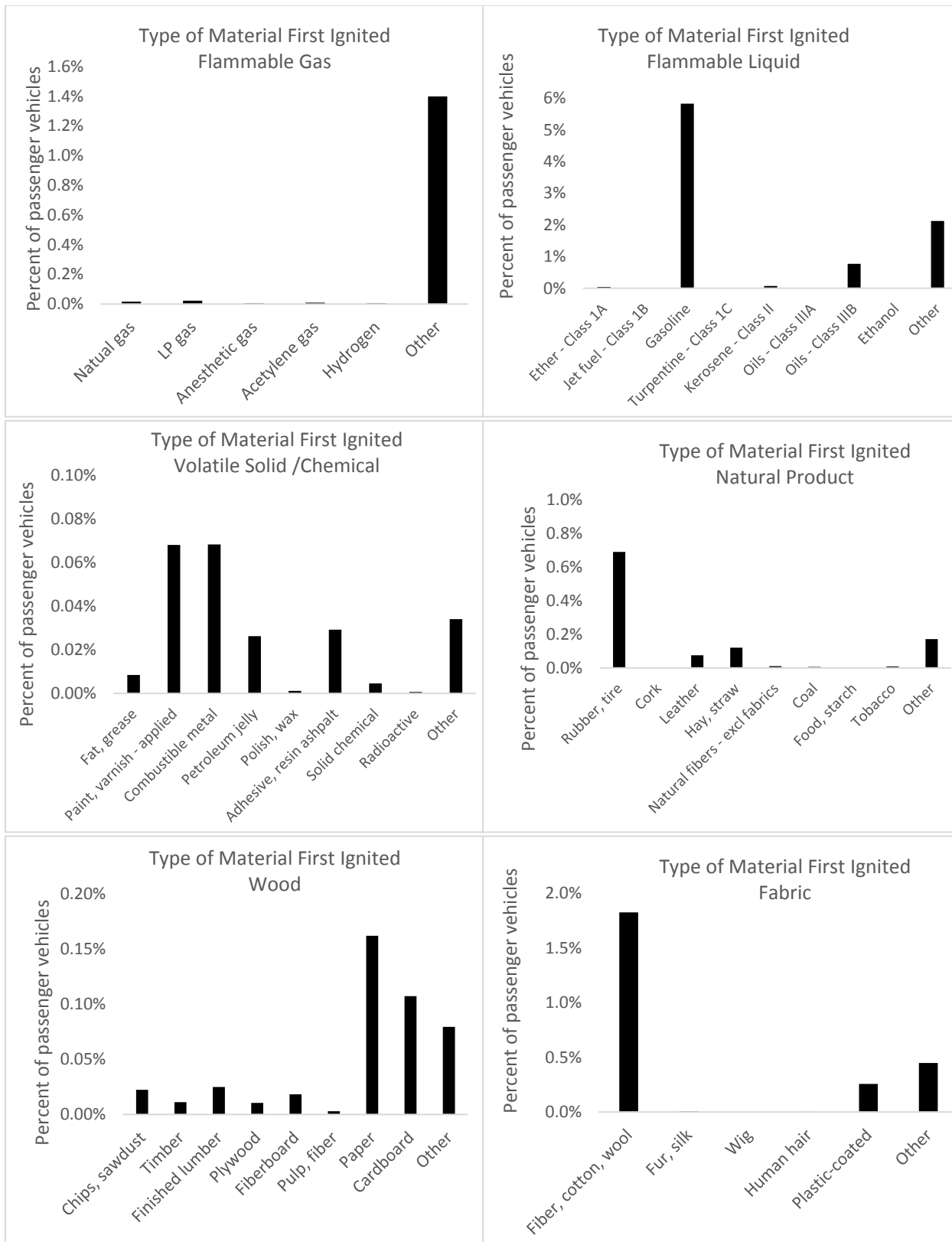


Figure B-7. Type of material first ignited by the heat source; detailed description of top 6 general materials (plastics are not further disaggregated) (NFIRS 2010-2014; Passenger Vehicles)

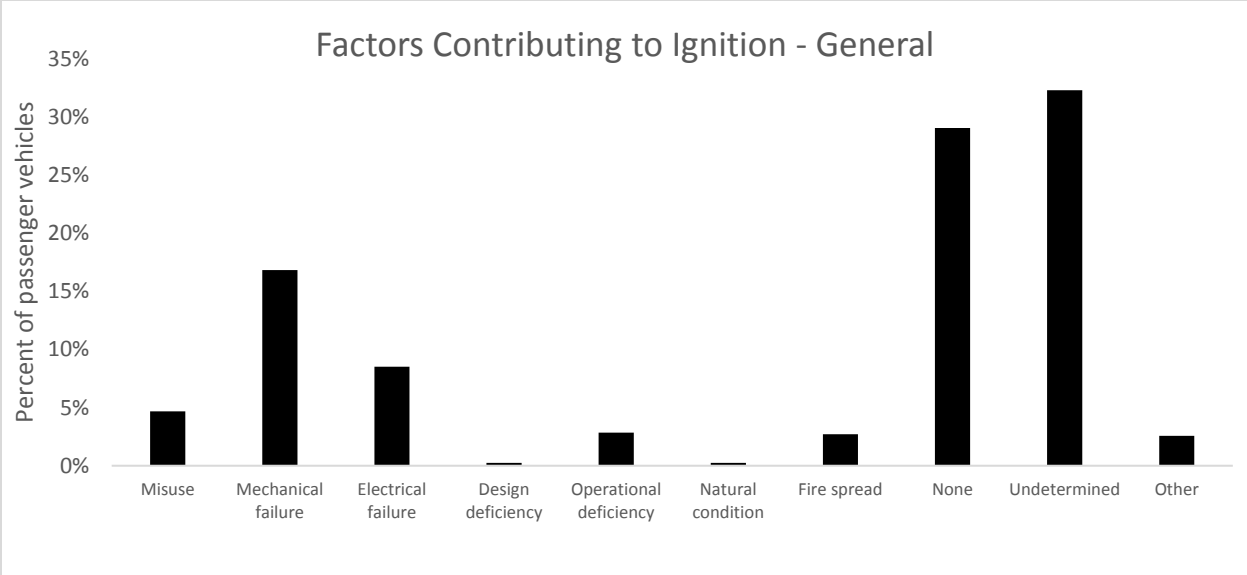


Figure B-8. Factors contributing to ignition; general description (NFIRS 2010-2014; Passenger Vehicles)

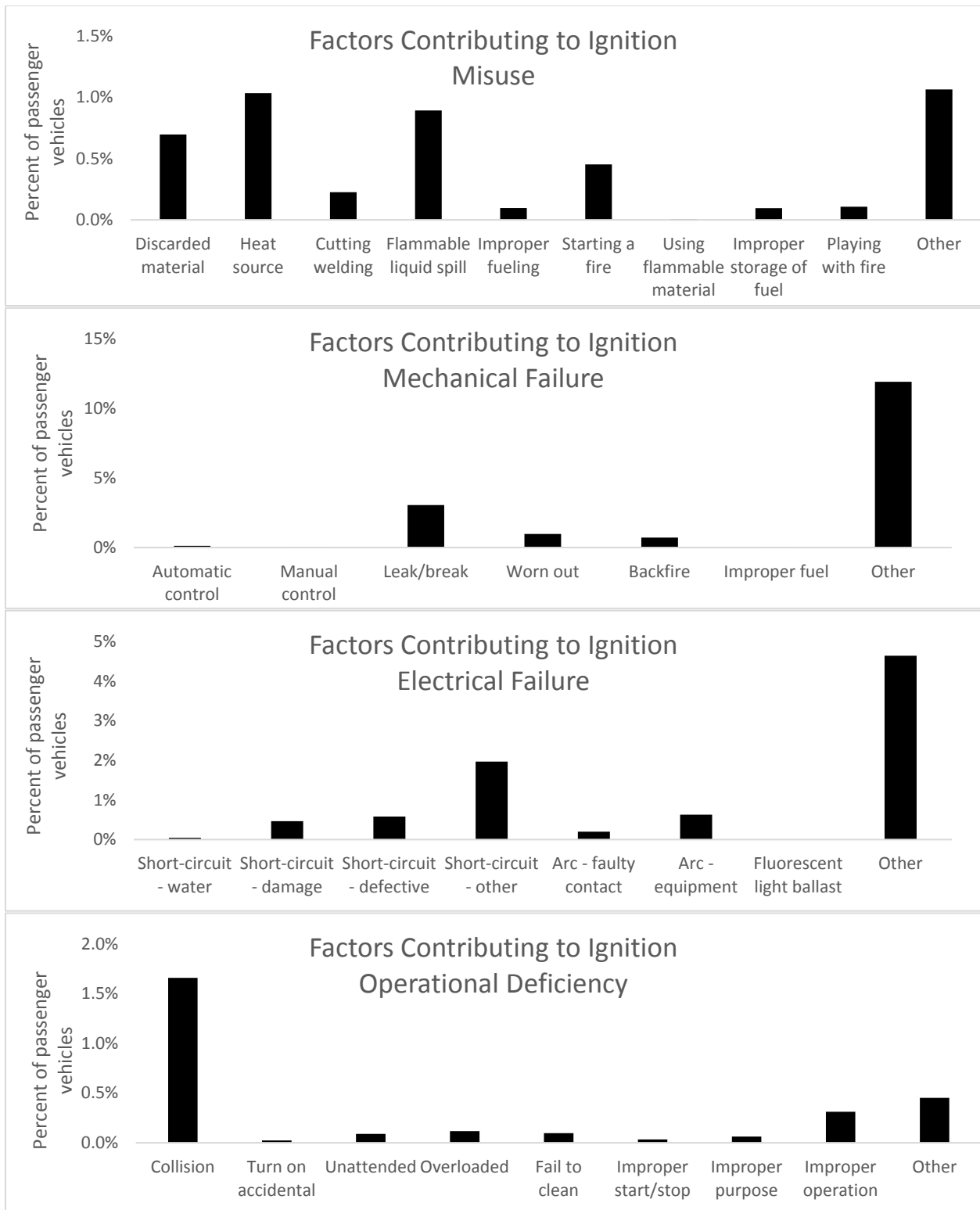


Figure B-9. Factors contributing to ignition; detailed description of 4 most common general factors (NFIRS 2010-2014; Passenger Vehicles)

3.2 NFIRS-5 (2010-2014; Passenger Vehicles - COLLISIONS)

The following results include only passenger vehicles that were coded with “collision” as a factor that contributed to fire ignition. There were a total of 7,390 vehicles identified as such, which represents 1.7 percent of all passenger vehicle fires. A breakdown by fire involvement type is provided in Table 4. A greater proportion of collision-related vehicle fires were identified with the vehicle as the ignition source than the overall population of vehicle fires.

Table B-4. Vehicle Fire Involvement Type (NFIRS 2010-2014; Passenger Vehicles)

NFIRS Reported Fire Involvement	Passenger Vehicles			
	COLLISION		ALL FIRES	
	n	%	n	%
Burned but not ignition source	240	3.2	41,499	9.5
Burned and was ignition source	7150	96.8	395,569	90.5
Total	7390	100	437,068	100

Fire area of origin was similar whether or not the vehicle was identified as the ignition source. Fires were predominantly identified as originating in the engine compartment while all other areas were relatively rare, as shown in Figure 10.

Operating equipment was the most common determinable primary heat source (Figure 11). “Hot objects” was the only other notable category of heat sources. The detailed breakdown of heat sources (Figure 12) indicates that electrical arcing, radiated heat, flames, and overheated tires are some of the most common heat sources.

Engine fuel, electrical wire, and tires are the most frequent items to ignite first (Figures 13 and 14). Furniture, which includes vehicle seats, was rarely coded as the first items to ignite. Similar results are recorded in a breakdown of the first material ignited (Figures 15 and 16). The most common materials that ignite first are flammable liquids and gases, plastics, and tires.

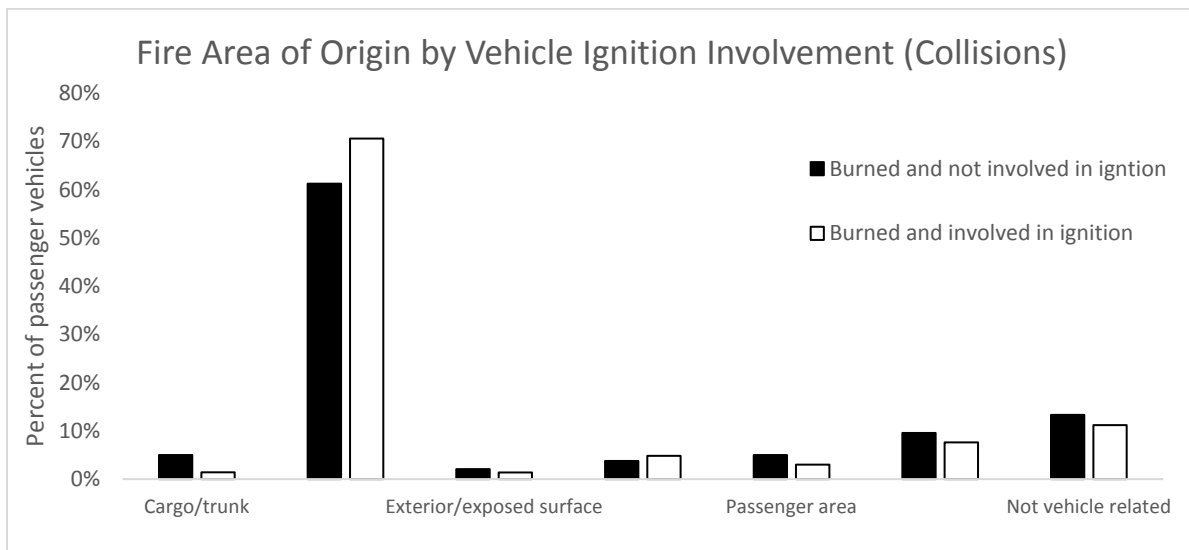


Figure B-10. Area of origin versus vehicle involvement for all passenger vehicles (NFIRS 2010-2014; Passenger Vehicles - COLLISIONS)

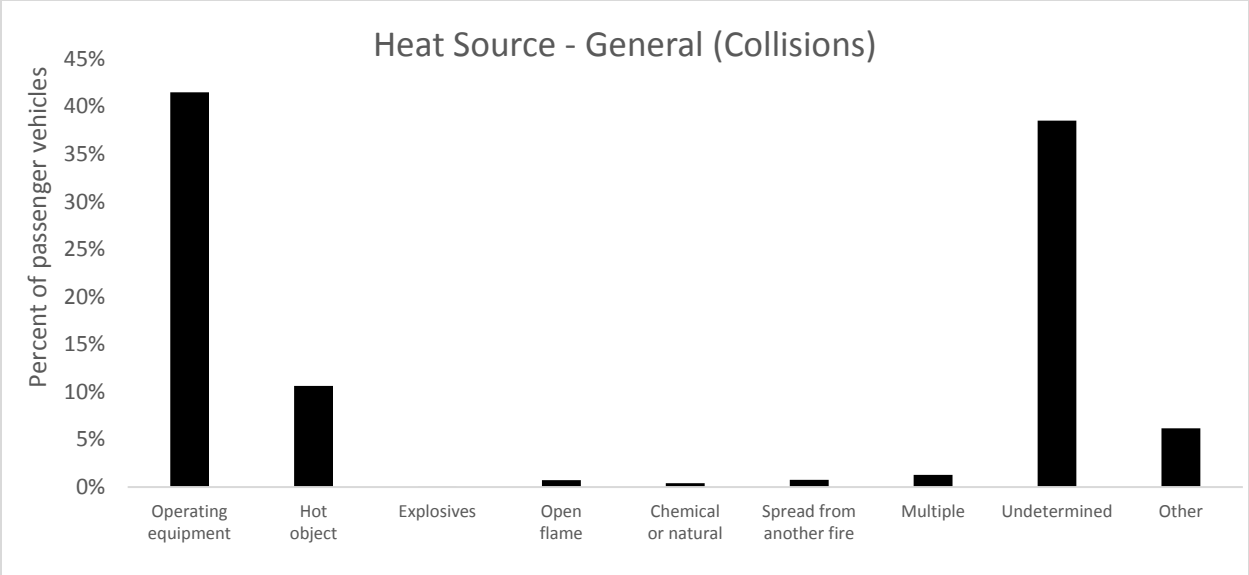


Figure B-11. Heat source that ignited the item first ignited to cause the fire; general description (NFIRS 2010-2014; Passenger Vehicles - COLLISIONS)

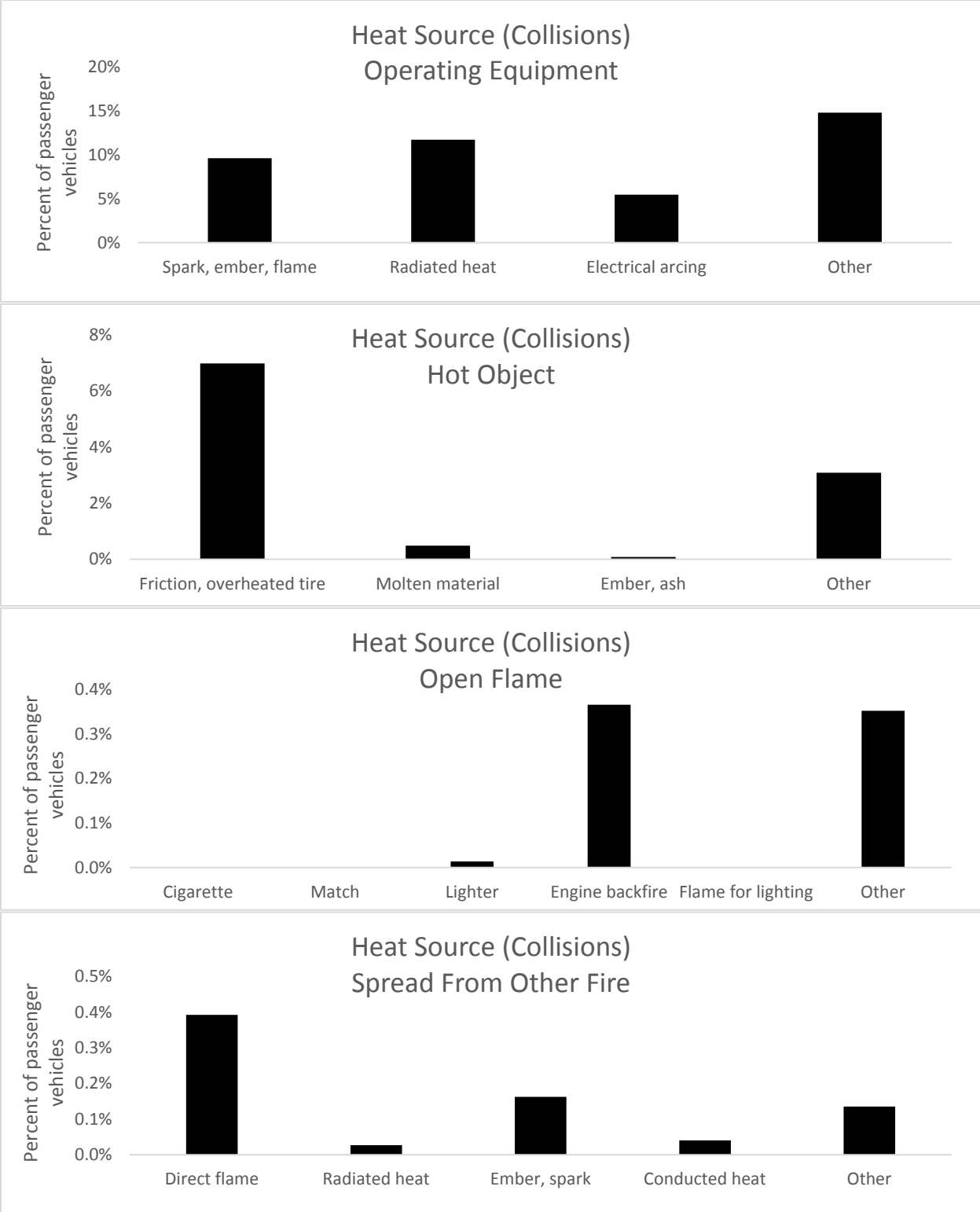


Figure B-12. Heat source that ignited the item first ignited to cause the fire; detailed description of top 4 known general sources (NFIRS 2010-2014; Passenger Vehicles - COLLISIONS)

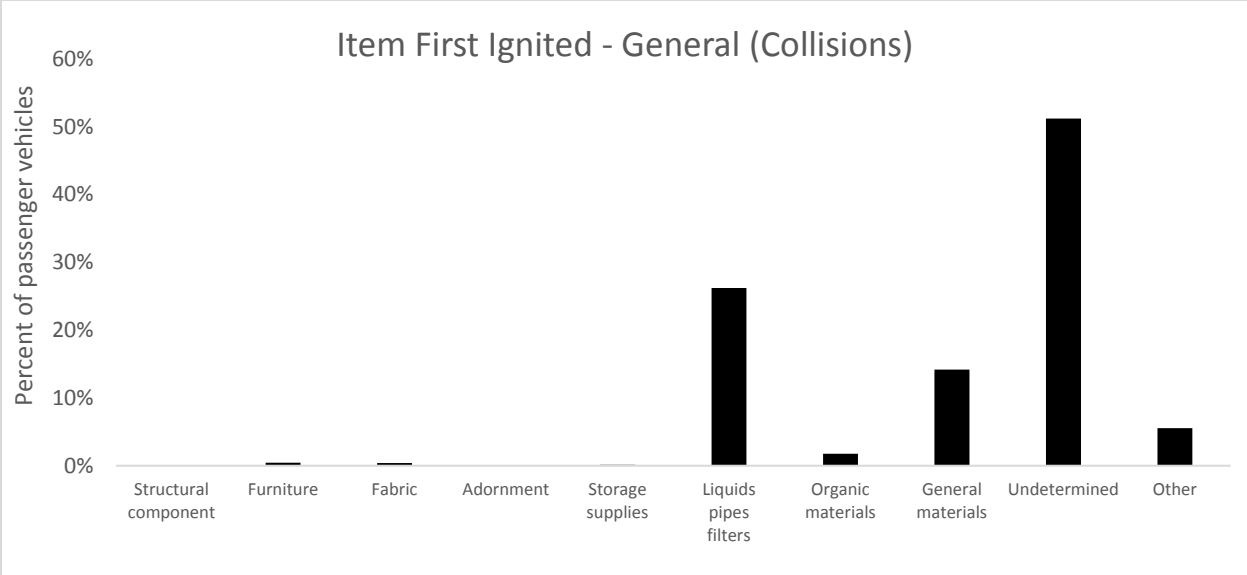


Figure B-13. Item first ignited; general description (NFIRS 2010-2014; Passenger Vehicles - COLLISIONS)

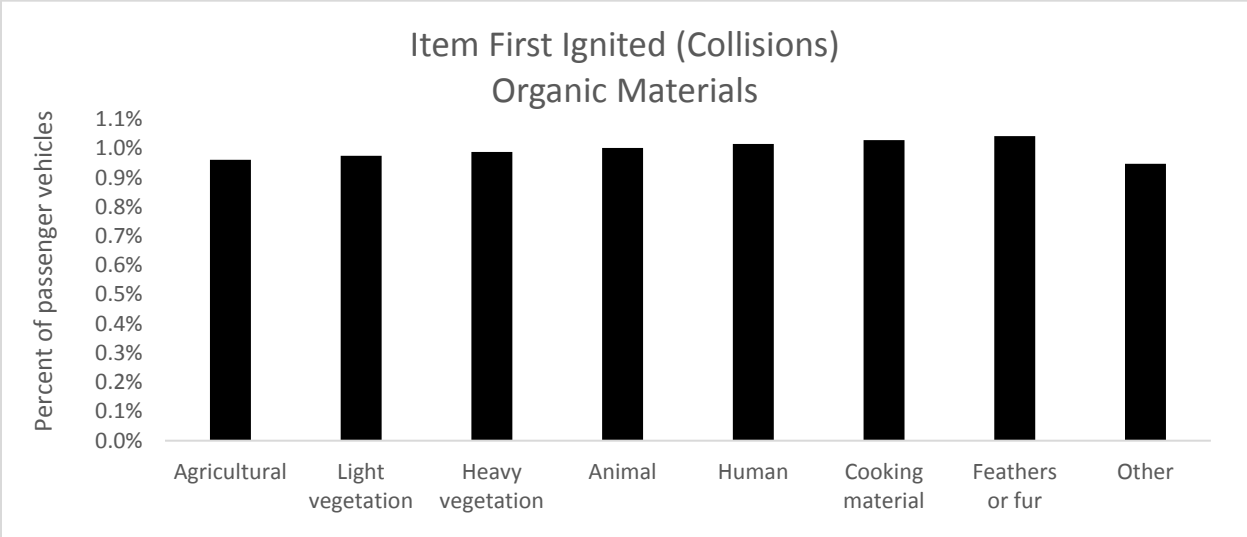
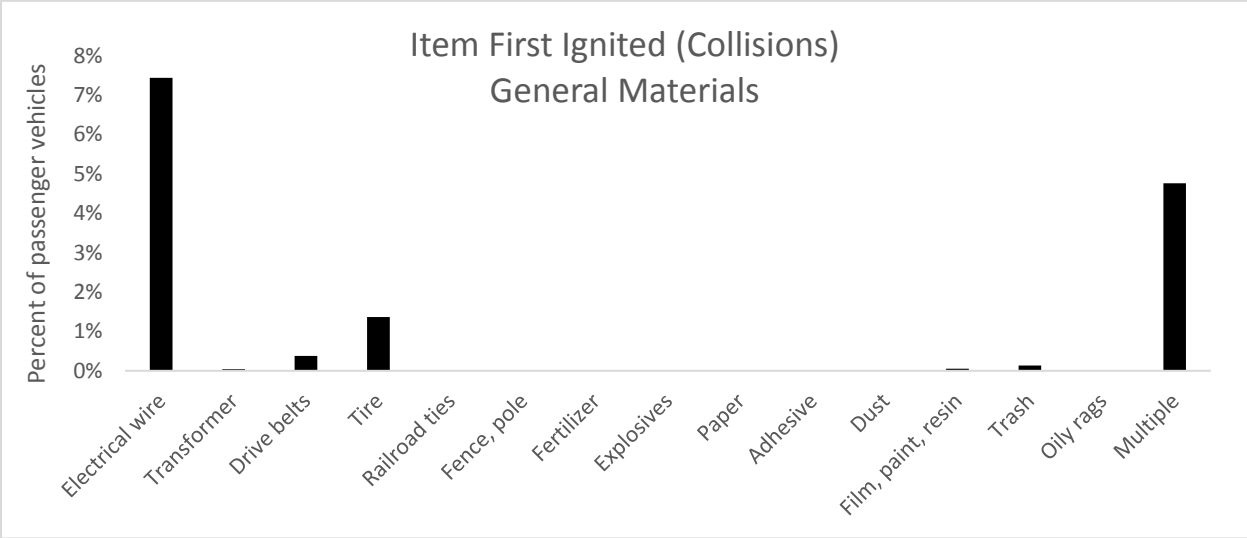
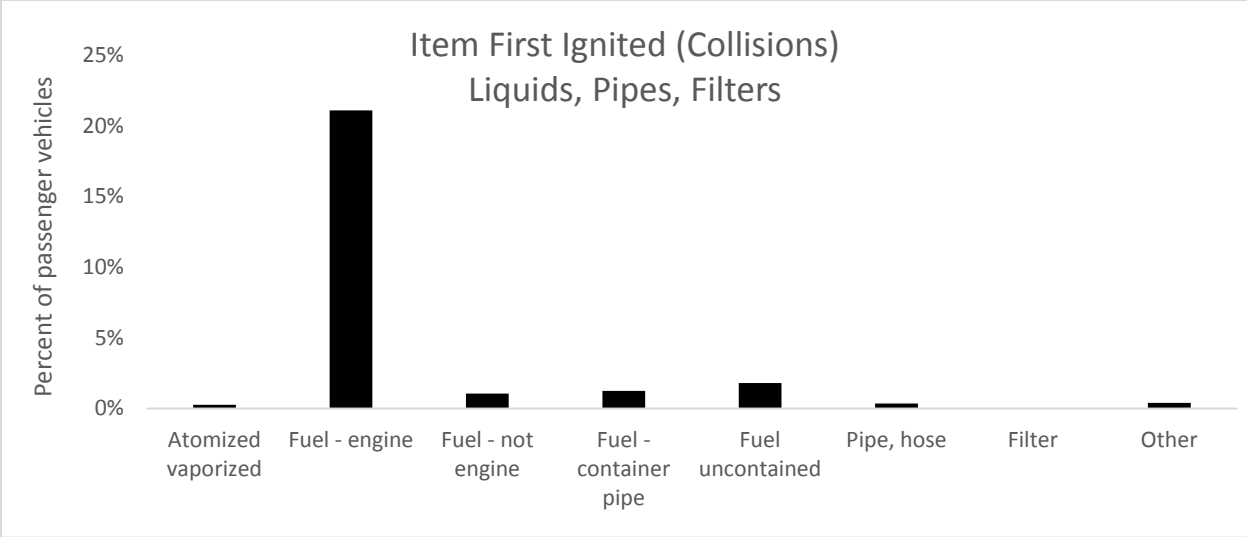


Figure B-14. Item first ignited; detailed description of top 3 known general items (NFIRS 2010-2014; Passenger Vehicles - COLLISIONS)

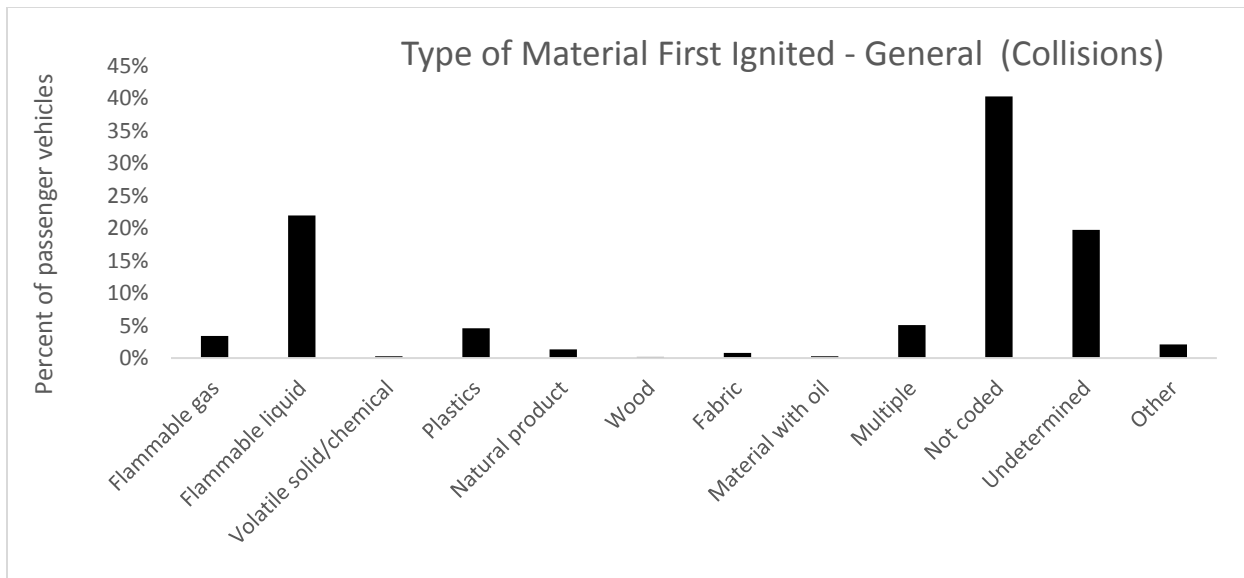


Figure B-15. Type of material first ignited by the heat source; general description (NFIRS 2010-2014; Passenger Vehicles - COLLISIONS)

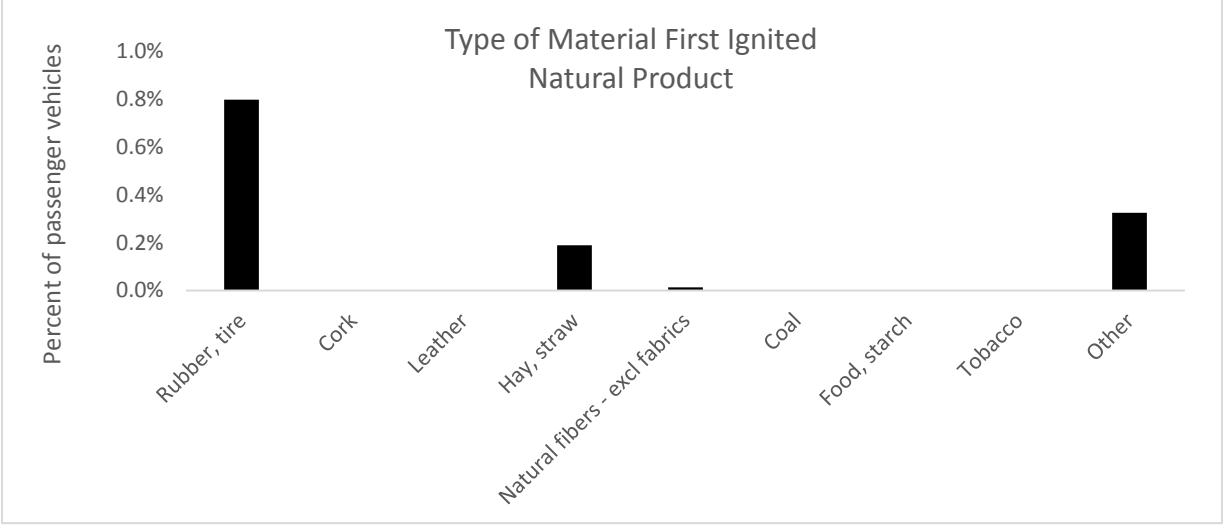
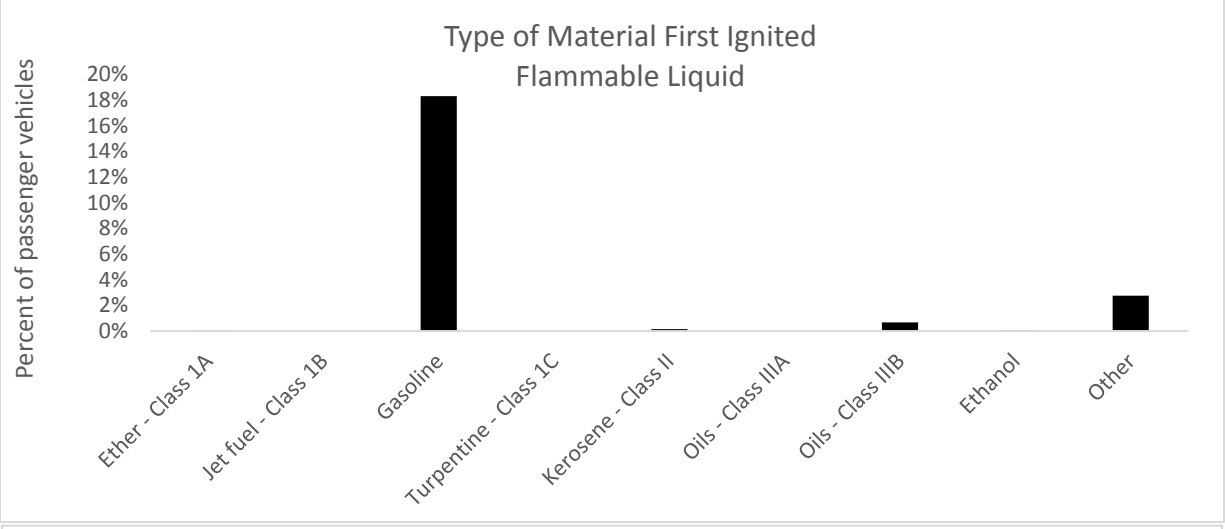
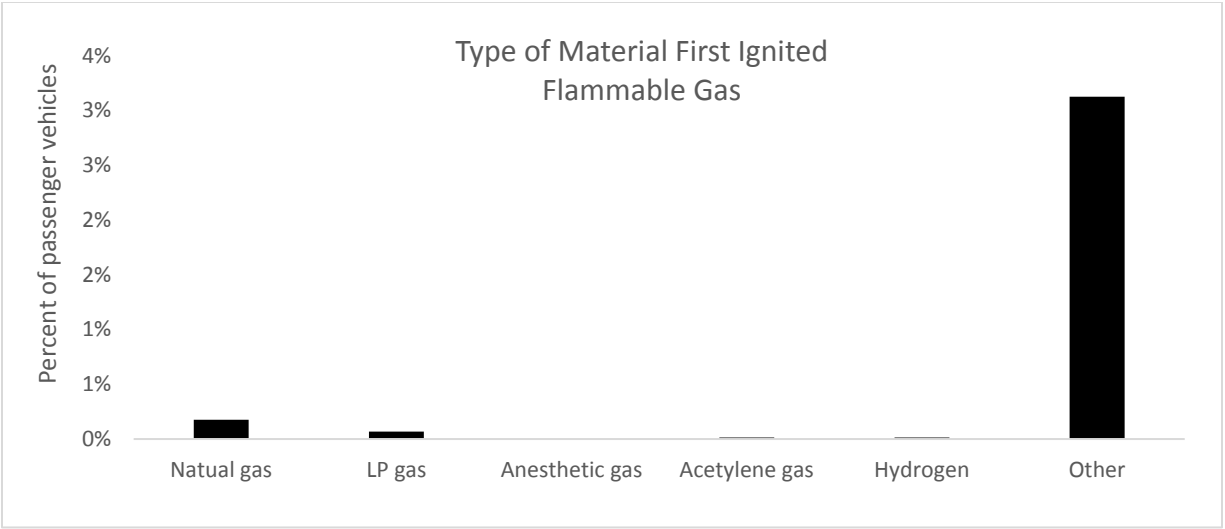


Figure B-16. Type of material first ignited by the heat source; detailed description of top 3 general materials (plastics are not further disaggregated) (NFIRS 2010-2014; Passenger Vehicles - COLLISIONS)

3.3 NFIRS-5 (2010-2014; Heavy Trucks)

The total number of heavy trucks identified in NFIRS from 2010 to 2014 that burned is listed in Table 5 and disaggregated by fire involvement. Those identified as having a collision as a factor contributing to the fire are also identified. Approximately 2 percent of all 27,898 heavy-truck fires were identified as having collision being a contributing factor to the fire initiation.

Table B-5. Vehicle Fire Involvement Type (NFIRS 2010-2014; Heavy Trucks)

NFIRS Reported Fire Involvement	Heavy Trucks			
	COLLISION		ALL FIRES	
	n	%	n	%
Burned but not ignition source	28	5.2	3742	13.4
Burned and was ignition source	512	94.8	24156	86.6
Total	540	100	27898	100

The engine/wheel area was the most frequently identified area of origin for all heavy-truck fires (Figures 17 and 18). The fuel tank/fuel line area was also commonly recorded as the fire origin area for heavy trucks that were involved in collisions. The cargo area was identified as the fire's area of origin in about 25 percent of fires for heavy trucks that were not coded as being involved in the fire ignition. The passenger compartment was coded as being the area of origin for a fire in less than 10 percent of cases.

Operating equipment and hot object were the most common determinable primary heat sources (Figure 19). The detailed breakdown of heat sources (Figure 20) indicates that radiated heat from operating equipment and overheated tires were the two most common heat sources.

Tires, electrical wire, and engine fuel are the most frequent items to ignite first (Figures 21 and 22). Vehicle seats were relatively rarely coded as the first items to ignite. Similar results are recorded in a breakdown of the first material ignited (Figures 23 and 24). The most common materials that ignite first are flammable liquids and gases, plastics, tires, and wood products.

The most commonly coded factors contributing to the ignition of a heavy-truck fire are mechanical or electrical failures (Figure 25). However, the detailed descriptions for these categories are most often coded as ““other.” Collision is only coded as a factor contributing to fire ignition for 1.9 percent of all heavy-truck fires (Figure 26).

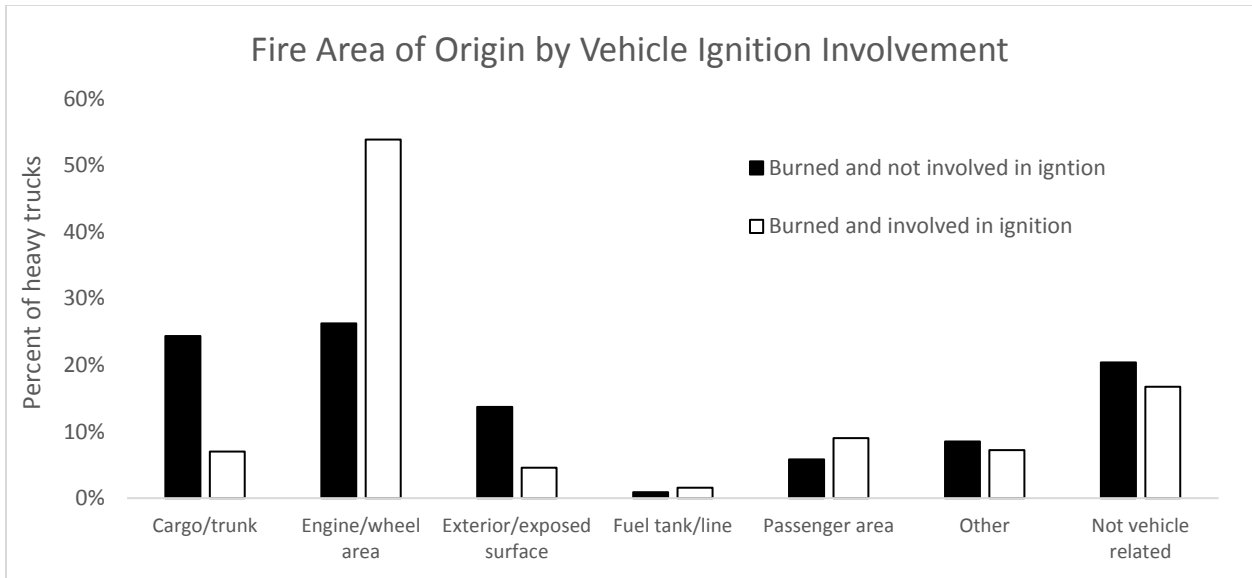


Figure B-17. Area Of Origin Versus Vehicle Involvement For All Heavy Trucks (NFIRS 2010-2014; Heavy Trucks)

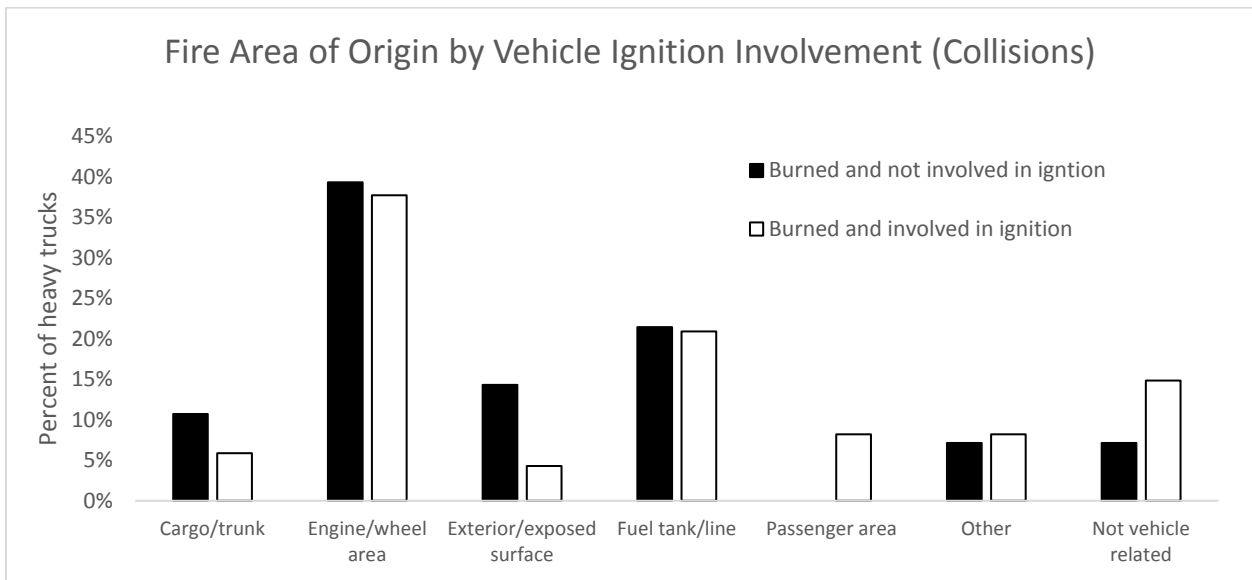


Figure B-18. Area of origin versus vehicle involvement for all heavy trucks involved in collisions (NFIRS 2010-2014; Heavy Trucks – COLLISIONS)

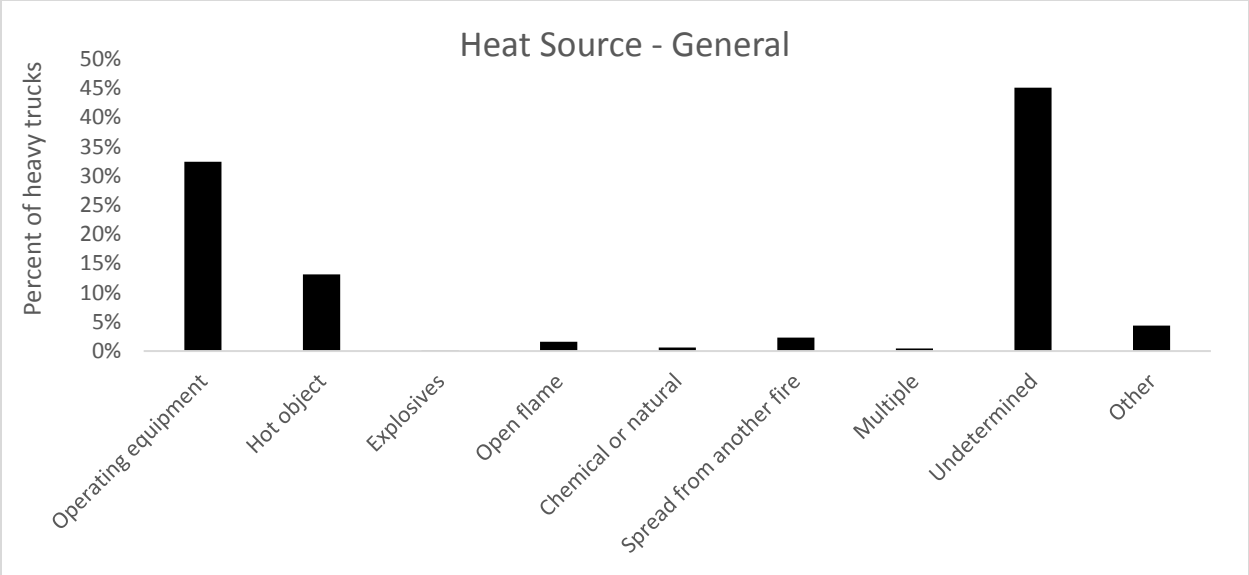


Figure B-19. Heat source that ignited the item first ignited to cause the fire; general description (NFIRS 2010-2014; Heavy Trucks)

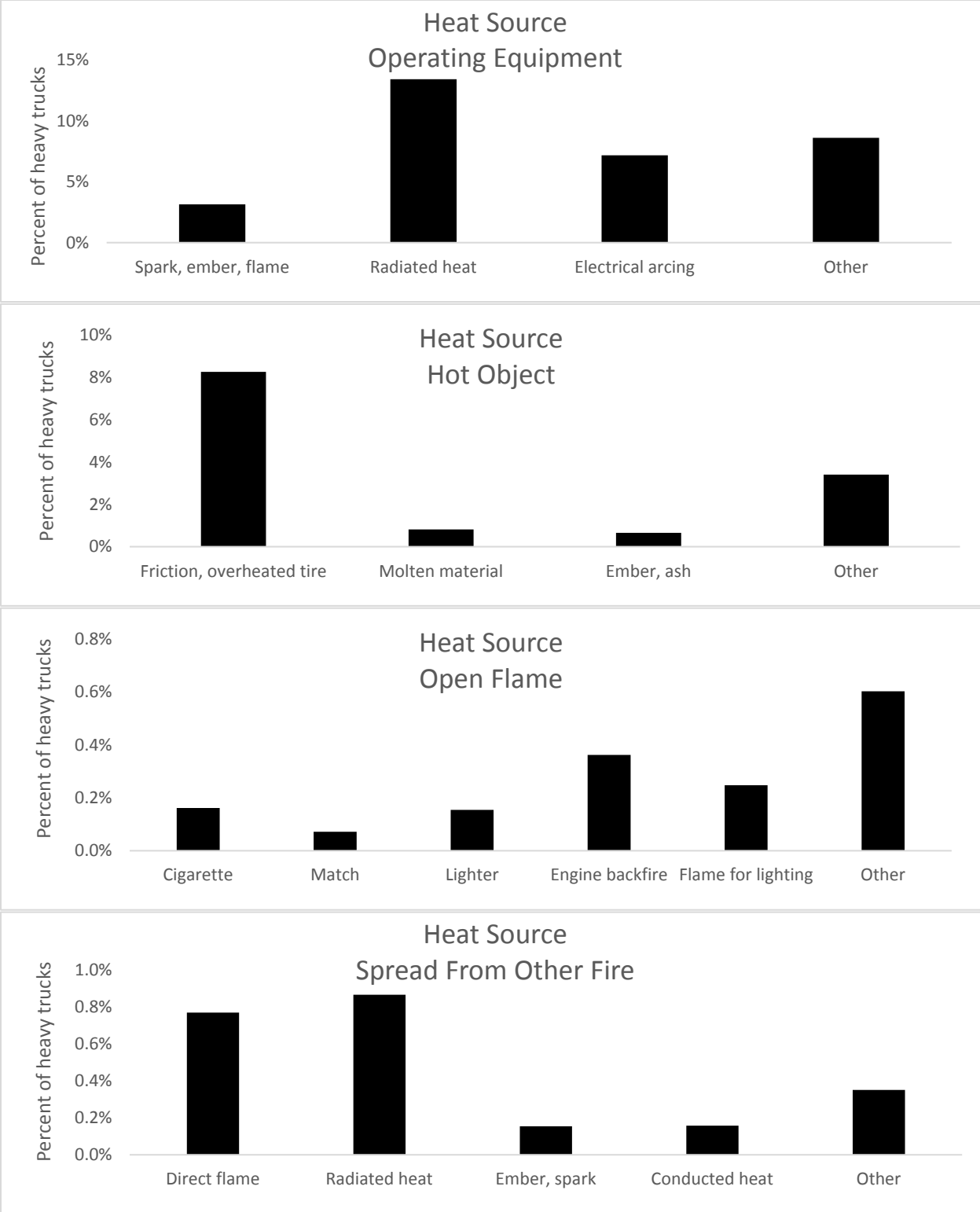


Figure B-20. Heat source that ignited the item first ignited to cause the fire; detailed description of top 4 known general sources (NFIRS 2010-2014; Heavy Trucks)

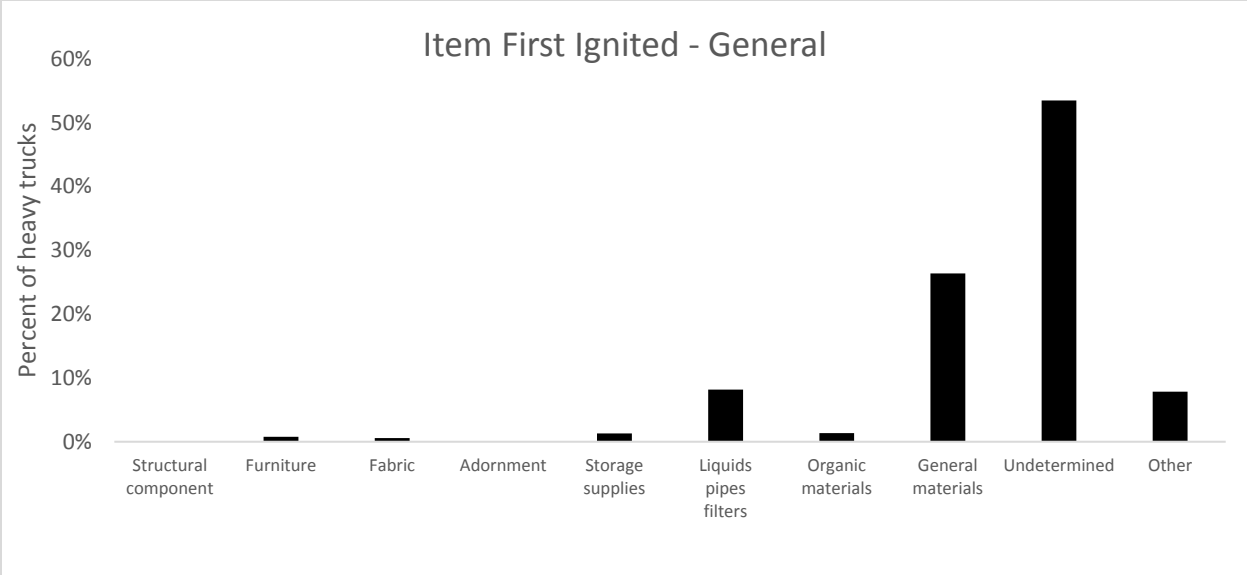


Figure B-21. Item first ignited; general description (NFIRS 2010-2014; Heavy Trucks)

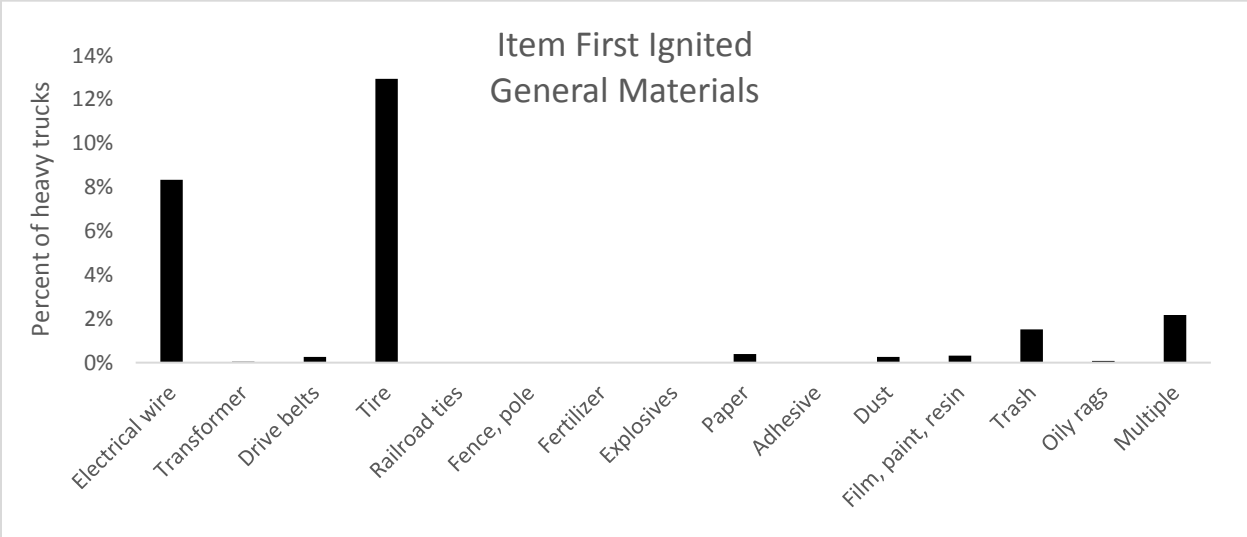
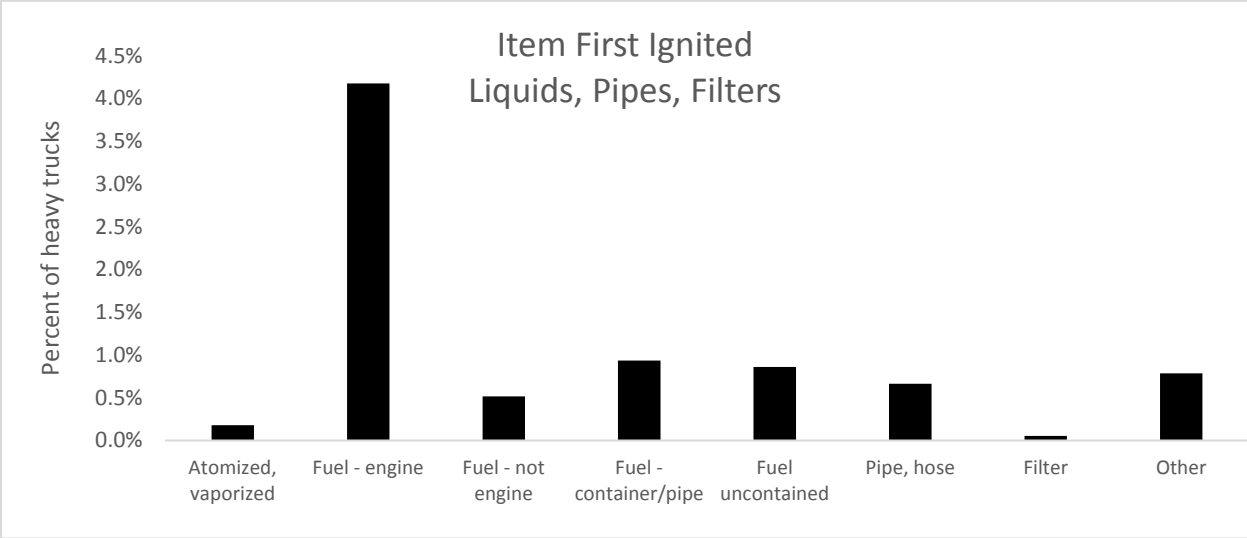
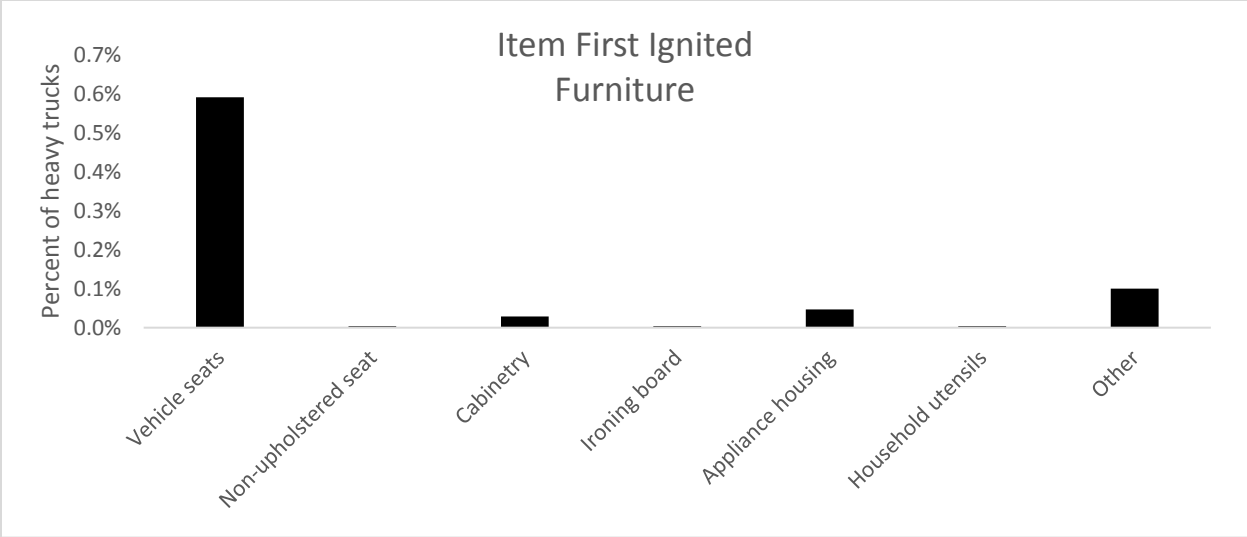


Figure B-22. Item first ignited; detailed description of 3 select general items (NFIRS 2010-2014; Heavy Trucks)

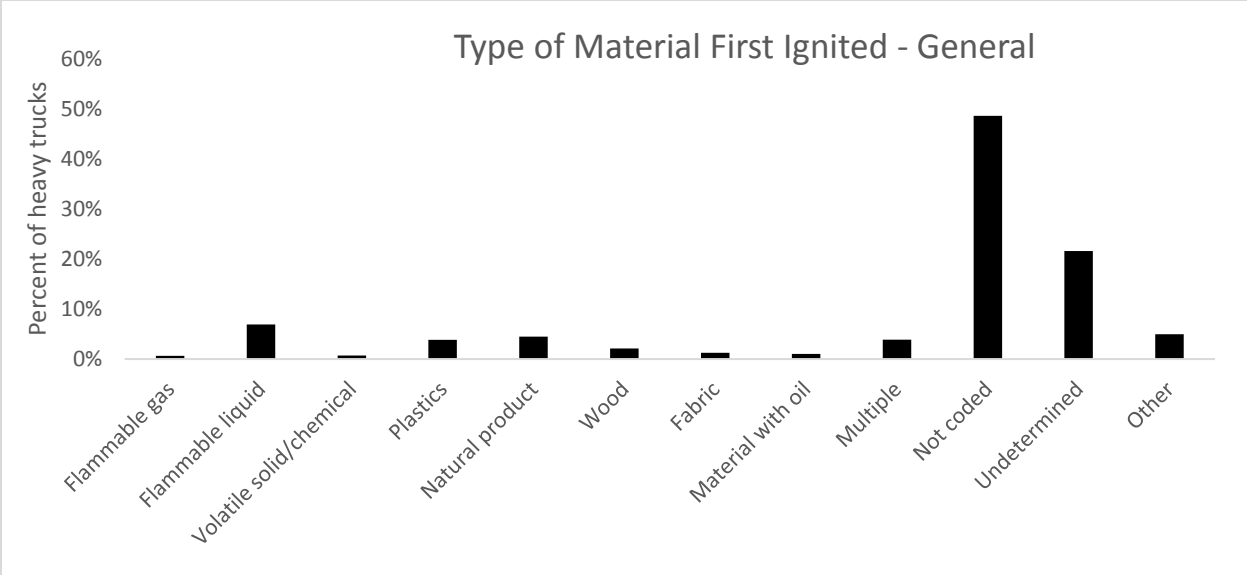


Figure B-23. Type of material first ignited by the heat source; general description (NFIRS 2010-2014; Heavy Trucks)

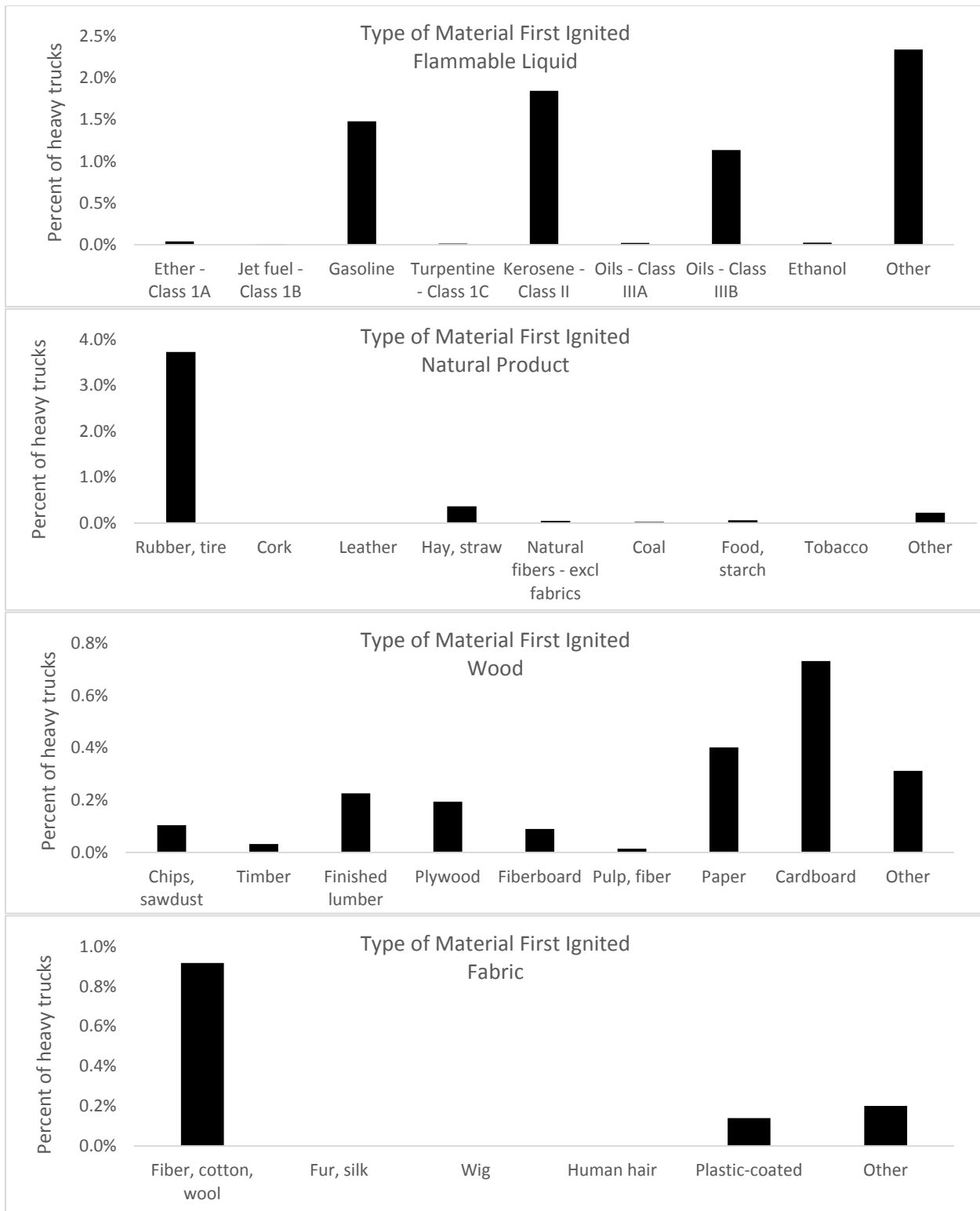


Figure B-24. Type of material first ignited by the heat source; detailed description of top 4 materials (plastics are not further disaggregated) (NFIRS 2010-2014; Heavy Trucks)

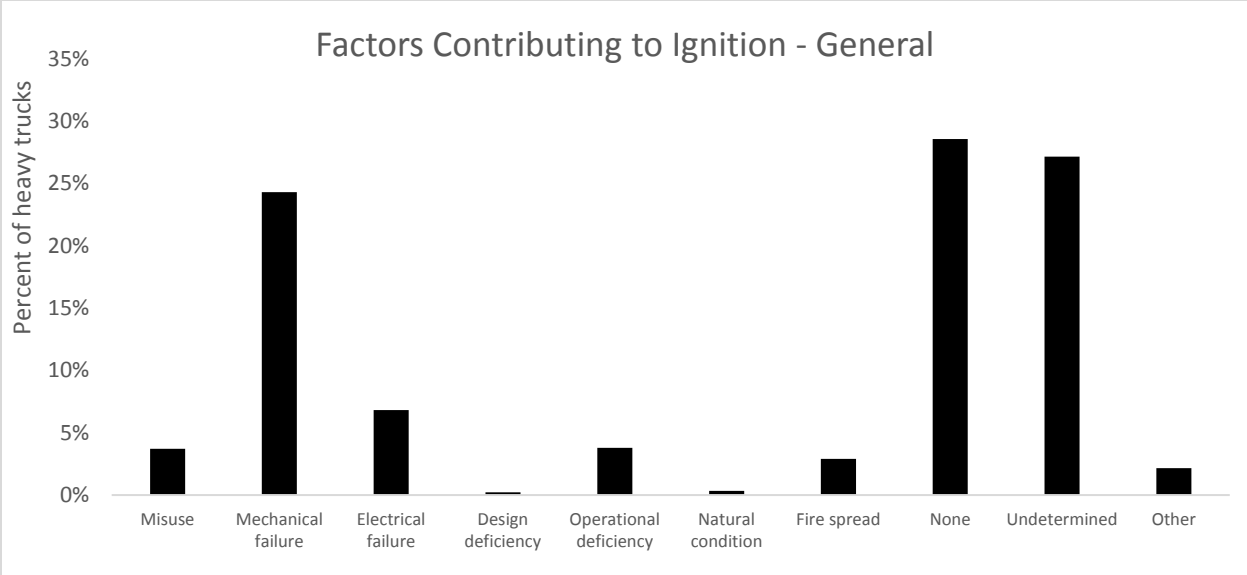


Figure B-25. Factors contributing to ignition; general description (NFIRS 2010-2014; Heavy Trucks)

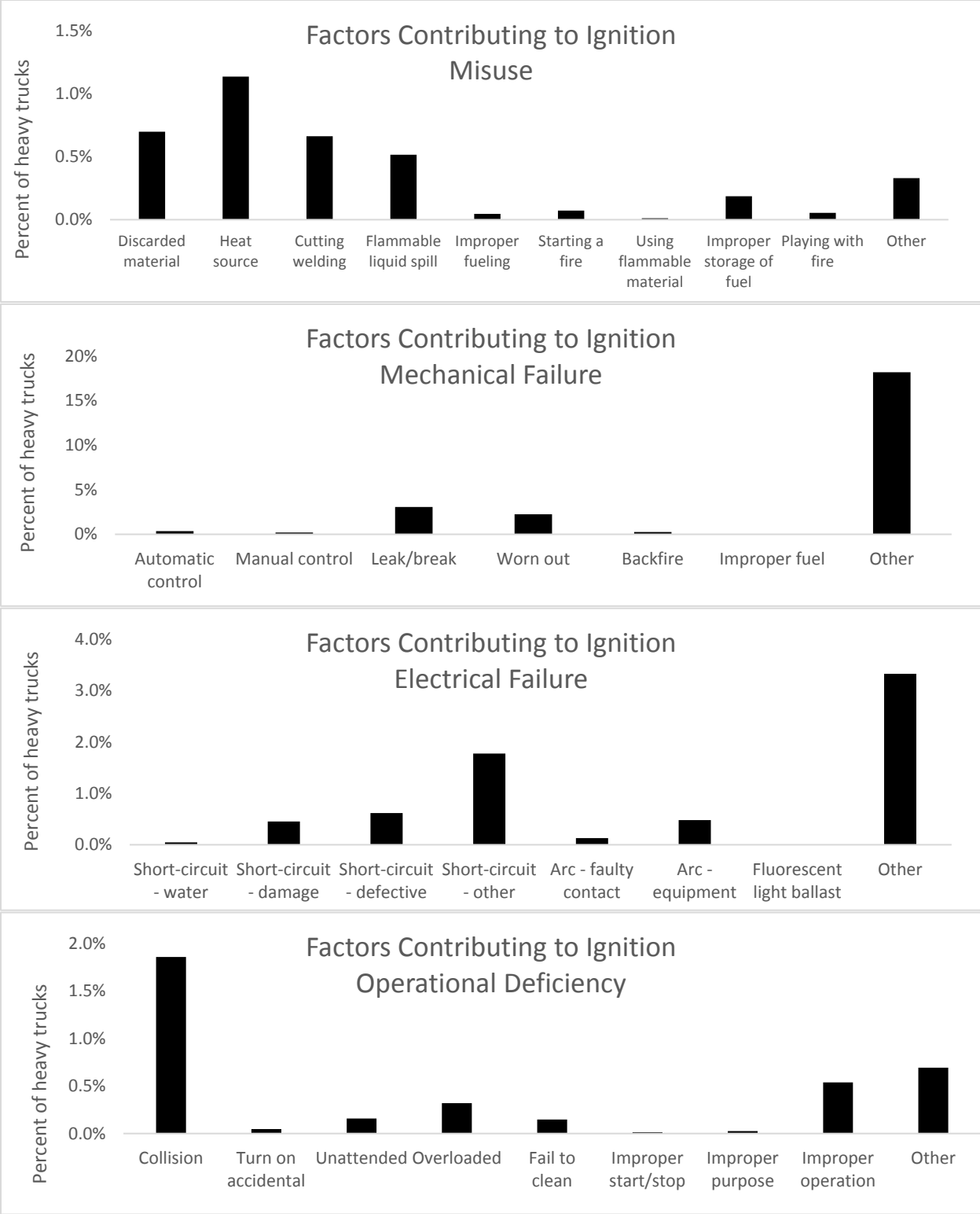


Figure B-26. Factors contributing to ignition; detailed description of 4 most common general factors (NFIRS 2010-2014; Heavy Trucks)

3.4 NFIRS-5 (2010-2014; Buses)

The total number of buses identified in NFIRS from 2010 to 2014 that burned is listed in Table 6 and disaggregated by fire involvement. Those identified as having a collision as a factor contributing to the fire are also identified. Approximately 0.3 percent of all 2,786 bus fires were identified as having a collision being a contributing factor to the fire initiation. The following results include data from all bus fires identified in the NFIRS database. Due to the low number of collision related fires for buses, the cases were not disaggregated by collision involvement.

Table B-6. Vehicle Fire Involvement Type (NFIRS 2010-2014; Buses)

NFIRS Reported Fire Involvement	Buses			
	Collision		All Fires	
	n	%	n	%
Burned but not ignition source	1	12.5	276	9.9
Burned and was ignition source	7	87.5	2510	90.1
Total	8	100	2786	100

The engine/wheel area was the most frequently identified area of origin for all bus fires (Figure 27). For buses that were not involved in the fire ignition, the passenger area was coded as the fire area of ignition 25 percent of the time. The fuel tank/fuel line area was rarely coded as the fire origin area for any bus fire.

Operating equipment and hot object were the most common determinable primary heat sources (Figure 28). The detailed breakdown of heat sources (Figure 29) indicates that radiated heat, electrical arcing, and sparks from operating equipment and overheated tires were the four most common heat sources.

Engine fuel, electrical wire, and tires are the most frequent items to be coded as first to ignite (Figures 30 and 31). Vehicle seats were coded as the first items to ignite in 1.2 percent of all bus fires. Similar results are recorded in a breakdown of the first material ignited (Figures 32 and 33). The most common materials that ignite first are flammable liquids and gases, plastics, tires, and fabrics.

The most commonly coded factors contributing to the ignition of a heavy-truck fire are mechanical or electrical failures (Figures 34 and 35). However, the detailed descriptions for these categories are most often coded as ““other.””

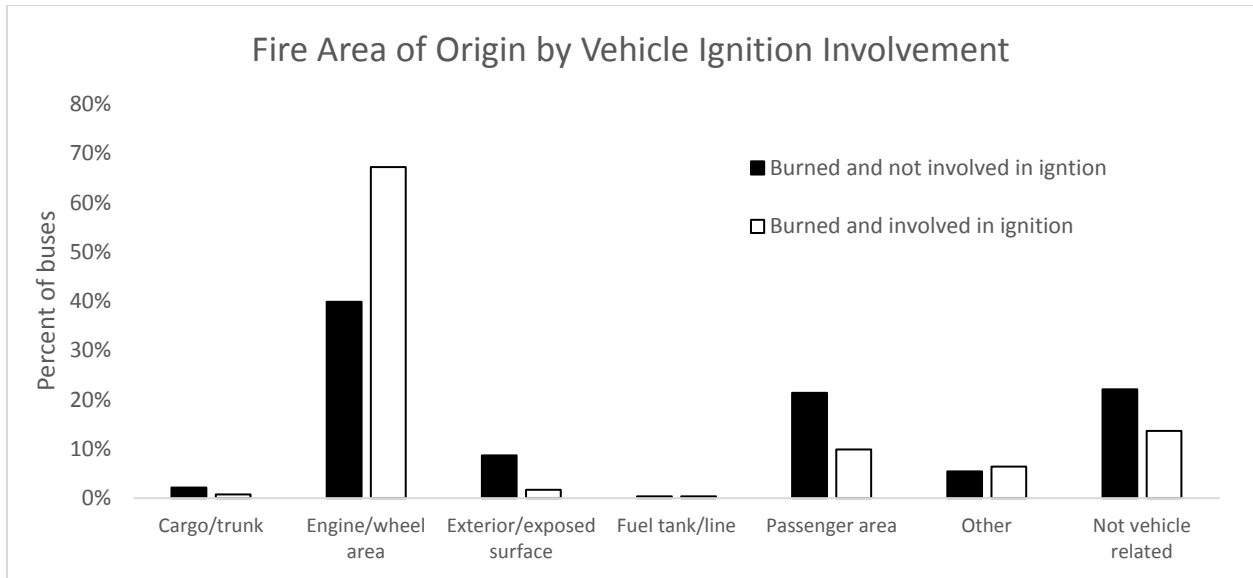


Figure B-27. Area Of Origin Versus Vehicle Involvement For All Buses (NFIRS 2010-2014; Buses)

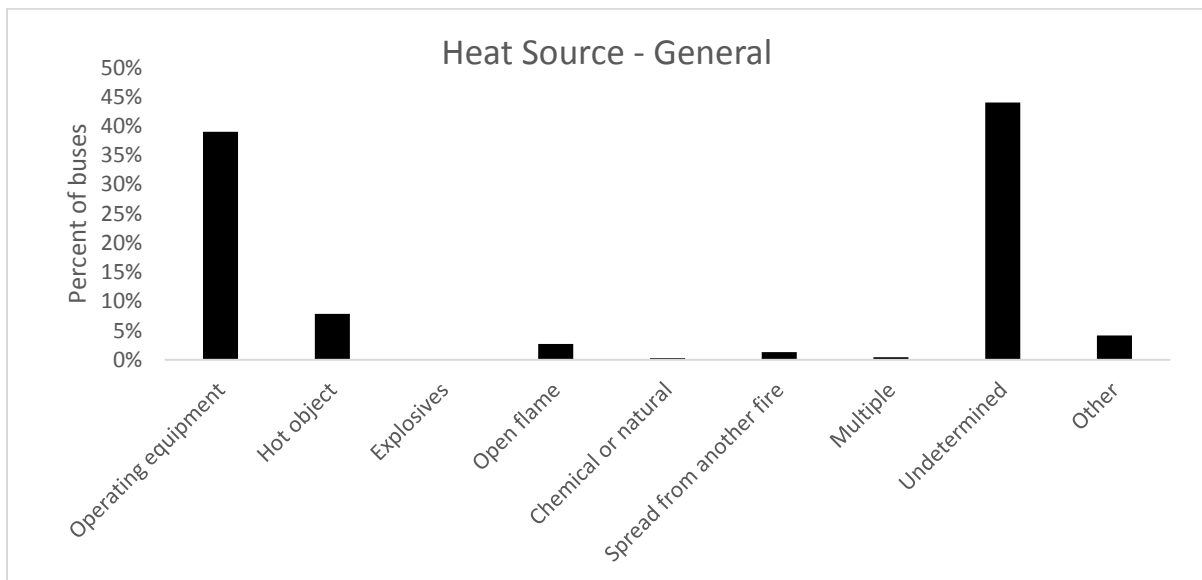


Figure B-28. Heat source that ignited the item first ignited to cause the fire; general description (NFIRS 2010-2014; Buses)

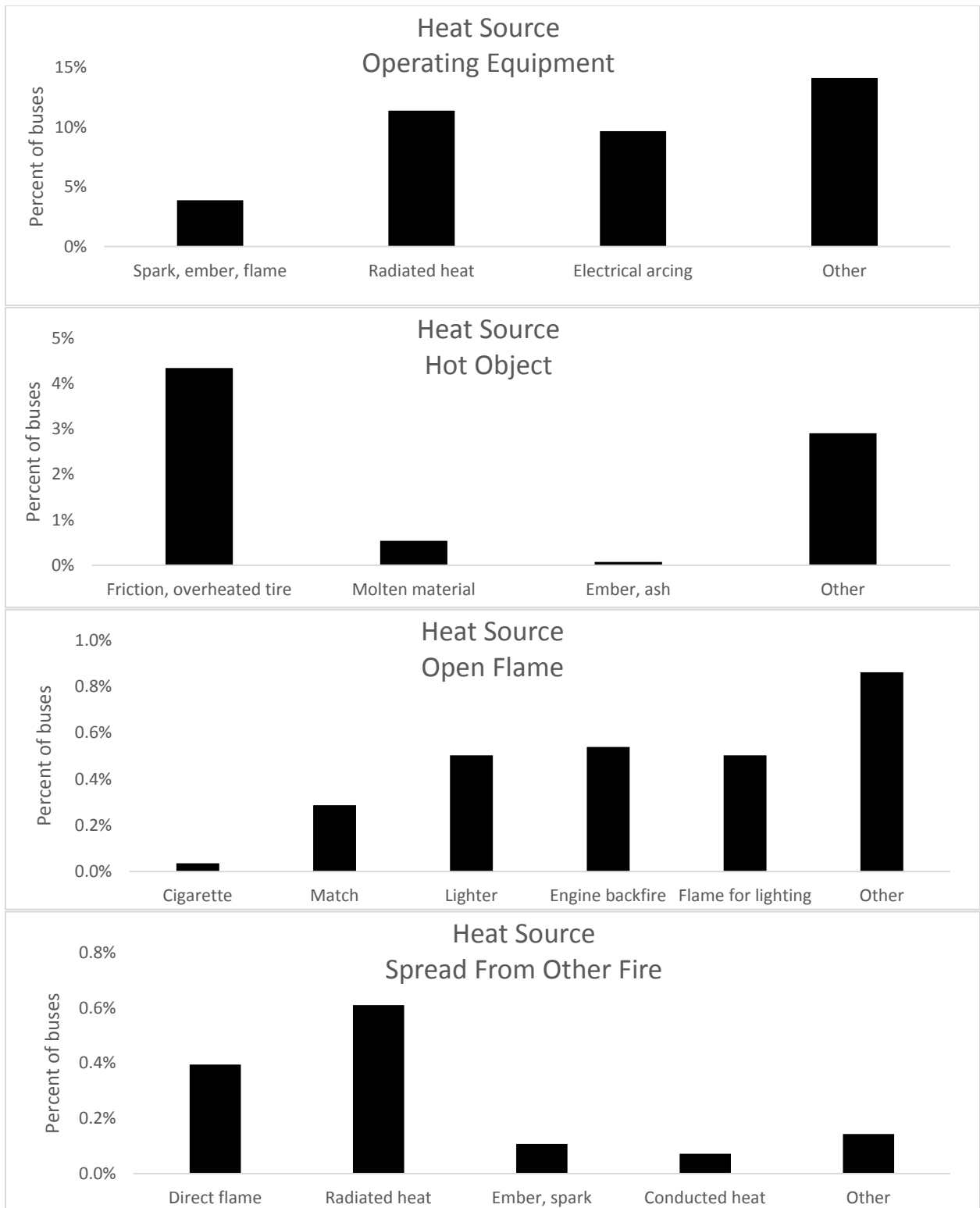


Figure B-29. Heat Source that ignited the item first ignited to cause the fire; detailed description of top 4 known general sources (NFIRS 2010-2014; Buses)

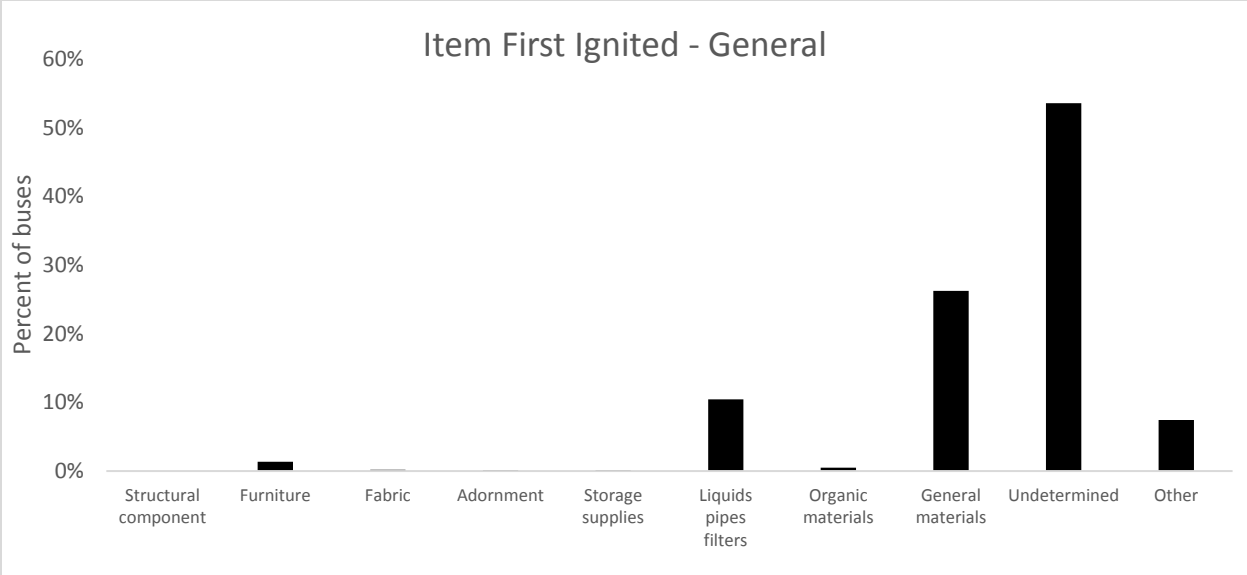


Figure B-30. Item First ignited; general description (NFIRS 2010-2014; Buses)

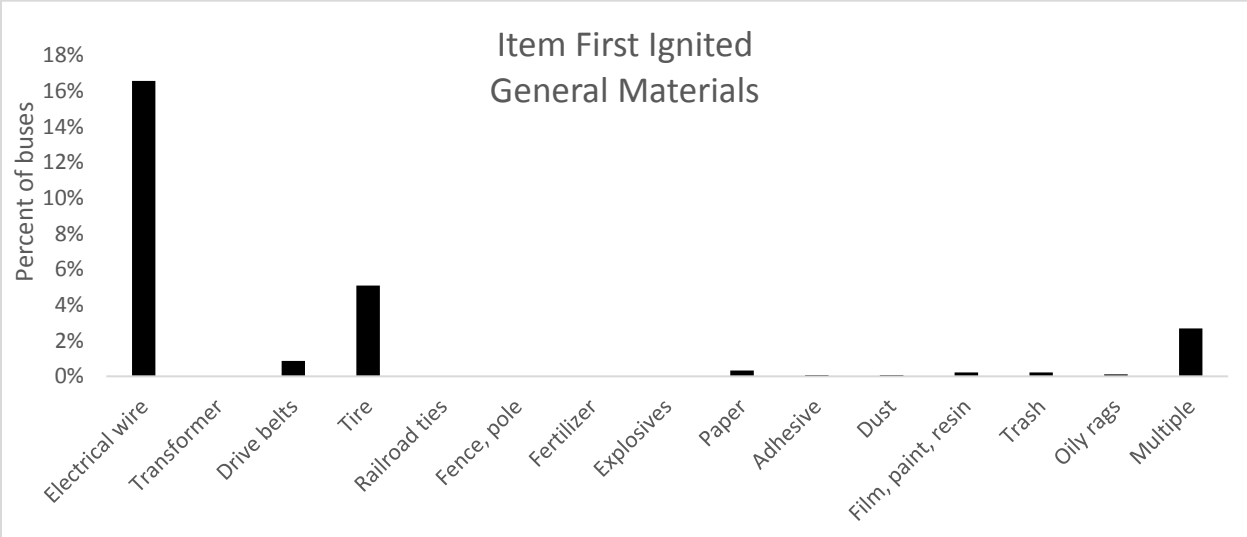
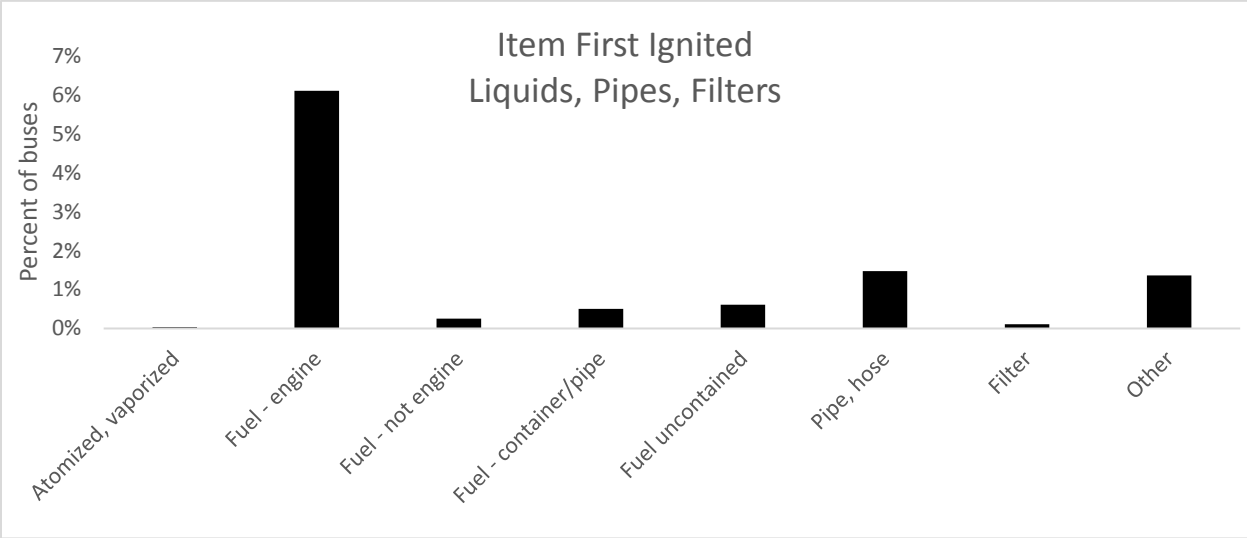
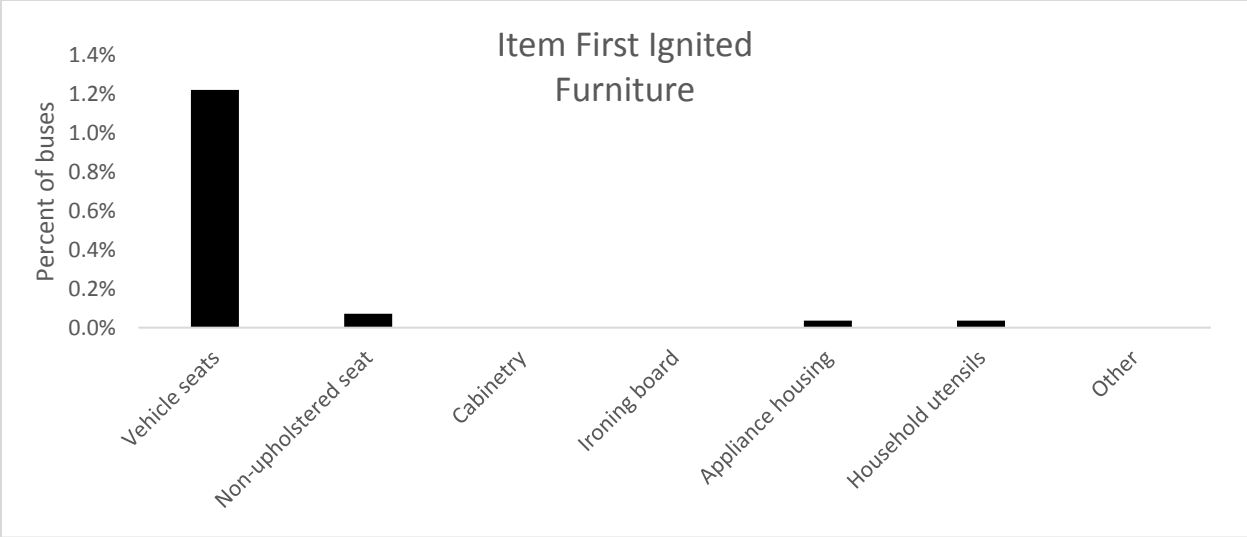


Figure B-31. Item First ignited; detailed description of 3 select general items (NFIRS 2010-2014; Buses)

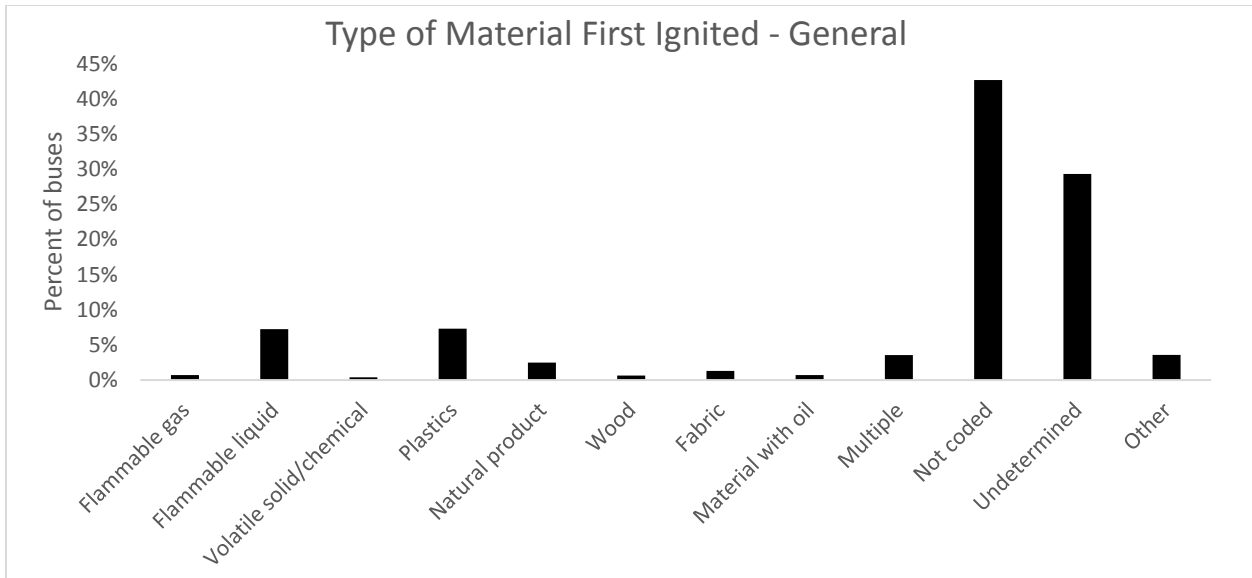


Figure B-32. Type of Material first ignited by the heat source; general description (NFIRS 2010-2014; Buses)

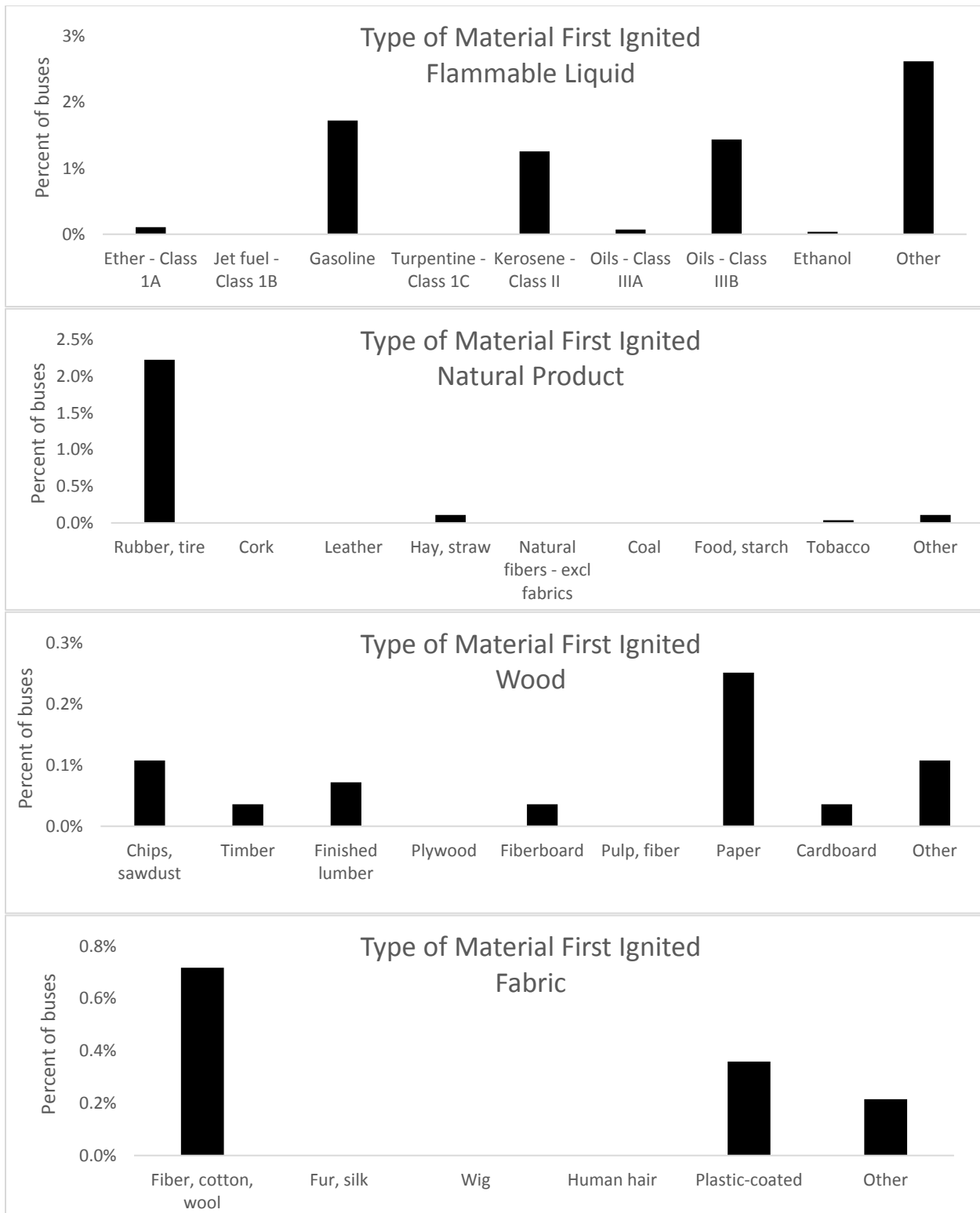


Figure B-33. Type of material first ignited by the heat source; detailed description of top 4 materials (plastics are not further disaggregated) (NFIRS 2010-2014; Buses)

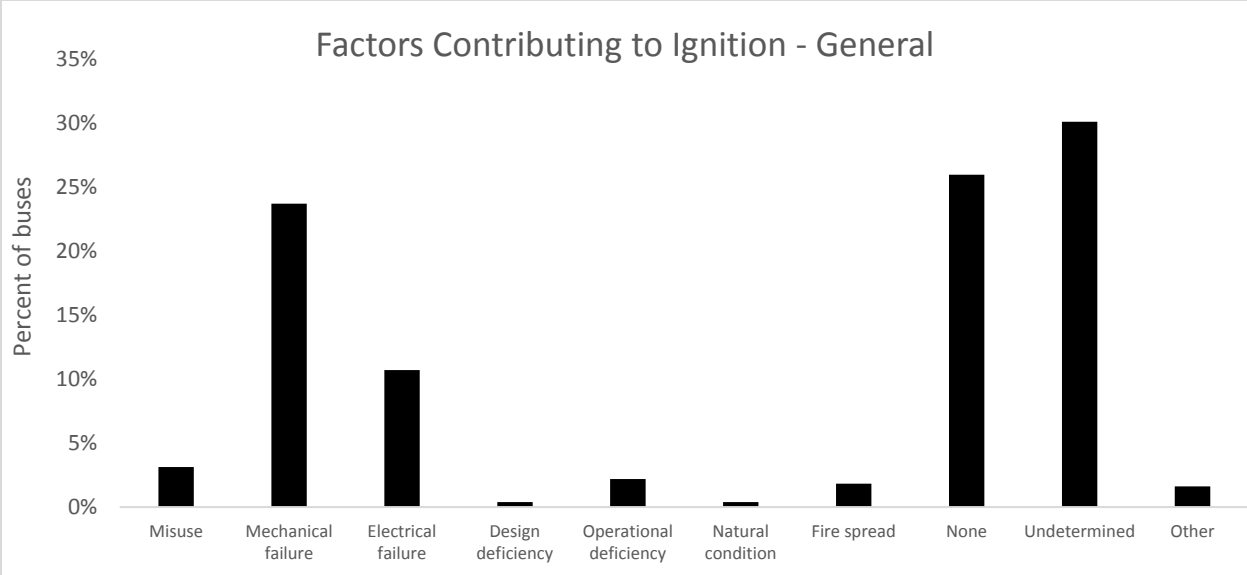


Figure B-34. Factors Contributing to ignition; general description (NFIRS 2010-2014; Buses)

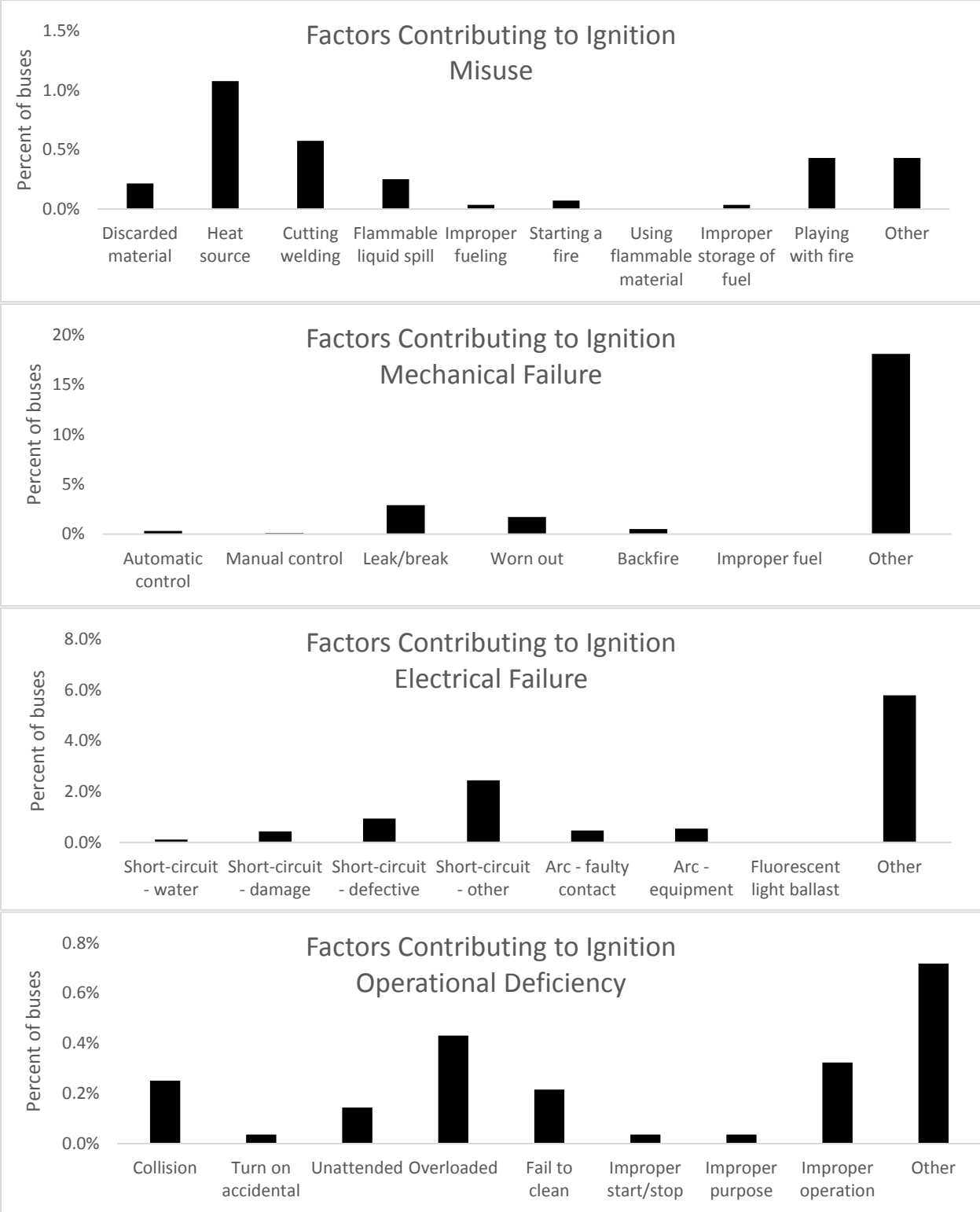


Figure B-35. Factors contributing to ignition; detailed description of 4 most common general factors (NFIRS 2010-2014; Buses)

3.5 NFIRS-5 (2010-2014; Modern Passenger Vehicles)

Fire departments do not respond to all incidents involving vehicle crashes, however they likely respond to the majority of those involving fire. Therefore, the rate of fire involvement for a given vehicle could not be determined from NFIRS data alone. To account for this, the number of vehicle fires experienced by a given make/model was normalized by its total number of fatal and police-reported crashes from FARS and GES, respectively.

The data in Table 7 include the number of vehicle fires identified in NFIRS that occurred from 2010 to 2014 for 56 unique model year 2006-2015 passenger vehicles. These 56 unique vehicle models make up the top 50 crashed vehicles identified in the FARS and GES databases from 2010 to 2014.

Figures 36 and 37 depict the normalized fire involvement rate that is defined as the number of NFIRS Fire Involvements divided by the number of fatal or police-reported crashes identified in FARS or GES for the same vehicle model for the same data years. The number of fatal or police-reported crashes for each of the 56 unique vehicle models are plotted along with the fire involvement rates. While the normalization method may not provide an accurate absolute fire involvement rate, for example not all fires in NFIRS involved a collision, it does provide a method to compare a relative rate across the selected vehicles. This method also provides a clear picture of the relationship between fire involvement and crash exposure.

There are varying fire involvement rates across vehicle models and across total crash numbers. The vehicles with the greatest number of crashes also have the greatest number of fires; a relationship likely based on vehicle sales and mileage.

Table B-7. Number of Fire Involvements (NFIRS 2010-2014; Modern Passenger Vehicles) for 56 Most Commonly Crashed Vehicles (FARS & GES 2010-2014; MY 2006+)

NFIRS Data years 2010-2014; Vehicle Model Years 2006+			
Vehicle	Vehicle fires (NFIRS)	Fatal Crashes with or without fire (FARS)	Police-reported crashes with or without fire (GES-weighted)
Ford F-Series Pickup	2,117	2,900	626,482
Chevrolet C, K, R, V Series Pickup	1,200	2,528	502,883
Nissan Altima	1,081	1,602	279,918
Dodge Ram Pickup	1,063	1,133	428,762
Dodge Charger	1,010	603	165,652
Chevrolet Impala	884	1,171	343,766
Toyota Camry	774	1,251	564,688
Chevrolet Malibu	549	842	299,302
Honda Accord	530	988	448,549
Chevrolet Cobalt	502	908	237,433
Honda Civic	433	1,096	474,173
GMC C, K, R, V Series Pickup	430	908	299,094
Ford Focus	425	370	119,906
Toyota Corolla	414	835	169,606
Chrysler 300	412	1,155	393,808
Ford Fusion	392	728	317,760
Hyundai Sonata	377	574	224,238
Jeep Wrangler	343	551	154,786
Dodge Grand Caravan	337	371	99,296
BMW 3-Series	329	390	125,587
Pontiac G6	327	258	120,539
Chevrolet Blazer	325	408	152,778
Ford Escape	321	572	279,418
Ford Taurus	313	537	170,820
Ford Mustang	307	459	138,698
Nissan Maxima	290	270	81,914
Ford Bronco/Explorer	281	346	132,807
Dodge Avenger	269	272	99,096
Nissan Sentra	266	471	163,530
Ford Crown Victoria	247	325	145,154
VW Jetta	241	426	164,792
Chevrolet Trailblazer	232	311	72,213
Chrysler Town and Country	228	484	115,664
Ford E-Series Van	218		154,150

NFIRS Data years 2010-2014; Vehicle Model Years 2006+			
Vehicle	Vehicle fires (NFIRS)	Fatal Crashes with or without fire (FARS)	Police-reported crashes with or without fire (GES-weighted)
Toyota Tundra	214	430	133,076
Chevrolet Equinox	193	445	142,548
Chevrolet HHR	191	353	161,529
Toyota RAV4	190	514	118,094
Dodge Caliber	184	349	108,021
Kia Optima	183	269	79,248
Toyota Tacoma	180	417	151,002
Mazda 3	177	263	84,056
Hyundai Elantra	156	262	162,934
Chevrolet Cruze	153	485	171,660
Honda Odyssey	148	270	98,784
Nissan Versa	138	377	120,048
Ford Ranger	136	280	72,694
Toyota Sienna	122	254	127,624
Ford Edge	117	280	113,114
Honda Pilot	112	426	211,588
Honda CR-V	110	247	112,581
Toyota Scion tC	93	429	171,480
Toyota Highlander	91	257	109,887
Toyota Prius	84	283	61,456
Jeep Cherokee	83	335	144,762
Toyota Yaris	79	274	81,841

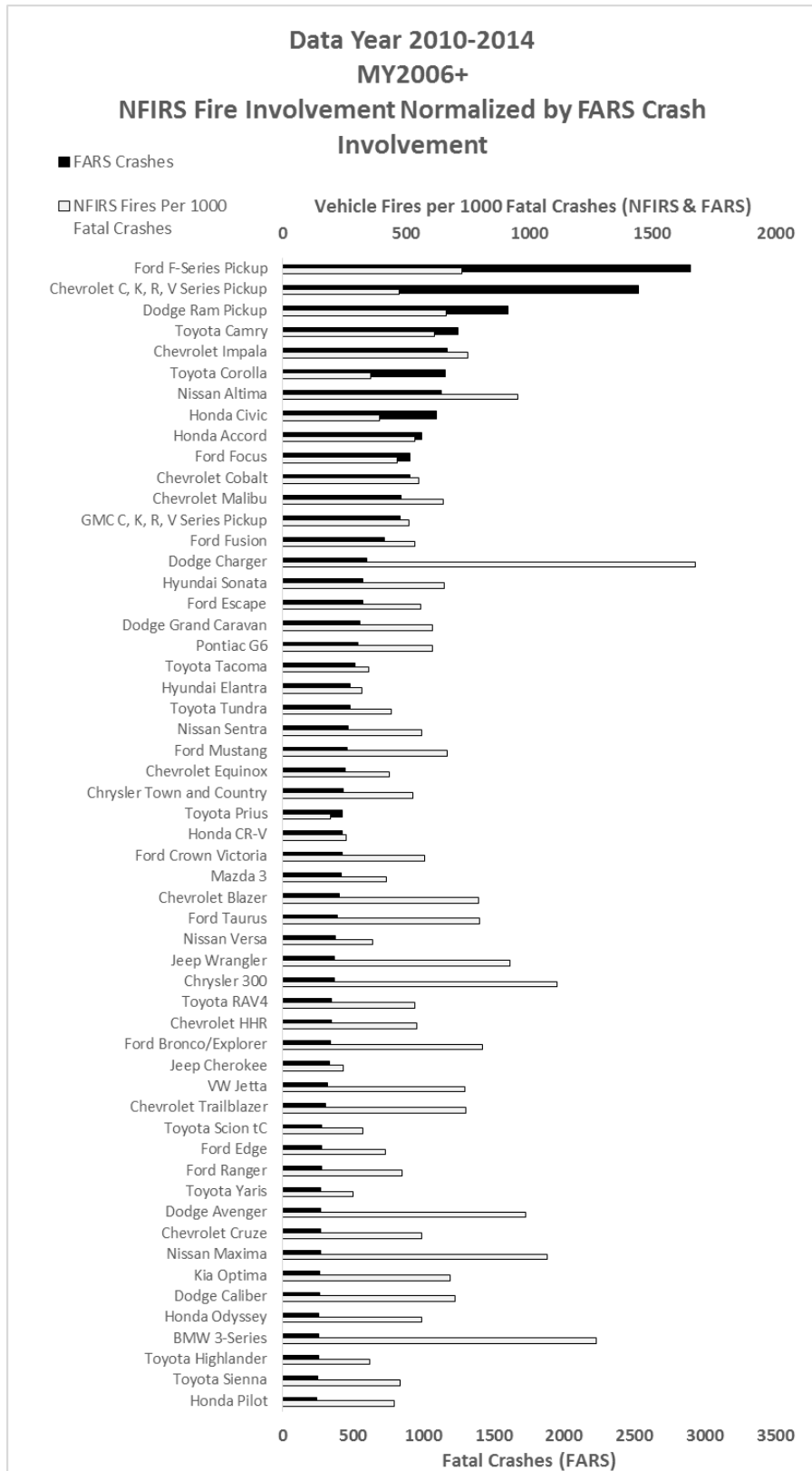


Figure B-36. Fire involvement (NFIRS) Normalized by fatal crash involvement (FARS); Sorted by descending number of fatal crashes

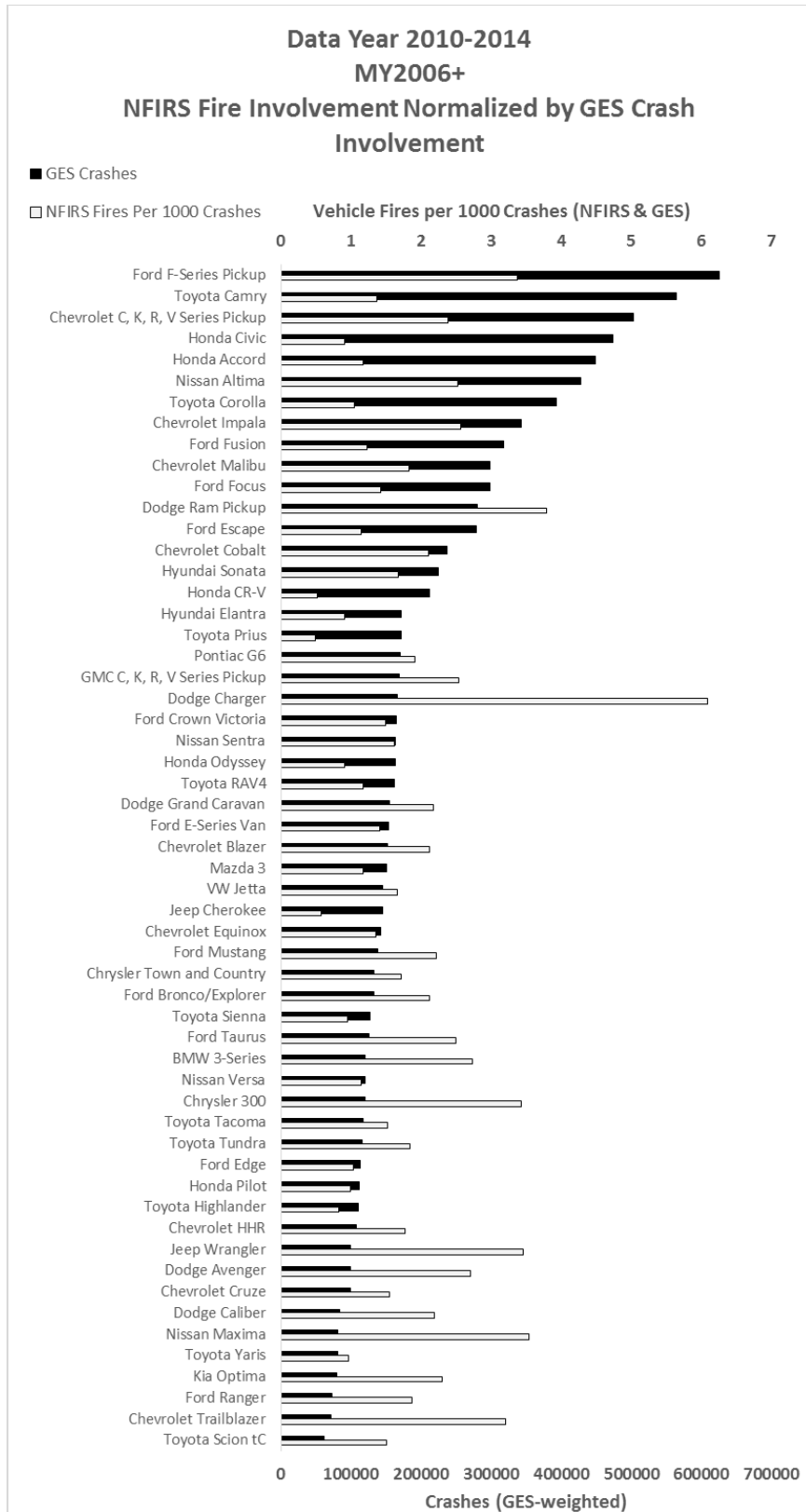


Figure B-37. Fire involvement (NFIRS) Normalized by crash involvement (GES); Sorted by descending number of crashes

3.6 NASS-GES (2000-2015)

Data in NASS_GES from 2000 to 2015 was interrogated to investigate the characteristics of vehicle fires. Tables 8 and 9 summarize the total number of crashes, with and without fire involvement, for light passenger vehicles and heavy trucks and buses. Approximately 0.1 percent of all passenger vehicles were coded as having been involved in fires, regardless of their specific body type. Medium/heavy trucks had 4 times the rate of fire involvement than passenger vehicles, while buses were rarely involved in fires.

The total number of crashes for all vehicle types has increased over the past 5 to 6 years, after abnormally low counts experienced partially as a result of effects from the global financial crisis (Figures 38 and 40). During that same time the fire occurrence rate for passenger vehicles has generally decreased from about 0.13 percent to 0.07 percent (Figure 39). The fire involvement rate for medium/heavy trucks, while somewhat erratic over the previous 5 years, has reached its lowest level for the previous 16 years (Figure 41). There were only 2 cases of bus fires identified in the GES, representing a weighted value of 30 cases.

Figures 42 and 43 describe the frequency of vehicles involved in crashes by initial contact point, defined as the area on each vehicle that produced the first instance of injury or that resulted in the first instance of damage. The vast majority of passenger vehicles involved in crashes sustained initial damage to the front, back, or sides. Similar results are obtained for trucks and buses. Initial contact points identified as front or non-collision made up approximately 40 percent of all cases resulting in passenger vehicle fires (Figure 44). The majority of the remaining 10 percent of passenger vehicles that burned were shared between right, left, or back initial contact points. For trucks and buses the initial contact point defined as non-collision made up approximately 63 percent of all vehicle fires with front contact points accounting for 23 percent.

Table B-8. Fire Occurrence For Passenger Vehicles In Police-Reported Crashes (NASS GES 2000-2015)

Fire Occurrence	Automobiles		Light trucks		Utility vehicles		Van-based light trucks	
	n	%	n	%	n	%	n	%
No Fire	92,172,357	99.9	27,751,280	99.9	25,558,390	99.9	11,044,487	99.9
Fire	89,291	0.1	35,593	0.1	22,769	0.1	14,589	0.1
Total	92,261,648	100	27,786,873	100	25,581,159	100	11,059,076	100

Table B-9. Fire Occurrence For Trucks and Buses In Police-Reported Crashes (NASS GES 2000-2015)

Fire Occurrence	Medium/heavy trucks		Buses	
	n	%	n	%
No Fire	5,623,175	99.6	917,999	100
Fire	25,243	0.4	30	0.0
Total	5,648,418	100	918,029	100

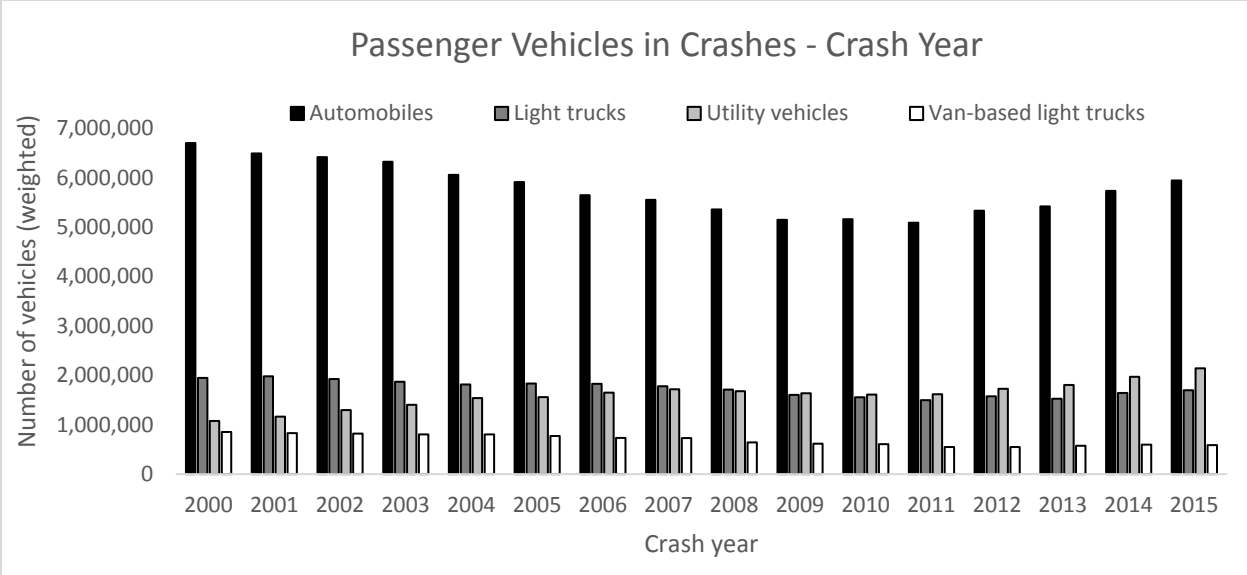


Figure B-38. Passenger Vehicle crash count by crash year (NASS GES 2000-2015)

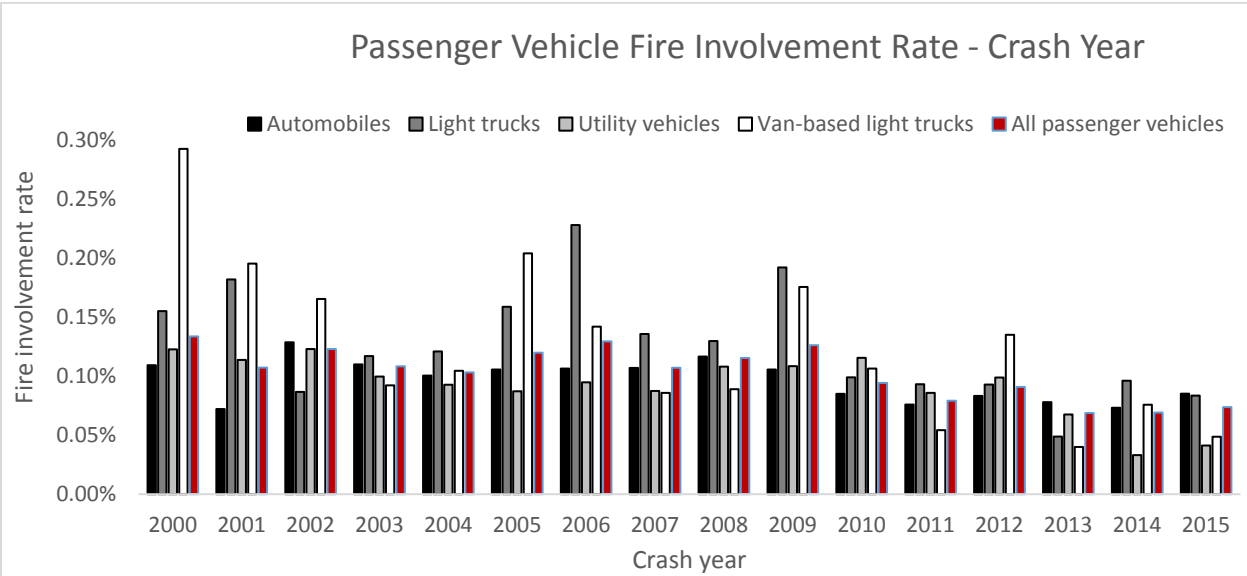


Figure B-39. Passenger vehicle fire involvement rate by crash year (NASS GES 2000-2015)

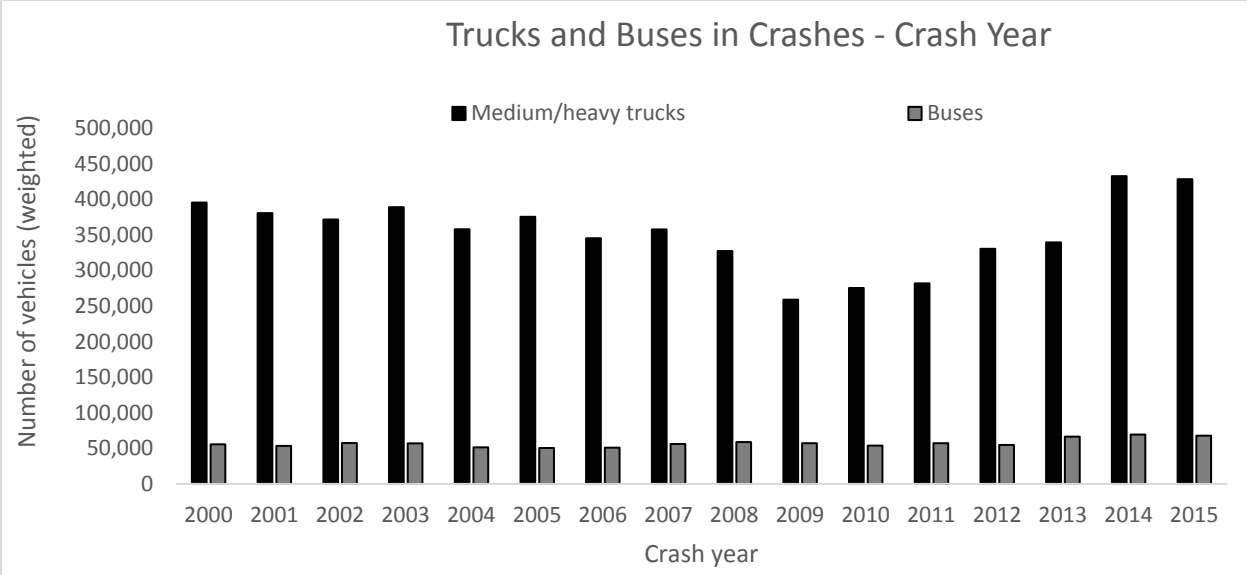


Figure B-40. Truck And bus crash count by crash year (NASS GES 2000-2015)

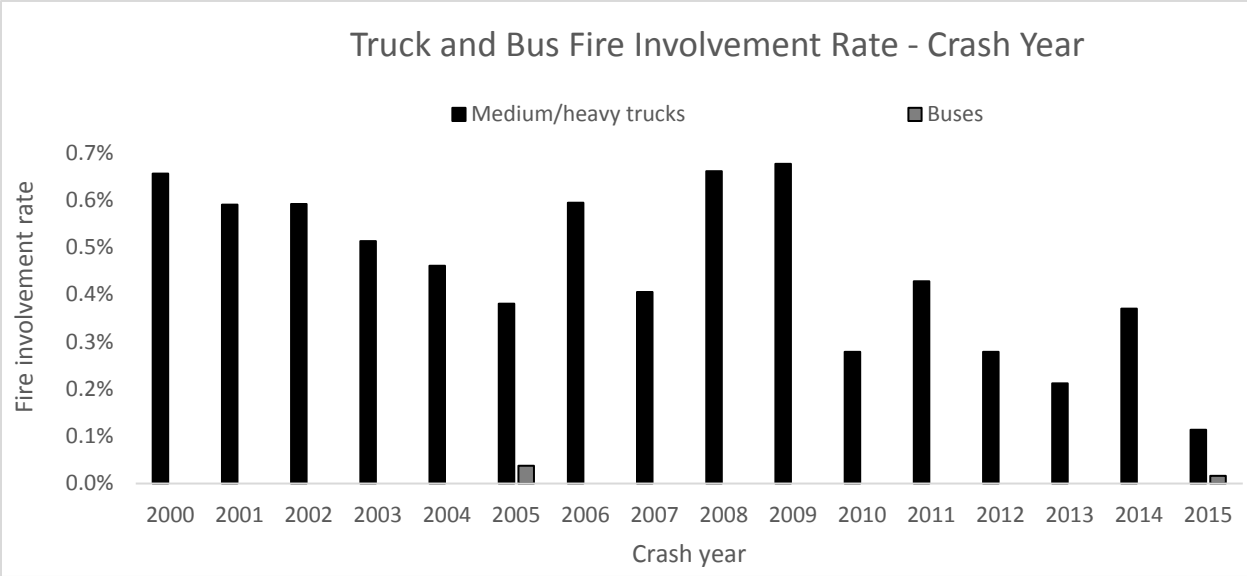


Figure B-41. Truck and bus crash fire involvement rate by crash year (NASS GES 2000-2015)

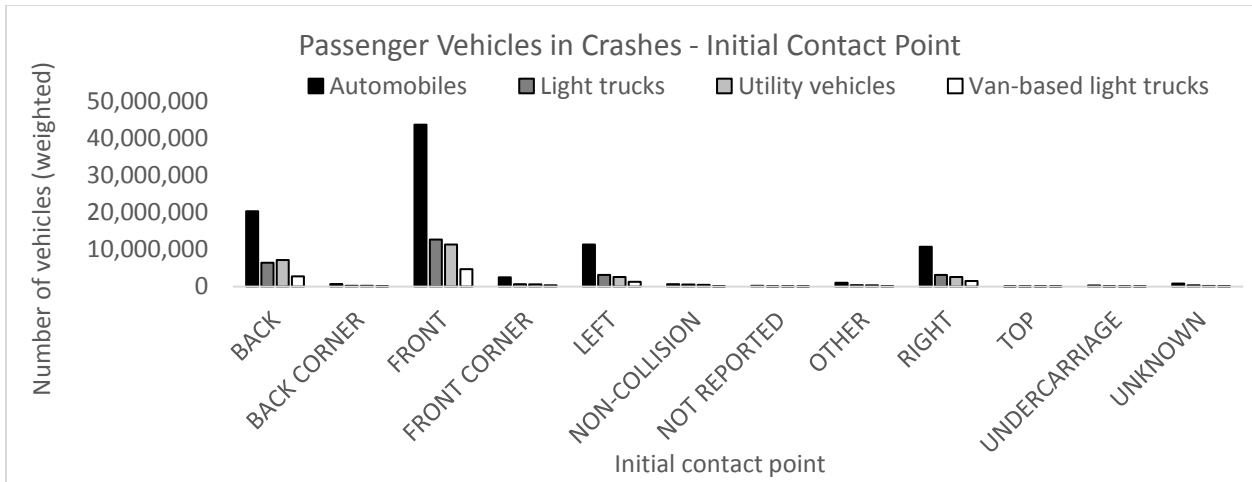


Figure B-42. Passenger vehicles in crashes by initial contact point (NASS GES 2000-2015)

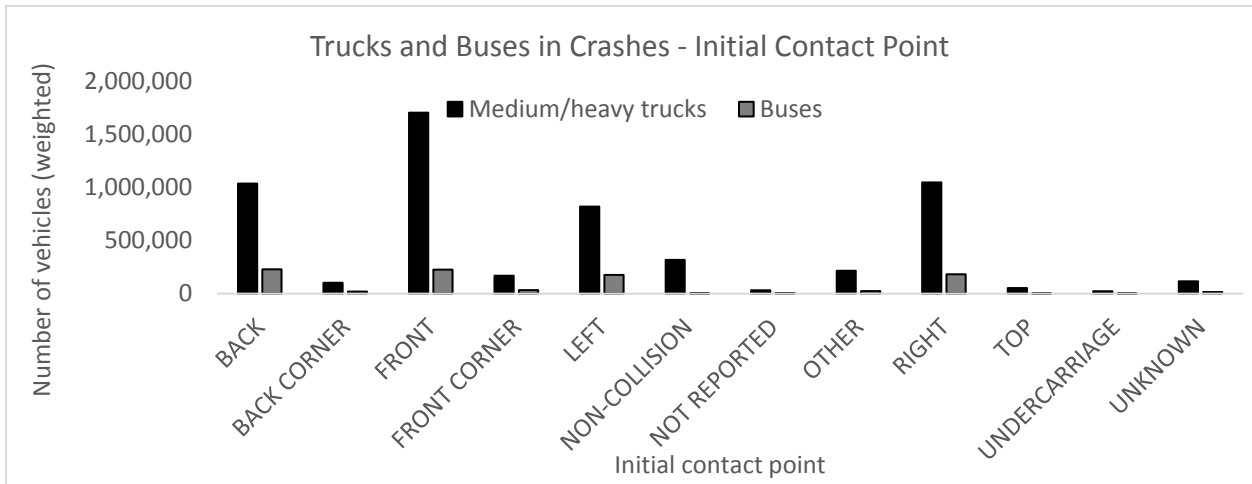


Figure B-43. Trucks and buses in crashes by initial contact point (NASS GES 2000-2015)

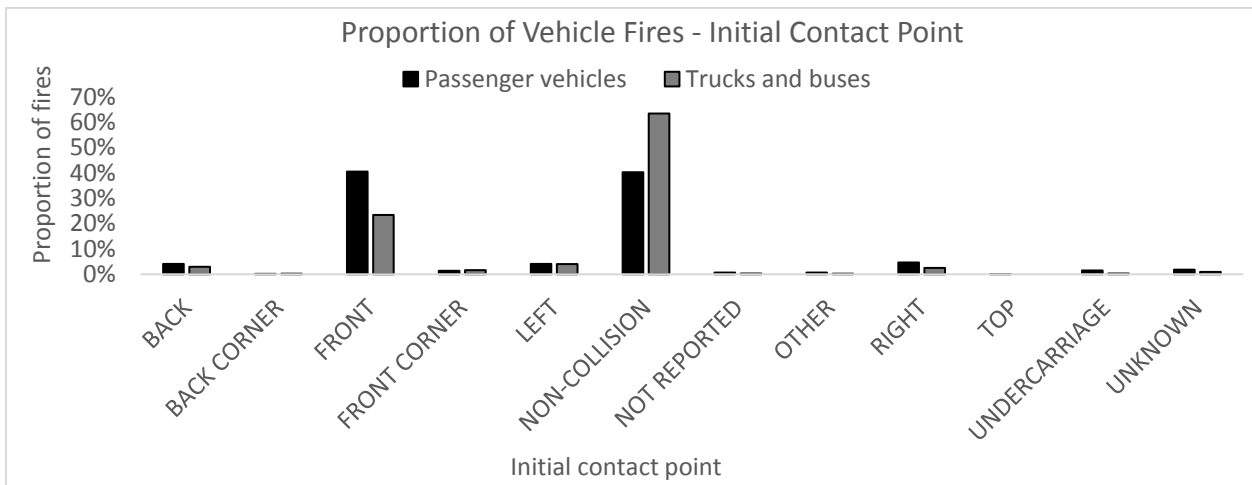


Figure B-44. Proportion of vehicle fires by initial contact point (NASS GES 2000-2015)

3.7 FARS – (1991-2015)

The average fire occurrence rate for passenger vehicles involved in fatal crashes is 2.8 percent over the past 25 years (Table 10). Medium/heavy trucks have twice the rate of passenger vehicles while buses have approximately one-quarter the rate of fire occurrence as that of passenger vehicles (Table 11). Automobiles comprise the largest number of vehicle fires, although light trucks and utility vehicles have slightly higher rates of fire occurrence.

The number of fatal crashes for passenger vehicles and medium/heavy trucks decreased from 2005 to 2011, and increased slightly from 2011 to 2015 (Figures 45 and 47). Over the past 25 years the rate of fire occurrence for passenger vehicles in fatal crashes has generally increased from 2.8 percent in 1991 to nearly 3.2 percent in 2015 (Figure 46). A similar increase has been observed for medium/heavy trucks with fire rates increasing from approximately 4.5 percent to over 6 percent from 1991 to 2015 (Figure 48).

Vehicles in fatal crashes were predominantly identified as having an initial point of contact to the front (Figures 49 and 50). This trend was also observed for fires that occurred in vehicles that were involved in fatal crashes. Approximately 70 percent of all passenger vehicle and truck/bus fires in fatal crashes were sustained by vehicles identified as having an initial point of contact to the front area (Figure 51).

Vehicle age is positively correlated to fire involvement rate for passenger vehicles involved in fatal crashes (Figure 52). Approximately 2.3 percent of passenger vehicles less than 5 years old sustain fires in fatal crashes. This rate nearly doubles for passenger vehicles over 20 years old. The opposite trend, while not as strong, is observed for trucks and buses, where older vehicles tend to have lower rates of fire involvement in fatal crashes.

Table B-10. Fire Occurrence For Passenger Vehicles In Fatal Crashes (NASS GES 2000-2015)

Fire Occurrence	Automobiles		Light trucks		Utility vehicles		Van-based light trucks	
	n	%	n	%	n	%	n	%
No Fire	608,172	97.2	241,545	97.0	141,628	97.1	75,568	97.7
Fire	17,462	2.8	7,423	3.0	4,169	2.9	1,740	2.3
Total	625,634	100	248,968	100	145,797	100	77,308	100

Table B-11. Fire Occurrence For Trucks and Buses In Fatal Crashes (NASS GES 2000-2015)

Fire Occurrence	Medium/heavy trucks		Buses	
	n	%	n	%
No Fire	104,900	94.4	6,852	99.2
Fire	6,184	5.6	57	0.8
Total	111,084	100	6,909	100

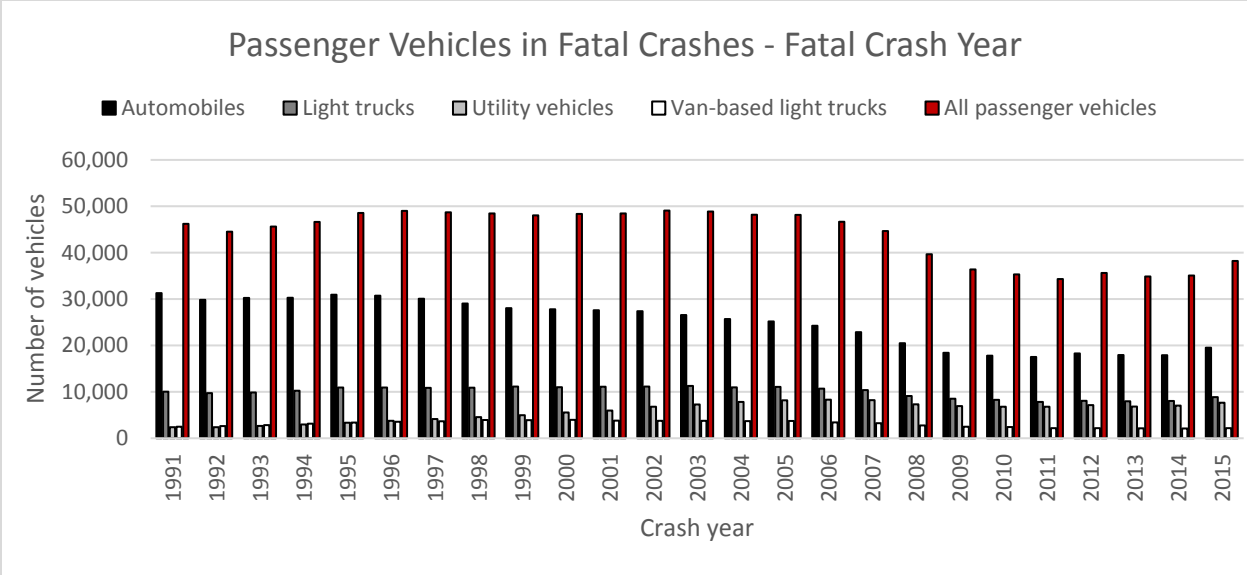


Figure B-45. Passenger vehicle fatal crash count by crash year (FARS 1991-2015)

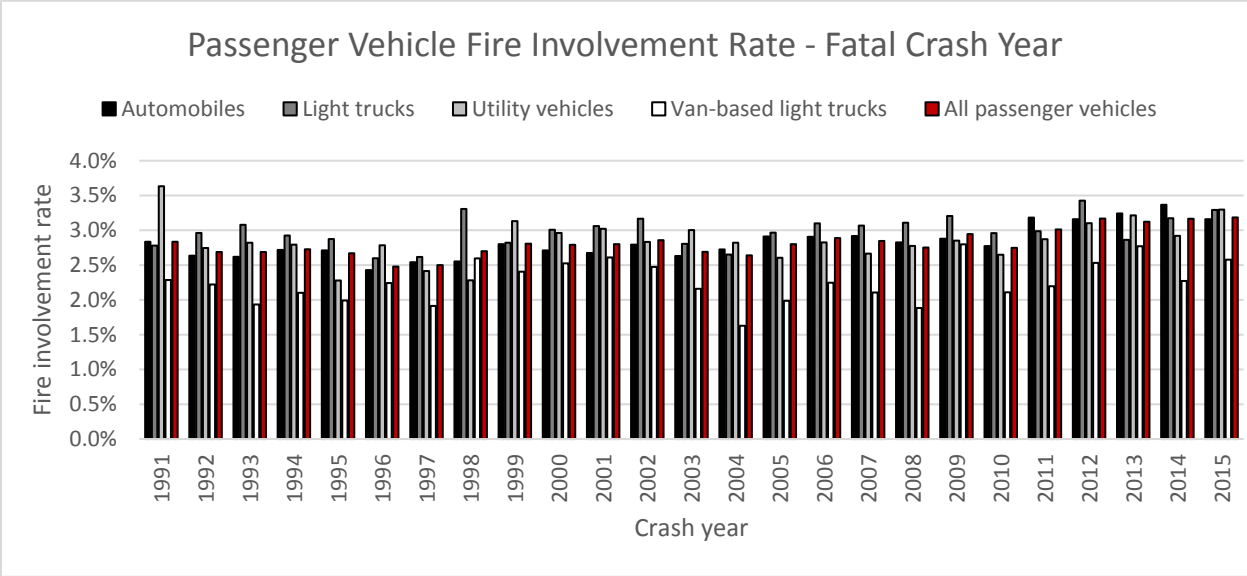


Figure B-46. Passenger vehicle fire involvement rate in fatal crashes by crash year (FARS 1991-2015)

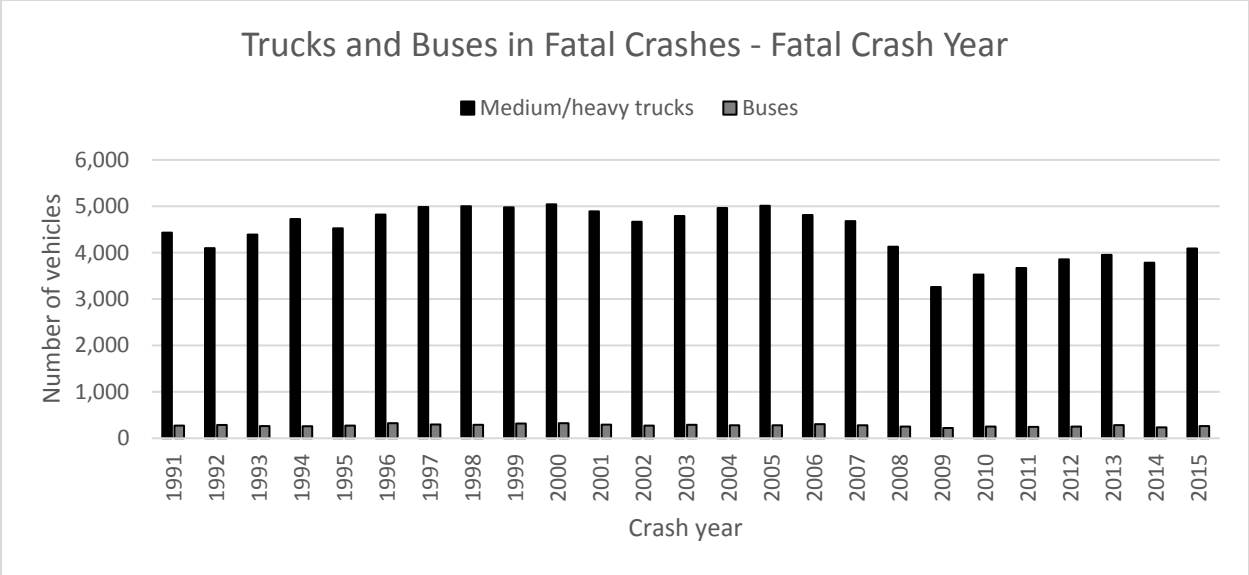


Figure B-47. Truck and bus fatal crash count by crash year (FARS 1991-2015)

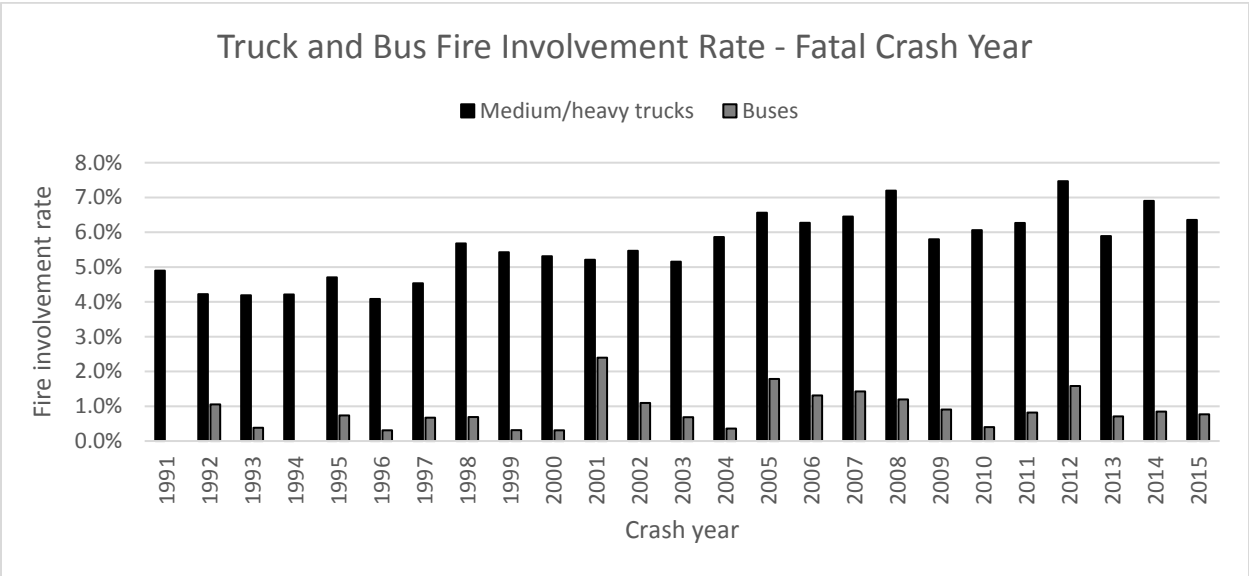


Figure B-48. Truck and bus fire involvement rate in fatal crashes by crash year (FARS 1991-2015)

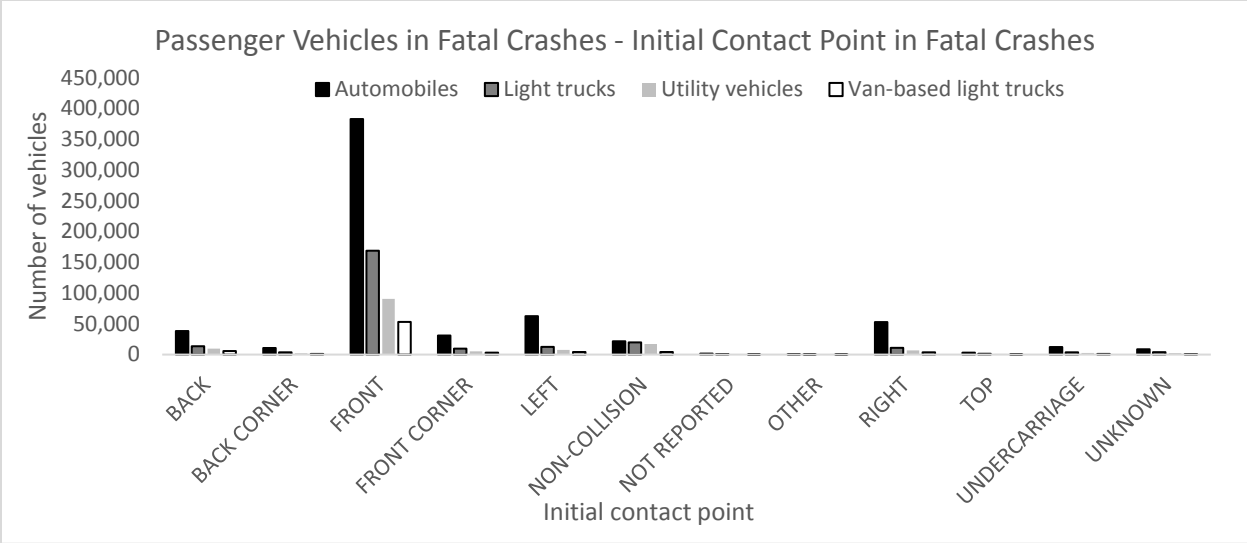


Figure B-49. Passenger vehicles in fatal crashes by initial contact point (FARS 1991-2015)

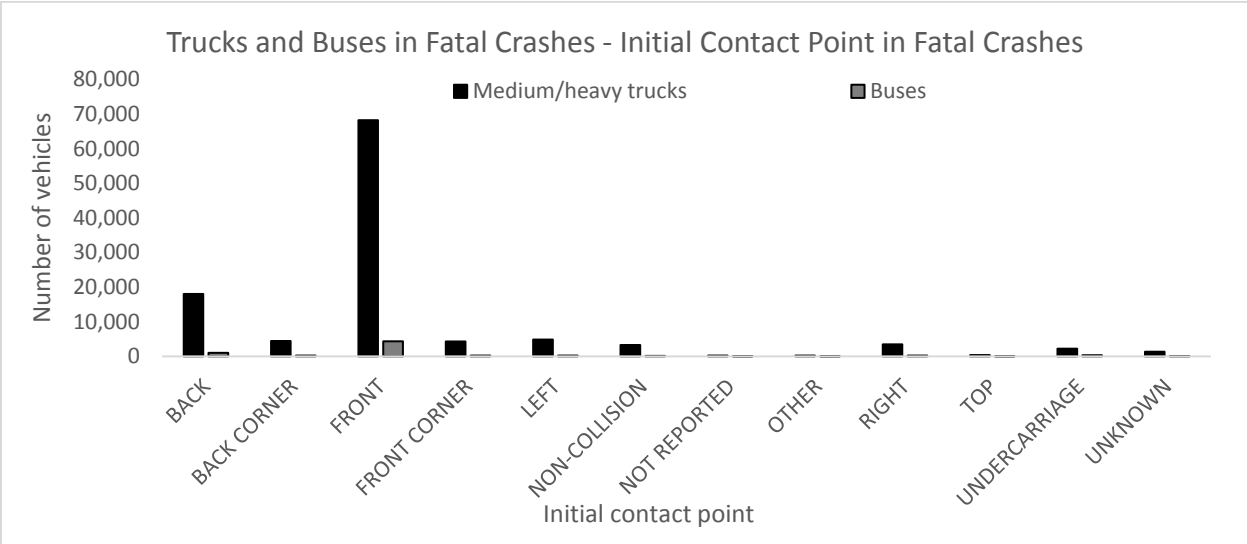


Figure B-50. Trucks and buses in fatal crashes by initial contact point (FARS 1991-2015)

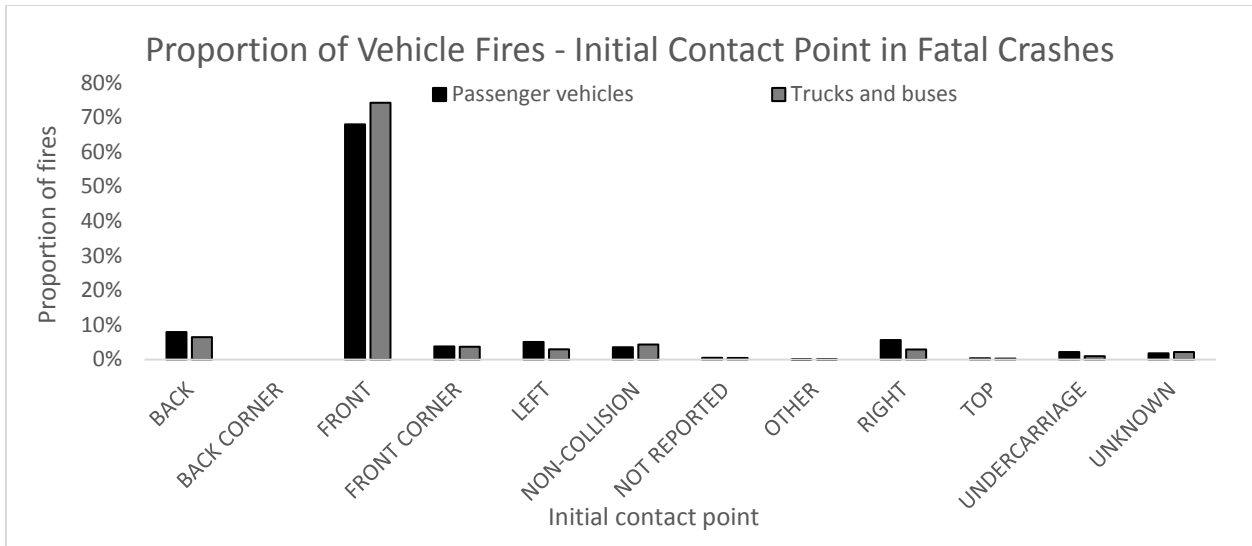


Figure B-51. Proportion of vehicle fires in fatal crashes by initial contact point (FARS 1991-2015)

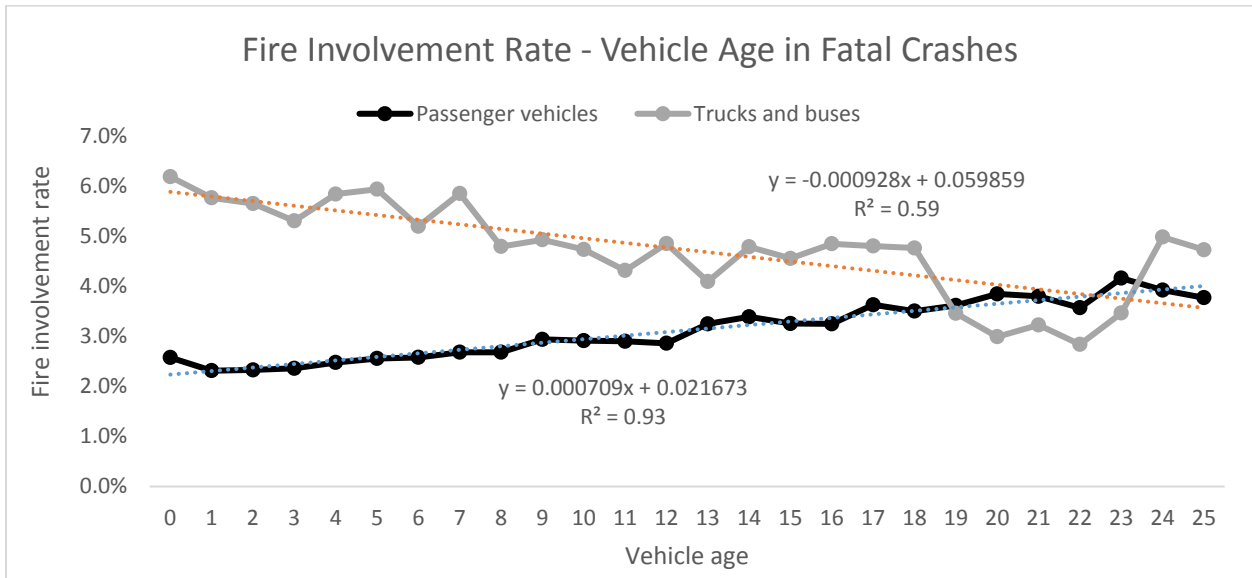


Figure B-52. Vehicle fire rate by vehicle age in fatal crashes (FARS 1991-2015)

3.8 NASS-CDS – (1995-2015)

Passenger vehicle fires from NASS CDS were investigated to determine the path of fire ingress and interior components that burned. A summary of all passenger vehicle fires in NASS CDS between 1995 and 2015 is provided in Table 12. Approximately 0.24 percent of crashes were identified as having a major or minor fire. Most fires, approximately 80 percent, were coded as originating in the engine compartment (Figure 53). The fuel tank was the next most common area of fire origin followed by the instrument panel.

Passenger vehicle fire cases from the CDS were reviewed individually on a case-by-case basis using the online XML viewer to determine methods of fire ingress into the occupant compartment. The cases were reviewed in order of increasing vehicle age starting with the 2015 model

year. A total of 228 cases were investigated that included vehicle model years from 2002 to 2015 and in crash years from 2002 to 2015.

For 74 percent of cases the fire damage was too extensive or the available pictures were too poor to be able to estimate the region of ingress (Figure 54). For those cases in which the ingress area could be identified “over dash” and “rear” were the most common regions. A determination of individual components that were damaged by fire was able to be undertaken for approximately 13 percent of passenger vehicle fire cases; those with moderate and minor fire damage as assessed in our investigation (Figure 55). Of the remaining cases, 60 percent had complete interior fire damage and 27 percent had no interior fire damage. The distribution of components damaged by fire in the 13 percent of vehicles with moderate or minor interior fire damage are outlined in Figure 56. The results indicate that the fire moves in a general front-to-rear and bottom-to-top direction. In general this includes, in order of decreasing frequency, fire damage to the top dash, sun visor, front headliner, mid dash, steering wheel, mid headliner, steering wheel air bag, and front seat backs.

In the “over dash” cases, it was found that the fire appeared to burn through the windshield (which may have been fractured in the crash or due to extreme heat) and then onto the dash. The fire then appeared to burn the headliner and make its way down the dash. It was noted that the upper dash always burned first prior to headliner, lower dash, or seats in these cases. The ingress area was always associated with a fractured windshield and often also included a deformed hood. Some example pictures are depicted in Figure 57. Rear fire ingress was commonly associated with significant rear damage, as shown in Figure 58. One incident with rear-fire ingress was identified in which no major damage was observed other than detachment of fuel lines caused by driving over a downed pole. Fire ingress through the firewall/dash was difficult to identify due to the fact that they can only be identified in cases that did not significantly burn and which fire ingress through the windshield/over the dash could be eliminated. While there is some evidence of fire ingress through heavily damaged firewalls (Figure 59), it appears that this mechanism results in a slow-moving fire that would be secondary in risk and danger to a fire progressing through the windshield.

Table B-12. Fire Occurrence In Crashes (NASS CDS 1995-2015)

NASS CDS Reported Fire Occurrence	Weighted		Raw		In-Depth Review
	n	%	n	%	n
No Fire	58,950,875	99.33	115,774	98.56	0
Minor Fire	56,797	0.1	437	0.37	81
Major Fire	80,575	0.14	607	0.52	147
Unknown	258,002	0.43	648	0.55	0
Total	59,346,249	100	117,466	100	228

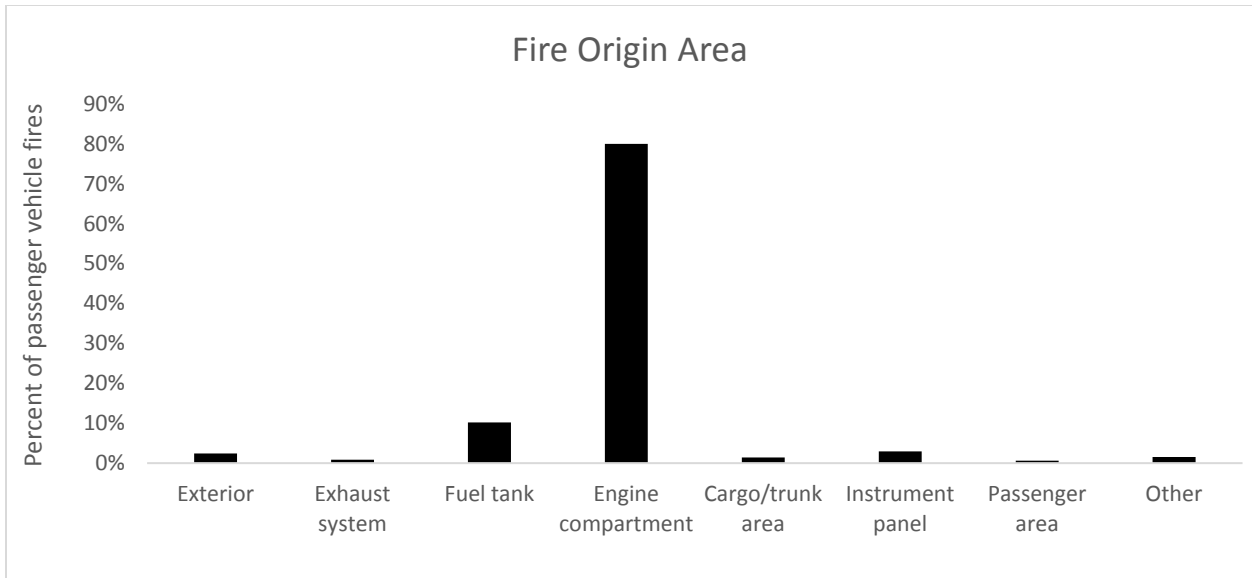


Figure B-53. Passenger vehicle fire area of origin (NASS CDS 1995-2015)



Figure B-54. Passenger vehicle fire ingress area (NASS CDS - 228 cases)

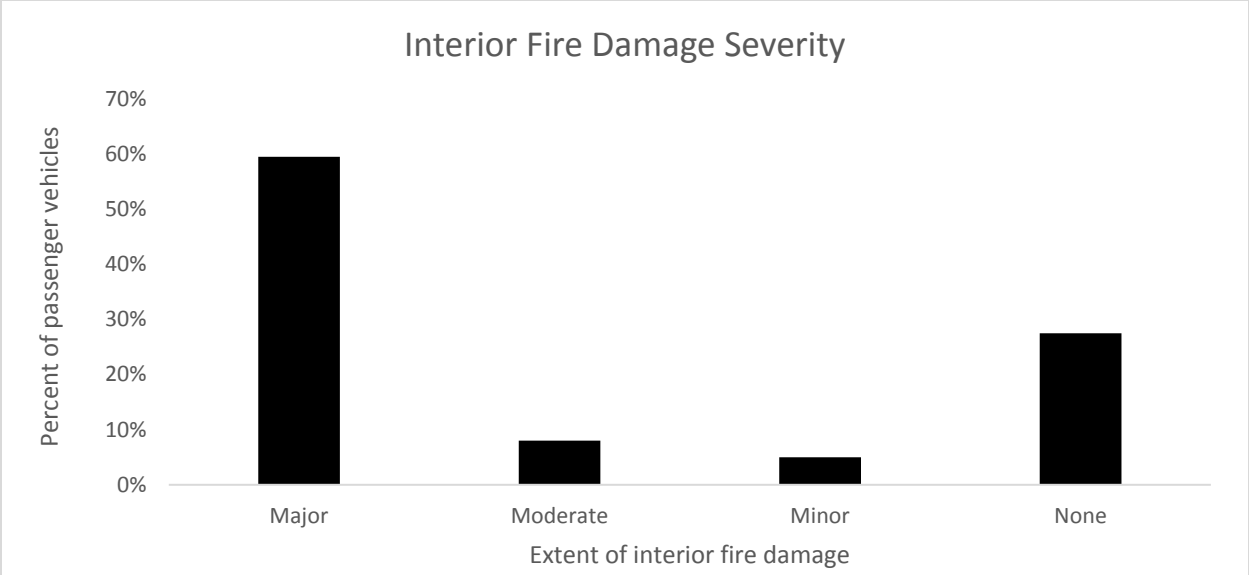


Figure B-55. Passenger vehicle interior fire damage severity (NASS CDS - 228 cases)

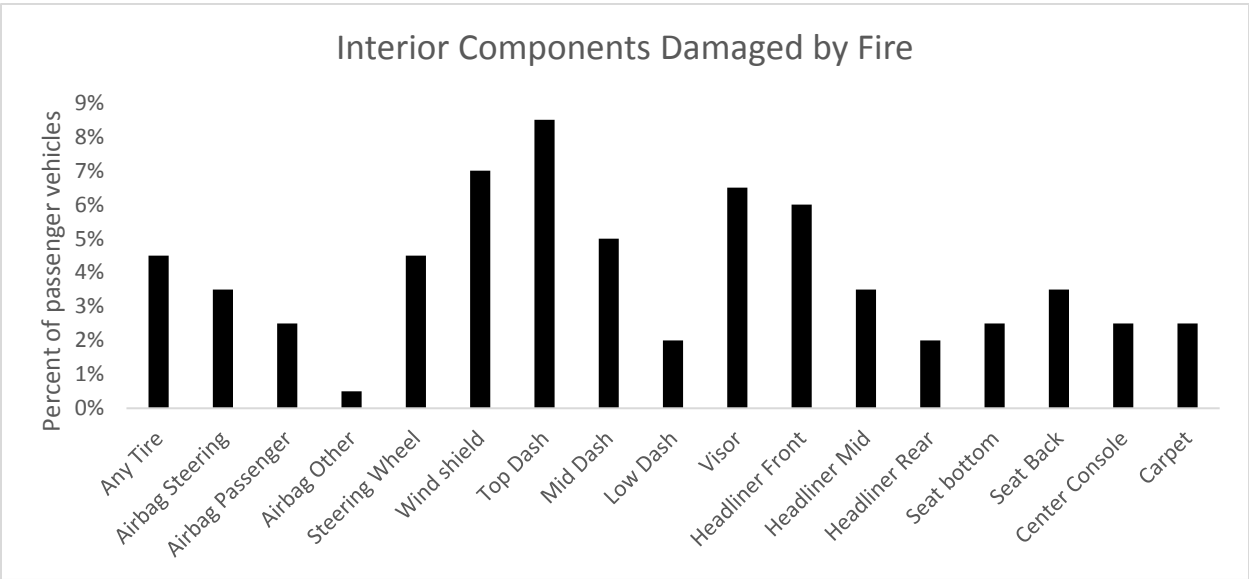


Figure B-56. Passenger vehicle interior component damaged by fire (NASS CDS - 228 cases)



Figure B-57. Example cases with fire ingress through the windshield and over the dash. top left (2004-02-65) top right (2011-09-38) bottom left (2005-50-147) bottom right (2005-43-215)



Figure B-58. Example cases with fire ingress from rear. Left (2013-81-125) right (2007-49-156)



Figure B-59. Example cases with fire ingress through dash/firewall. Left (2009-45-186) right (2011-78-134)

4 Discussion

The number and rate, per police-reported crash, of passenger vehicle fires has decreased over the past decade. This is true for all passenger vehicle fires as well as crash-related fires. However, the rate of fire involvement for passenger vehicles involved in fatal crashes has increased over the past 26 years. This is likely due to improved vehicle crashworthiness that has resulted in a relative increase in the severity of fatal crashes over the same time period; i.e., occupants of contemporary vehicles are surviving more severe crashes than those in older vehicles. Thus, this result is likely more indicative that fire involvement increases with crash severity than with crash year or model year.

The last 5 years of NFIRS data indicate the overall number of heavy-truck fires, with or without crash-involvement, has increased. Yet there has been a reduction in the number and rate of crash-involved heavy-truck fires, similar to passenger vehicles. Bus fire and crash exposure was relatively low and no real trend was observed.

Vehicle fires were most often initiated without crash involvement. Approximately 1.6 percent of passenger vehicle fires and 1.9 percent of heavy-truck fires were associated with some type of collision. Crash events were only coded as being a factor in 0.3 percent of bus fires.

The characteristics of all vehicle fires were generally similar across all vehicle types and databases. For vehicles involved in collisions, fires most often originated in the engine compartment due to frontal impact damage. The passenger area was only noted as relatively common area of fire origin for events in which crashes were not a factor. Heavy-truck fires, in general, most frequently originated in the engine compartment or cargo area. However, in crash-related heavy-truck fires the fuel tank and fuel lines were noted as the area of origin 10 times more often than in non-crash-related heavy-truck fires.

The types of materials that burned consisted mostly of flammable liquids in the engine compartment or fuel lines, electrical wires, tires, and interior fabrics. Operating equipment was, by far, the main source of heat attributed to initiating the fire. Overheated tires were noted as a common heat source. Vehicle seats made up a relatively large proportion of items first ignited in passenger vehicles. However, vehicle seats were rarely coded as the first item ignited when passenger vehicle fires were restricted to those in which a collision was identified as factor contributing to the fire.

The fire rate, per crash, was found to vary widely for different vehicle makes and models. This may be due to factors such as driver demographics, engine compartment and firewall design, and types of materials used throughout the vehicle. Vehicle age was also noted to be associated with fire involvement rates for both passenger vehicles and heavy trucks. Interestingly, the rate of fire involvement increased with vehicle age for passenger vehicles while it decreased with vehicle age for heavy trucks.

An in-depth investigation of crashes involving fires in the NASS CDS highlighted some characteristics of passenger vehicle fires. Frontal crashes were the predominant crash mode resulting in fires and the engine compartment was most often indicated as the fire origin area. In vehicle fires originating in the engine compartment the method of fire ingress into the passenger compartment was most often through the windshield and over the dash. It appears that the fire progresses through the windshield, which was either damaged by crash forces or thermal effects, and then ignites the vehicle interior, often the top of the dash. The fire then moves upward and rearward

through the interior of the vehicle. A secondary method of ingress may include propagation through a damaged firewall, though evidence for this was rarely directly observed. Another common scenario for ingress was through the rear of the vehicle often associated with rear impact damage.

Appendix C: FMVSS 302 Data

FMVSS 302 Data

Results Description	Appendix C Table Number
FMVSS 302 Results for School Bus Seat Materials	C-1
FMVSS 302 Results for Motorcoach Materials	C-2
FMVSS 302 Results for Vehicle Interior Materials	C-3
FMVSS 302 Results for Vehicle Interior Materials (Backside)	C-4
Thin Materials	C-5
Water Mist Foams	C-6
Child Restraint Seat Foams	C-7

Nomenclature for Appendix C

D_{\max} = maximum flame spread distance from the front edge of the specimen (in.)

m_f = final FMVSS 302 specimen mass (g)

m_i = initial FMVSS 302 specimen mass (g)

t_{fo} = time to flameout (s)

$t_{\text{mark } 1}$ = time for the flame to spread to the first mark at 1.5 in. from the front edge (s)

$t_{\text{mark } 2}$ = time for the flame to spread to the second mark at 11.5 in. from the front edge (s)

Table C-1. FMVSS 302 Results for School Bus Seat Materials

Test No.	Material Description	t _{mark 1} (s)	t _{mark 2} (s)	t _{fo} (s)	D _{max} (in.)	Burn Rate (mm/min)	m _i (g)	m _f (g)	P/F
1	Blue Bird Seat Cover	NA	NA	NA	1.1	NA			Pass
2	Blue Bird Seat Cover	NA	NA	NA	1.0	NA			Pass
3	Blue Bird Seat Cover	NA	NA	NA	1.0	NA			Pass
4	Blue Bird Seat Cover	NA	NA	NA	1.0	NA			Pass
5	Blue Bird Seat Cover	NA	NA	NA	1.0	NA			Pass
Average:		NA	NA	NA	1.0	0			Pass
Standard Deviation:		NA	NA	NA	0.0	0.0			
1	Blue Bird Seat Padding	63	422	607	12.5	42			Pass
2	Blue Bird Seat Padding	186	817	1071	12.5	24			Pass
3	Blue Bird Seat Padding	135	727	1065	12.5	26			Pass
4	Blue Bird Seat Padding	128	741	1516	12.5	25			Pass
5	Blue Bird Seat Padding	134	615	1076	12.5	32			Pass
Average:		129	664	1067	12.5	30			Pass
Standard Deviation:		43.8	154	321	0.0	7.7			
1	Starcraft Seat Cover	13	NA	97	3.9	44			Pass
2	Starcraft Seat Cover	9	NA	132	6.1	57			Pass
3	Starcraft Seat Cover	NA	NA	82	1.0	NA			Pass
4	Starcraft Seat Cover	10	NA	117	5.7	60			Pass
5	Starcraft Seat Cover	15	NA	79	1.9	8			Pass
Average:		11.8	NA	101.4	3.7	42			Pass
Standard Deviation:		2.8	NA	22.8	2.3	23.6			
1	Starcraft Seat Padding	77	NA	352	5.2	20			Pass
2	Starcraft Seat Padding	NA	NA	141	1.4	NA			Pass
3	Starcraft Seat Padding	NA	NA	NA	0.7	NA			Pass
4	Starcraft Seat Padding	81	730	900	12.5	23			Pass
5	Starcraft Seat Padding	93	807	927	12.5	21			Pass
Average:		84	769	580	6.4	22			Pass
Standard Deviation:		8.3	54	395	5.8	1.6			
1	Trans Tech Seat Cover	27	NA	68	1.7	NA			Pass
2	Trans Tech Seat Cover	16	NA	108	4.8	55			Pass
3	Trans Tech Seat Cover	22	NA	128	5.9	63			Pass
4	Trans Tech Seat Cover	25	NA	106	3.5	37			Pass
5	Trans Tech Seat Cover	22	NA	104	2.9	26			Pass
Average:		22	NA	103	3.8	45			Pass
Standard Deviation:		4.2	NA	22	1.6	16.9			
1	Trans Tech Seat Padding	NA	NA	NA	2.2	NA			Pass
2	Trans Tech Seat Padding	NA	NA	NA	2.2	NA			Pass
3	Trans Tech Seat Padding	NA	NA	NA	2.6	NA			Pass
4	Trans Tech Seat Padding	NA	NA	NA	2.3	NA			Pass
5	Trans Tech Seat Padding	NA	NA	NA	2.3	NA			Pass
Average:		NA	NA	NA	2.3	0			Pass
Standard Deviation:		NA	NA	NA	0.2	0.0			

Table C-2. FMVSS 302 Results for Motorcoach Materials

Test No.	Material Description	t _{mark 1} (s)	t _{mark 2} (s)	t _{fo} (s)	D _{max} (in.)	Burn Rate (mm/min)	m _i (g)	m _f (g)	P/F
1	Green Cover Seat Padding	52	527	697	12.5	32			Pass
2	Green Cover Seat Padding	37	529	585	12.5	31			Pass
3	Green Cover Seat Padding	47	NA	156	1.9	6			Pass
4	Green Cover Seat Padding	NA	NA	6	1.5	NA			Pass
5	Green Cover Seat Padding	NA	NA	51	1.5	NA			Pass
Average:		45	528	299	6.0	23			Pass
Standard Deviation:		7.6	1.4	319	6.0	14.8			
1	Seat Cover - Green	10	395	407	12.1	40			Pass
2	Seat Cover - Green	12	379	495	12.5	42			Pass
3	Seat Cover - Green	14	387	471	12.5	41			Pass
4	Seat Cover - Green	19	483	546	12.5	33			Pass
5	Seat Cover - Green	17	472	498	12.5	33			Pass
Average:		14	423	483	12.4	38			Pass
Standard Deviation:		3.6	50.0	50.6	0.2	4.2			
1	Seat Backing - Blue	NA	NA	23	1.0	NA			Pass
2	Seat Backing - Blue	NA	NA	15	0.9	NA			Pass
3	Seat Backing - Blue	NA	NA	14	0.9	NA			Pass
4	Seat Backing - Blue	NA	NA	14	1.4	NA			Pass
5	Seat Backing - Blue	NA	NA	12	1.5	NA			Pass
Average:		NA	NA	15.6	1.1	0			Pass
Standard Deviation:		NA	NA	4.3	0.3	0.0			
1	Seat Cover - Pattern Blue	NA	NA	29	0.7	NA			Pass
2	Seat Cover - Pattern Blue	NA	NA	31	1.0	NA			Pass
3	Seat Cover - Pattern Blue	NA	NA	73	1.0	NA			Pass
4	Seat Cover - Pattern Blue	NA	NA	55	1.1	NA			Pass
5	Seat Cover - Pattern Blue	NA	NA	32	1.1	NA			Pass
Average:		NA	NA	44.0	1.0	0			Pass
Standard Deviation:		NA	NA	19.4	0.2	0.0			
1	Seat Backing - Gray	18	305	372	12.5	53			Pass
2	Seat Backing - Gray	10	311	357	12.5	51			Pass
3	Seat Backing - Gray	12	305	390	12.5	52			Pass
4	Seat Backing - Gray	13	475	603	12.5	33			Pass
5	Seat Backing - Gray	36	441	515	12.5	38			Pass
Average:		18	367	447	12.5	45			Pass
Standard Deviation:		10.6	83.6	107	0.0	9.3			
1	Door of Luggage Rack	202	1573	2453	12.5	11			Pass
2	Door of Luggage Rack	235	915	1631	12.5	22			Pass
3	Door of Luggage Rack	266	788	1310	12.5	29			Pass
4	Door of Luggage Rack	177	1565	2069	12.5	11			Pass
5	Door of Luggage Rack	196	1000	1866	12.5	19			Pass
Average:		215	1168	1866	12.5	19			Pass
Standard Deviation:		35.3	374	433	0.0	7.8			

Table C-2. FMVSS 302 Results for Motorcoach Materials (Continued)

Test No.	Material Description	t _{mark 1} (s)	t _{mark 2} (s)	t _{fo} (s)	D _{max} (in.)	Burn Rate (mm/min)	m _i (g)	m _f (g)	P/F
1	Floor Covering	NA	NA	1	1.1	NA			Pass
2	Floor Covering	NA	NA	120	1.0	NA			Pass
3	Floor Covering	NA	NA	1	0.9	NA			Pass
4	Floor Covering	NA	NA	61	0.7	NA			Pass
5	Floor Covering	NA	NA	1	1.1	NA			Pass
Average:		NA	NA	37	1.0	0			Pass
Standard Deviation:		NA	NA	53	0.1	0.0			
1	Headliner	NA	NA	5	1.7	NA			Pass
2	Headliner	NA	NA	17	1.8	NA			Pass
3	Headliner	NA	NA	19	1.6	NA			Pass
4	Headliner	NA	NA	19	1.4	NA			Pass
5	Headliner	NA	NA	19	1.6	NA			Pass
Average:		NA	NA	16	1.6	0			Pass
Standard Deviation:		NA	NA	6.1	0.2	0.0			
1	Blue Cover Seat Padding	8	NA	74	5.25	87			Pass
2	Blue Cover Seat Padding	5	NA	90	6.00	81			Pass
3	Blue Cover Seat Padding	1	NA	48	5.00	113			Fail
Average:		5	NA	70.7	5.4	94			Pass
Standard Deviation:		3.5	NA	21.2	0.5	17.5			

Table C-3. FMVSS 302 Results for Vehicle Interior Materials

Test No.	Material Description	t _{mark 1} (s)	t _{mark 2} (s)	t _{fo} (s)	D _{max} (in.)	Burn Rate (mm/min)	m _i (g)	m _f (g)	P/F
1	Carpet Ford F250	64	763	1068	12.5	22	68.3	45.1	Pass
2	Carpet Ford F250	91	892	1335	12.5	19	73.5	38.9	Pass
3	Carpet Ford F250	71	810	1063	12.5	21	67.0	41.1	Pass
4	Carpet Ford F250	55	853	1159	12.5	19	66.7	43.5	Pass
5	Carpet Ford F250	35	900	1155	12.5	18	65.1	42.1	Pass
Average:		63	844	1156	12.5	20	68.1	41.4	Pass
Standard Deviation:		21	58	110	0.0	1.6	3.2	2.3	
1	Carpet Mercedes	121	837	1324	12.5	21	170.6	121.9	Pass
2	Carpet Mercedes	308	NA	690	4.5	12	245.1	239.5	Pass
3	Carpet Mercedes	125	NA	996	6.5	9	180.9	174.1	Pass
4	Carpet Mercedes	73	1005	1520	12.5	16	148.8	102.4	Pass
5	Carpet Mercedes	175	1147	1364	12.5	16	169.0	163.7	Pass
Average:		160	996	1179	9.7	15	185.9	169.9	Pass
Standard Deviation:		90.1	155.2	333	3.9	4.7	36.7	53.2	
1	Dashboard Ford F250	184	1036	1327	12.5	18	115.1	71.7	Pass
2	Dashboard Ford F250	166	700	1133	12.5	29	102.8	64.3	Pass
3	Dashboard Ford F250	177	855	1301	12.5	22	116.8	75.1	Pass
4	Dashboard Ford F250	140	1130	1616	12.5	15	102.0	65.7	Pass
5	Dashboard Ford F250	313	1608	2416	12.5	12	164.1	102.5	Pass
Average:		196	1066	1559	12.5	19	121.4	76.9	Pass
Standard Deviation:		68	345	510	0.0	6.5	25.5	15.5	
1	Dashboard Mercedes	NA	NA	8	0.5	NA	245.1	244.8	Pass
2	Dashboard Mercedes	37	426	3120	12.5	39	250.1	168.4	Pass
3	Dashboard Mercedes	107	433	1057	12.5	47	187.4	181.0	Pass
4	Dashboard Mercedes	24	490	636	12.5	33	245.0	208.8	Pass
5	Dashboard Mercedes	21	455	580	12.5	35	200.0	166.9	Pass
Average:		47	451	1080	10.1	38	220.6	181.3	Pass
Standard Deviation:		40	29	1200	5.4	6.2	29.5	33.0	
1	Headliner Camaro	41	739	933	12.5	22	32.1	23.8	Pass
2	Headliner Camaro	77	1110	1277	12.5	15	30.9	27.5	Pass
3	Headliner Camaro	58	707	850	12.5	23	30.6	23.2	Pass
4	Headliner Camaro	57	734	903	12.5	23	29.6	23.0	Pass
5	Headliner Camaro	61	641	881	12.5	26	30.4	22.5	Pass
Average:		59	786	969	12.5	22	30.4	24.1	Pass
Standard Deviation:		13	185	175	0.0	4.3	0.9	2.0	
1	Headliner Ford	NA	NA	67	1.2	NA	38.0	37.5	Pass
2	Headliner Ford	92	NA	104	1.6	NA	38.6	37.9	Pass
3	Headliner Ford	NA	NA	65	1.4	NA	38.4	37.8	Pass
4	Headliner Ford	66	NA	104	1.8	NA	41.9	40.9	Pass
5	Headliner Ford	NA	NA	12	1.3	NA	39.1	38.3	Pass
Average:		79	NA	70	1.5	0	39.2	38.5	Pass
Standard Deviation:		18	NA	38	0.2	0.0	1.5	1.4	

Table C-3. FMVSS 302 Results for Vehicle Interior Materials (Continued)

Test No.	Material Description	t _{mark 1} (s)	t _{mark 2} (s)	t _{fo} (s)	D _{max} (in.)	Burn Rate (mm/min)	m _i (g)	m _f (g)	P/F
1	Seat Cover Camaro	12	192	230	12.5	85	20.8	13.4	Pass
2	Seat Cover Camaro	22	215	327	12.5	79	19.9	14.9	Pass
3	Seat Cover Camaro	11	197	251	12.5	82	21.1	15.1	Pass
4	Seat Cover Camaro	10	200	253	12.5	80	21.6	15.6	Pass
5	Seat Cover Camaro	20	252	370	12.5	66	26.8	15.2	Pass
Average:		15	211	286	12.5	78	22.3	15.2	Pass
Standard Deviation:		5.6	24.4	60	0.0	7.4	2.7	0.8	
1	Seat Cover Mercedes	32	307	592	12.5	55	37.1	30.2	Pass
2	Seat Cover Mercedes	NA	NA	4	0.7	NA	38.8	38.6	Pass
3	Seat Cover Mercedes	30	NA	324	9.5	41	49.8	46.8	Pass
4	Seat Cover Mercedes	26	409	471	11.5	34	40.7	37.9	Pass
5	Seat Cover Mercedes	23	355	468	12.5	46	45.0	41.7	Pass
Average:		28	357	372	9.3	44	42.3	39.0	Pass
Standard Deviation:		4.0	51.0	226	5.0	8.9	5.1	6.1	
1	Seat Padding Camaro	NA	NA	3	1.3	NA	28.2	27.8	Pass
2	Seat Padding Camaro	NA	NA	1	1.0	NA	21.6	21.5	Pass
3	Seat Padding Camaro	NA	NA	6	1.3	NA	22.1	22.1	Pass
4	Seat Padding Camaro	NA	NA	1	0.8	NA	24.7	24.6	Pass
5	Seat Padding Camaro	NA	NA	1	0.8	NA	19.2	19.1	Pass
Average:		NA	NA	2.4	1.0	0	21.9	21.8	Pass
Standard Deviation:		NA	NA	2.2	0.2	0.0	3.4	3.3	
1	Seat Padding Mercedes	NA	NA	1	1.8	NA	39.2	38.9	Pass
2	Seat Padding Mercedes	NA	NA	1	1.7	NA	31.1	30.9	Pass
3	Seat Padding Mercedes	NA	NA	1	1.2	NA	29.2	28.9	Pass
4	Seat Padding Mercedes	NA	NA	0	1.5	NA	31.9	31.7	Pass
5	Seat Padding Mercedes	NA	NA	2	1.7	NA	41.9	41.6	Pass
Average:		NA	NA	1	1.6	0	34.7	34.4	Pass
Standard Deviation:		NA	NA	1	0.2	0.0	5.5	5.5	

Table C-4. FMVSS 302 Results for Vehicle Interior Materials (Backside Surface Tested)

Test No.	Material Description	t _{mark 1} (s)	t _{mark 2} (s)	t _{fo} (s)	D _{max} (in.)	Burn Rate (mm/min)	m _i (g)	m _f (g)	P/F
1	Carpet Ford F250	18	NA	264	2.3	5	63.4	63.1	Pass
2	Carpet Ford F250	72	651	1164	12.5	26	59.2	41.1	Pass
3	Carpet Ford F250	106	978	1421	12.5	17	57.4	31.8	Pass
4	Carpet Ford F250	77	751	1733	12.5	23	53.8	41.6	Pass
5	Carpet Ford F250	132	1027	1285	12.5	17	68.1	46.2	Pass
Average:		81	852	1173	10.5	18	59.6	40.2	Pass
Standard Deviation:		43	180	551	4.6	8.2	5.5	11.5	
1	Dashboard Ford F250	548	NA	920	2.0	2	136.1	133.3	Pass
2	Dashboard Ford F250	151	841	1316	12.5	22	115.9	74.6	Pass
3	Dashboard Ford F250	218	941	1275	12.5	21	119.0	74.3	Pass
4	Dashboard Ford F250								Pass
5	Dashboard Ford F250								Pass
Average:		306	891	1170	9.0	15	117.5	74.4	Pass
Standard Deviation:		213	71	218	6.1	11.3	10.9	34.0	
1	Headliner Camaro	37	1022	1256	12.5	15	32.1	27.2	Pass
2	Headliner Camaro	33	644	836	12.5	25	31.4	26.1	Pass
3	Headliner Camaro	47	980	1187	12.5	16	33.9	28.6	Pass
4	Headliner Camaro	45	576	762	12.5	29	32.5	24.7	Pass
5	Headliner Camaro	40	737	978	12.5	22	33.9	27.6	Pass
Average:		40	792	1004	12.5	21	32.9	26.8	Pass
Standard Deviation:		5.7	200	215	0.0	5.6	1.1	1.5	
1	Seat Cover Camaro	25	247	336	12.5	69	17.0	10.7	Pass
2	Seat Cover Camaro	29	254	346	12.5	68	22.8	16.8	Pass
3	Seat Cover Camaro	34	222	420	12.5	81	28.8	16.2	Pass
4	Seat Cover Camaro	30	NA	64	3.5	NA	36.9	36.5	Pass
5	Seat Cover Camaro	NA	NA	8	0.5	NA	24.1	23.9	Pass
Average:		30	241	235	8.3	72	28.2	23.4	Pass
Standard Deviation:		3.7	16.8	185	5.8	7.4	7.4	9.9	

Table C-5. FMVSS 302 Results for Thin Materials

Test No.	Material Description	t _{mark 1} (s)	t _{mark 2} (s)	t _{fo} (s)	D _{max} (in.)	Burn Rate (mm/min)	m _i (g)	m _f (g)	P/F
1	Acrylate	78	389	586	12.5	49	59.6	32.6	Pass
2	Acrylate	103	520	714	12.5	37	65.4	35.4	Pass
3	Acrylate	108	450	691	12.5	45	65.3	30.8	Pass
4	Acrylate	105	430	678	12.5	47	62.1	34.8	Pass
5	Acrylate	107	578	990	12.5	32	68.1	37.1	Pass
Average:		100	473	732	12.5	42	65.2	34.5	Pass
Standard Deviation:		12.6	75.3	152	0.0	7.1	2.47	2.67	
1	Corrugated Cardboard	25	265	302	12.5	64	18.0	11.5	Pass
2	Corrugated Cardboard	25	289	342	12.5	58	17.7	12.0	Pass
3	Corrugated Cardboard	31	334	391	12.5	50	17.4	11.4	Pass
4	Corrugated Cardboard	30	286	342	12.5	60	17.4	11.7	Pass
5	Corrugated Cardboard	27	235	281	12.5	73	17.2	10.6	Pass
Average:		28	282	332	12.5	61	17.4	11.4	Pass
Standard Deviation:		2.8	36.3	42.4	0.0	8.4	0.31	0.50	
1	HDPE Thick	62	577	851	12.5	30	52.9	35.3	Pass
2	HDPE Thick	60	462	632	12.5	38	53.3	34.2	Pass
3	HDPE Thick	59	433	1153	12.5	41	53.2	34.9	Pass
4	HDPE Thick	49	459	617	12.5	37	53.1	34.4	Pass
5	HDPE Thick	46	473	641	12.5	36	53.6	34.7	Pass
Average:		55	481	779	12.5	36	53.3	34.6	Pass
Standard Deviation:		7.2	55.7	230	0.0	4.1	0.25	0.42	
1	HDPE Thin	16	257	482	12.5	63	27.3	18.2	Pass
2	HDPE Thin	19	254	490	12.5	65	27.3	17.9	Pass
3	HDPE Thin	12	222	318	12.5	73	27.4	19.1	Pass
4	HDPE Thin	14	235	342	12.5	69	27.3	18.5	Pass
5	HDPE Thin	14	232	347	12.5	70	27.4	18.5	Pass
Average:		15	240	396	12.5	68	27.3	18.5	Pass
Standard Deviation:		2.6	15.0	83.1	0.0	3.8	0.04	0.44	
1	Manila File Folder	15	179	186	12.5	93	7.32	4.23	Pass
2	Manila File Folder	16	138	173	12.5	125	7.12	4.15	Fail
3	Manila File Folder	18	134	160	12.5	131	7.17	4.19	Fail
4	Manila File Folder	14	128	158	12.5	134	6.77	3.97	Fail
5	Manila File Folder	14	141	173	12.5	120	7.05	4.11	Fail
Average:		15	144	170	12.5	121	7.03	4.11	Fail
Standard Deviation:		1.7	20.2	11	0.0	16.4	0.20	0.10	
1	Acrylate (Insulated)	119	732	1388	12.5	25	61.6	41.0	Pass
1	Cardboard (Insulated)	20	NA	78	3.0	NA	17.7	17.2	Pass
1	HDPE Thick (Insulated)	57	529	802	12.5	32	53.4	37.8	Pass
1	HDPE Thin (Insulated)	20	256	397	12.5	65	27.2	19.8	Pass
1	Manila Folder (Insulated)	7	147	189	12.5	109	7.1	4.4	Fail
1	Acrylate (Protected)	308	2966	3574	12.5	6	58.8	31.9	Pass

Table C-6. FMVSS 302 Results for Water Mist Foams

Test No.	Material Description	t _{mark 1} (s)	t _{mark 2} (s)	t _{fo} (s)	D _{max} (in.)	Burn Rate (mm/min)	m _i (g)	m _f (g)	P/F
1	SF Foam (¼ in.)	2	108	125	12.5	144			Fail
2	SF Foam (¼ in.)	2	132	148	12.5	117			Fail
3	SF Foam (¼ in.)	1	93	110	12.5	166			Fail
4	SF Foam (¼ in.)								
5	SF Foam (¼ in.)								
Average:		1.7	111	128	12.5	142			Fail
Standard Deviation:		0.6	20	19	0.0	24.2			
1	SF Foam (½ in.)	15	173	265	12.5	96	13.7	7.7	Pass
2	SF Foam (½ in.)	15	171	203	12.5	98	13.7	9.0	Pass
3	SF Foam (½ in.)	10	150	190	12.5	109	11.2	7.9	Fail
4	SF Foam (½ in.)	10	160	188	12.5	102	13.1	6.9	Pass
5	SF Foam (½ in.)	9	160	202	12.5	101	12.7	9.2	Pass
Average:		12	163	210	12.5	101	12.7	8.2	Pass
Standard Deviation:		2.9	9.4	32	0.0	4.8	1.0	1.0	
1	SM Foam (¼ in.)	1	130	159	12.5	118	8.8	6.9	Fail
2	SM Foam (¼ in.)	1	128	150	12.5	120	9.8	7.1	Fail
3	SM Foam (¼ in.)	1	134	159	12.5	115	9.2	7.1	Fail
4	SM Foam (¼ in.)	1	121	150	12.5	127	8.5	7.0	Fail
5	SM Foam (¼ in.)	4	148	180	12.5	106	9.1	6.7	Fail
Average:		1.6	132	160	12.5	117	9.1	7.0	Fail
Standard Deviation:		1.3	10.0	12.3	0.0	7.8	0.5	0.2	
1	SM Foam (½ in.)	12	201	388	12.5	81	20.3	13.1	Pass
2	SM Foam (½ in.)	15	195	322	12.5	85	18.2	12.4	Pass
3	SM Foam (½ in.)	11	209	540	12.5	77	18.7	15.0	Pass
4	SM Foam (½ in.)	13	191	295	12.5	86	16.7	10.4	Pass
5	SM Foam (½ in.)	13	201	315	12.5	81	19.7	11.8	Pass
Average:		13	199	372	12.5	82	18.3	12.4	Pass
Standard Deviation:		1.5	6.8	100	0.0	3.5	1.4	1.7	

Table C-7. FMVSS 302 Results for Child Restraint Seat Foams

Test No.	Material Description	t _{1.5 in.} (s)	t _{10.5 in.} (s)	t _{fo} (s)	D _{max} (in.)	Burn Rate (mm/min)	m _i (g)	m _f (g)	P/F
1	Chicco KeyFit	1	NA	35	3.3	NA			Pass
2	Chicco KeyFit	1	NA	15	3.0	NA			Pass
1	Peg Perego Primo Viaggio	5	NA	14	2.5	NA			Pass
1	UPPAbaby Mesa	1	127	146	12.5	121			Fail

Appendix D: ASTM D3801 Data

ASTM D3801 Data

Results Description	Appendix D Table Number
ASTM D3801 Results for School Bus Seat Materials	D-1
ASTM D3801 Results for Motorcoach Materials	D-2
ASTM D3801 Results for Vehicle Interior Materials	D-3

Nomenclature for Appendix D

- t₁ = duration of flaming after the end of the first 10 s burner flame application (s)
- t₂ = duration of flaming after the end of the second 10 s burner flame application (s)
- t₃ = duration of glowing after the end of the second 10 s burner flame application (s)

Table D-1. ASTM D3801 Results for School Bus Seat Materials

Test No.	Material Description	t ₁ (s)	t ₂ (s)	Σ(t ₁ +t ₂) (s)	t ₃ (s)	Flame/Glow to Clamp?	Cotton Ignited?	V-Rating
1	Blue Bird Seat Cover	0.0	3.0	15.0	0.0	No	No	V-0
2	Blue Bird Seat Cover	0.0	1.0		0.0	No	No	V-0
3	Blue Bird Seat Cover	0.0	2.0		0.0	No	No	V-0
4	Blue Bird Seat Cover	0.0	0.0		0.0	No	No	V-0
5	Blue Bird Seat Cover	6.0	3.0		0.0	No	No	V-0
Average:		1.2	1.8					V-0
Standard Deviation:		2.7	1.3					
1	Blue Bird Seat Padding	0.0	1.0	41.0	0.0	No	Yes	V-2
2	Blue Bird Seat Padding	0.0	11.0		0.0	No	Yes	V-2
3	Blue Bird Seat Padding	0.0	0.0		0.0	No	Yes	V-2
4	Blue Bird Seat Padding	0.0	3.0		0.0	No	Yes	V-2
5	Blue Bird Seat Padding	0.0	26.0		0.0	Yes	Yes	V-2
Average:		0.0	8.2					V-2
Standard Deviation:		0.0	10.8					
1	Starcraft Seat Cover	23.0	42.0	203.0	0.0	Yes	Yes	NR
2	Starcraft Seat Cover	29.0	0.0		0.0	Yes	Yes	NR
3	Starcraft Seat Cover	11.0	14.0		0.0	No	No	V-1
4	Starcraft Seat Cover	9.0	22.0		0.0	Yes	Yes	NR
5	Starcraft Seat Cover	37.0	16.0		0.0	No	No	NR
Average:		21.8	18.8					NR
Standard Deviation:		11.9	15.3					
1	Starcraft Seat Padding	7.0	51.0	267.0	0.0	Yes	Yes	NR
2	Starcraft Seat Padding	51.0	0.0		0.0	Yes	Yes	NR
3	Starcraft Seat Padding	48.0	0.0		0.0	Yes	Yes	NR
4	Starcraft Seat Padding	59.0	0.0		0.0	Yes	Yes	NR
5	Starcraft Seat Padding	51.0	0.0		0.0	Yes	Yes	NR
Average:		43.2	10.2					NR
Standard Deviation:		20.6	22.8					
1	Trans Tech Seat Cover	1.0	4.0	42.0	0.0	No	No	V-0
2	Trans Tech Seat Cover	2.0	11.0		0.0	No	No	V-1
3	Trans Tech Seat Cover	0.0	1.0		0.0	No	No	V-0
4	Trans Tech Seat Cover	3.0	14.0		0.0	No	No	V-1
5	Trans Tech Seat Cover	2.0	4.0		0.0	No	No	V-0
Average:		1.6	6.8					V-1
Standard Deviation:		1.1	5.4					
1	Trans Tech Seat Padding	1.0	0.0	22.0	0.0	Yes	Yes	NR
2	Trans Tech Seat Padding	5.0	0.0		0.0	Yes	Yes	NR
3	Trans Tech Seat Padding	6.0	0.0		0.0	Yes	No	NR
4	Trans Tech Seat Padding	4.0	0.0		0.0	Yes	No	NR
5	Trans Tech Seat Padding	6.0	0.0		0.0	Yes	No	NR
Average:		4.4	0.0					NR
Standard Deviation:		2.1	0.0					

Table D-2. ASTM D3801 Results for Motorcoach Materials

Test No.	Material Description	t ₁ (s)	t ₂ (s)	Σ(t ₁ +t ₂) (s)	t ₃ (s)	Flame/Glow to Clamp?	Cotton Ignited?	V-Rating
1	Green Cover Seat Padding	4.0	0.0	96.0	0.0	Yes	Yes	NR
2	Green Cover Seat Padding	15.0	0.0		0.0	Yes	Yes	NR
3	Green Cover Seat Padding	22.0	0.0		0.0	Yes	Yes	NR
4	Green Cover Seat Padding	25.0	0.0		0.0	Yes	Yes	NR
5	Green Cover Seat Padding	30.0	0.0		0.0	Yes	Yes	NR
Average:		19.2	0.0					NR
Standard Deviation:		10.1	0.0					
1	Seat Cover - Green	57.0	0.0	321.0	0.0	Yes	Yes	NR
2	Seat Cover - Green	57.0	0.0		0.0	Yes	Yes	NR
3	Seat Cover - Green	56.0	0.0		0.0	Yes	Yes	NR
4	Seat Cover - Green	53.0	0.0		0.0	Yes	Yes	NR
5	Seat Cover - Green	98.0	0.0		0.0	Yes	Yes	NR
Average:		64.2	0.0					NR
Standard Deviation:		19.0	0.0					
1	Seat Backing - Blue	73.0	0.0	385.0	0.0	Yes	No	NR
2	Seat Backing - Blue	83.0	0.0		0.0	Yes	No	NR
3	Seat Backing - Blue	81.0	0.0		0.0	Yes	No	NR
4	Seat Backing - Blue	77.0	0.0		0.0	Yes	No	NR
5	Seat Backing - Blue	71.0	0.0		0.0	Yes	No	NR
Average:		77.0	0.0					NR
Standard Deviation:		5.1	0.0					
1	Seat Cover - Pattern Blue	60.0	55.0	389.0	0.0	Yes	No	NR
2	Seat Cover - Pattern Blue	70.0	0.0		0.0	Yes	No	NR
3	Seat Cover - Pattern Blue	65.0	0.0		0.0	Yes	Yes	NR
4	Seat Cover - Pattern Blue	63.0	0.0		0.0	Yes	No	NR
5	Seat Cover - Pattern Blue	76.0	0.0		0.0	Yes	Yes	NR
Average:		66.8	11.0					NR
Standard Deviation:		6.3	24.6					
1	Seat Backing - Gray	143.0	0.0	761.0	0.0	Yes	Yes	NR
2	Seat Backing - Gray	106.0	0.0		0.0	Yes	Yes	NR
3	Seat Backing - Gray	101.0	0.0		0.0	Yes	Yes	NR
4	Seat Backing - Gray	191.0	0.0		0.0	Yes	Yes	NR
5	Seat Backing - Gray	220.0	0.0		0.0	Yes	Yes	NR
Average:		152.2	0.0					NR
Standard Deviation:		52.3	0.0					
1	Door of Luggage Rack	100.0	0.0	609.0	0.0	Yes	Yes	NR
2	Door of Luggage Rack	111.0	0.0		0.0	Yes	Yes	NR
3	Door of Luggage Rack	120.0	0.0		0.0	Yes	Yes	NR
4	Door of Luggage Rack	128.0	0.0		0.0	Yes	Yes	NR
5	Door of Luggage Rack	150.0	0.0		0.0	Yes	Yes	NR
Average:		121.8	0.0					NR
Standard Deviation:		18.9	0.0					

Table D-2. ASTM D3801 Results for Motorcoach Materials (Continued)

Test No.	Material Description	t ₁ (s)	t ₂ (s)	Σ(t ₁ +t ₂) (s)	t ₃ (s)	Flame/Glow to Clamp?	Cotton Ignited?	V-Rating
1	Floor Covering	44.0	38.0	292.0	0.0	No	No	NR
2	Floor Covering	50.0	1.0		0.0	No	No	NR
3	Floor Covering	64.0	1.0		0.0	No	No	NR
4	Floor Covering	49.0	2.0		0.0	No	No	NR
5	Floor Covering	35.0	8.0		0.0	No	No	NR
Average:		48.4	10.0					NR
Standard Deviation:		10.5	15.9					
1	Headliner	57.0	0.0	261.0	0.0	Yes	Yes	NR
2	Headliner	43.0	0.0		0.0	Yes	Yes	NR
3	Headliner	56.0	0.0		0.0	Yes	Yes	NR
4	Headliner	45.0	0.0		0.0	Yes	Yes	NR
5	Headliner	60.0	0.0		0.0	Yes	No	NR
Average:		52.2	0.0					NR
Standard Deviation:		7.7	0.0					

Table D-3. ASTM D3801 Results for Vehicle Interior Materials

Test No.	Material Description	t ₁ (s)	t ₂ (s)	Σ(t ₁ +t ₂) (s)	t ₃ (s)	Flame/Glow to Clamp?	Cotton Ignited?	V-Rating
1	Carpet Ford F250	79	0	347	0	Yes	Yes	NR
2	Carpet Ford F250	66	0		0	Yes	Yes	NR
3	Carpet Ford F250	64	0		0	Yes	Yes	NR
4	Carpet Ford F250	76	0		0	Yes	Yes	NR
5	Carpet Ford F250	62	0		0	Yes	Yes	NR
Average:		69.4	0.0					NR
Standard Deviation:		7.6	0.0					
1	Carpet Mercedes	112	0	835	0	Yes	Yes	NR
2	Carpet Mercedes	85	0		0	Yes	Yes	NR
3	Carpet Mercedes	104	0		0	Yes	Yes	NR
4	Carpet Mercedes	264	0		0	Yes	Yes	NR
5	Carpet Mercedes	270	0		0	Yes	Yes	NR
Average:		167.0	0.0					NR
Standard Deviation:		91.8	0.0					
1	Dashboard Ford F250	152	0	763	0	Yes	Yes	NR
2	Dashboard Ford F250	143	0		0	Yes	Yes	NR
3	Dashboard Ford F250	166	0		0	Yes	Yes	NR
4	Dashboard Ford F250	158	0		0	Yes	Yes	NR
5	Dashboard Ford F250	144	0		0	Yes	Yes	NR
Average:		152.6	0.0					NR
Standard Deviation:		9.7	0.0					
1	Headliner Camaro	73	0	330	0	Yes	No	NR
2	Headliner Camaro	61	0		0	Yes	No	NR
3	Headliner Camaro	61	0		0	Yes	No	NR
4	Headliner Camaro	67	0		0	Yes	No	NR
5	Headliner Camaro	68	0		0	Yes	No	NR
Average:		66.0	0.0					NR
Standard Deviation:		5.1	0.0					
1	Headliner Ford	81	0	343	0	Yes	No	NR
2	Headliner Ford	65	0		0	Yes	No	NR
3	Headliner Ford	61	0		0	Yes	No	NR
4	Headliner Ford	72	0		0	Yes	No	NR
5	Headliner Ford	64	0		0	Yes	No	NR
Average:		68.6	0.0					NR
Standard Deviation:		8.0	0.0					
1	Seat Cover Camaro	31	0	177	0	Yes	Yes	NR
2	Seat Cover Camaro	39	0		0	Yes	Yes	NR
3	Seat Cover Camaro	10	19		0	Yes	Yes	NR
4	Seat Cover Camaro	41	0		0	Yes	Yes	NR
5	Seat Cover Camaro	37	0		0	Yes	Yes	NR
Average:		31.6	3.8					NR
Standard Deviation:		12.6	8.5					

Table D-3. ASTM D3801 Results for Vehicle Interior Materials (Continued)

Test No.	Material Description	t ₁ (s)	t ₂ (s)	Σ(t ₁ +t ₂) (s)	t ₃ (s)	Flame/Glow to Clamp?	Cotton Ignited?	V-Rating
1	Seat Cover Mercedes	83	0	424	0	Yes	No	NR
2	Seat Cover Mercedes	76	0		0	Yes	No	NR
3	Seat Cover Mercedes	99	0		0	Yes	No	NR
4	Seat Cover Mercedes	84	0		0	Yes	No	NR
5	Seat Cover Mercedes	82	0		0	Yes	No	NR
Average:		84.8	0.0					NR
Standard Deviation:		8.5	0.0					
1	Seat Padding Camaro	0	7	20	0	No	Yes	V-2
2	Seat Padding Camaro	0	2		0	No	Yes	V-2
3	Seat Padding Camaro	1	2		0	No	Yes	V-2
4	Seat Padding Camaro	1	4		0	No	Yes	V-2
5	Seat Padding Camaro	2	1		0	No	No	V-2
Average:		0.8	3.2					V-2
Standard Deviation:		0.8	2.4					
1	Seat Padding Mercedes	1	2	35	0	No	Yes	V-2
2	Seat Padding Mercedes	5	5		0	No	Yes	V-2
3	Seat Padding Mercedes	2	9		0	No	Yes	V-2
4	Seat Padding Mercedes	2	3		0	No	Yes	V-2
5	Seat Padding Mercedes	1	5		0	No	Yes	V-2
Average:		2.2	4.8					V-2
Standard Deviation:		1.6	2.7					

Appendix E: ASTM E1354 Data

ASTM E1354 Data

Results Description	Appendix E Table Number
ASTM E1354 Results for School Bus Seat Materials	E-1
ASTM E1354 Results for Motorcoach Materials	E-2
ASTM E1354 Results for Vehicle Interior Materials	E-3

Nomenclature for Appendix E

HOC = effective heat of combustion (MJ/kg)

HRR_{peak} = first peak heat release rate (kW/m²)

HRR₆₀ = average heat release rate over the first 60 s from ignition (kW/m²)

SEA = specific smoke extinction area (m²/kg)

t_{ig} = time to sustained ignition (s)

t_{end} = time from start to end of test (s)

THR = total heat release (MJ/m²)

Table E-1. ASTM E1354 Results for School Bus Seat Materials

Test No.	Material Description	t _{ig} (s)	t _{end} (s)	HRR _{peak} (kW/m ²)	HRR ₆₀ (kW/m ²)	THR (MJ/m ²)	HOC (MJ/kg)	SEA (m ² /kg)
1	Blue Bird - Seat Assembly	12	430	313	187	75.1	23.1	561
2	Blue Bird - Seat Assembly	15	353	382	233	74.3	22.0	521
3	Blue Bird - Seat Assembly	14	551	234	161	82.6	22.2	497
4	Blue Bird - Seat Assembly	15	478	364	219	80.1	22.1	514
5	Blue Bird - Seat Assembly	12	504	246	183	91.2	23.1	463
6	Blue Bird - Seat Assembly	15	528	280	145	85.3	22.7	508
Average:		13.8	474	303	188	81.4	22.5	511
Standard Deviation:		1.5	73	61	34	6.4	0.5	32
1	Starcraft - Seat Assembly	12	780	283	231	94.4	22.1	582
2	Starcraft - Seat Assembly	11	426	298	213	89.0	22.1	675
3	Starcraft - Seat Assembly	12	486	273	212	96.2	21.6	662
Average:		11.7	564	285	219	93.2	21.9	640
Standard Deviation:		0.6	189	12	11	3.8	0.3	51
1	Trans Tech - Seat Assembly	13	218	262	216	25.5	18.2	720
2	Trans Tech - Seat Assembly	15	285	268	232	27.6	19.7	677
3	Trans Tech - Seat Assembly	12	313	264	217	26.1	18.8	682
Average:		13.3	272	265	222	26.4	18.9	693
Standard Deviation:		1.5	49	3	9	1.1	0.7	23

Table E-2. ASTM E1354 Results for Motorcoach Materials

Test No.	Material Description	t _{ig} (s)	t _{end} (s)	HRR _{peak} (kW/m ²)	HRR ₆₀ (kW/m ²)	THR (MJ/m ²)	HOC (MJ/kg)	SEA (m ² /kg)
1	Green Seat Assembly (Grid)	44	708	207	157	68.6	24.8	197
2	Green Seat Assembly (Grid)	40	691	212	168	84.6	24.8	202
3	Green Seat Assembly (Grid)	49	633	228	175	66.1	24.5	203
Average:		44.3	677	216	166	73.1	24.7	201
Standard Deviation:		4.5	39	11	9	10.0	0.2	3
1	Bue Seat Assembly	37	924	267	152	85.0	24.5	164
2	Blue Seat Assembly	46	832	232	133	77.4	24.1	201
3	Blue Seat Assembly	47	184	234	143	12.0	18.0	251
Average:		43.3	647	244	143	58.1	22.2	205
Standard Deviation:		5.5	403	20	10	40.1	3.7	44
1	Blue Seat Assembly (Grid)	83	767	156	100	60.8	23.1	167
2	Blue Seat Assembly (Grid)	48	178	147	92	11.8	15.4	302
3	Blue Seat Assembly (Grid)	69	188	186	139	11.9	13.0	236
Average:		66.7	378	163	110	28.2	17.1	235
Standard Deviation:		17.6	337	21	25	28.3	5.3	68
1	Seat Backing - Gray	20	251	431	242	59.6	31.5	532
2	Seat Backing - Gray	18	417	436	272	56.7	29.8	450
3	Seat Backing - Gray	19	296	393	239	59.7	30.3	515
1	Seat Backing - Gray	21	277	448	258	56.1	31.6	522
2	Seat Backing - Gray	22	268	462	270	58.4	29.9	519
3	Seat Backing - Gray	21	545	466	273	67.9	30.0	472
Average:		20.2	342	440	259	59.7	30.5	502
Standard Deviation:		1.5	116	26	16	4.3	0.8	33
1	Door of Luggage Rack	50	858	685	460	187.7	27.8	1053
2	Door of Luggage Rack	52	830	630	424	195.5	29.7	1092
3	Door of Luggage Rack	47	1040	670	445	197.7	28.9	1019
Average:		49.7	909	662	443	193.6	28.8	1055
Standard Deviation:		2.5	114	29	18	5.2	0.9	37
1	Floor Covering	28	283	263	210	32.9	14.2	1050
2	Floor Covering	25	296	264	204	33.0	14.5	1009
3	Floor Covering	25	267	275	211	34.5	14.7	1076
Average:		26.0	282	267	208	33.5	14.5	1045
Standard Deviation:		1.7	15	7	4	0.9	0.3	34
1	Headliner	14	153	280	147	14.1	16.5	176
2	Headliner	29	182	257	90	12.1	14.1	170
3	Headliner	71	158	281	179	11.7	14.4	160
Average:		38.0	164	273	139	12.6	15.0	169
Standard Deviation:		29.5	16	14	45	1.2	1.3	8

Table E-3. ASTM E1354 Results for Interior Vehicle Materials

Test No.	Material Description	t _{ig} (s)	t _{end} (s)	HRR _{peak} (kW/m ²)	HRR ₆₀ (kW/m ²)	THR (MJ/m ²)	HOC (MJ/kg)	SEA (m ² /kg)
1	Carpet Ford F250	29	426	399	252	67.3	31.6	585
2	Carpet Ford F250	33	436	433	272	69.6	30.9	590
3	Carpet Ford F250	32	387	478	263	68.9	31.3	564
Average:		31.3	416	437	262	68.6	31.3	580
Standard Deviation:		2.1	26	40	10	1.2	0.3	14
1	Carpet Mercedes	69	632	332	252	79.1	31.0	499
2	Carpet Mercedes	59	1612	326	248	66.2	25.6	255
3	Carpet Mercedes	75	779	293	228	86.8	31.0	404
Average:		67.7	1008	317	243	77.4	29.2	386
Standard Deviation:		8.1	529	21	13	10.4	3.1	123
1	Dashboard Ford F250	56	875	362	269	150.8	39.4	664
2	Dashboard Ford F250	55	1249	358	270	151.9	37.5	586
3	Dashboard Ford F250	51	1106	396	277	151.4	38.5	556
Average:		54.0	1077	372	272	151.4	38.5	602
Standard Deviation:		2.6	189	21	4	0.6	1.0	56
1	Dashboard Mercedes	20	1088	389	299	193.7	31.1	545
2	Dashboard Mercedes	22	776	411	286	170.8	32.5	549
3	Dashboard Mercedes	21	608	388	274	130.5	30.7	596
Average:		21.0	824	396	287	165.0	31.4	563
Standard Deviation:		1.0	244	13	12	32.0	0.9	29
1	Headliner Camaro	6	226	284	201	17.9	25.2	465
2	Headliner Camaro	6	186	295	206	16.6	27.6	556
3	Headliner Camaro	9	174	321	216	16.6	26.6	575
Average:		7.0	195	300	208	17.0	26.5	532
Standard Deviation:		1.7	27	19	8	0.8	1.2	59
1	Headliner Ford	7	141	347	187	16.7	25.4	589
2	Headliner Ford	6	134	351	163	13.3	21.2	525
3	Headliner Ford	9	132	331	167	13.7	19.6	483
Average:		7.3	136	343	173	14.6	22.1	532
Standard Deviation:		1.5	5	10	13	1.8	3.0	53
1	Seat Assembly Camaro	23	511	279	180	82.6	25.4	315
2	Seat Assembly Camaro	24	531	259	184	79.7	25.6	255
3	Seat Assembly Camaro	28	481	299	200	79.6	24.6	286
Average:		25.0	508	279	188	80.6	25.2	286
Standard Deviation:		2.6	25	20	11	1.7	0.5	30
1	Seat Assembly Mercedes	10	478	198	160	61.5	22.0	463
2	Seat Assembly Mercedes	10	636	214	169	65.0	21.4	324
3	Seat Assembly Mercedes	9	493	212	168	60.4	22.6	392
Average:		9.7	536	208	166	62.3	22.0	393
Standard Deviation:		0.6	87	8	5	2.4	0.6	70

Appendix F: ASTM D7309 Data

ASTM D7309 Data

Results Description	Appendix F Table Number
ASTM D7309 Results for School Bus Seat Materials	F-1
ASTM D7309 Results for Motorcoach Materials	F-2
ASTM D7309 Results for Motorcoach Blue Cover Seat Padding	F-3
ASTM D7309 Results for Vehicle Interior Materials	F-4
ASTM D7309 Results for Surface Layer of Selected Vehicle Interior Materials	F-5
ASTM D7309 Results for Cryo-Milled Samples of Various Materials	F-6
ASTM D7309 Results for Thin Materials	F-7
ASTM D7309 Results for Water Mist Foams	F-8
ASTM D7309 Results for Britax Parkway and Chicco KeyFit Materials	F-9
ASTM D7309 Results for Peg Perego Primo Viaggio and UP-PAbaby Mesa Materials	F-10

Nomenclature for Appendix F

h_c = specific heat release (kJ/g)

$h_{c,gas}$ = heat of combustion of the specimen gases (kJ/g)

m_f = final MCC sample mass (mg)

m_i = initial MCC sample mass (mg)

Q = specific heat release rate (W/g)

Q_{max} = maximum specific heat release rate (W/g)

T = pyrolysis chamber temperature ($^{\circ}C$ or K)

T_{max} = pyrolysis chamber temperature when Q_{max} is reached ($^{\circ}C$ or K)

Y_p = pyrolysis residue relative to the initial sample mass (g/g)

β = heating rate (K/s)

η_c = heat release capacity, calculated as Q_{max}/β (J/kg·K)

Table F-1. ASTM D7309 Results for School Bus Seat Materials

Test No.	Material Description	m_i (mg)	m_f (mg)	η_c (J/g·K)	Q_{max} (W/g)	T_{max} (°C)	h_c (kJ/g)	Y_p (g/g)	$h_{c, gas}$ (kJ/g)
1	Blue Bird Seat Cover	4.07	0.97	151	154	248	8.16	0.24	10.7
2	Blue Bird Seat Cover	4.38	1.11	178	182	251	8.31	0.25	11.1
3	Blue Bird Seat Cover	4.57	1.06	178	183	251	8.31	0.23	10.8
Average:		4.34	1.05	169	173	250	8.26	0.24	10.9
Standard Deviation:		0.25	0.07	15.3	16.0	1.7	0.08	0.01	0.21
1	Blue Bird Seat Padding	3.11	0.09	416	421	415	18.0	0.03	18.6
2	Blue Bird Seat Padding	3.51	0.13	372	377	415	16.7	0.04	17.3
3	Blue Bird Seat Padding	3.09	0.16	325	329	429	21.0	0.05	22.2
Average:		3.24	0.13	371	376	420	18.6	0.04	19.4
Standard Deviation:		0.24	0.04	45.4	45.7	7.6	2.20	0.01	2.50
1	Starcraft Seat Cover	3.89	0.82	133	136	300	10.0	0.21	12.7
2	Starcraft Seat Cover	3.66	0.71	132	135	297	10.1	0.19	12.5
3	Starcraft Seat Cover	3.32	0.72	112	114	291	9.53	0.22	12.2
Average:		3.62	0.75	125	128	296	9.86	0.21	12.4
Standard Deviation:		0.29	0.06	11.9	12.5	4.6	0.29	0.01	0.25
1	Starcraft Seat Padding	4.86	0.43	419	423	410	18.6	0.09	20.4
2	Starcraft Seat Padding	4.91	0.22	380	384	413	16.6	0.04	17.4
3	Starcraft Seat Padding	4.97	0.3	272	274	413	14.2	0.06	15.1
Average:		4.91	0.32	357	360	412	16.5	0.06	17.7
Standard Deviation:		0.06	0.11	76.5	77.2	1.8	2.23	0.02	2.68
1	Trans Tech Seat Cover	3.67	0.81	128	130	294	9.62	0.22	12.3
2	Trans Tech Seat Cover	3.73	0.76	129	131	300	9.37	0.20	11.8
3	Trans Tech Seat Cover	3.87	0.79	132	135	299	9.61	0.20	12.1
Average:		3.76	0.79	129	132	298	9.53	0.21	12.1
Standard Deviation:		0.10	0.03	2.2	2.3	3.4	0.14	0.01	0.29
1	Trans Tech Seat Padding	4.18	0.19	303	306	413	16.7	0.05	17.5
2	Trans Tech Seat Padding	4.21	0.11	374	378	409	14.3	0.03	14.7
3	Trans Tech Seat Padding	4.83	0.08	372	375	408	14.1	0.02	14.4
Average:		4.41	0.13	350	353	410	15.1	0.03	15.5
Standard Deviation:		0.37	0.06	40.6	41.0	2.9	1.46	0.01	1.75

Table F-2. ASTM D7309 Results for Motorcoach Materials

Test No.	Material Description	m_i (mg)	m_f (mg)	η_c (J/g·K)	Q_{max} (W/g)	T_{max} (°C)	h_c (kJ/g)	Y_p (g/g)	$h_{c, gas}$ (kJ/g)
1	Green Cover Seat Padding	5.05	0.2	544	542	348	18.4	0.04	19.2
2	Green Cover Seat Padding	5.08	0.23	NA	NA	355	18.3	0.05	19.1
3	Green Cover Seat Padding	5.08	0.54	532	531	362	18.9	0.11	21.1
Average:		5.07	0.32	538	537	355	18.52	0.06	19.8
Standard Deviation:		0.02	0.19	8.3	7.9	7.2	0.31	0.04	1.12
1	Seat Cover - Green	3.33	0.06	259	264	442	14.9	0.02	15.2
2	Seat Cover - Green	3.13	0.06	261	264	447	14.9	0.02	15.2
3	Seat Cover - Green	NA	NA	NA	NA	NA	NA	NA	NA
Average:		3.23	0.06	260	264	444	14.9	0.02	15.2
Standard Deviation:		0.14	0.00	1.1	0.5	3.5	0.00	0.00	0.01
1	Seat Backing - Blue	3.08	0.58	101	102	372	8.60	0.19	10.6
2	Seat Backing - Blue	3.3	0.43	88	89	377	8.90	0.13	10.2
3	Seat Backing - Blue	3.98	0.67	89	90	366	8.50	0.17	10.2
Average:		3.45	0.56	93	93	372	8.67	0.16	10.3
Standard Deviation:		0.47	0.12	7.1	7.1	5.3	0.21	0.03	0.21
1	Seat Cover - Pattern Blue	4.36	0.81	121	121	423	13.4	0.19	16.4
2	Seat Cover - Pattern Blue	4.07	0.7	124	124	422	12.4	0.17	15.0
3	Seat Cover - Pattern Blue	4.54	0.88	130	130	425	12.9	0.19	15.9
Average:		4.32	0.80	125	125	423	12.9	0.18	15.8
Standard Deviation:		0.24	0.09	4.5	4.5	1.9	0.47	0.01	0.72
1	Seat Backing - Gray	3.50	0.01	1027	1027	490	37.9	0.00	38.0
2	Seat Backing - Gray	3.00	0.01	985	985	489	37.0	0.00	37.1
3	Seat Backing - Gray	3.87	0.04	796	796	489	29.0	0.01	29.3
Average:		3.46	0.02	936	936	489	34.6	0.01	34.8
Standard Deviation:		0.44	0.02	122.7	122.7	0.7	4.89	0.00	4.79
1	Door of Luggage Rack	4.03	0.2	383	388	430	28.2	0.05	29.7
2	Door of Luggage Rack	3.91	0.2	378	384	440	28.8	0.05	30.3
3	Door of Luggage Rack	3.96	0.17	376	380	439	28.0	0.04	29.3
Average:		3.97	0.19	379	384	436	28.3	0.05	29.8
Standard Deviation:		0.06	0.02	3.7	4.0	5.3	0.40	0.00	0.53
1	Floor Covering	3.80	3.16	104	106	309	7.13	0.83	42.3
2	Floor Covering	3.85	2.95	92	94	306	6.96	0.77	29.8
3	Floor Covering	3.84	3.06	107	108	308	7.48	0.80	36.8
Average:		3.83	3.06	101	103	308	7.19	0.80	36.3
Standard Deviation:		0.03	0.11	7.7	7.8	1.6	0.26	0.03	6.29
1	Headliner	3.38	0.05	98	100	527	3.96	0.01	4.0
2	Headliner	NA	NA	NA	NA	NA	NA	NA	NA
3	Headliner	3.86	0.07	116	117	494	4.07	0.02	4.1
Average:		3.62	0.06	107	109	510	4.0	0.02	4.1
Standard Deviation:		0.34	0.01	12.1	12.1	23.0	0.08	0.00	0.09

Table F-3. ASTM D7309 Results for Motorcoach Blue Cover Seat Padding

Test No.	Material Description	m_i (mg)	m_f (mg)	η_c (J/g·K)	Q_{max} (W/g)	T_{max} (°C)	h_c (kJ/g)	Y_p (g/g)	$h_{c,gas}$ (kJ/g)
1	Blue Cover Padding (Int)	2.95	0.27	436	436	406	23.4	0.09	25.7
2	Blue Cover Padding (Int)	2.97	0.10	440	435	407	23.5	0.03	24.3
3	Blue Cover Padding (Int)	2.95	0.23	429	424	406	23.1	0.08	25.0
Average:		2.96	0.20	435	432	406	23.3	0.07	25.0
Standard Deviation:		0.01	0.09	5.5	7.0	0.1	0.20	0.03	0.71
4	Blue Cover Padding (Int)	3.03	0.34	427	417	406	22.7	0.11	25.6
5	Blue Cover Padding (Int)	3.02	0.18	470	458	404	24.1	0.06	25.7
6	Blue Cover Padding (Int)	3.00	0.24	447	443	407	23.9	0.08	26.0
Average:		3.02	0.25	448	439	405	23.6	0.08	25.7
Standard Deviation:		0.02	0.08	21.5	20.4	1.5	0.78	0.03	0.24
1	Blue Cover Padding (Surf)	3.03	0.17	417	413	403	24.4	0.06	25.9
2	Blue Cover Padding (Surf)	3.02	0.17	423	416	406	23.5	0.06	24.9
3	Blue Cover Padding (Surf)	3.00	0.18	424	421	403	23.7	0.06	25.2
Average:		3.02	0.17	421	417	404	23.9	0.06	25.3
Standard Deviation:		0.02	0.01	3.9	4.0	1.5	0.47	0.00	0.48
4	Blue Cover Padding (Surf)	3.02	0.15	428	425	405	23.5	0.05	24.8
5	Blue Cover Padding (Surf)	3.05	0.16	430	424	406	24.4	0.05	25.8
6	Blue Cover Padding (Surf)	3.01	0.22	424	416	405	24.0	0.07	25.9
Average:		3.03	0.18	427	422	405	24.0	0.06	25.5
Standard Deviation:		0.02	0.04	3.3	4.7	0.8	0.45	0.01	0.62
Average (Int):		2.99	0.23	441	435	406	23.4	0.08	25.4
Standard Deviation (Int):		0.04	0.08	15.8	14.2	1.1	0.53	0.03	0.62
Average (Surf):		3.02	0.18	424	419	405	23.9	0.06	25.4
Standard Deviation (Surf):		0.02	0.02	4.7	4.8	1.3	0.42	0.01	0.50
Average (All):		3.00	0.20	433	427	405	23.7	0.07	25.4
Standard Deviation (All):		0.03	0.06	14.2	13.2	1.3	0.52	0.02	0.54

Table F-4. ASTM D7309 Results for Vehicle Interior Materials

Test No.	Material Description	m_i (mg)	m_f (mg)	η_c (J/g·K)	Q_{max} (W/g)	T_{max} (°C)	h_c (kJ/g)	Y_p (g/g)	$h_{c,gas}$ (kJ/g)
1	Carpet Ford F250	5.05	0.20	922	938	482	40.8	0.04	42.5
2	Carpet Ford F250	5.08	0.23	955	970	483	41.0	0.05	43.0
3	Carpet Ford F250	5.08	0.54	851	864	481	38.7	0.11	43.3
Average:		5.07	0.32	909	924	482	40.2	0.06	42.9
Standard Deviation:		0.02	0.19	53.2	54.3	0.80	1.29	0.04	0.40
1	Carpet Mercedes	5.00	1.35	213	217	415	20.0	0.27	27.4
2	Carpet Mercedes	5.04	1.35	201	206	411	18.9	0.27	25.8
3	Carpet Mercedes	4.98	0.82	246	250	416	22.4	0.16	26.8
Average:		5.01	1.17	220	224	414	20.4	0.23	26.7
Standard Deviation:		0.03	0.31	23.4	23.2	2.5	1.76	0.06	0.81
1	Dashboard Ford F250	4.85	0.70	1246	1074	491	38.2	0.14	44.7
2	Dashboard Ford F250	4.84	0.64	1055	1072	493	38.4	0.13	44.2
3	Dashboard Ford F250	4.94	0.75	1034	1054	492	37.4	0.15	44.1
Average:		4.88	0.70	1112	1066	492	38.0	0.14	44.3
Standard Deviation:		0.06	0.06	116.6	11.0	0.9	0.51	0.01	0.28
1	Dashboard Mercedes	5.03	0.19	322	326	412	25.5	0.04	26.5
2	Dashboard Mercedes	5.12	0.18	329	333	411	24.7	0.04	25.6
3	Dashboard Mercedes	5.02	0.25	315	319	411	24.8	0.05	26.1
Average:		5.06	0.21	322	326	411	25.0	0.04	26.1
Standard Deviation:		0.06	0.04	6.9	6.8	0.4	0.46	0.01	0.47
1	Headliner Camaro	5.02	1.26	181	183	465	16.4	0.25	21.9
2	Headliner Camaro	4.97	1.11	178	180	456	15.4	0.22	19.8
3	Headliner Camaro	5.04	1.48	201	204	469	16.4	0.29	23.2
Average:		5.01	1.28	187	189	463	16.1	0.26	21.6
Standard Deviation:		0.04	0.19	12.9	12.8	7.0	0.57	0.04	1.70
1	Headliner Ford	4.97	1.49	125	128	431	16.2	0.30	23.1
2	Headliner Ford	4.88	1.10	133	136	419	18.8	0.23	24.2
3	Headliner Ford	4.86	1.40	156	160	426	17.6	0.29	24.7
Average:		4.90	1.33	138	141	425	17.5	0.27	24.0
Standard Deviation:		0.06	0.20	16.5	16.7	6.4	1.30	0.04	0.82
1	Seat Cover Camaro	5.02	0.52	320	323	445	18.1	0.10	20.1
2	Seat Cover Camaro	5.01	0.46	322	325	442	18.3	0.09	20.1
3	Seat Cover Camaro	5.01	0.46	332	336	445	17.9	0.09	19.7
Average:		5.01	0.48	325	328	444	18.1	0.10	20.0
Standard Deviation:		0.01	0.03	6.6	7.0	1.4	0.19	0.01	0.25
1	Seat Cover Mercedes	5.65	0.83	288	295	283	14.4	0.15	16.9
2	Seat Cover Mercedes	5.07	0.67	263	268	285	12.8	0.13	14.8
3	Seat Cover Mercedes	5.51	0.78	255	262	281	12.8	0.14	14.9
Average:		5.41	0.76	269	275	283	13.3	0.14	15.5
Standard Deviation:		0.30	0.08	16.9	17.5	2.0	0.92	0.01	1.18

Table F-4. ASTM D7309 Results for Vehicle Interior Materials (Continued)

Test No.	Material Description	m_i (mg)	m_f (mg)	η_c (J/g·K)	Q_{max} (W/g)	T_{max} (°C)	h_c (kJ/g)	Y_p (g/g)	$h_{c,gas}$ (kJ/g)
1	Seat Padding Camaro	4.97	0.16	510	516	409	21.5	0.03	22.2
2	Seat Padding Camaro	5.01	0.19	477	483	408	21.5	0.04	22.3
3	Seat Padding Camaro	5.00	0.10	502	507	408	21.5	0.02	21.9
Average:		4.99	0.15	496	502	409	21.5	0.03	22.1
Standard Deviation:		0.02	0.05	17.3	17.5	0.6	0.02	0.01	0.20
1	Seat Padding Mercedes	4.96	0.30	526	533	408	23.5	0.06	25.0
2	Seat Padding Mercedes	4.92	0.27	524	528	409	23.6	0.05	25.0
3	Seat Padding Mercedes	4.96	0.39	524	512	409	23.2	0.08	25.2
Average:		4.95	0.32	525	524	409	23.4	0.06	25.0
Standard Deviation:		0.02	0.06	1.3	11.0	0.6	0.21	0.01	0.10

Table F-5. ASTM D7309 Results for Surface Layer of Selected Vehicle Interior Materials

Test No.	Material Description	m_i (mg)	m_f (mg)	η_c (J/g·K)	Q_{max} (W/g)	T_{max} (°C)	h_c (kJ/g)	Y_p (g/g)	$h_{c,gas}$ (kJ/g)
1	Carpet Ford F250	3.00	0.03	927	948	474	41.1	0.01	41.5
2	Carpet Ford F250	3.03	0.09	969	960	472	41.3	0.03	42.6
3	Carpet Ford F250	3.05	0.09	952	943	471	41.4	0.03	42.6
Average:		3.03	0.07	949	950	472	41.2	0.02	42.2
Standard Deviation:		0.03	0.03	21.4	8.6	1.5	0.16	0.01	0.64
1	Carpet Mercedes	3.05	0.09	609	604	459	30.0	0.03	30.9
2	Carpet Mercedes	3.04	0.23	581	577	456	28.1	0.08	30.4
3	Carpet Mercedes	3.00	0.00	642	637	458	29.8	0.00	29.8
Average:		3.03	0.11	611	606	458	29.3	0.04	30.4
Standard Deviation:		0.03	0.12	30.5	30.5	1.6	1.04	0.04	0.55
1	Dashboard Mercedes	3.00	0.21	264	261	372	27.0	0.07	29.0
2	Dashboard Mercedes	3.00	0.06	294	290	388	27.4	0.02	28.0
3	Dashboard Mercedes	3.02	0.07	324	321	389	27.1	0.02	27.7
Average:		3.01	0.11	294	291	383	27.2	0.04	28.2
Standard Deviation:		0.01	0.08	29.8	30.4	9.8	0.21	0.03	0.69
1	Headliner Camaro	3.00	0.35	210	209	416	18.7	0.12	21.1
2	Headliner Camaro	3.04	0.32	227	226	422	19.0	0.11	21.3
3	Headliner Camaro	3.01	0.35	253	249	438	18.2	0.12	20.5
Average:		3.02	0.34	230	228	425	18.6	0.11	21.0
Standard Deviation:		0.02	0.02	21.6	19.8	11.5	0.44	0.01	0.38
1	Headliner Ford	3.01	0.30	303	302	442	17.9	0.10	19.9
2	Headliner Ford	3.00	0.23	249	245	442	20.7	0.08	22.4
3	Headliner Ford	3.00	0.42	290	289	438	17.3	0.14	20.1
Average:		3.00	0.32	281	279	441	18.6	0.11	20.8
Standard Deviation:		0.01	0.10	28.1	29.8	2.1	1.79	0.03	1.38
1	Seat Cover Camaro	3.03	0.52	368	364	439	16.7	0.17	20.1
2	Seat Cover Camaro	3.00	0.46	389	385	435	16.7	0.15	19.7
3	Seat Cover Camaro	3.03	0.46	398	394	438	16.7	0.15	19.7
Average:		3.02	0.48	385	381	438	16.7	0.16	19.9
Standard Deviation:		0.02	0.03	15.1	15.5	2.1	0.02	0.01	0.25

Table F-6. ASTM D7309 Results for Cryo-Milled Samples of Various Materials

Test No.	Material Description	m_i (mg)	m_f (mg)	η_c (J/g·K)	Q_{max} (W/g)	T_{max} (°C)	h_c (kJ/g)	Y_p (g/g)	$h_{c, gas}$ (kJ/g)
1	Blue Bird - Seat Cover	3.70	0.60	140	143	249	14.5	0.16	17.3
2	Blue Bird - Seat Cover	3.50	0.30	106	107	435	14.6	0.09	16.0
3	Blue Bird - Seat Cover	3.80	0.90	156	158	244	14.8	0.24	19.4
Average:		3.67	0.60	134	136	310	14.6	0.16	17.5
Standard Deviation:		0.15	0.30	25.5	26.0	108.85	0.16	0.08	1.70
1	Blue Bird - Seat Padding	3.40	0.00	528	536	402	28.1	0.00	28.1
2	Blue Bird - Seat Padding	3.20	0.20	564	574	402	30.9	0.06	33.0
3	Blue Bird - Seat Padding	3.30	0.00	523	531	400	28.5	0.00	28.5
Average:		3.30	0.07	538	547	401	29.2	0.02	29.9
Standard Deviation:		0.10	0.12	22.5	23.3	1.4	1.55	0.04	2.73
1	Blue Bird - Padding BS	3.00	0.00	388	395	411	24.4	0.00	24.4
2	Blue Bird - Padding BS	2.90	0.10	393	399	414	25.4	0.03	26.4
3	Blue Bird - Padding BS	2.80	0.20	420	426	414	26.5	0.07	28.6
Average:		2.90	0.10	400	407	413	25.4	0.04	26.4
Standard Deviation:		0.10	0.10	17.0	17.0	2.0	1.07	0.04	2.10
1	Starcraft - Seat Padding	3.70	0.00	330	335	414	22.9	0.00	22.9
2	Starcraft - Seat Padding	3.70	0.20	386	392	411	26.9	0.05	28.4
3	Starcraft - Seat Padding	3.70	0.00	435	443	411	29.1	0.00	29.1
Average:		3.70	0.07	383	390	412	26.3	0.02	26.8
Standard Deviation:		0.00	0.12	52.6	54.0	1.8	3.15	0.03	3.40
1	Trans Tech - Seat Padding	3.70	0.60	415	421	406	28.9	0.16	34.5
2	Trans Tech - Seat Padding	3.40	0.00	417	424	408	30.1	0.00	30.1
3	Trans Tech - Seat Padding	3.70	0.20	378	384	409	27.9	0.05	29.5
Average:		3.60	0.27	403	410	408	29.0	0.07	31.4
Standard Deviation:		0.17	0.31	21.9	22.2	1.6	1.08	0.08	2.74
1	Door of Luggage Rack	4.03	0.20	631	645	446	39.2	0.05	41.3
2	Door of Luggage Rack	3.91	0.20	649	651	444	40.0	0.05	42.2
3	Door of Luggage Rack	3.96	0.17	588	591	443	34.0	0.04	35.5
Average:		3.97	0.19	623	629	444	37.7	0.05	39.6
Standard Deviation:		0.06	0.02	31.8	33.4	1.5	3.28	0.00	3.62
1	Headliner	3.20	0.00	111	112	374	12.0	0.00	12.0
2	Headliner	3.20	0.00	132	134	368	15.0	0.00	15.0
3	Headliner	3.20	0.00	126	128	373	15.0	0.00	15.0
Average:		3.20	0.00	123	125	372	14.0	0.00	14.0
Standard Deviation:		0.00	0.00	10.7	11.0	3.4	1.73	0.00	1.73
1	Carpet Mercedes	3.90	1.30	130	132	488	15.7	0.33	23.5
2	Carpet Mercedes	3.80	1.30	131	133	487	12.9	0.34	19.6
3	Carpet Mercedes	4.00	1.20	134	149	488	12.8	0.30	18.3
Average:		3.90	1.27	132	138	488	13.8	0.33	20.5
Standard Deviation:		0.10	0.06	2.3	9.7	0.9	1.62	0.02	2.69

Table F-6. ASTM D7309 Results for Cryo-Milled Samples of Various Materials (Continued)

Test No.	Material Description	m_i (mg)	m_f (mg)	η_c (J/g·K)	Q_{max} (W/g)	T_{max} (°C)	h_c (kJ/g)	Y_p (g/g)	$h_{c, gas}$ (kJ/g)
1	Headliner Ford	3.00	0.60	147	150	400	20.2	0.20	25.3
2	Headliner Ford	3.00	0.30	155	157	400	24.5	0.10	27.2
3	Headliner Ford	3.30	0.60	144	144	401	20.2	0.18	24.7
Average:		3.10	0.50	149	150	401	21.7	0.16	25.7
Standard Deviation:		0.17	0.17	5.7	6.7	0.66	2.48	0.05	1.33
1	Seat Padding Camaro	4.00	0.10	502	560	406	28.4	0.03	29.1
2	Seat Padding Camaro	4.00	0.10	505	560	406	28.2	0.03	29.0
3	Seat Padding Camaro	4.00	0.10	487	542	404	27.4	0.03	28.1
Average:		4.00	0.10	498	554	405	28.0	0.03	28.7
Standard Deviation:		0.00	0.00	9.9	10.4	1.2	0.52	0.00	0.53
1	Acrylate	3.10	0.00	411	457	384	27.2	0.00	27.2
2	Acrylate	3.10	0.00	421	467	387	26.8	0.00	26.8
3	Acrylate	2.90	0.00	427	475	396	27.1	0.00	27.1
Average:		3.03	0.00	420	466	389	27.0	0.00	27.0
Standard Deviation:		0.12	0.00	7.9	8.8	6.1	0.18	0.00	0.18

Table F-7. ASTM D7309 Results for Thin Materials

Test No.	Material Description	m_i (mg)	m_f (mg)	η_c (J/g·K)	Q_{max} (W/g)	T_{max} (°C)	h_c (kJ/g)	Y_p (g/g)	$h_{c,gas}$ (kJ/g)
1	Acrylate	5.12	0.08	406	412	385	25.8	0.02	26.3
2	Acrylate	4.81	0.05	400	404	408	25.4	0.01	25.7
3	Acrylate	5.86	0.07	407	412	407	26.2	0.01	26.5
Average:		5.26	0.07	404	409	400	25.8	0.01	26.2
Standard Deviation:		0.54	0.02	3.9	4.5	13.1	0.38	0.00	0.41
1	Corrugated Cardboard	4.51	0.88	125	127	363	9.1	0.20	11.3
2	Corrugated Cardboard	4.17	0.81	145	146	365	9.3	0.19	11.6
3	Corrugated Cardboard	4.52	0.86	150	152	363	9.9	0.19	12.3
Average:		4.40	0.85	140	142	364	9.5	0.19	11.7
Standard Deviation:		0.20	0.04	13.0	13.0	1.0	0.42	0.00	0.48
1	HDPE	4.69	0.07	1104	1125	505	42.8	0.01	43.5
2	HDPE	4.11	0.05	1241	1261	504	44.4	0.01	44.9
3	HDPE	4.57	0.07	1124	1143	503	42.9	0.02	43.6
Average:		4.46	0.06	1156	1176	504	43.4	0.01	44.0
Standard Deviation:		0.31	0.01	73.7	73.6	0.8	0.89	0.00	0.83
1	Manila File Folder	4.44	0.48	211	213	366	10.3	0.11	11.5
2	Manila File Folder	4.61	0.54	212	214	364	11.0	0.12	12.4
3	Manila File Folder	4.73	0.55	222	224	366	10.8	0.12	12.2
Average:		4.59	0.52	215	217	365	10.7	0.11	12.1
Standard Deviation:		0.15	0.04	5.9	6.0	1.0	0.36	0.00	0.47

Table F-8. ASTM D7309 Results for Water Mist Foams

Test No.	Material Description	m_i (mg)	m_f (mg)	η_c (J/g·K)	Q_{max} (W/g)	T_{max} (°C)	h_c (kJ/g)	Y_p (g/g)	$h_{c,gas}$ (kJ/g)
1	Water Mist SF Foam	3.04	0.00	642	636	388	27.3	0.00	27.3
2	Water Mist SF Foam	3.02	0.00	618	608	382	27.6	0.00	27.6
3	Water Mist SF Foam	3.03	0.00	660	652	385	27.3	0.00	27.3
Average:		3.03	0.00	640	632	385	27.4	0.00	27.4
Standard Deviation:		0.01	0.00	20.8	22.1	3.0	0.17	0.00	0.17
1	Water Mist SM Foam	3.18	0.03	540	532	389	26.9	0.01	27.1
2	Water Mist SM Foam	3.18	0.03	524	517	389	26.0	0.01	26.3
3	Water Mist SM Foam	3.20	0.00	569	558	384	27.3	0.00	27.3
Average:		3.19	0.02	544	536	387	26.7	0.01	26.9
Standard Deviation:		0.01	0.02	22.4	20.9	2.7	0.67	0.01	0.57

Table F-9. ASTM D7309 Results for Britax Parkway and Chicco KeyFit Materials

Test No.	Material Description	m_i (mg)	m_f (mg)	η_c (J/g·K)	Q_{max} (W/g)	T_{max} (°C)	h_c (kJ/g)	Y_p (g/g)	$h_{c,gas}$ (kJ/g)
1	Britax Base Plastic	3.00	0.00	1246	1237	471	44.8	0.00	44.8
2	Britax Base Plastic	3.06	0.00	1225	1215	470	43.8	0.00	43.8
3	Britax Base Plastic	3.06	0.00	1237	1236	467	44.5	0.00	44.5
Average:		3.04	0.00	1236	1229	469	44.4	0.00	44.4
Standard Deviation:		0.03	0.00	10.4	12.5	1.71	0.54	0.00	0.54
1	Britax Fabric	3.25	0.49	340	337	442	15.7	0.15	18.4
2	Britax Fabric	3.26	0.45	332	330	441	16.0	0.14	18.6
3	Britax Fabric	3.27	0.47	331	329	442	15.9	0.14	18.5
Average:		3.26	0.47	334	332	442	15.9	0.14	18.5
Standard Deviation:		0.01	0.02	5.0	4.5	0.6	0.19	0.01	0.08
1	Britax Padding	3.27	0.38	333	329	439	15.6	0.12	17.7
2	Britax Padding	3.29	0.47	333	331	440	15.7	0.14	18.3
3	Britax Padding	3.28	0.53	329	326	440	15.5	0.16	18.5
Average:		3.28	0.46	332	329	440	15.6	0.14	18.2
Standard Deviation:		0.01	0.08	2.5	2.7	0.6	0.07	0.02	0.43
1	Britax Padding & Fabric	3.18	0.51	340	337	442	15.9	0.16	19.0
2	Britax Padding & Fabric	3.19	0.39	352	348	445	16.8	0.12	19.1
3	Britax Padding & Fabric	3.18	0.53	347	346	443	15.7	0.17	18.8
Average:		3.18	0.48	346	344	443	16.1	0.15	19.0
Standard Deviation:		0.01	0.08	5.9	6.2	1.2	0.57	0.02	0.14
1	Chicco Base Plastic	3.03	0.02	1151	1139	469	44.3	0.01	44.6
2	Chicco Base Plastic	3.02	0.00	1156	1139	470	44.4	0.00	44.4
3	Chicco Base Plastic	3.06	0.06	1142	1141	471	43.3	0.02	44.2
Average:		3.04	0.03	1149	1140	470	44.0	0.01	44.4
Standard Deviation:		0.02	0.03	7.2	0.9	0.6	0.57	0.01	0.18
1	Chicco Fabric	3.05	0.08	1235	1227	473	42.0	0.03	43.1
2	Chicco Fabric	3.05	0.03	1280	1266	474	43.7	0.01	44.1
3	Chicco Fabric	3.02	0.02	1224	1210	473	42.8	0.01	43.1
Average:		3.04	0.04	1246	1234	473	42.8	0.01	43.5
Standard Deviation:		0.02	0.03	29.7	28.9	0.5	0.83	0.01	0.57
1	Chicco Padding	2.99	0.00	330	326	386	26.5	0.00	26.5
2	Chicco Padding	3.04	0.10	318	312	385	25.2	0.03	26.0
3	Chicco Padding	3.01	0.01	334	324	385	26.6	0.00	26.7
Average:		3.01	0.04	327	321	385	26.1	0.01	26.4
Standard Deviation:		0.03	0.06	8.3	7.6	0.8	0.77	0.02	0.32
1	Chicco Padding & Fabric	3.11	0.03	256	254	387	31.3	0.01	31.6
2	Chicco Padding & Fabric	3.13	0.04	260	257	468	33.7	0.01	34.2
3	Chicco Padding & Fabric	3.10	0.03	289	286	410	34.1	0.01	34.4
Average:		3.11	0.03	268	266	422	33.1	0.01	33.4
Standard Deviation:		0.02	0.01	17.8	17.9	41.5	1.49	0.00	1.54

Table F-10. ASTM D7309 Results for Peg Perego Primo Viaggio and UPPAbaby Mesa Materials

Test No.	Material Description	m_i (mg)	m_f (mg)	η_c (J/g·K)	Q_{max} (W/g)	T_{max} (°C)	h_c (kJ/g)	Y_p (g/g)	$h_{c,gas}$ (kJ/g)
1	Peg Perego Base Plastic	3.11	0.00	1215	1202	470	45.4	0.00	45.4
2	Peg Perego Base Plastic	3.12	0.05	1162	1147	467	43.7	0.02	44.5
3	Peg Perego Base Plastic	3.12	0.02	1182	1163	470	44.3	0.01	44.6
Average:		3.12	0.02	1186	1171	469	44.5	0.01	44.8
Standard Deviation:		0.01	0.03	26.5	28.1	1.78	0.86	0.01	0.53
1	Peg Perego Fabric	3.06	0.49	322	319	442	15.7	0.16	18.7
2	Peg Perego Fabric	3.06	0.38	331	331	443	16.0	0.12	18.2
3	Peg Perego Fabric	3.06	0.43	331	326	439	16.2	0.14	18.8
Average:		3.06	0.43	328	325	441	15.9	0.14	18.6
Standard Deviation:		0.00	0.06	5.3	6.3	2.3	0.25	0.02	0.32
1	Peg Perego Padding	3.30	0.08	518	511	391	25.4	0.02	26.1
2	Peg Perego Padding	3.35	0.08	526	515	391	25.7	0.02	26.4
3	Peg Perego Padding	3.37	0.00	497	487	388	25.2	0.00	25.2
Average:		3.34	0.05	513	504	390	25.4	0.02	25.9
Standard Deviation:		0.04	0.05	15.2	15.2	1.6	0.28	0.01	0.62
1	Peg Perego Assembly	3.23	0.34	229	227	387	19.9	0.11	22.2
2	Peg Perego Assembly	3.22	0.33	187	187	442	19.1	0.10	21.3
3	Peg Perego Assembly	3.21	0.29	249	245	387	20.0	0.09	22.0
Average:		3.22	0.32	222	220	405	19.7	0.10	21.8
Standard Deviation:		0.01	0.03	31.8	29.6	31.7	0.46	0.01	0.47
1	UPPAbaby Base Plastic	3.00	0.04	1275	1262	470	44.0	0.01	44.6
2	UPPAbaby Base Plastic	2.98	0.00	1231	1220	471	44.0	0.00	44.0
3	UPPAbaby Base Plastic	2.98	0.00	1308	1299	471	45.4	0.00	45.4
Average:		2.99	0.01	1271	1261	471	44.5	0.00	44.6
Standard Deviation:		0.01	0.02	38.8	39.9	0.4	0.81	0.01	0.69
1	UPPAbaby Fabric	3.12	0.59	130	129	395	14.5	0.19	17.9
2	UPPAbaby Fabric	3.12	0.57	121	120	391	14.7	0.18	18.0
3	UPPAbaby Fabric	3.11	0.56	120	119	388	14.7	0.18	18.0
Average:		3.12	0.57	124	123	391	14.7	0.18	18.0
Standard Deviation:		0.01	0.02	5.7	5.6	3.7	0.12	0.00	0.06
1	UPPAbaby Padding	3.27	0.38	582	575	391	27.7	0.12	31.3
2	UPPAbaby Padding	3.29	0.47	574	571	391	27.4	0.14	32.0
3	UPPAbaby Padding	3.28	0.53	556	547	392	28.0	0.16	33.4
Average:		3.28	0.46	571	564	391	27.7	0.14	32.2
Standard Deviation:		0.01	0.08	13.1	14.8	0.6	0.29	0.02	1.05
1	UPPAbaby Assembly	3.18	0.51	265	261	401	17.4	0.16	20.8
2	UPPAbaby Assembly	3.19	0.39	258	254	401	17.7	0.12	20.2
3	UPPAbaby Assembly	3.18	0.53	282	279	402	18.3	0.17	22.0
Average:		3.18	0.48	269	265	401	17.8	0.15	21.0
Standard Deviation:		0.01	0.08	12.3	13.1	0.6	0.44	0.02	0.91

Appendix G: ASTM E2574 Data

ASTM E2574 Data

Results Description	Appendix G Table Number
ASTM E2574 Results for MC Green Seats – Top Gas Burner Ignition Source	G-1
ASTM E2574 Results for MC Green Seats – Paper Bag Ignition Source	G-2
ASTM E2574 Results for MC Blue Seats – Top Gas Burner Ignition Source	G-3
ASTM E2574 Results for MC Blue Seats – Paper Bag Ignition Source	G-4
ASTM E2574 Results for Bluebird SB Seats – Paper Bag Ignition Source	G-5

**SUMMARY OF
LARGE-SCALE CALORIMETRY TESTING OF MOTORCOACH SEATING
GREEN SEATS - TOP SEAT GAS BURNER IGNITION SOURCE**

Peak HRR_{total}	560 kW	at	11 min	19 sec
Average HRR_{total}	157 kW			
Total Heat Released	236 MJ			
Peak HRR_{conv}	269 kW	at	11 min	35 sec
Average HRR_{conv}	123 kW			
Convective Heat Released	185 MJ			
Steady State Convective Fraction	78%			
Steady State Radiative Fraction	22%			
Peak Heat Flux from Seat Flame	54.7 kW/m ²	at	3 min	15 sec
Maximum CO Production Rate	1.024 *10 ⁻³ m ³ /s	at	5 min	55 s
Maximum CO Release Rate	1.172 g/s			
Maximum CO ₂ Production Rate	0.018 *10 ⁻³ m ³ /s	at	11 min	45 s
Maximum CO ₂ Release Rate	33.19 g/s			

Figure G-1: ASTM E2574 results for MC Green Seats – top gas burner ignition source

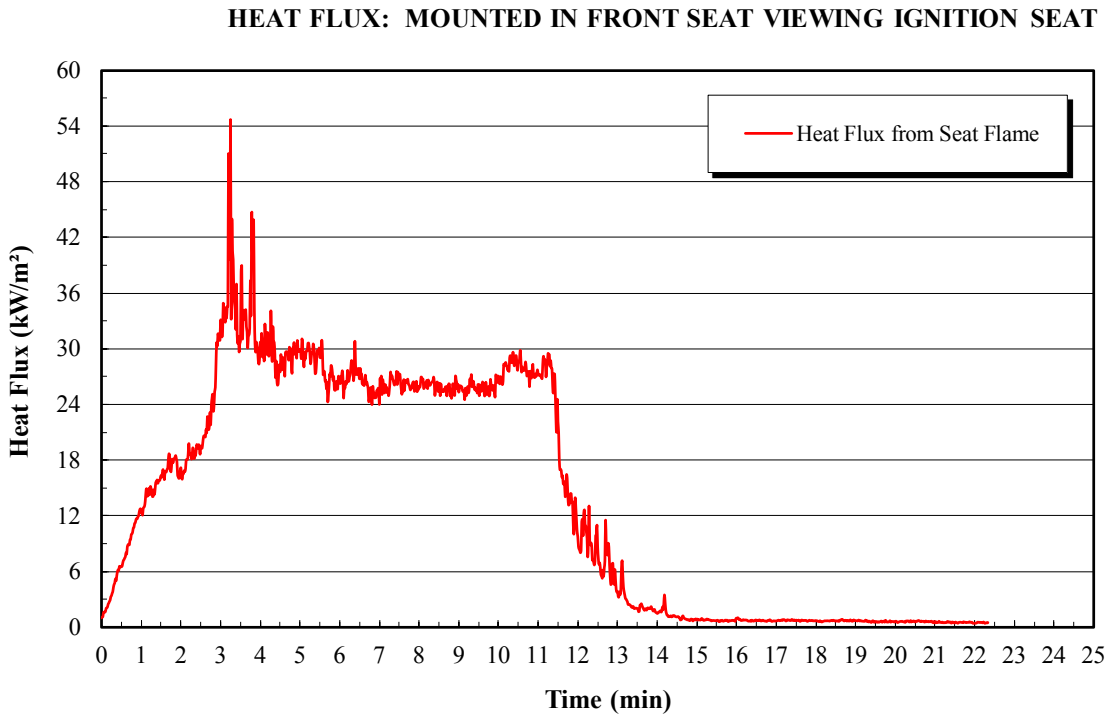
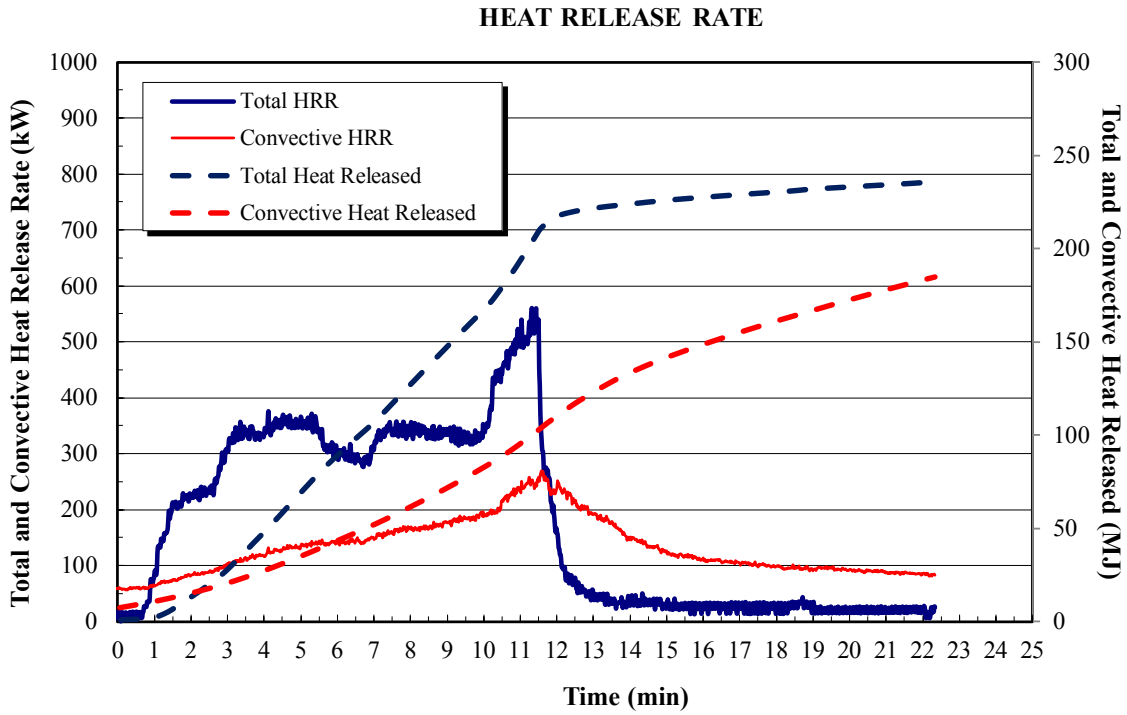
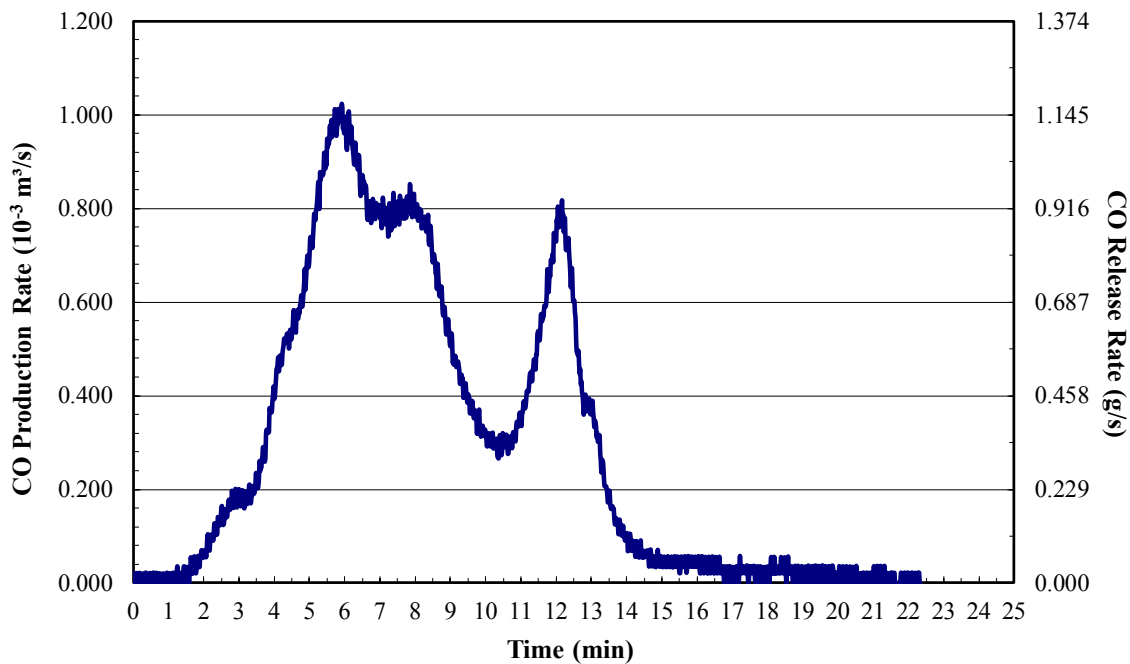


Figure G-1: ASTM E2574 results for MC Green Seats – top gas burner ignition source (continued)

CARBON MONOXIDE (CO) PRODUCTION RATE



CARBON DIOXIDE (CO₂) PRODUCTION RATE

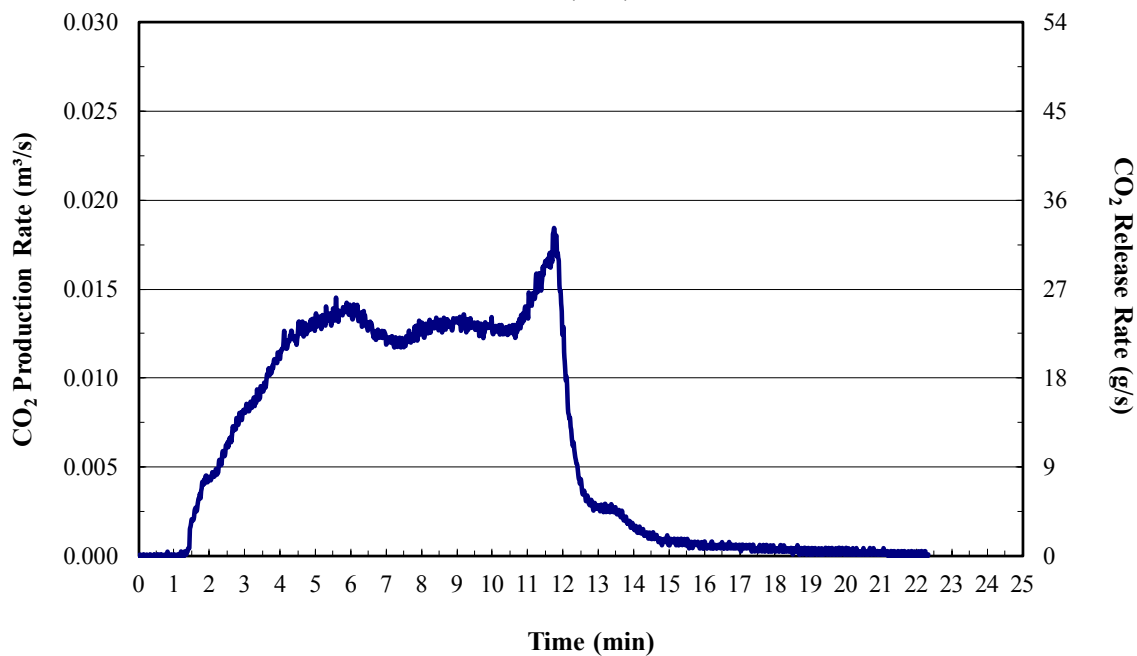


Figure G-1: ASTM E2574 results for MC Green Seats – top gas burner ignition source (continued)

**SUMMARY OF
LARGE-SCALE CALORIMETRY TESTING OF MOTORCOACH SEATING
GREEN SEATS - TOP SEAT PAPER BAG IGNITION SOURCE**

Peak HRR _{total}	422 kW	at	17 min	23 sec
Average HRR _{total}	254 kW			
Total Heat Released	838 MJ			
Peak HRR _{conv}	268 kW	at	28 min	58 sec
Average HRR _{conv}	198 kW			
Convective Heat Released	654 MJ			
Steady State Convective Fraction	78%			
Steady State Radiative Fraction	22%			
Peak Heat Flux from Seat Flame	44.1 kW/m ²	at	18 min	1 sec
Maximum CO Production Rate	1.107 *10 ⁻³ m ³ /s	at	5 min	56 s
Maximum CO Release Rate	1.267 g/s			
Maximum CO ₂ Production Rate	0.015 *10 ⁻³ m ³ /s	at	6 min	13 s
Maximum CO ₂ Release Rate	27.78 g/s			

Figure G-2: ASTM E2574 results for MC Green Seats – paper bag ignition source

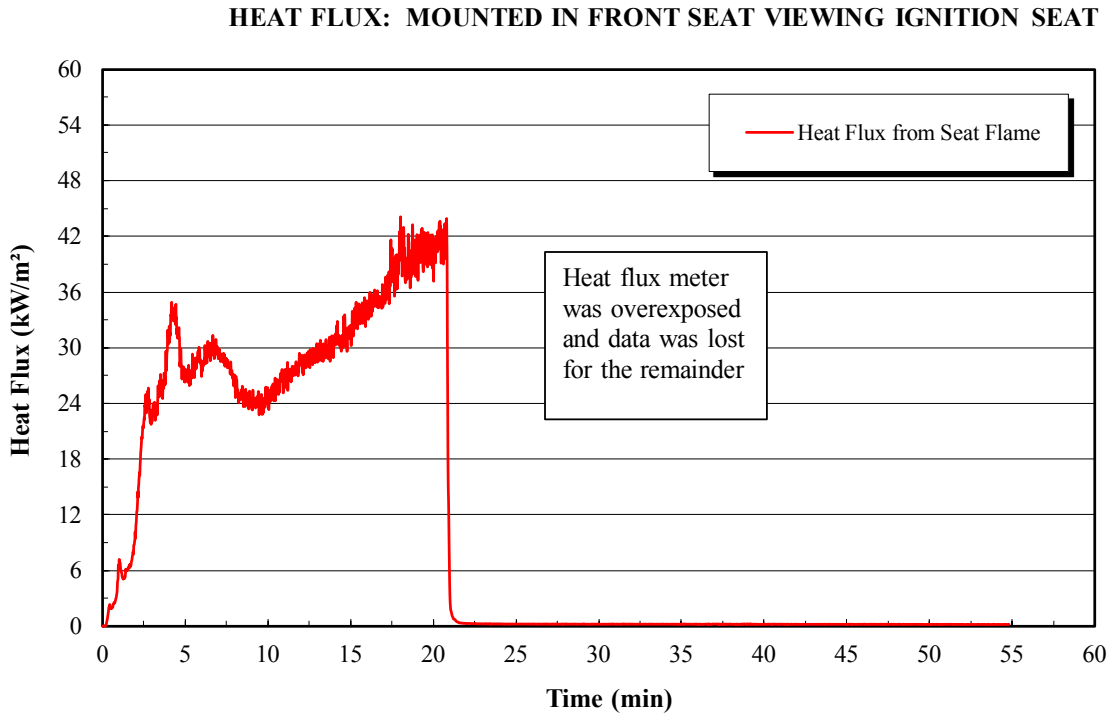
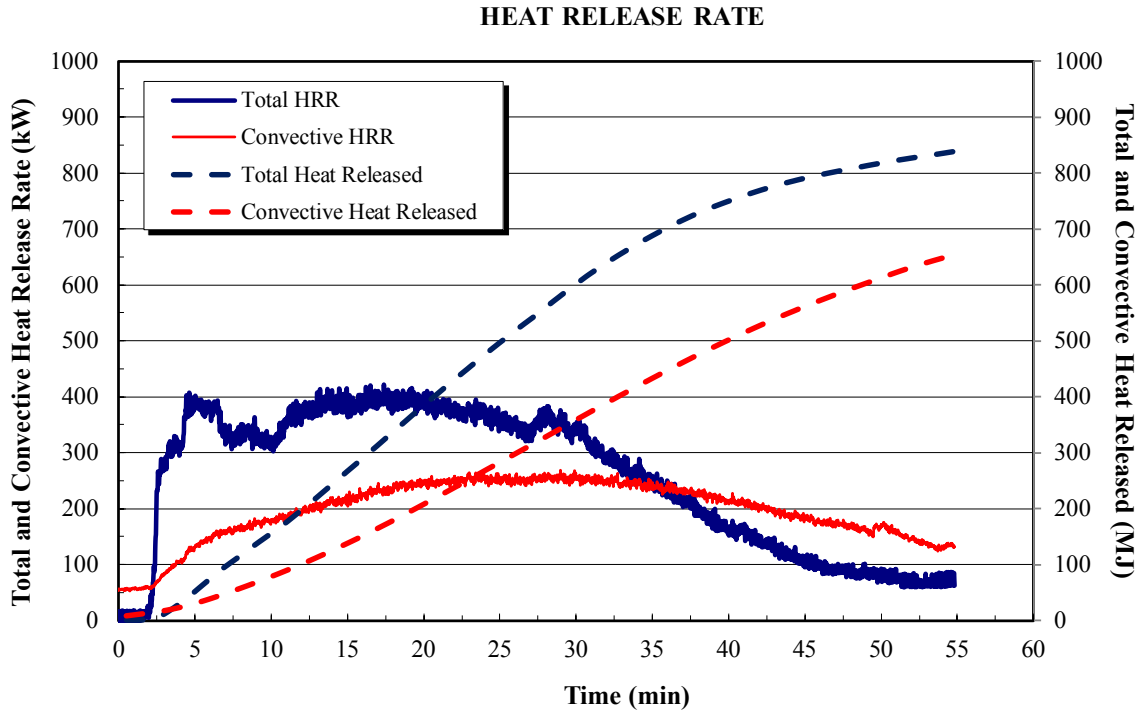


Figure G-2: ASTM E2574 results for MC Green Seats – paper bag ignition source (continued)

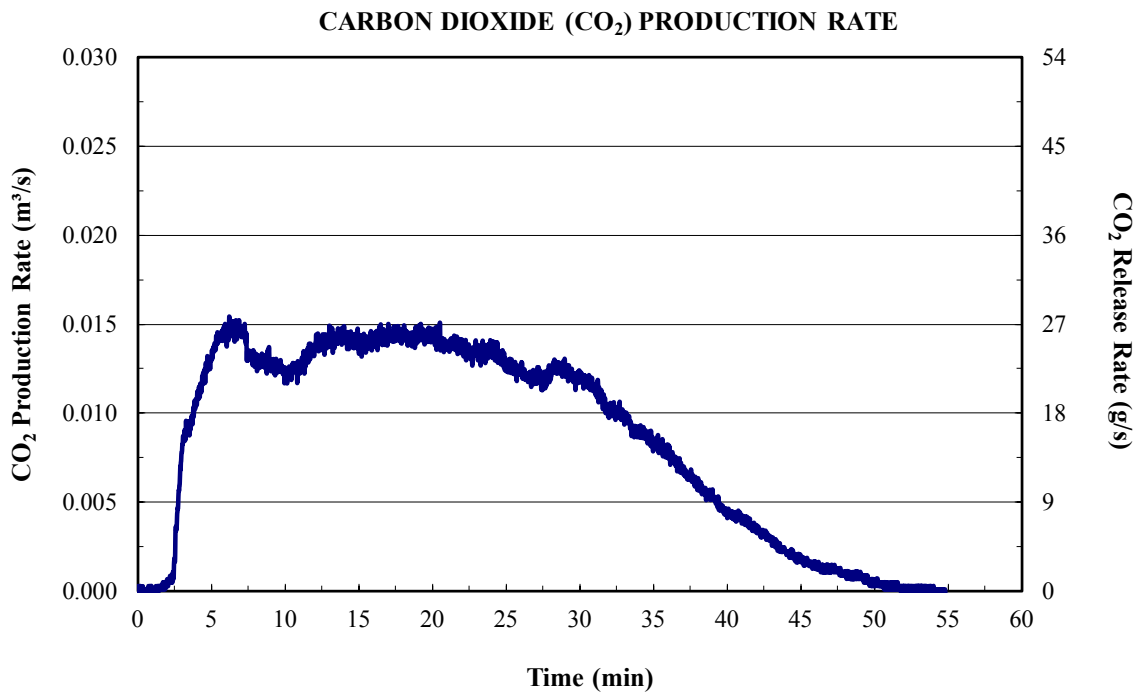
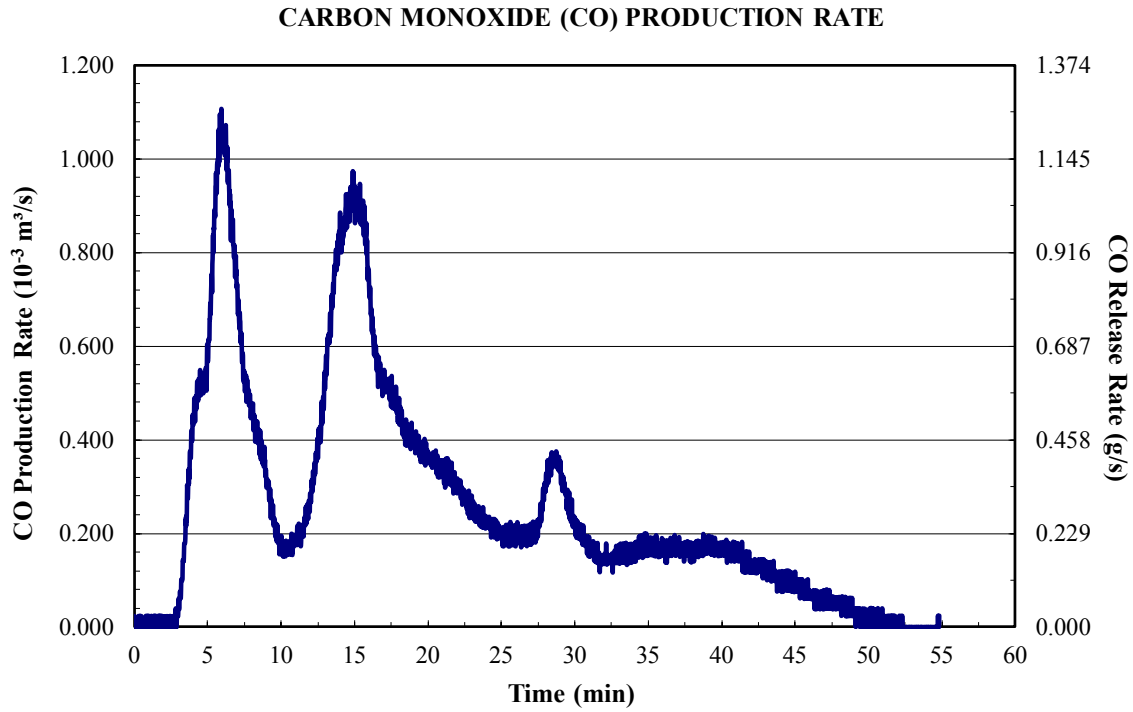


Figure G-2: ASTM E2574 results for MC Green Seats – paper bag ignition source (continued)

**SUMMARY OF
LARGE-SCALE CALORIMETRY TESTING OF MOTORCOACH SEATING
BLUE SEATS - TOP SEAT GAS BURNER IGNITION SOURCE**

Peak HRR _{total}	430 kW	at	18 min	32 sec
Average HRR _{total}	259 kW			
Total Heat Released	854 MJ			
Peak HRR _{conv}	256 kW	at	34 min	9 sec
Average HRR _{conv}	168 kW			
Convective Heat Released	556 MJ			
Steady State Convective Fraction	65%			
Steady State Radiative Fraction	35%			
Peak Heat Flux from Seat Flame	0.3 kW/m ²	at	8 min	13 sec
Maximum CO Production Rate	1.169 *10 ⁻³ m ³ /s	at	17 min	7 s
Maximum CO Release Rate	1.338 g/s			
Maximum CO ₂ Production Rate	0.016 *10 ⁻³ m ³ /s	at	9 min	24 s
Maximum CO ₂ Release Rate	28.35 g/s			

Figure G-3: ASTM E2574 results for MC Blue Seats – top gas burner ignition source

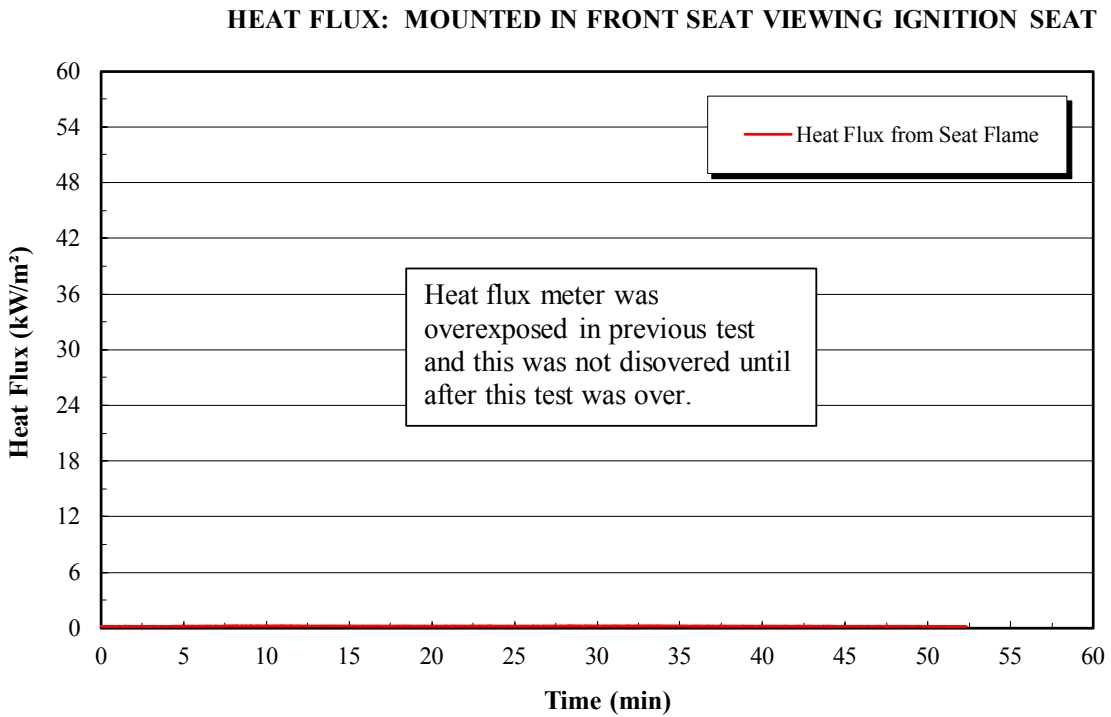
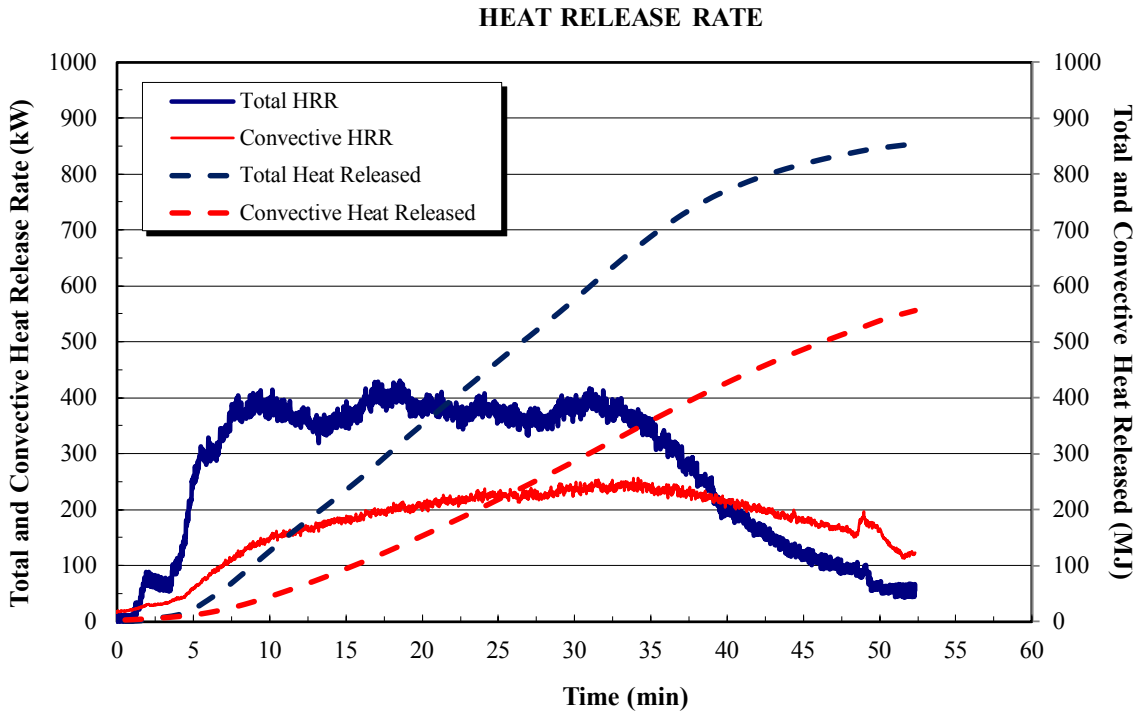


Figure G-3: ASTM E2574 results for MC Blue Seats – top gas burner ignition source (continued)

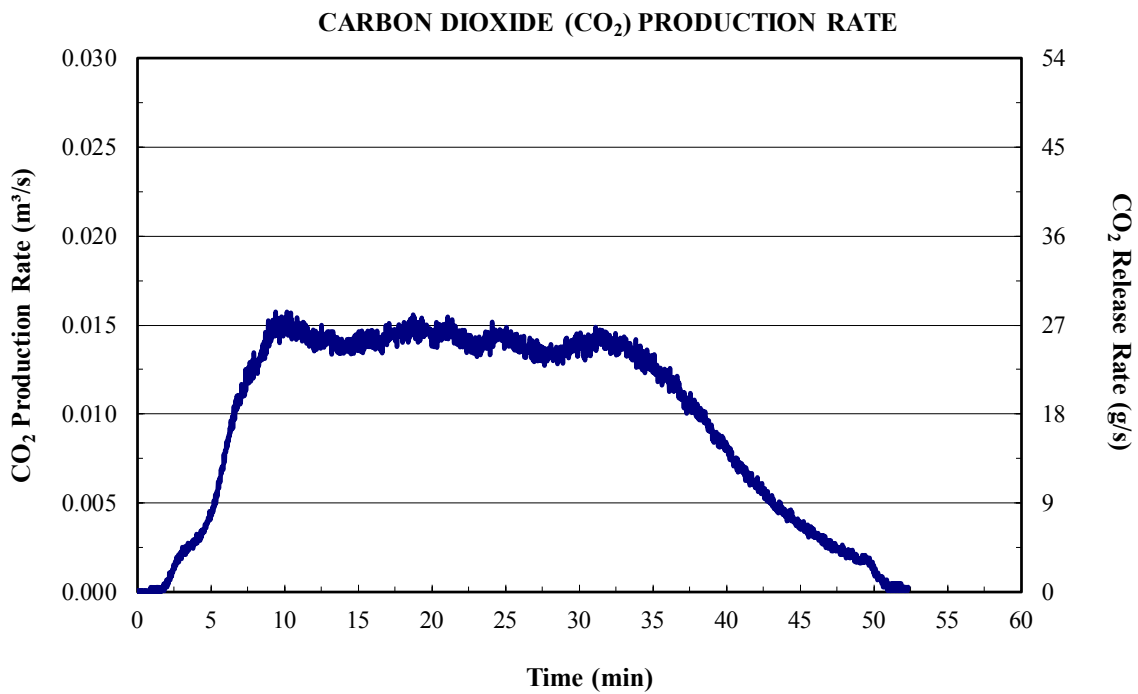
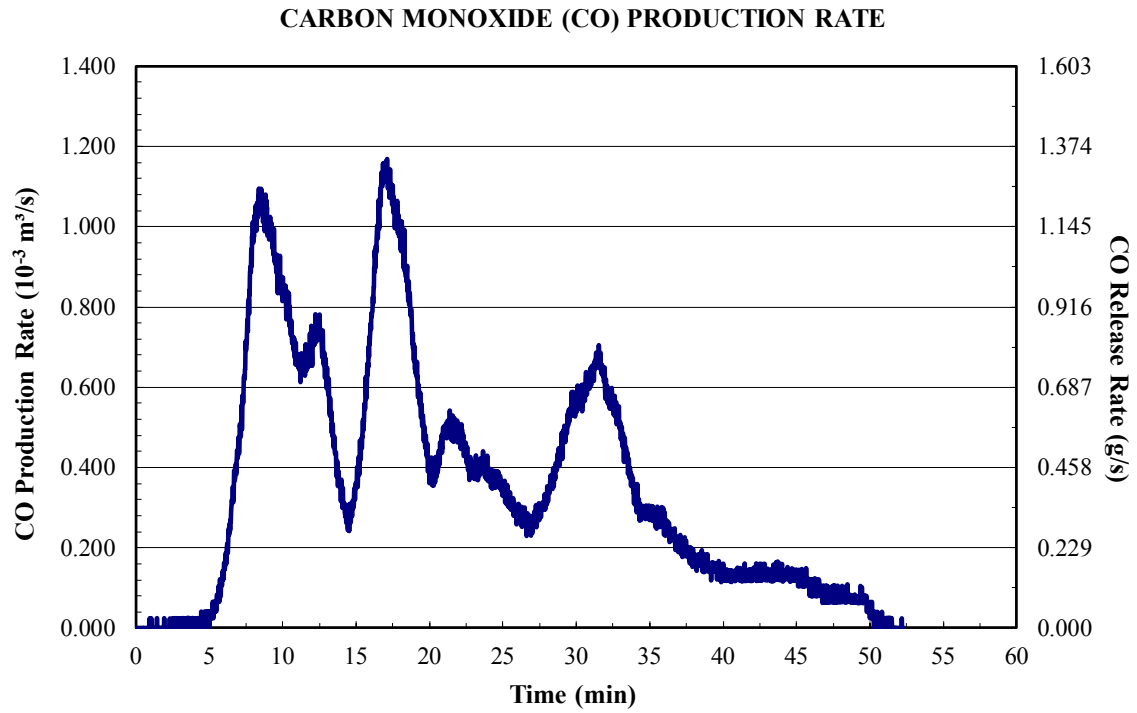


Figure G-3: ASTM E2574 results for MC Blue Seats – top gas burner ignition source (continued)

**SUMMARY OF
LARGE-SCALE CALORIMETRY TESTING OF MOTORCOACH SEATING
BLUE SEATS - TOP SEAT PAPER BAG IGNITION SOURCE**

Peak HRR _{total}	440 kW	at	22 min	25 sec
Average HRR _{total}	244 kW			
Total Heat Released	807 MJ			
Peak HRR _{conv}	301 kW	at	34 min	44 sec
Average HRR _{conv}	196 kW			
Convective Heat Released	648 MJ			
Steady State Convective Fraction	80%			
Steady State Radiative Fraction	20%			
Peak Heat Flux from Seat Flame	67.0 kW/m ²	at	35 min	51 sec
Maximum CO Production Rate	2.096 *10 ⁻³ m ³ /s	at	18 min	4 s
Maximum CO Release Rate	2.400 g/s			
Maximum CO ₂ Production Rate	0.016 *10 ⁻³ m ³ /s	at	13 min	44 s
Maximum CO ₂ Release Rate	29.16 g/s			

Figure G-4: ASTM E2574 results for MC Blue Seats – paper bag ignition source

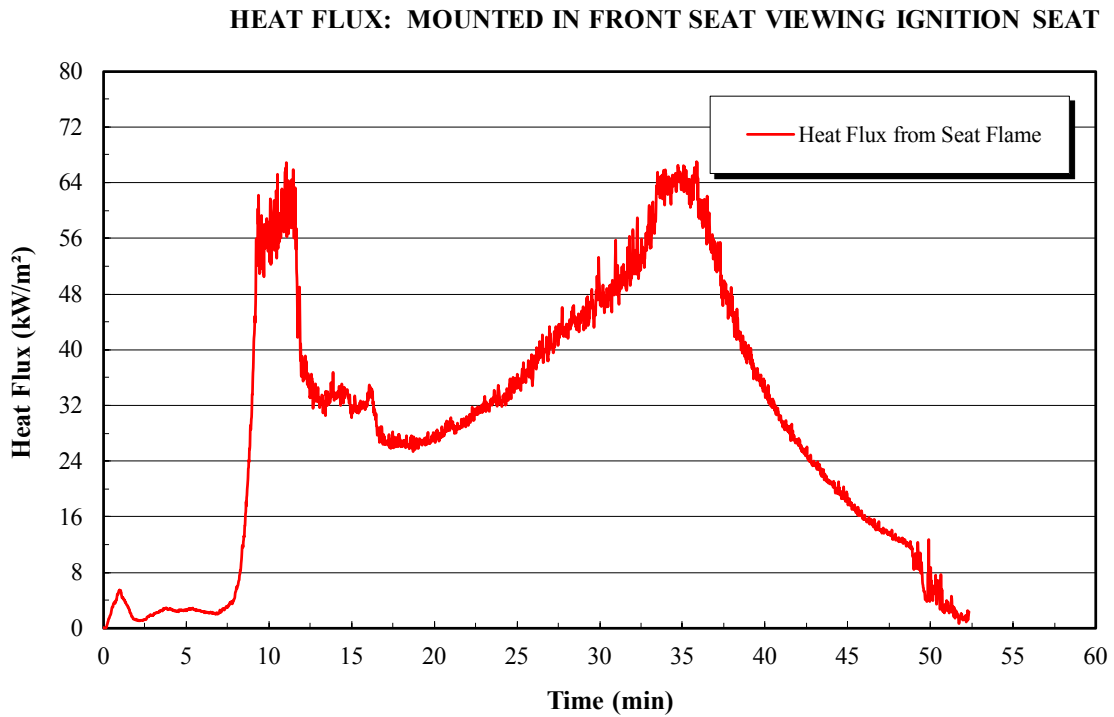
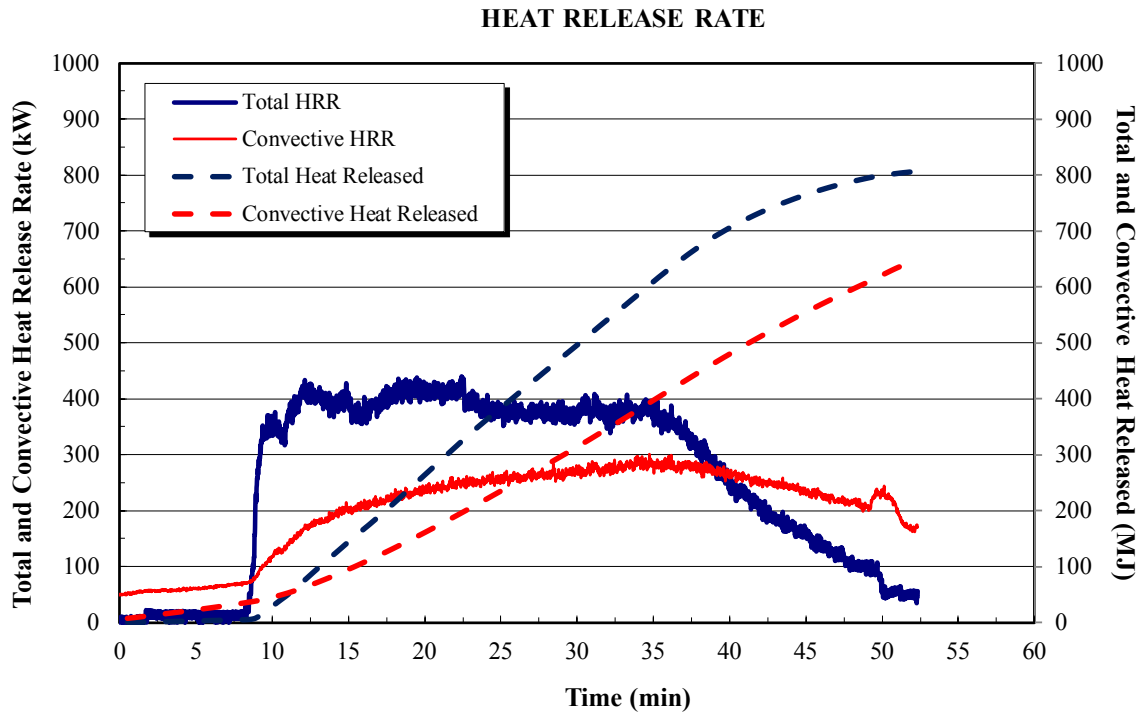


Figure G-4: ASTM E2574 results for MC Blue Seats – paper bag ignition source (continued)

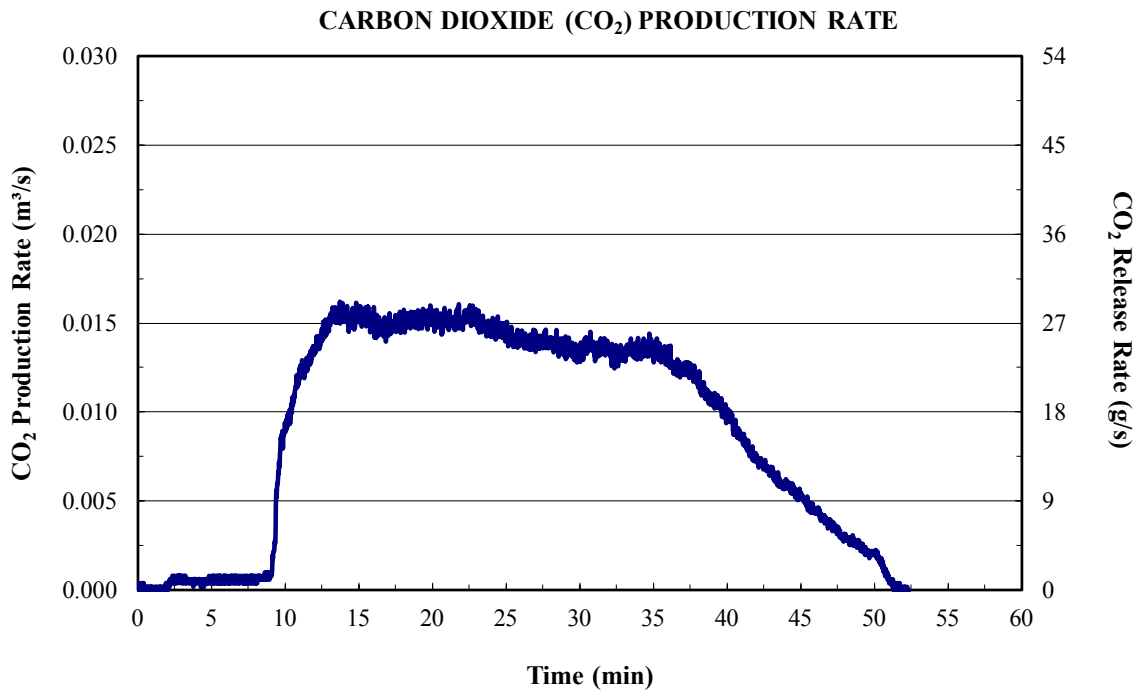
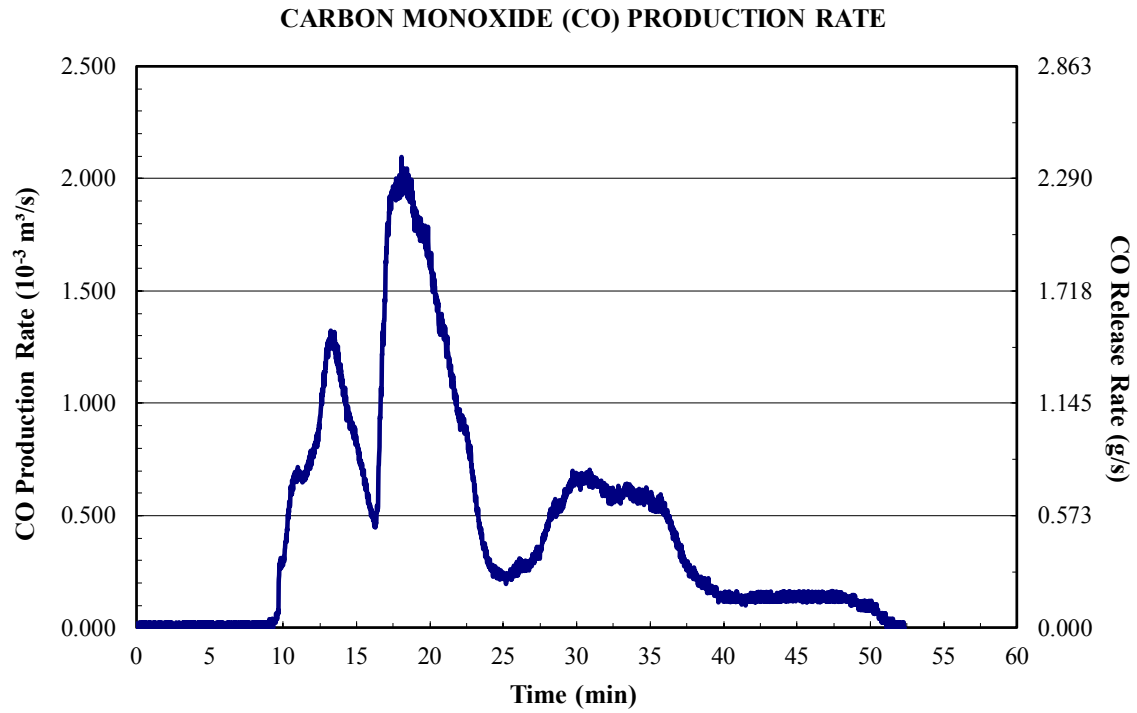


Figure G-4: ASTM E2574 results for MC Blue Seats – paper bag ignition source (continued)

**SUMMARY OF
LARGE-SCALE CALORIMETRY TESTING OF SCHOOL BUS SEATING
BLUEBIRD SEATS - TOP SEAT PAPER BAG IGNITION SOURCE**

Peak HRR_{total}	37 kW	at	3 min 25 sec
Average HRR_{total}	11 kW		
Total Heat Released	15 MJ		
Peak HRR_{conv}	26 kW	at	20 min 1 sec
Average HRR_{conv}	17 kW		
Convective Heat Released	23 MJ		
Steady State Convective Fraction	-		
Steady State Radiative Fraction	-		
Peak Heat Flux from Seat Flame	4.5 kW/m ²	at	2 min 15 sec
Maximum CO Production Rate	0.026 *10 ⁻³ m ³ /s	at	5 min 13 s
Maximum CO Release Rate	0.030 g/s		
Maximum CO ₂ Production Rate	0.001 *10 ⁻³ m ³ /s	at	3 min 26 s
Maximum CO ₂ Release Rate	1.34 g/s		

Figure G-5: ASTM E2574 results for Bluebird SB seats – paper bag ignition source

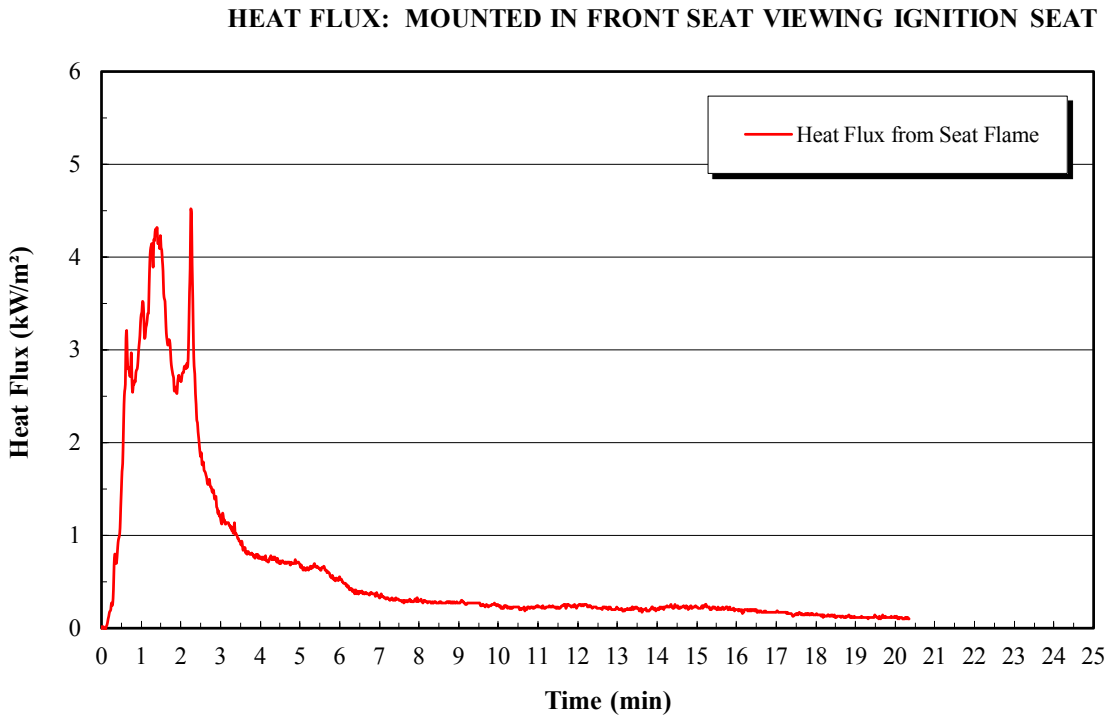
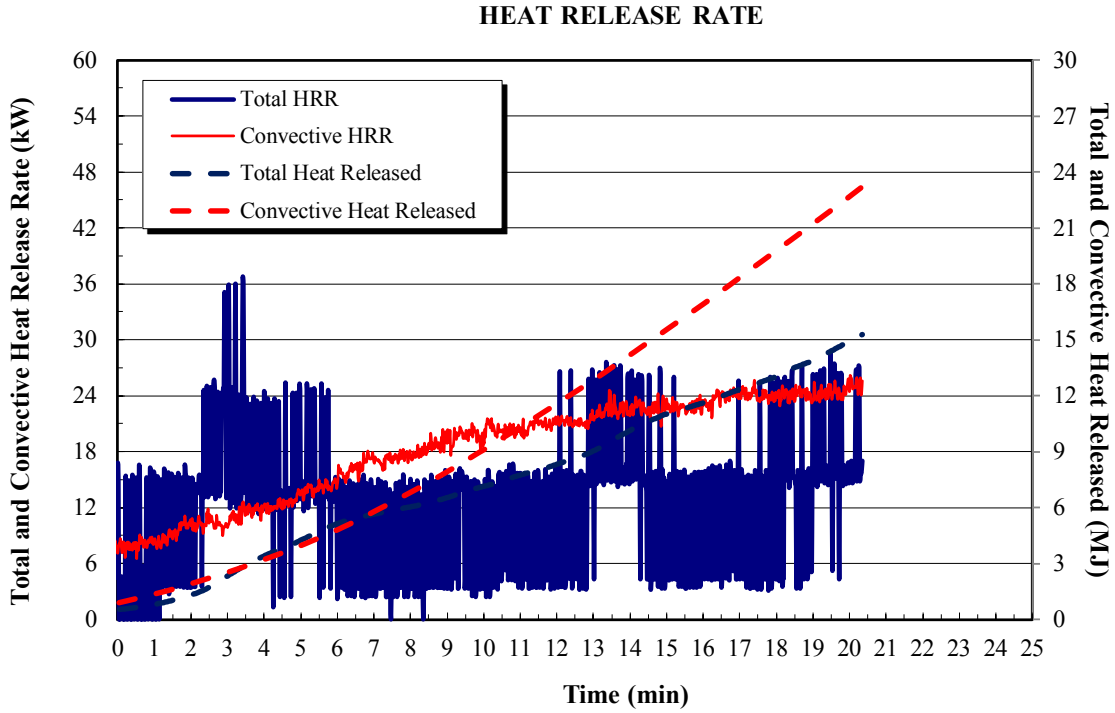


Figure G-5: ASTM E2574 results for Bluebird SB seats – paper bag ignition source (continued)

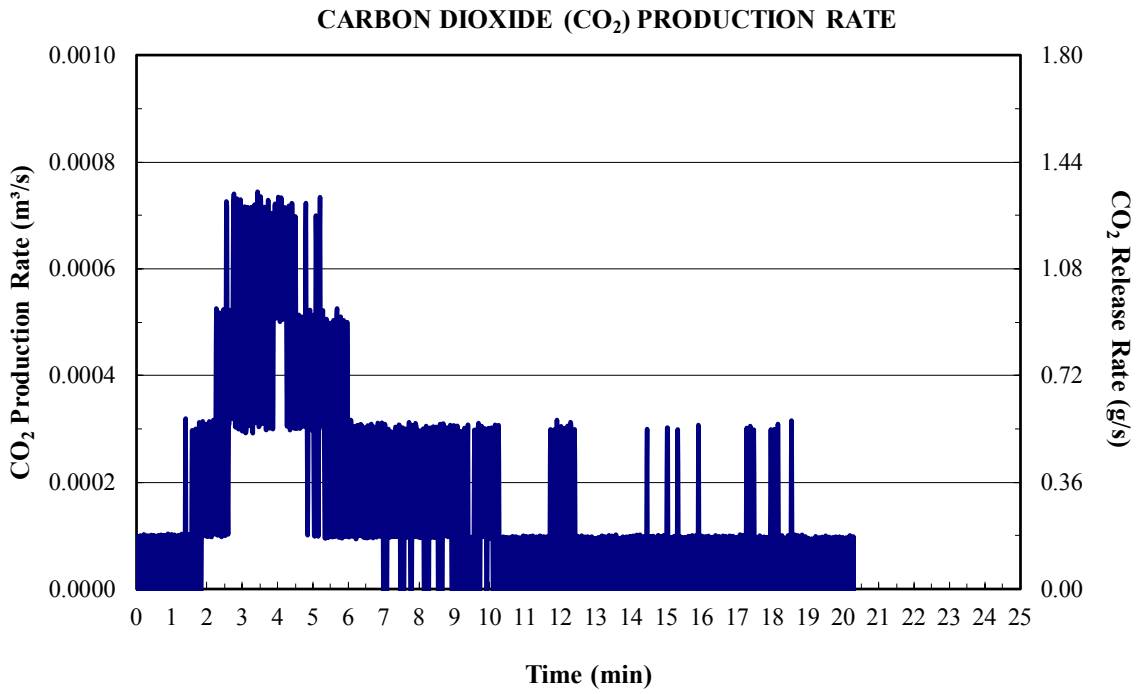
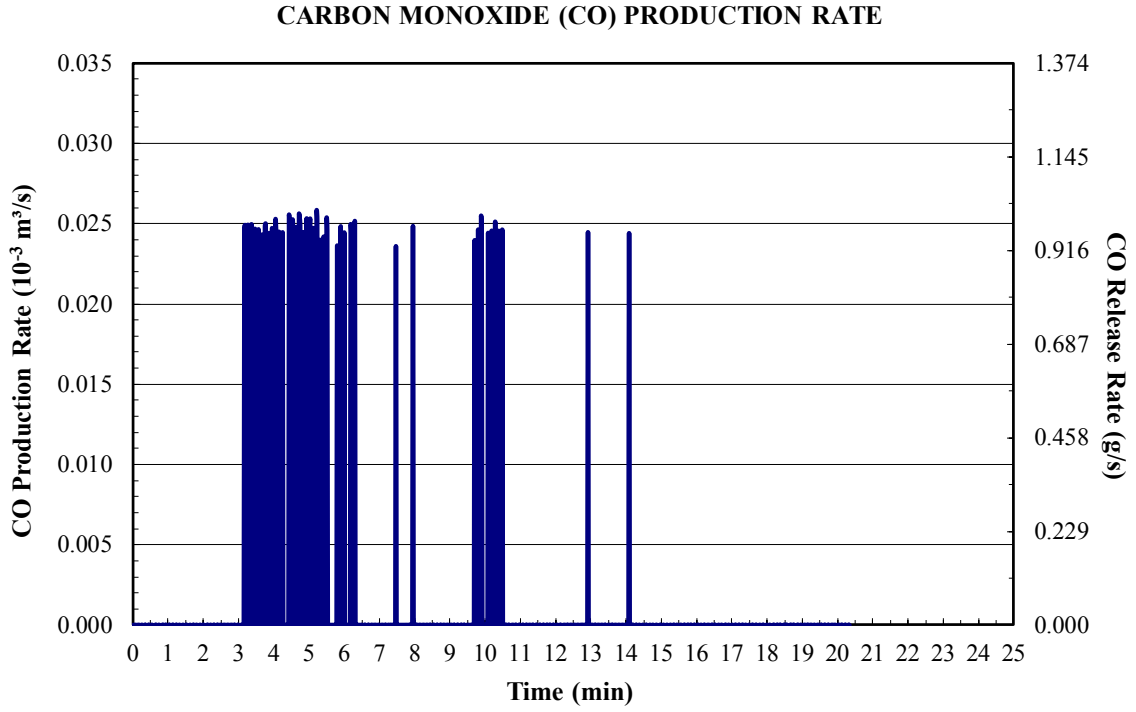


Figure G-5: ASTM E2574 results for Bluebird SB seats – paper bag ignition source (continued)

Appendix H: Child Restraint Seat Calorimetry Data

Child Restraint Seat Calorimetry Data

Results Description	Appendix H Figure Number
ASTM E2067 Results for Britax Parkway CRS	H-1
ASTM E2067 Results for Chicco KeyFit CRS	H-2
ASTM E2067 Results for Peg Perego Primo Viaggio CRS	H-3
ASTM E2067 Results for UPPAbaby Mesa CRS	H-4

SUMMARY OF

CUSTOM CALORIMETRY TESTING OF BRITAX PARKWAY SEAT

**TEST 1: ABORTED AFTER SEAT FELL, TEST 2: LOAD CELL DATA CABLE WAS
DAMAGAGED DURING TESTING, TEST 3: NO EXPERIMENTAL PROBLEMS**

	Test 1	Test 2	Test 3
Peak HRR _{total} (kW)	73	588	917
Average HRR _{total} (kW)	12	90	123
Total Heat Released (MJ)	7	108	147
Peak HRR _{conv} (kW)	32	296	440
Average HRR _{conv} (kW)	5	53	70
Convective Heat Released (MJ)	3	64	84
Steady State Convective Fraction (%)	44	59	57
Steady State Radiative Fraction (%)	56	41	43
Peak Smoke Production Rate (m ² /s)	0.34	5.16	5.72
Total Smoke Released (m ²)	37	1095	1113
Optical Density (-)	0.19	1.09	0.99
Total Mass Loss (kg)	4.92	2.82	5.21
Peak Mass Loss Rate (g/s)	50.88	14.97	33.65
Average Effective Heat of Combustion (kJ/g)	1.4	38.5	28.2
Maximum CO Production Rate (*10 ⁻³ m ³ /s)	0.026	0.276	0.434
Maximum CO Release Rate (g/s)	0.030	0.316	0.496
Maximum CO ₂ Production Rate (*10 ⁻³ m ³ /s)	0.001	0.020	0.028
Maximum CO ₂ Release Rate (g/s)	2.18	36.08	50.76

Figure H-1: ASTM E2067 results for Britax Parkway CRS

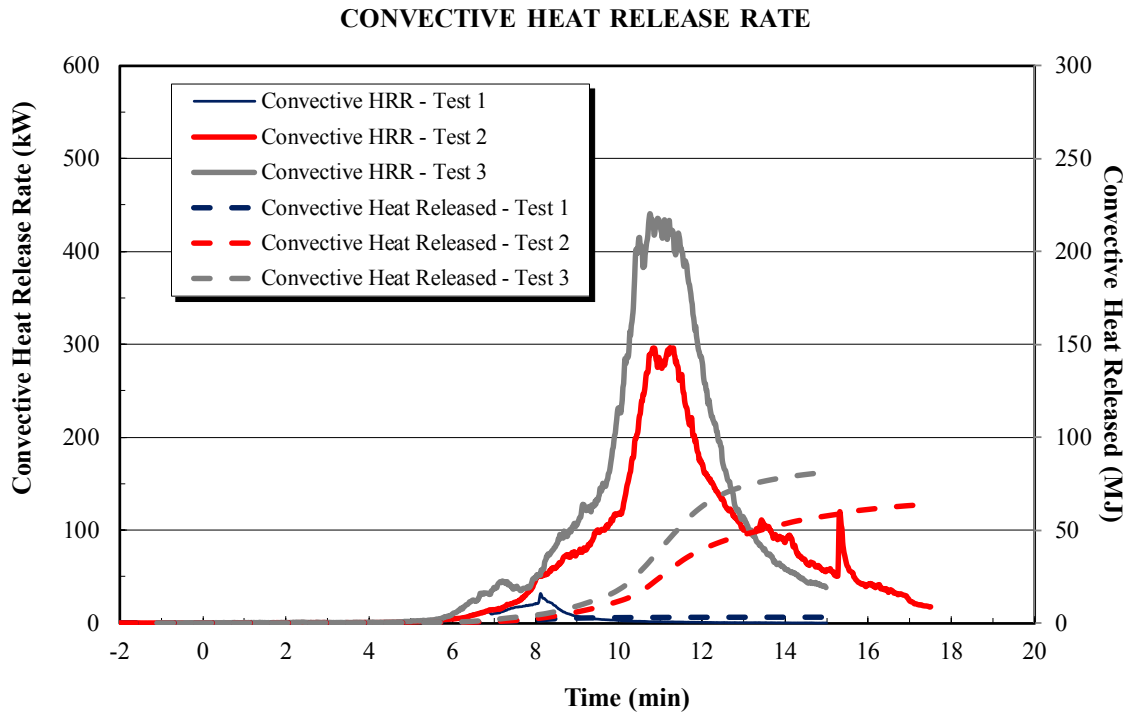
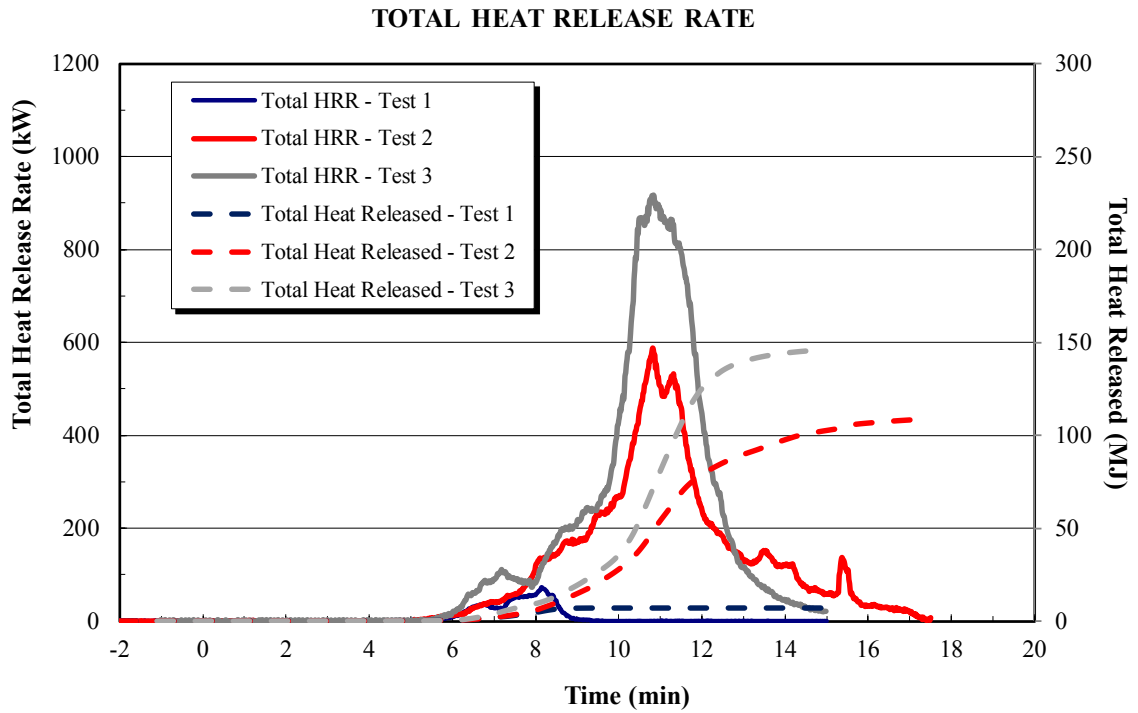


Figure H-1: ASTM E2067 results for Britax Parkway CRS (continued)

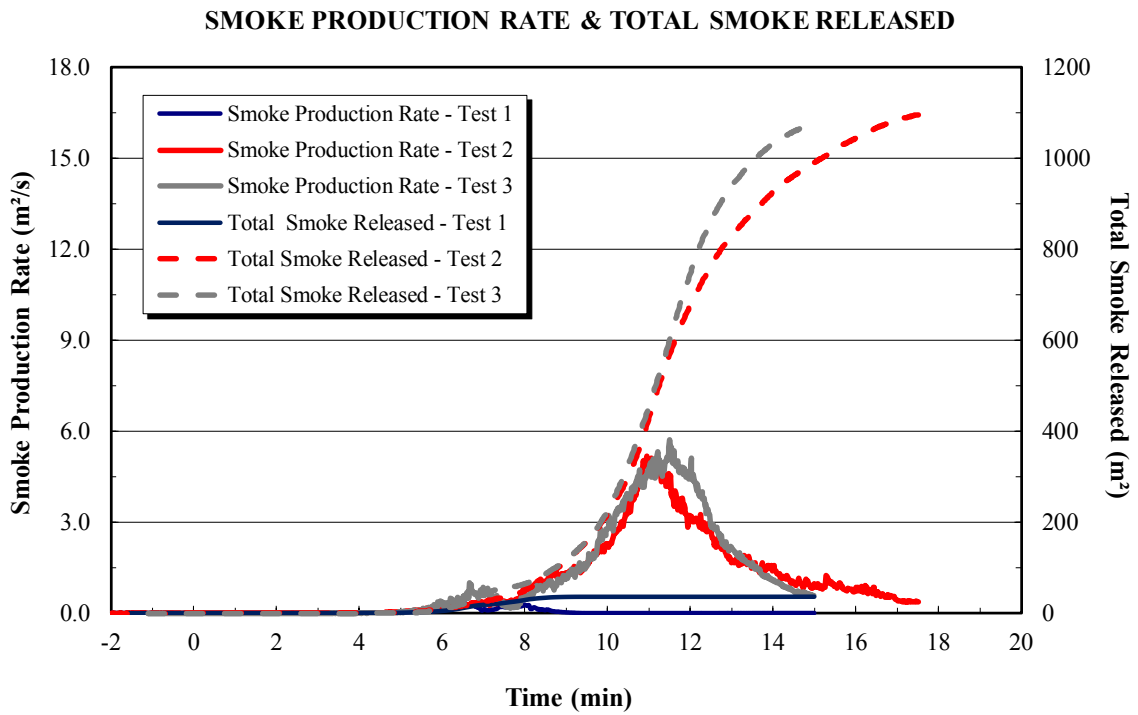
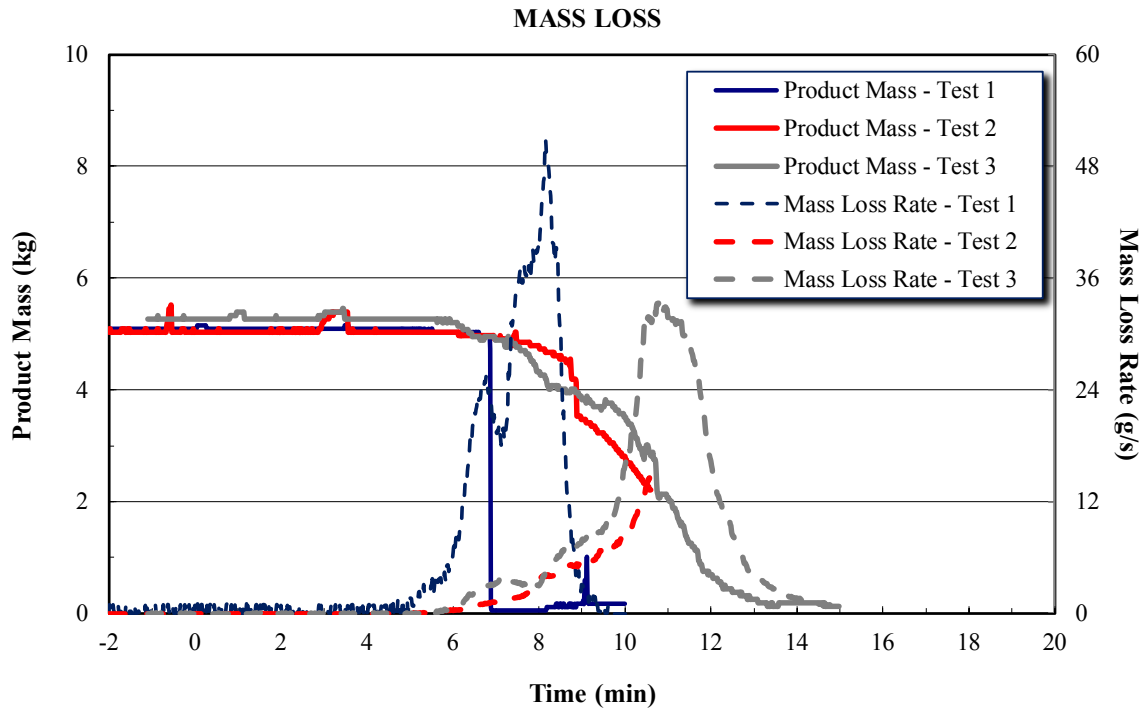


Figure H-1: ASTM E2067 results for Britax Parkway CRS (continued)

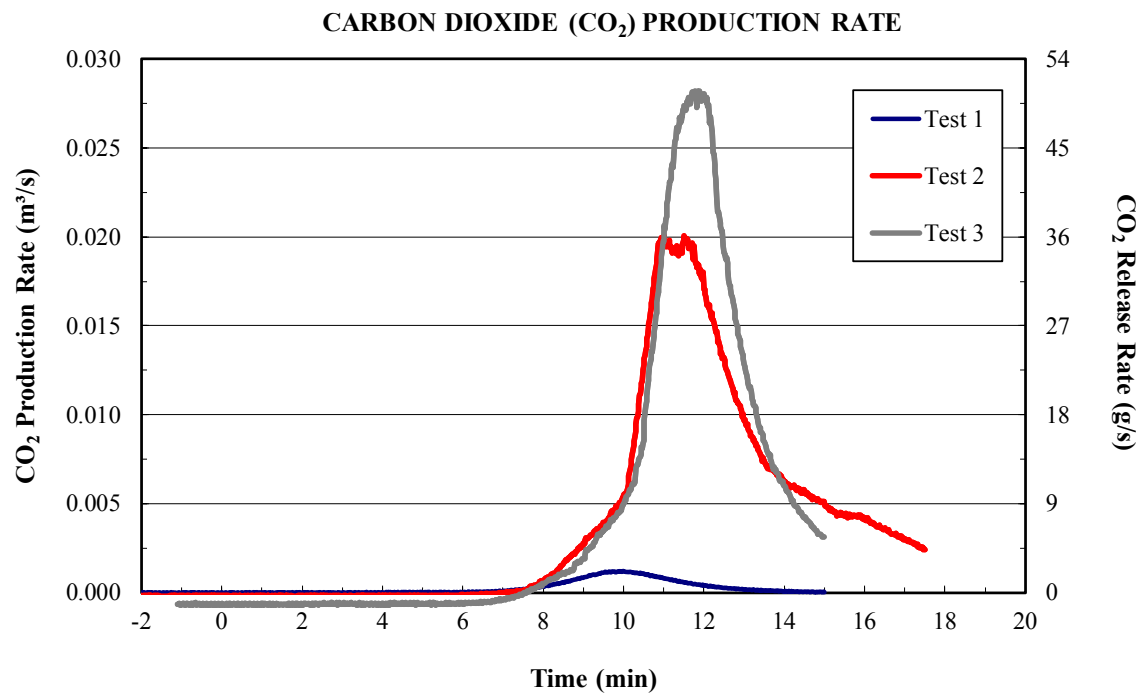
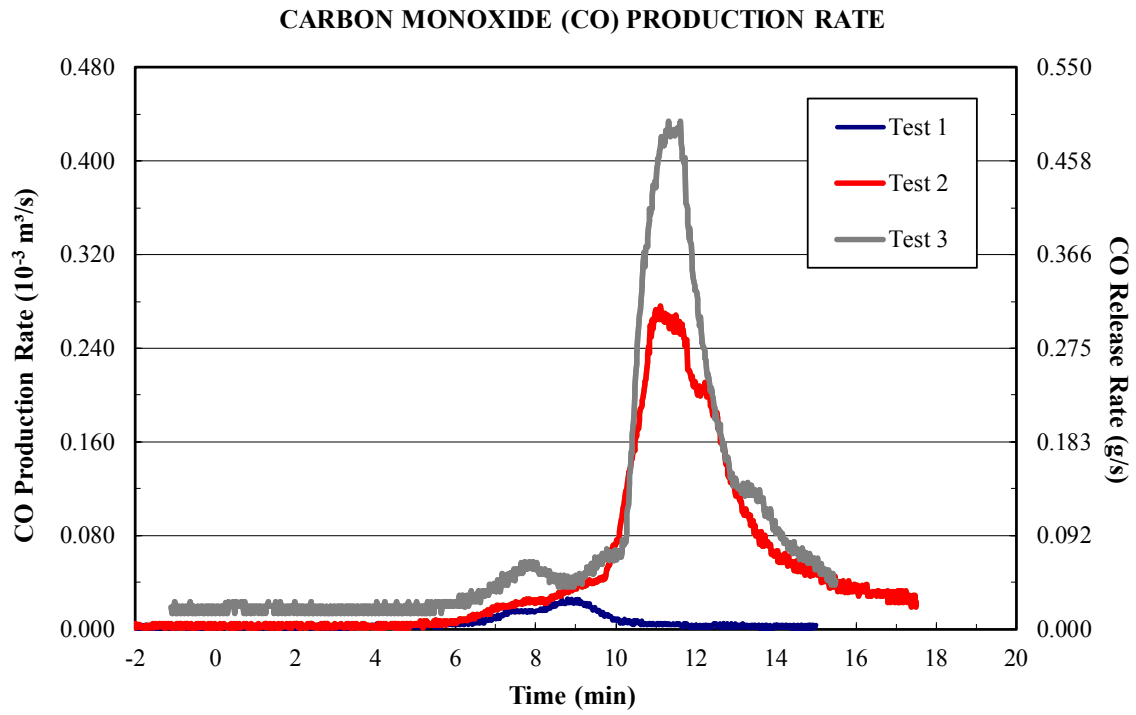


Figure H-1: ASTM E2067 results for Britax Parkway CRS (continued)

**SUMMARY OF
CUSTOM CALORIMETRY TESTING OF CHICCO KEYFIT SEAT
TEST 1-2: SEAT AND BASE, TEST 3: SEAT ONLY, TEST 4: BASE ONLY**

	Test 1	Test 2	Test 3	Test 4
Peak HRR _{total} (kW)	940	795	594	113
Average HRR _{total} (kW)	163	147	87	26
Total Heat Released (MJ)	195	176	105	63
Peak HRR _{conv} (kW)	498	436	329	58
Average HRR _{conv} (kW)	105	89	54	13
Convective Heat Released (MJ)	126	107	65	31
Steady State Convective Fraction (%)	64	61	62	50
Steady State Radiative Fraction (%)	36	39	38	50
Peak Smoke Production Rate (m ² /s)	7.62	6.03	4.09	1.15
Total Smoke Released (m ²)	1670	1444	850	354
Optical Density (-)	1.06	0.90	0.61	0.19
Total Mass Loss (kg)	7.91	7.79	4.08	2.13
Peak Mass Loss Rate (g/s)	38.10	35.15	33.87	6.67
Average Effective Heat of Combustion (kJ/g)	24.7	22.6	25.6	29.3
Maximum CO Production Rate (*10 ⁻³ m ³ /s)	0.343	0.289	0.185	0.038
Maximum CO Release Rate (g/s)	0.392	0.331	0.212	0.044
Maximum CO ₂ Production Rate (*10 ⁻³ m ³ /s)	0.031	0.025	0.019	0.004
Maximum CO ₂ Release Rate (g/s)	56.48	45.39	33.30	6.54

Figure H-2: ASTM E2067 results for Chicco KeyFit CRS

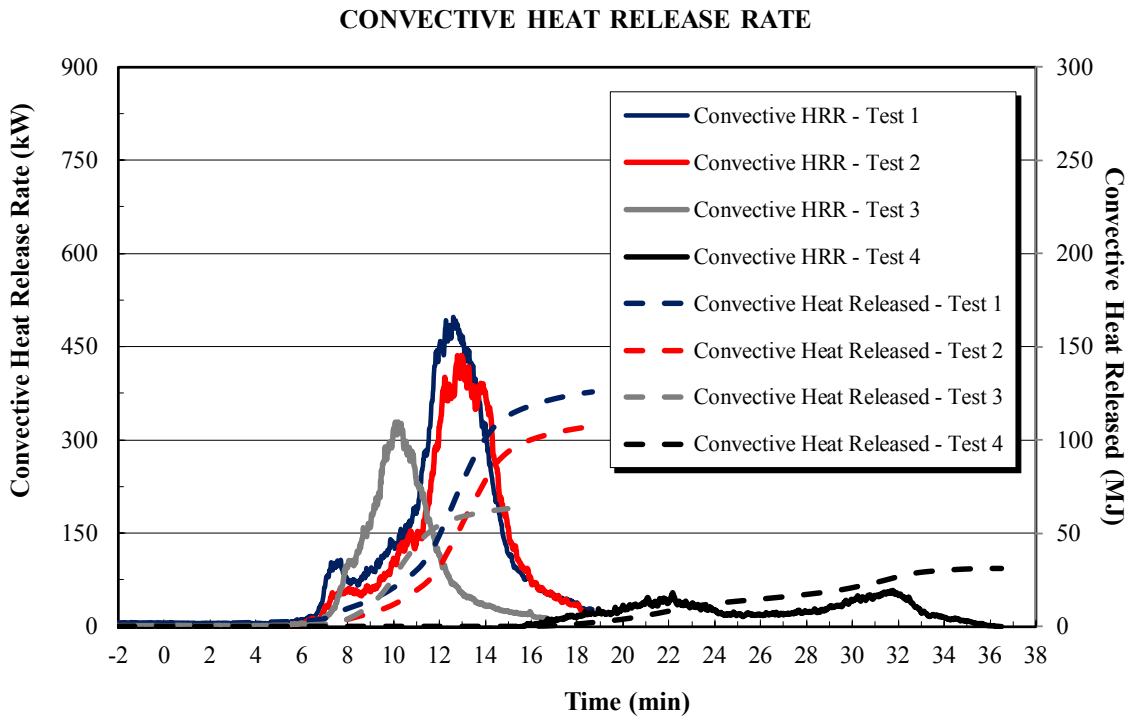
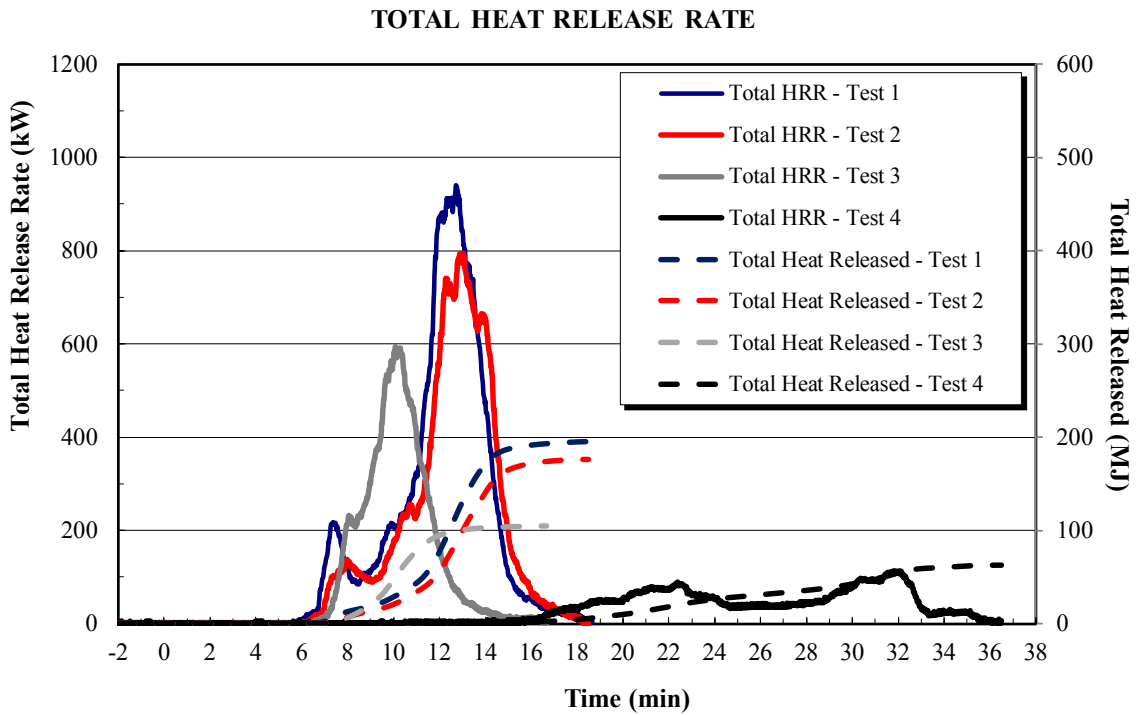


Figure H-2: ASTM E2067 results for Chicco KeyFit CRS (continued).

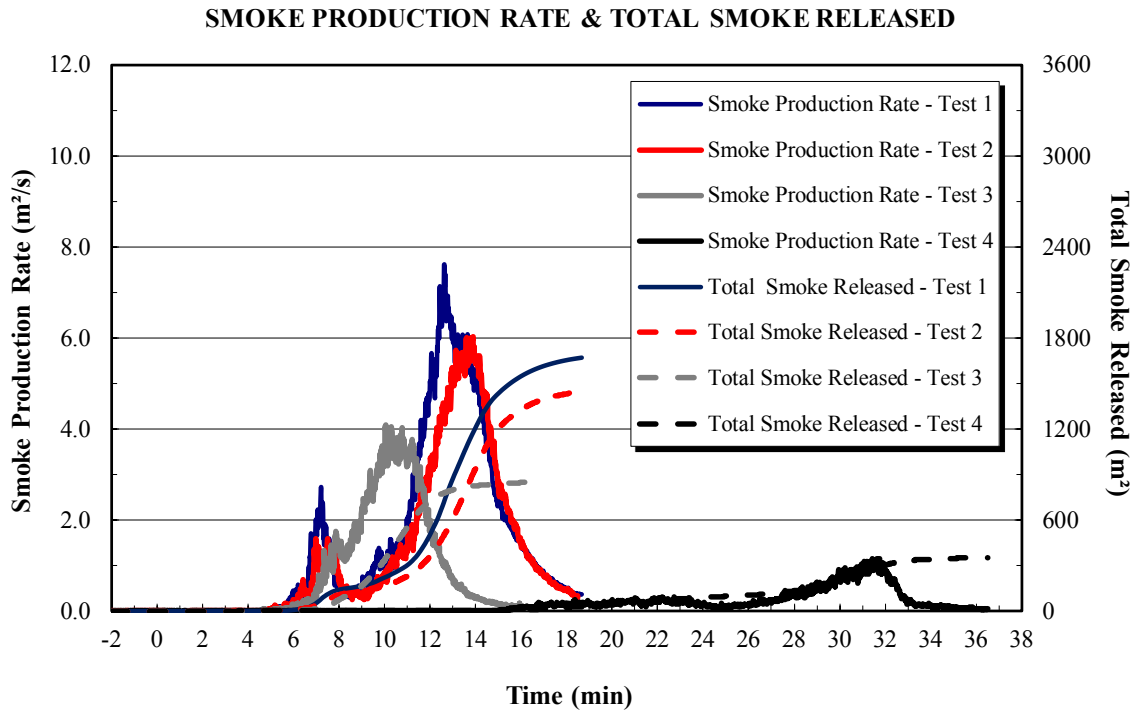
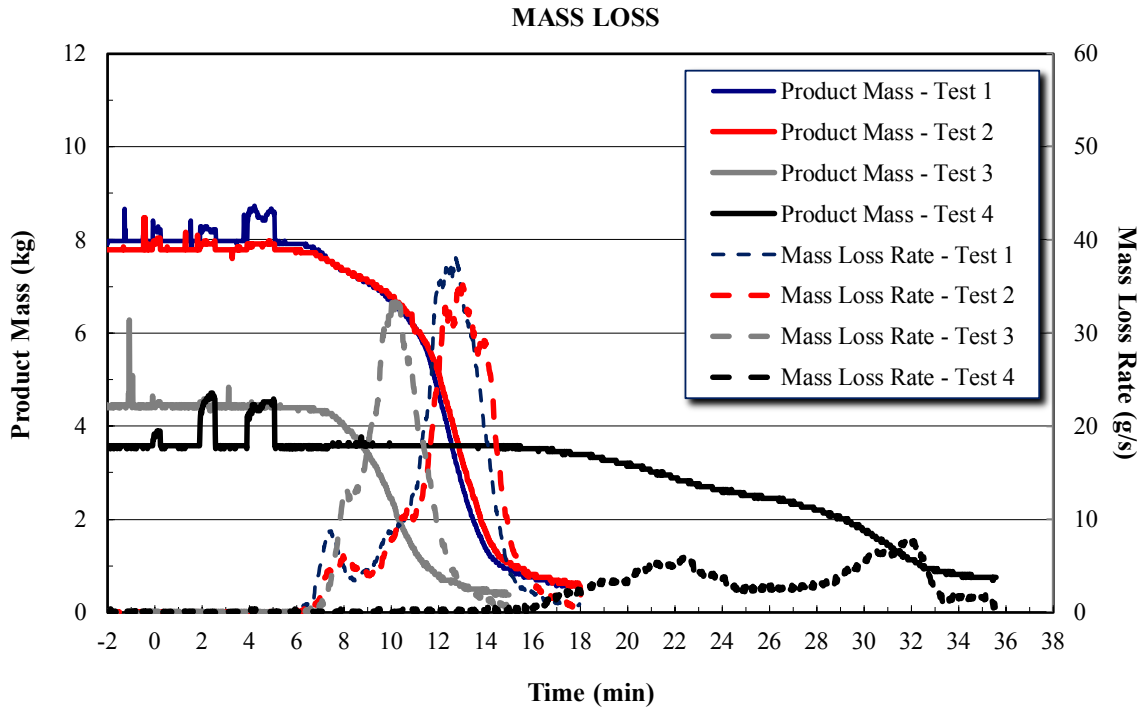


Figure H-2: ASTM E2067 results for Chicco KeyFit CRS (continued)

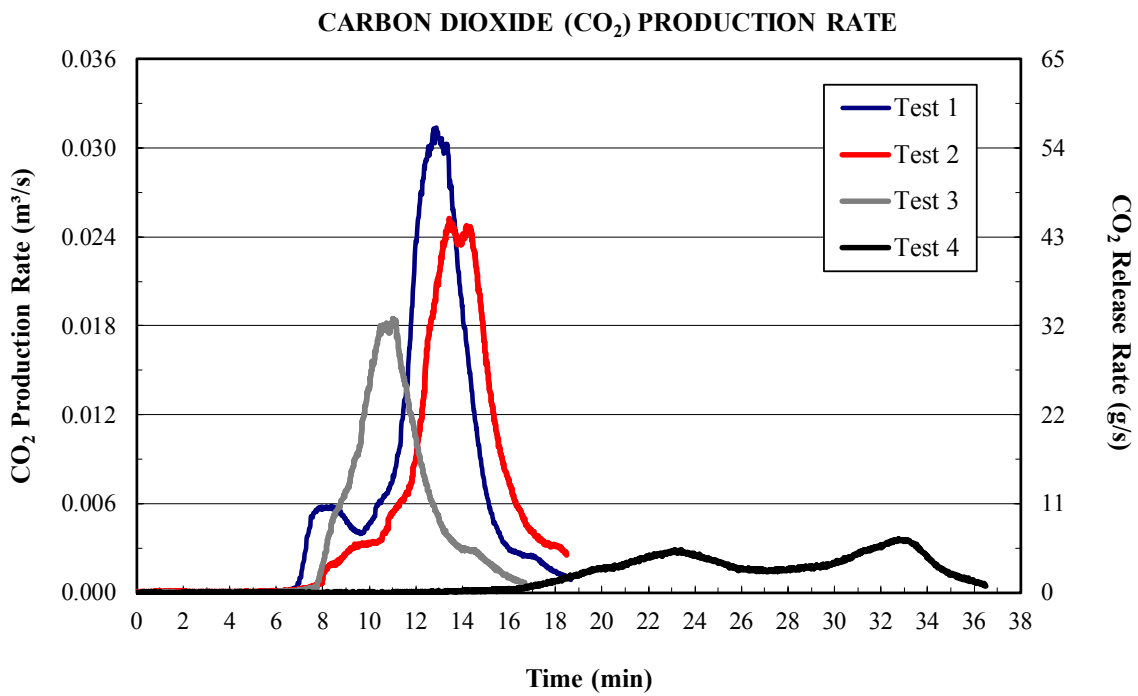
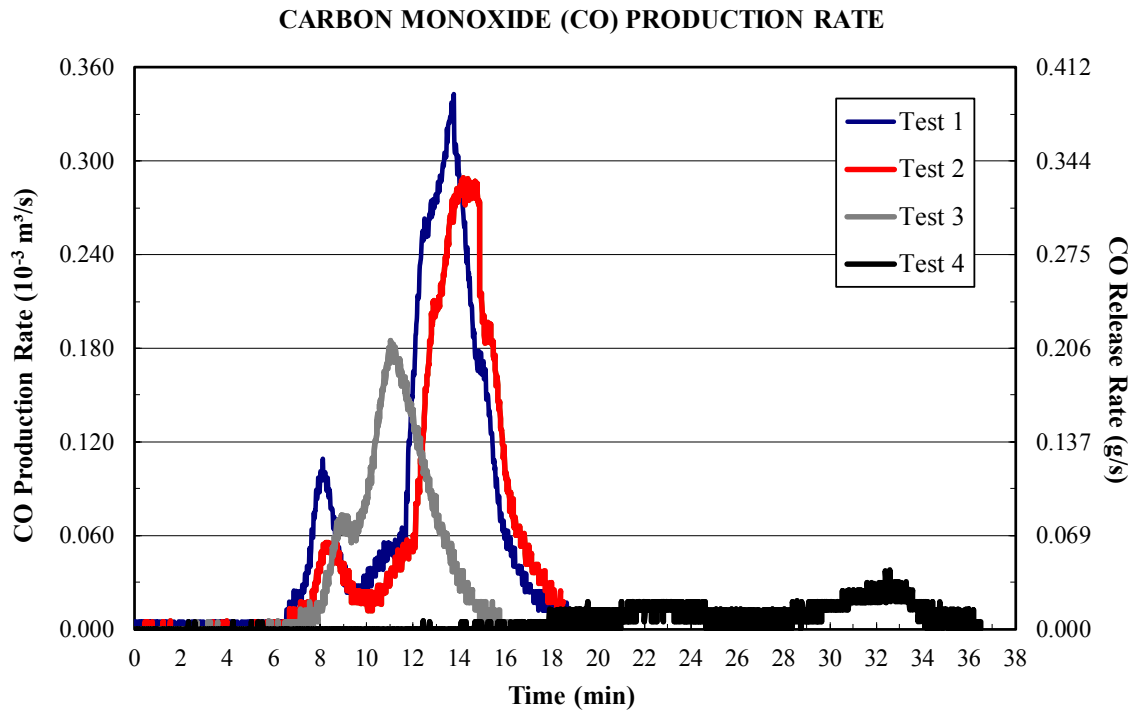


Figure H-2: ASTM E2067 results for Chicco KeyFit CRS (continued)

**SUMMARY OF
CUSTOM CALORIMETRY TESTING OF PEG PEREGO PRIMO VIAGGIO
TEST 1: SEAT AND BASE (ONLY ONE FULL SEAT AND BASE AVAILABLE)**

	Test 1
Peak HRR _{total} (kW)	693
Average HRR _{total} (kW)	186
Total Heat Released (MJ)	223
Peak HRR _{conv} (kW)	400
Average HRR _{conv} (kW)	119
Convective Heat Released (MJ)	143
Steady State Convective Fraction (%)	64
Steady State Radiative Fraction (%)	36
Peak Smoke Production Rate (m ² /s)	6.11
Total Smoke Released (m ²)	2059
Optical Density (-)	0.91
Total Mass Loss (kg)	7.35
Peak Mass Loss Rate (g/s)	22.76
Average Effective Heat of Combustion (kJ/g)	30.4
Maximum CO Production Rate (*10 ⁻³ m ³ /s)	0.236
Maximum CO Release Rate (g/s)	0.270
Maximum CO ₂ Production Rate (*10 ⁻³ m ³ /s)	0.022
Maximum CO ₂ Release Rate (g/s)	38.79

Figure H-3: ASTM E2067 results for Peg Perego Primo Viaggio CRS

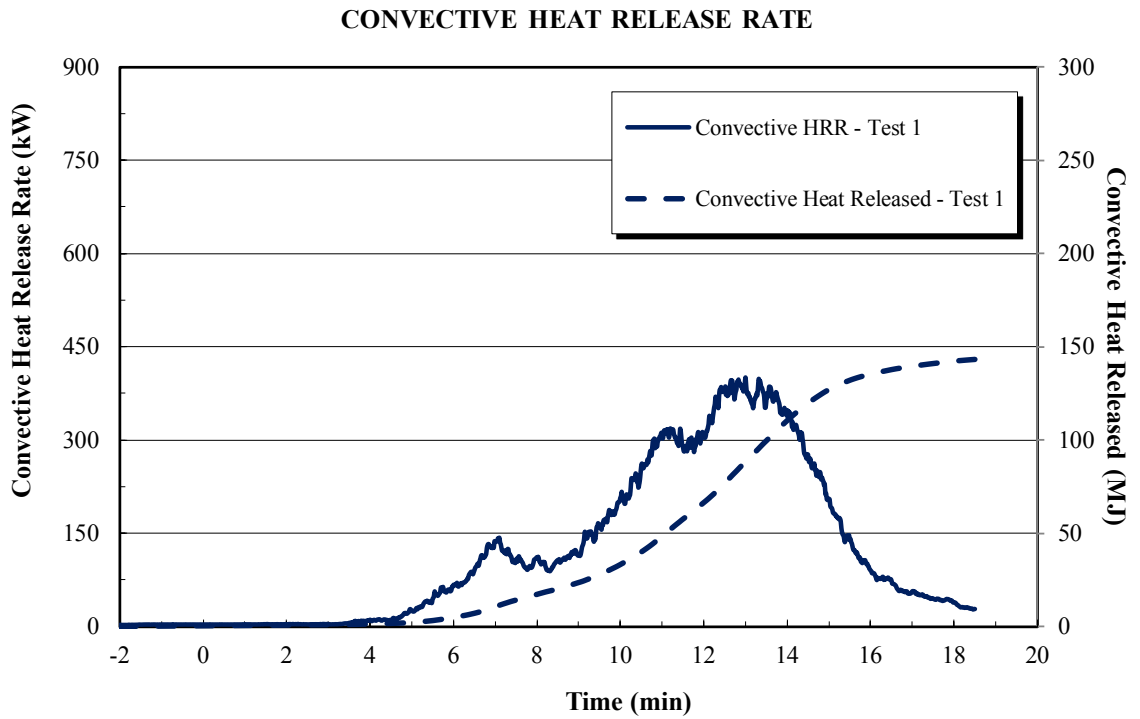
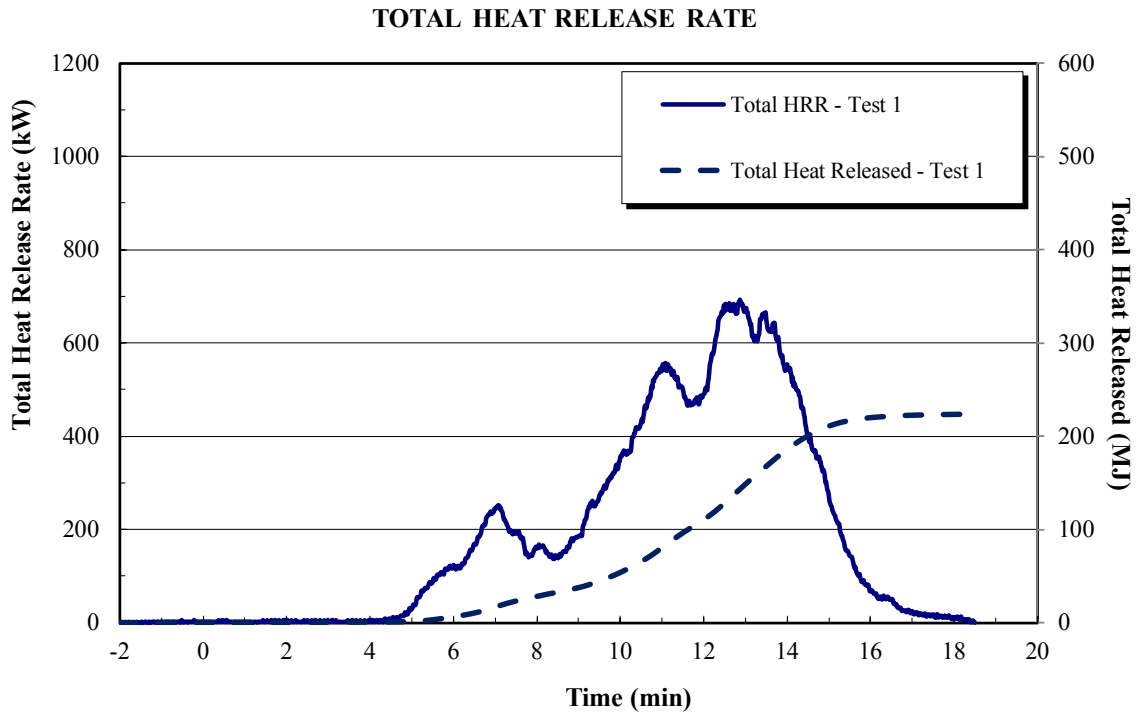


Figure H-3: ASTM E2067 results for Peg Perego Primo Viaggio CRS (continued).

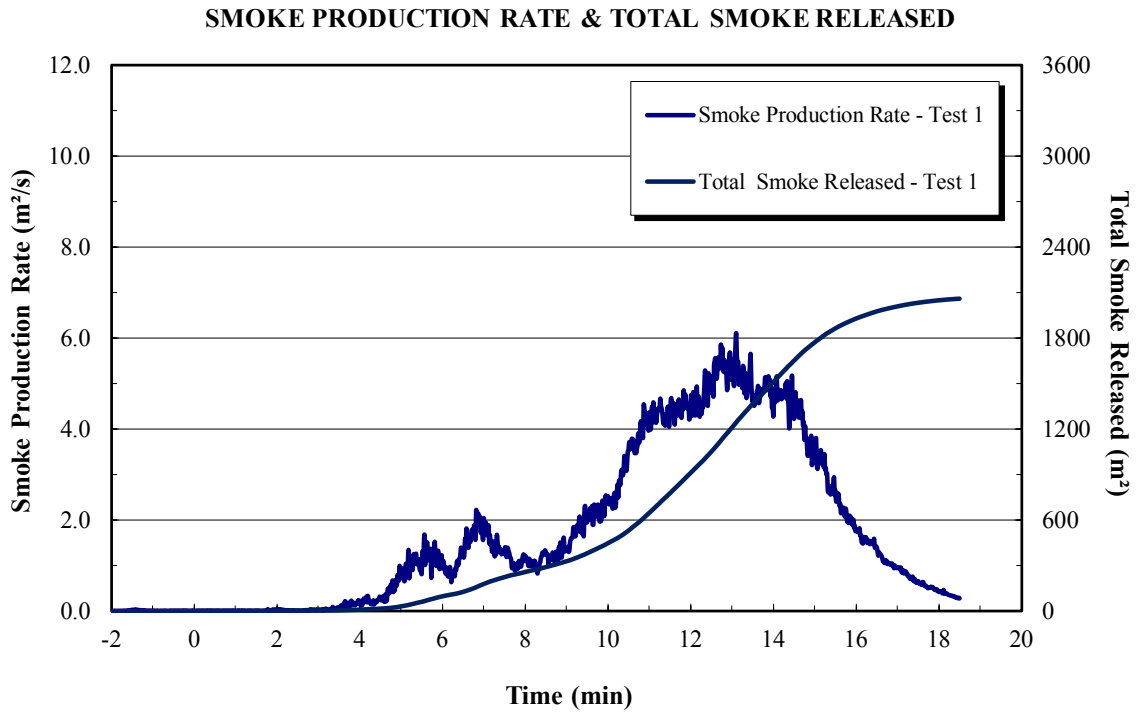
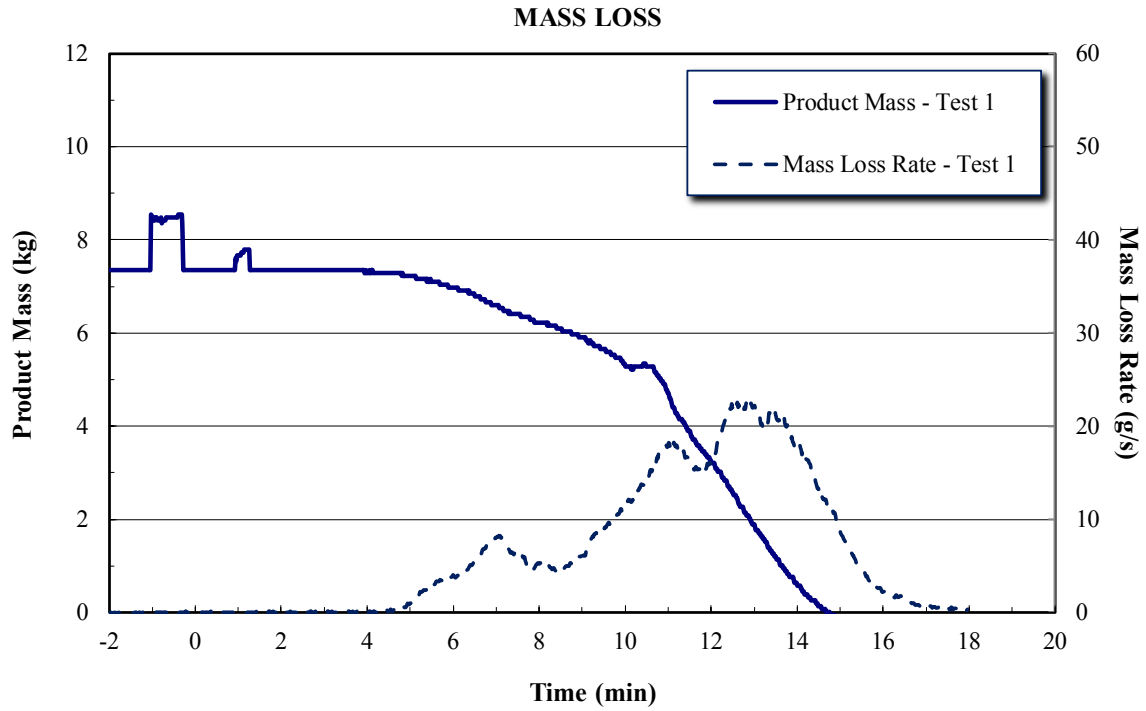


Figure H-3: ASTM E2067 results for Peg Perego Primo Viaggio CRS (continued)

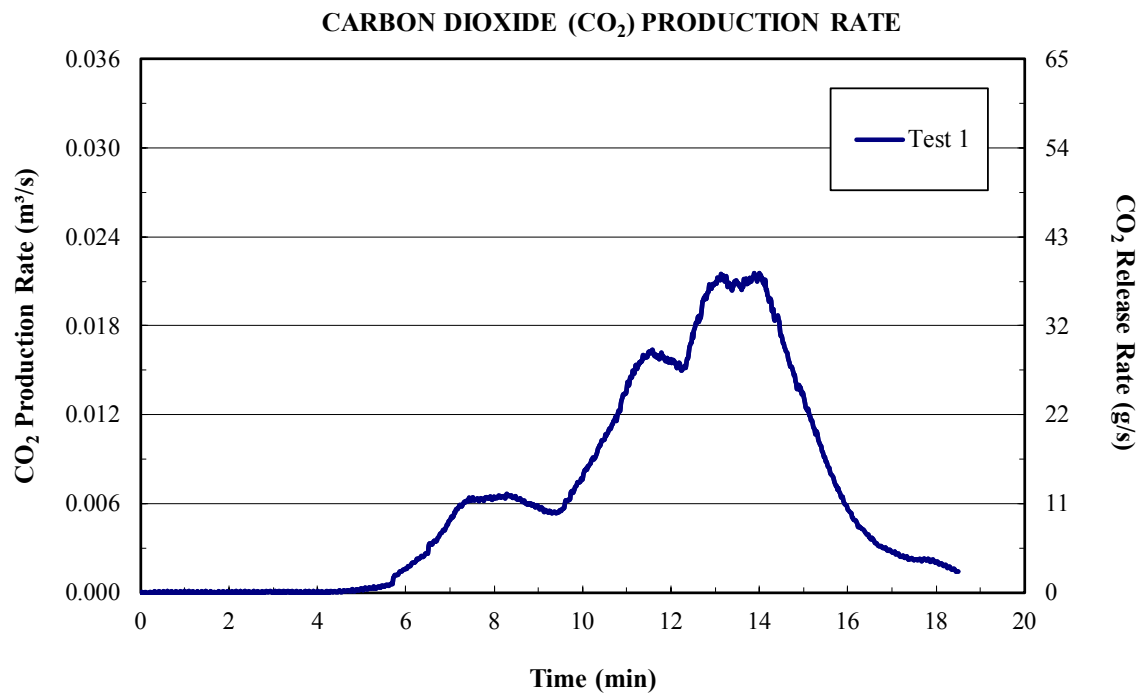
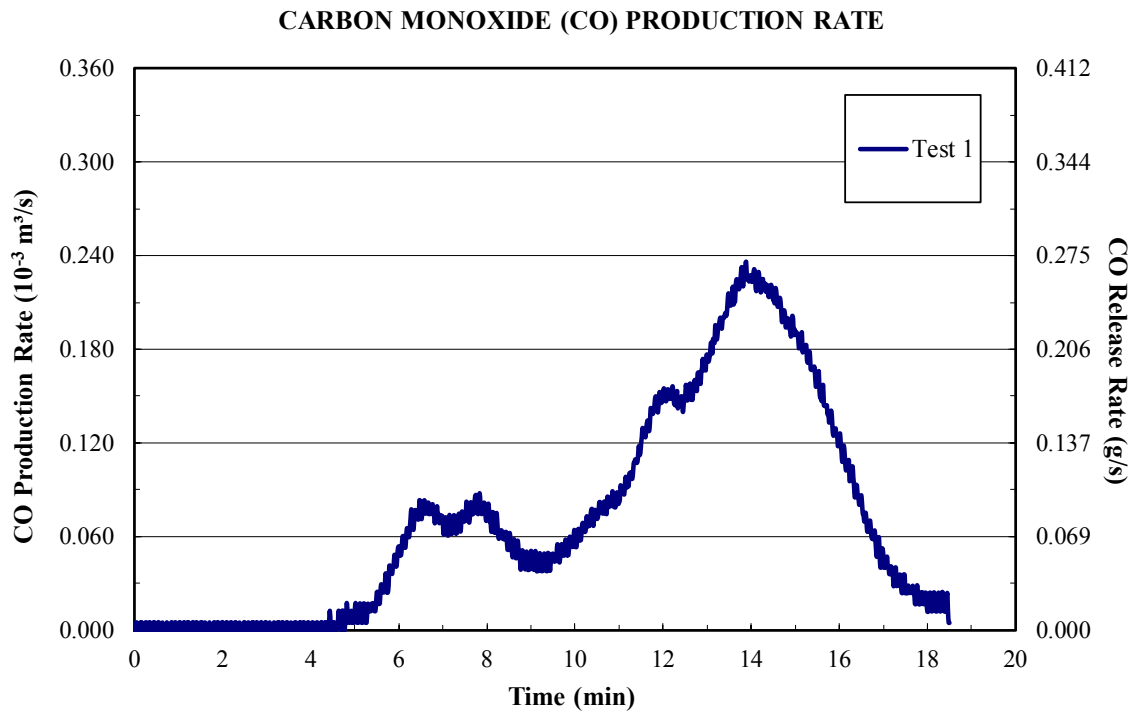


Figure H-3: ASTM E2067 results for Peg Perego Primo Viaggio CRS (continued)

**SUMMARY OF
CUSTOM CALORIMETRY TESTING OF UPPA BABY MESA SEAT
TEST 1-2: SEAT AND BASE, TEST 3: SEAT ONLY, TEST 4: BASE ONLY**

	Test 1	Test 2	Test 3	Test 4
Peak HRR _{total} (kW)	854	873	682	360
Average HRR _{total} (kW)	201	160	106	48
Total Heat Released (MJ)	241	249	127	101
Peak HRR _{conv} (kW)	470	486	328	188
Average HRR _{conv} (kW)	115	92	64	26
Convective Heat Released (MJ)	138	144	77	55
Steady State Convective Fraction (%)	57	58	60	54
Steady State Radiative Fraction (%)	43	42	40	46
Peak Smoke Production Rate (m ² /s)	7.04	7.59	4.29	2.54
Total Smoke Released (m ²)	2112	2267	991	628
Optical Density (-)	0.95	1.02	0.93	0.40
Total Mass Loss (kg)	8.71	8.54	4.46	3.32
Peak Mass Loss Rate (g/s)	30.89	29.93	26.87	16.12
Average Effective Heat of Combustion (kJ/g)	27.6	29.1	28.6	30.4
Maximum CO Production Rate (*10 ⁻³ m ³ /s)	0.229	0.265	0.186	0.093
Maximum CO Release Rate (g/s)	0.262	0.304	0.213	0.106
Maximum CO ₂ Production Rate (*10 ⁻³ m ³ /s)	0.026	0.028	0.020	0.011
Maximum CO ₂ Release Rate (g/s)	46.20	50.10	36.14	18.99

Figure H-4: ASTM E2067 results for UPPAbaby Mesa CRS

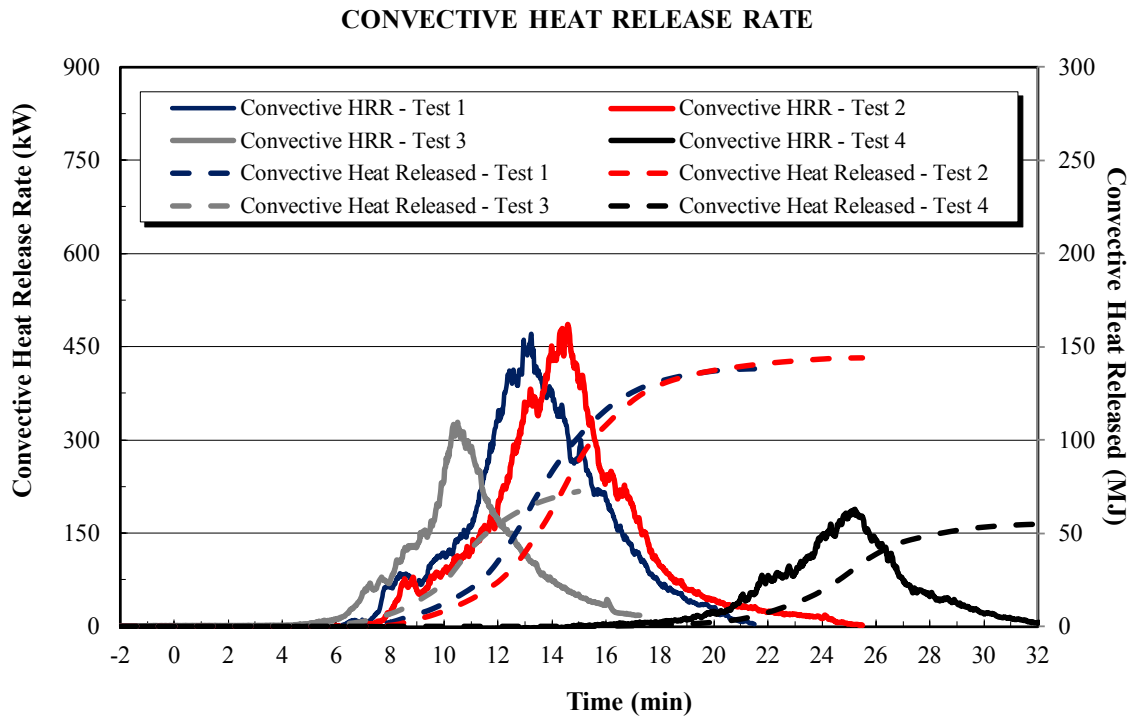
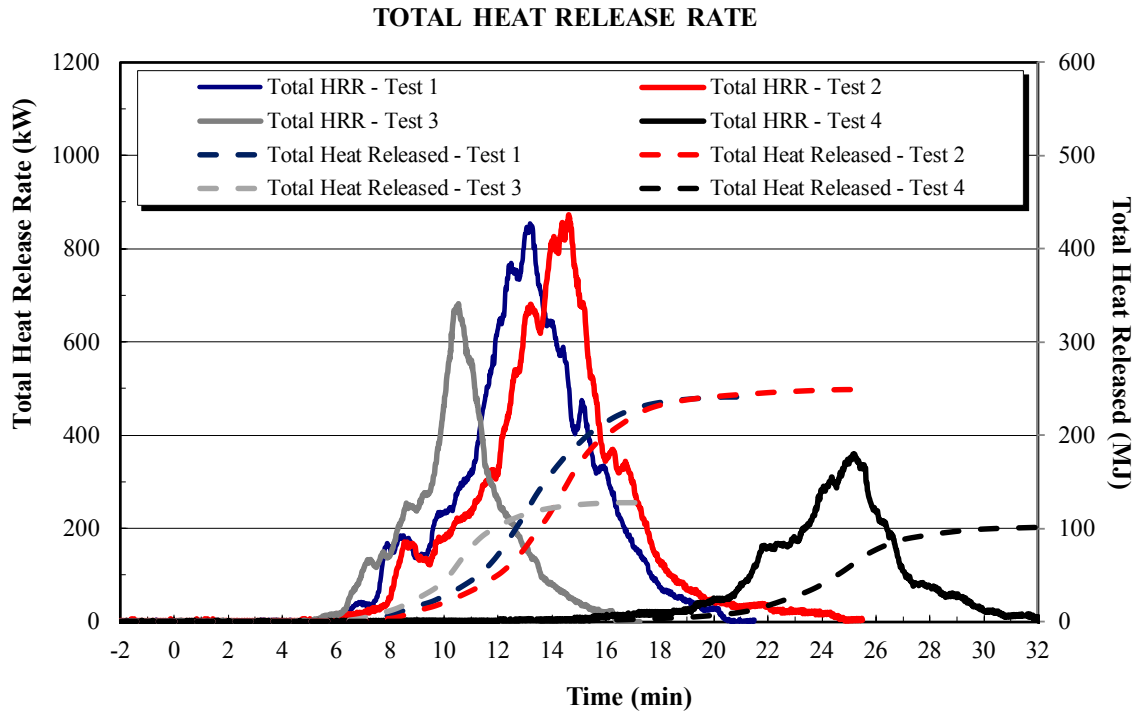


Figure H-4: ASTM E2067 results for UPPAbaby Mesa CRS (continued)

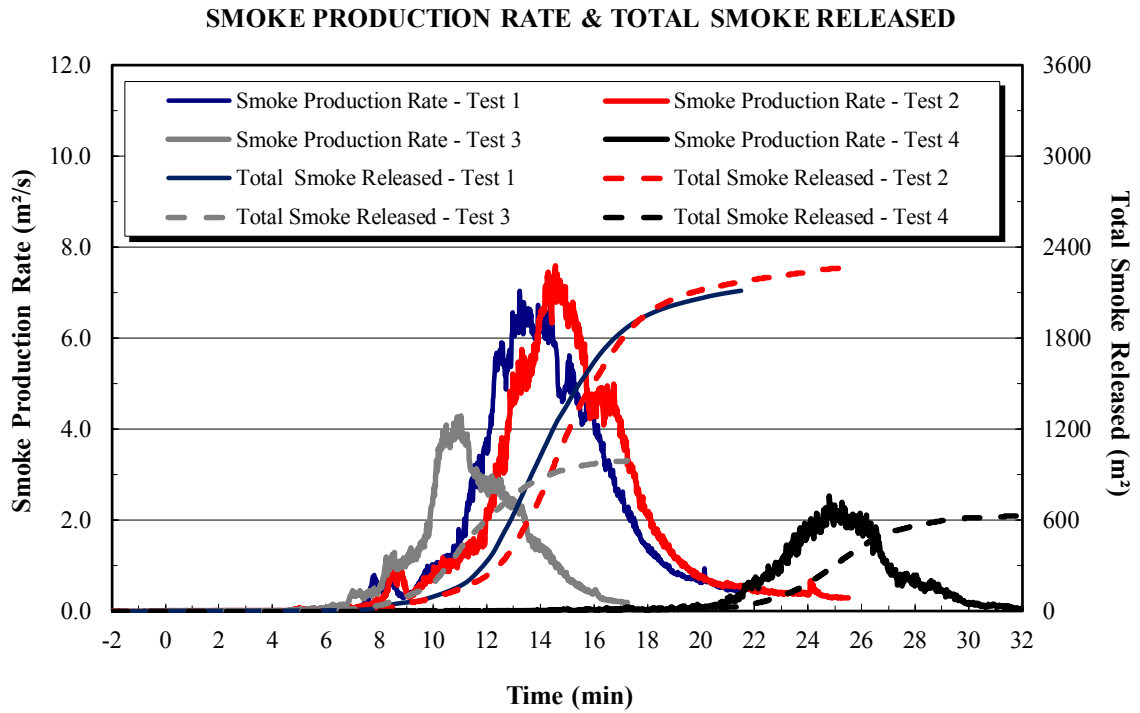
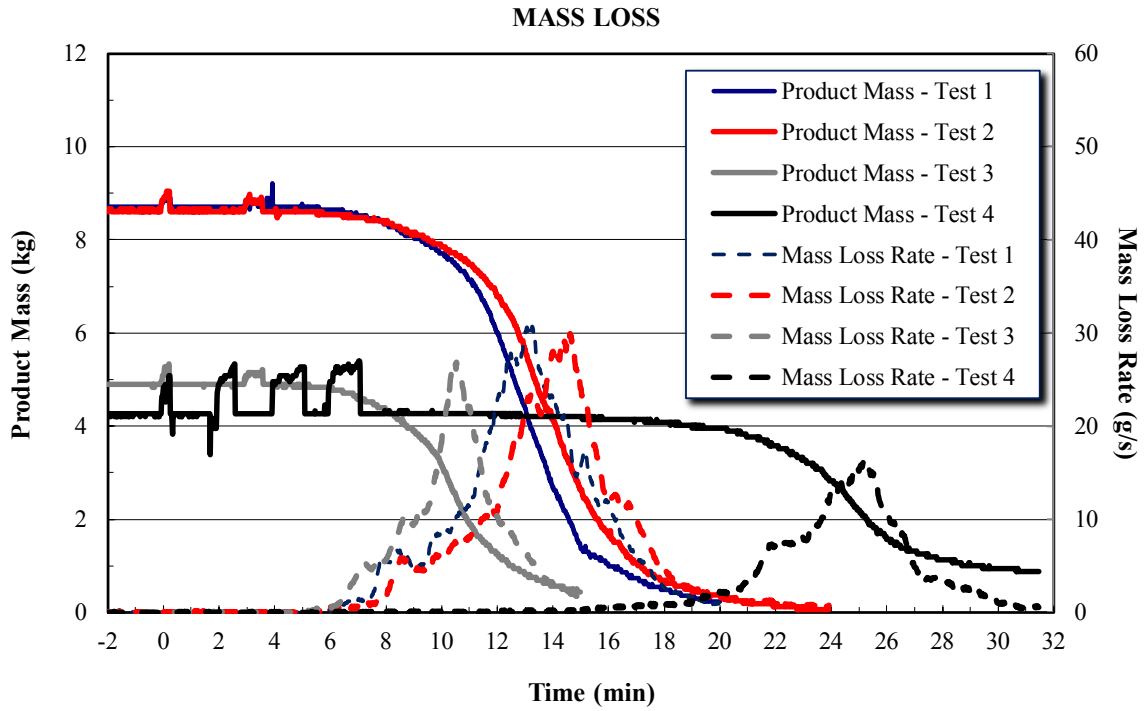


Figure H-4: ASTM E2067 results for UPPAbaby Mesa CRS (continued)

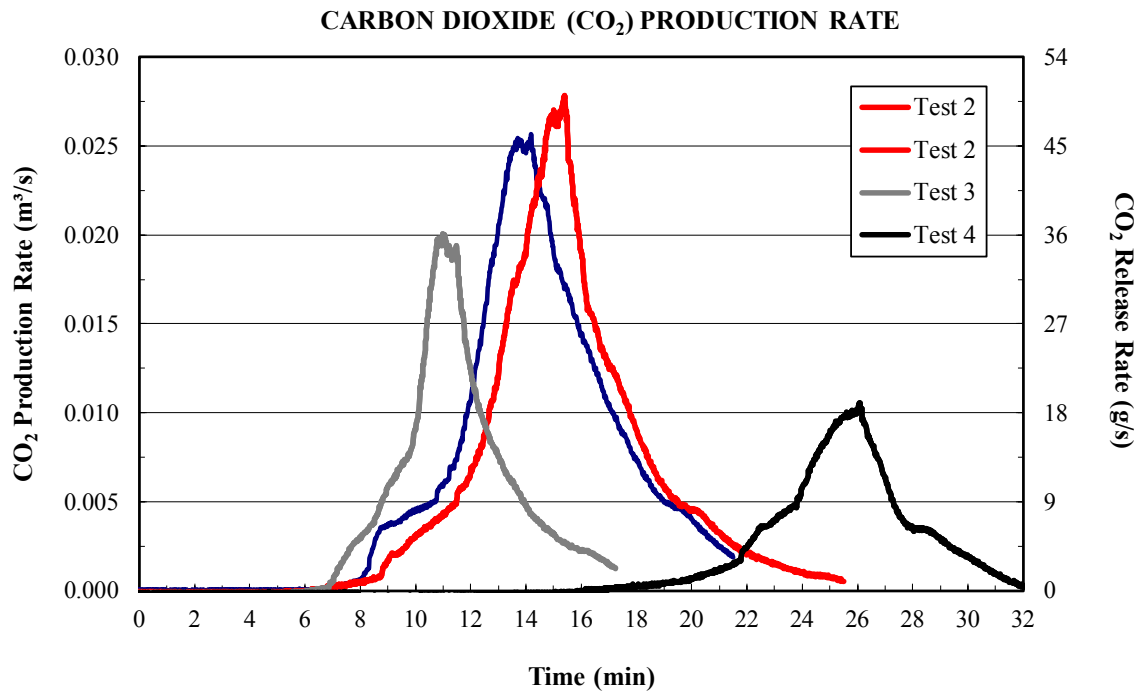
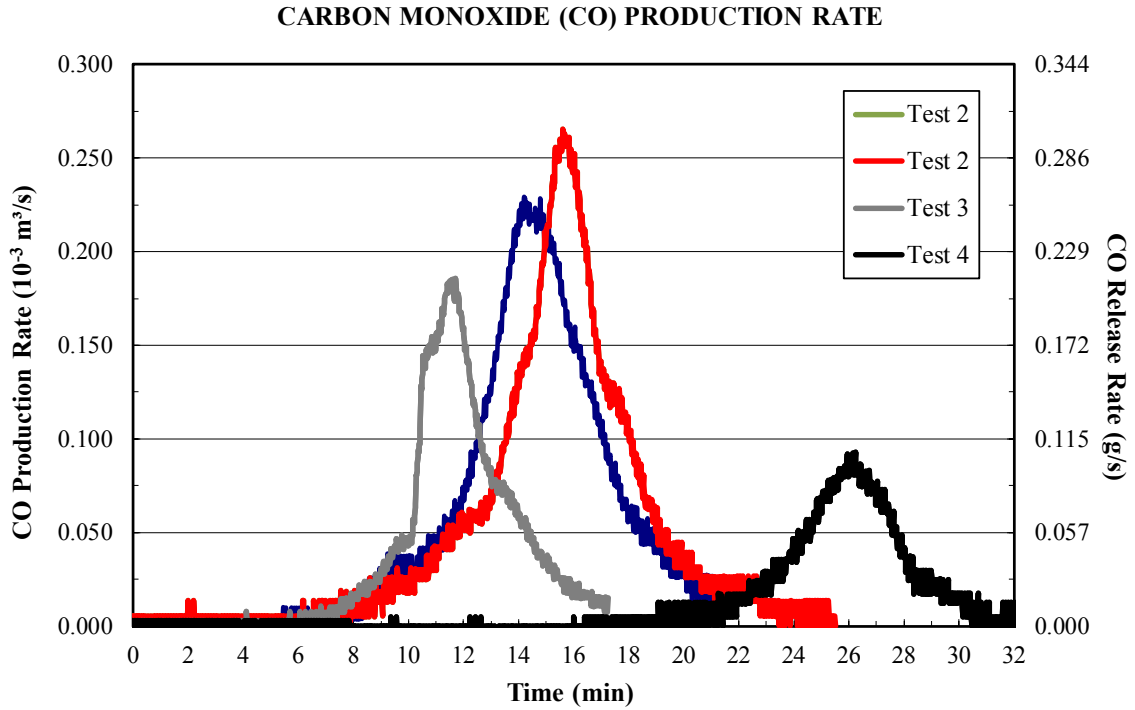


Figure H-4: ASTM E2067 results for UPPAbaby Mesa CRS (continued)

Appendix I: Chemical Composition Data

Chemical Composition Data

Results Description	Appendix I Table Number
Chemical Composition Results for Passenger Vehicle Materials	I-1
Chemical Composition Results for School Bus Seat Materials	I-2
Chemical Composition Results for CRS Seat Materials	I-3
Chemical Composition Results for Motorcoach Materials	I-4
Chemical Composition Results for Control Materials	I-5

The red color coding signifies FR present based on analysis.

The yellow color coding signifies FR plausible based on analysis.

The green color coding signifies FR absent based on analysis.

The final decision, reflected by the color coding, was made after the secondary analysis.

Table I-1: Chemical Composition Results for Passenger Vehicle Materials

Sample Number	#1	#2	#2	#3	#3	#4	#4
Sample Designation	M20170114_Camaro 2 of 5	M20170114_Camaro 2 of 5	M20170114_Camaro 2 of 5	4/5 carpet	4/5 carpet	M 1/5 carpet M20174300	M 1/5 carpet M20174300
Sample Section	light foam	gray, light interior portion	back, dark portion	fibrous portion	black rubber portion	gray portion	black portion
Search It Result	Future Foam 90270 yellow: polyurethane foam	Hyfonic 1 (combustion - modified polyether polyurethane)	Poly(ethylene terephthalate)	Poly(ethylene terephthalate)	Ritawax (lanolin alcohol based)	Polyurethane foam	Nylon 6
HQI	98.54	97.53	97.55	97.7	96.44	94.31	98.52
FRX Database Result	Conathane EN-2545 Part B (polyurethane encapsulant)	Expyrol CF (AFFF) 6% (foam concentrate for fighting fires)	Valox 420-SEO (glass filled PBT (polybutyl terephthalate)resin, thermoplastic), Brominated ER	Valox 420-SEO (glass filled PBT (polybutyl terephthalate)resin, thermoplastic), Brominated FR	Duro FR-H	Conathane EN-2545 Part B (polyurethane encapsulant)	Vydyne M-340 (nylon modified with flame retardant additives)
HQI	82.9	81.16	87.29	87.62	95.13	80.06	97.15
Mixture Analysis Compilation	4 components, fairly good compilation match	5 components, fairly good compilation match	performed but did not like or accept matches	N/A	Software sees 1.00 % weight Ritawax	4 components, fairly good compilation match	3 components, fairly good compilation match
HQI	99.2	99.06	N/A	N/A	96.66	97.81	98.94
Mixture Analysis Components	polyglycol, polyurethane, thermo plastic urethane, D, L-Methadone	styrene copolymer, polyurethane, cellulose, diisopropyl-D-tartrate	N/A	N	N/A	Genamin D (PP glycol that acts as a curing agent), pyrolyzate, polyurethane, plaza insulation	nylon 6, akulon K136 (polyamide) and bis-phosphonic acid
Probability of FR presence: (Likely/Plausible/Unlikely)	Plausible	Likely	FR in alternate piece of this sample	Need secondary analysis	Need secondary analysis	FR in alternate piece of this sample	Likely
Justification/Notes	The FR correlation is used for circuit boards, electrical assemblies, not sure it would be in vehicle foam.	All searches match to the foam component and Search It correlates with a combustion modified material.	FRX HQI below 90% and key peaks missing: FR is in the gray portion of this textile	FR correlation is used in automotive exterior and interior parts. Has a peak span between 750-500cm ⁻¹ .	Since the software only sees the ritawax in the mixture, I question whether a flame retardant material is present. DURO FR-H appears to be used in locker construction.	FRX match is less than 90% and does not correlate well	Nice correlation between core material and FRX spectral match. FR is a Nylon 6 composition.
Review Notes after scan of FR Controls	Does share a peak in the P=O range at 1223 cm ⁻¹	Has 1141 peak (P=O)		Need a PET control	Need a Control		Need a Control (for Nylon)
Conclusion Drawn				Scanned PET control with no flame retardant (negative control); sample almost perfect fit with exceptions around 950 and 850 cm ⁻¹ which do not represent peaks of interest			
Presence or Absence of Brominated peaks (1360-1340 and 1325 cm⁻¹); only PP-FR control shows these peaks.	No	No	No	1339 peak but not a match for Brominated FR	No	No	No
Presence or Absence of Brominated peaks (750-500 cm⁻¹); only ABS-FR control shows this peak.	650 peak; that Foam control does not have	No	No	NO	No	No	No

Table I-1: Chemical Composition Results for Passenger Vehicle Materials (Continued)

Sample Number	#5	#5	#6	#6	#7	#8	#8
Sample Designation	3/5 Head	3/5 Head	F-Head	F-Head	Ford dash	Dashboard	Dashboard
Sample Section	gray portion	black portion	rigid, gray foam portion	soft gray portion	silver of inner compar	black rubber portion	gray foam portion
Search It Result	Rimthane CPR 2138-70D-controlled pyrolyzate (urethane elastomer)	Poly(ethylene terephthalate)	Millox ?	Polyurethane foam	Kraton G-7827 (styrene-butadiene-isop-rubber)	Neorez R-967 (water-borne urethane polymer)	Polyurethane foam
HQI	94.83	97.65	95.33	98.65	95.37	94.53	95.25
FRX Database Result	Thurane (Flame retardant rigid polyurethane foam insulation)	Valox 420-SEO (glass filled brominated, flame retardant PBT resin, thermoplastic)	Thurane (Flame retardant rigid polyurethane foam insulation)	Expyrol CF (AFFF) 6% (foam concentrate for fighting fires)	Tridecyl acid phosphate	FR-222	Conathane EN-2545 Part B (polyurethane encapsulant)
HQI	90.01	97.72	92.02	80.79	86.05	83.58	79.59
Mixture Analysis Compilation	4 components, fairly good compilation match	4 components, fairly good compilation match	5 components, compilation overall is off on level of intensity due to Helastic WC-6912 component	4 components, fairly good compilation match	3 components, not a perfect fit	5 components, fairly good compilation match	4 components, fairly good compilation match
HQI	98.4	98.73	98.36	99.22	97.33	98.87	98.25
Mixture Analysis Components	plaza insulation, pyrolyzate, polystyrene, polyurethane	PET, Melinex (polyester film), Andur 7500-DP prepolymer, Styrene copolymer	pyrolyzate, polyurethane, plaza insulation, n-phenyl-1-naphthylamine, Helastic WC-6912 (polyurethane dispersion)	Future Foam, aromatic prepolymer, poron	PET, thermocomp MF-1002HS (PP), Plaslude PP (PP-based resin)	polyglycol, cortisone, Hyfonic 1, polyurethane, ethyl carbamate	PP, polyurethane, pyrolyzate, plaza insulation
Probability of FR presence: (Likely/Plausible/Unlikely)	FR in alternate piece of this sample	Likely	Need secondary analysis	Need secondary analysis	Need secondary analysis	Plausible	Need secondary analysis
Justification/Notes	mixture analysis correlates with FR insulation found on FRX database	Brominated peak is present (~750-500 cm ⁻¹ and 450cm ⁻¹).	FR insulation is showing up in mixture analysis; secondary analysis required	FR identified does not show up in mixture analysis; might be at a very low percent	Small P peak around 1140 cm ⁻¹	Not a good spectral match under FRX database. Don't agree with all of the mixture analysis but Hyfonic is present.	Poor correlation on FRX database.
Review Notes after scan of FR Controls			Intensity of peaks differs but similar peaks to PU control.	Almost identical peaks to PU control, except at 700 cm ⁻¹	compare sample to PET control; no FR. Could we get PET control with FR?		Sample has unique spectral features that the PU-FR control does not; not a good match
Conclusion Drawn							
Presence or Absence of Brominated peaks (1360-1340 and 1325 cm⁻¹); only PP-FR control shows these peaks.	Possible shifted area (1373-1341)	Possible shifted area (1384-1372)	No	1373-1341	1376-1359	1372-1344	1372-1345
Presence or Absence of Brominated peaks (750-500 cm⁻¹); only ABS-FR control shows this peak.	No	722	No	No	No	No	No

Table I-2: Chemical Composition Results for School Bus Seat Materials

Sample Number	#18	#18	#19	#20
Sample Designation	School Bus_Blue Bird cover	School Bus_Blue Bird cover	School Bus_Blue Bird padding	School Bus_Starcraft cover
Sample Section	gray portion	gray portion attached to threading	whole, intact	whole, intact (scanned on gray side)
Search It Result	D-11 (blend of monostearates with polysorbate 60)	D-11 (blend of monostearates with polysorbate 60)	Future Foam 100180 Yellow (polyurethane foam)	Turco Guard 100-66 (modified acrylic coating)
HQI	91.6	91.22	97.72	92.29
FRX Database Result	FR-222 (fire resistant ketone peroxides in plasticizer)	FR-222 (fire resistant ketone peroxides in plasticizer)	Thurane (Flame retardant rigid polyurethane foam insulation)	Fire Snuf 25 32 F. S. White (fiberglass panels)
HQI	83.74	84.52	80.72	86.37
Mixture Analysis Compilation	5 components; intensity is way off	5 components; intensity is way off	3 components, fairly good compilation fit	5 components; picked up on adhesives and lacquers
HQI	98.2	98.05	98.96	96.66
Mixture Analysis Components			Future Foam, 2-amino-5-chlorobenzophenone and Resokaempferol	2-part polyurethane adhesive, silicone modified alkyds, acrylic lacquer, vinyl chloride homopolymer, polyvinyl acetate copolymer
Probability of FR presence: (Likely/Plausible/Unlikely)	Secondary Analysis	Secondary Analysis	Plausible	Unlikely
Justification/Notes	Picked up on a Phosphorus compounds	Picked up on a Phosphorus compounds		
Review Notes after scan of FR Controls	Has peaks between 1320-1140; which represents the P double bond O region.	Has peaks between 1320-1140; which represents the P double bond O region.	Only 1 peak differs from Foam w/FR control at around 950 cm ⁻¹ ; this gives the impression that this sample might have the FR in it	No great control for comparison
Conclusion Drawn	No great control for this sample	No great control for this sample		
Presence or Absence of Brominated peaks (1360-1340 and 1325 cm⁻¹); only PP-FR control shows these peaks.	No	No	1373-1340	No
Presence or Absence of Brominated peaks (750-500 cm⁻¹); only ABS-FR control shows this peak.	No	No	No	No

Table I-2: Chemical Composition Results for School Bus Seat Materials (Continued)

Sample Number	#21	#22	#23	#23
Sample Designation	School Bus_Starcraft padding	School Bus_Trans Tech cover	School Bus_Trans Tech padding	School Bus_Trans Tech padding
Sample Section	whole, intact	gray portion attached to threading	foam portion	lining portion
Search It Result	Expyrol CF (AFFF) 6% (synthetic foam compound that contains fluorocarbon surfactants); FRX database	Polyethylene glycol methacrylate phosphate	Future Foam 100180 Yellow (polyurethane foam)	Poly (ethylene terephthalate)
HQI	82.37	90.3	98.66	90.69
FRX Database Result	Hyfonic (combustion modified polyether polyurethane foam)	Pluracol 463 (flame retardant for urethane foams)	Verel Type A natural Bright 3 DEN/Filament (modacrylic fiber)	Pyrovatex CP (flame retardant finish for textiles of cellulose fibers and fabric blends)
HQI	90.33	89.41	74.67	84.1
Mixture Analysis Compilation	5 components	5 components; picked up on chlorinated phosphate	3 components; nice overall match	5 components; does not all make sense
HQI	98.95	96.6	99.21	96.75
Mixture Analysis Components	polyurethane foam, styrene copolymers, polyamides and questionable matches	part of 2-part polyurethane adhesive, misc. polymers, Fyroflex 2800 (chlorinated phosphate), phthalate	polyurethane foam, acrylonitrile, and Desmodur E15 (aromatic polyisocyanate prepolymer)	PET and resins and a possible carcinogen (o-Dianisidine)
Probability of FR presence: (Likely/Plausible/Unlikely)	Secondary Analysis	Plausible	Unlikely	Secondary Analysis
Justification/Notes	Not the best spectra (noise areas); Search It provides an FRX match but not the same when you isolate just the FRX database.	Mixture analysis sees Cl and P.	Very low FRX correlation.	
Review Notes after scan of FR Controls	Intensity and structure of peaks vary between 1000-700cm ⁻¹ when compared to Foam-FR control. Has representation peaks in the areas of phosphate regions (2440-2275 and 1320-1140 when compared to control	No great control for this sample.		
Conclusion Drawn				Do not have a PET sample with FR control.
Presence or Absence of Brominated peaks (1360-1340 and 1325 cm⁻¹); only PP-FR control shows these peaks.	1373-1340	1382-1365 (shifted); 1325	1373-1340 shifted	1340 peak
Presence or Absence of Brominated peaks (750-500 cm⁻¹); only ABS-FR control shows this peak.	No	some individual peaks	No	No

Table I-3: Chemical Composition Results for CRS Seat Materials

Sample Number	#9	#10	#10	#11	#12	#13	#13
Sample Designation	Baby Seat, Peg Perego foam sample intact	Baby Seat, Britax parking cover foam portion	Baby Seat, Britax parking cover fabric portion	Baby Seat, Britax Parkway foam sample intact	Baby Seat, Uppa Baby plastic sample intact	Baby Seat, Uppa Baby cover foam portion	Baby Seat, Uppa Baby cover fabric portion
Sample Section							
Search It Result	Polystyrene, monohydroxy terminated	Poly (ethylene terephthalate)	Poly (ethylene terephthalate)	Polystyrene, monohydroxy terminated	Fortilene 5401 (polypropylene)	Future Foam 55240 white (polyurethane foam)	Silk Fibroin (polyamides)
HOI	97.95	98.74	98.36	99.69 (real tight fit)	98.91	99.09	94.55
FRX Database Result	Pelaspn FR 333 natural (flame retardant expandable polystyrene); <u>brominated</u>	Valox 420-SEO (thermoplastic, glass-reinforced polyester resin); <u>brominated</u> flame retardant	Valox 420-SEO (thermoplastic, glass-reinforced polyester resin); <u>brominated</u> flame retardant	Pelaspn FR 333 natural (flame retardant expandable polystyrene); <u>brominated</u>	Fire Resistive C.I. Mastic 65-05 (vapor barrier and weather coating); used in outdoor materials	Conathane EN-2545 Part B (polyurethane encapsulant)	Tutogen FP (fluoroprotein foam)
HOI	94.96	88.68	88.88	96.79	94.84	82.56	88.66
Mixture Analysis Compilation	5 components, nice match with minor residual	2 components	3 components	3 components	3 components	5 components	5 components
HOI	99.04	98.97	98.99	99.86	99.54	99.36	97.15
Mixture Analysis Components	copolymer styrene-stat-styrene azide, polystyrene monocarboxy terminated, styrene/allyl alcohol copolymer, D-Phenylglycinol, styrene co MA trimethoxysilane	PET, hexafluoropropyl phosphonic acid	PET, Melinex 442/142 (PET film) and Vycron Type 12 (PET)	Polystyrene, monohydroxy terminated, copolymer styrene-stat-styrene azide, Bio Beads S-X8.6 400 mesh	Polypropylene-graft--maleic anhydride, Fortilene 1201A, Polypropylene P7673-960	Future Foam white, Polyglycol B 01/40, Desmodur (E14) (prepolymer toluene diisocyanate), Terpolymer Toluene diisocyanate-Propylene glycol, poron 4701-01 (cellular urethane)	Gafite (polyester), Zetol, 2-Cyanoethylhydrazin, 4-methyl-1-(alpha-methylbenzylidene)-3, estane 58810 (thermoplastic polyurethane)
Probability of FR presence: (Likely/Plausible/Unlikely)	Likely	Likely	FR in alternate piece of this sample	Likely	Need secondary analysis	Need secondary analysis	Need secondary analysis
Justification/Notes	Highly probably PS with flame retardant. Appears to have brominated and possibly Cl peaks.	Spectra has peaks that hover in the spectral regions for <u>B</u> and <u>P</u> . Mixture analysis sees the PET with a <u>phosphorus</u> component	Mixture analysis sees only the polymers	Main constituent fits FRX match, tight spectral fit	Mixture analysis sees just polymers		not a good spectral interpretation for the correlation. Major shifts and intensity differences for peaks.
Review Notes after scan of FR Controls	No PS control	2323-2286 P range		No PS control	Compared to PP Control with Br-FR; samples does not have 1320 peak or 1140 but has something at 1166 (shared with control).	Almost identical match to the Foam_FR control provided	
Conclusion Drawn					Unlikely		no comparison for the fabric
Presence or Absence of Brominated peaks (1360-1340 and 1325 cm⁻¹); only PP-FR control shows these peaks.	No	1370-1340	just 1340	1328	No	1141	No
Presence or Absence of Brominated peaks (750-500 cm⁻¹); only ABS-FR control shows this peak.	3 unique peaks in this region: 754, 695, 538	No	No	3 unique peaks in this region: 753, 695, 538	No	No	No

Note: Sample #13 is the removable foam pad part of the seat, which is comprised of fabric adhered to a thin foam padding. In the table above, there is information for the foam part and the fabric part of this overall seat component. The disposition for the fabric portion of this component is yellow and therefore plausible, but really this is unknown, since there was not a good match for any positive control.

Sample #16 in the table on the next page is also identified as foam from the UppaBaby seat. This foam is polystyrene based, as opposed to #13, which is polyurethane, and is adhered to the rigid plastic from the seat back, molded into a contour similar to the other seats.

Table I-3: Chemical Composition Results for CRS Seat Materials (Continued)

Sample Number	#14	#15	#16	#17	#17	#17
Sample Designation	Baby Seat_Britax Parkway plastic	Baby Seat_Peg Perego plastic	Baby Seat_Uppa Baby foam	Baby Seat_Peg Perego cover	Baby Seat_Peg Perego cover	Baby Seat_Peg Perego cover
Sample Section	sample intact	sample intact	sample intact	fabric top	foam portion	fabric bottom
Search It Result	Hostalen PPN VP 8018 (polymer mixture: PP and Poly (ethylene-co-propylene); impact resistant especially for automobile fender coatings	Hostalen PPN VP 8018 (polymer mixture: PP and Poly (ethylene-co-propylene); impact resistant especially for automobile fender coatings	Fortilene 4141F (PP copolymer)	Poly (ethylene terephthalate)	Scott Pyrell Foam (flexible polyurethane foam)	Poly (ethylene terephthalate)
HQI	98.65	99.07	99.46	95.08	96.66	98.79
FRX Database Result	Fire Resistive C.I. Mastix 65-05 (vapor barrier and weather coating)	Fire Resistive C.I. Mastix 65-05 (vapor barrier and weather coating)	Fire Resistive C.I. Mastix 65-05 (vapor barrier and weather coating)	Valox 420-SEO (polyester resin, glass reinforced); brominated	Industrial Foam (SIF); (flexible, ester-type of polyurethane foam)	Valox 420-SEO (polyester resin, glass reinforced); brominated
HQI	94.35	95.38	94.03	86.58	98.94	90.24
Mixture Analysis Compilation	2 components	2 components	2 components	3 components	3 components	3 components; matching to Search It ID
HQI	99.34	99.18	99.47	98.81	99.59	99.25
Mixture Analysis Components	Polypropylene-graft--maleic anhydride, Rexene PP 11S5 (propylene homopolymer)	Polypropylene-graft--maleic anhydride, Polypropylene, isotactic	Polypropylene, isotactic and IR 310 (polyisoprene)	Poly (ethylene terephthalate), Scott Foam 100Q (polyester urethane foam) and Polyester from glutamic acid hydrochloride	Scott Foam 60 (polyester foam), Scott Foam 100Q, Wellamid MRGF 30/10 (reinforced nylon resin)	Poly (ethylene terephthalate), 1-Benzylpyrrole and Chlordiazepoxide hydrochloride
Probability of FR presence: (Likely/Plausible/Unlikely)	Need secondary analysis	Need secondary analysis	Need secondary analysis	FR in alternate piece of this sample	Likely	FR in alternate piece of this sample
Justification/Notes	Residual spectra not accounted for is not in a flame retardant spectral region. Mixture analysis sees PP polymers.	Mixture analysis sees PP polymers.	Mixture analysis sees PP polymers.	Less than 90% on FRX; fabric does not appear glass-reinforced, but some peak overlap specific regions	Nice overlay of spectral matching and high correlation.	
Review Notes after scan of FR Controls	PP control has unique 1322 peak that samples does not	Sample is missing the signature 1360-1340 cm ⁻¹ peak; believe it to be FR free	Based on comparison to PP control with brominated FR, this sample is missing key peaks at 1320, 1140 and 1060 cm ⁻¹ . FR library match also primarily used in outside service applications.			
Conclusion Drawn						
Presence or Absence of Brominated peaks (1360-1340 and 1325 cm⁻¹); only PP-FR control shows these peaks.	1359-1330	No	No	No	No	No
Presence or Absence of Brominated peaks (750-500 cm⁻¹); only ABS-FR control shows this peak.	No	small 750 peak	No	No	3 unique peaks in this region	No

Table I-4: Chemical Composition Results for Motorcoach Materials

Sample Number	#24	#25	#25	#26	#26
Sample Designation	Motorcoach_seat padding	Motorcoach_Headliner	Motorcoach_Headliner	Motorcoach_Floor covering	Motorcoach_Floor covering
Sample Section	whole, intact	top blue portion	bottom portion	fibrous portion	rubber portion
Search It Result	Future Foam 55240 white (polyurethane foam)	Nylon 4		Pharmcal PM-150-C (polyester films)	Poly (vinyl chloride), plasticized with phthalate ester
HQI	96.79	96.35		96.43	95.83
FRX Database Result	Oncor 23A (flame retardants for chlorinated resin compounds)	Grilon A28 VO natural (flame retarded Nylon 6)		Valox DR-48 (polyester resin with 15% glass reinforced); brominated	ECP-4515 (emulsifiable brominated organic)
HQI	78.89	88.35		86.02	88.29
Mixture Analysis Compilation	5 components; sees just the urethane	3 components		5 components	4 components; sees Bromoform
HQI	98.52	99.32		98.52	98.36
Mixture Analysis Components	all urethane compounds	all spectra seeing enzymatic material		PET, polyester, acrylic polymer resin	PVC injection molding compound, polyvinyl chloride, Bromoform and a hydrate
Probability of FR presence: (Likely/Plausible/Unlikely)	Plausible	Secondary Analysis	Secondary Analysis	Likely	Likely
Justification/Notes	Possible C-BR peak.	Odd results reported, need to re-run sample.	Not a good spectra collection; no data		Brominated organic detected.
Review Notes after scan of FR Controls	Couple of different peaks from the Foam-FR control	No control sample	No control sample		
Conclusion Drawn					
Presence or Absence of Brominated peaks (1360-1340 and 1325 cm⁻¹); only PP-FR control shows these peaks.	1373-1340			1380-1338 (shifted)	1355-1328
Presence or Absence of Brominated peaks (750-500 cm⁻¹); only ABS-FR control shows this peak.	No			723	

Table I-4: Chemical Composition Results for Motorcoach Materials (Continued)

Sample Number	#27	#27	#28	#29	#30
Sample Designation	Motorcoach_Door of luggage	Motorcoach_Door of luggage	Motorcoach_HVAC control panel	Motorcoach_Seat Backing gray	Motorcoach_Seat Cover
Sample Section	foam portion	gray plastic portion	whole, intact	whole, intact	blue top portion
Search It Result	Cuvertin UK 1430 (poly ether urethane)	Cyclolac EPB 3570 C (acrylonitrile/butadiene styrene)	Styrene/acrylonitrile copolymer 75/25	Rexene PP 23R2A (random polypropylene copolymers)	Nylon 4
HQI	94.62	96.35	96.43	94.96	96.62
FRX Database Result	Thurane (Flame retardant rigid polyurethane foam insulation)	Pelaspas FR 333 natural (flame retardant expandable polystyrene)	Pelaspas FR 333 natural (flame retardant expandable polystyrene)	Sure-Stick Clear I-C 205 (high strength FR adhesive)	Grilon A28 VO natural (flame retarded Nylon 6)
HQI	75.45	90.81	93.51	89.18	90.87
Mixture Analysis Compilation	5 components; sees polyurethane components	5 components	5 components	3 components	4 components
HQI	97.95	98.95	98.99	97.05	99.28
Mixture Analysis Components	polyurethane foams...	Copolymer (styrene-phosphonic monomer), acrylonitrile/butadiene styrene...	Copolymer (styrene-phosphonic monomer), acrylonitrile/butadiene styrene, styrene resin...	Polypropylenes, water-resistant adhesive and 3-nitrobenzoic acid	nylon monofilament
Probability of FR presence: (Likely/Plausible/Unlikely)	FR in alternate piece of this sample	Likely	Likely	Secondary Analysis	Plausible
Justification/Notes	Very low FRX correlation.	Nice spectral match; high FRX correlation. Has peaks in FR regions.	Nice spectral match; high FRX correlation. Has peaks in FR regions.	Could not find info on the FR adhesive.	strange matches to enzymes; must be something in the fabric glues. Most certainly a nylon.
Review Notes after scan of FR Controls				Don't see key peaks around 1300 in the sample as compared to the PP control	No control sample
Conclusion Drawn					
Presence or Absence of Brominated peaks (1360-1340 and 1325 cm⁻¹); only PP-FR control shows these peaks.	No	No	No	No	
Presence or Absence of Brominated peaks (750-500 cm⁻¹); only ABS-FR control shows this peak.	No	3 peaks (758, 697, 542)	3 peaks (758, 698, 542)	No	

Table I-4: Chemical Composition Results for Motorcoach Materials (Continued)

Sample Number	#30	#31	#31	#32	#32
Sample Designation	Motorcoach_Seat Cover	Motorcoach_Seat Cover green	Motorcoach_Seat Cover green	Motorcoach_Seat Cover patterned blue	Motorcoach_Seat Cover patterned blue
Sample Section	blue bottom portion	top portion	bottom portion	top portion	bottom portion
Search It Result	D-11 (blend of monostearates with polysorbate 60)	Poly (ethylene terephthalate)	Baycrl L 461 W-55% (acrylic & methacrylic polymer dispersion)	alpha-Chymotrypsin (seeing this enzyme; must be something in a glue or adhesive in these textiles) or is not a good correlation	Sure-Lag I-C 130 (water base lagging adhesive)
HQI	93.69	98.82	91.87	97.74	92.31
FRX Database Result	Virchem FR-53	Valox 420-SEO (thermoplastic, glass-reinforced polyester resin); brominated flame retardant	FR-222 (fire resistant ketone peroxides in plasticizer)	Tutogen U (protein-based fire extinguishing air foam)	Sure-Lag I-C 130 (water base lagging system)
HQI	86.92	88.92	87.5	92.67	92.31
Mixture Analysis Compilation	no good mixture analysis results	4 components	no good mixture analysis results	2 components	4 components
HQI		99.07		99.28	97.73
Mixture Analysis Components		Poly (ethylene terephthalate), Melinex polyester film, PET with brightener		alpha-Chymotrypsin and a polymer phenolic resin	Acrylic latex caulk; polyamide-PP polymer blend, poly vinyl acetate, natural organic coloring
Probability of FR presence: (Likely/Plausible/Unlikely)	Secondary Analysis	Likely	Plausible	Secondary Analysis	Plausible
Justification/Notes	Not a good spectral correlation.	Brominated peak present	Based on peak in the regions of 750nm and 1100 to 1300nm	Not sure what FR Tutogen U is?	FRX correlation shows up for main constituent. Mixture analysis format is not a great correlation. Not able to find info on Sure-Lag product.
Review Notes after scan of FR Controls	No control sample			From comparison with the controls; it appears to relate mostly to the Foam control but has a very diffèrent representation in the fingerprint region	From comparison with the controls; it appears to relate mostly to the Foam control but has a very diffèrent representation in the fingerprint region
Conclusion Drawn					
Presence or Absence of Brominated peaks (1360-1340 and 1325 cm⁻¹); only PP-FR control shows these peaks.		1340		No	1408-1340 (shifted)
Presence or Absence of Brominated peaks (750-500 cm⁻¹); only ABS-FR control shows this peak.			No	No	No

Table I-5: Chemical Composition Results for Control Materials

<u>Sample Number</u>	CONTROL	CONTROL	CONTROL	CONTROL
<u>Sample Designation</u>	Manilla Folder	PMMA	HDPE	Thick Cardboard
<u>Sample Section</u>	whole, intact	whole, intact	whole, intact	whole, intact
<u>Search It Result</u>	cellulose (20 micron)	Poly (methyl methacrylate)	polyethylene (Petrothene LB 924-HDPE)	cellulose (100 micron)
<u>HQI</u>	99.22	99.62	99.53	98.63
<u>FRX Database Result</u>	Pyroset Flame Retardant TKP	Coustex	PE-2FR (flame retardant polyethylene)	Pyroset Flame Retardant TKP
<u>HQI</u>	91.12	80.85	97.73	92.5
<u>Mixture Analysis Compilation</u>	0.91% weight is cellulose; trace of purine	N/A	N/A	N/A
<u>HQI</u>	N/A	N/A	N/A	N/A
<u>Mixture Analysis Components</u>	N/A	N/A	N/A	N
<u>Probability of FR presence: (Likely/Plausible/Unlikely)</u>	Unlikely	Unlikely	Unlikely	Unlikely
<u>Justification/Notes</u>	spectra is almost spot on for pure cellulose; forced match under FRX database does not align.	nice matching spectra for PMMA; below 90% for FR and spectra does not align.	The FR correlation has 2 tiny peaks that overall spectra does not account for.	spectra is almost spot on for pure cellulose; forced match under FRX database does not align.
<u>Review Notes after scan of FR Controls</u>				
<u>Conclusion Drawn</u>				
<u>Presence or Absence of Brominated peaks (1360-1340 and 1325 cm⁻¹); only PP-FR control shows these peaks.</u>	No	No	No	No
<u>Presence or Absence of Brominated peaks (750-500 cm⁻¹); only ABS-FR control shows this peak.</u>	No	No	No	No

Appendix J: Ignition Temperature Analysis

Ignition Temperature Analysis

	Ignition Temperature Analysis Results Description	Figure Number
School Bus	Blue Bird Seat Cover	J-1
	Blue Bird Seat Padding	J-2
	Starcraft Seat Cover	J-3
	Starcraft Seat Padding	J-4
	Trans Tech Seat Cover	J-5
	Trans Tech Seat Padding	J-6
Motor Coach Materials	Green Cover Seat Padding	J-7
	Green Seat Cover	J-8
	Blue Seat Backing	J-9
	Blue Seat Cover	J-10
	Grey Seat Backing	J-11
	Luggage Rack Door	J-12
	Floor Covering	J-13
	Headliner	J-14
	Blue Seat Cover Padding (Interior Samples 1-3)	J-15
	Blue Seat Cover Padding (Interior Samples 4-6)	J-16
	Blue Seat Cover Padding (Surface Samples 1-3)	J-17
	Blue Seat Cover Padding (Surface Samples 4-6)	J-18
Motor Vehicle Interior	Ford F250 Carpet	J-19
	Mercedes Carpet	J-20
	Ford F250 Dashboard	J-21
	Mercedes Dashboard	J-22
	Camaro Headliner	J-23
	Ford Headliner	J-24
	Camaro Seat Cover	J-25
	Mercedes Seat Cover	J-26
	Camaro Seat Padding	J-27
	Mercedes Seat Padding	J-28
Surface Layer	Ford F250 Carpet	J-29
	Mercedes Carpet	J-30
	Mercedes Dashboard	J-31
	Camaro Headliner	J-32
	Ford Headliner	J-33
	Camaro Seat Cover	J-34
Thin	Acrylate	J-35
	Corrugated Cardboard	J-36
	High Density Polyethylene (HDPE)	J-37
	Manila Folder Cardboard	J-38
	Water Mist Test Simulated Furniture (SM) Foam	J-39
	Water Mist Test Simulated Furniture (SM) Foam	J-40

	Material Description	Figure Number
Cryo-milled Samples	Blue Bird School Bus Seat Cover	J-41
	Blue Bird School Bus Seat Padding	J-42
	Blue Bird School Bus Seat Padding (Back Side)	J-43
	Starcraft School Bus Seat Padding	J-44
	Trans Tech School Bus Seat Padding	J-45
	Motor Coach Luggage Rack Door	J-46
	Motor Coach Headliner	J-47
	Mercedes Carpet	J-48
	Ford Headliner	J-49
	Camaro Seat Padding	J-50
	Thin Acrylate Sheet	J-51
	Childseat Materials	Britax Parkway Base
Chicco KeyFit Base		J-53
Peg Perego Primo Viaggio Base		J-54
UPPAbaby Mesa Base		J-55
Britax Parkway Fabric		J-56
Chicco KeyFit Fabric		J-57
Peg Perego Primo Viaggio Fabric		J-58
UPPAbaby Mesa Fabric		J-59
Britax Parkway Padding		J-60
Chicco KeyFit Padding		J-61
Peg Perego Primo Viaggio Padding		J-62
UPPAbaby Mesa Padding		J-63
Britax Parkway Fabric and Padding Assembly		J-64
Chicco KeyFit Fabric and Padding Assembly		J-65
Peg Perego Primo Viaggio Fabric and Padding Assembly		J-66
UPPAbaby Mesa Fabric and Padding Assembly	J-67	

Nomenclature for Appendix J

A	=	frequency factor (s^{-1})
E	=	activation energy (kJ/mol)
h_c	=	specific heat release (kJ/g)
$h_{c,gas}$	=	heat of combustion of the specimen gases (kJ/g)
m_i	=	initial MCC sample mass (mg)
m_f	=	final MCC sample mass (mg)
n	=	reaction order
Q	=	specific heat release rate (W/g)
Q_{max}	=	maximum specific heat release rate (W/g)
$Q_{max,1}$	=	maximum specific heat release rate for the first (or only) reaction (W/g)
T	=	pyrolysis chamber temperature ($^{\circ}C$ or K)
T_{ig}	=	pyrolysis chamber temperature corresponding to sustained ignition ($^{\circ}C$ or K)
T_{max}	=	pyrolysis chamber temperature when Q_{max} is reached ($^{\circ}C$ or K)
$T_{max,1}$	=	pyrolysis chamber temperature when $Q_{max,1}$ is reached ($^{\circ}C$ or K)
$T_{\alpha=0.01}$	=	pyrolysis chamber temperature when $\alpha = 0.01$ ($^{\circ}C$ or K)
$T_{\alpha=0.02}$	=	pyrolysis chamber temperature when $\alpha = 0.02$ ($^{\circ}C$ or K)
$T_{\alpha=0.03}$	=	pyrolysis chamber temperature when $\alpha = 0.03$ ($^{\circ}C$ or K)
$T_{\alpha=0.04}$	=	pyrolysis chamber temperature when $\alpha = 0.04$ ($^{\circ}C$ or K)
$T_{\alpha=0.05}$	=	pyrolysis chamber temperature when $\alpha = 0.05$ ($^{\circ}C$ or K, also defined a T_1)
$T_{\alpha=0.95}$	=	pyrolysis chamber temperature when $\alpha = 0.95$ ($^{\circ}C$ or K, also defined a T_2)
Y_p	=	pyrolysis residue relative to the initial sample mass (g/g)
α	=	conversion or degree of advancement of the reaction (see Equation 2)
α_{ig}	=	conversion when $T = T_{ig}$
β	=	heating rate (K/s)
η_c	=	heat release capacity, calculated as Q_{max}/β (J/kg·K)
$\eta_{c,ig}$	=	value of Q/β when $T = T_{ig}$ (J/kg·K)
$\eta_{c,max,1}$	=	value of $Q_{max,1}/\beta$ (J/kg·K)

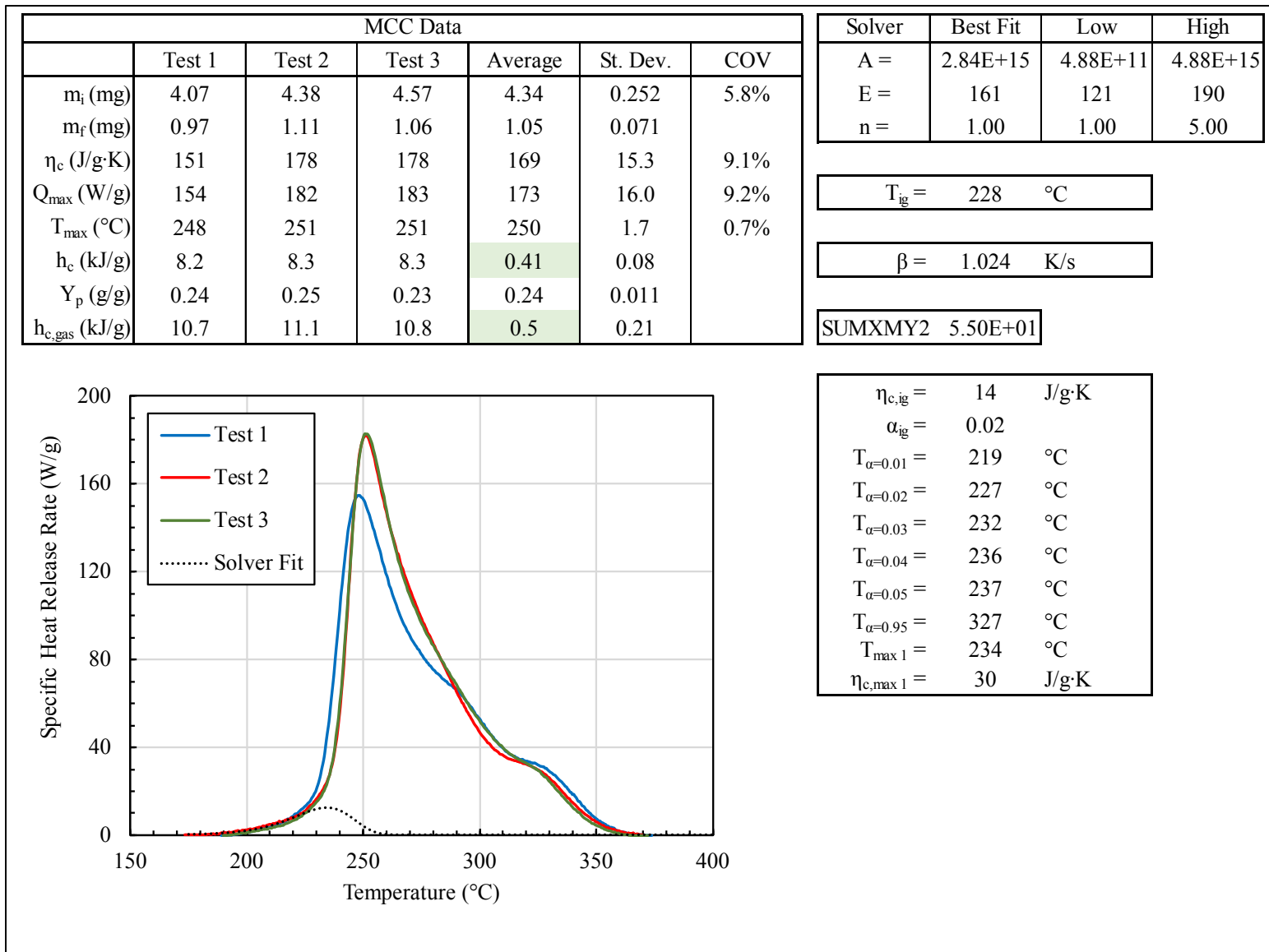


Figure J-1. Ignition temperature analysis results for Blue Bird School Bus seat material

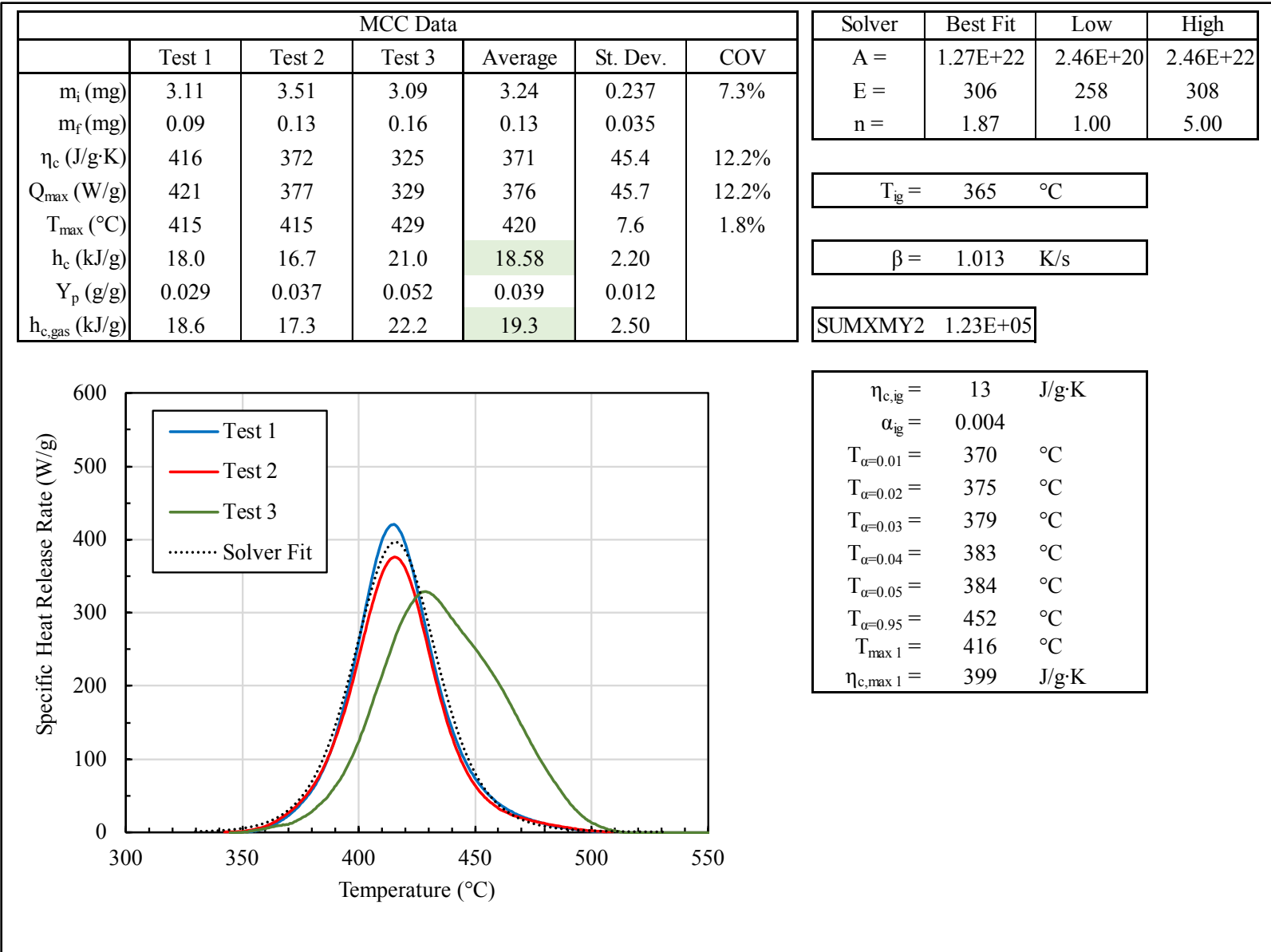


Figure J-2. Ignition temperature analysis results for Blue Bird School Bus seat padding

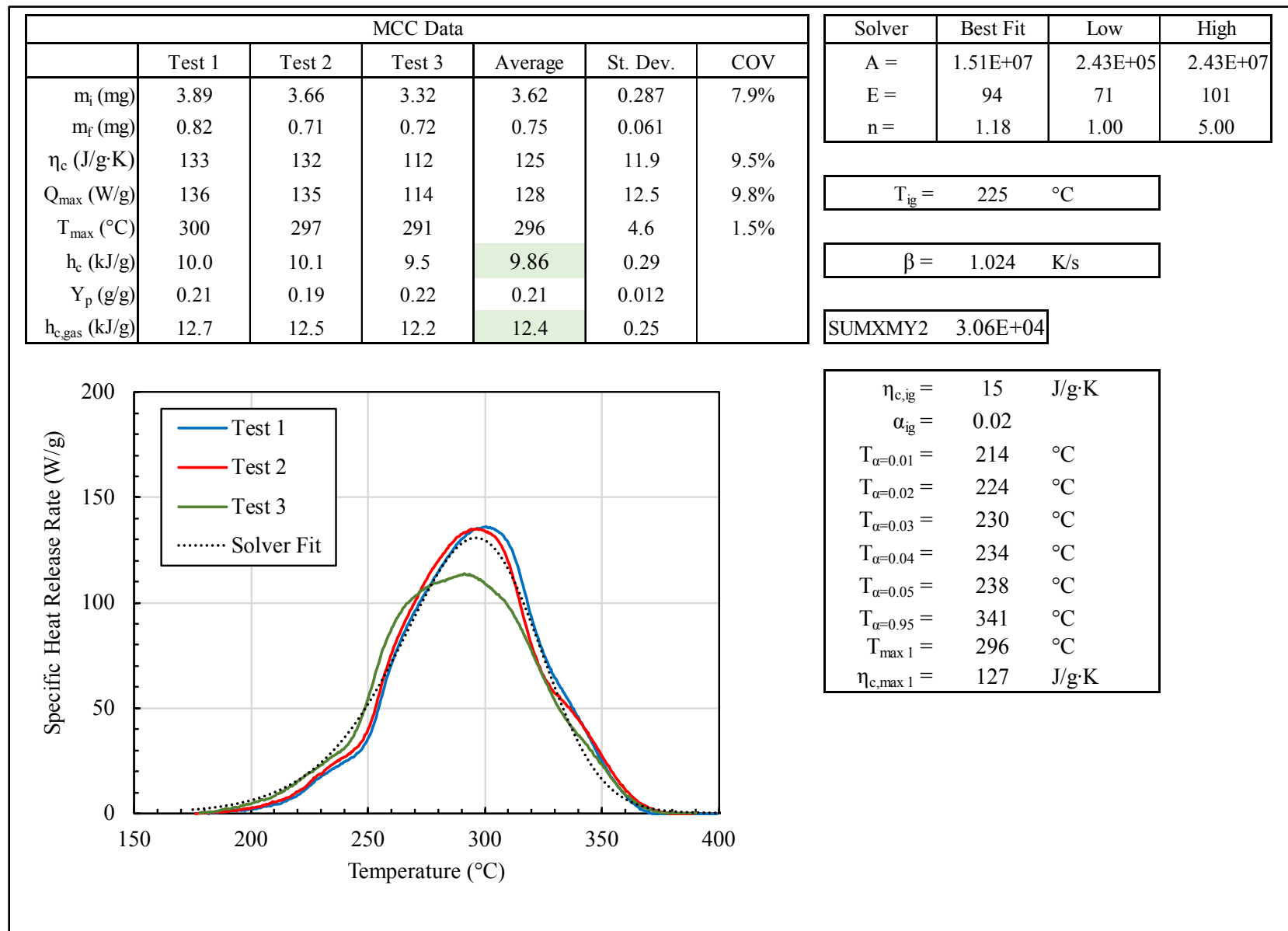


Figure J-3. Ignition temperature analysis results for Starcraft School Bus seat cover

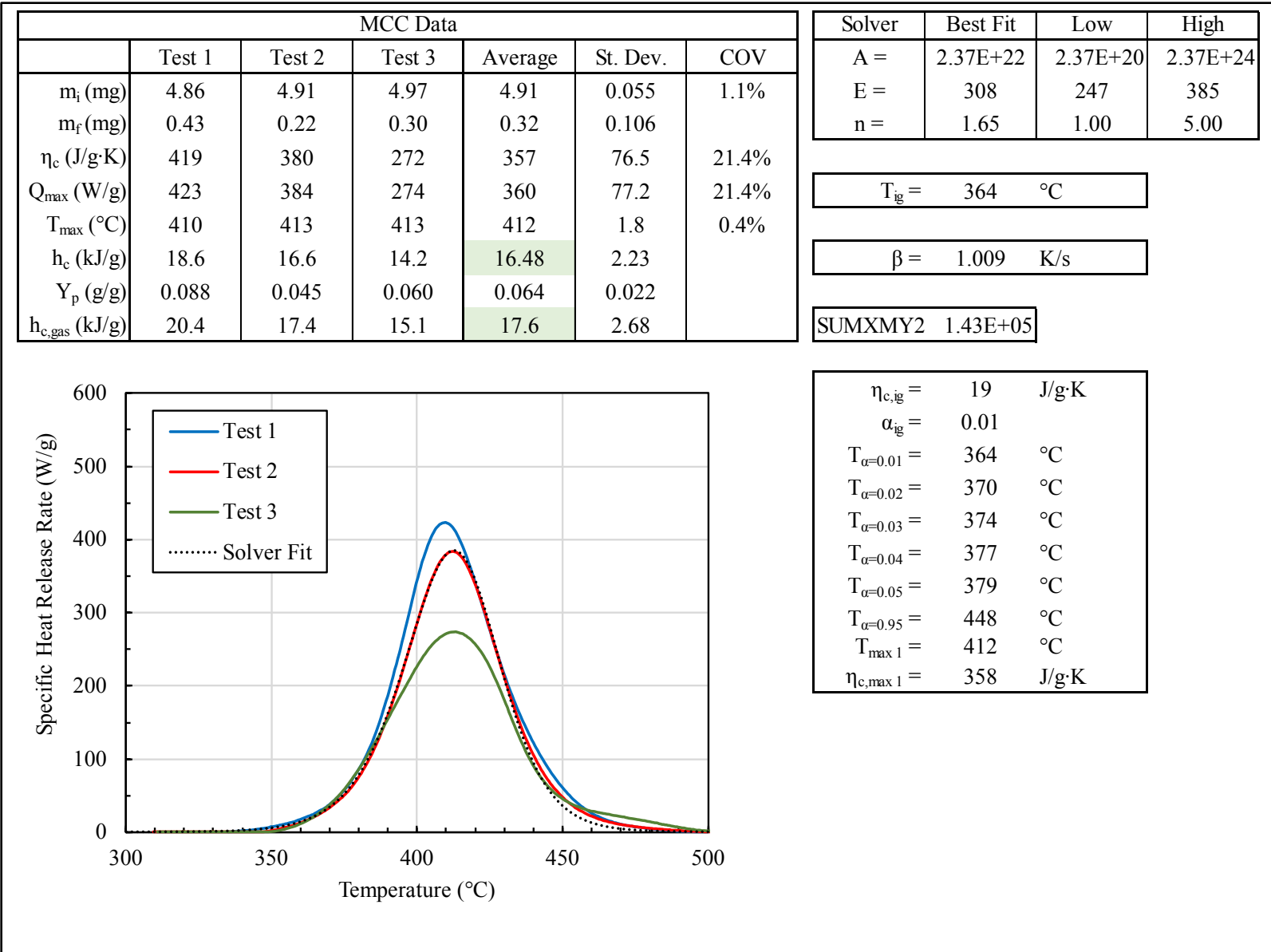


Figure J-4. Ignition temperature analysis results for Starcraft School Bus seat padding

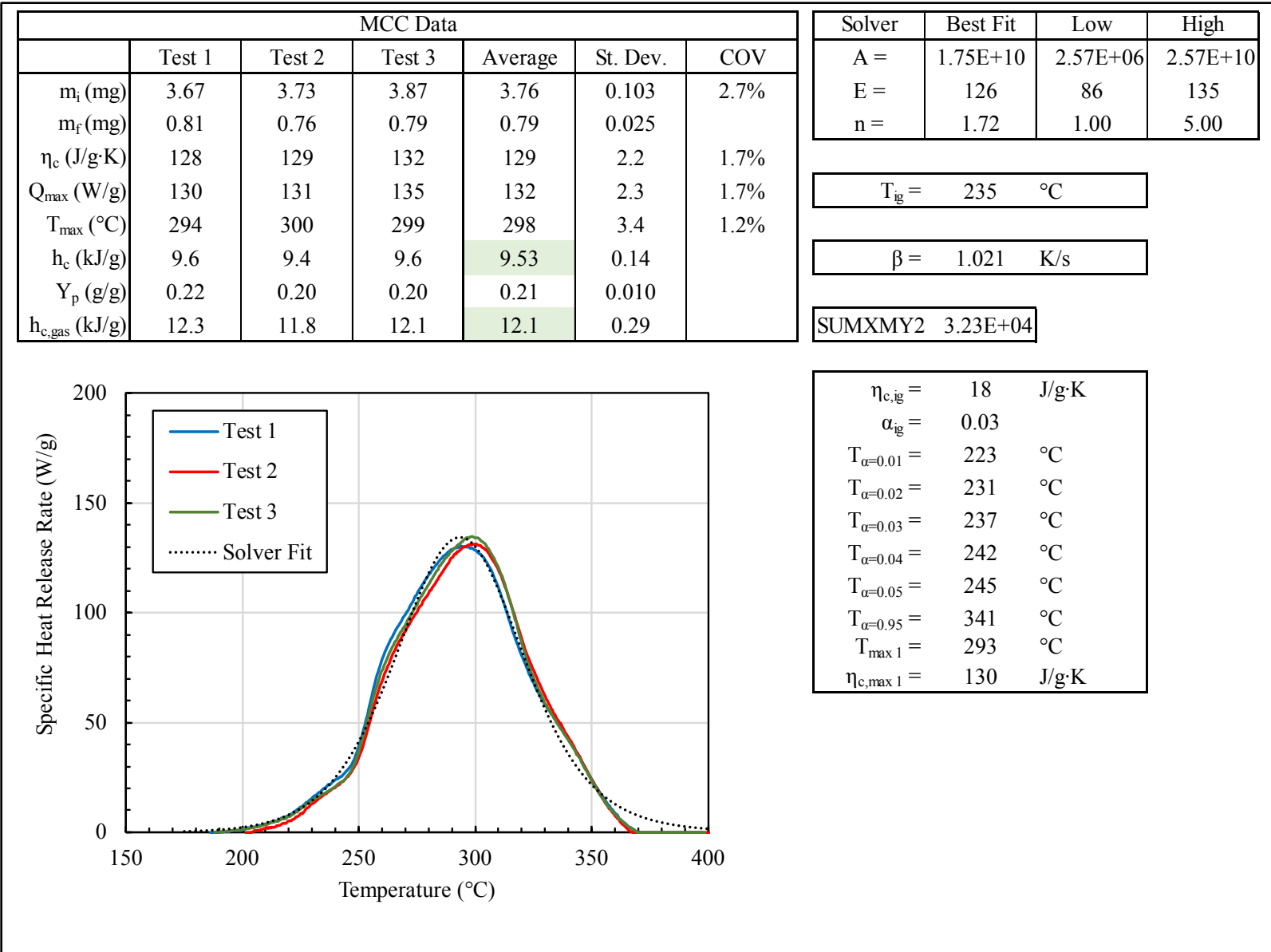


Figure J-5. Ignition temperature analysis results for Trans Tech School Bus seat cover

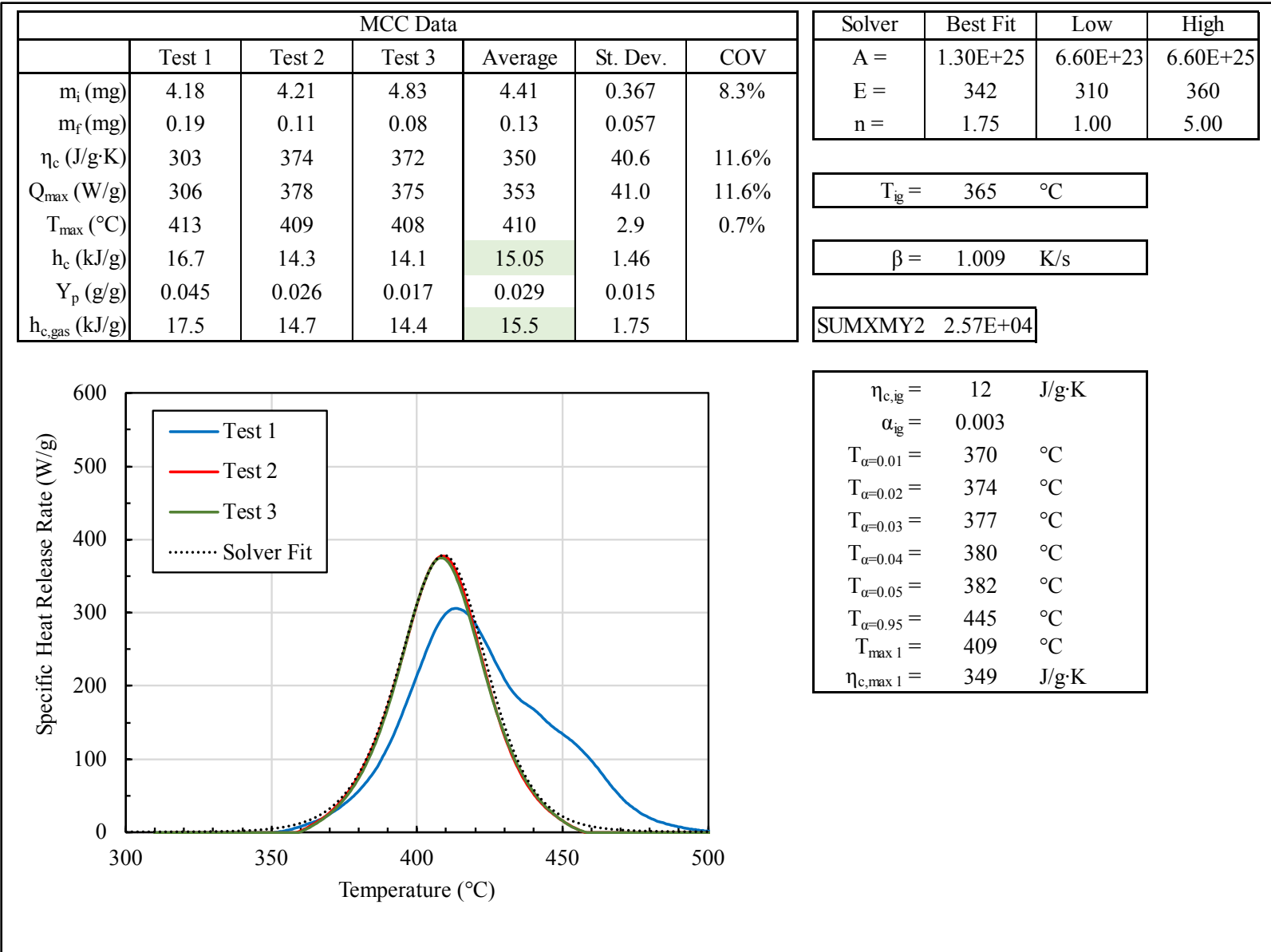


Figure J-6. Ignition temperature analysis results for Trans Tech School Bus seat padding

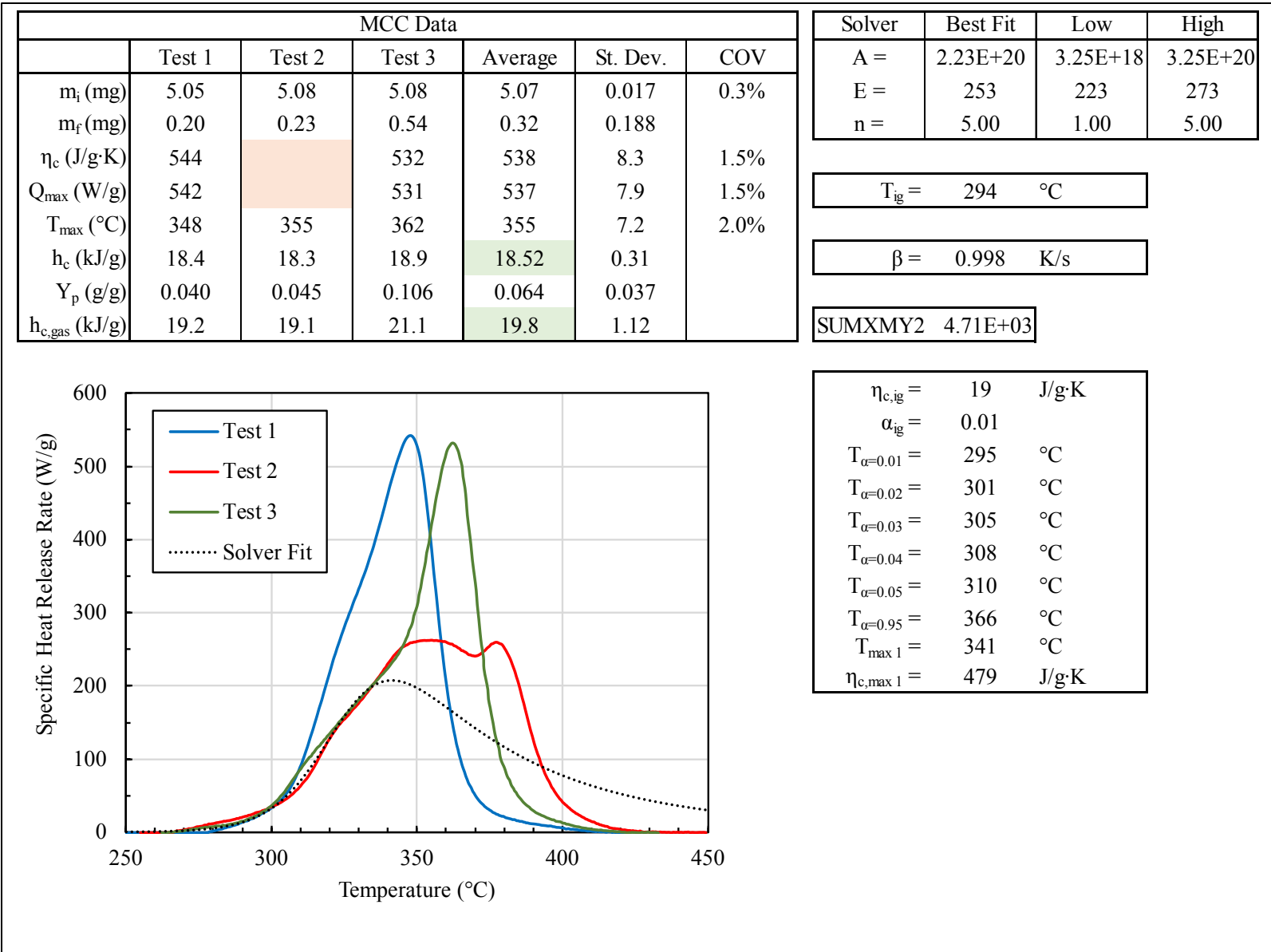


Figure J-7. Ignition temperature analysis results for Green Cover Motor Coach seat padding

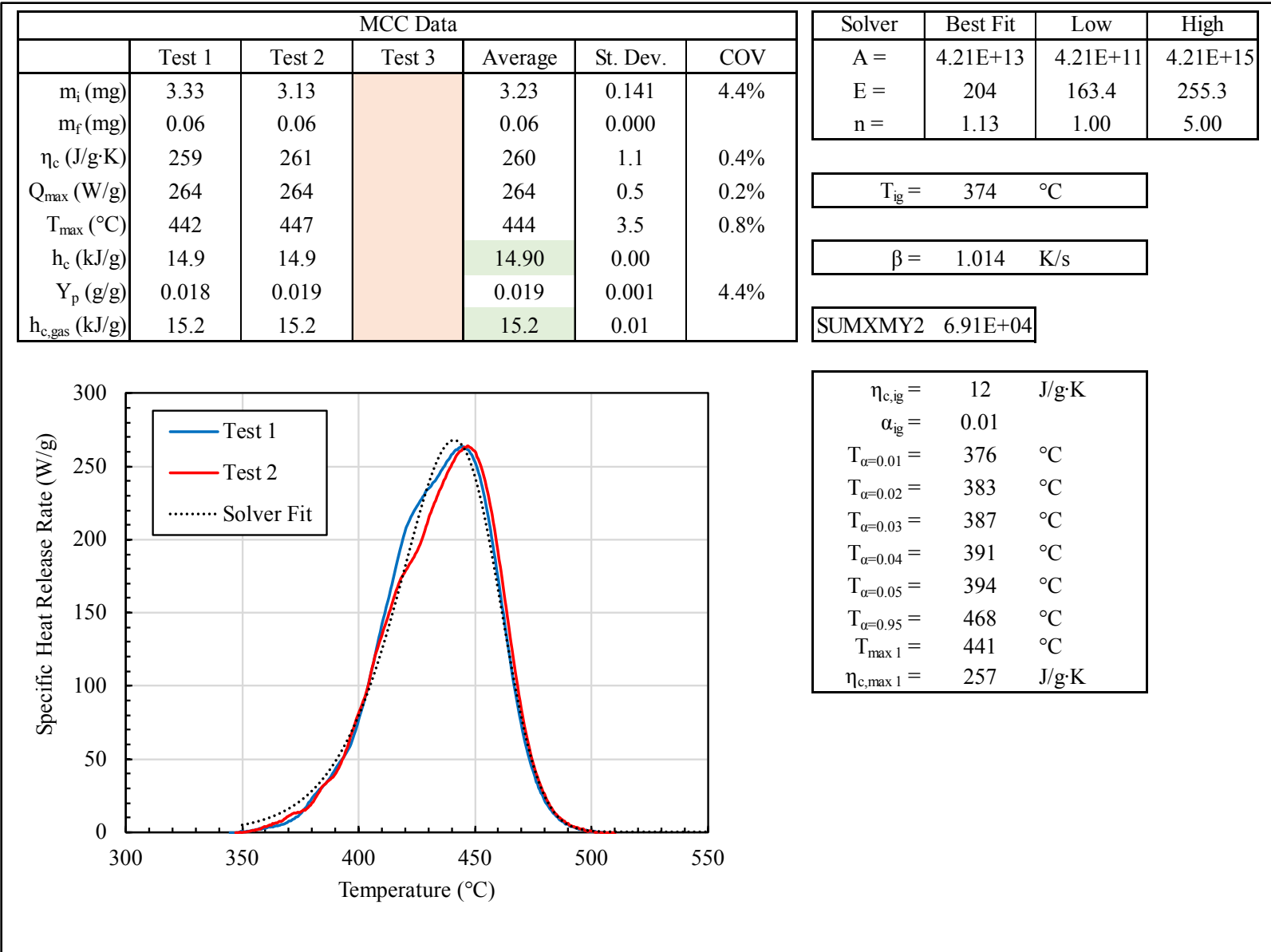


Figure J-8. Ignition temperature analysis results for Green Motor Coach seat cover

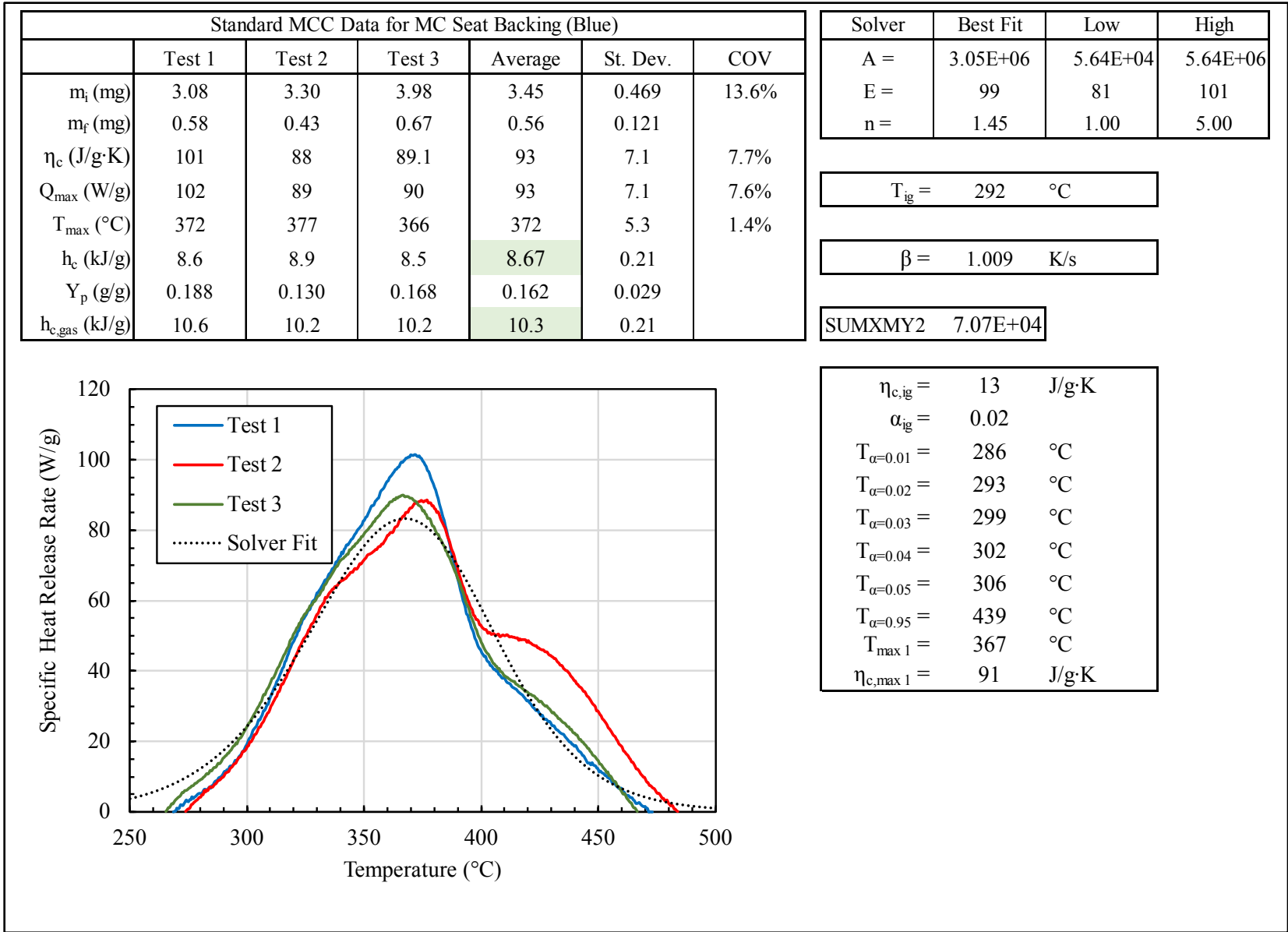


Figure J-9. Ignition temperature analysis results for Blue Motor Coach seat backing

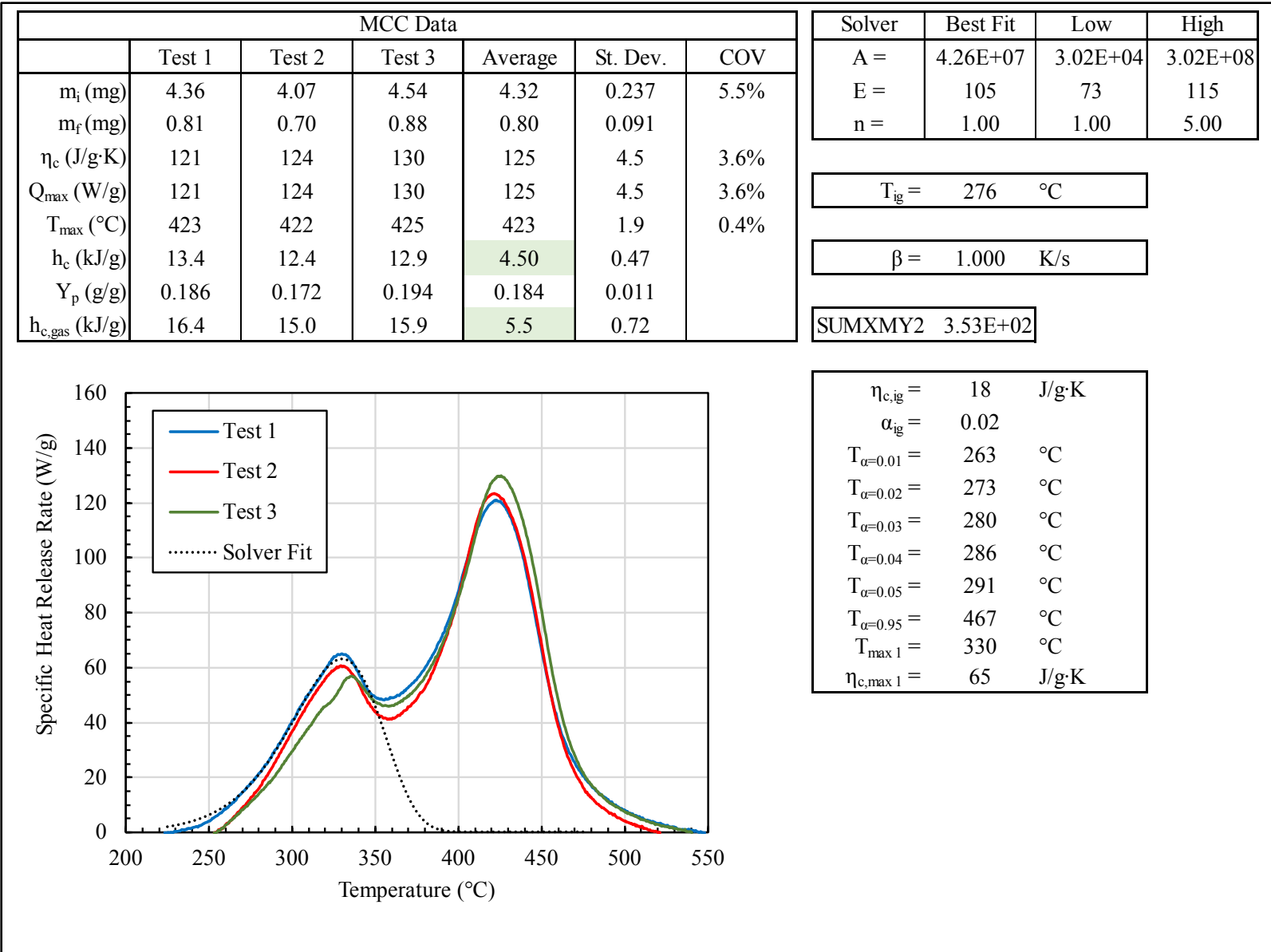


Figure J-10. Ignition temperature analysis results for Blue Motor Coach seat cover

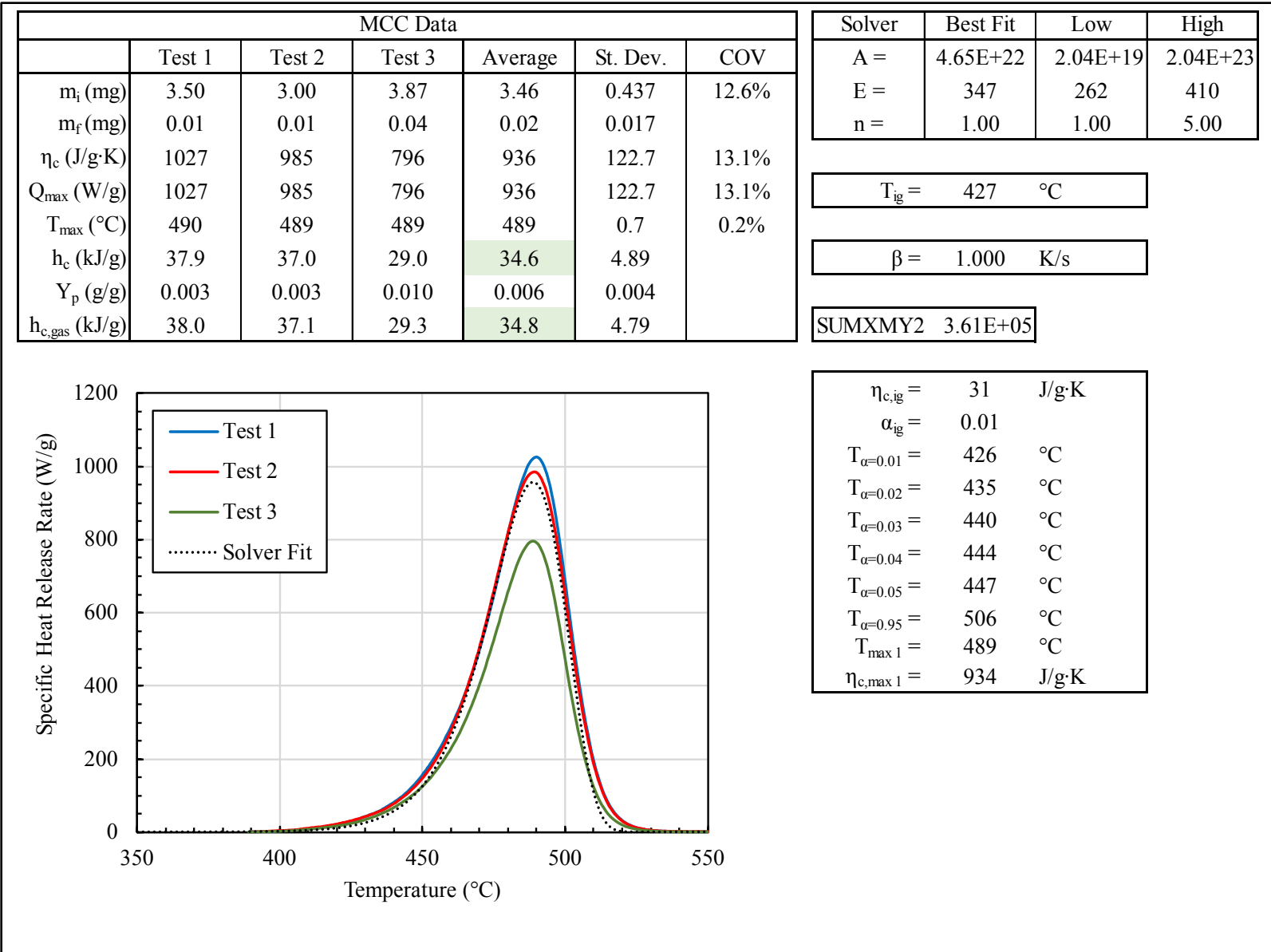


Figure J-11. Ignition temperature analysis results for Grey Motor Coach seat backing

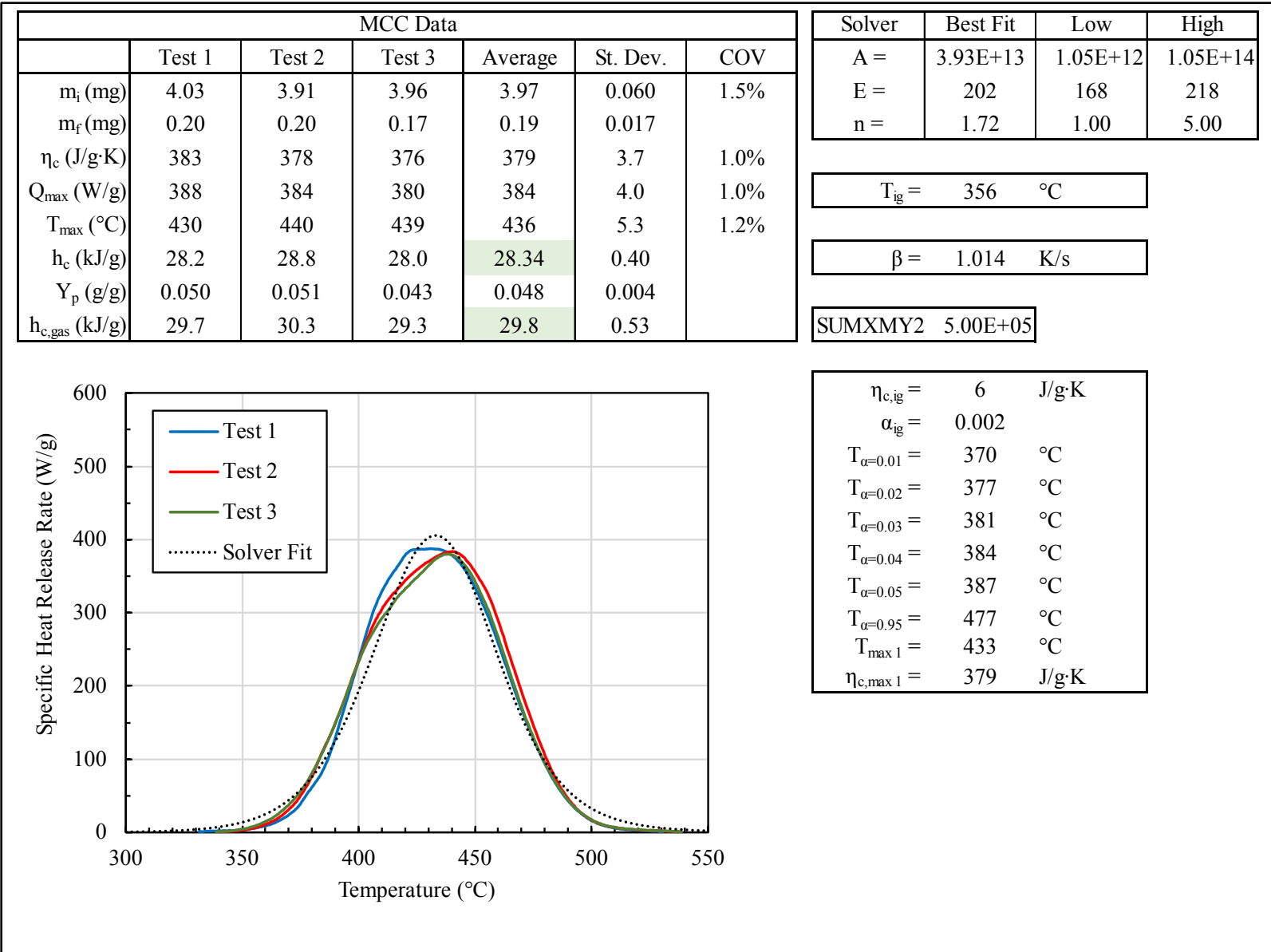


Figure J-12. Ignition temperature analysis results for Motor Coach luggage rack door

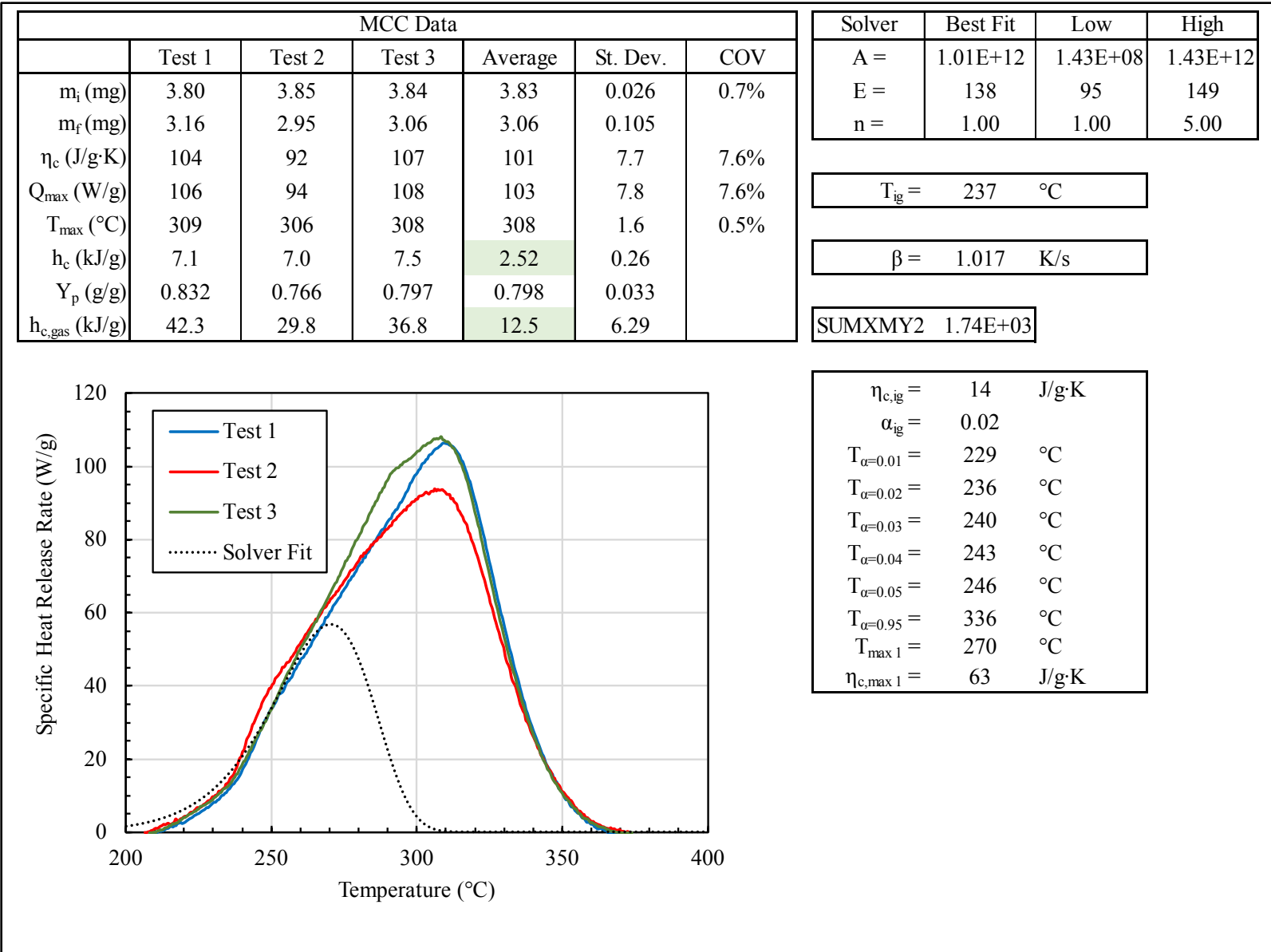


Figure J-13. Ignition temperature analysis results for Coach floor covering

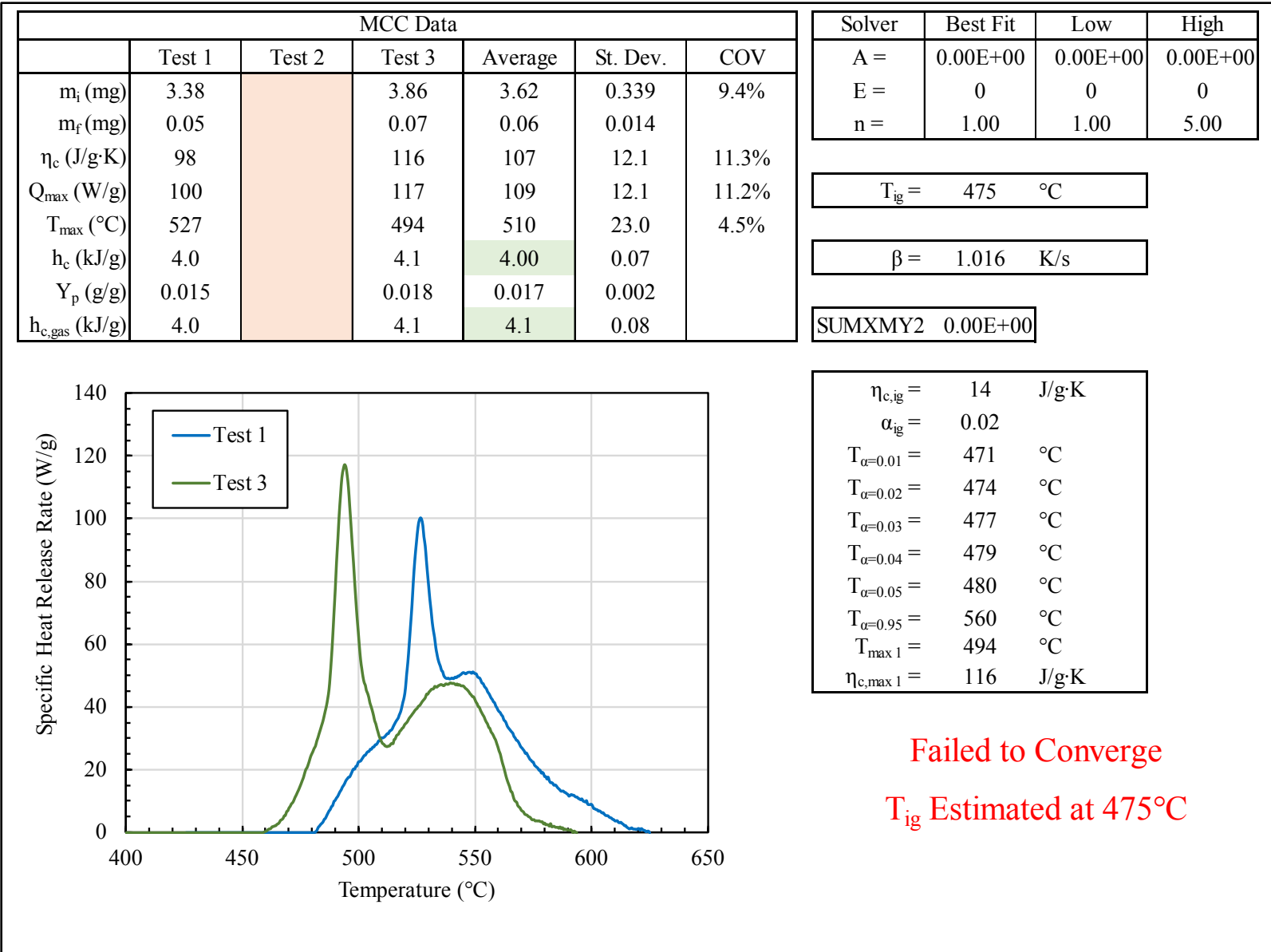


Figure J-14. Ignition temperature analysis results for Motor Coach Headliner

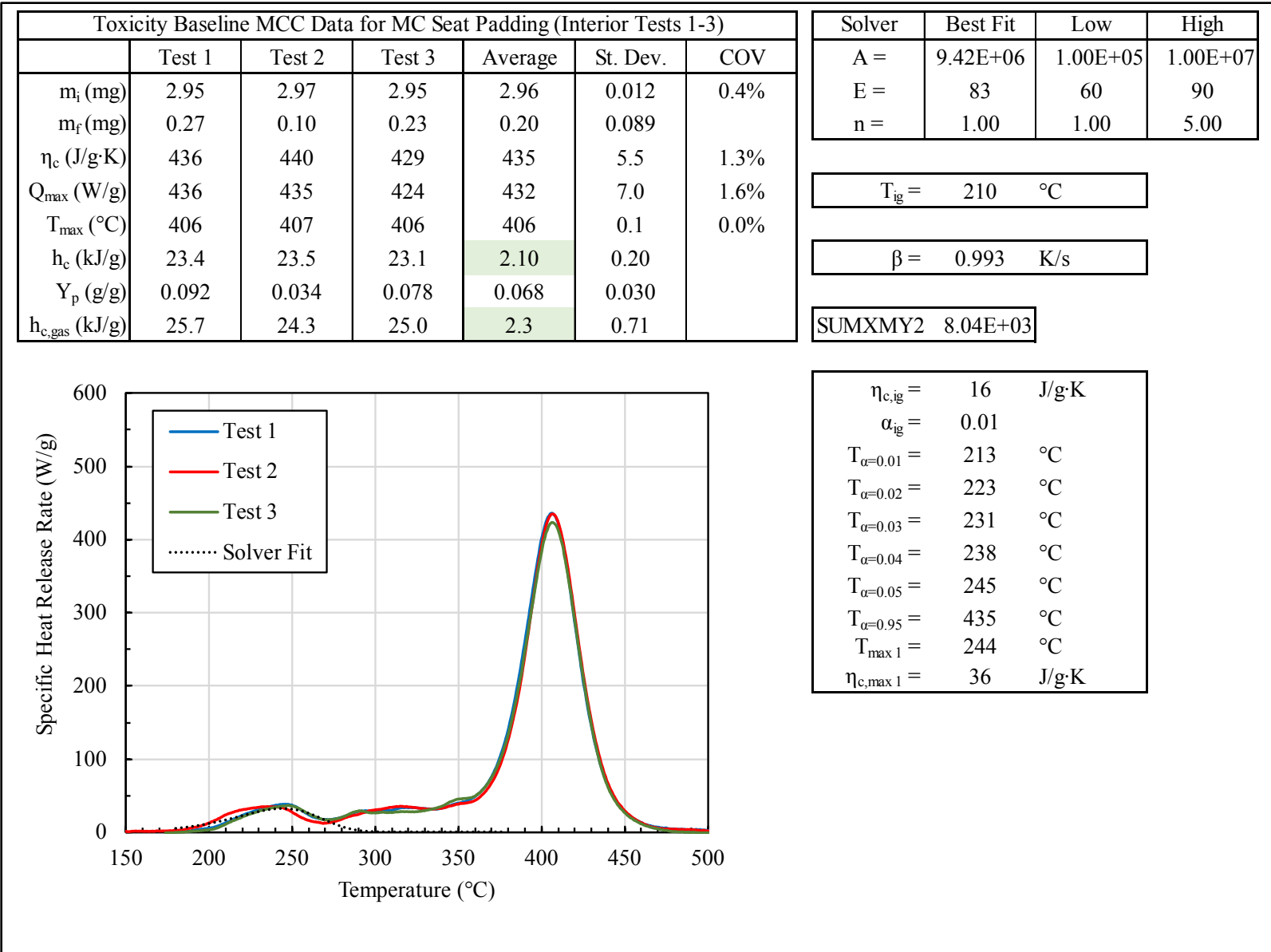


Figure J-15. Ignition temperature analysis results for Motor Coach Blue seat cover padding (interior samples 1-3)

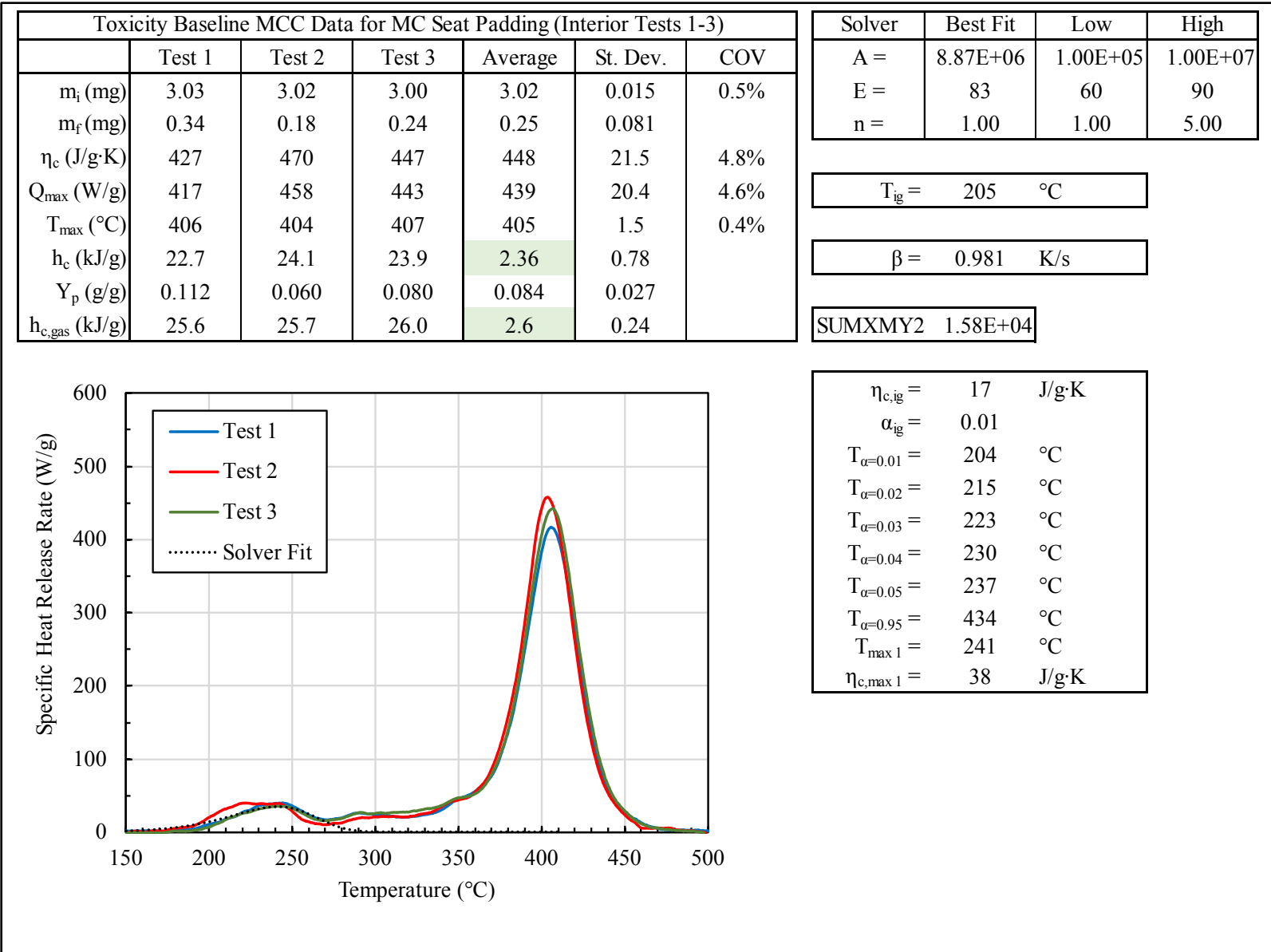


Figure J-16. Ignition temperature analysis results for Motor Coach Blue seat cover padding (interior samples 4-6)

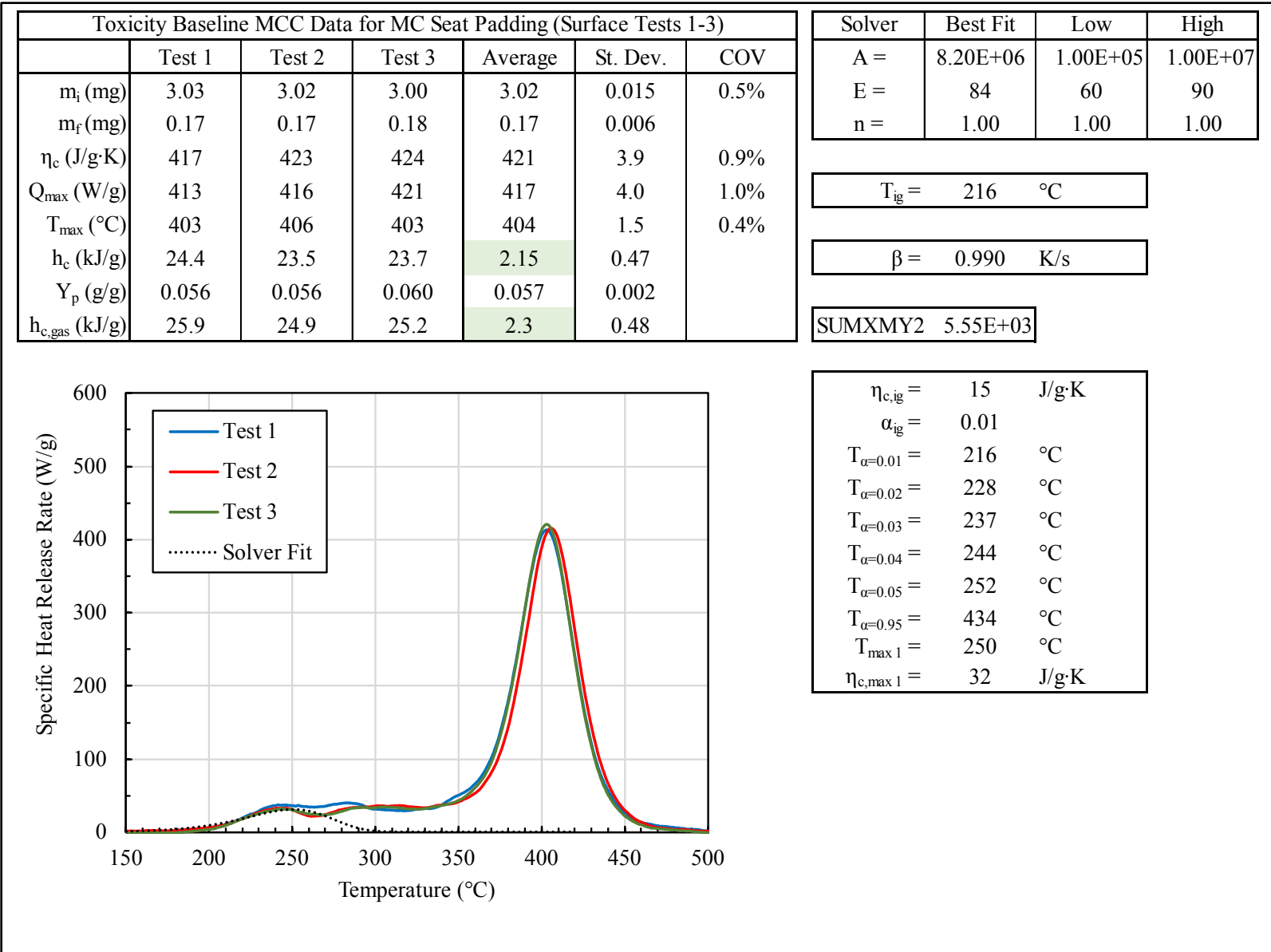


Figure J-17. Ignition temperature analysis results for Motor Coach Blue seat cover padding (surface samples 1-3)

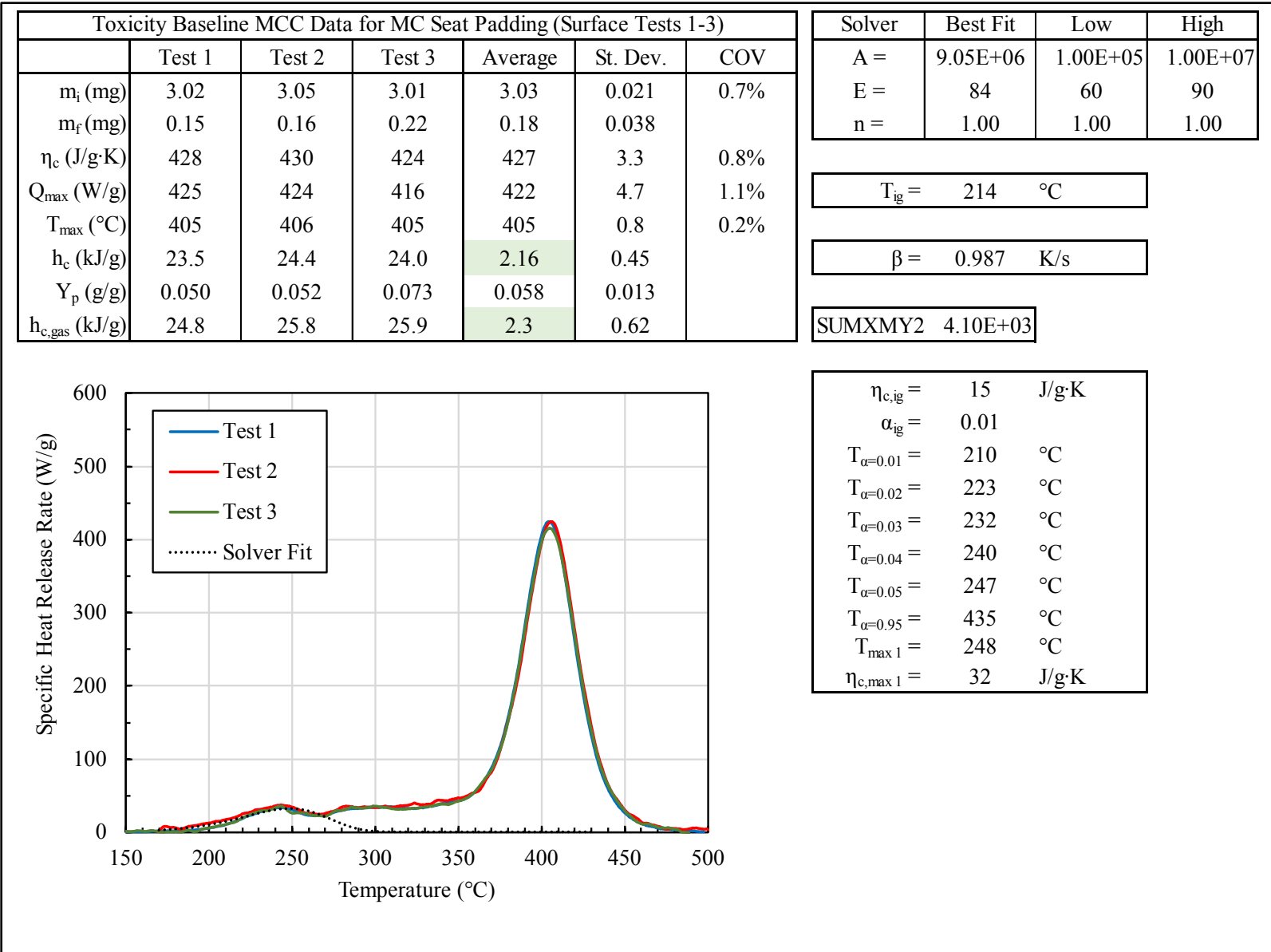


Figure J-18. Ignition temperature analysis results for Motor Coach Blue seat cover padding (surface samples 4-6)

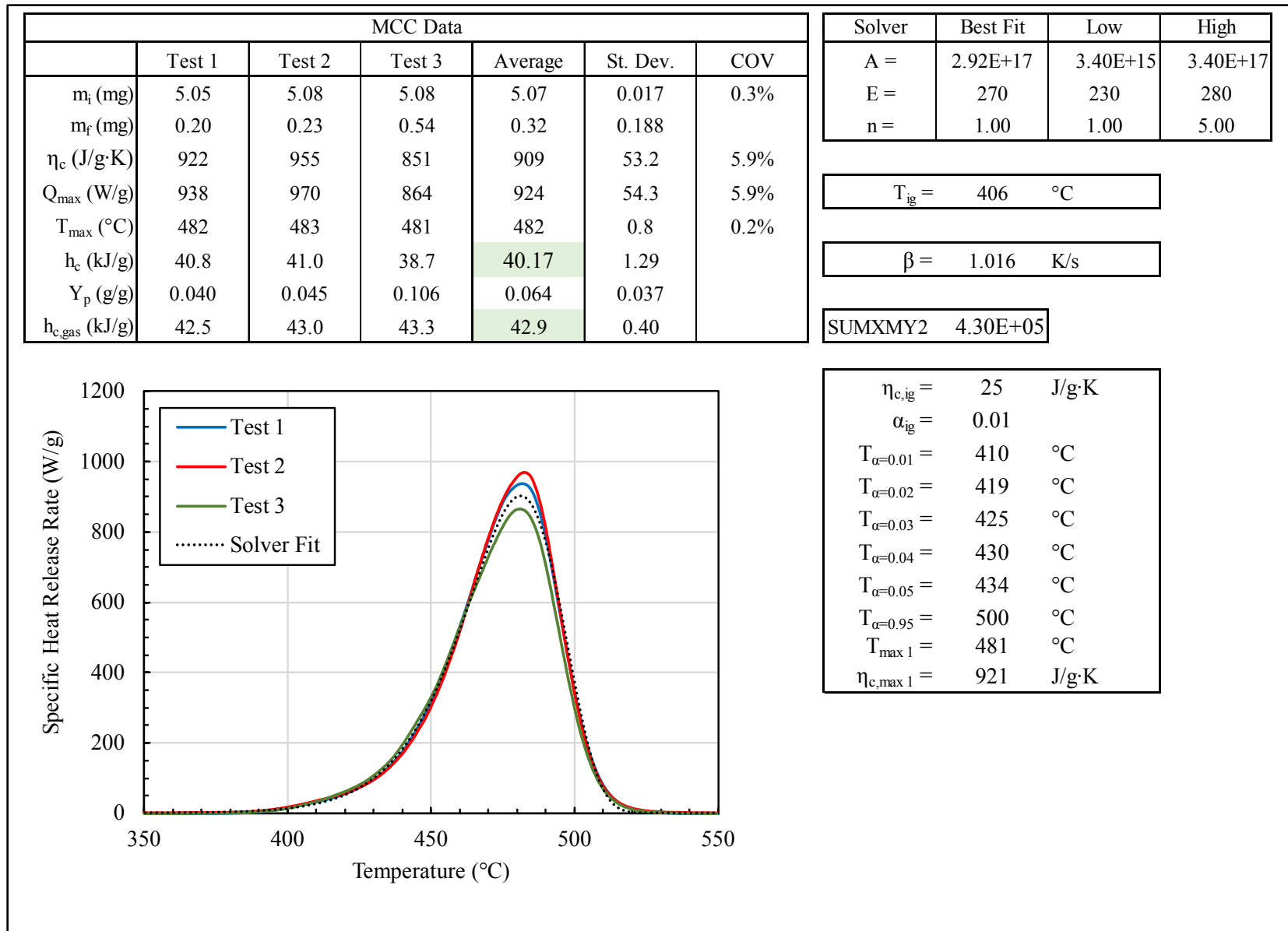


Figure J-19. Ignition temperature analysis results for Ford F250 carpet

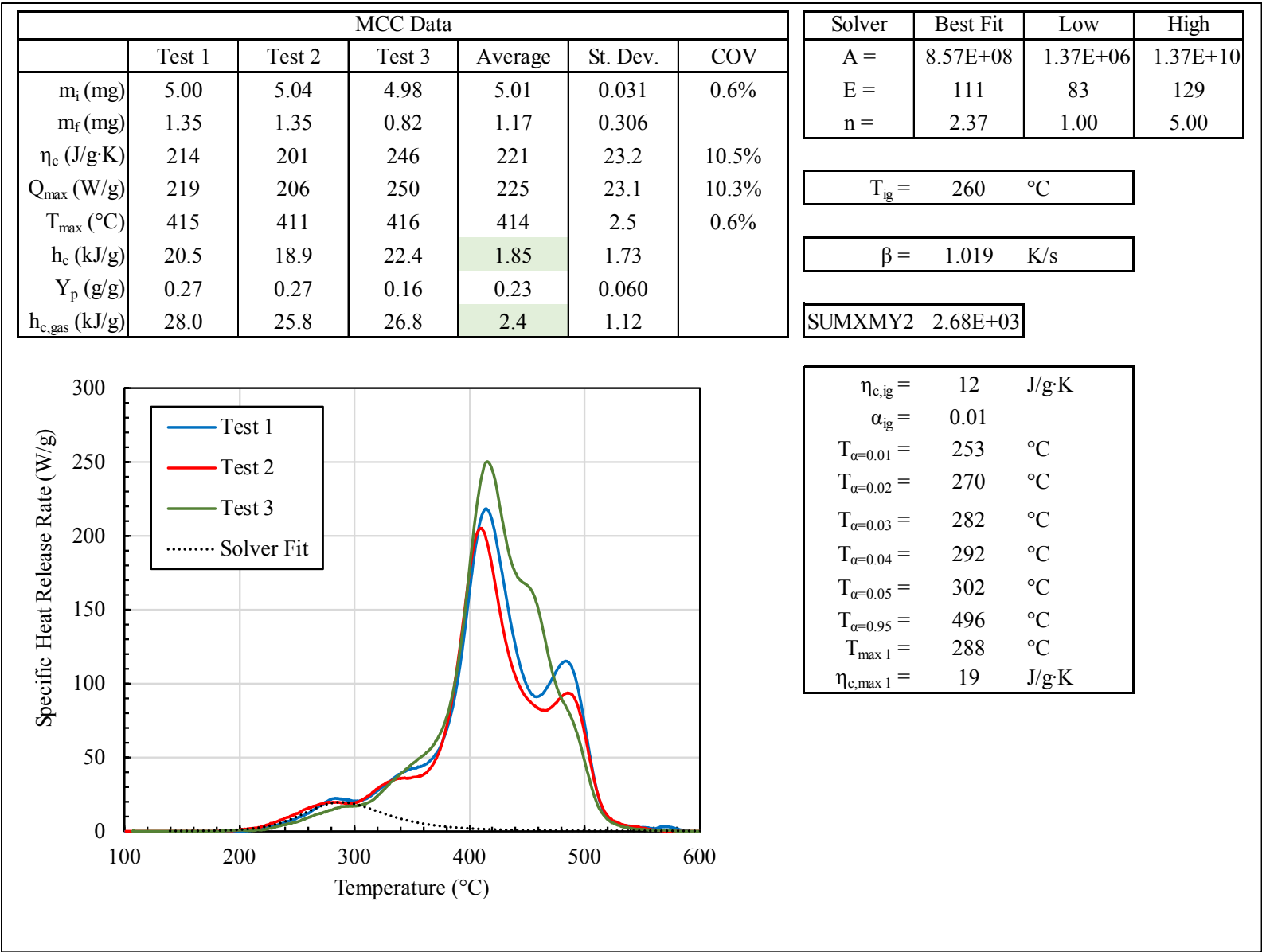


Figure J-20. Ignition temperature analysis results for Mercedes carpet

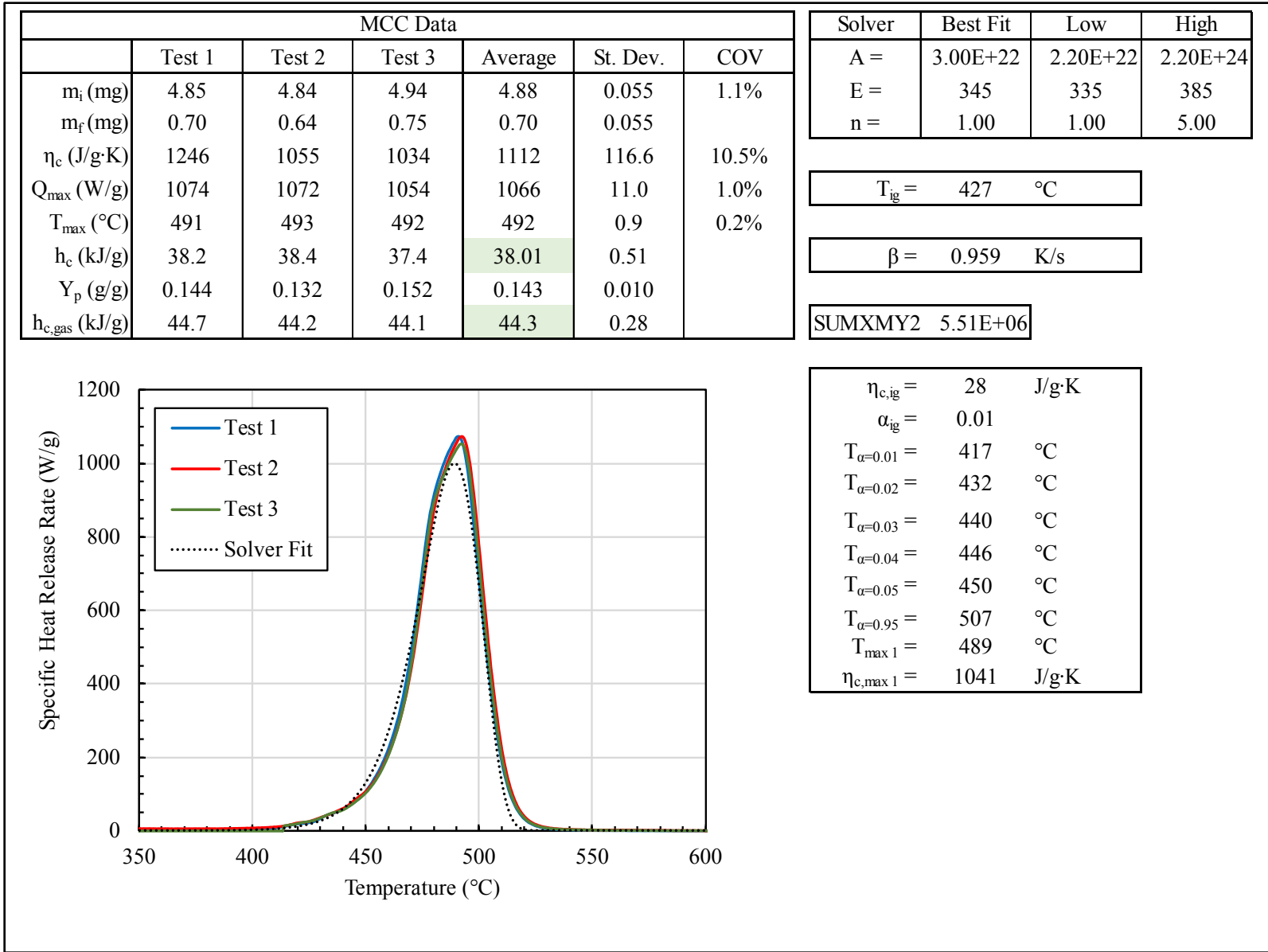


Figure J-21. Ignition temperature analysis results for Ford F250 dashboard

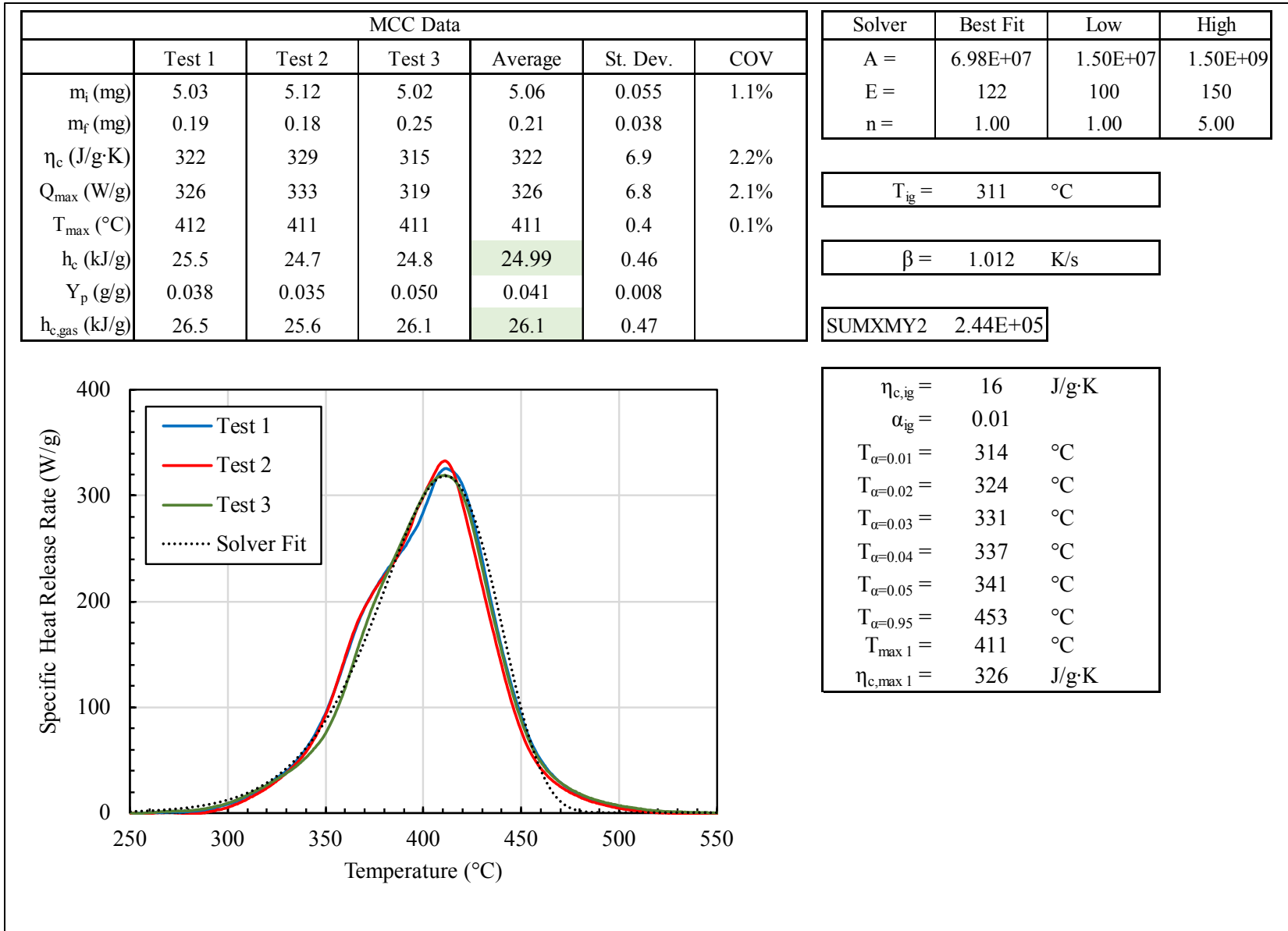


Figure J-22. Ignition temperature analysis results for Mercedes dashboard

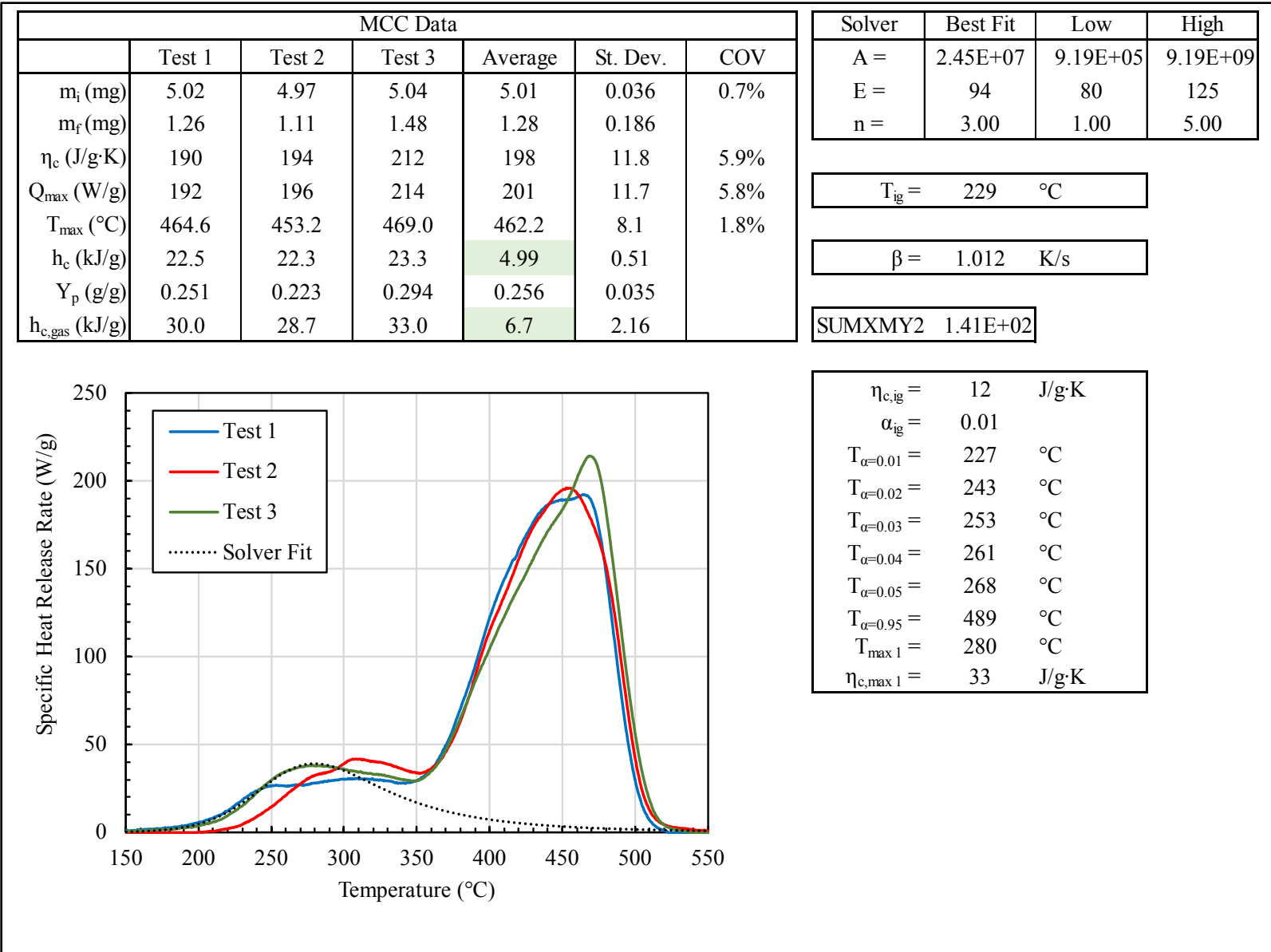


Figure J-23. Ignition temperature analysis results for Camaro Headliner

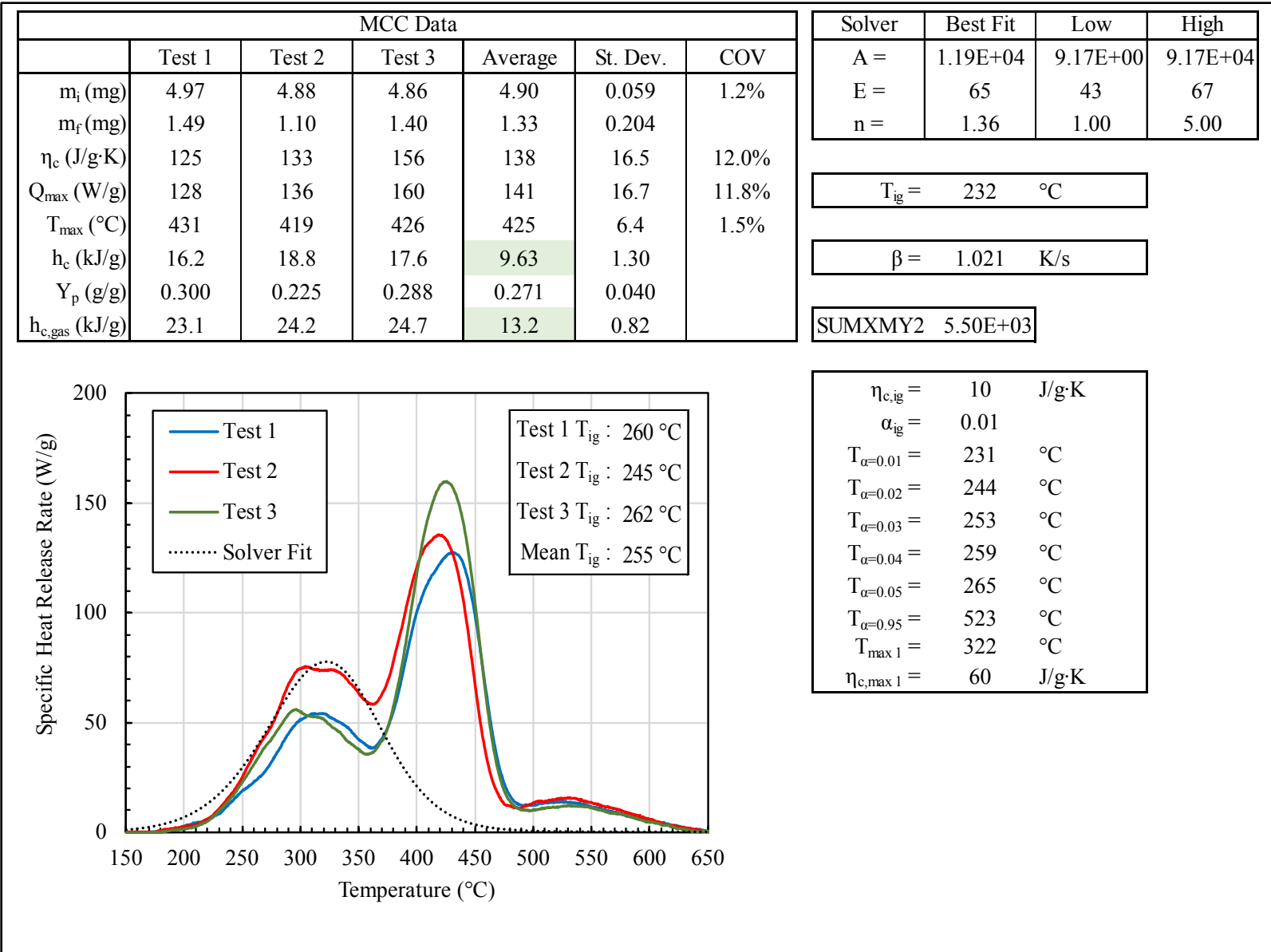


Figure J-24. Ignition temperature analysis results for Ford Headliner

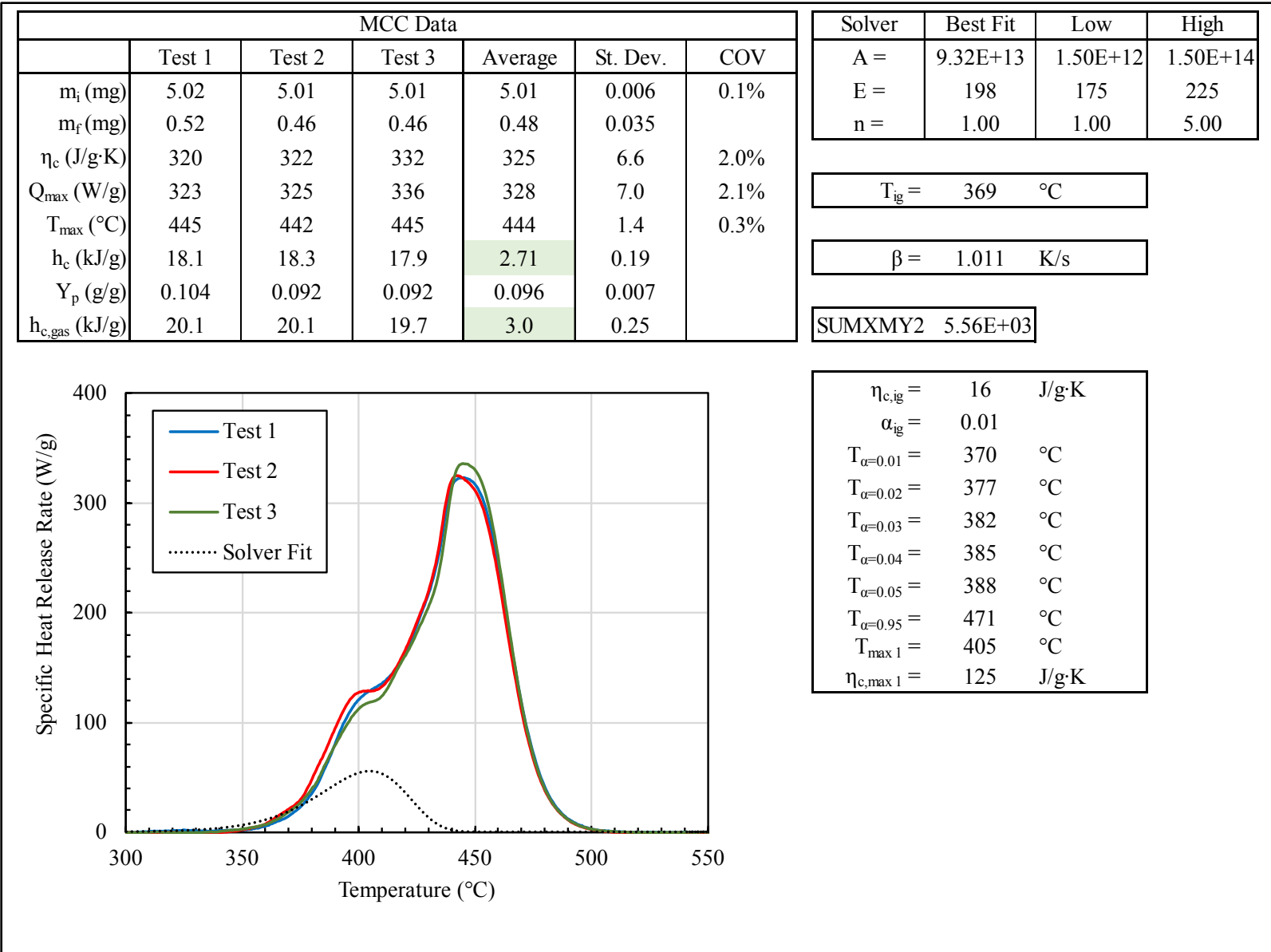


Figure J-25. Ignition temperature analysis results for Camaro seat cover

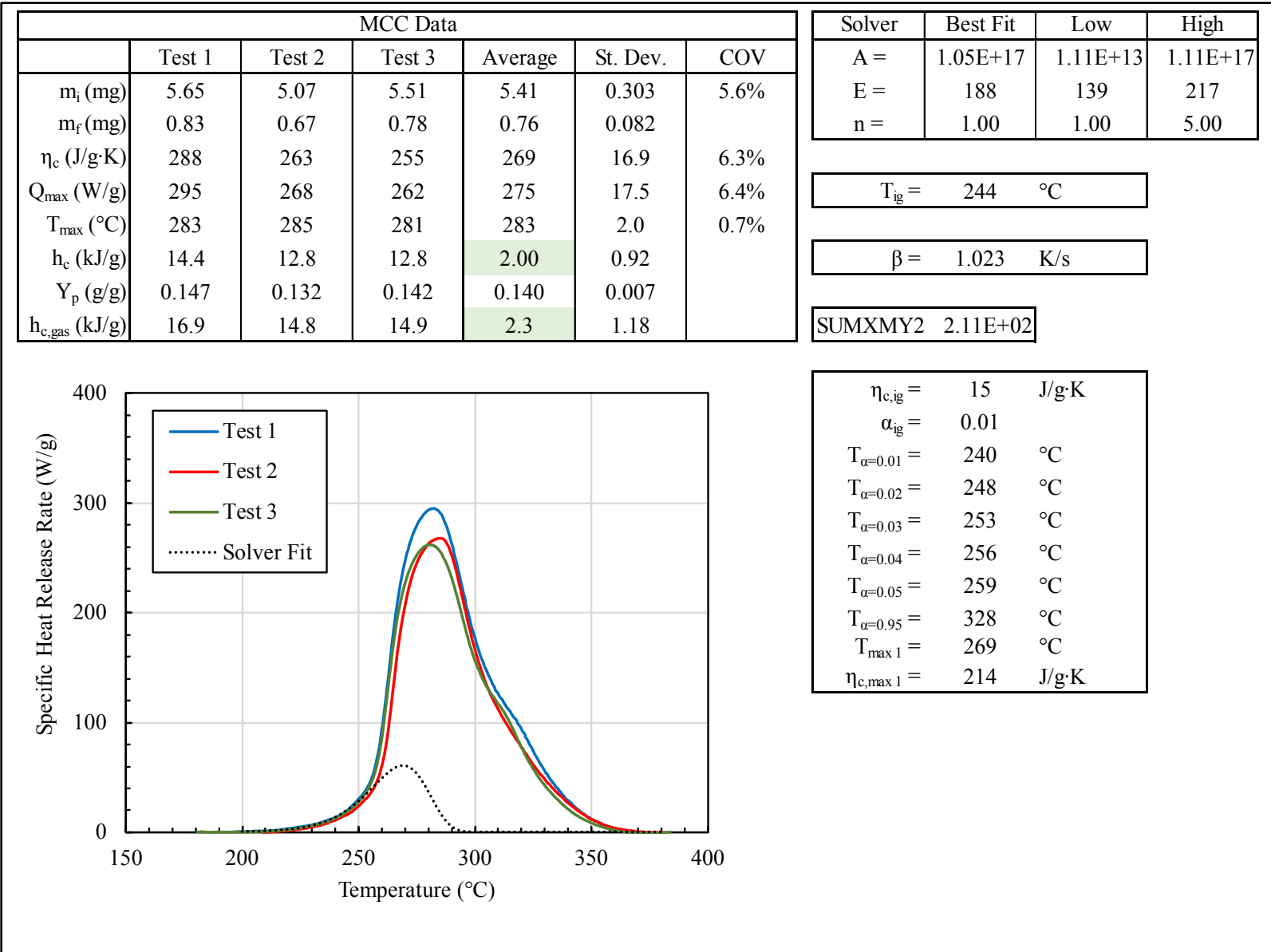


Figure J-26. Ignition temperature analysis results for Mercedes seat cover

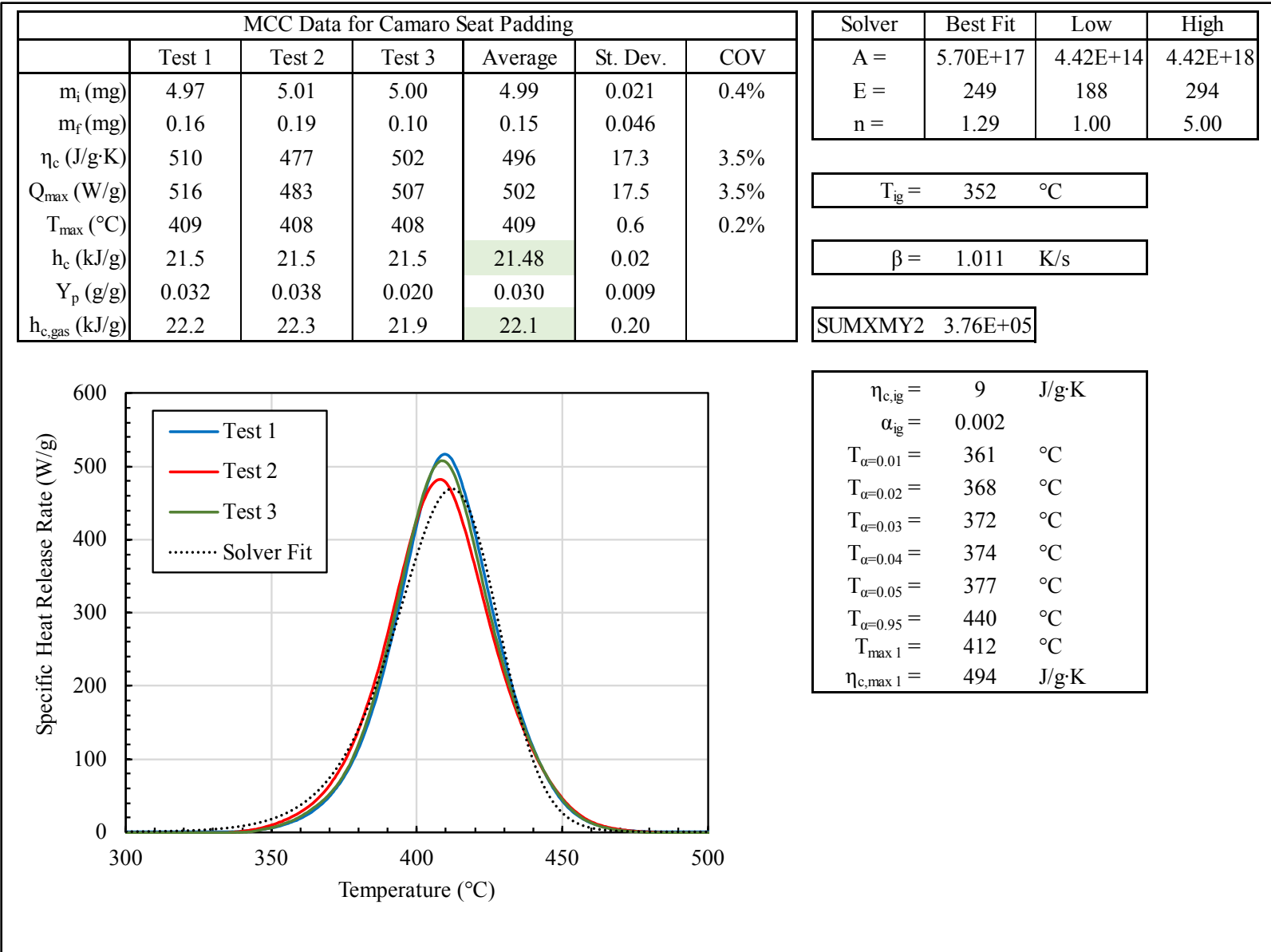


Figure J-27. Ignition temperature analysis results for Camaro seat padding

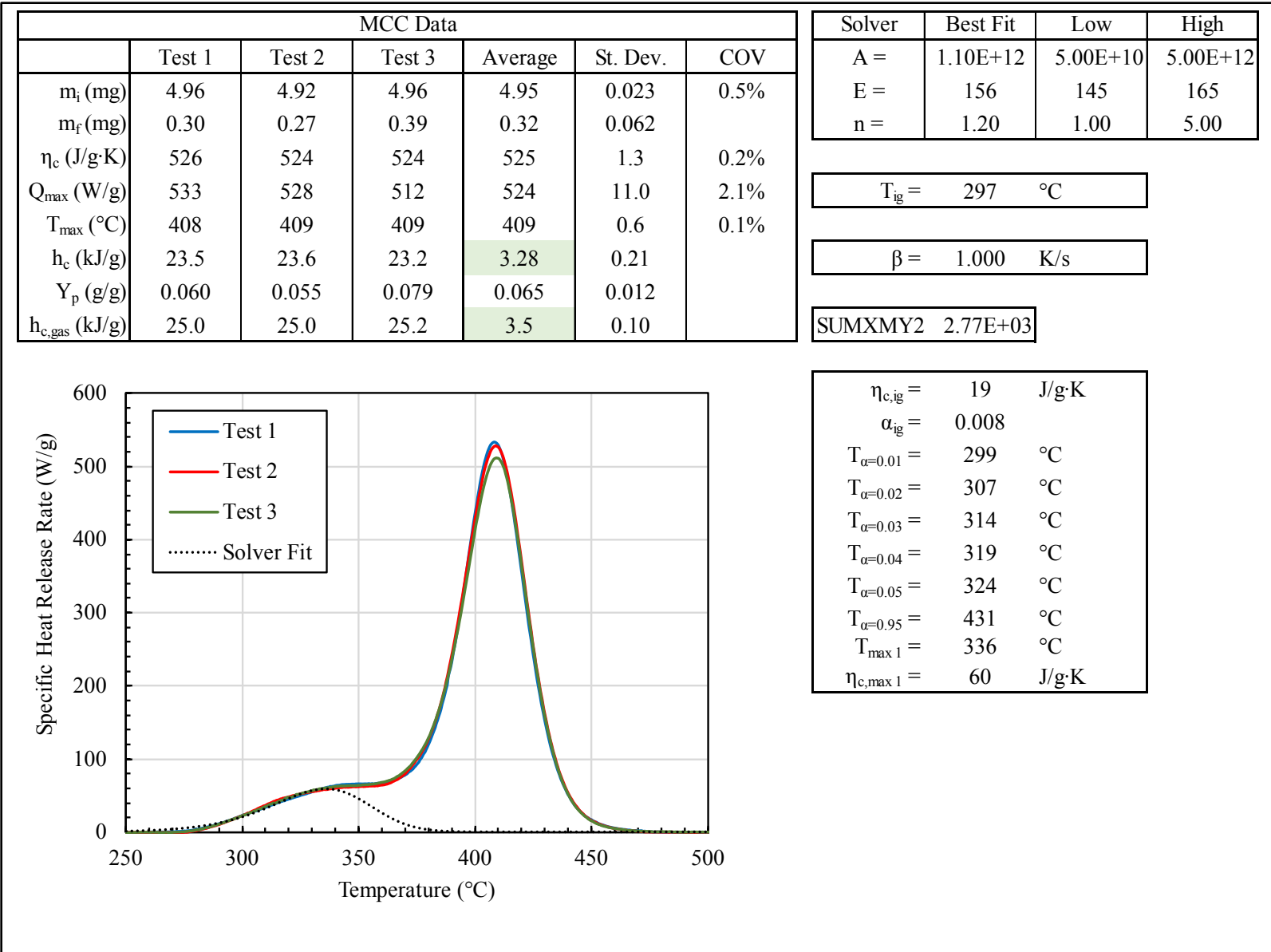


Figure J-28. Ignition temperature analysis results for Mercedes seat padding

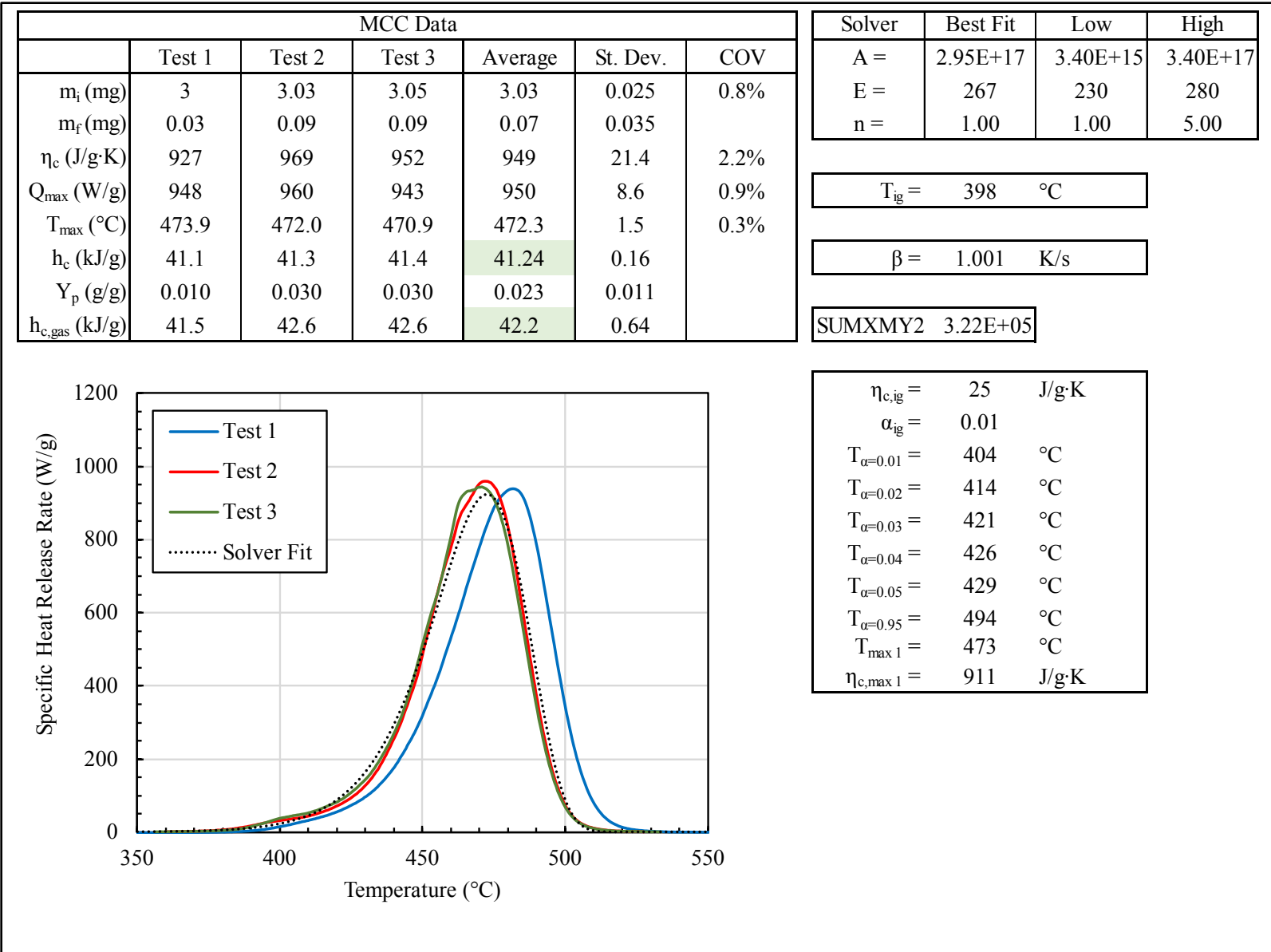


Figure J-29. Ignition temperature analysis results for Ford F250 carpet (surface layer)

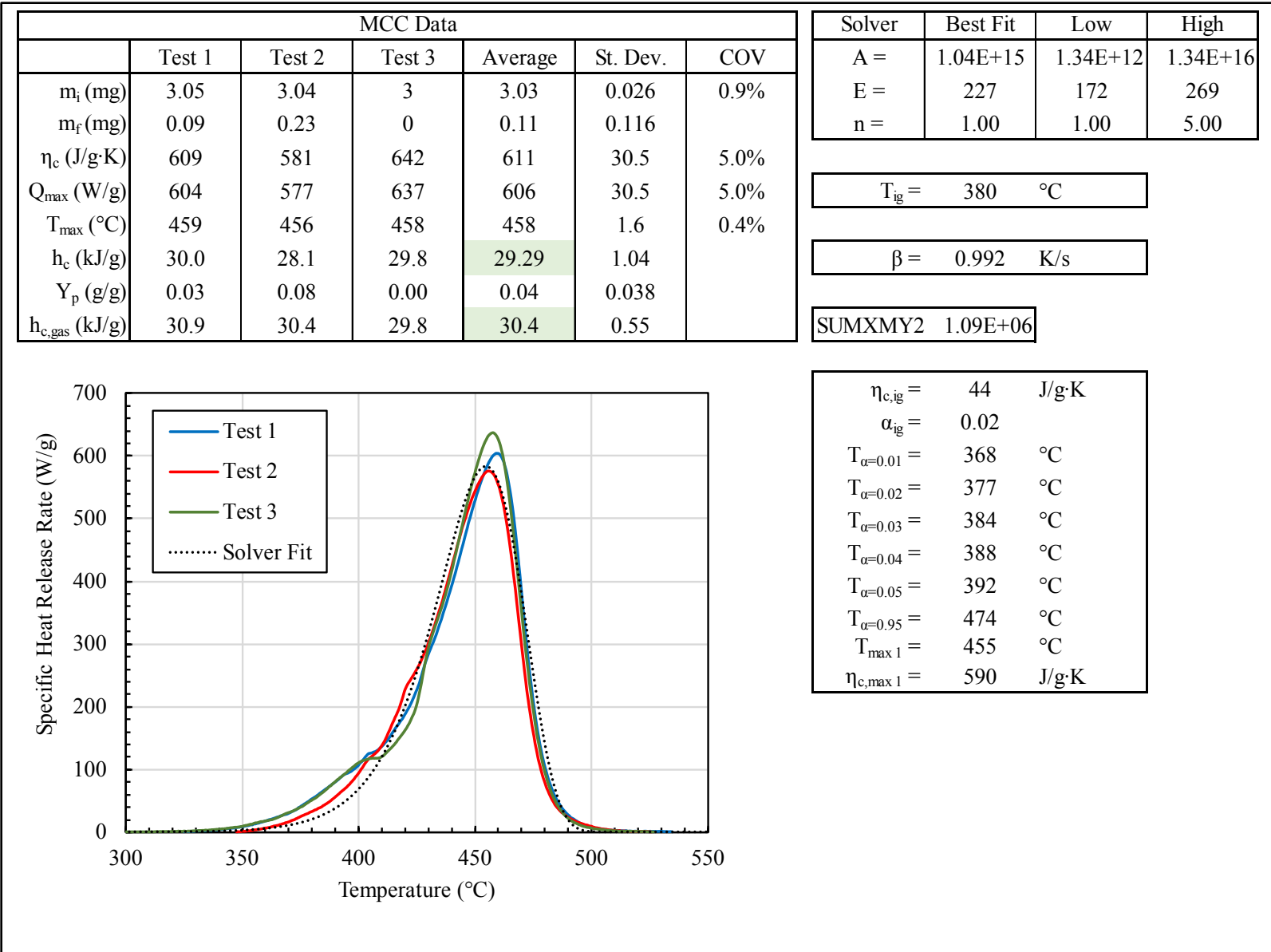


Figure J-30. Ignition temperature analysis results for Mercedes carpet (surface layer)

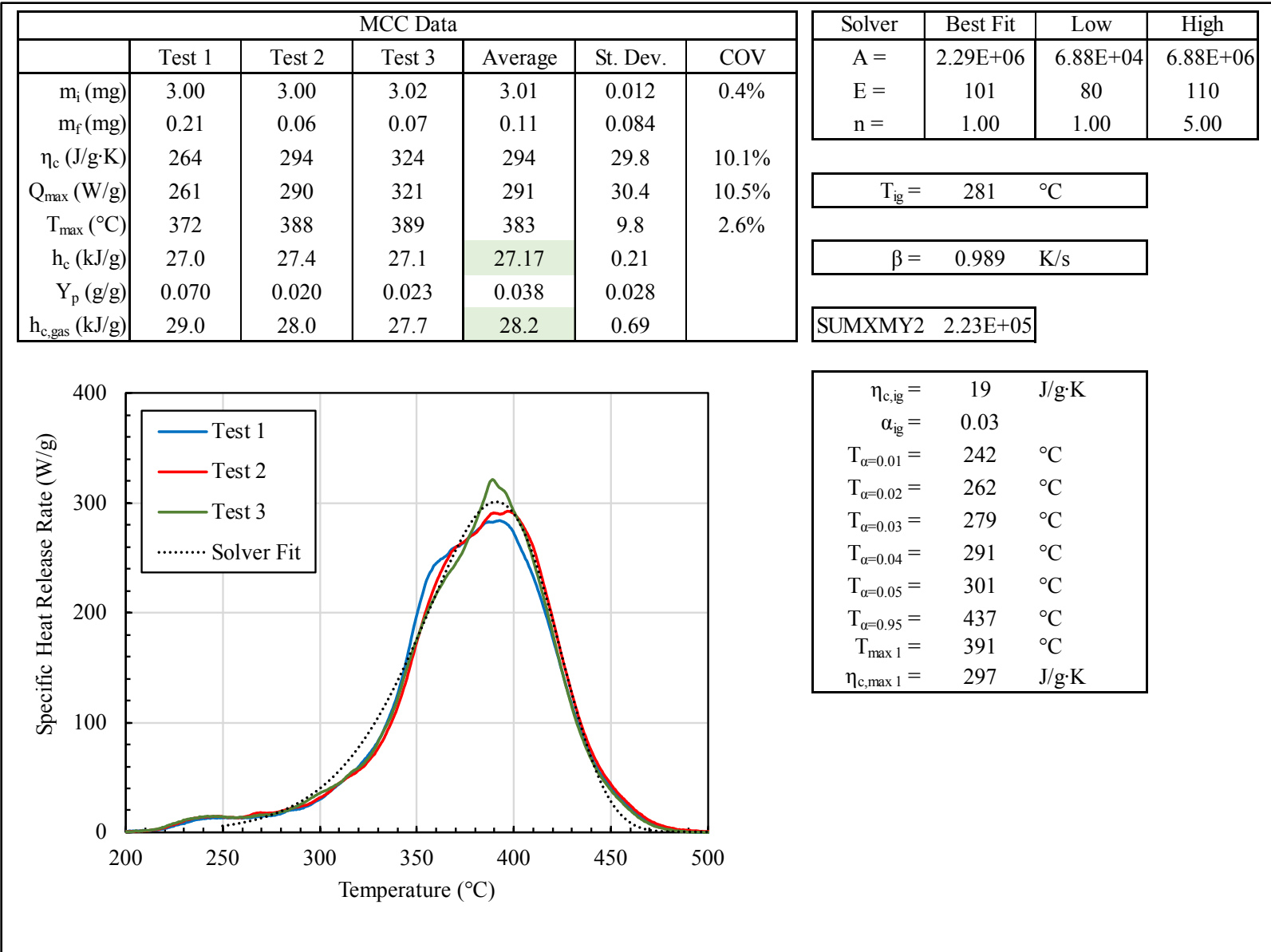


Figure J-31. Ignition temperature analysis results for Mercedes Dashboard (surface layer)

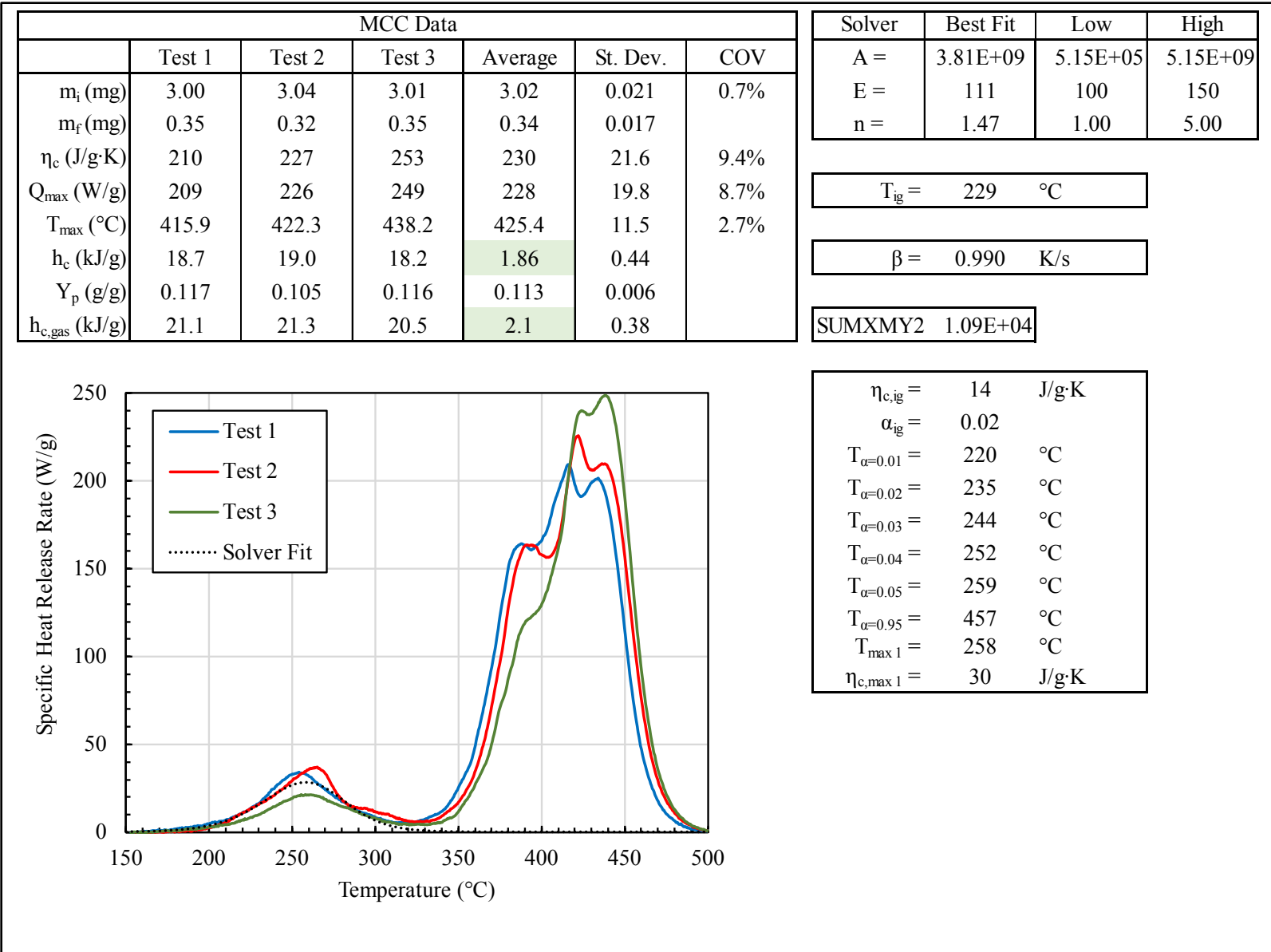


Figure J-32. Ignition temperature analysis results for Camaro Headliner (surface layer)

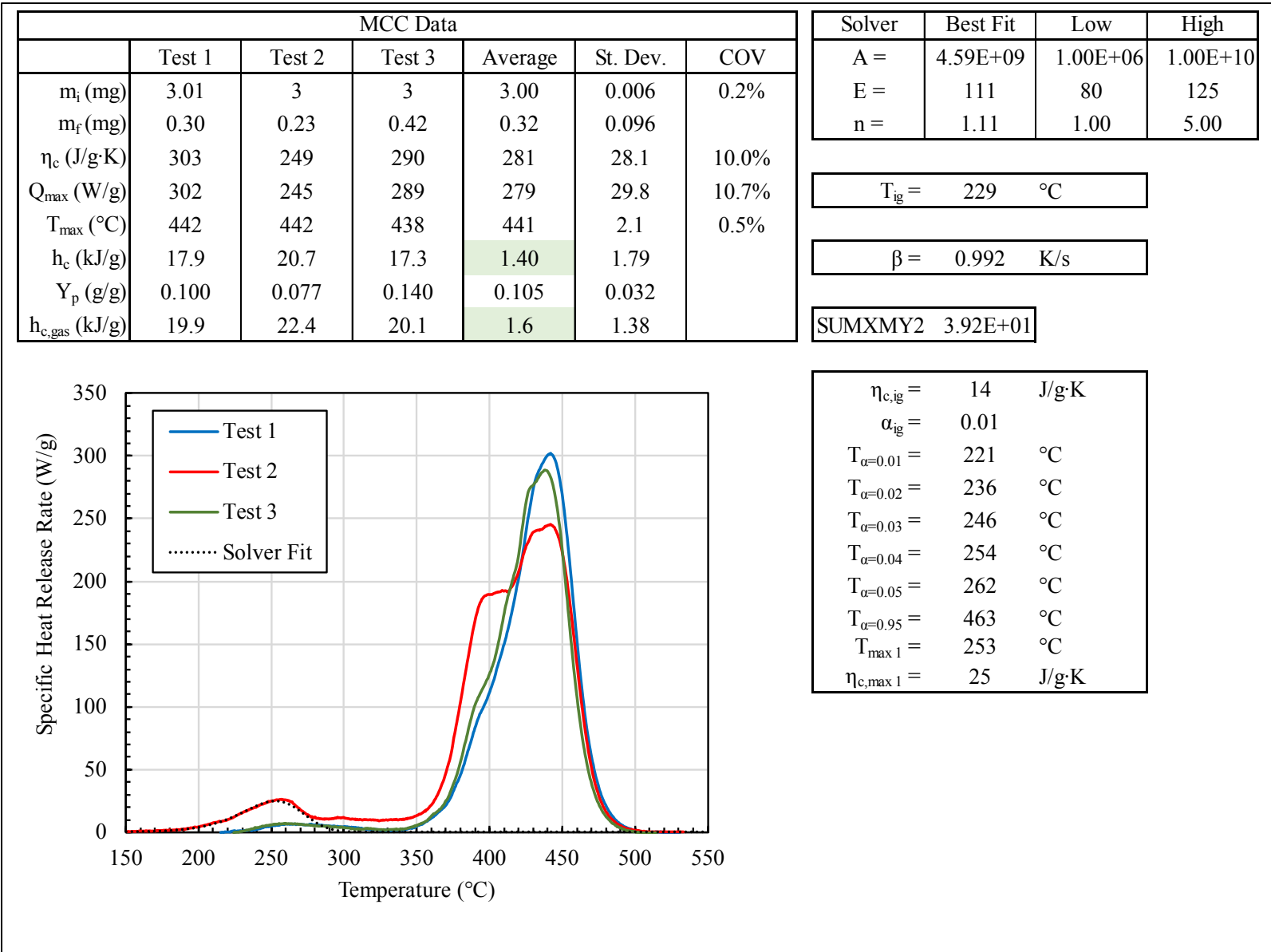


Figure J-33. Ignition temperature analysis results for Ford Headliner (surface layer)

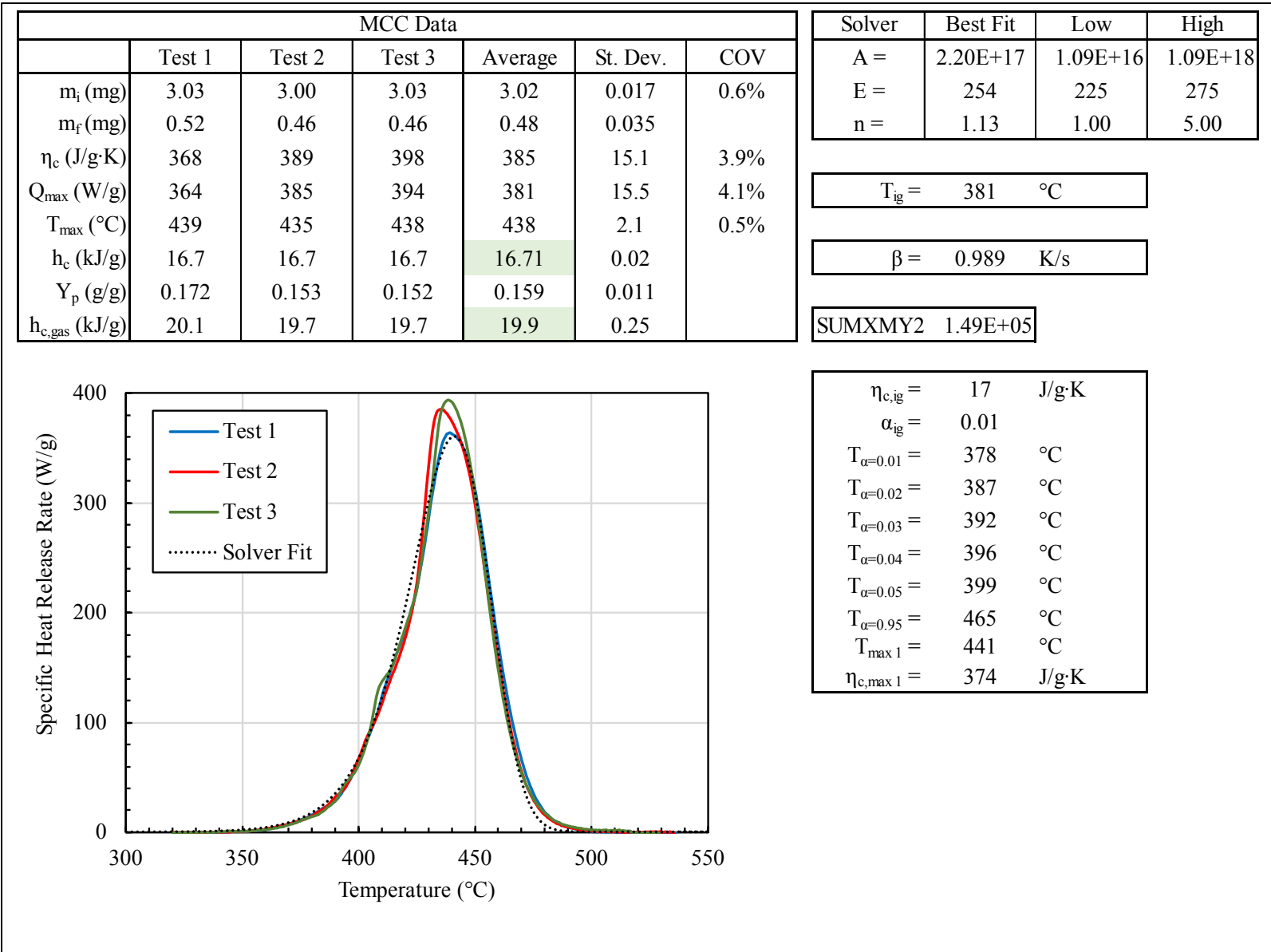


Figure J-34. Ignition temperature analysis results for Camaro seat cover (surface layer)

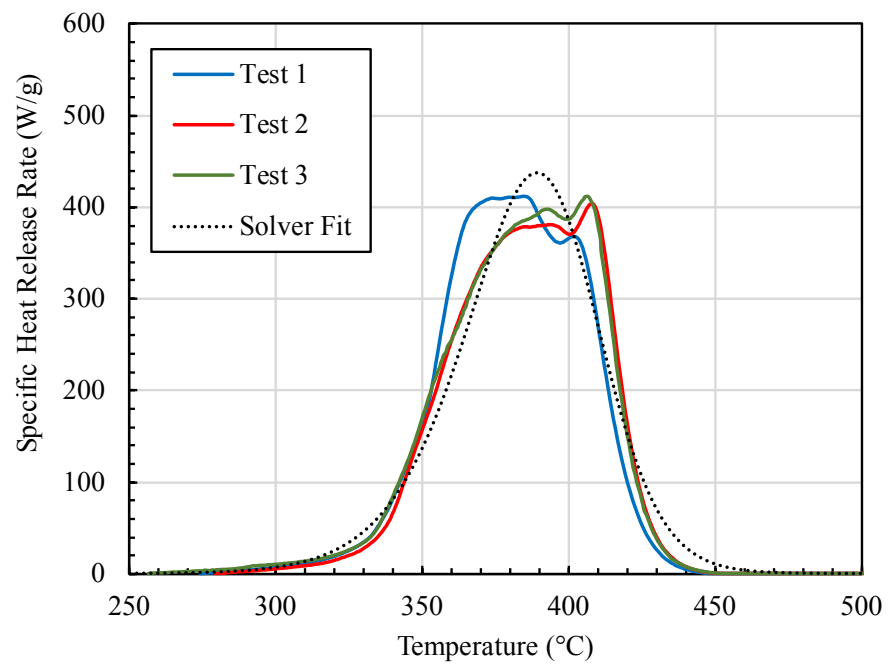
MCC Data						
	Test 1	Test 2	Test 3	Average	St. Dev.	COV
m_i (mg)	5.12	4.81	5.86	5.26	0.539	10.2%
m_f (mg)	0.08	0.05	0.07	0.07	0.015	
η_c (J/g·K)	406	400	407	404	3.9	1.0%
Q_{max} (W/g)	412	404	412	409	4.5	1.1%
T_{max} (°C)	385	408	407	400	13.1	3.3%
h_c (kJ/g)	25.8	25.4	26.2	25.82	0.38	
Y_p (g/g)	0.016	0.010	0.012	0.013	0.003	
$h_{c,gas}$ (kJ/g)	26.3	25.7	26.5	26.2	0.41	

Solver	Best Fit	Low	High
A =	2.00E+13	2.00E+11	2.00E+13
E =	185	150	200
n =	1.38	1.0	5.0

$T_{ig} = 316 \text{ } ^\circ\text{C}$

$\beta = 1.011 \text{ K/s}$

SUMXMY2 1.39E+06



$\eta_{c,ig}$	=	14	J/g·K
α_{ig}	=	0.01	
$T_{\alpha=0.01}$	=	315	°C
$T_{\alpha=0.02}$	=	328	°C
$T_{\alpha=0.03}$	=	335	°C
$T_{\alpha=0.04}$	=	339	°C
$T_{\alpha=0.05}$	=	342	°C
$T_{\alpha=0.95}$	=	417	°C
$T_{max 1}$	=	389	°C
$\eta_{c,max 1}$	=	390	J/g·K

Figure J-35. Ignition temperature analysis results for Acrylate (thin material)

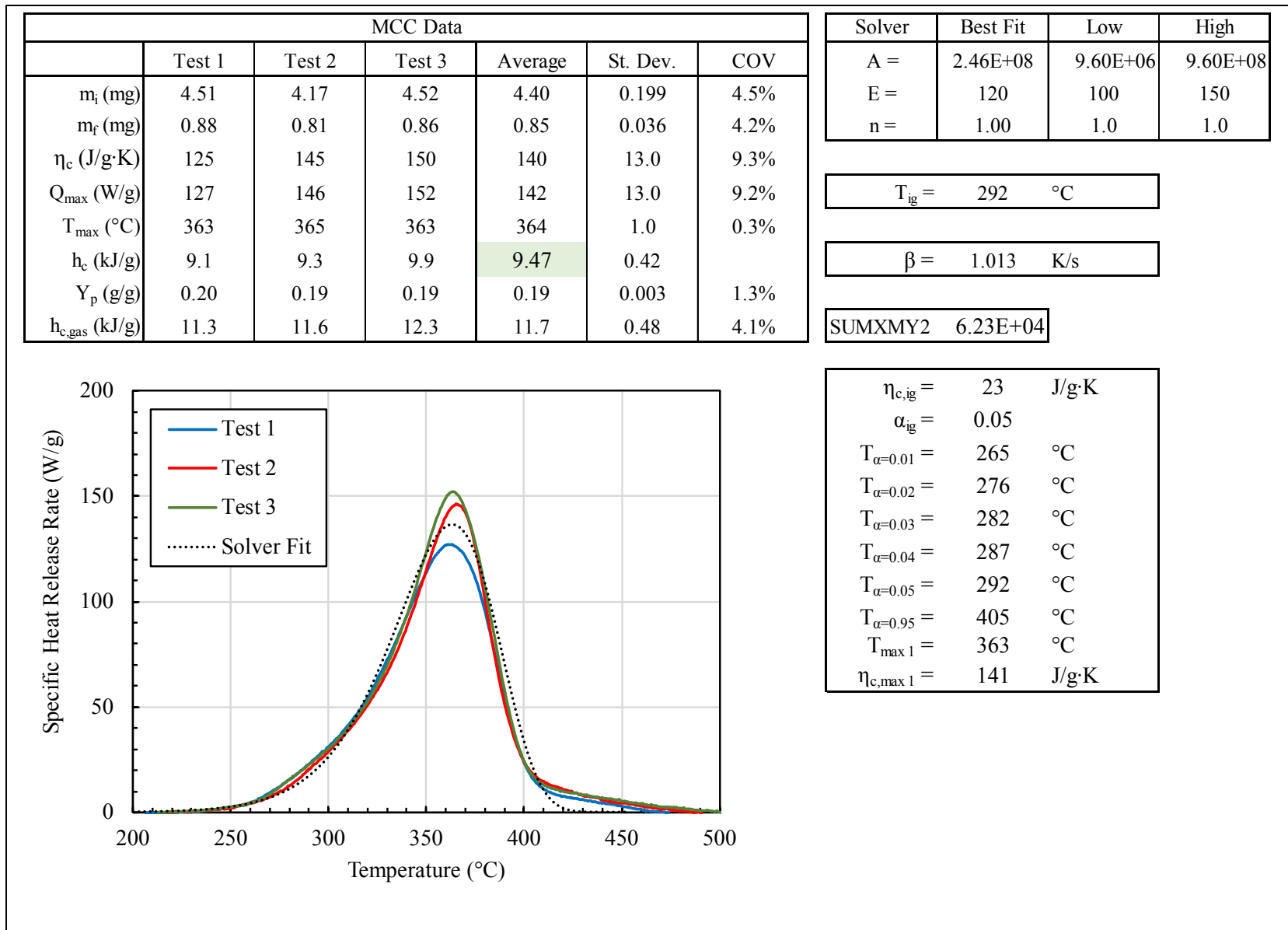


Figure J-36. Ignition temperature analysis results for corrugated cardboard (thin material)

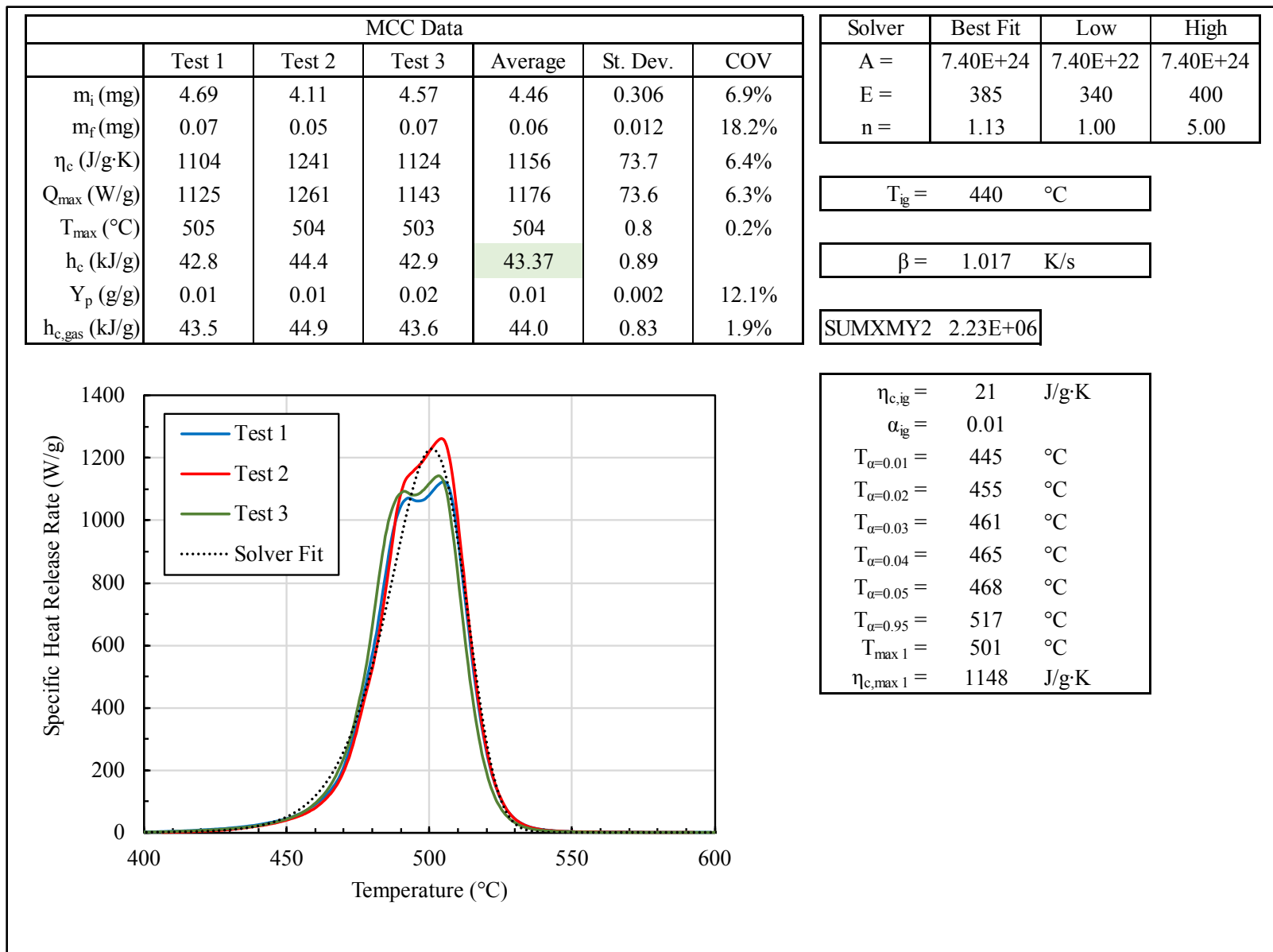


Figure J-37. Ignition temperature analysis results for HDPE (thin material)

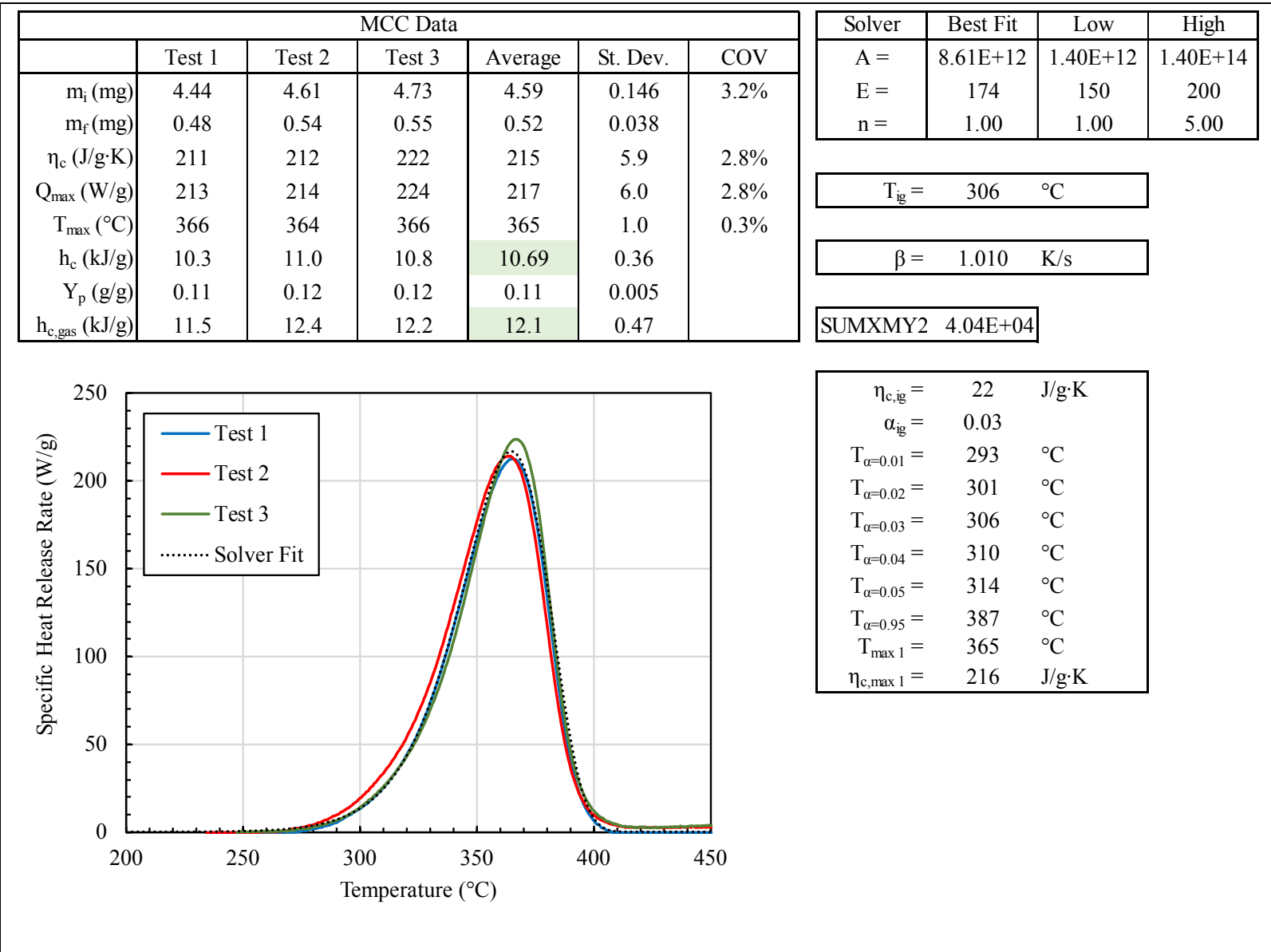


Figure J-38. Ignition temperature analysis results for Manila Folder Cardboard (thin material)

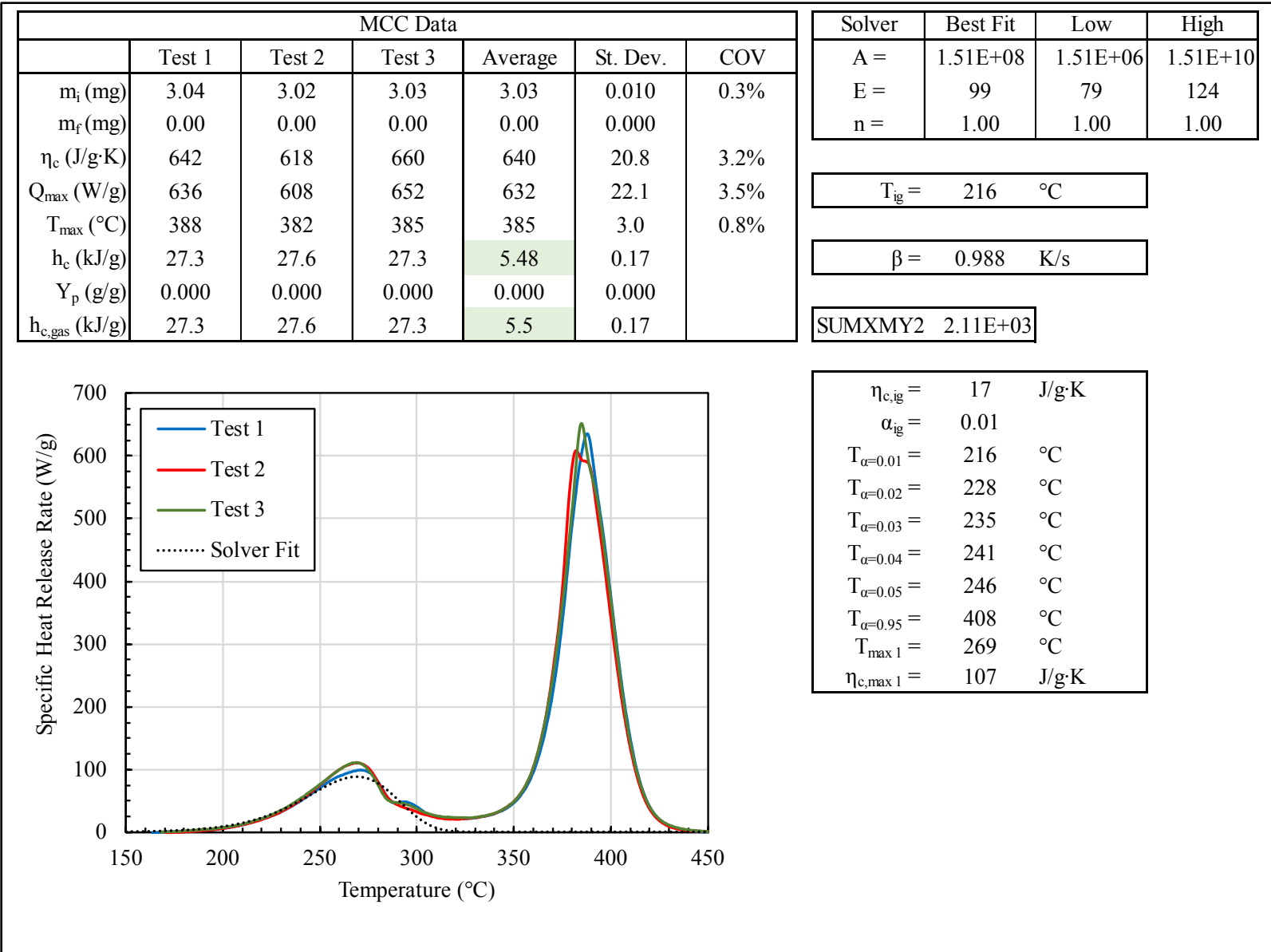


Figure J-39. Ignition temperature analysis results for Water Mist Test Simulated Furniture Foam (SF)

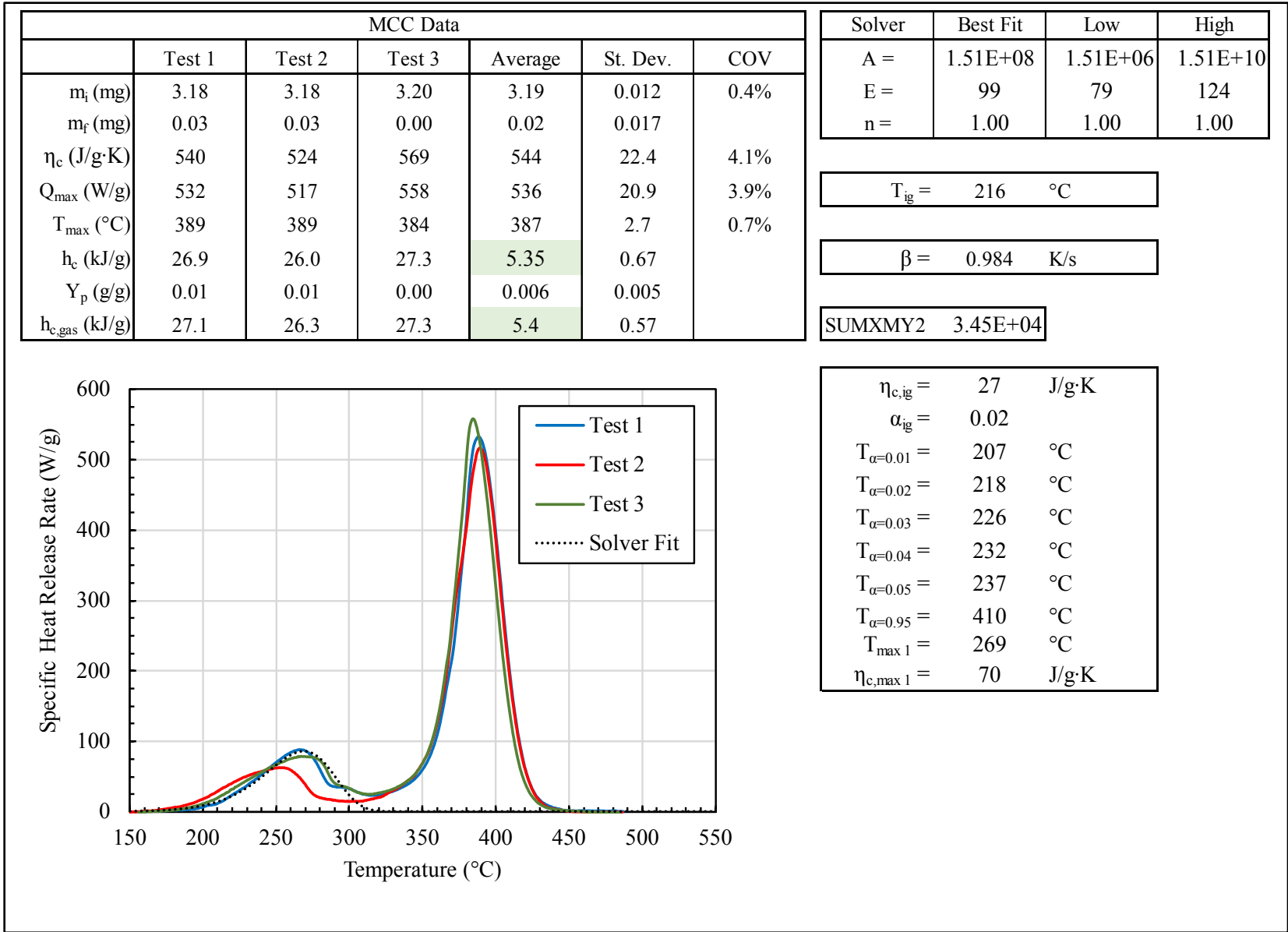


Figure J-40. Ignition temperature analysis results for Water Mist Test Simulated Mattress Foam (SM)

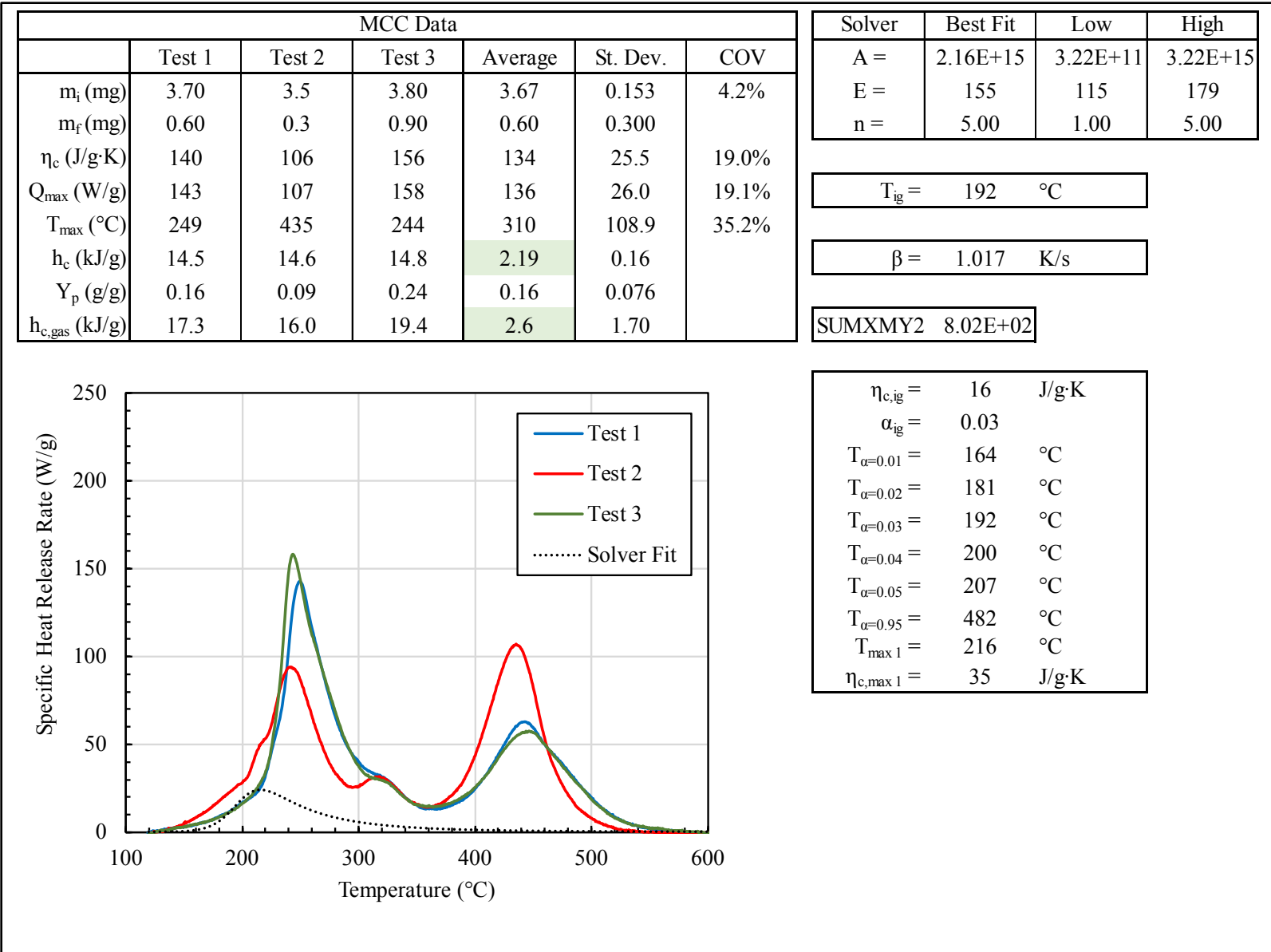


Figure J-41. Ignition temperature analysis results for Blue Bird School Bus seat cover (Cryo-milled)

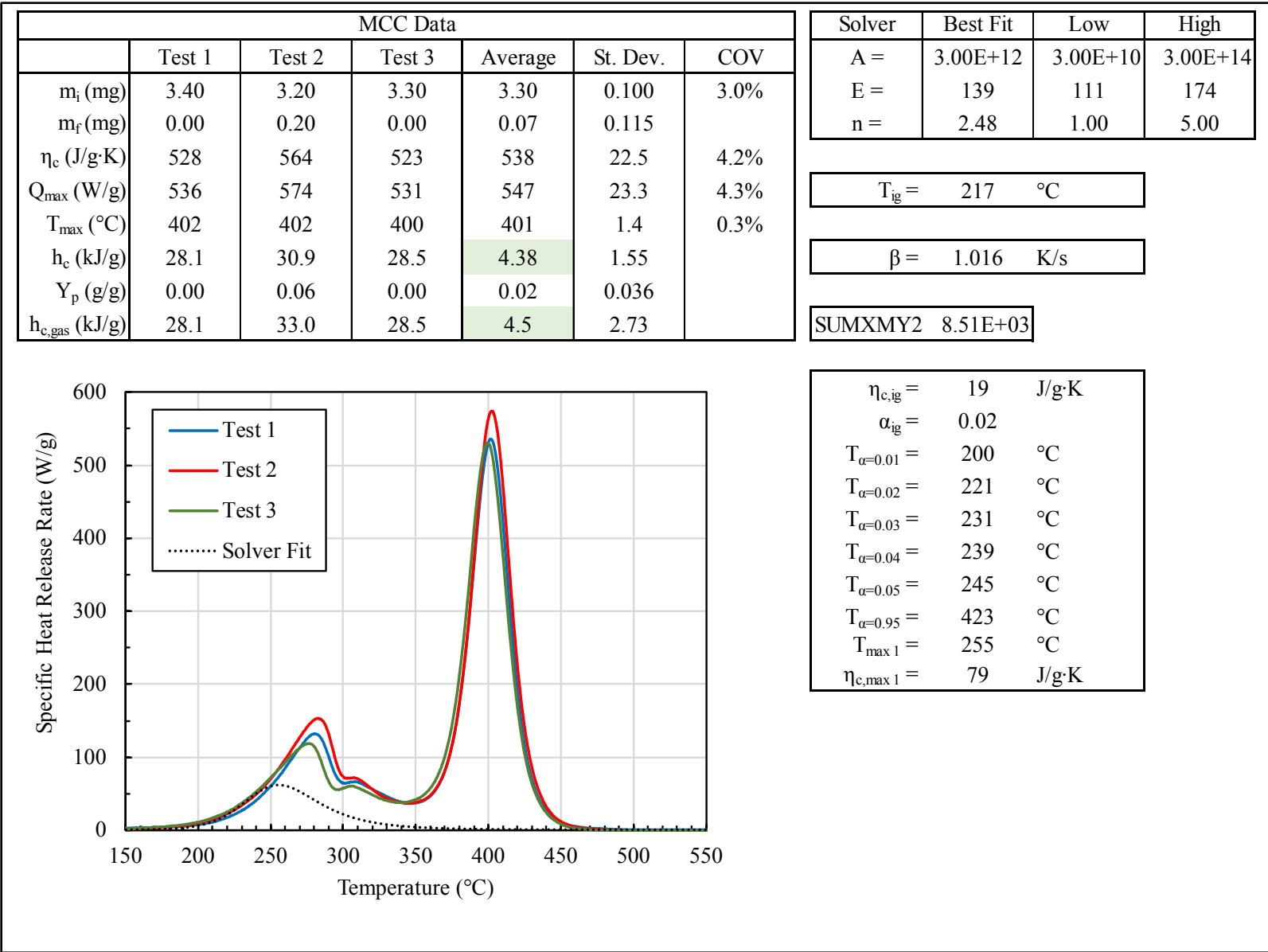


Figure J-42. Ignition temperature analysis results for Blue Bird School Bus seat padding (Cryo-milled)

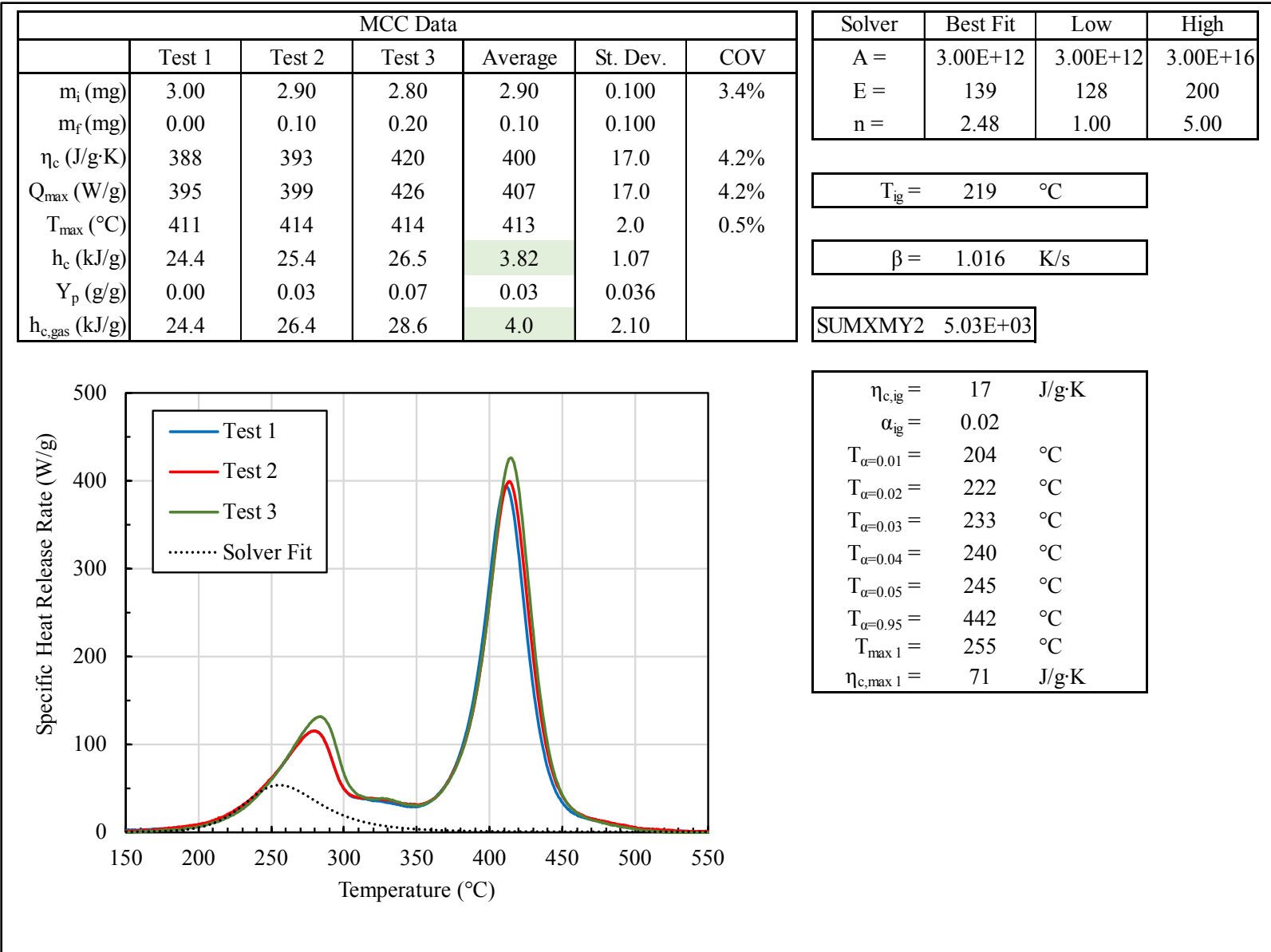


Figure J-43. Ignition temperature analysis results for Blue Bird School Bus seat padding (back side)

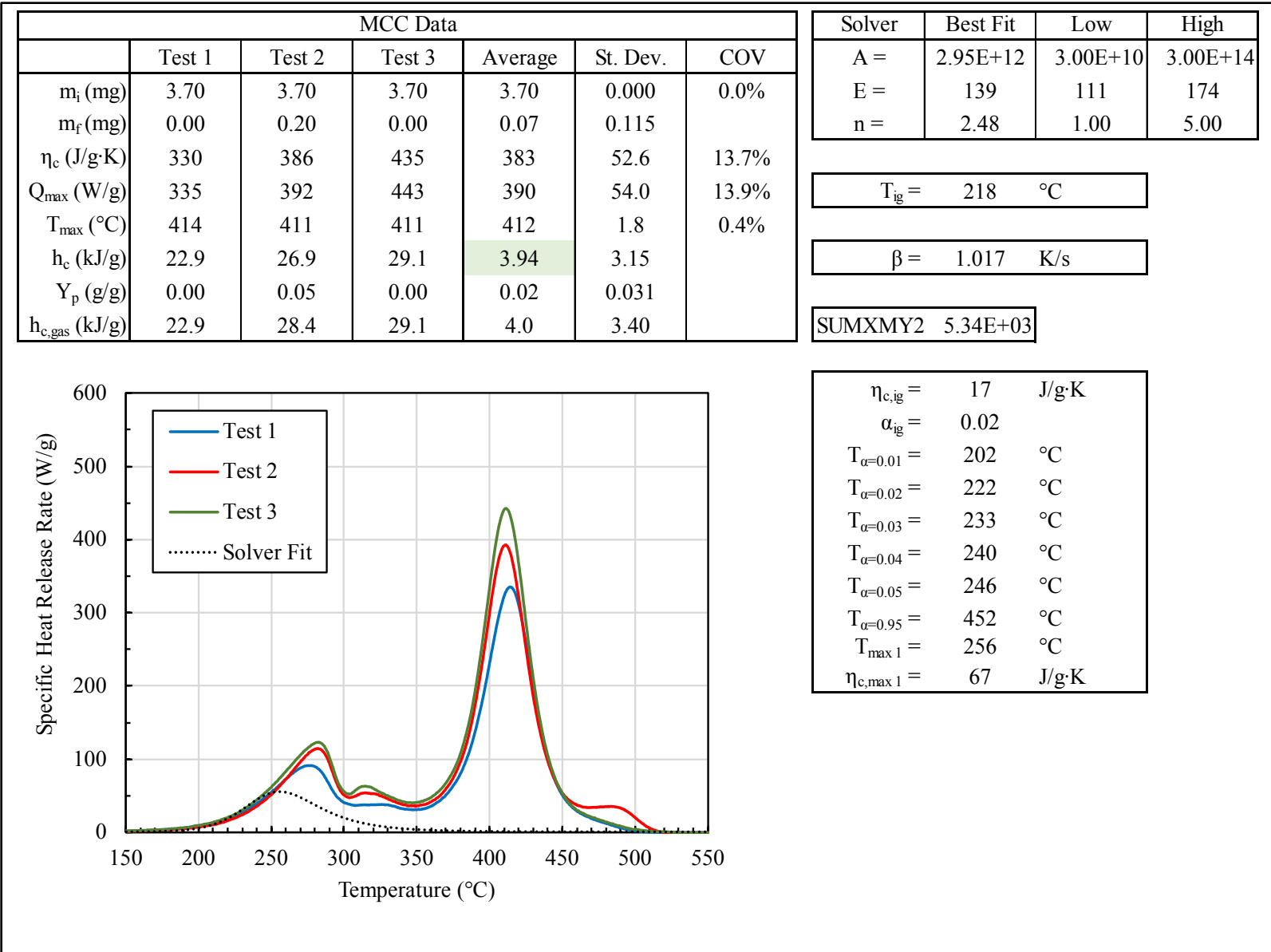


Figure J-44. Ignition temperature analysis results for Starcraft School Bus seat padding (Cryo-milled)

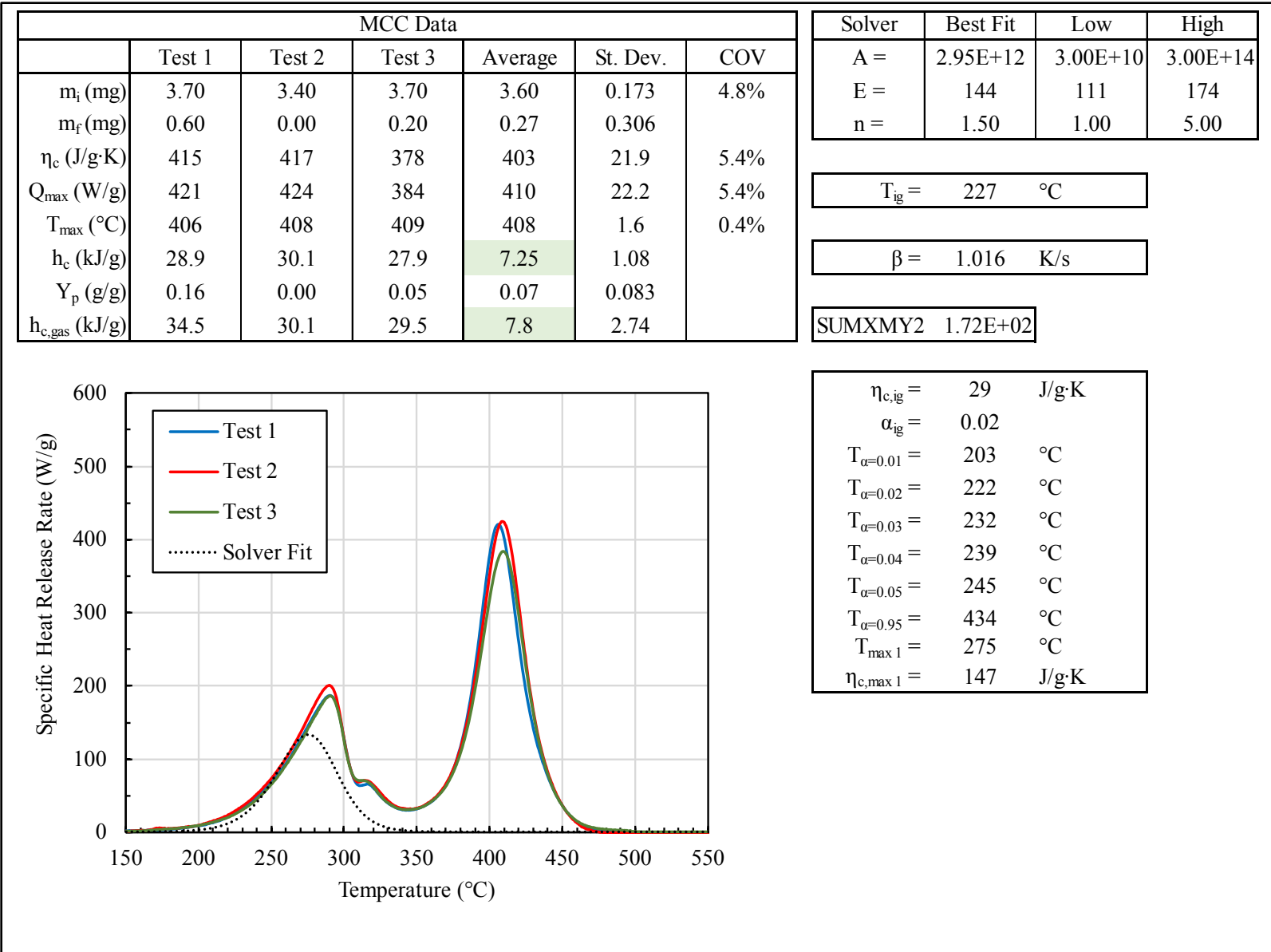


Figure J-45. Ignition temperature analysis results for Trans Tech School Bus seat padding (Cryo-milled)

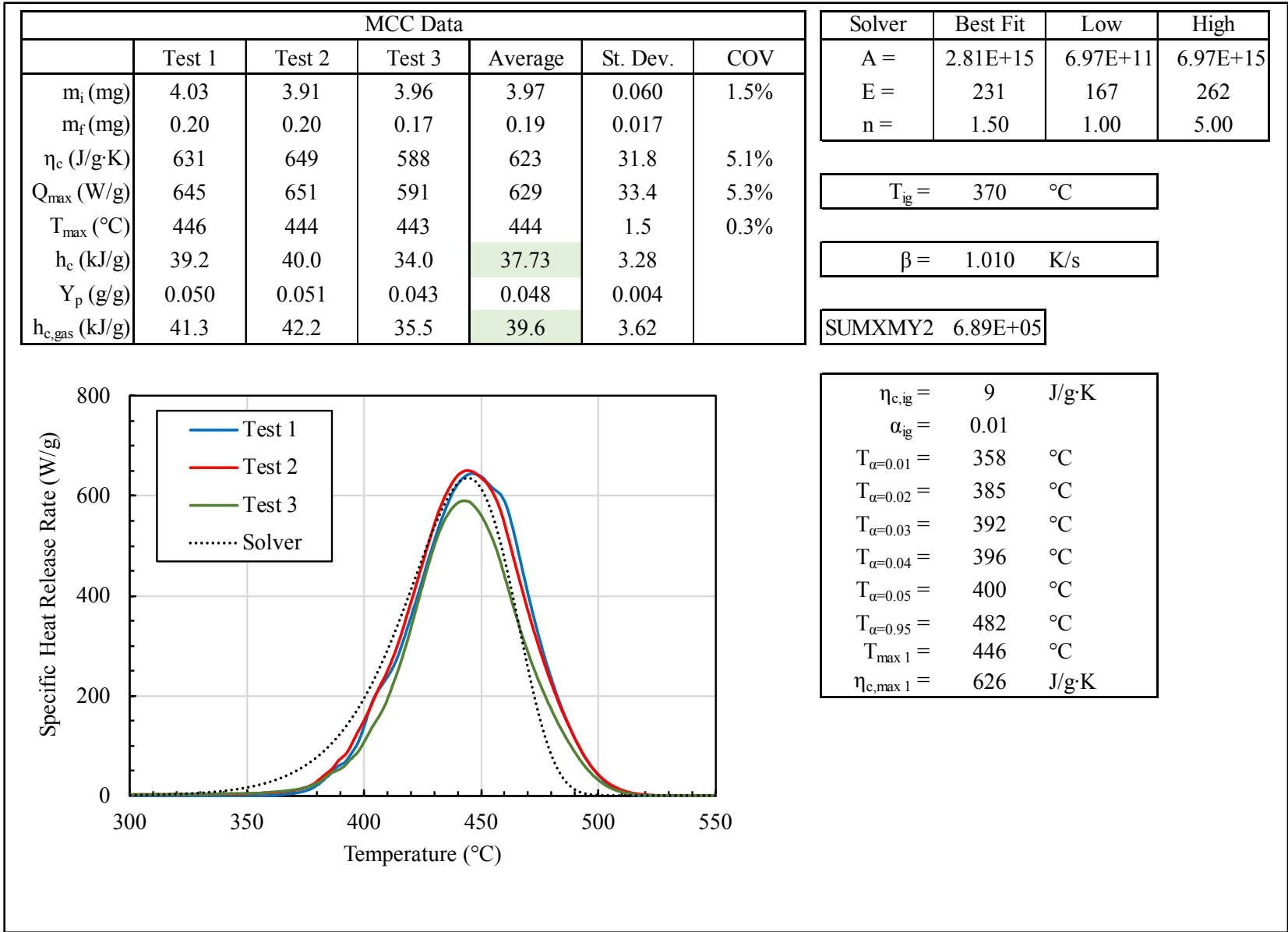


Figure J-46. Ignition temperature analysis results for r Motor Coach luggage rack door (Cryo-milled)

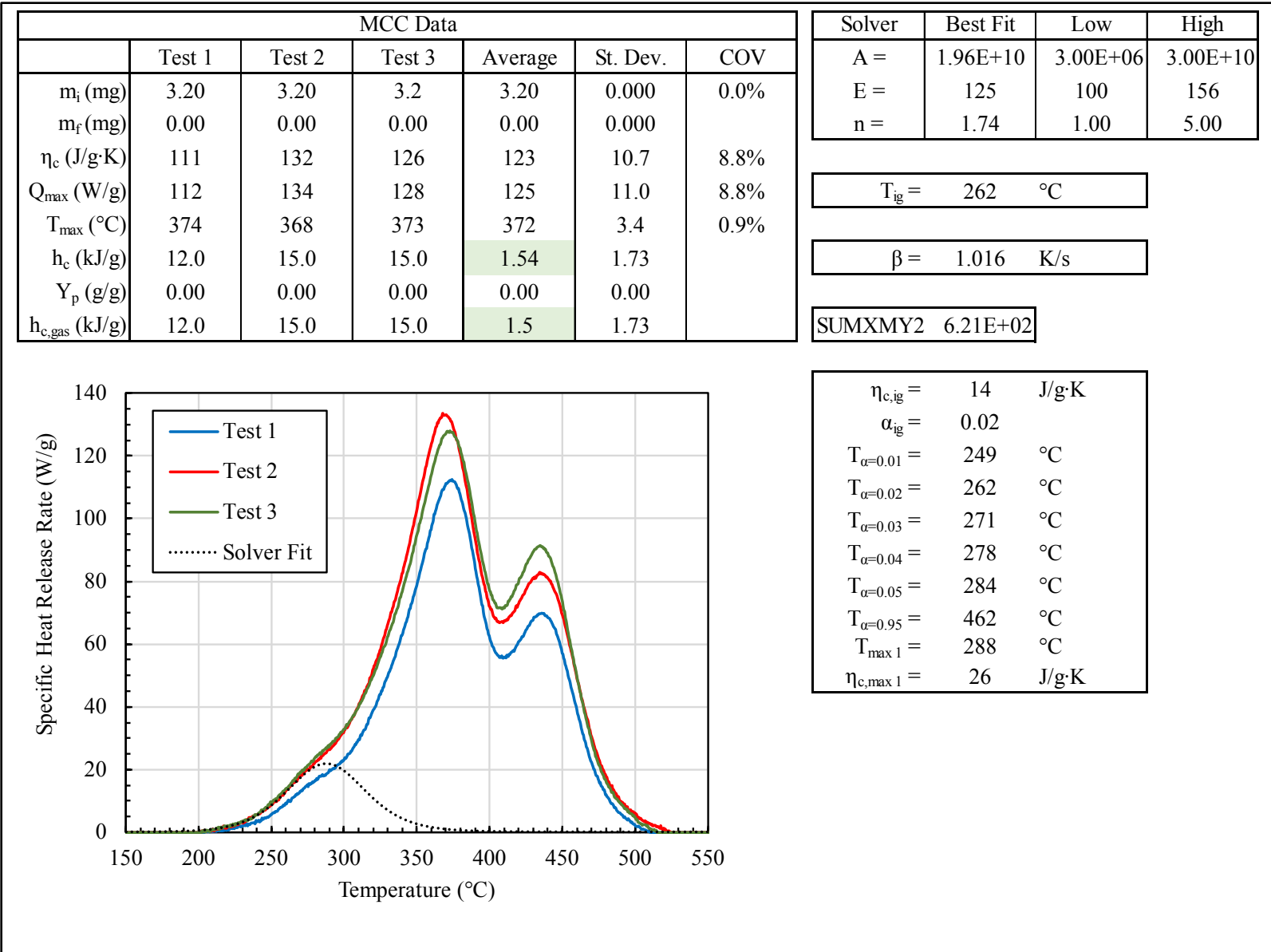


Figure J-47. Ignition temperature analysis results for Motor Coach Headliner (Cryo-milled)

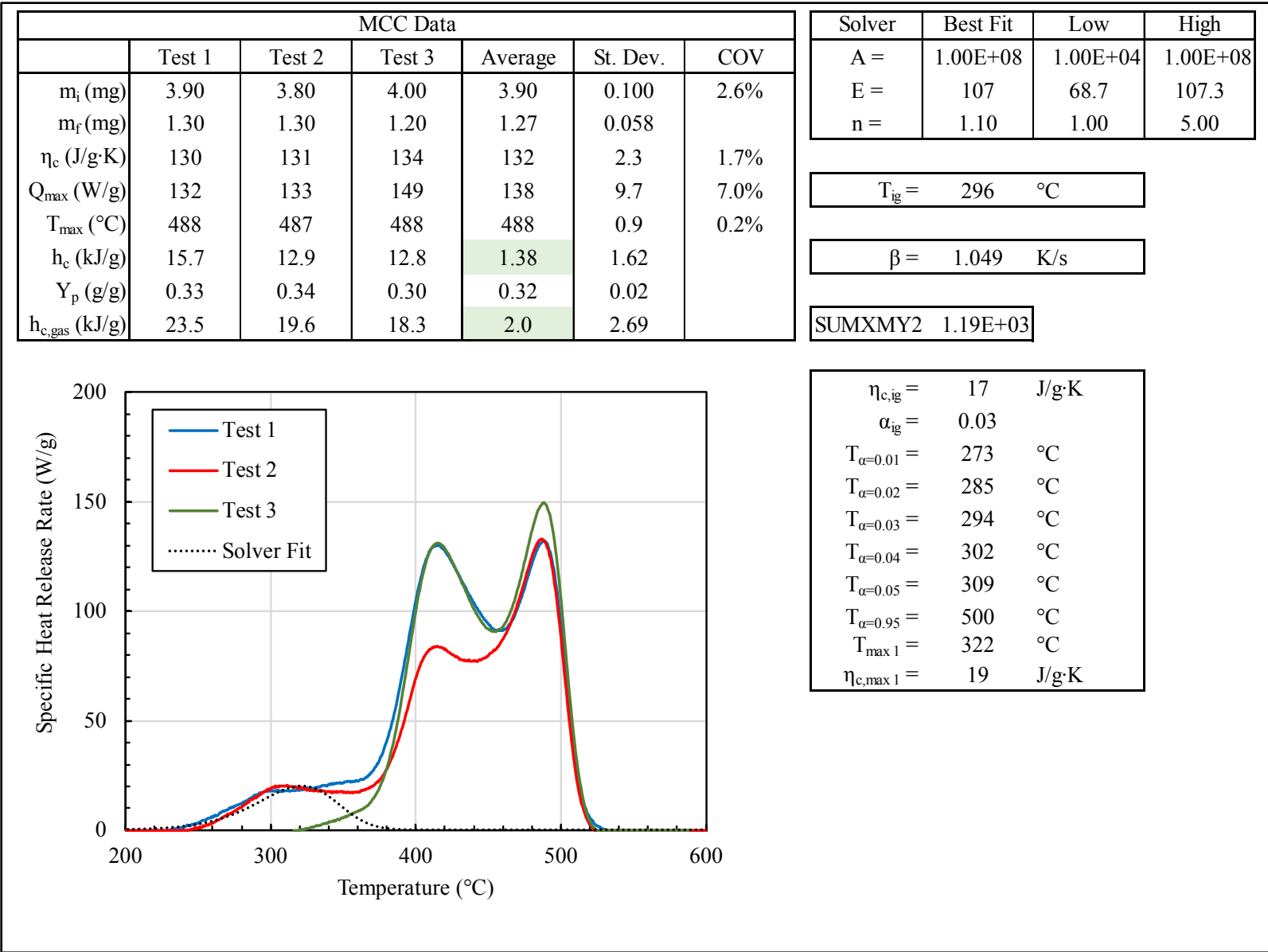


Figure J-48. Ignition temperature analysis results for Mercedes carpet (Cryo-milled)

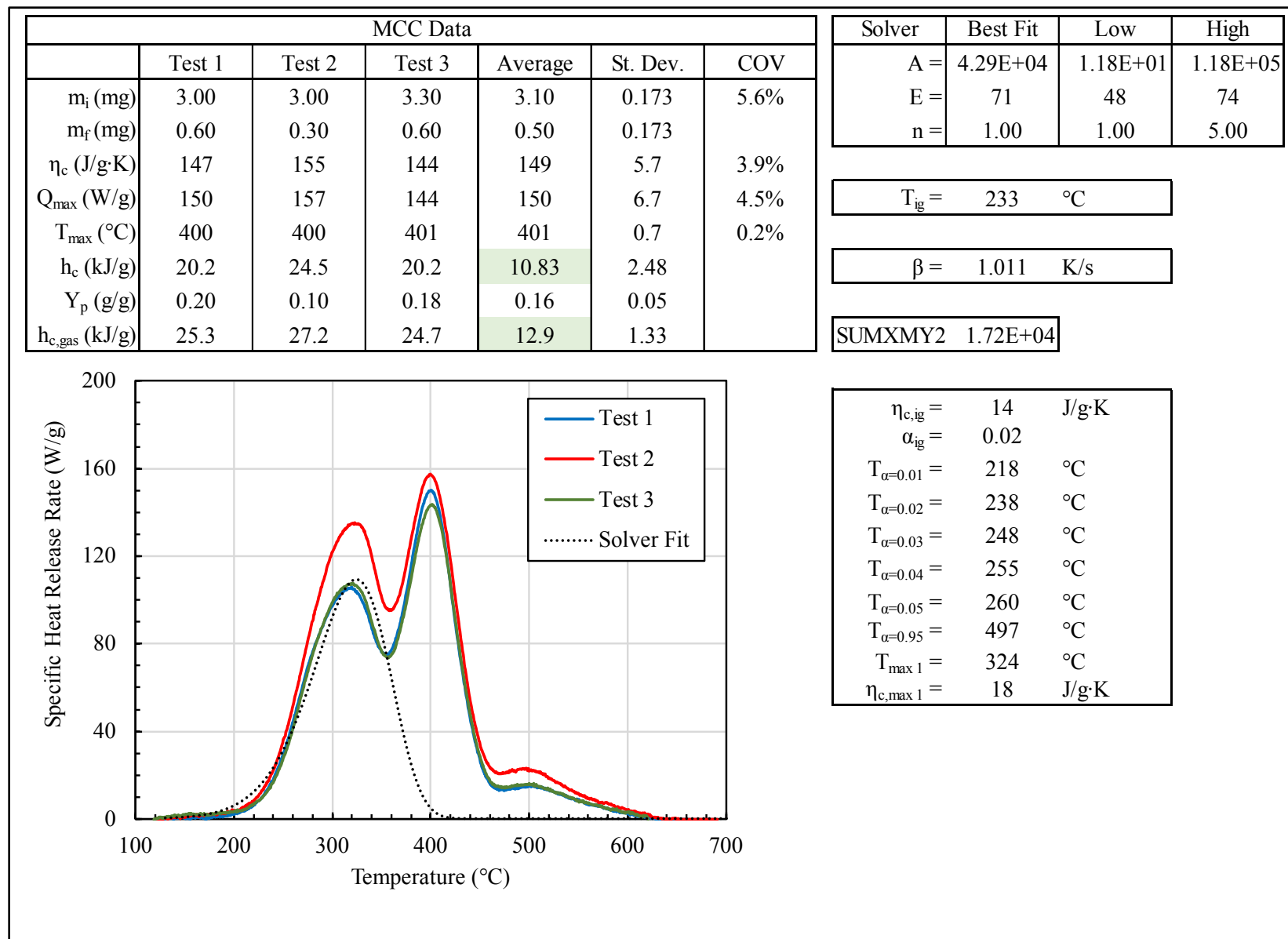


Figure J-49. Ignition temperature analysis results for Ford Headliner (Cryo-milled)

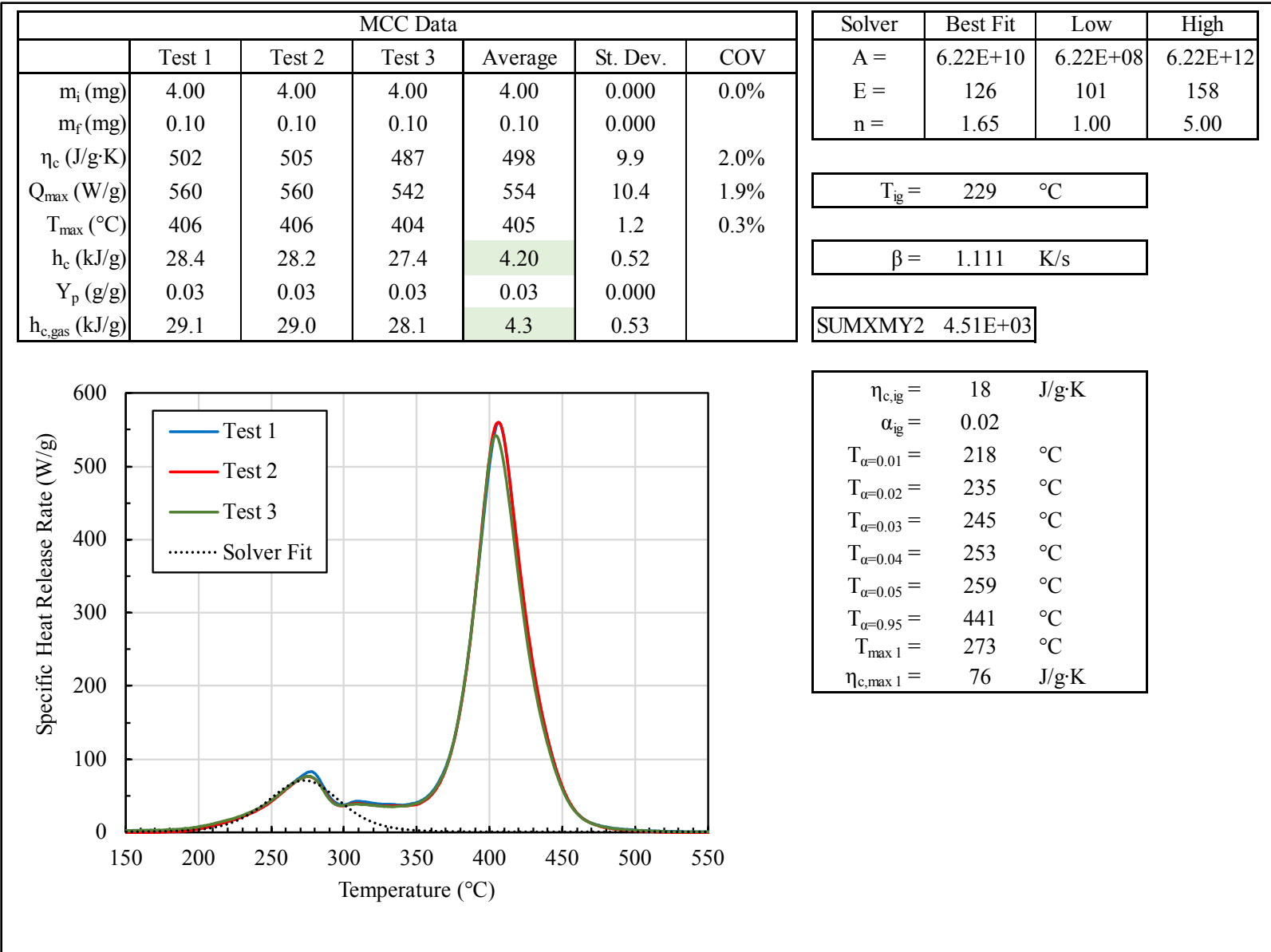


Figure J-50. Ignition temperature analysis results for Camaro seat padding (Cryo-milled)

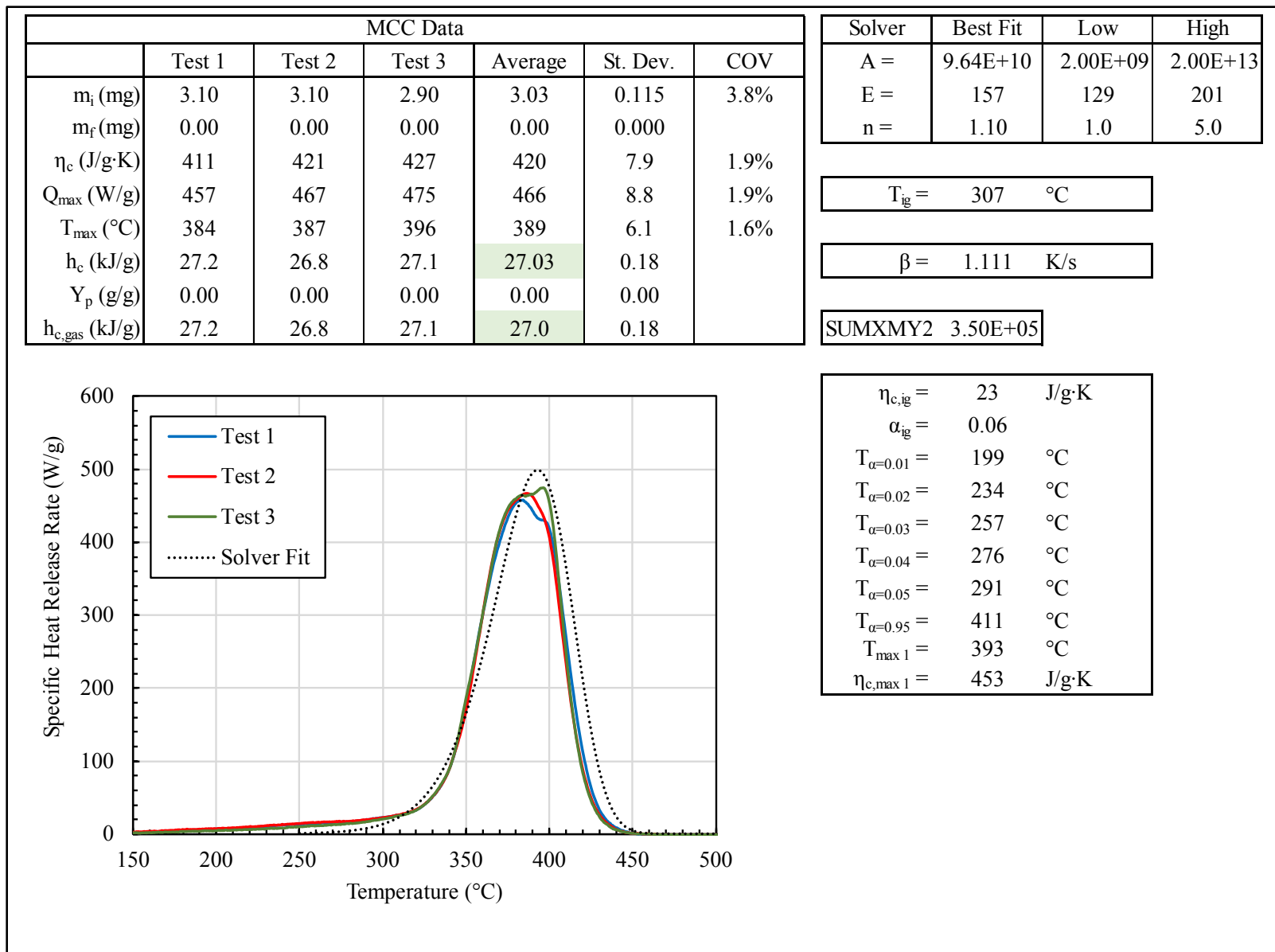


Figure J-51. Ignition temperature analysis results for Thin Acrylate Sheet (Cryo-milled)

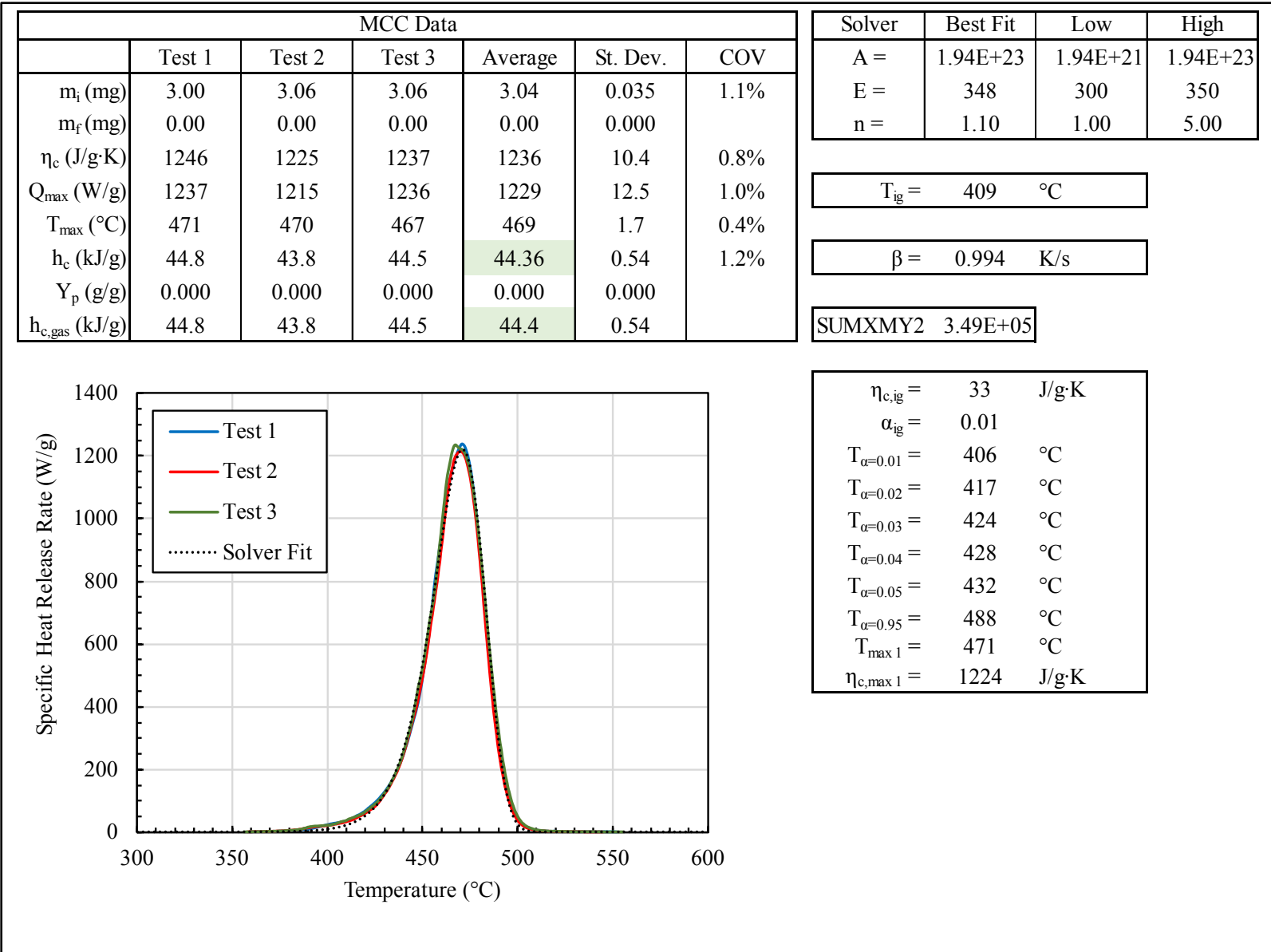


Figure J-52. Ignition temperature analysis results for Britax Parkway base

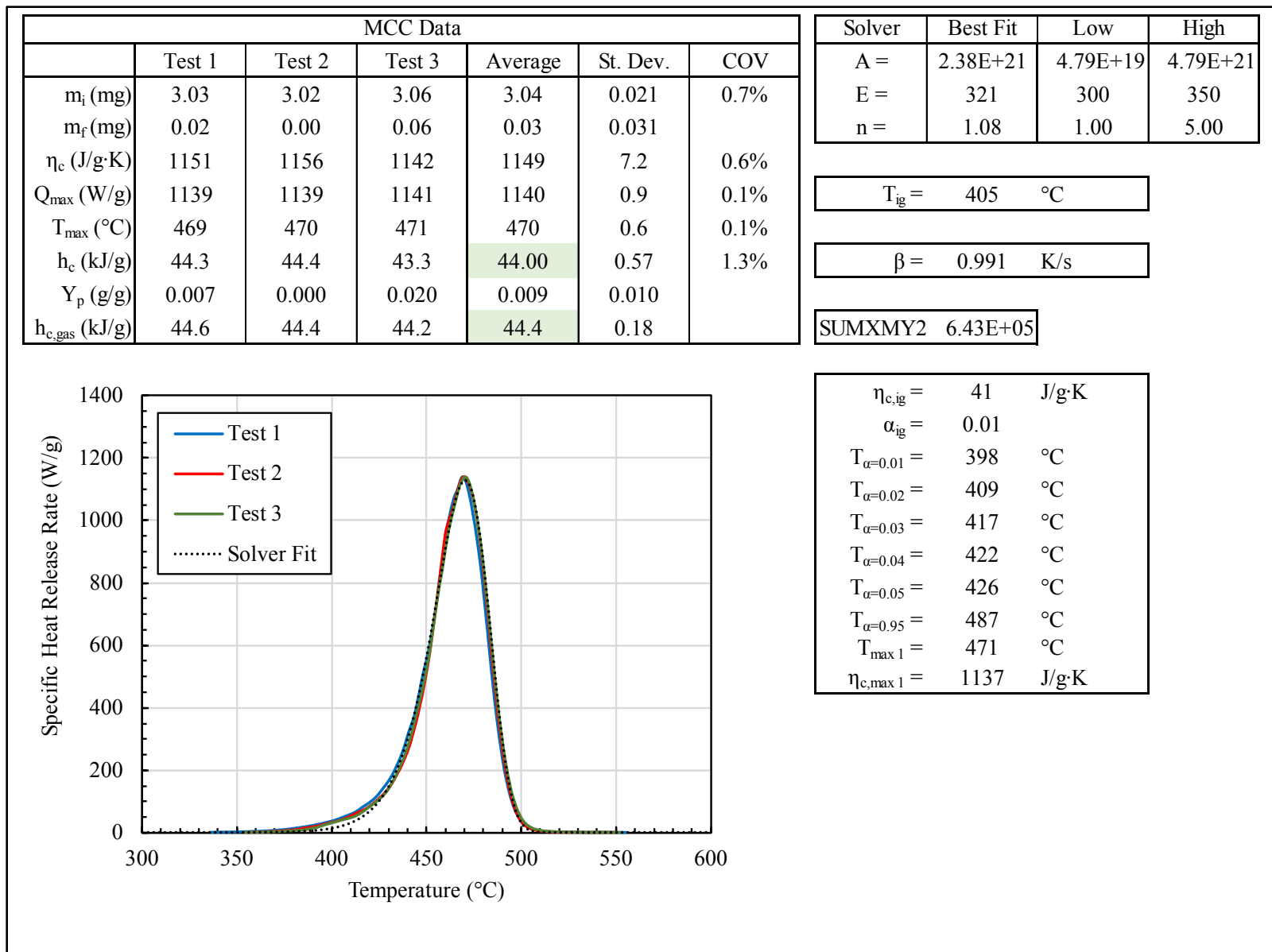


Figure J-53. Ignition temperature analysis results for Chicco KeyFit base

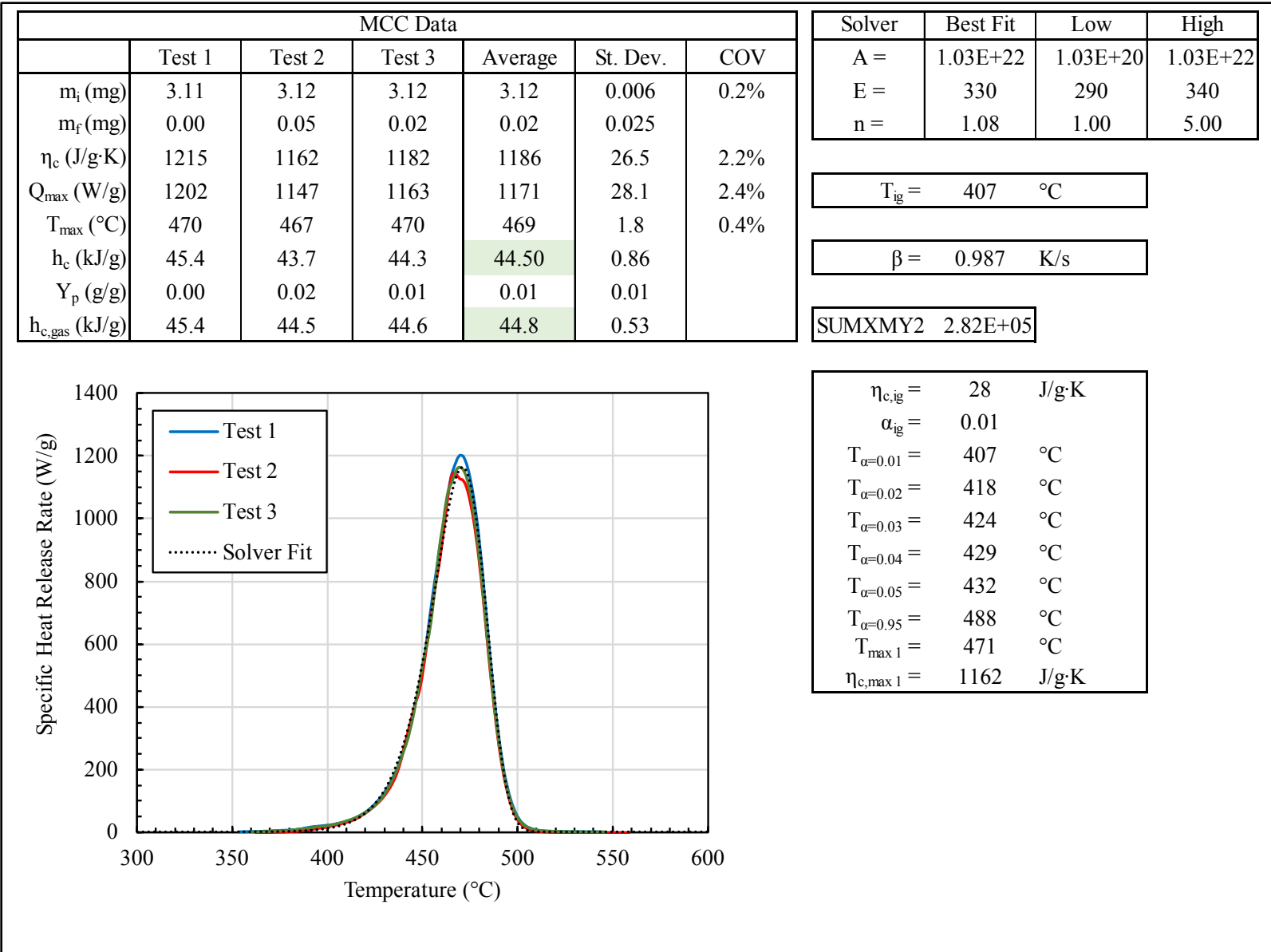


Figure J-54. Ignition temperature analysis results for Peg Perego Primo Viaggio base

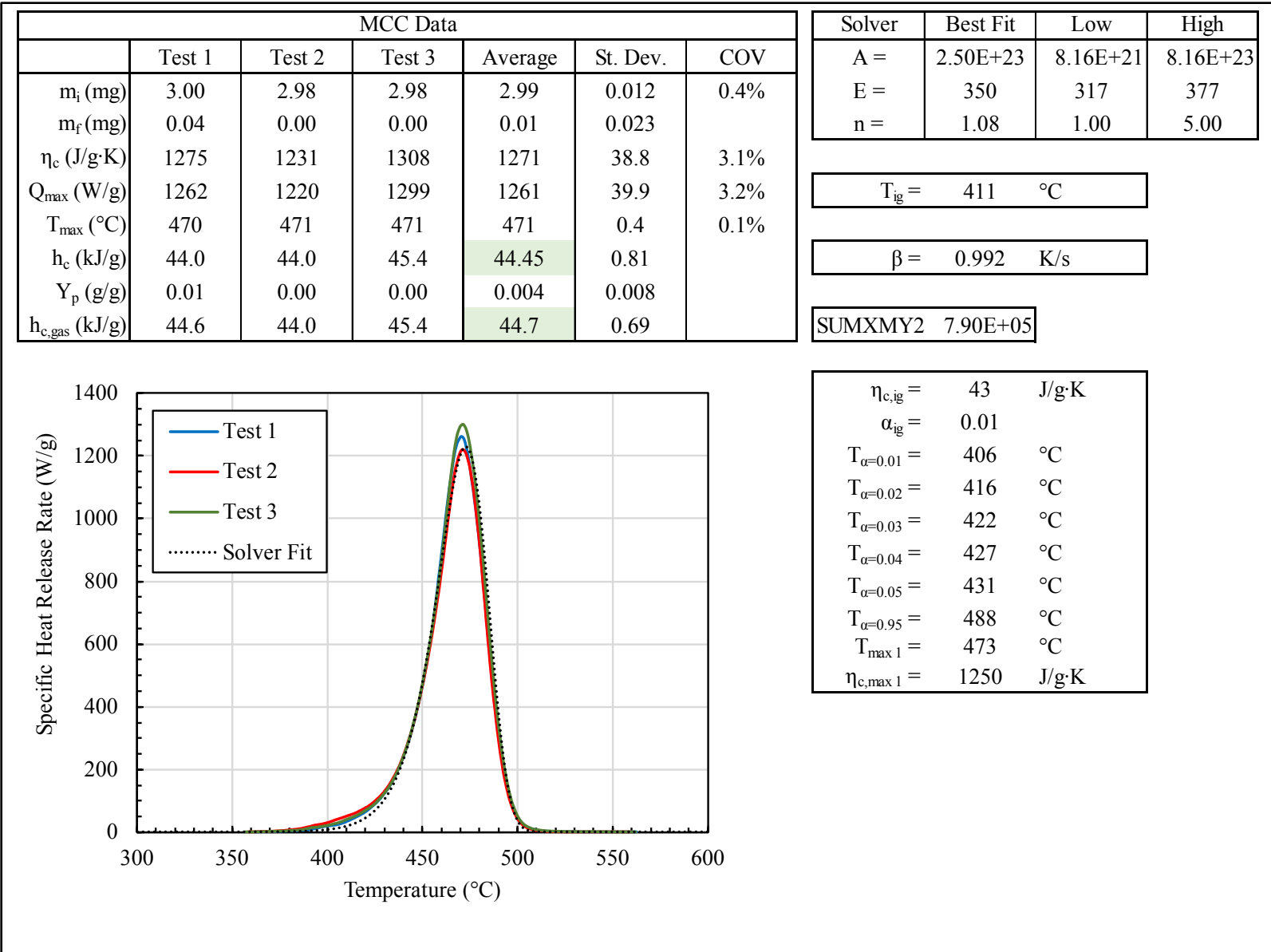


Figure J-55. Ignition temperature analysis results for UPPAbaby Mesa base

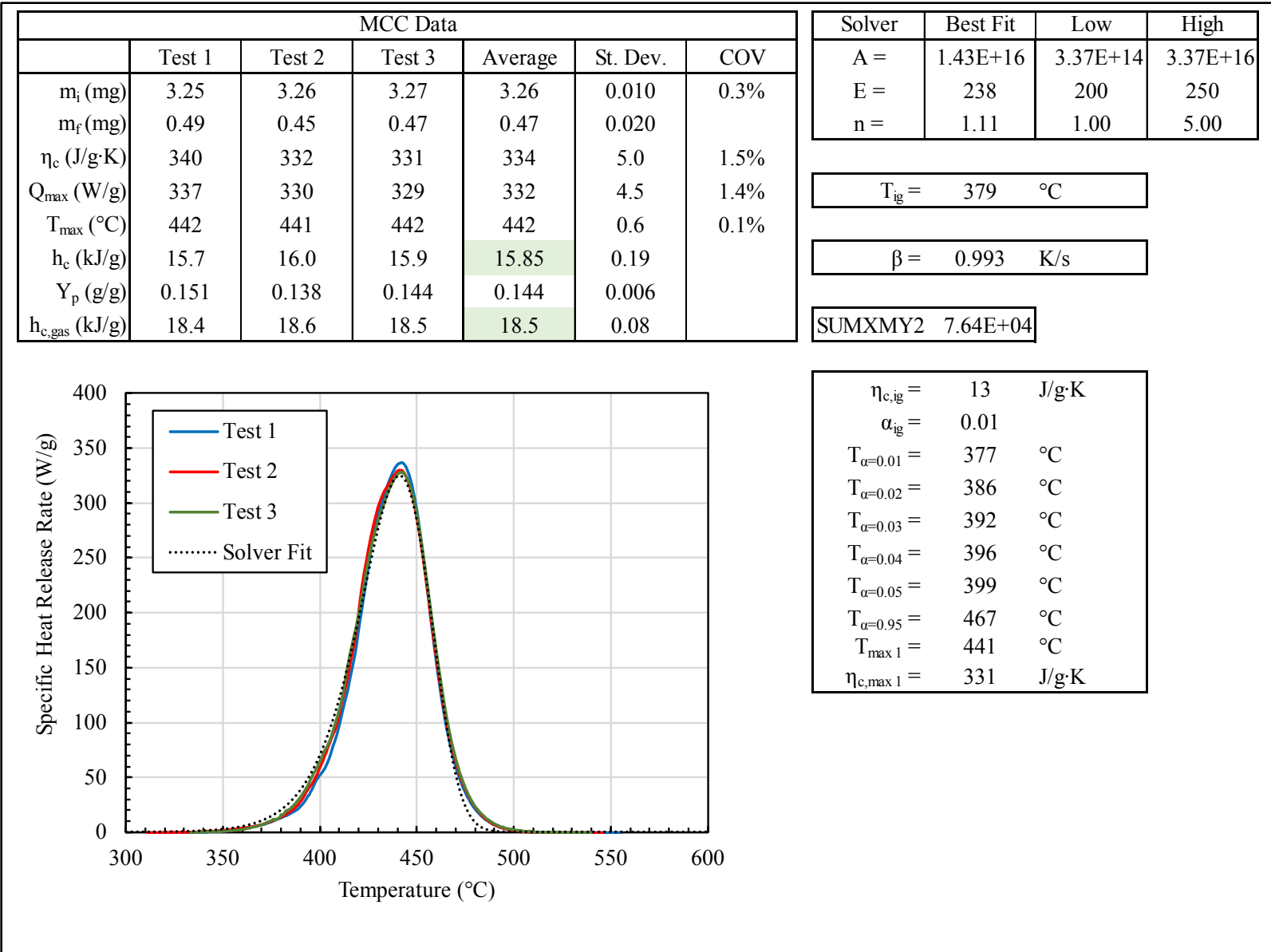


Figure J-56. Ignition temperature analysis results for Britax Parkway fabric

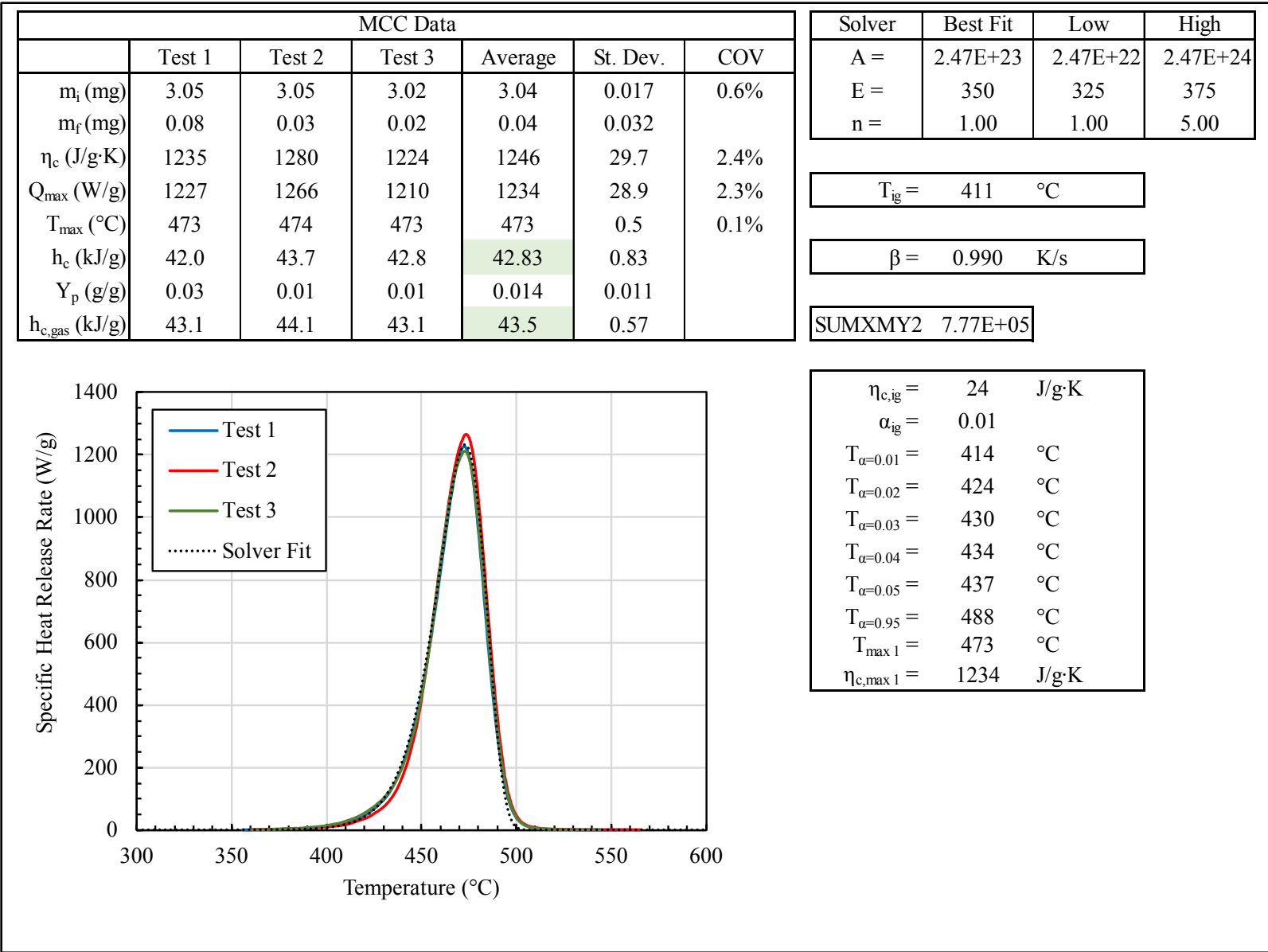


Figure J-57. Ignition temperature analysis results for Chicco KeyFit fabric

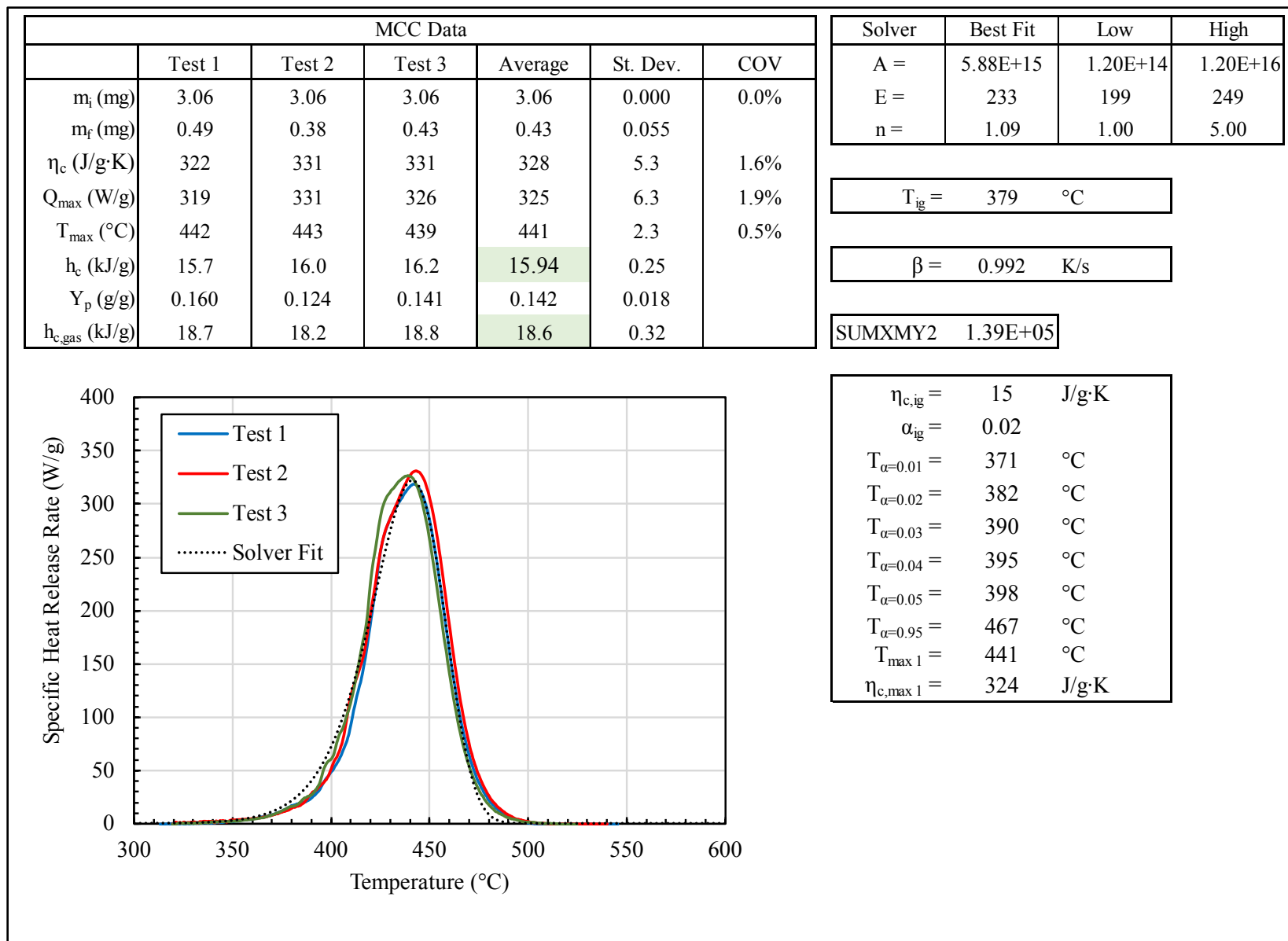


Figure J-58. Ignition temperature analysis results for Peg Perego Primo Viaggio fabric

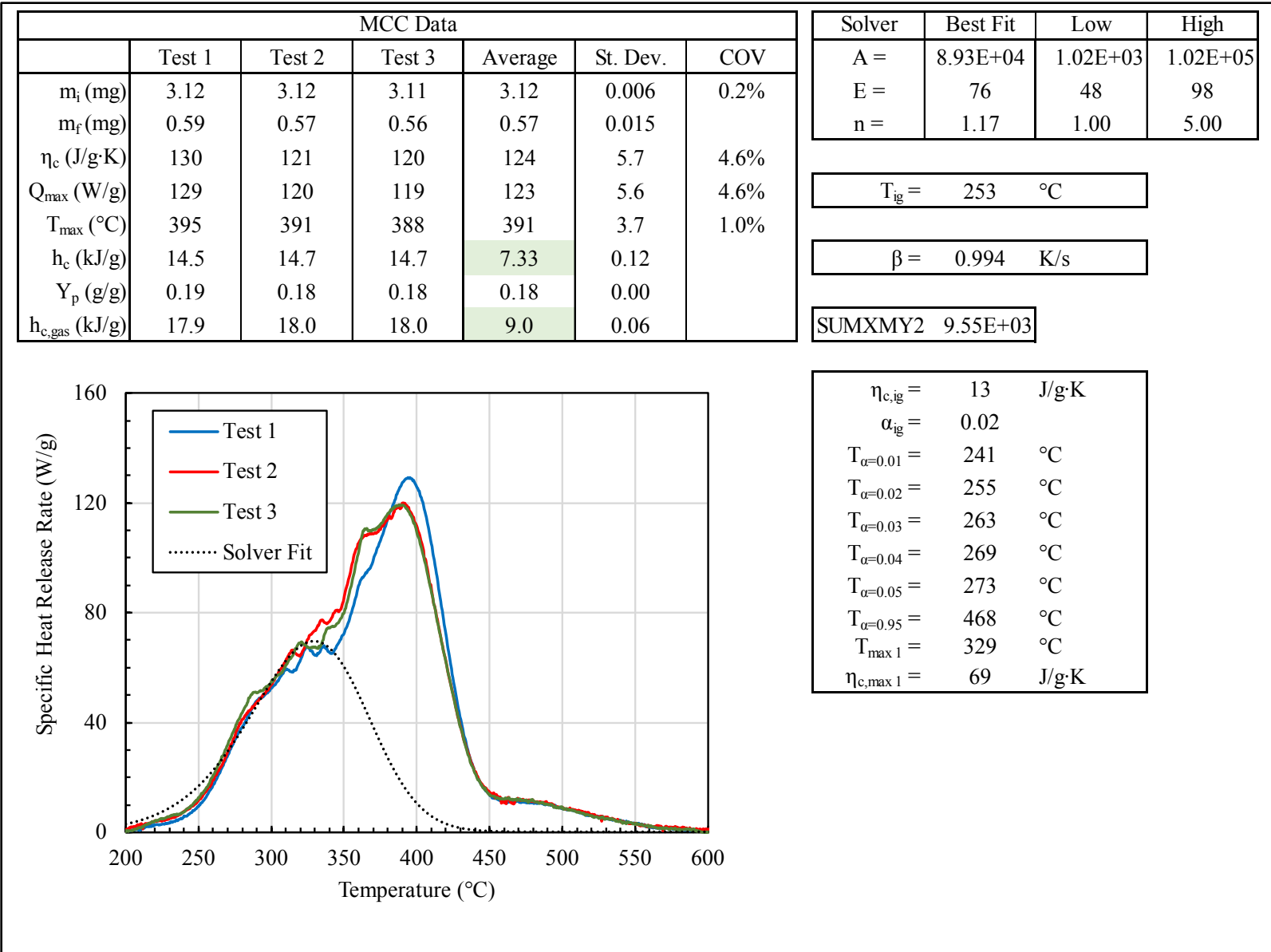


Figure J-59. Ignition temperature analysis results for UPPAbaby Mesa fabric

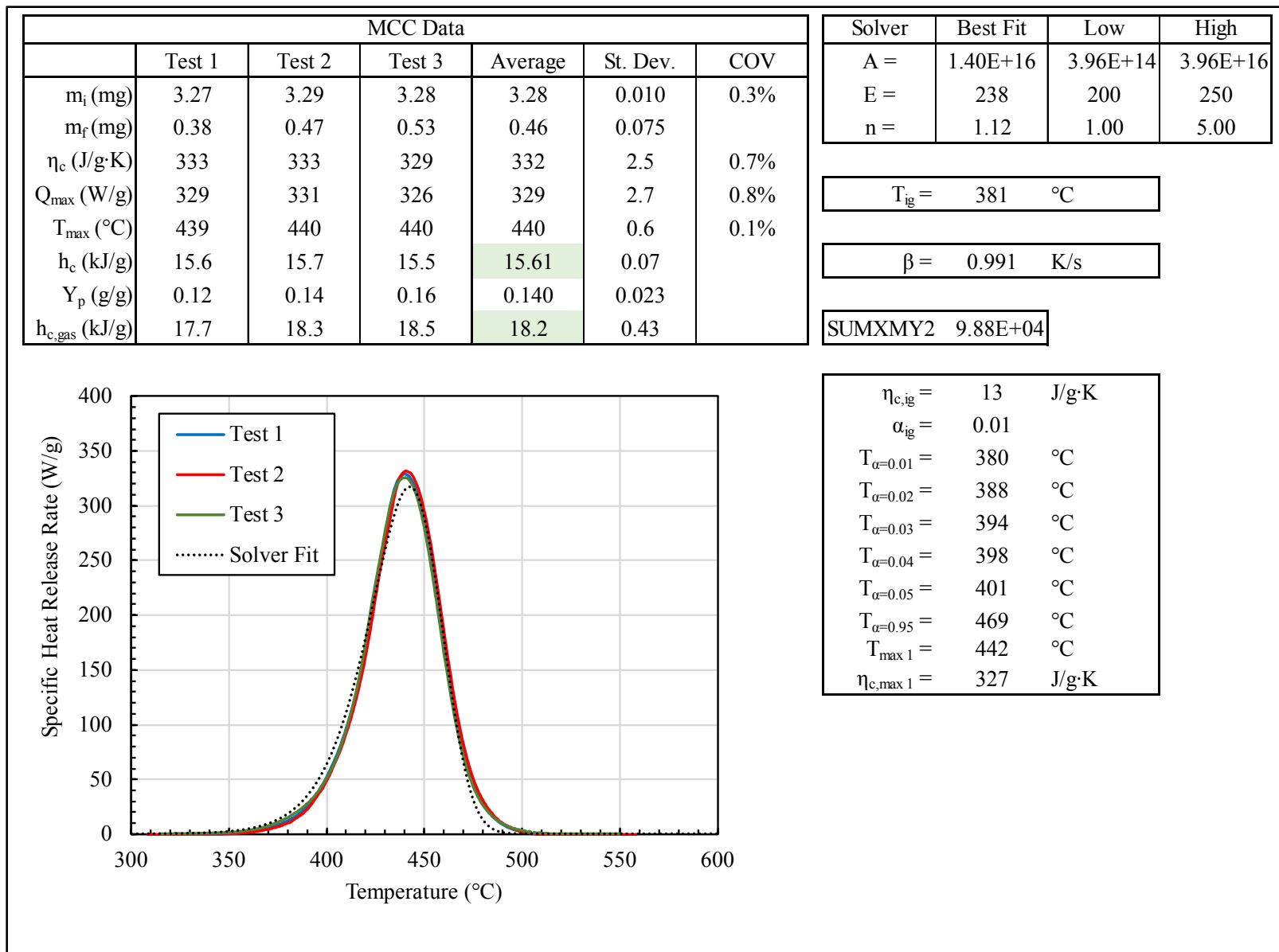


Figure J-60. Ignition temperature analysis results for Britax Parkway padding

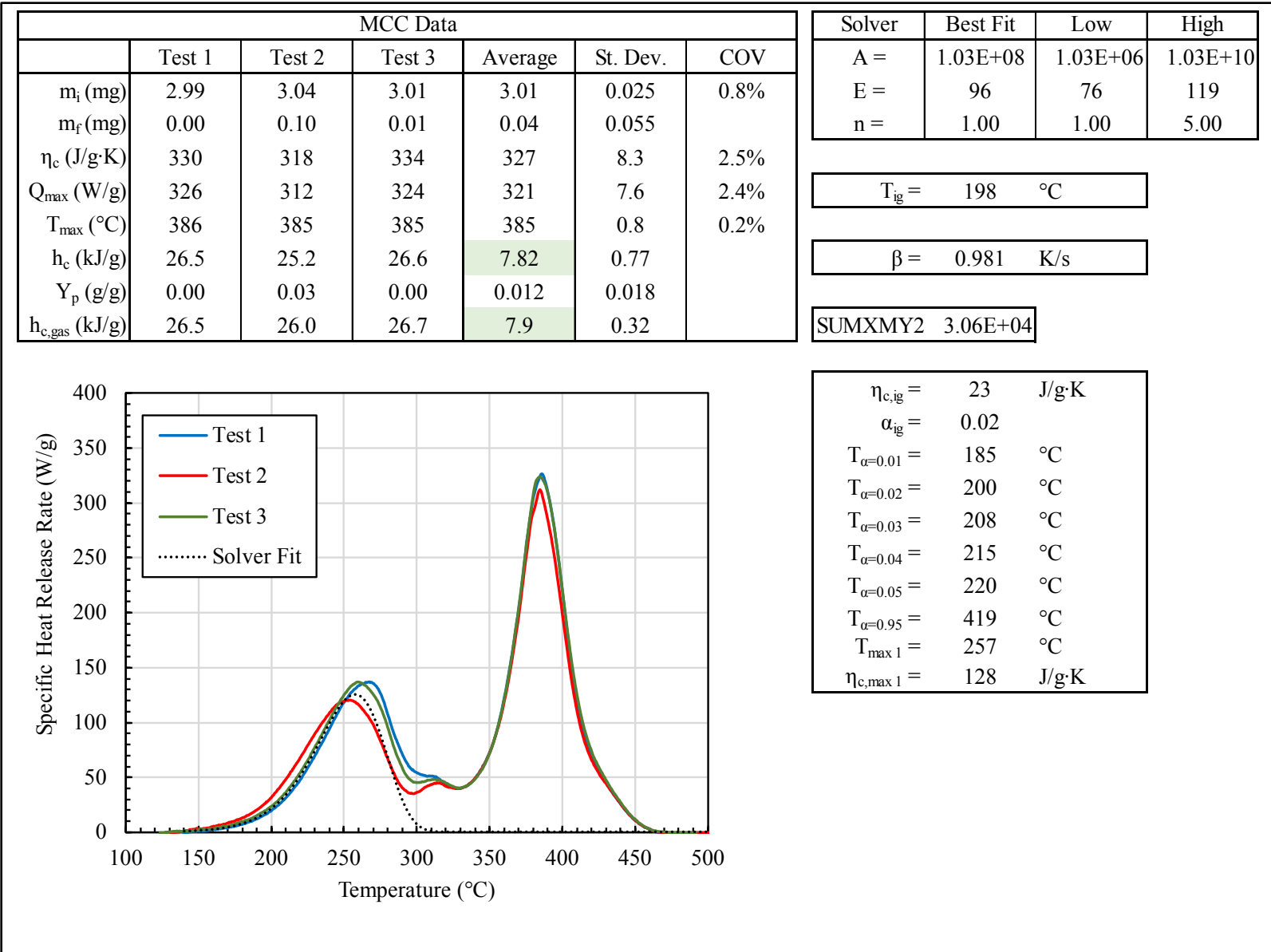


Figure J-61. Ignition temperature analysis results for Chicco KeyFit padding

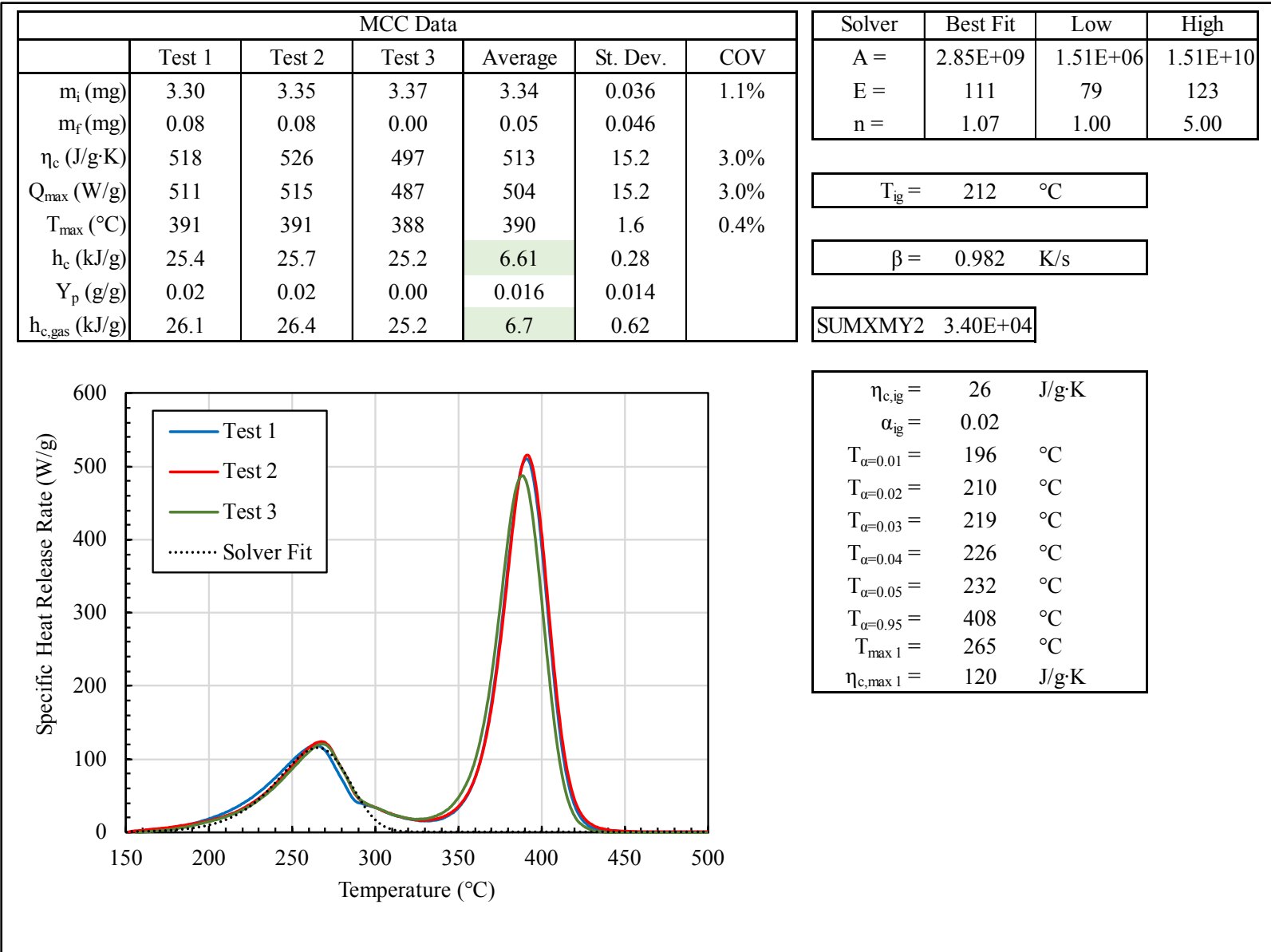


Figure J-62. Ignition temperature analysis results for Peg Perego Primo Viaggio padding

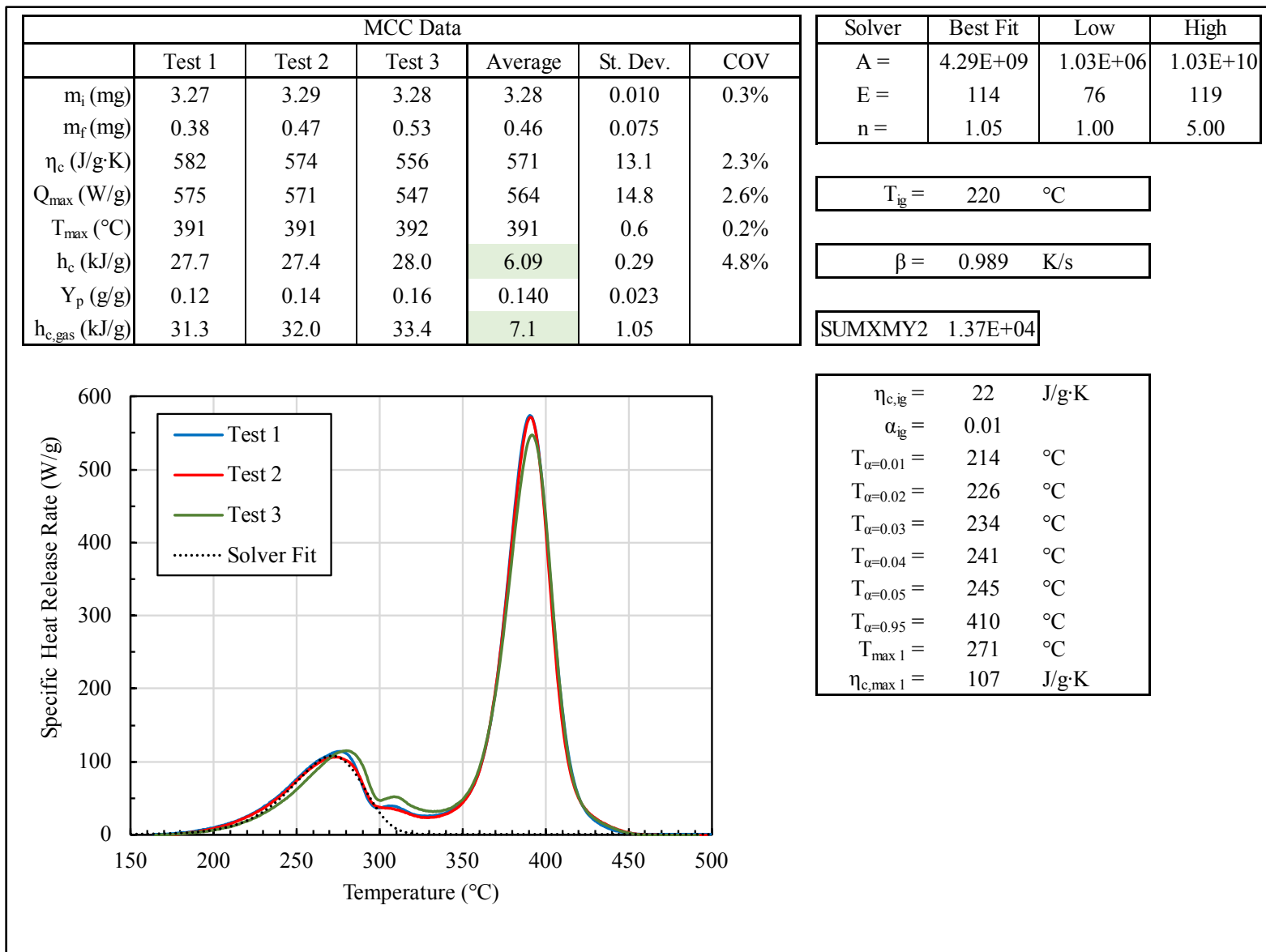


Figure J-63. Ignition temperature analysis results for UPPAbaby Mesa padding

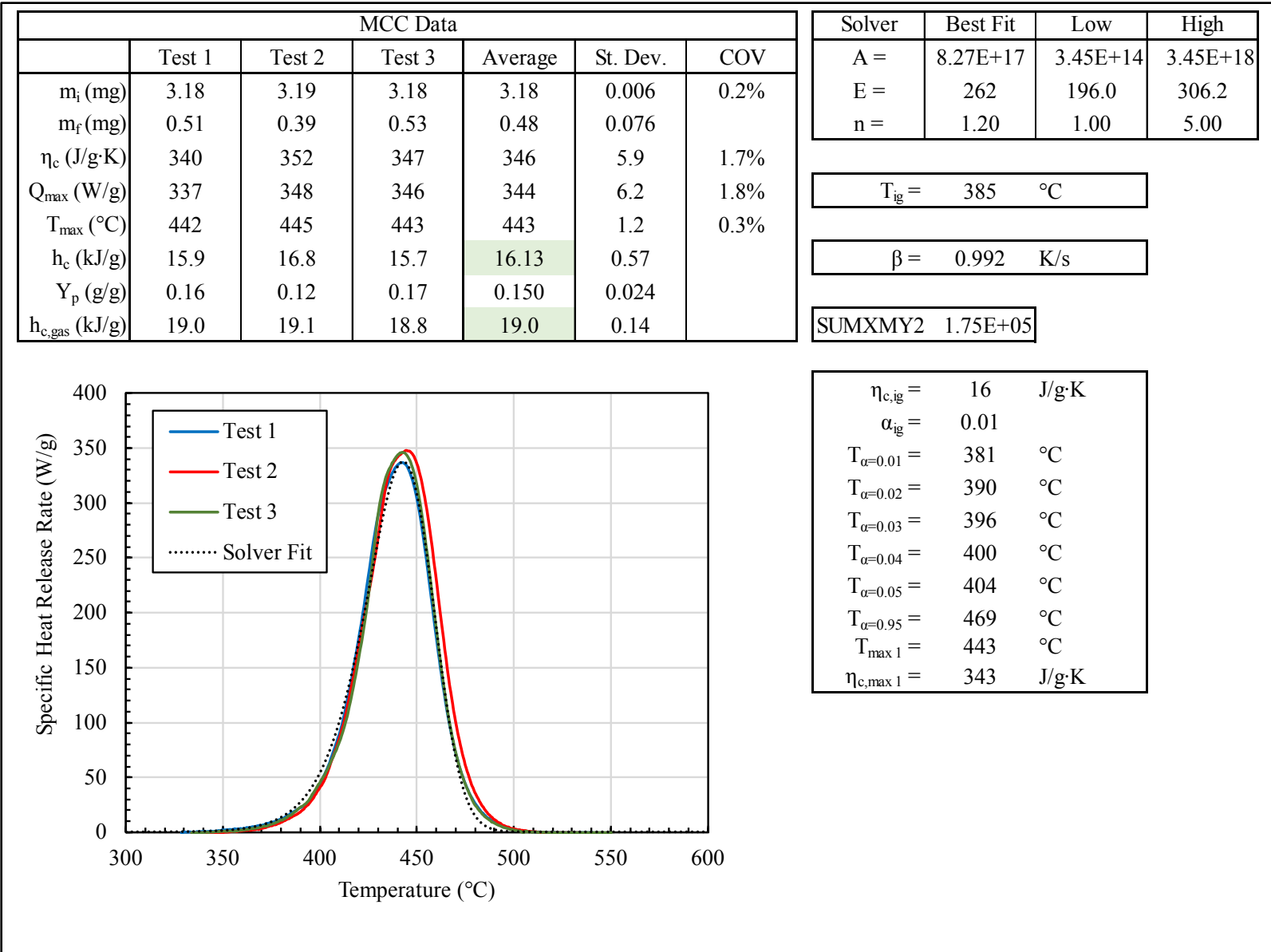


Figure J-64. Ignition temperature analysis results for Britax Parkway fabric and padding assembly

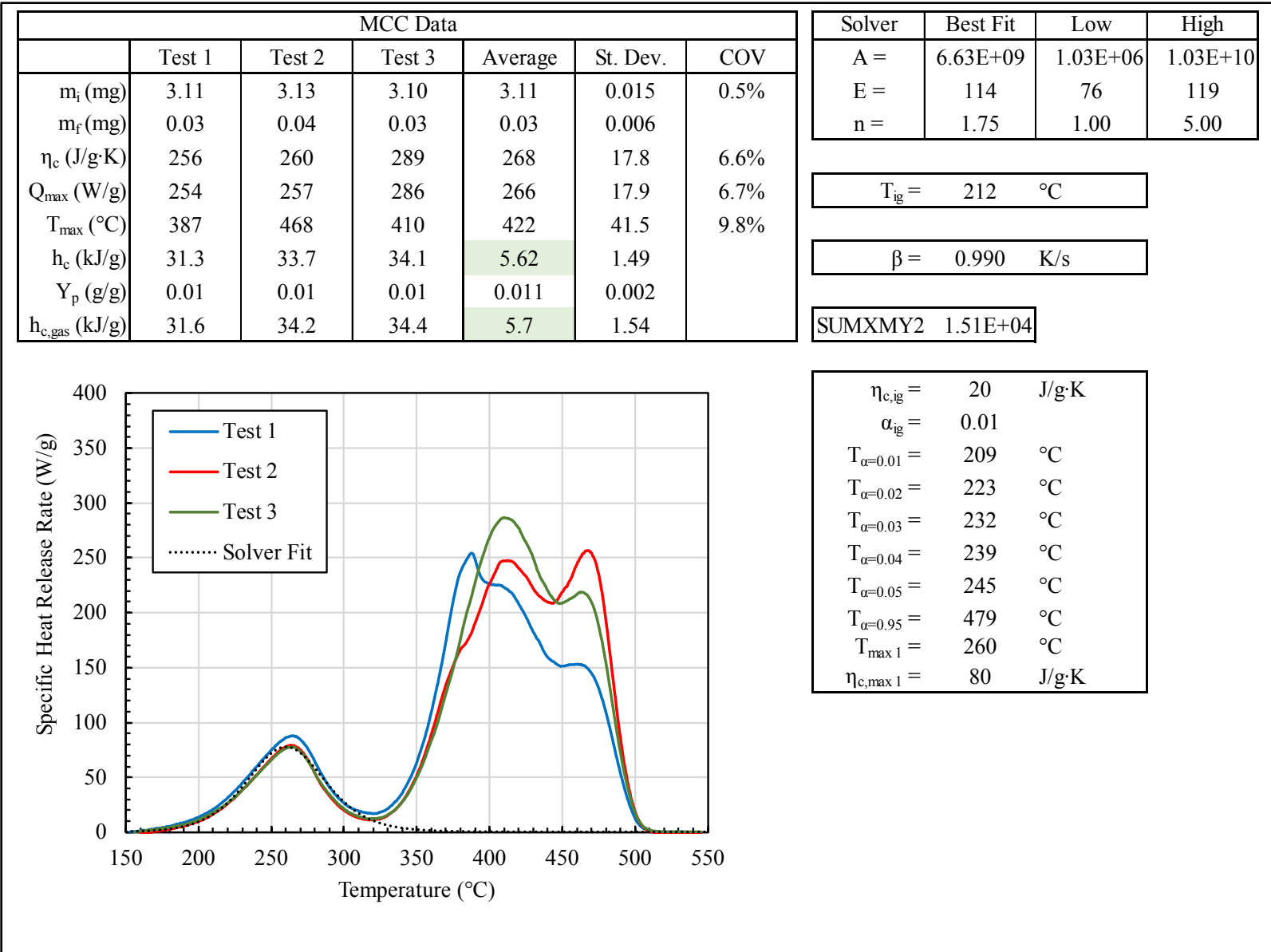


Figure J-65. Ignition temperature analysis results for Chicco KeyFit fabric and padding assembly

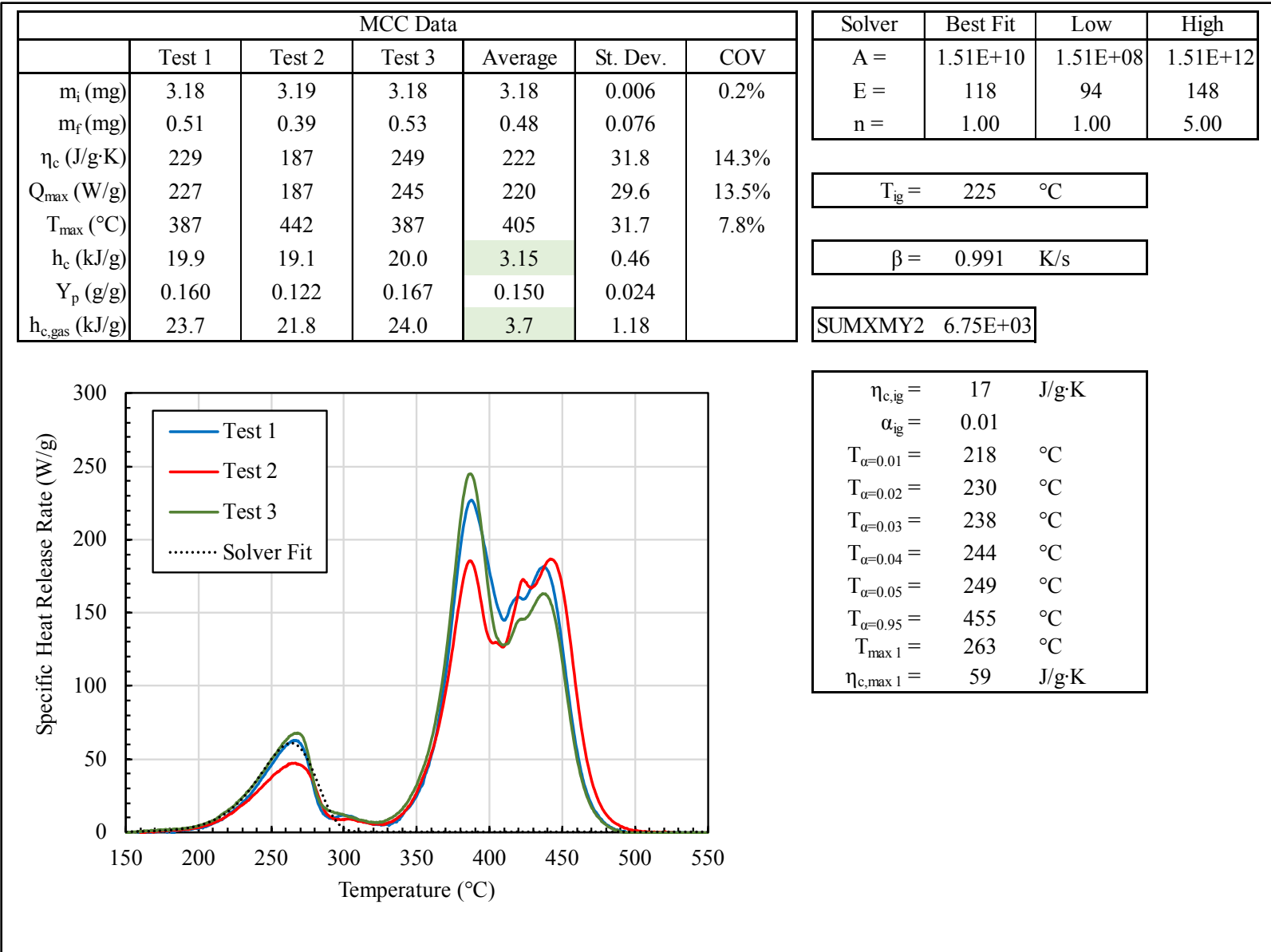


Figure J-66. Ignition temperature analysis results for Peg Perego Primo Viaggio fabric and padding assembly

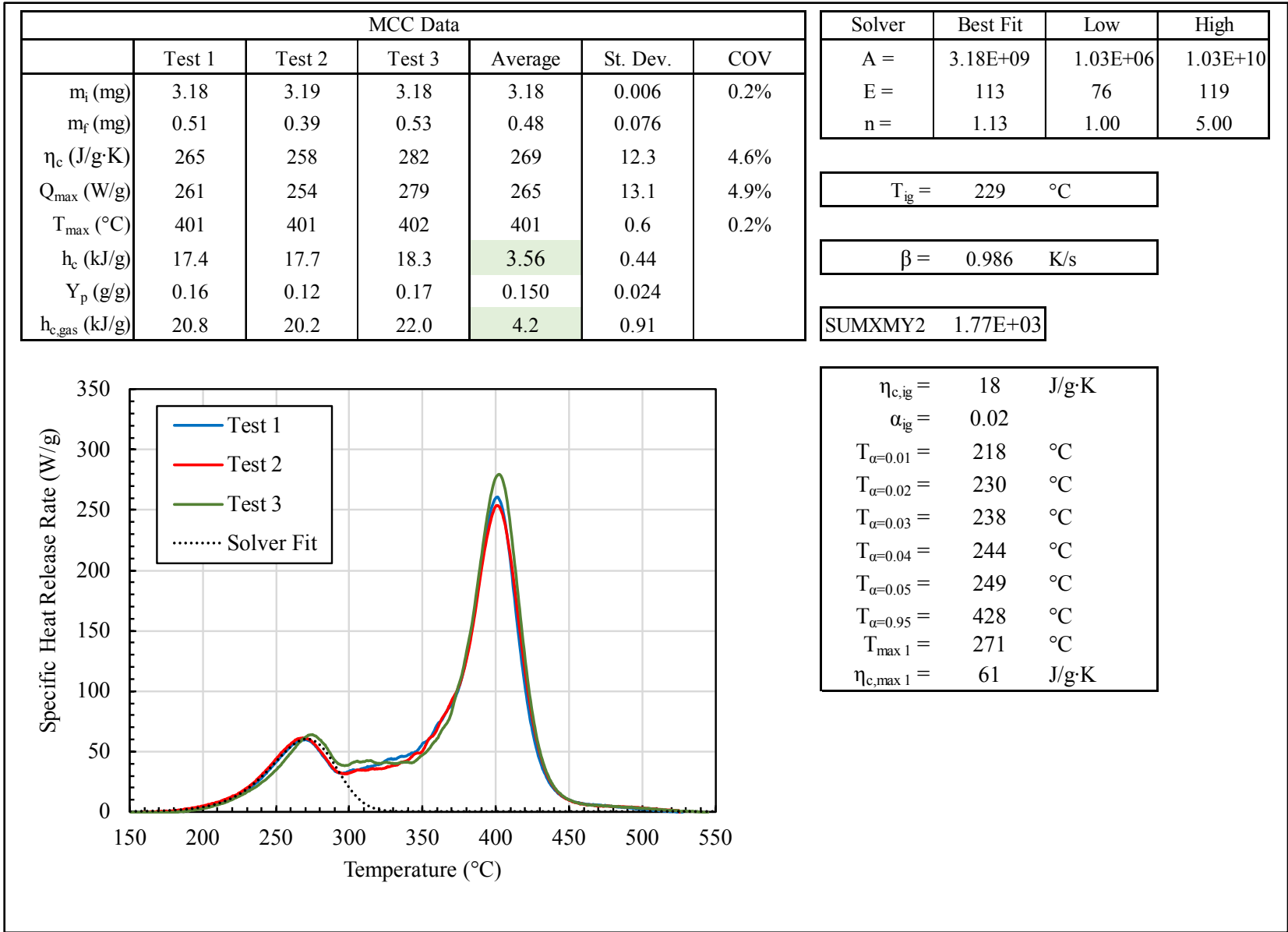


Figure J-67. Ignition temperature analysis results for Uppababy Mesa fabric and padding assembly

DOT HS 812 091
April 2021



U.S. Department
of Transportation
**National Highway
Traffic Safety
Administration**

